

**National Institute of Mental Health
Psychoactive Drug Screening Program
(NIMH PDSP)**

**ASSAY PROTOCOL BOOK
Version III**

March 2018

Bryan L. Roth, MD, PhD

Department of Pharmacology
University of North Carolina at Chapel Hill

This is an updated version as of March 2018 of the previous PDSP assay protocol book (2012), and contains detailed descriptions of experimental procedures, data analysis, and representative figures for radioligand binding and functional assays performed by the NIMH-PDSP.

Table of Contents

1. Radioligand binding assays

1.1. Drug plate preparation (Hamilton ASM[®] and STAR[®])

1.2. Cell culture and membrane fraction preparation

1.2.1. Calcium phosphate precipitation transfection – adherent HEK293 T

1.2.2. Suspension HEK293 transfection

1.2.3. Membrane preparations from cultured cells

1.2.4. Membrane preparations from tissues (general)

1.2.5. Membrane preparations from rat brain for specific targets

1.2.6. List of cell lines that PDSP maintains

1.2.7. Media recipes

1.3. Saturation binding assay

1.4. Primary and secondary binding assay

1.5. Radioligand binding assays for nicotinic acetylcholine receptors

1.5.1. Cell culture and membrane preparation

1.5.2. Radioligand binding assay

1.5.3. Primary and Secondary binding assay

1.5.4. Data analysis and result reporting

1.6. General binding data entry, analysis, and quality control (non nAChRs)

1.6.1. Built-in analysis tool in the PDSP Database

1.6.1.1. Saturation binding results analysis and reporting

1.6.1.2. Primary binding results analysis and reporting

1.6.1.3. Secondary binding results analysis and reporting

1.6.2. Data analysis using Microsoft Excel and Prism v5.0

1.6.2.1. Saturation binding results analysis

1.6.2.2. Primary binding results analysis

1.6.2.3. Secondary binding results analysis

1.7. Table of conditions for binding assays and representative figures

2. Functional assays

2.1. Drug plate preparations for functional assays

2.2. General procedures for PDSP functional assays

2.3. Data analysis for functional assays

2.3.1. Agonist activity

2.3.2. Antagonist activity

2.3.3. Schild plot analysis

2.3.4. Quantifying bias

2.3.5. Allosteric operational analysis

2.3.6. List of available functional assays at NIMH-PDSP

2.4. Functional assays for G_q coupled GPCRs:

2.4.1. Calcium mobilization assays (FLIPR^{TETRA})

2.4.2. Intracellular inositol phosphate accumulation

2.4.3. Table of G_q coupled GPCRs with functional assays done by the PDSP

- 2.4.4. Representative figures
- 2.5. Functional assays for G_i or G_s coupled GPCRs: split luciferase based biosensor cAMP assay (GloSensor® cAMP assay)
 - 2.5.1. Cell culture and transfection
 - 2.5.2. Split luciferase based cAMP assay – Luciferin first protocol
 - 2.5.3. Split luciferase based cAMP assay – Drug first protocol
 - 2.5.4. Data processing and analysis
 - 2.5.5. Table of G_i or G_s coupled GPCRs with functional assays done by the PDSP
 - 2.5.6. Representative figures
- 2.6. Functional assays for G-protein independent β -arrestin recruitment
 - 2.6.1. GPCR Tango construct design and HTLA cells
 - 2.6.2. GPCR Tango assay design
 - 2.6.3. Data processing and analysis
 - 2.6.4. Table of GPCR Tango constructs with representative curves
 - 2.6.5. Representative curves (agonist and antagonist activity)
- 2.7. PRESTO-GPCRome screening
 - 2.7.1. HTLA cell culture and plating
 - 2.7.2. GPCRome Tango (DNA) plate preparation
 - 2.7.3. Reverse transfection with Calcium phosphate precipitation method
 - 2.7.4. Compound addition and stimulation
 - 2.7.5. Data processing, analysis, representative figures

- 2.8. BRET-based transducerome screening platform
 - 2.8.1. Introduction
 - 2.8.2. Assay design and optimization
 - 2.8.3. Assay procedure and representative figures
 - 2.8.4. Additional resources
- 2.9. hERG functional assay: Thallium (Tl⁺) flux assay (FluxOR)
 - 2.9.1. HEK293 hERG cell culture
 - 2.9.2. Tl⁺ flux assays (FluxOR) for hERG inhibitors
 - 2.9.3. Tl⁺ flux assays (FluxOR) for hERG trafficking modulators
 - 2.9.4. Data processing and analysis
 - 2.9.5. Representative figures
- 2.10. hERG electrophysiology: automated patch-clamp PatchXpress assay
 - 2.10.1. External and internal solutions
 - 2.10.2. HEK293 hERG cell preparation
 - 2.10.3. Drug plate preparation
 - 2.10.4. Patch procedure
 - 2.10.5. Data processing and analysis
 - 2.10.6. Representative figures
- 2.11. Neurotransmitter transporter functional assay
 - 2.11.1. Neurotransmitter transporter uptake assay kit and background
 - 2.11.2. Assay procedure

- 2.11.3. Data processing and analysis
- 2.11.4. Representative figures
- 2.12. Multidrug resistance transporter -1 (MDR-1) modulation assay
 - 2.12.1. MDR assay background
 - 2.12.2. MDR assay procedure
 - 2.12.3. Data processing and analysis
 - 2.12.4. Representative figures
- 2.13. Histone Deacetylase (HDAC) assay
 - 2.13.1. HDAC assay kit and principle
 - 2.13.2. HDAC assay procedure
 - 2.13.3. Data processing and analysis
 - 2.13.4. Representative figures
- 2.14. Monoamine Oxidase (MAO) activity assay
 - 2.14.1. MAO assay kit and principle
 - 2.14.2. Assay procedure
 - 2.14.3. Data processing and analysis
 - 2.14.4. Representative figures
- 2.15. Protein Kinase C (PKC) activity assay
 - 2.15.1. PKC assay kit and principle
 - 2.15.2. PKC assay procedure
 - 2.15.3. Data processing and analysis

2.15.4. Representative figures

2.16. Checkpoint Kinase 2 (CHK2) activity assay

2.16.1. CHK2 assay kit and principle

2.16.2. CHK2 assay procedure

2.16.3. Data processing and analysis

2.16.4. Representative figures

2.17. Nicotinic acetylcholine receptor functional assay – $^{86}\text{Rb}^+$ efflux

2.17.1. nAChR $^{86}\text{Rb}^+$ efflux assay introduction

2.17.2. nAChR $^{86}\text{Rb}^+$ efflux assay procedure

2.17.2.1. Primary functional assay

2.17.2.2. Secondary functional assay

2.17.3. Data processing and analysis

2.17.4. Representative figures

3. Master table of targets at NIMH-PDSP

4. References

Section 1: Radioligand binding assays

1.1. Drug plate preparation for radioligand binding assays: Hamilton ASM® and STAR®

The NIMH PDSP uses an **Integrated Sample Storage, Retrieval & Liquid Handling Robotic System** (see SOW) to prepare assay plates for the research staff to perform experiments. Briefly, the system consists of a refrigerated storage module that stores the PDSP samples and reference compounds; a retrieval module that selects, thaws, uncaps and delivers the compounds; and a multi-station liquid handling platform to transfer the samples and standards to make assay plates. The system is controlled by four PC computers utilizing Hamilton's Microlab STAR Venus One and Sample Manager software suites. Considerable training is required to operate the system. Advanced training is required to program and trouble-shoot the system.

A set of steps to instruct the machines to create a plate is called a "method." Each method has hundreds of lines of instructions. Below is an overview of the steps required to create assay plates for primary and secondary assay plates. This is an overview of the liquid handling and major plate movement steps. Robotic movements for tip set-up, tip movements, tip recycling, plate staging, etc. are not included.

A. Primary Plate Preparation:

1. A "work list" is created by a senior staff member utilizing our PDSP Database.
2. The work list is downloaded onto the ASM computer.
3. The "run control" program is opened on ASM server computer.
4. The assay method corresponding to the assay to be run is selected; the ASM server and storage module, de-capper and robotic arms perform self-checks.
5. The user is prompted to select the work list to be run.
6. The "run control" program verifies the work list, prompts the user to select start and thaw time variables or defaults.
7. Sample retrieval begins in ASM storage module, which sends messages to appropriate liquid handling station.

B. The ASM storage module retrieves samples using the 2-dimensional bar code on each tube

- C. Samples are collected in an empty rack, inside the ASM Storage module.
 - D. When all samples are collected, the rack is sent to the ASM server via an automated trolley and the server's internal single-grip arm.
 - E. Samples are thawed with forced hot air according to protocol, with an option to enter thaw time.
 - F. The rack is then delivered via the ASM Server single-grip arm and hand-off arm to the Capper/Decapper
 - G. Sample tubes are uncapped and sent to the appropriate STAR deck
8. The user prepares the STAR liquid handler deck with proper plates, buffers and pipette tips. (Steps 8-14 are performed in parallel to step 7.)
 9. The STAR computer run control program (this is a separate instance from the ASM run control program) prompts the user for tip-counting verification; user also confirms that the protocol and plate count are correct.
 10. STAR platform begins plating procedure.
 11. Assay plates are distributed to the STAR deck (1 per final plate); the plate barcode is recorded and used throughout the remainder of the process to verify the integrity of sample tracking.
 12. 97.5 microliters of buffer are added to rows A and E of each assay plate.
 13. DMSO (vehicle control) is added to wells A1 and E1 of each assay plate.
 14. STAR platform pauses with user input, and waits for drug delivery from the ASM (step 7f above).
 15. Samples are mixed after step 7G is completed and the sample rack is delivered to the STAR deck.
 16. 2.5 microliters of control reference compound are aspirated from the sample tube and distributed into the assay plate in wells A12 and E12 using the eight single-channel pipettors.
 17. 2.5 microliters of each sample is aspirated from sample tubes and distributed into the assay plate in wells A2 through A11 and E2 through E11 using the eight single-channel pipettors.
 18. Row A is then mixed and aliquoted from A to B and A to C and A to D with a single-row selection of pipette tips by the 96-well head, each well then has 25 microliters of combined sample and buffer.

19. Step 18 is repeated for row E-H to make replicates.
20. A plate map is created corresponding to the plate bar-code, samples added and receptor assigned.
21. Steps 16-20 are repeated for each assay plate. (See Figure 1 for primary drug plate map).

B. Secondary Plate Preparation:

1. A “work list” is created by a senior staff member utilizing our PDSP Database.
2. The work list is down-loaded onto the ASM computer.
3. The “run control” program is opened by the user on the ASM server computer.
4. The assay “method” corresponding to the assay to be run is selected; the ASM server and storage module, de-capper and robotic arms perform self-checks.
5. The user is prompted to select the work list to be run.
6. The “run control” program verifies the work list, prompts the user to select start and thaw time variables or defaults.
7. Sample retrieval begins in the ASM storage module, and sends messages to the appropriate liquid handling station.
 - A. The ASM storage module retrieves samples using the 2-dimensional bar code on each tube
 - B. Samples are collected into an empty rack, inside the ASM storage module
 - C. When all required samples are collected, the rack is sent to the ASM server via an automated trolley and the server’s internal single-grip arm.
 - D. Samples are thawed with forced hot air according to protocol with an option to enter thaw time.
 - E. The rack is then delivered via the ASM Server single-grip arm and hand-off arm to the Capper/Decapper
 - F. Sample tubes are uncapped and sent to the appropriate STAR deck
8. The user prepares the STAR liquid handler deck with proper plates, buffer and pipette tips. (Steps 8-14 are performed in parallel to step 7.)
9. The STAR computer run control program (this is a separate instance from the ASM run control) prompts the user for tip-counting verification; the user also confirms that the protocol and plate count are correct.

10. The STAR platform begins the plating procedure.
11. Assay plates are distributed to the STAR deck (1 dilution plate and 3 plates for replicates per set); the plate barcodes are recorded and are used throughout our process to verify the integrity of sample tracking.
12. 180 microliters of buffer are added to all wells of each assay plate with the 96CORE head.
13. 15 microliters of buffer are added to column 12, 40 microliters are aspirated from column 11.
14. The STAR platform pauses and waits for drug delivery from ASM (step 7f above).
15. Samples are mixed.
16. 5 microliters of sample (or control compound) is aspirated from the sample tubes and distributed into the first dilution plate in column 12 using the eight single-channel pipettors.
17. 40 microliters of buffer are removed from column 11.
18. After mixing, 60 microliters are aspirated from column 12 and dispensed into column 11.
19. A serial dilution is performed; 20 microliters is aspirated from/dispensed to col 12 to 10, col 10 to 8, col 8 to 6, col 6 to 4, col 4 to 2, col 11 to 9, col 9 to 7, col 7 to 5 and, col 5 to 3.
20. The entire plate is mixed again and then three replicates with 25 microliters per well are made.
21. Steps 16-20 are repeated for each additional set of four plates.
22. Plate maps are created corresponding to the plate barcode, samples added and receptor assigned for all plates on the deck. (See Figure 2 for secondary drug plate map).

Managing the workflow of the automated system is extremely important. First, the overall flow, i.e., what assays to select, when to make assay plates and, assigning assays to a researcher must be performed by a senior staff member. Second, the workflow for the system also requires careful planning and scheduling. Operating the system can be performed by a researcher. The operation of the system *requires* careful attention to detail and significant planning in order to achieve optimal performance. Preparing the liquid handling deck for a method, being attentive to tip usage, having all the reagents ready prior to start, having all consumables ready prior to start, as well as the sequence of primary versus secondary methods to minimize transition time between runs are all required to have the system operate at 35-plus hours per week (its current utilization).

	1	2	3	4	5	6	7	8	9	10	11	12
A		a	c	e	g	i	k	m	o	q	s	
B		a	c	e	g	i	k	m	o	q	s	
C		a	c	e	g	i	k	m	o	q	s	
D		a	c	e	g	i	k	m	o	q	s	
E		b	d	f	h	j	l	n	p	r	t	
F		b	d	f	h	j	l	n	p	r	t	
G		b	d	f	h	j	l	n	p	r	t	
H		b	d	f	h	j	l	n	p	r	t	

Input Barcodes:

- BAGS33

Primary Binding Plates:

Barcode: BAGS33

Receptor: H3-0 Primary BAGS33 03

Date: 3-14-2013 09-13-18

	1	2	3	4	5	6	7	8	9	10	11	12
A	Empty	27054	22578	22580	22581	22582	22583	22584	22585	26656	26657	Histamine
B	Empty	27054	22578	22580	22581	22582	22583	22584	22585	26656	26657	Histamine
C	Empty	27054	22578	22580	22581	22582	22583	22584	22585	26656	26657	Histamine
D	Empty	27054	22578	22580	22581	22582	22583	22584	22585	26656	26657	Histamine
E	Empty	26658	26772	26787	26788	26789	26790	26791	26793	26794	26796	Histamine
F	Empty	26658	26772	26787	26788	26789	26790	26791	26793	26794	26796	Histamine
G	Empty	26658	26772	26787	26788	26789	26790	26791	26793	26794	26796	Histamine
H	Empty	26658	26772	26787	26788	26789	26790	26791	26793	26794	26796	Histamine

Figure 1. 96-well drug plate setup diagram (up) and an actual barcoded plate (bottom) for primary radioligand binding assays. The drug plate is designed to contain 20 compounds (compound “a” to compound “t” in Columns 2 - 11, each in quadruplicate) and one reference compound (Column 12), 25 μ l per well at 50 μ M (5x of final assay concentration of 10 μ M). Column 1 contains buffer only, and is therefore designated for total binding (0% inhibition). Column 12 contains reference compound (histamine in this case) is designated as nonspecific binding (100% inhibition).

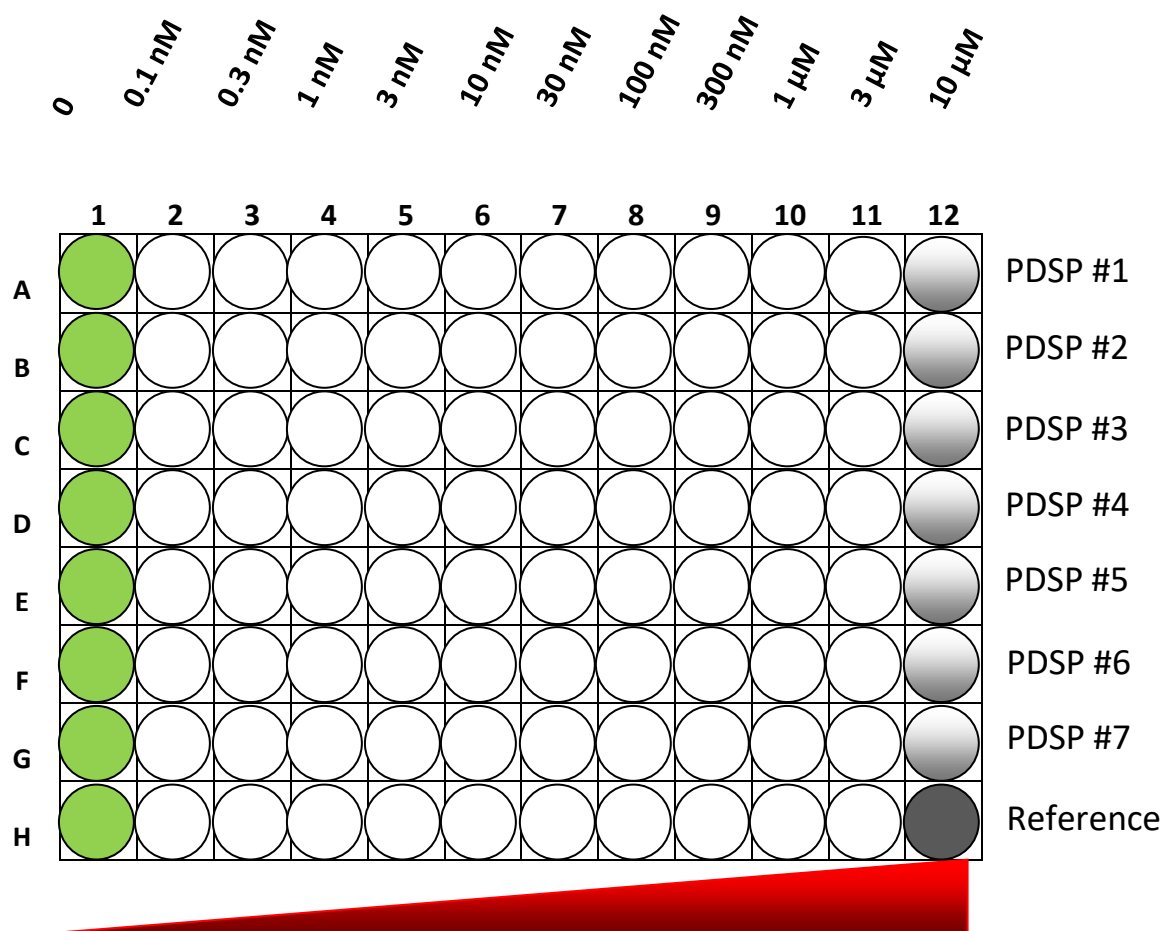


Figure 2a. 96-well drug plate map for secondary radioligand binding assays. The drug plate is designed to contain 7 PDSP compounds (Rows A to G) and 1 reference compound (Row H) as indicated at right of the plate, one compound per row and 25 μ l per well at 5x of final concentrations as indicated on top of the plate. Well H12 is designated for nonspecific binding and column 1 is designated for total binding for the plate. Each secondary assay consists of 3 sets of identical 96-well plates.

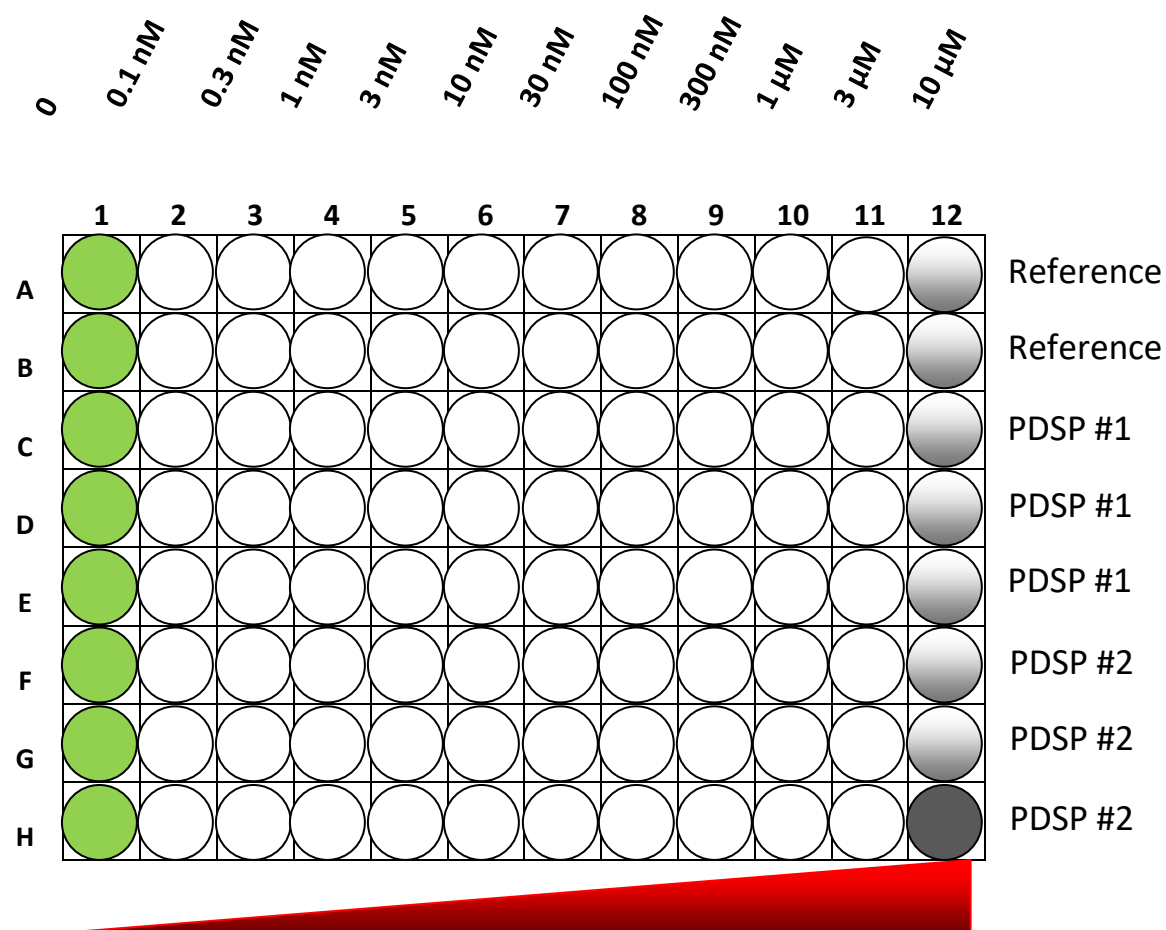


Figure 2b. 96-well drug plate map for secondary radioligand binding assays. The drug plate is designed to contain 2 PDSP compounds (Rows C to H) and 1 reference compound (Rows A and B) as indicated at right of the plate, therefore each PDSP compound is assayed in triplicate and the reference compound in duplicate. Each well contains 25 μ l at 5x of final concentrations as indicated above the plate.

1.2. Cell culture and membrane fraction preparation

The majority of binding assays performed by the NIMH PDSP staff employ stably or transiently transfected cell lines expressing mainly human recombinant receptors, monoamine transporters, or ion channels. A detailed description of the cell lines, the culture and sub-culture conditions, and the appropriate media are listed in **Table 1**.

1.2.1. Calcium phosphate precipitation transfection for adherent HEK293 T cells.

2x HBS: 140 mM NaCl, 1.5 mM Na₂HPO₄, 50 mM HEPES, pH 7.05, room temperature.

The calcium phosphate precipitation method was adapted from Jordan et al (1996)(1). In brief, HEK293T cells are subcultured into 15-cm dishes at a density of 8 – 10 million cells per dish and incubated overnight. For each dish of 15-cm, 18 µg DNA, 100 µl of 2.5 M CaCl₂, 100 µl of TE (1 mM Tris HCl, 0.1 mM EDTA, pH 7.60) are diluted into a final volume of 1 ml water. The mixture is then quickly added to an equal volume of 2x HBS and added dropwise to cells. The cells are then incubated overnight and for another day or two in fresh growth medium. For transient transfections with 5-HT receptors, we use medium containing dialyzed FBS overnight before harvesting. Cells are usually harvested 48 – 72 hours after transfection.

1.2.2. Suspension HEK293 transfection.

The PDSP also uses suspension HEK293 cells to obtain high levels of protein expression for binding assays (2). HEK293 suspension culture is maintained in flasks (115 rpm, 37°C, and 8% CO₂) with the Expi293 Expression Medium with GlutaMax-1 (Life Technologies) supplemented with Pen/Strep (such as 30 ml medium in a 125 ml flask), and passaged when they reach a density of 5 – 7 million cells per ml. When seeding for a new passage, cell density is maintained at 0.5 – 0.75 million cells per ml. For transfection, we use the ExpiFectamine 293 Transfection Kit (Life Technologies). Cells are first subcultured in the Expi293 medium without Pen/Strep at a density of 3 million cells per ml for 25.5 ml in a 125 ml flask. To make the transfection mix (for each 125 ml flask), 30 µg receptor DNA is mixed in 1.5 ml OptiMEM medium in one tube and 80 µl of ExpiFetamine reagent is mixed in 1.5 ml OptiMEM medium in another tube. Both tubes are incubated for 5 min separately at RT and then for

20-30 min after being mixed together at RT. The mixture is then added to cells for overnight incubation at 115 rpm, 37°C, and 8% CO₂. At 16-20 hr after the initial transfection, 0.15 ml Enhancer #1 and 1.5 ml Enhancer #2 are added and the culture are incubated for another 20-28 hrs to enhance protein expression (3). Cells are then collected for membrane preparation or kept at -80°C until membrane preparation (next section).

1.2.3. Membrane preparations from stable or transiently transfected cells. To make membrane fractions from stably transfected cell lines, cells are subcultured into 15-cm dishes and grown to 90% confluency. For 5-HT receptors, cells are incubated overnight in either serum-free medium or medium containing 1% dialyzed fetal bovine serum. The next day, the cells are rinsed with PBS, scraped off into 50 ml conical tubes, and pelleted by centrifugation (1000 x g, 10 min at 4°C). The cell pellet is resuspended in chilled (4°C) lysis buffer (50 mM Tris HCl buffer, pH 7.4) and triturated gently for hypotonic lysis. The suspension is then centrifuged at 21,000 x g for 20 min (4°C) to obtain a crude membrane fraction pellet. The fresh membrane pellet is then resuspended in cold lysis buffer with 3x volumes of the pellet size and is immediately subjected to the Bradford protein assay to determine protein concentration, followed by a saturation binding assay (see following section for details) to determine receptor expression level and the affinity of the selected radioligand. Based on the receptor expression level and the K_d value, fresh membrane suspensions are stored at -80 °C in small aliquots such that one aliquot is enough for one 96-well plate to have at least 500 cpm/well when assayed at 0.5 – 1.0x K_d value of the hot ligand.

1.2.4. Membrane preps from tissues. To make membrane fractions from tissues, crude membrane fractions are prepared from rodent (typically rat or guinea pig brain or kidney, purchased from PelFreeze Biologicals). Here is the general procedure for membrane preparations unless otherwise stated. Frozen tissue (maintained at -80°C) is thawed on ice, homogenized on ice in 10 volumes of cold lysis buffer (50 mM Tris HCl, pH 7.4, containing protease inhibitor cocktail from Roche) using a Polytron homogenizer (6 pulses and 10 seconds per pulse). The homogenate is centrifuged at 1,000 x g for 10 min at 4°C to obtain supernatant. The supernatant is then centrifuged at 40,000 x g for 20 min, and then the resulting supernatant is decanted and replaced with the same ice-cold lysis buffer. Two or three additional rounds of homogenization-centrifugation are performed to ensure thorough

homogenization and also to wash out endogenous ligands (particularly important for GABA assays). The final pellet is resuspended in the same buffer and homogenized one last time. The fresh suspension is subjected to protein concentration measurement, saturation binding, and aliquoted for storage at -80°C for future use. Aliquots are also made such that each aliquot is enough for one binding assay in one 96-well plate to have at least 500 cpm/well when assayed with a 0.5 – 1.0x K_d level of the corresponding hot ligand.

1.2.5. Membrane preps from rat brain for NMDA radioligand binding assays. The protocol is adapted from Chiu et al., 1999 (4). In brief, rat brain is thawed on ice in SHE buffer (300 mM Sucrose, 10 mM HEPES, 2 mM EDTA, pH 7.3) and homogenized on ice in 20 ml ice-cold SHE buffer per gram of wet tissue using glass homogenizer (at least 6 strokes). The homogenate is centrifuged at 1,000 x g for 20 min at 4°C to collect supernatant. The supernatant is then centrifuged at 16,000 x g for 1h at 4°C. The pellet is suspended in the same SHE buffer and stored in aliquots (10 mg per aliquot after protein concentration determination) at -80°C until use. Protein concentration is determined using the Bradford method. Immediately prior to assay, the aliquoted pellet is resuspended in 1 ml HE buffer (20 mM HEPES, 1 mM EDTA, pH 7.0) and centrifuged briefly in desktop centrifuge at 4°C to remove the sucrose. The pellet is then resuspended in 0.5 ml of HE buffer and incubated at 37°C for 30 min. The suspension is then centrifuged at 13,000 x g for 10 min at 4°C. The pellet is washed four times by resuspending it in 1 ml HE buffer, followed by centrifugation. The final pellet is resuspended to about 2 mg/ml concentration after protein concentration determination and is then used in binding assays at 100 ug per well, using the HE buffer supplemented with 100 µM sodium glutamate and 100 µM glycine.

1.2.6. List of cell lines and targets that PDSP uses for binding assays.

Table 1. List of cell lines and targets that PDSP uses for making membrane pellets for binding assays. All clones are stable lines, while transient cells are marked with “*”. Most clones are of human origin unless noted, such as (rat) behind receptor name. Detailed info about media is listed below the table.

Receptor	Note	Parental cells	Media (see details below the table)
Serotonin (5HT)			
5-HT _{1A}		stable CHO	500 G418
5-HT _{1B}		stable HEK	500 G418
5-HT _{1D}	*	HEKT	COS/HEK
5-HT _{1E}		stable HEK	500 G418
5-HT _{2A} (rat)		stable 3T3	500 G418
5-HT _{2A}	*	HEKT	COS/HEK
5-HT _{2B}		stable HEK	2 µg/ml Puromycin
5-HT _{2C}		HEK T	COS/HEK
5-HT ₃	*	HEKT	COS/HEK
5-HT ₄		HEK T	COS/HEK
5-HT _{5A}		Flp-In CHO	DMEM/F-12 200 µg/ml Hygromycin B
5-HT ₆		stable HEK	500 G418
5-HT _{7A}		Stable HEK	2 µg/ml Puromycin
Dopamine			
D ₁	*	HEKT	COS/HEK
D ₂		stable fibroblast	COS/HEK
D _{2L}		stable CHO	F-12/10%FBS 400G418
D ₃ (rat)	*	HEKT	COS/HEK
D ₃	*	HEKT	COS/HEK
D ₄		Stable HEK	DMEM/F12 10% CS Fe+
D ₅	*	HEKT	COS/HEK
Opioid			
DOR		stable HEK	200 G418
MOR		stable HEK	200 G418
KOR (rat)		stable HEK	500 G418
KOR		stable HEK	500 G418
NOP	*	HEKT	COS/HEK
Neurotransmitter Transporters			
SERT		stable HEK	500 G418
NET		stable HEK	hNET (250 G418)
DAT		stable HEK	hDAT (350 G418)
Vasopressin and Oxytocin			
V _{1A}		stable CHO	V1A & OT media
V _{1B}		stable CHO	V2 & V1B media
V ₂		stable CHO	V2 & V1B media
OT		stable CHO	V1A & OT media
Prostaglandin			
EP-3	*	HEKT	COS/HEK
EP-4	*	HEKT	COS/HEK
Adrenergic			
α _{1A}		stable	500 G418
α _{1B}	*	HEKT	

Receptor	Note	Parental cells	Media (see details below the table)
α_{1D}		stable	500 G418
α_{2A}		stable MDCK	500 G418
α_{2B}	*	HEKT	COS/HEK
α_{2C}		stable MDCK	500 G418
β_1		CHO Flp-In	DMEM/F12 200 μ g/ml Hygromycin B
β_2		HEK Flp-In	DMEM 100 μ g/ml Hygromycin B
β_3		HEK Flp-In	DMEM 100 μ g/ml Hygromycin B
Muscarinic acetylcholine			
M ₁		stable CHO	250 G418
M ₂		stable CHO	500 G418
M ₃		stable CHO	500 G418
M ₃ D (DREADD)		CHO Flp-In	DMEM/F12 100 μ g/ml Hygromycin B
M ₄		stable CHO	10% FBS F12
M ₄ D (DREADD)		HEKT	COS/HEK
M ₅		stable CHO	250 G418
Nicotinic acetylcholine			
$\alpha_2\beta_3$		HEK	500 G418
$\alpha_2\beta_4$		HEK	500 G418
$\alpha_3\beta_2$		HEK	500 G418
$\alpha_3\beta_4$		HEK	500 G418
$\alpha_4\beta_2$		HEK	500 G418
$\alpha_4\beta_4$		HEK	500 G418
α_7		HEK	500 G418
Histamine			
H ₁		stable HEK	500 G418
H ₂		Stable HEK	In Progress
H ₃		HEK Flp-In	DMEM 100 μ g/ml Hygromycin B
H ₄		HEK T	COS/HEK
Cannabinoid			
CB ₁		HEK	500 G418, In Progress
CB ₁		HEK Flp-In	DMEM 100 μ g/ml Hygromycin B
CB ₂		HEK Flp-In	DMEM 100 μ g/ml Hygromycin B
Adenosine			
A ₁	*	HEKT	COS/HEK
A _{2A}	*	HEKT	COS/HEK
A _{2A}		HEK	500 G418
A _{2B}	*	HEKT	COS/HEK
A ₃	*	HEKT	COS/HEK
Melanocortin			
MC ₁	*	HEKT	COS/HEK
MC ₂	*	HEKT	COS/HEK
MC ₃	*	HEKT	COS/HEK

Receptor	Note	Parental cells	Media (see details below the table)
MC ₄	*	HEKT	COS/HEK
MC ₅	*	HEKT	COS/HEK
Purinergic P2Y			
P2Y1		Astrocyte line	500 G418
P2Y2		Astrocyte line	500 G418
P2Y4		Astrocyte line	500 G418
P2Y6		Astrocyte line	500 G418
P2Y11		Astrocyte line	500 G418
P2Y12		Astrocyte line	500 G418
Trace Amine			
TA-1	*	HEKT	COS/HEK
TA-3	*	HEKT	COS/HEK
TA-4	*	HEKT	COS/HEK
TA-5	*	HEKT	COS/HEK
Lysophospholipid (LPA)			
LPA1	*	HEKT	COS/HEK
LPA2	*	HEKT	COS/HEK
LPA3	*	HEKT	COS/HEK
Tachykinin (NK)			
NK ₁		HEK	500 G418
NK ₂		HEK	500 G418
NK ₃		HEK	500 G418
mGluR			
mGlu ₁	*	HEKT	In progress
mGlu ₂	*	HEKT	In progress
mGlu ₃	*	HEKT	In progress
mGlu ₄	*	HEKT	In progress
mGlu ₅		CHO	2 µg/ml Puromycin
mGlu ₅	*	HEKT	In progress
mGlu ₆	*	HEKT	In progress
mGlu ₇	*	HEKT	In progress
mGlu ₈	*	HEKT	In progress
Others			
Ghrelin		HEK Flp-In	DMEM 100 µg/ml Hygromycin B
PAR1		Lung Fibroblast, PAR1 KO	500 G418
SMO	*	HEKT	COS/HEK
SMO		HEK	500 G418, in progress
CCK ₂		CHO	500 G418
Orexin-2	*	HEKT	COS/HEK
RXFP1	*	HEKT	
RXFP2	*	HEKT	
RXFP3	*	HEKT	
RXFP4	*	HEKT	

Receptor	Note	Parental cells	Media (see details below the table)
GPR39	*	HEKT	
GPR4	*	HEKT	
GPR40	*	HEKT	COS/HEK
GPR41	*	HEKT	COS/HEK
GPR43	*	HEKT	COS/HEK
GPR58	*	HEKT	COS/HEK
GPR61	*	HEKT	COS/HEK
GPR62	*	HEKT	COS/HEK
GPR65	*	HEKT	COS/HEK
GPR68	*	HEKT	COS/HEK
GPR88	*	HEKT	COS/HEK
Il-1 imidazoline	*	HEKT	COS/HEK
HERG-K ⁺ Channel		HEK	500ug/ml G418
PC12			COS/HEK
Cav1.2		HEK	
Sigma1	*	HEKT	
Sigma2	*	HEKT	

1.2.7. Media Recipes

Details of media composition for cells are as follows (please note that DMEM is purchased as 1X high D-glucose (4,500 mg/L) with L-glutamine and supplemented upon receipt with penicillin/streptomycin (100 U/ml).

1. COS/HEK Medium (10% serum) – 1 L: also used for transient transfection

1L DMEM, 100 ml FBS, 10 ml Pen/Strep

2. Standard G418 Media (500 µg/ml; 10% serum) – 1L

1 L DMEM, 500 mg G418, 100 ml FBS, 10 ml Pen/Strep

3. Standard Puromycin Medium (2 µg/ml Puromycin:10% Serum) - 1L

1 L DMEM, 2 aliquots (1mg/ml Puro in PBS), 100 ml FBS, 10 ml Pen/Strep

4. Standard Puromycin Medium +G418 Selection Medium

1L DMEM, 2 aliquots (1mg/ml Puro in PBS), 500 mg geneticin, 100 ml FBS, 10 ml Pen/Strep

5. Dialyzed Medium (1% dialyzed serum) – 1 L

1 L DMEM, 10 ml Dialyzed FBS, 10 ml Pen/Strep

6. hNET Medium (250 µg/mL G418; 10% serum) – 1 L

1 L DMEM, 250 mg geneticin, 100 ml FBS, 10 ml Pen/Strep

7. hDAT Medium (350 µg/ml G418; 10% serum) - 1L

1L DMEM, 350mg geneticin, 100ml FBS, 10ml Pen/Strep

8. V1A and OT Medium (400 µg/ml G418, 10% FBS, 15 mM HEPES) – 1L

1L Hams F12, 400 mg Geneticin, 100 ml Calf serum, 15 ml HEPES (1M stock), 10 ml Pen/Strep

9. V2 & V1B Medium (150 µg/mL Zeocin; 10% Serum; 15 mM Hepes) – 500 mL

1L Hams F12, 1.5 ml Zeocin (100mg/mL), 100ml Calf Serum, 15 ml Hepes (1M), 10 ml Pen/Strep

10. MOR/DOR selection medium (200 µg/ml G418, 10% serum) – 1L

1 L DMEM, 200 mg G418, 100 ml FBS, 10 ml Pen/Strep

11. Alpha 1A and 1D selection medium (500 µg/ml G418, 10% serum) – 1L

1 L DMEM, 500 mg G418, 100 ml FBS, 10 ml Pen/Strep

12. M4 medium (10% serum) - 1L

1L Hams F12, 100 ml FBS, 10 ml Pen/Strep

13. D4 medium (10% serum) – 1L

1L DMEM/F12, 15mM HEPES; with pyridoxine HCl, 100 ml Donor Calf Serum with Iron, 10 ml Pen/Strep

14. FLP-In CHO medium (10% serum) – 1L

1L DMEM/F12 50/50, 10% FBS, 200 µg/ml Hygromycin B, 10 ml Pen/Strep

15. FLP-In HEK medium (10% serum) – 1L

1L DMEM, 10% FBS, 100 µg/ml Hygromycin B, 10 ml Pen/Strep

16. PC-12 medium (10% serum) – 1L

1L DMEM, 5% Horse Serum, 5% FBS, 10 ml Pen/Strep

17. HTLA medium – 1L

1L DMEM, 100 ml FBS, 100 µg/ml Hygromycin B, 5 µg/ml Puromycin, 10 ml Pen/Strep

18. Inositol/Inositol-free medium

500 ml BME (BME purchased from LONZA), 5 ml Pen/Strep, 5 ml L-Glutamine

19. McCoy medium for U2OS – 1L

1L McCoy, 100 ml dialyzed FBS, 50 µg/ml Hygromycin B, 200 µg/ml Zeocin, 100 µg/ml G418, 0.1 mM non-essential AA, 25 mM HEPES, 1 mM Sodium Pyruvate, 10 ml Pen/Strep.

20. Expi293 Expression Medium – 1L

1L Expi293 Expression Medium with GlutaMax-1, 10 ml Pen/Strep.

1.3. Saturation binding assays

Saturation binding assays, usually performed immediately after the membrane fraction is obtained and protein concentration is determined (see above section for membrane preparations), are routinely carried out to measure receptor expression level (B_{\max}) and binding affinity (K_d) of a selected radioligand. **Tables 2-24** lists the identity of hot ligands, reference compounds, and buffers for each family of targets. Saturation binding assays are carried out in 96-well plates in a final volume of 125 μ l per well. In brief, 25 μ l of radioligand is added to a 96-well plate according to the setup in **Figure 3**; followed by addition of 25 μ l binding buffer (for total binding) or 25 μ l reference compound at a final concentration of 10 μ M (for nonspecific binding). The reaction starts upon addition of 75 μ l of fresh membrane protein (typically 25 to 50 μ g per well) and the reaction is usually incubated in the dark at room temperature for 90 min. The reaction is stopped by vacuum filtration onto cold 0.3% polyethyleneimine (PEI) soaked 96-well filter mats using a 96-well Packard Filtermate harvester, followed by three washes with cold wash buffers (for details, see following **Tables 2 to 24**). Scintillation cocktail is then melted onto microwave-dried filters on a hot plate and radioactivity is counted in a Microbeta counter.

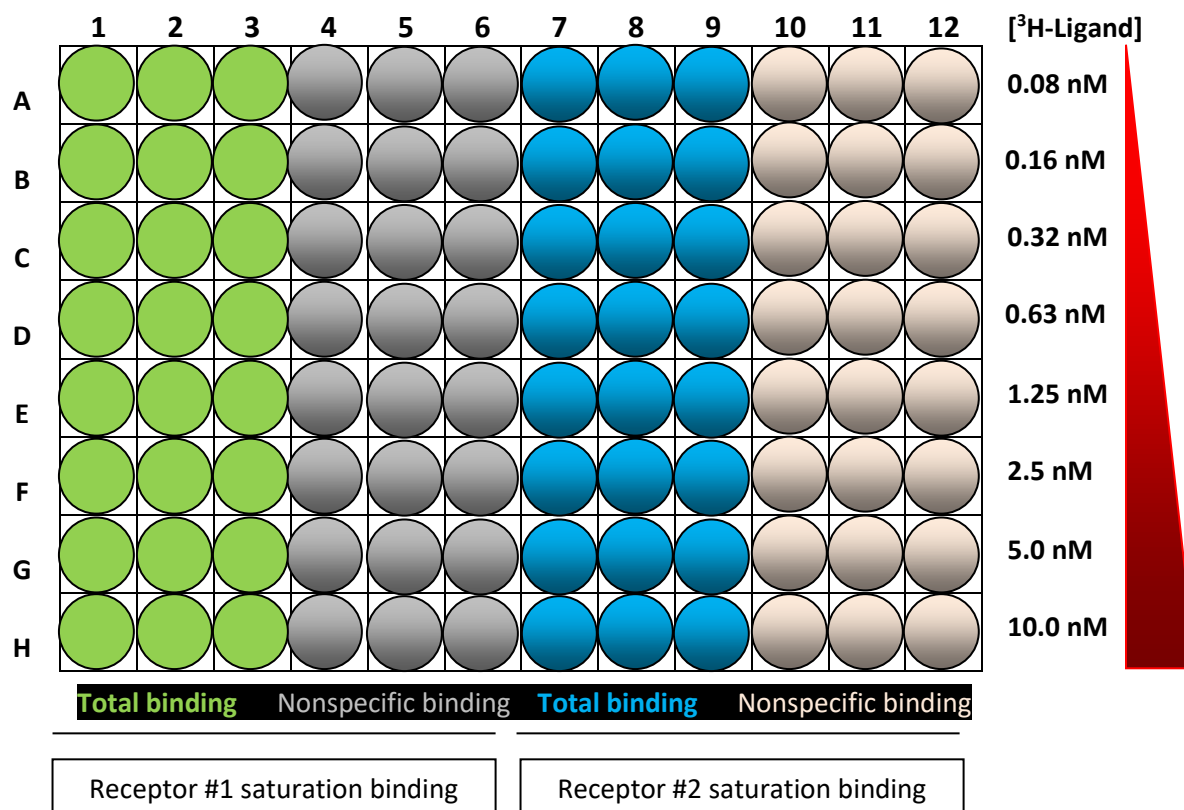


Figure 3. Radioligand saturation binding plate set up in a 96-well plate. Total and nonspecific binding are determined in the absence and presence of 10 μ M of the appropriate reference compound, respectively, in the indicated final concentrations of hot ligand (nM). Final radioligand concentrations are shown as an example and different concentration ranges are used for different receptors, dependent on their K_d values for selected radioligand. The K_d value is usually in the middle, i.e. Row D or E. Amount of membrane protein (μ g/well) are adjusted so that bound radioactivity is less than 10% of the total added radioactivity.

1.4. Primary and secondary radioligand binding assays

Compounds are typically subjected to primary radioligand binding assays at targets selected by PIs and approved by the PDSP Director, Dr Bryan Roth. In primary binding assays, compounds are usually tested at a single concentration (10 μ M) and in quadruplicate in 96-well plates (see **Figure 1** for drug

plate map). Compounds showing a minimum of 50% inhibition at 10 μ M are tagged for secondary radioligand binding assays to determine equilibrium binding affinity at specific targets. In secondary binding assays, selected compounds are usually tested at 11 concentrations (0.1, 0.3, 1, 3, 10, 30, 100, 300 nM, 1, 3, 10 μ M) and in triplicate (3 sets of 96-well plates, see **Figure 2a** for drug plate map). An alternative drug plate set up is shown in **Figure 2b** which contains 2 PDSP test compounds and 1 reference compound. The drug map in **Figure 2a** is more efficient than the one in **Figure 2b**; the **Figure 2b** drug plate is usually made manually for urgent projects with a small number of high priority compounds to be tested immediately upon request.

Both primary and secondary radioligand binding assays are carried out in a final volume of 125 μ l per well in appropriate binding buffers (for details, see **Tables 2 to 24**). The hot ligand concentration is usually at a concentration close to the K_d (unless otherwise indicated). Total binding and nonspecific binding are determined in the absence and presence of 10 μ M of the appropriate reference compound, respectively. In brief, plates are usually incubated at room temperature and in the dark for 90 min (unless otherwise indicated). Reactions are stopped by vacuum filtration onto 0.3% polyethyleneimine (PEI) soaked 96-well filter mats using a 96-well Filtermate harvester, followed by three washes with cold wash buffers (for details, see **Tables 2 to 24**). Scintillation cocktail is then melted onto the microwave-dried filters on a hot plate and radioactivity is counted in a Microbeta counter. A general procedure for binding assays is shown below (unless otherwise stated, such as radioligand binding assays for nAChRs; see details in the next section for nAChR binding assays).

1. Receive barcoded primary drug plate or secondary drug plates from Hamilton STAR®
2. Check out drug plates and mark them “in progress” in PDSP database
3. Prepare appropriate binding buffers and wash buffers
4. Check out membrane pellets
5. Check pellet box to obtain K_d and concentration to use for the radioligand
6. Prepare 2.5x of final concentration of radioligand working solution
7. Count 50 μ l of radioligand working solution to confirm radioligand concentration and activity

8. Add 50 μ l radioligand to each well
9. Add 50 μ l membrane suspension to each well
10. Mix by gentle and brief shaking
11. Incubate the plates in the dark for desired time (usually 60 – 90 min at RT)
12. Soak filters in cold 0.3% PEI
13. Stop the reaction by vacuum filtration and washing
14. Dry the filters using microwave oven
15. Melt scintillation cocktail on top of filters
16. Wrap filters in plastic wrap
17. Count radioactivity
18. Download results, process and upload to PDSP database
19. Preview and submit results
20. Report progress in the PDSP database (completion or redo or repeat) after receiving approval email

1.5. Radioligand binding assays for nicotinic acetylcholine receptors (nAChRs). Radioligand binding assays with nAChRs follow slightly different protocols from those outlined in the above sections and are detailed in the following sections, modified from previously published procedures (5, 6).

1.5.1. Cell culture. The six stable cell lines expressing human $\alpha 2\beta 2$, $\alpha 2\beta 4$, $\alpha 3\beta 2$, $\alpha 3\beta 4$, $\alpha 4\beta 2$, or $\alpha 4\beta 4$ subtype were established by stably co-transfecting HEK293 cells with a combination of one α nicotinic receptor subtype gene and one β subunit gene. The cell line expressing $\alpha 7$ nAChRs were established by stably transfecting HEK293 cells with the rat $\alpha 7$ nAChR subunit. Cells are grown in minimum essential medium (MEM) supplemented with 10% fetal bovine serum, 100 units/ml penicillin G, 100 μ g/ml streptomycin, and selective antibiotics at 37°C with 5% CO₂ in a humidified incubator.

1.5.2. Radioligand binding assays. Radioligand binding assays of nAChRs (displacement of [³H]-epibatidine) use the above stably expressed nAChRs as well as rat forebrain tissue. In brief, cells

stably expressing nAChRs are harvested in 50 mM Tris HCl (pH 7.4), washed, homogenized with a Brinkmann polytron homogenizer and centrifuged at 36,000 g. The resulting washed membranes are then incubated with [3 H] epibatidine for 4h at room temperature in a final volume of 0.5 ml. Nonspecific binding is assessed in parallel incubations in the presence of 300 μ M nicotine. Bound and free ligands are separated by vacuum filtration through Whatman GF/C filters treated with 0.5% polyethylenimine. The filter-retained radioactivity is measured by liquid scintillation counting. Specific binding is defined as the difference between total binding and nonspecific binding.

1.5.3. Primary and secondary nAChR binding assays. Primary binding assays are performed with 100 pM [3 H]-epibatidine and a single concentration of a PDSP test compound (10 μ M) in quadruplicate. Results are expressed as percentage inhibition of [3 H]-epibatidine specific binding. Compounds with a minimum of 25% inhibition are subjected to secondary binding assays to determine binding affinity. In the secondary binding assays, 0.5 nM [3 H]-epibatidine and 10 concentrations of the PDSP test compound are used to generate a competition binding curve. Results are analyzed in Prism 5.0 with nonlinear least-square regression to obtain K_i values. Nicotine at 300 μ M is included in all assays to define nonspecific binding and a nicotine dose-response curve is included as a positive control in the secondary binding assays.

1.5.4. Nicotinic acetylcholine receptor binding data entry and reporting. Binding assay results with nAChRs are analyzed as indicated in above sections and K_i values are then manually entered into the PDSP database. Figures and raw data are available to corresponding investigators upon request.

1.6. General binding data entry, analysis, and quality control for targets other than nAChRs.

Except for radioligand binding results with nAChRs, whose analysis is outlined in the above sections, binding assays for targets other than nAChRs are analyzed and reported as outlined in the following sections. Raw cpm data from the Microbeta counter are uploaded into the PDSP database and analyzed online using built-in analysis tools in the PDSP database. If necessary, binding assay results are also analyzed in Microsoft Excel (for primary binding results) or Prism v5.0 (for saturation binding and secondary binding results). The following sections provide detailed procedures for binding result

analysis and reporting, using both built-in tools in the PDSP database or third party software (Microsoft Excel and GraphPad Prism).

1.6.1. Result analysis using built-in tools in the PDSP database. The PDSP database is programmed to analyze results from saturation binding and competition binding assays (primary and secondary binding assays). The code for analyzing saturation and competition binding results is written in PHP using external library JQuery UI. The non-linear regression calculation is computed by the R statistical programming language using an Automatic Differentiation Model Builder (ADMB) to support robust non-linear regression calculation. To use built-in tools in the PDSP database to analyze binding assay results, technicians can upload raw counting results in Excel spreadsheets from the Microbeta counters directly into the PDSP database through corresponding reporting systems designed for saturation binding, primary binding, or secondary binding assays. The online reporting system and analysis tools are designed to optimize data processing and quality control.

1.6.1.1. Saturation binding result analysis. Saturation binding assays are carried out whenever a new membrane preparation is made. The Protein amount per well is adjusted so that less than 10% of the total added radioligand is bound. Upon completion of saturation binding assays, technicians can upload saturation binding results in Excel spreadsheets directly to the membrane pellet section of the PDSP database. During the uploading and reporting process, technicians must provide (1) receptor identity and species information; (2) stable line or transient transfection or animal tissue; (3) amount of protein per well used; (4) radioligand identity and concentration. An automatic email will be sent to the designated PDSP administrator when saturation binding results are submitted and results are placed in a list pending review and approval as indicated in **Figure 4**. The PDSP database is programmed to analyze saturation binding results and generate a hyperbolic curve using a non-linear least squares curve-fitting algorithm to determine B_{max} and K_d values. The PDSP administrator will review and analyze the binding results online with options to (1) reject the whole set of results; (2) exclude apparent outliers among replicates; (3) request a repeat; or (4) approve the data set. **Figure 5** shows a screen captured when a saturation binding assay is being reviewed. When the data set is approved, the PDSP administrator decides on (1) amount of protein per well and (2) radioligand

concentration to use for inhibition binding assays. Upon approval, the saturation binding curve is immediately available in approved membrane pellet section with a unique timestamp associated with each batch of membrane preparation. Technicians make aliquots accordingly so that each aliquot is enough for one binding assay plate at the decided concentration of radioligand. Aliquots are stored in 1.5 ml eppendorf tubes at -80°C until their use at the specified concentration of radioligand and one aliquot per plate.

1.6.1.2. Primary binding assay result analysis. Upon completion of primary binding assays, technicians upload raw results in Excel spreadsheets directly into the PDSP database via the primary binding assay reporting menu. When uploading primary binding results, technicians must identify plates by barcodes and match those generated by the Hamilton STAR liquid handling system when the drug plates were made. A designated PDSP administrator double checks the plate identity and sample order before making the results available online for reviewing. The PDSP database is programmed to calculate the percentage inhibition for each assay plate with total binding (with buffer) as 0% inhibition and nonspecific binding (in the presence of 10 μ M of reference compound) as 100% inhibition. It also calculates an average value from 4 replicates for each sample. The PDSP database automatically marks those entries with 50% or higher inhibition for secondary binding assays; also highlights those with variances greater than 20% among the quadruplicate determinations for further inspection.

Saturation Binding Analysis Tool

Pellets pending approval:

PelletID	Receptor	Radioligand	Date Created	Technician
673	5-HT1A	[3H]WAY100635	2013-03-19	tom

PDSP Home Ki DB Home Tracer Database Roth Lab U N C Binding Assay
[Home](#) [Log Out](#) [Add...](#) [Edit...](#) [View...](#)

View Pending Experiments

Primary Binding Analysis Tool

Experiment Name	Experiment Type
TC312135HT2B	primaryBindingExperiments
TC312135HT2C	primaryBindingExperiments
TC31213ALPHA2A2	primaryBindingExperiments
TC31213ALPHA2C1	primaryBindingExperiments
TC31213D1	primaryBindingExperiments
TC31213D2	primaryBindingExperiments
TC31213D3	primaryBindingExperiments
TC31213D4	primaryBindingExperiments
TC31213D5	primaryBindingExperiments
899-Beta1ASMa tjm	primaryBindingExperiments

Secondary Binding Analysis Tool

Plates pending approval:

PlateID	Receptor	Compounds	Technician
2336	BZP Rat Brain Site 90001		rwh
2871	5-HT5a	1, 2, 3, 4, 5, 6, 90001	sal
4345	DAT	27103, 27266, 27267, 27101, 27364, 27365	jfw
4896	DAT	26610, 26611, 26614, 26615, 26616, 26617, 26618	jfw

Figure 4. Representative pending lists for Saturation binding (Top), Primary binding (Middle), and Secondary binding (bottom) results. When binding assay results are reported and uploaded into the PDSP database, they are placed in separate pending lists.

Alternatively, compounds with negative inhibition (more binding in the presence of test compound) by over 20% are also highlighted for inspection. For any compound, there are four options available: “Redo” would delete the data from database and put the compound back on the “scheduled” list; “Repeat” would accept the results and put the compound back on the “scheduled” list for a repeat; “Force Secondary” would accept the primary results and add the compound on the “scheduled” list for secondary assays, even if the primary inhibitory percentage is less than 50%; “Approve” would accept the results, and database puts the compound on secondary “schedule” list if primary inhibition is over 50%. Either “Repeat”, or “Force Secondary”, or “Approve” immediately makes primary binding results available online to investigators. A representative screen capture (**Figure 6**) shows a reviewing screen for primary binding assay results.

1.6.1.3. Secondary binding assay result analysis. Upon completion of secondary binding results, technicians can upload raw results in Excel spreadsheets directly into the PDSP database via the secondary binding assay reporting menu. Differently from primary binding results, the PDSP database analysis tools can accept two types of 96-well drug plate layouts as indicated in **Figures 2a and 2b**, either manually made or made by the Hamilton STAR®. When uploading and submitting secondary binding results, technicians must match drug plate maps and barcodes with those generated by the Hamilton STAR® liquid handling system when the drug plates were made. They also need to choose buffers, radioligand identity, and reference compounds from pull-down menus and enter the total radioligand activity (dpm), specific activity, and K_d values (from saturation binding assay, see above) for the radioligand; the latter values will be used by the PDSP database to calculate the radioligand concentration used for the assay and to convert IC_{50} to K_i values. A representative screen capture (**Figure 7**) is shown below as technicians are uploading secondary binding results for submission. Technicians can view and examine the preliminary curves per plate or individually before submission.

After secondary binding results are submitted, the PDSP database treats results from 3 replicates of 96-well plates as a single file, assigns it a serial number with extra information such as receptor identity and PDSP compound numbers, and places the results in a pending list for review (**Figure 4**).

When PDSP administrators review and analyze the results for approval by clicking on any set of results in the pending list, the PDSP database will parse the uploaded file, and generate an editable table along with a preliminary graph for the purpose of analysis (**Figure 8**). Clicking on individual PDSP compounds leads to a new screen (**Figure 9**) showing a curve of the selected compound along with the reference curve. The raw data for both the selected compound and the reference are shown in tables at left. The PDSP database is also programmed to run a **Robust regression and Outlier removal (ROUT)** algorithm to identify and highlight potential outliers. PDSP administrators can either exclude or include the potential outliers when reviewing each data set. The raw data tables are also editable and allow for excluding points that are known to be in error, e.g., when a mistake is noticed in pipetting radioligand or membrane by a technician.

As an internal control, each secondary binding assay contains a reference dose-response curve, also in triplicate. The reference K_i value is automatically compared with its historical average value and/or that in our K_i database. If the reference K_i is larger than 3 fold different than its historical average value, the entire data set is flagged for further inspection. Senior PDSP scientists work with technicians to determine underlying causes and arrive at solutions. Typically, the secondary binding assay is repeated or the old reference stock is replaced with a fresh one, if the same reference has a low K_i value in multiple data sets.

Each curve has its K_i value listed at the right side and can be marked as either “Redo” or “Accept”. If a curve is marked as “Accept”, a new graph is generated for the PDSP compound, together with a reference curve and the status of the assay is flagged as “completed”; the result is then immediately available online to the investigator. Otherwise, “Redo” puts the compound back on to PDSP “scheduled” list. When an assay is approved, the PDSP database checks whether that compound has been previously tested at the same receptor. If so, database compares the results and generates a warning email if it finds that one K_i value is at least 4x different (0.6 log unit) from another one. All the secondary assays with the same compound will then be put into the “Experiments under review” list. PDSP administrators will review and decide what to do next with the compounds. Options include (1) one more repeat with the same stock; (2) one more repeat with a fresh stock; (3) approval

with no more action since lowest K_i value could be 4x away from highest K_i value, but they are less than 3x away from mean value. If the PDSP database has multiple accepted entries for the same compound, the database will calculate an average from all previous repeats. If a compound shows allosteric potentiation in radioligand binding assays, the result is usually extracted and analyzed separately using Prism v5.0 (See representative figures for 5-HT_{1E} secondary binding below).

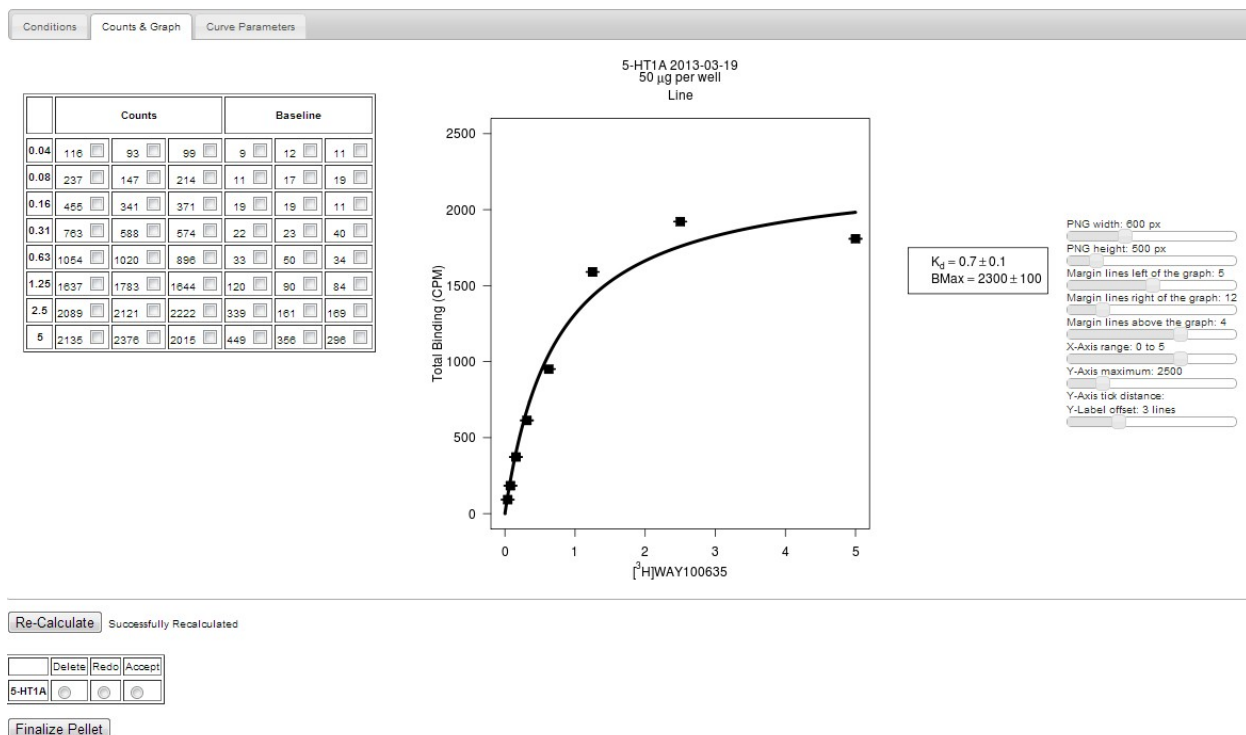


Figure 5. A representative screen capture showing the saturation binding result reviewing process. Both total and nonspecific binding (cpm/well) are shown in the tables on the left. Specific binding is fitted to a hyperbolic curve to determine B_{max} (cpm/well) and K_d (nM); both values are listed to the right of the curve. The pellet information is listed on top of the figure, showing that this is a 5-HT_{1A} membrane pellet, made from a stable line, assayed at 50 µg/well protein on March 19, 2013.

New Tab x View Pending Experiment x

https://pdspdb.unc.edu/html/pdspV2/web/views/viewPendingExperiment.php?pendingExpID=23193

Google Chrome Gateways PDSP UNC Journals GPCR Tech Chinese Company Followups Local Sports Android Reviews Camera Travel Science Books Imported

PDSP Home Ki DB Home Tracer Database Roth Lab U N C Binding Assay Functional Assay Publications AFCS-Nature

Home Log Out Add Edit View Admin Help Log Out

View Pending Experiment

Experiment: TC312135HT2C
 Receptor: 5-HT2C
 Date Completed: 2013-03-12

Compound	Total 1	Total 2	Mean Specific	Mean % Inhibition	Total 3	Total 4	Mean Specific	Mean % Inhibition	Mean % Inhibition (N=4)	Redo	Repeat	Force Secondary	Approve
None	2341	2128	2187	0	2961	2100	2465	0.00	0				
27475	881	757	771.5	84.723365	1085	877	915.5	62.86	63.791702				
27476	1653	1982	1770	19.067215	2370	2057	2148	12.86	15.963627				
27478	1315	1156	1188	45.679012	1384	2008	1630.5	33.85	39.766483				
27782	303	464	336	84.636488	494	525	444	81.99	83.312158				
27796	2049	2303	2128.5	2.6748971	2285	2397	2275.5	7.69	5.1812619				
27797	1515	1894	1657	24.234110	2517	1751	1568.5	36.37	30.301639				
27798	1407	1798	1555	28.898033	1913	2029	1905.5	22.70	25.797901				
27799	3434	2463	2901	-32.64746	2149	2786	2402	2.56	-15.04584				
27800	428	537	435	80.109739	658	770	648.5	73.69	76.900711				
27801	1728	1896	1864.5	23.891175	2126	920	1457.5	40.87	32.381693				

EN 1:00 AM 3/17/2013

Figure 6. A representative screen capture showing a reviewing screen of primary binding assay results. The barcoded plate is for 5-HT_{2B} binding assays carried out on March 12, 2013. Total binding is shown in the top row and PDSP compounds are shown below. Nonspecific binding is at the bottom of the screen and not shown in the figure. Highlighted in yellow are the the samples with more than 50% inhibition; these samples will be tagged for secondary binding assays automatically. Highlighted in red are samples with more 20% variation among the 4 replicates. There are four options for each compound: “Redo”, “Repeat”, “Force Secondary”, and “Approve”, as indicated at the right side of the screen capture.

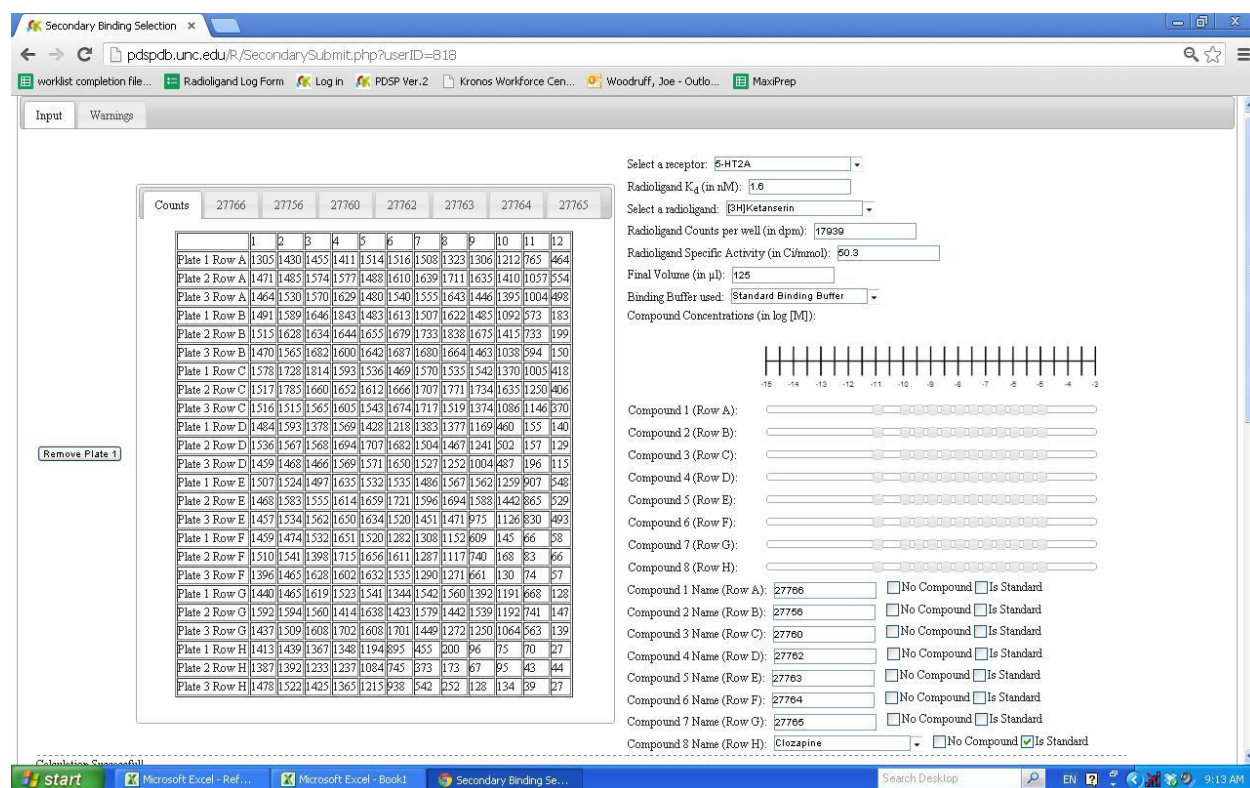


Figure 7. A representative screen capture showing the final stage in an actual secondary binding result submission. On the left, one complete set of raw data are pooled together from 3 96-well plates (Plate 7, Plate 8, and Plate 9) and organized from Rows A to G from top to bottom with PDSP compound # showing at the top of the table. On the upper right, detailed information for the binding assay is shown, including target receptor identity (5-HT_{2A} receptor in this case), K_d value (1.6 nM) for the radioligand [3H]-ketanserin, total radioactivity (17939 dpm) added to each well, specific activity of the radioligand (50.3 Ci/mmol), and final volume of the assay (125 µl/well) in standard binding buffer. On the lower right, detailed information on the tested compounds (PDSP numbered compounds and reference with corresponding concentrations) is shown. The concentrations for each compound are set at default values, but can be changed individually by sliding the corresponding bar button, if necessary.

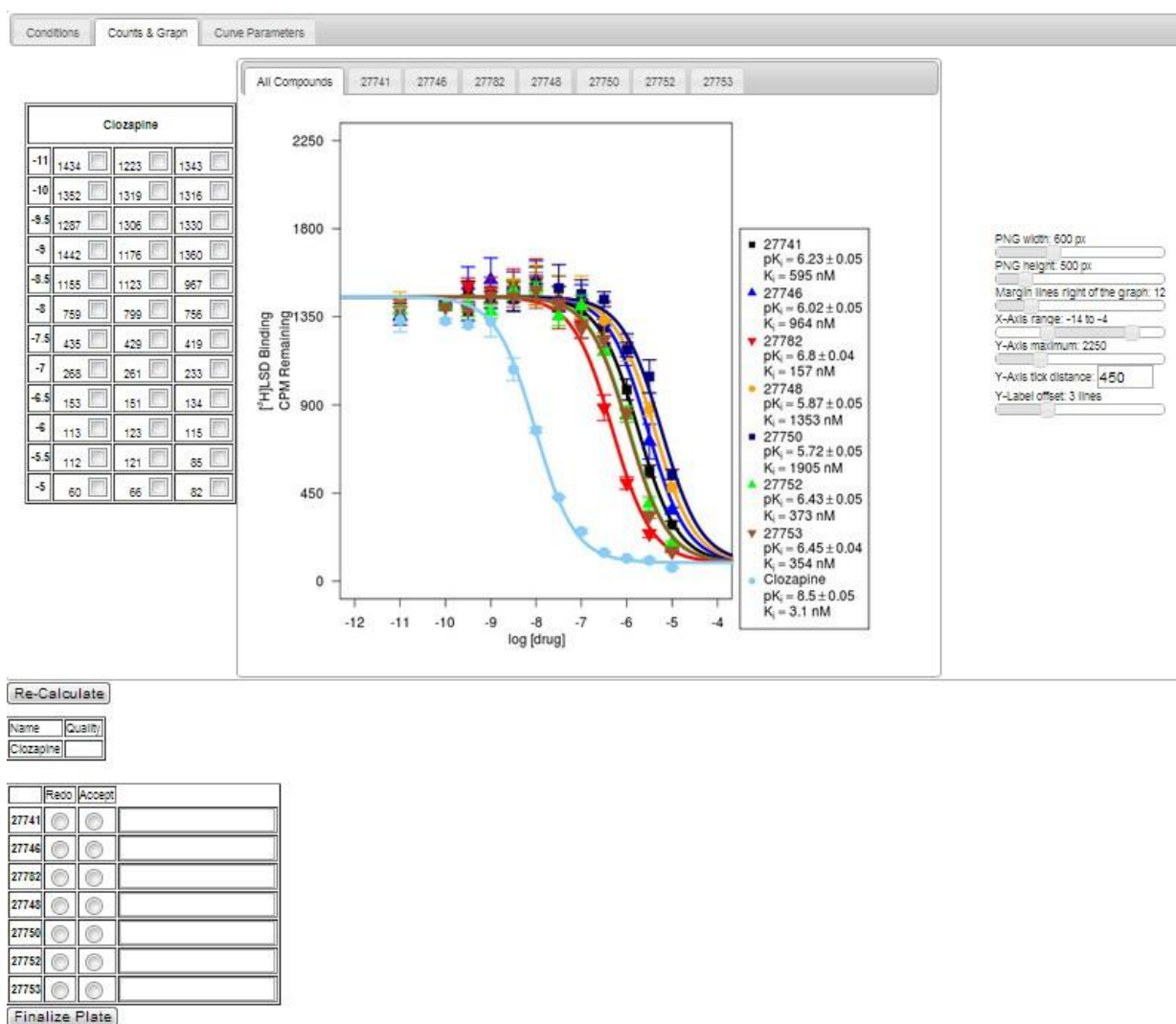


Figure 8. A screen capture showing a representative overview of a set of secondary binding results. On the left, detailed counts (cpm/well) for the reference compounds are shown in a table. In the middle, up to 8 curves are shown on the same graph with pre-determined color scheme with PDSP numbers on top of the graph (one on each tab) and corresponding pK_i and K_i values on the right. Clicking on any PDSP number brings up a graph showing the selected compound and reference, see Figure 9.

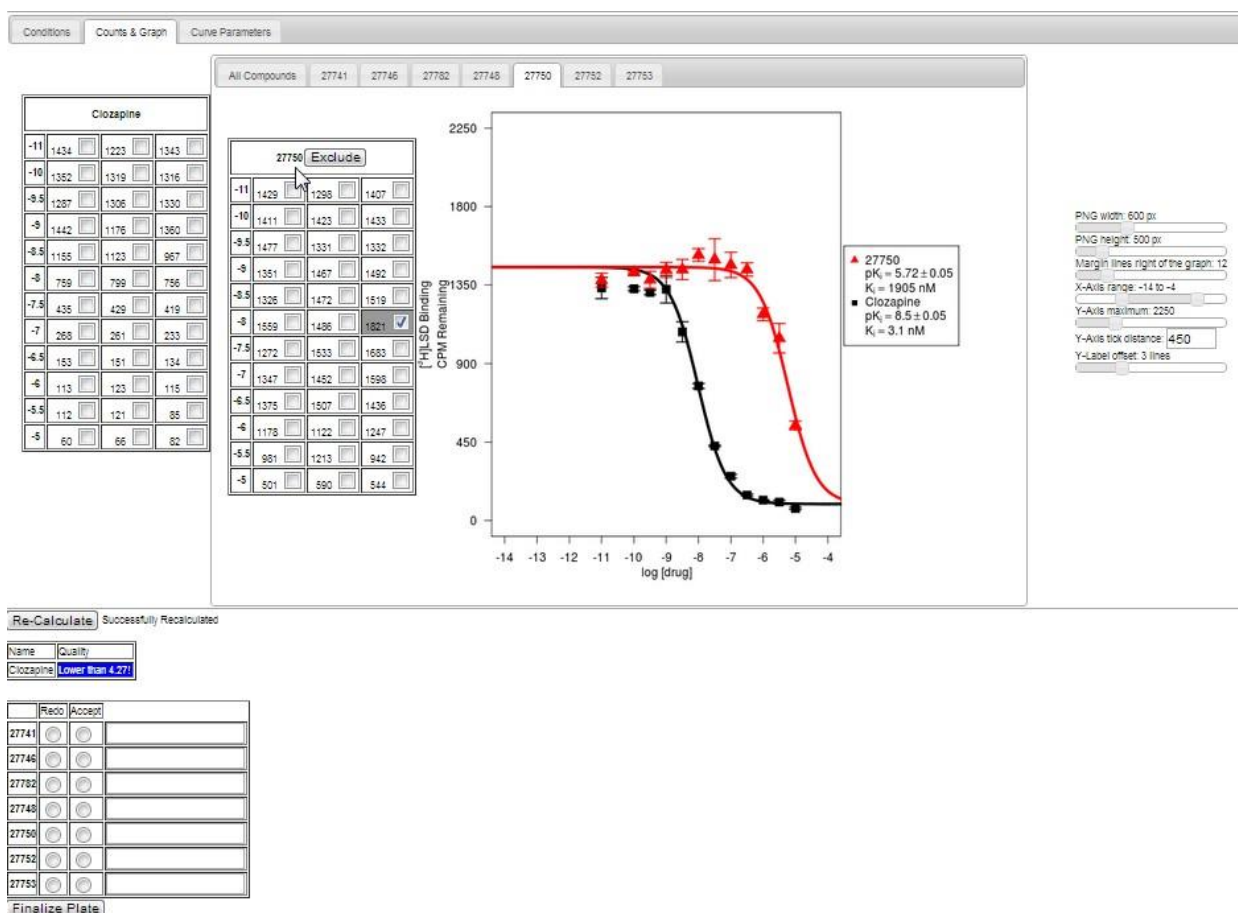


Figure 9. A screen capture showing a representative reviewing process. This screen shows when a PDSP compound is clicked on its tab in **Figure 8**. On the right, detailed counts (cpm/well) for both reference compound and the selected PDSP compound are shown in corresponding tables. One potential outlier has been highlighted (in dark gray with a checkmark “✓”) by the PDSP database using a robust outlier identification algorithm. In the middle, the selected compound is plotted side by side with the reference compound, with corresponding pK_i and K_i values listed on the right. At the lower left corner, each compound can be marked either “Redo” or “Accept” and there is a box for a brief note.

1.6.2. Binding assay result analysis using Prism v5.0: Binding assay results are also analyzed in Prism v5.0, if necessary, using Prism built-in functions for corresponding assay types. The following sections provide detailed procedures for binding assay data analysis.

1.6.2.1. Saturation binding result analysis. For saturation binding results, total binding and nonspecific binding results are analyzed in Prism v5.0 by fitting results to the following equations to determine B_{\max} and K_d values. To do this, total binding values in cpm must be entered in column A and nonspecific binding values in cpm must be entered in column B, corresponding to concentrations of the free radioligand.

$$\begin{aligned} \text{Nonspecific binding} &= NS * X + \text{Background} \\ \text{Total binding} &= \text{Nonspecific binding} + \frac{B_{\max} * X}{(X + K_d)} \end{aligned}$$

in which “**Nonspecific binding**” and “**Total binding**” are measured radioactivity (cpm per well) in the absence and presence of 10 μ M reference compound, respectively, at corresponding concentration [X] in nM. B_{\max} is receptor expression level in cpm/well or fmol/mg protein; K_d is the equilibrium binding affinity, corresponding to the radioligand concentration at which point 50% of B_{\max} is bound to the radioligand; NS and Background are two fitting values for nonspecific binding and background counts.

1.6.2.2. Primary binding result analysis. For primary binding results, non-specific binding in the presence of 10 μ M of an appropriate reference compound is set as 100% inhibition; total binding in the absence of test compound or reference compound is set as 0% inhibition. The radioactivity in the presence of test compound is calculated with the following equation and expressed as a percentage inhibition:

$$\% \text{ Inhibition} = 100 - \frac{\text{Sample cpm} - \text{Nonspecific cpm}}{\text{Total cpm} - \text{nonspecific cpm}} \times 100$$

1.6.2.3. Secondary binding result analysis. For secondary binding results, counts (cpm/well) are pooled and fitted to a three-parameter logistic function for competition binding in Prism v 5.0 to determine IC₅₀ values,

$$Y = \text{Bottom} + \frac{(\text{Top} - \text{Bottom})}{1 + 10^{X - \text{LogIC}_{50}}}$$

in which **Y** is the total binding in the presence of corresponding concentration of test compound (**X**); **Top** and **Bottom** are the total and nonspecific binding in the absence and presence of 10 µM reference antagonist; **IC₅₀** is the concentration at which 50% observed binding was inhibited and is converted to K_i according to the Cheng-Prusoff equation (7),

$$K_i = \frac{IC_{50}}{1 + \frac{L}{K_d}} \text{ or } \text{Log}K_i = \text{Log}IC_{50} - \text{Log}\left(1 + \frac{L}{K_d}\right)$$

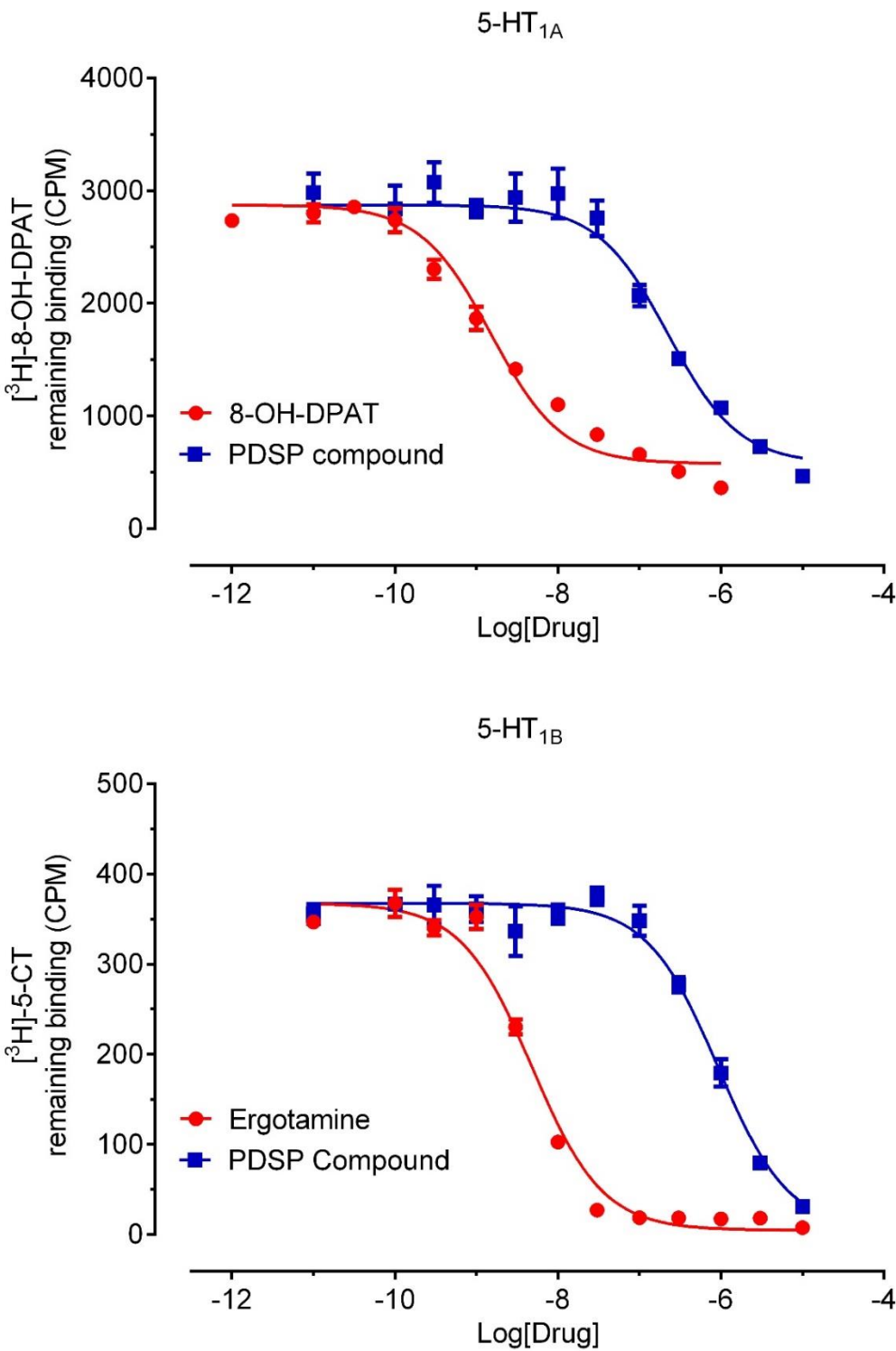
in which **L** is the radioligand concentration used in the competition binding assay; **K_d** is the radioligand equilibrium binding affinity determined in above saturation binding assays. In the curve-fitting analysis, top and bottom values are shared among all binding curves from the same plate if necessary.

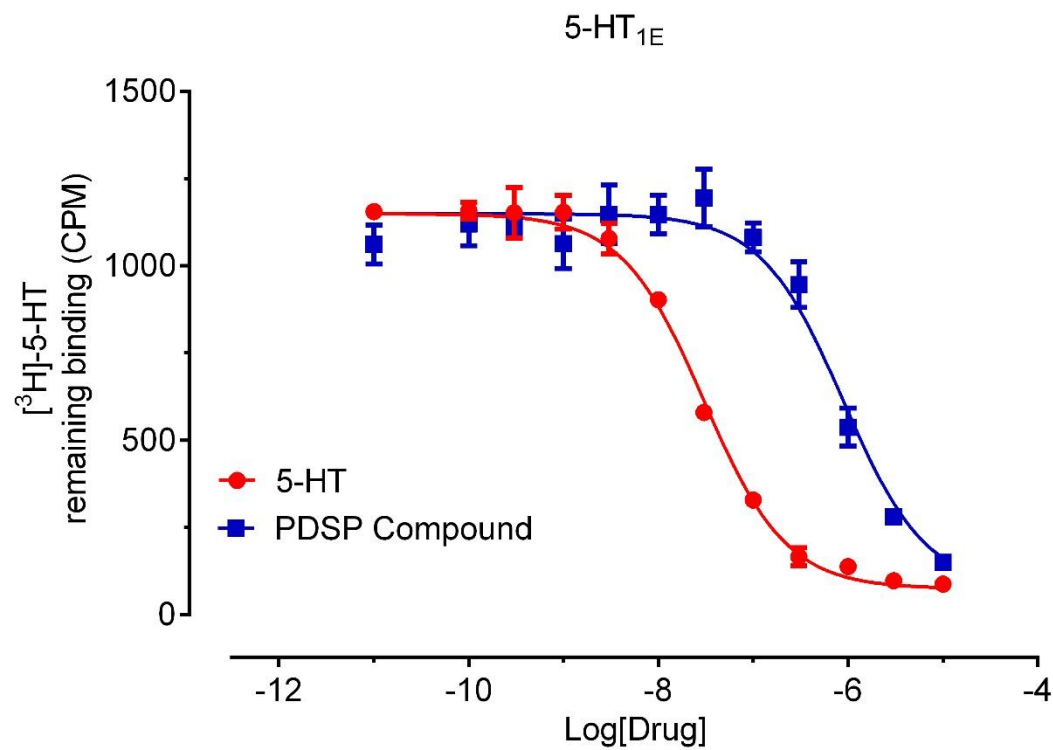
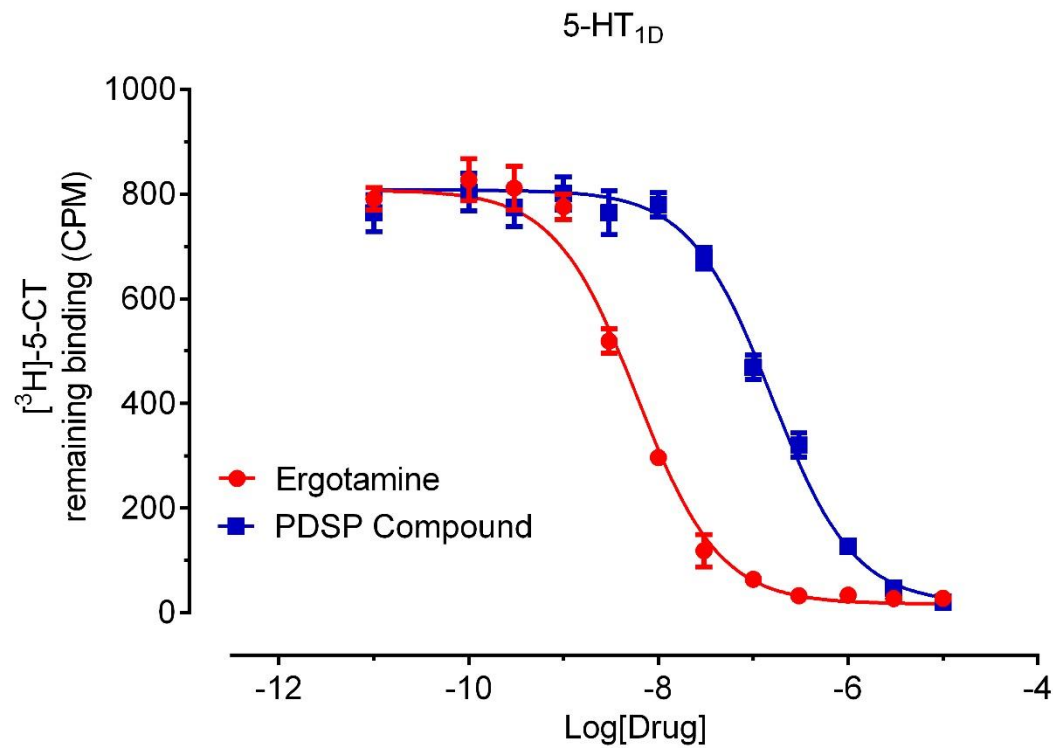
1.7. Tables of binding assay conditions and representative figures

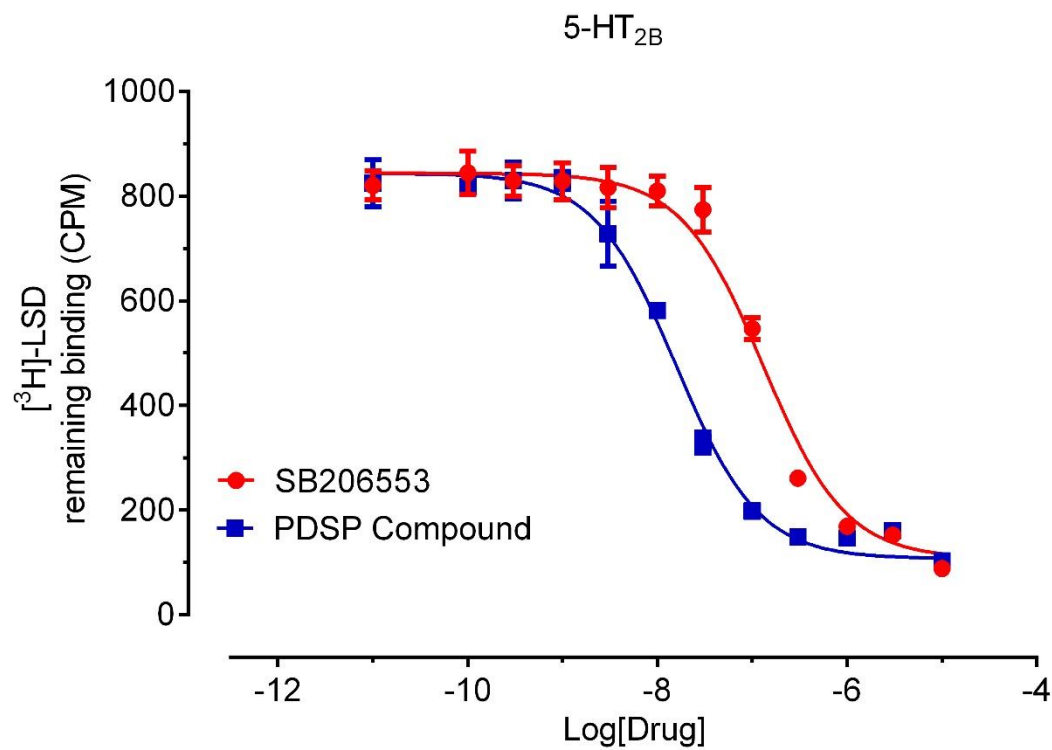
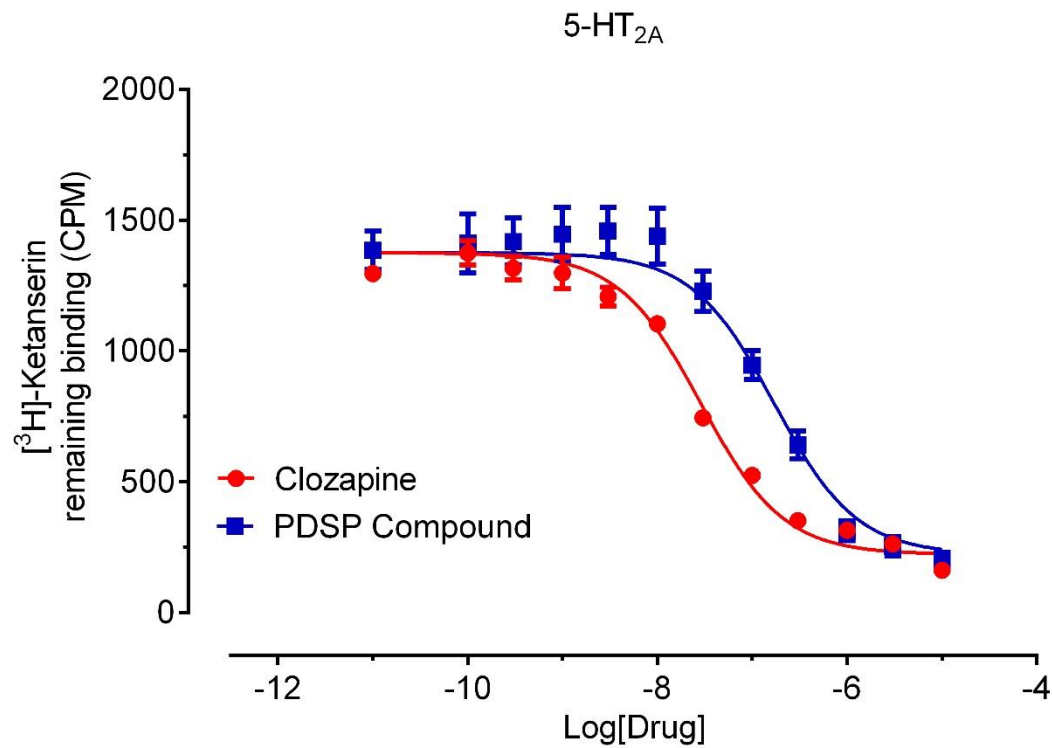
Table 2. 5-HT receptors, radioligands and corresponding concentrations, reference compounds, and buffers for primary and secondary radioligand binding assays. BB for binding buffer; WB for wash buffer. Historical reference K_i values from the last 2 years are also listed.

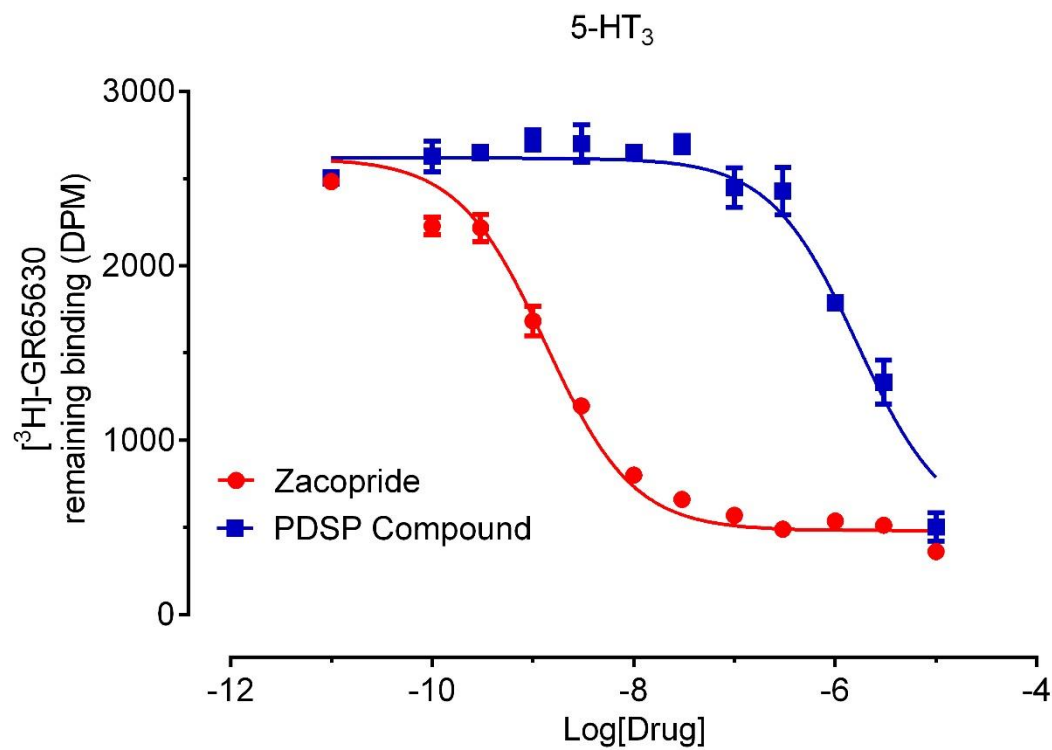
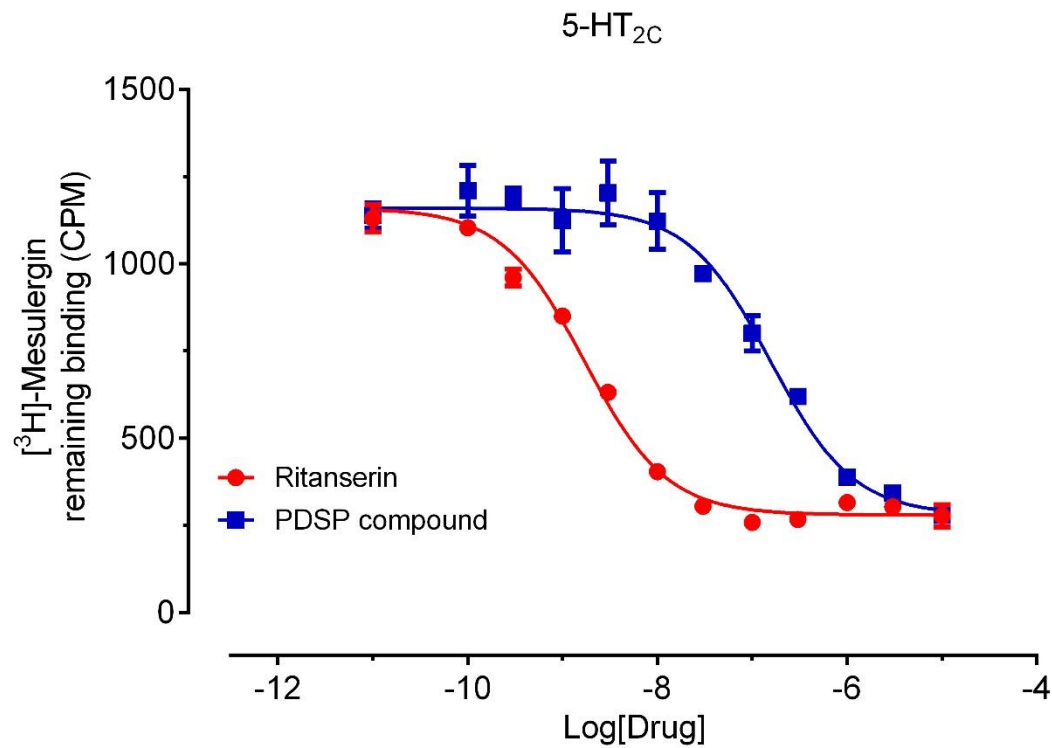
5-HT receptors				
Standard BB (SBB): 50 mM Tris HCl, 10 mM MgCl ₂ , 0.1 mM EDTA, pH 7.4, RT Standard WB (SWB): 50 mM Tris HCl, pH 7.4, cold				
Target	Radioligand $pK_d \pm SEM (K_d, nM)$	Radioligand used (nM)	Reference Ligand $pK_i \pm SEM (K_i, nM)$	Literature
5-HT _{1A}	[³ H]-Way100635 9.30 ± 0.04 (0.50)	0.5 – 1.0	8-OH-DPAT 9.18 ± 0.02 (0.66)	(8)
5-HT _{1B}	[³ H]5-CT 9.06 ± 0.09 (0.87)	0.6 – 1.5	Ergotamine 8.84 ± 0.03 (1.44)	(9, 10)
5-HT _{1D}	[³ H]5-CT 9.06 ± 0.06 (0.86)	1.0 – 2.0	Ergotamine 8.32 ± 0.02 (4.83)	(9, 10)
5-HT _{1E}	[³ H]5-HT 8.42 ± 0.06 (3.82)	2.1 – 5.0	5-HT 8.05 ± 0.03 (8.82)	(11–13)
5-HT _{1F}				
5-HT _{2A}	[³ H]-Ketanserin 8.92 ± 0.04 (1.20)	1.2 – 2.4	Clozapine 8.23 ± 0.01 (5.91)	(14–16)
5-HT _{2B}	[³ H]-LSD 8.93 ± 0.03 (1.19)	1.0 – 2.0	SB206553 7.84 ± 0.01 (14.39)	(17–19)
5-HT _{2C}	[³ H]-Mesulergine 5.85 ± 0.06 (2.66)	1.0 – 2.5	Ritanserin 8.84 ± 0.02 (1.44)	(17, 20)
5-HT ₃	[³ H]GR65630 8.46 ± 0.14 (3.48)	1.0 – 2.0	Zacopride 9.23 ± 0.02 (0.58)	(21, 22)
5-HT ₄	[³ H]GR113808 8.66 ± 0.17 (2.19)	0.5 – 2.0	SDZ205557 7.94 ± 0.09 (11.44)	(23–27)
5-HT _{5A}	[³ H]-LSD 8.72 ± 0.03 (1.91)	2.0 - 3.3	Ergotamine 7.61 ± 0.03 (24.60)	(28, 29)
5-HT ₆	[³ H]-LSD 8.37 ± 0.04 (4.27)	2.0 – 4.0	Clozapine 8.28 ± 0.02 (5.27)	(30)
5-HT _{7A}	[³ H]-LSD 8.13 ± 0.06 (7.48)	5.0 – 6.0	Clozapine 7.99 ± 0.02 (10.33)	(31)

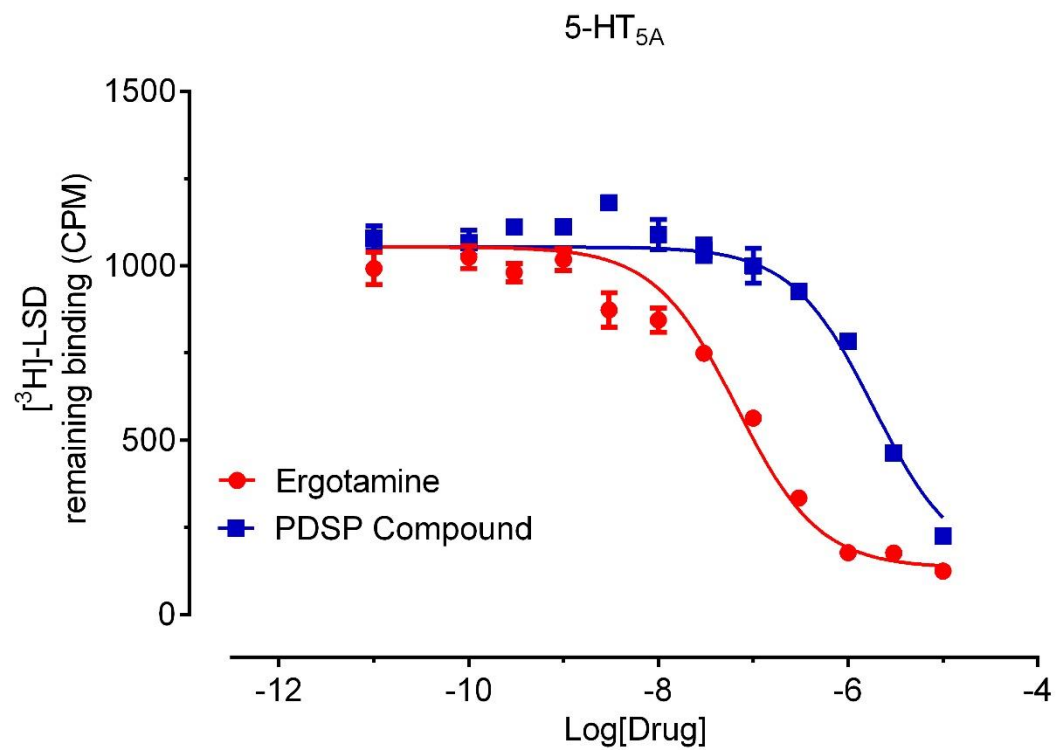
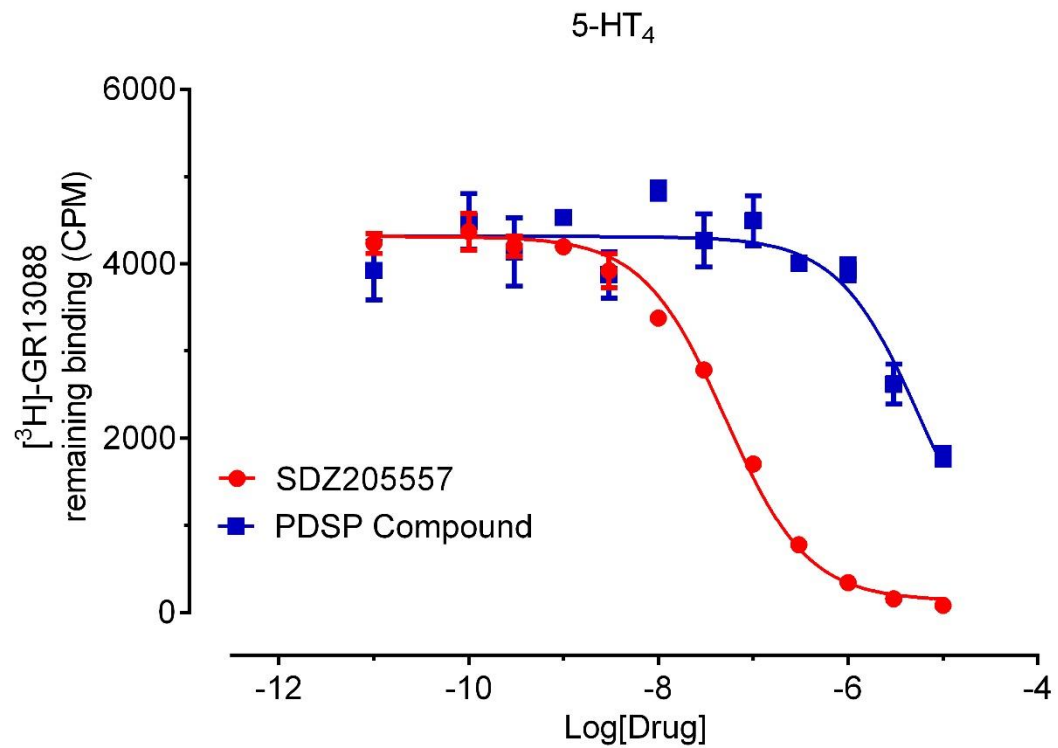
Figure 10. Representative competition binding curves with 5-HT receptors











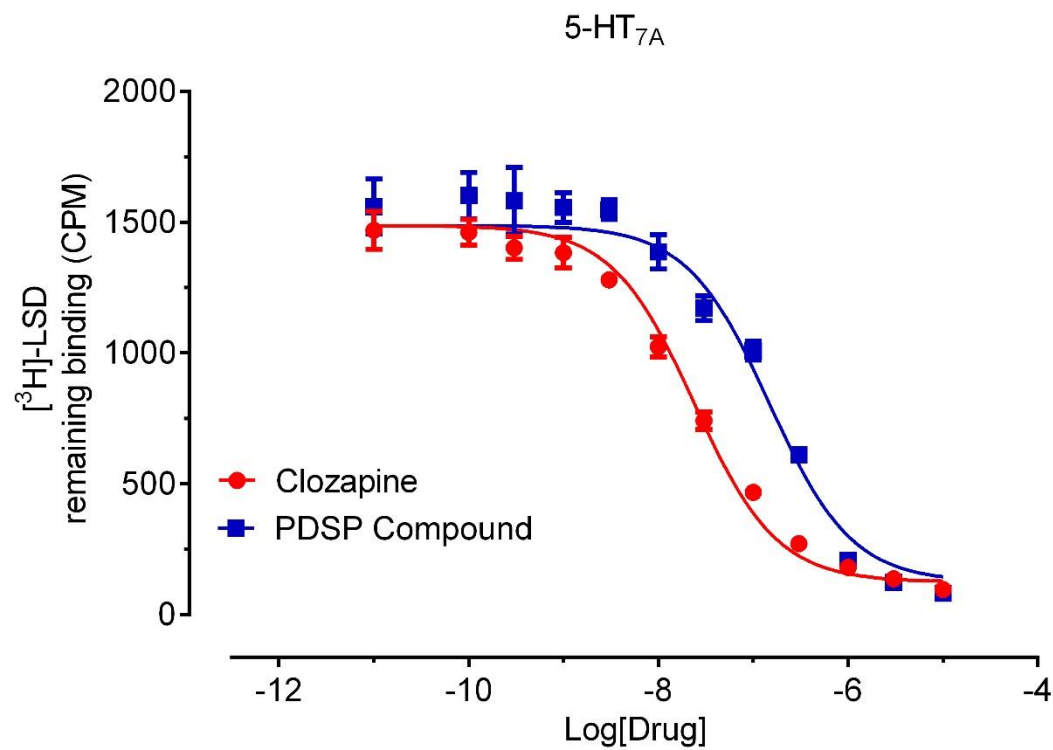
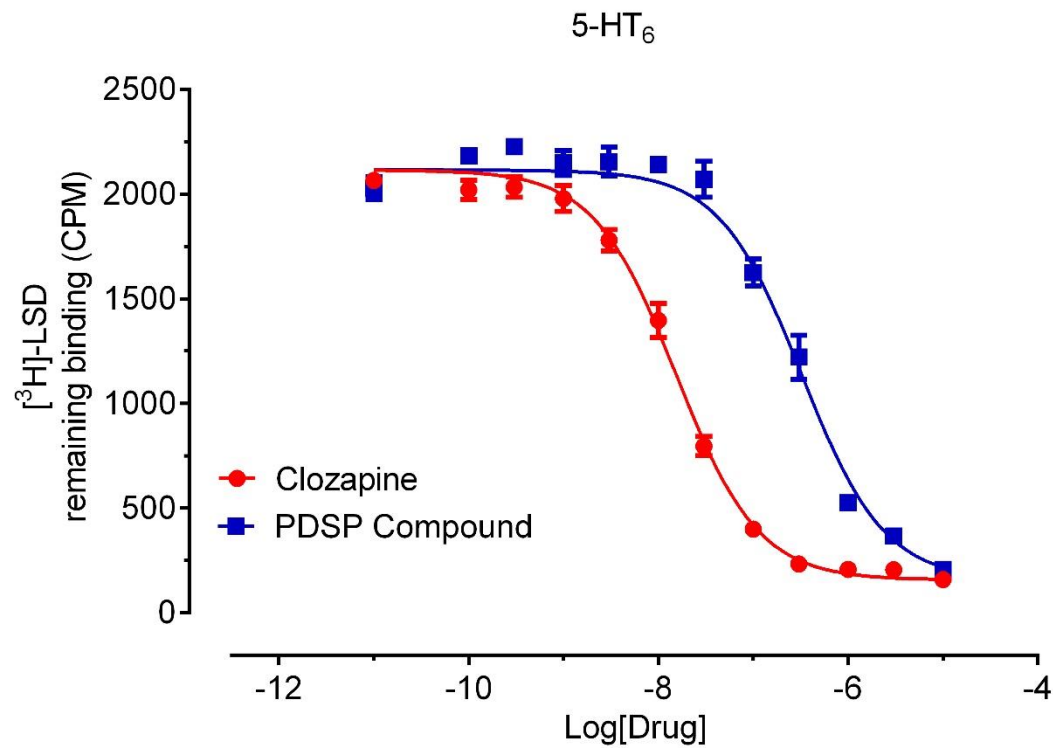
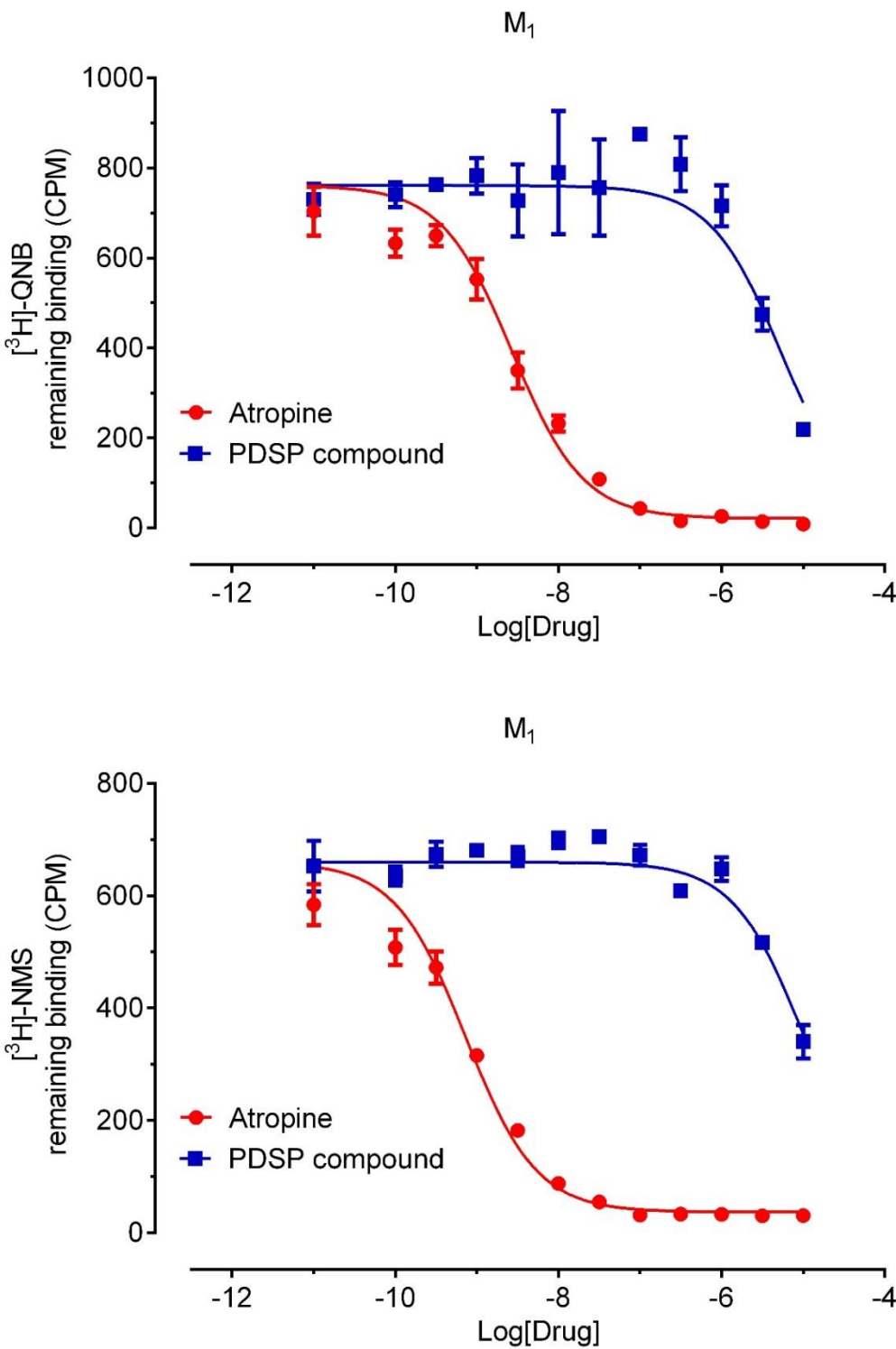
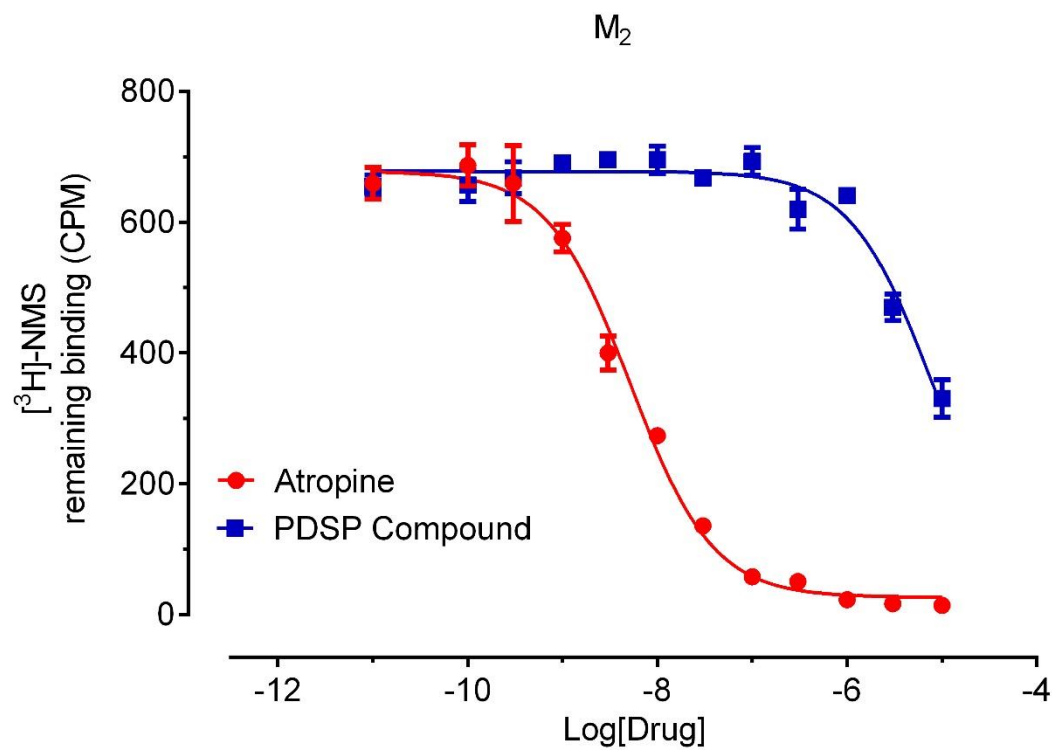
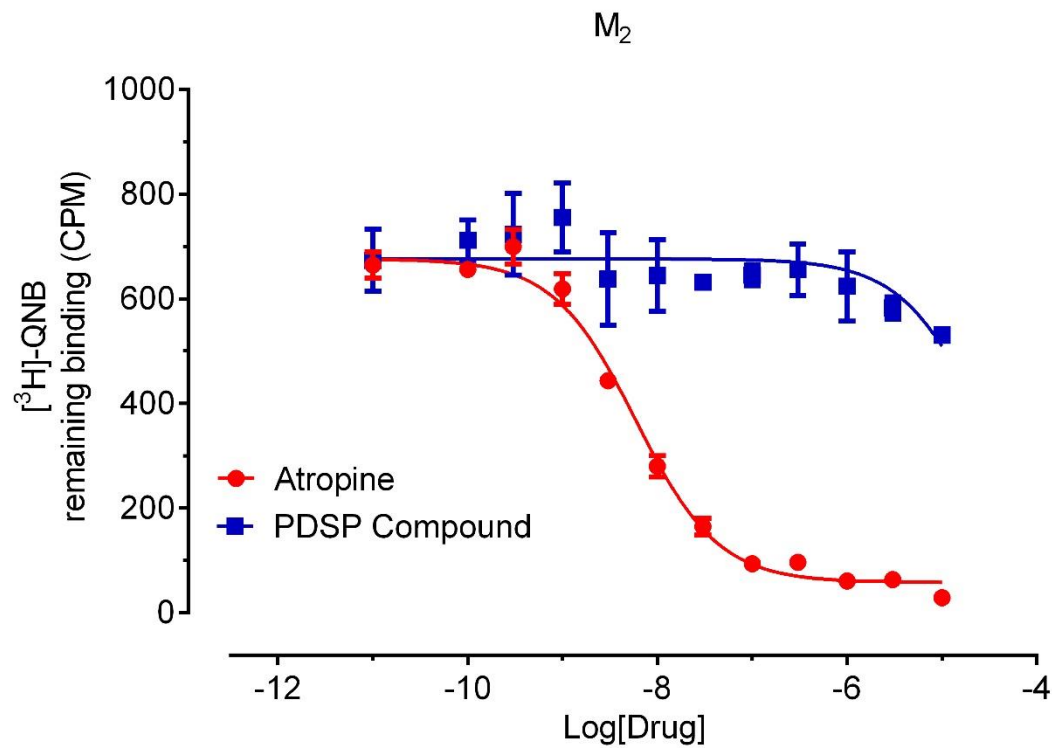


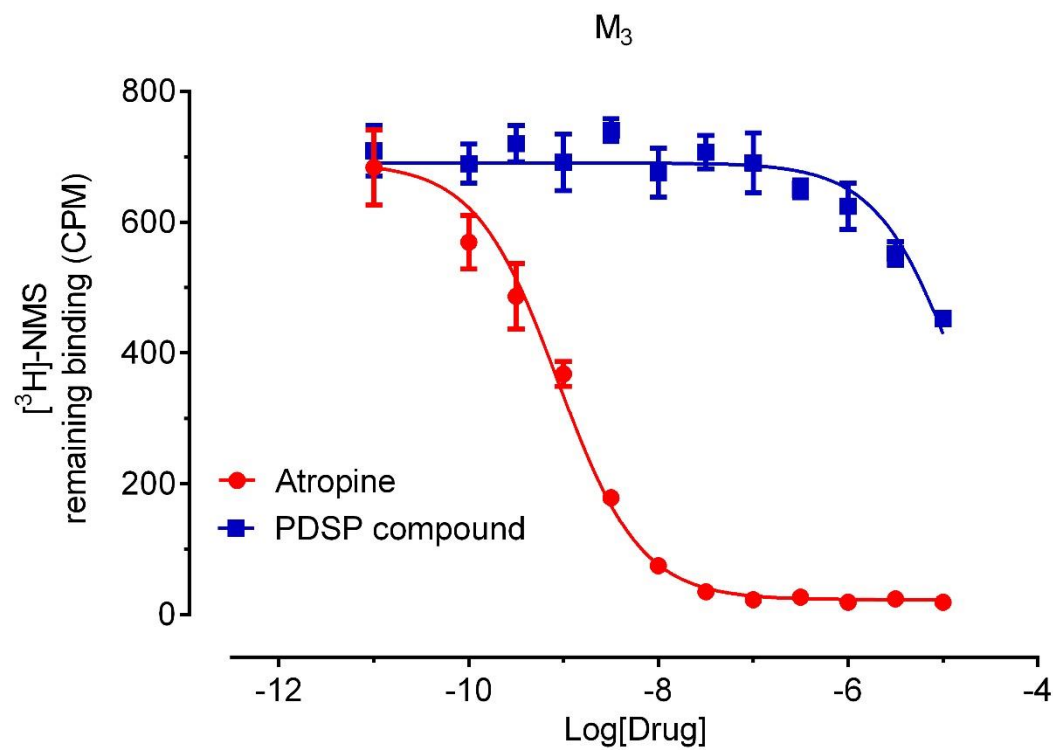
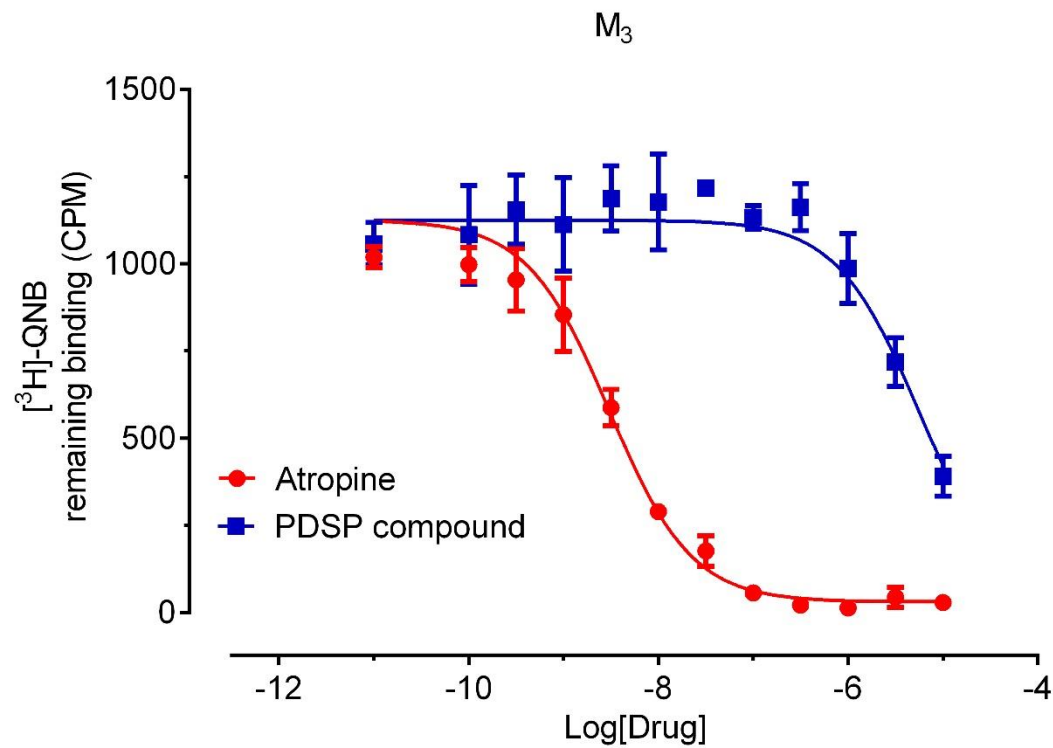
Table 3. Muscarinic acetylcholine receptors, radioligands and corresponding K_d values, reference compounds, and buffers for primary and secondary radioligand binding assays. BB for binding buffer; WB for wash buffer. Historical reference K_i values from over last years are also included.

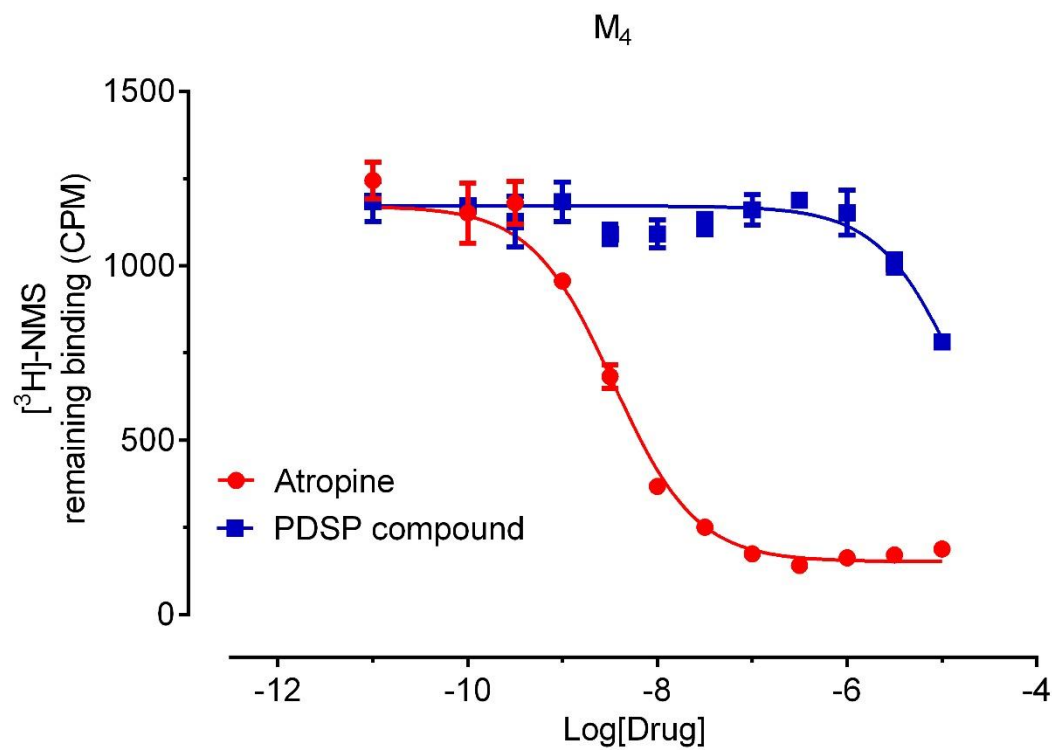
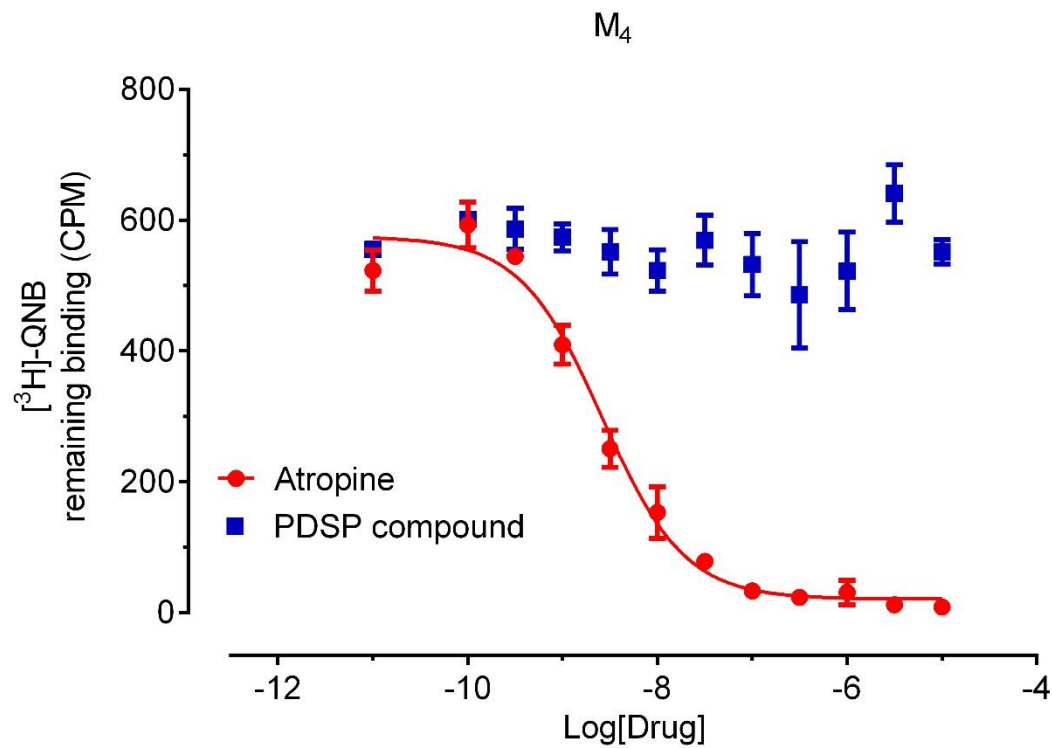
Muscarinic acetylcholine receptors				
Muscarinic BB (MBB) #1: 50 mM Tris HCl, pH 7.7, RT + SWB				
Muscarinic BB (MBB) #2: 25 mM Sodium Phosphate, 5 mM MgCl ₂ , pH 7.4, RT (cold for washing)				
Muscarinic wash buffer #2: Same as muscarinic binding buffer #2, cold				
Target	Radioligand $pK_d \pm SEM (K_d, nM)$	Radioligand used (nM)	Reference Ligand $pK_i \pm SEM (K_i, nM)$	Literature
M ₁	[³ H]-QNB 9.21 \pm 0.18 (0.62)	0.3 – 1.2	Atropine 8.92 \pm 0.03 (1.21)	(32, 33)
M ₁	[³ H]-NMS 9.26 \pm 0.21 (0.54)	0.5 – 0.9	Atropine 8.86 \pm 0.08 (1.39)	(34, 35)
M ₂	[³ H]-QNB 9.57 \pm 0.05 (0.27)	0.2 – 1.0	Atropine 8.63 \pm 0.03 (2.36)	(32)
M ₂	[³ H]-NMS 9.67 \pm 0.10 (0.21)	0.2 - 1.0	Atropine 9.11 \pm 0.34 (0.77)	(34)
M ₃	[³ H]-QNB 9.37 \pm 0.06 (0.43)	0.3 – 1.0	Atropine 9.30 \pm 0.03 (0.50)	(32)
M ₃	[³ H]-NMS 9.53 \pm 0.08 (0.30)	0.3 – 1.0	Atropine 9.19 \pm 0.12 (0.64)	(34)
M ₃ D	[³ H]-QNB 9.13 \pm 0.19 (0.74)	0.5 – 1.0	Atropine 8.30 \pm 0.12 (4.97)	(36, 37)
M ₄	[³ H]-QNB 9.64 \pm 0.06 (0.23)	0.3 – 1.0	Atropine 9.25 \pm 0.04 (0.56)	(32, 33)
M ₄	[³ H]-NMS 9.72 \pm 0.11 (0.19)	0.3-1.0	Atropine 8.89 \pm 0.07 (1.28)	(33, 34)
M ₄ D	[³ H]-QNB 8.74 \pm 0.14 (1.80)	1.0 – 2.5	Atropine 8.46 \pm 0.08 (3.47)	(37, 38)
M ₅	[³ H]-QNB 9.31 \pm 0.06 (0.49)	0.2 – 1.0	Atropine 9.26 \pm 0.02 (0.55)	(34)
M ₅	[³ H]-NMS 9.49 \pm 0.05 (0.32)	0.2 – 1.0	Atropine 8.99 \pm 0.08 (1.03)	(34, 39)

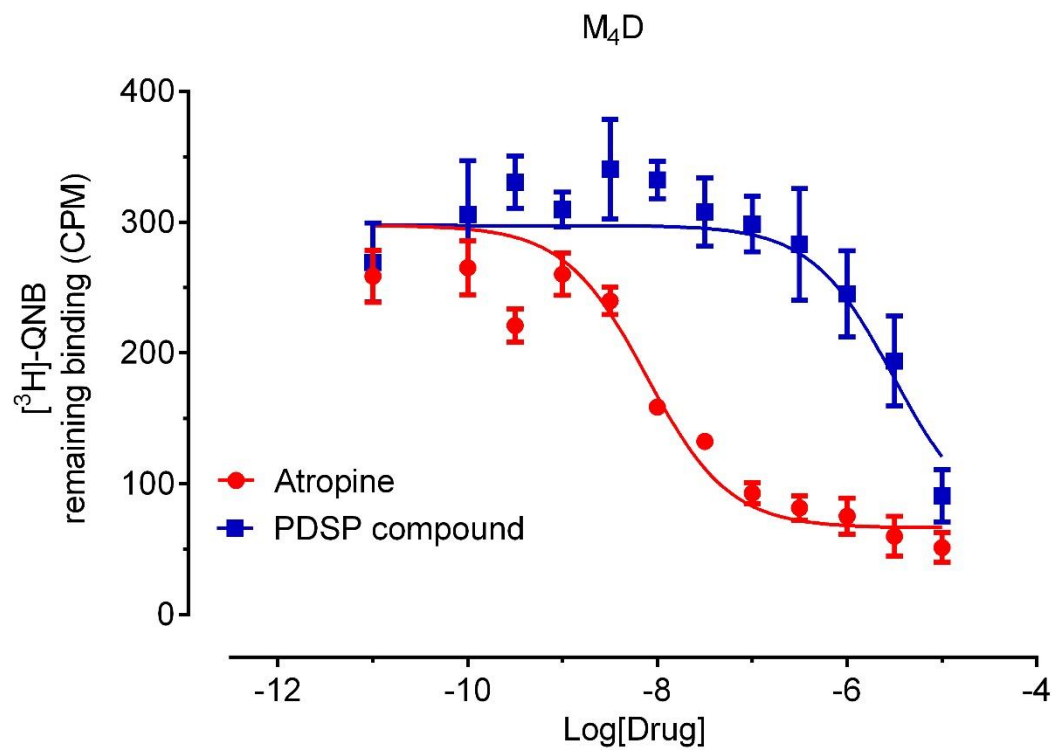
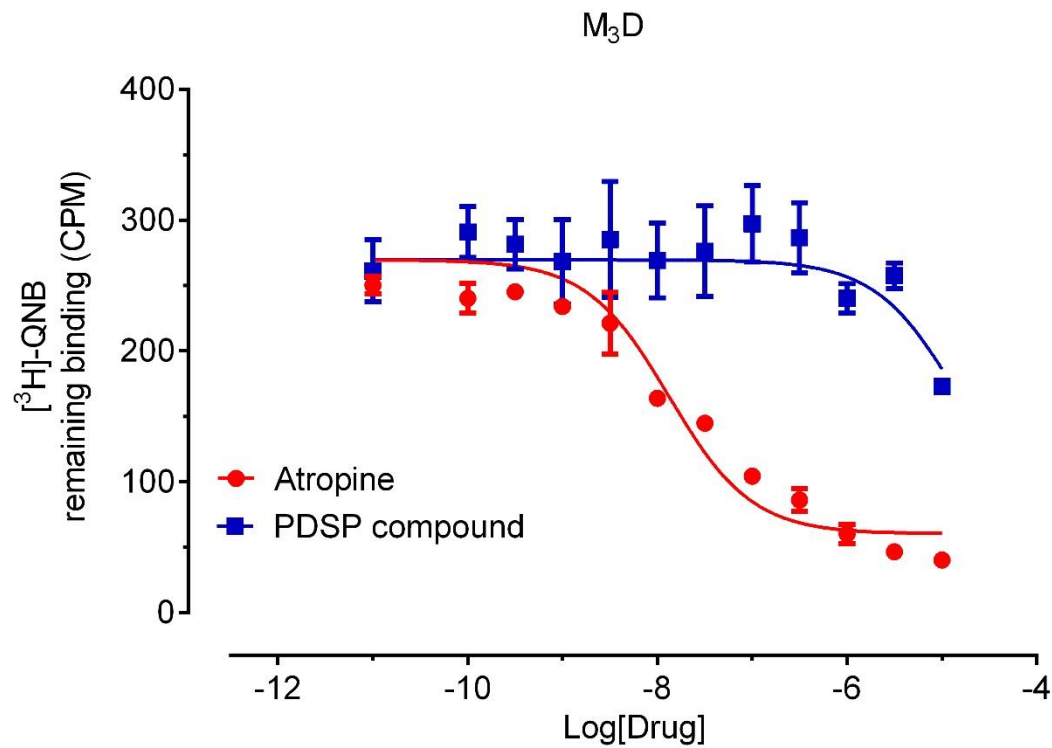
Figure 11. Representative competition binding curves with muscarinic acetylcholine receptors











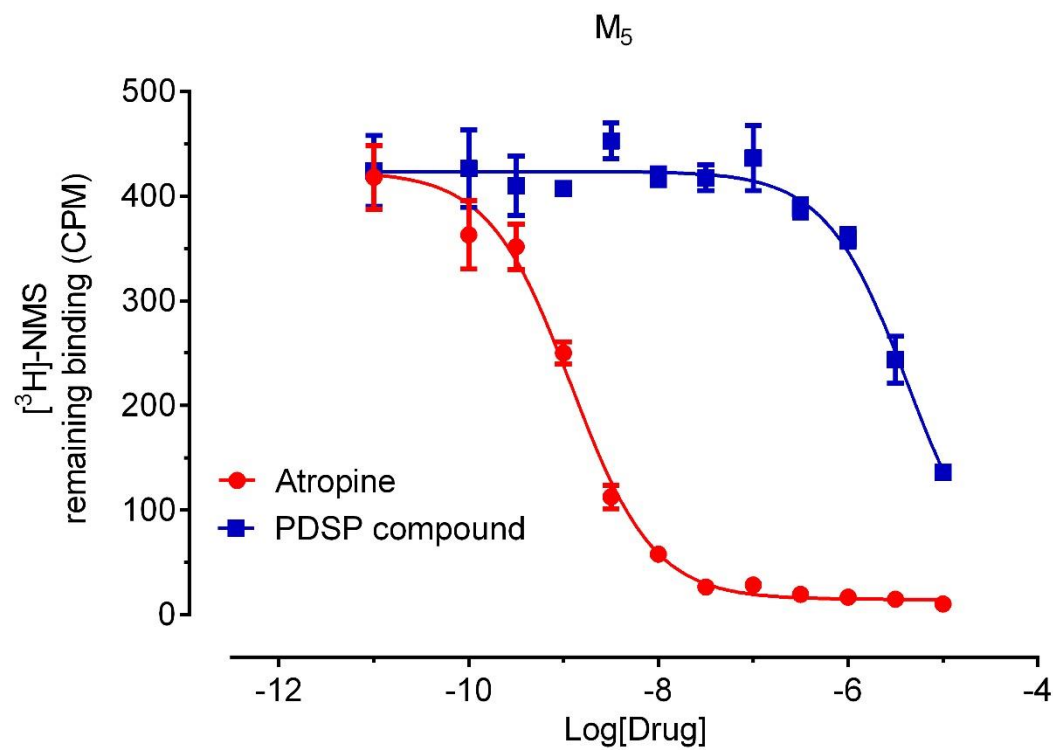
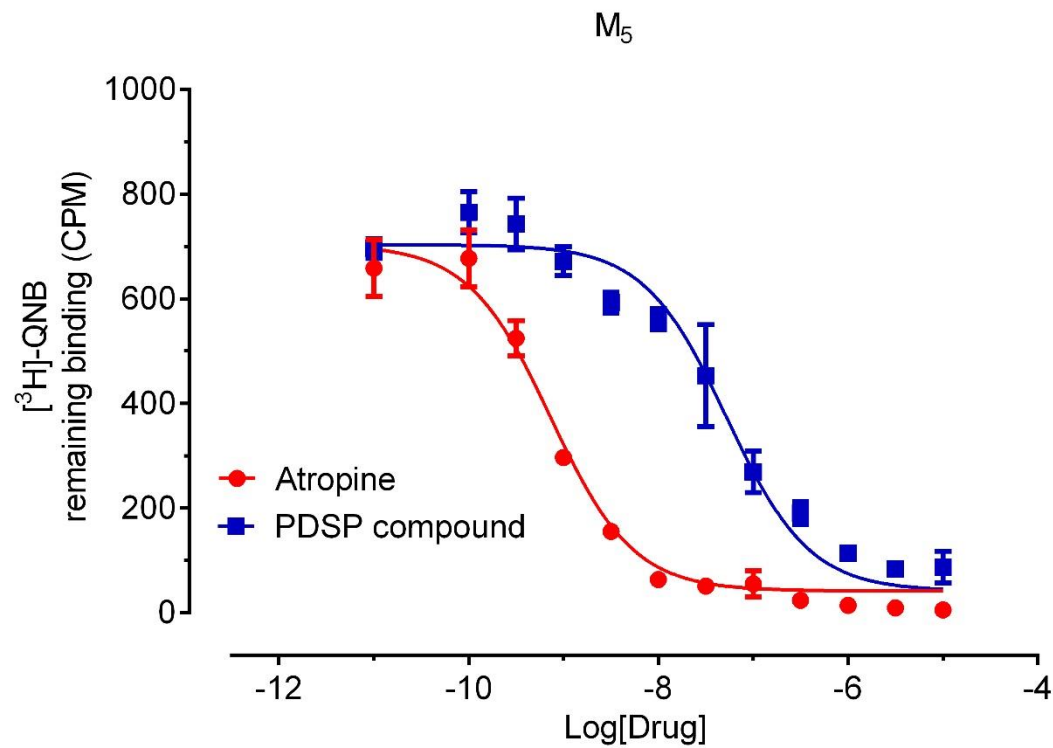
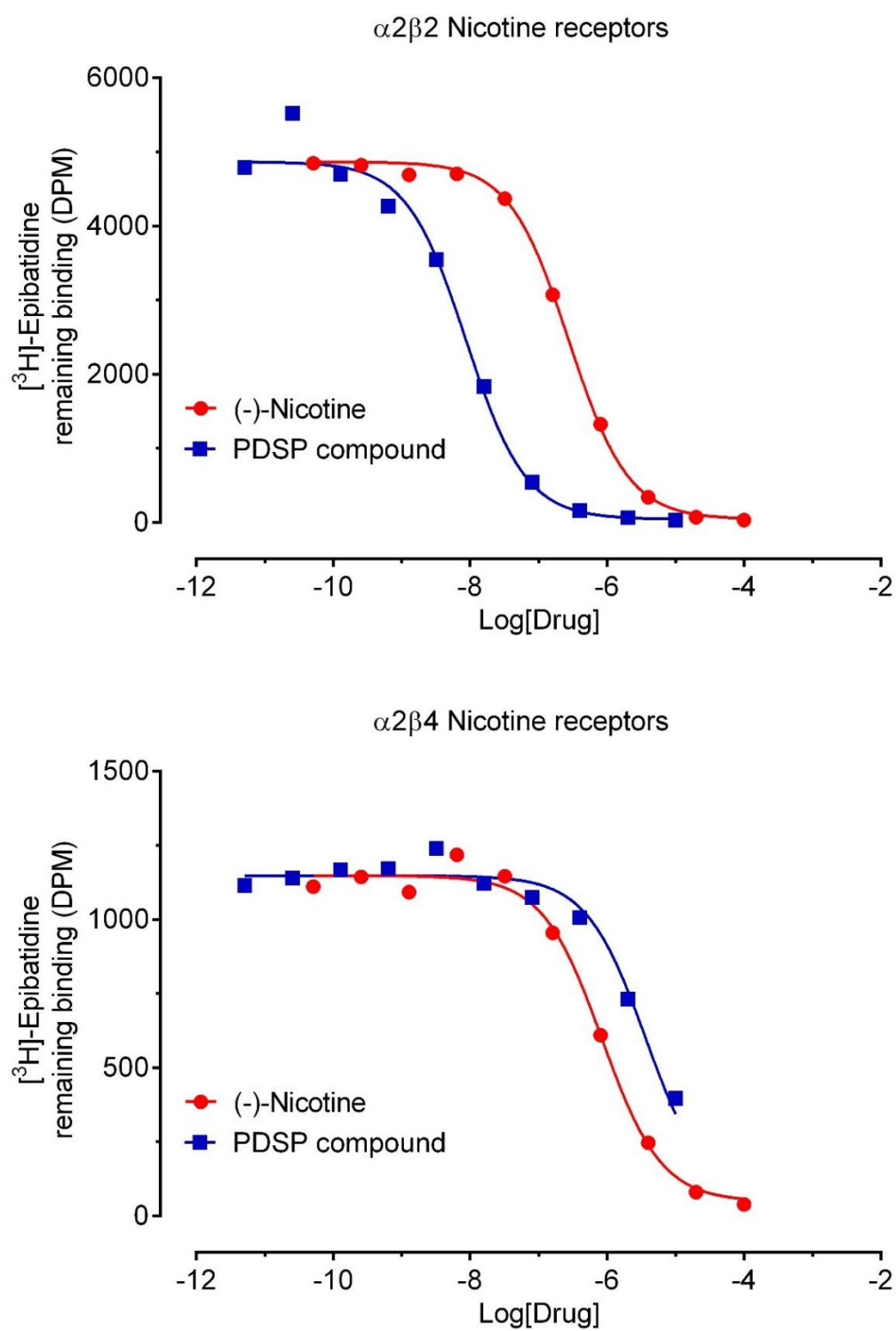


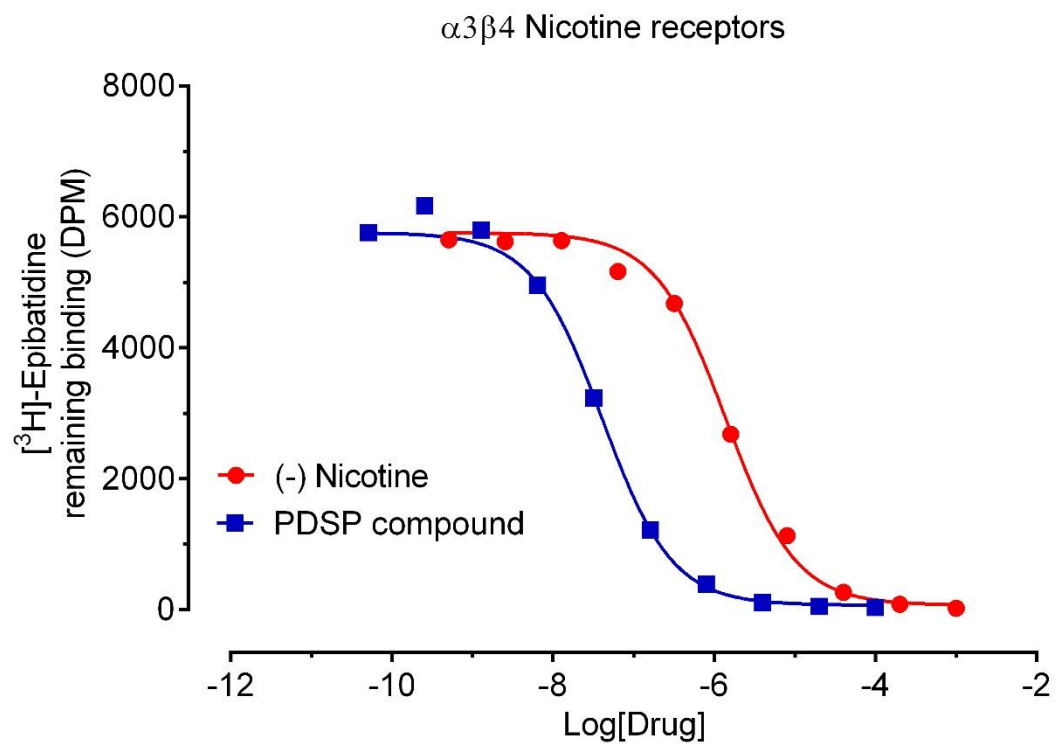
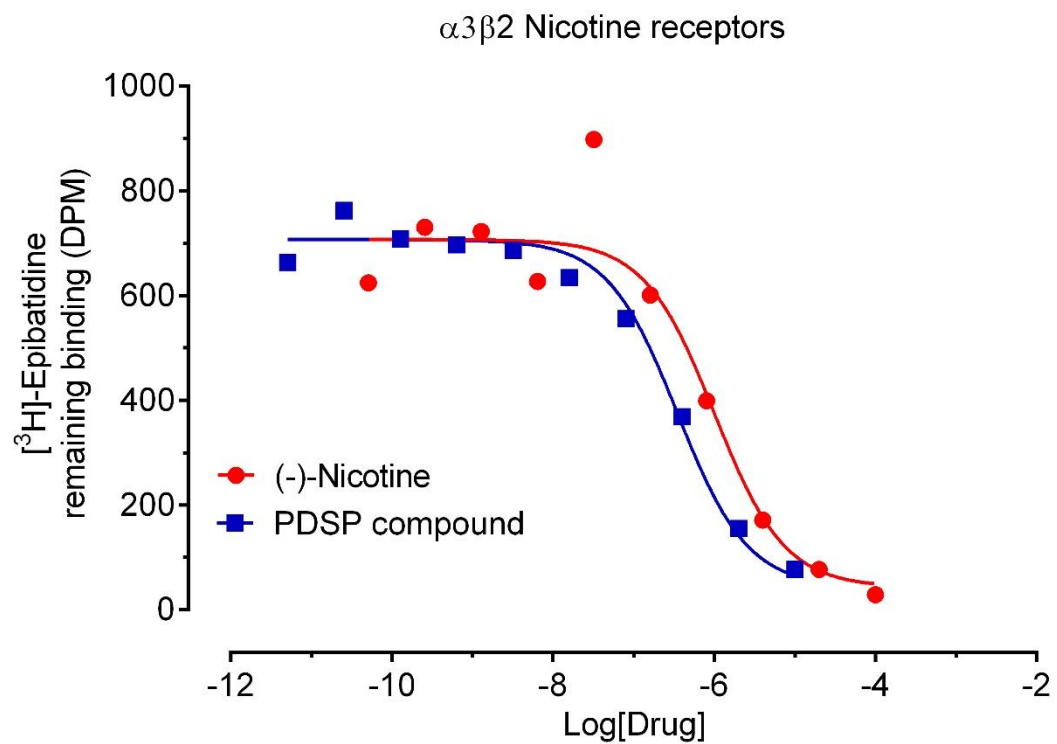
Table 4. Radioligand binding assays for nAChRs. Primary binding assays used 100 pM of [³H]-epibatidine and secondary binding assays used 0.5 -2.3 nM [³H]-epibatidine. Historical reference K_i values from last > 2 years are also included for quality control.

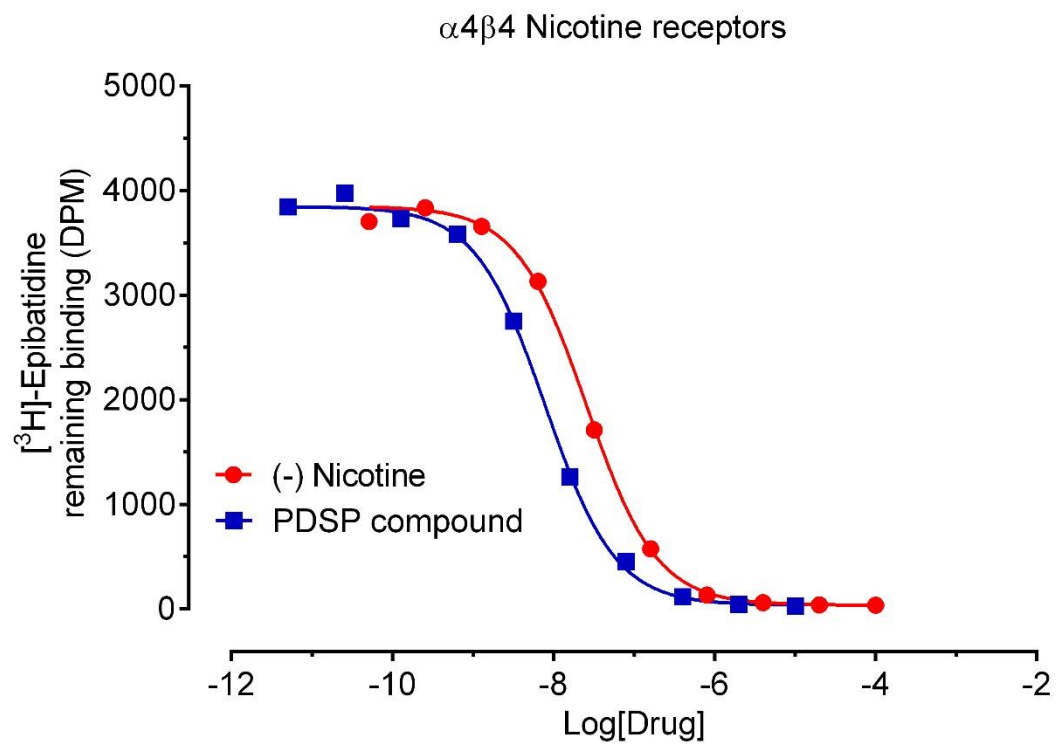
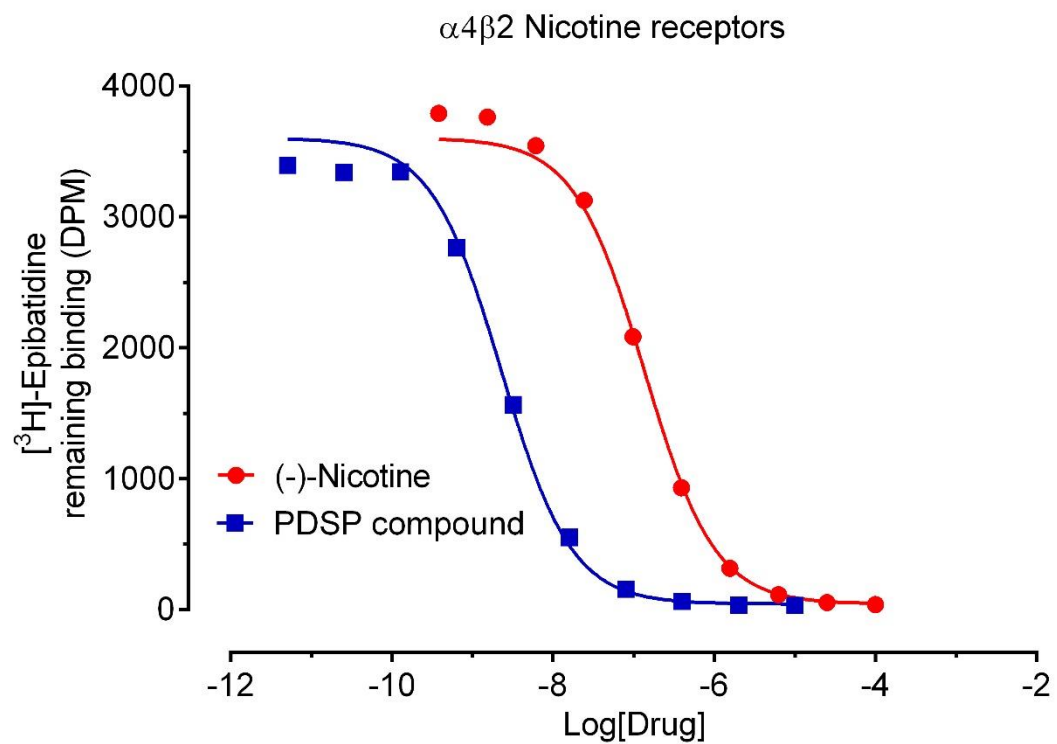
Nicotinic acetylcholine receptors (nAChRs)				
Nicotinic acetylcholine receptor binding buffer: 50 mM Tris HCl, pH 7.4, RT Standard wash buffer: 50 mM Tris HCl, pH 7.4, cold				
Target	Radioligand Avg K _d (nM)	Radioligand used (nM)	Reference pK _i ± SEM (K _i ,nM)	Literature
α2β2	[³ H]-Epibatidine 0.010	0.46 – 0.53	Nicotine 8.25 ± 0.06 (5.60)	(5, 6)
α2β4	[³ H]-Epibatidine 0.040	0.46 – 0.53	Nicotine 7.12 ± 0.03 (76.5)	
α3β2	[³ H]-Epibatidine 0.015	0.46 – 0.53	Nicotine 8.12 ± 0.02 (7.59)	
α3β4	[³ H]-Epibatidine 0.080	0.46 – 0.53	Nicotine 6.51 ± 0.03 (311)	
α4β2	[³ H]-Epibatidine 0.030	0.46 – 0.53	Nicotine 8.18 ± 0.04 (6.65)	
α4β2*	[³ H]-Epibatidine 0.050	0.46 – 0.53	Nicotine 8.04 ± 0.03 (9.03)	
α4β4	[³ H]-Epibatidine 0.080	0.46 – 0.53	Nicotine 7.56 ± 0.02 (27.5)	
α7, rat	[³ H]-Epibatidine 1.36	1.79 – 2.31	Nicotine 6.50 ± 0.05 (316)	
Cortex, rat	[³ H]-Epibatidine 0.04	0.46 – 0.53	Nicotine 8.20 ± 0.03 (6.27)	

* Rat forebrain

Figure 12. Representative competition binding curves with nicotinic acetylcholine receptors







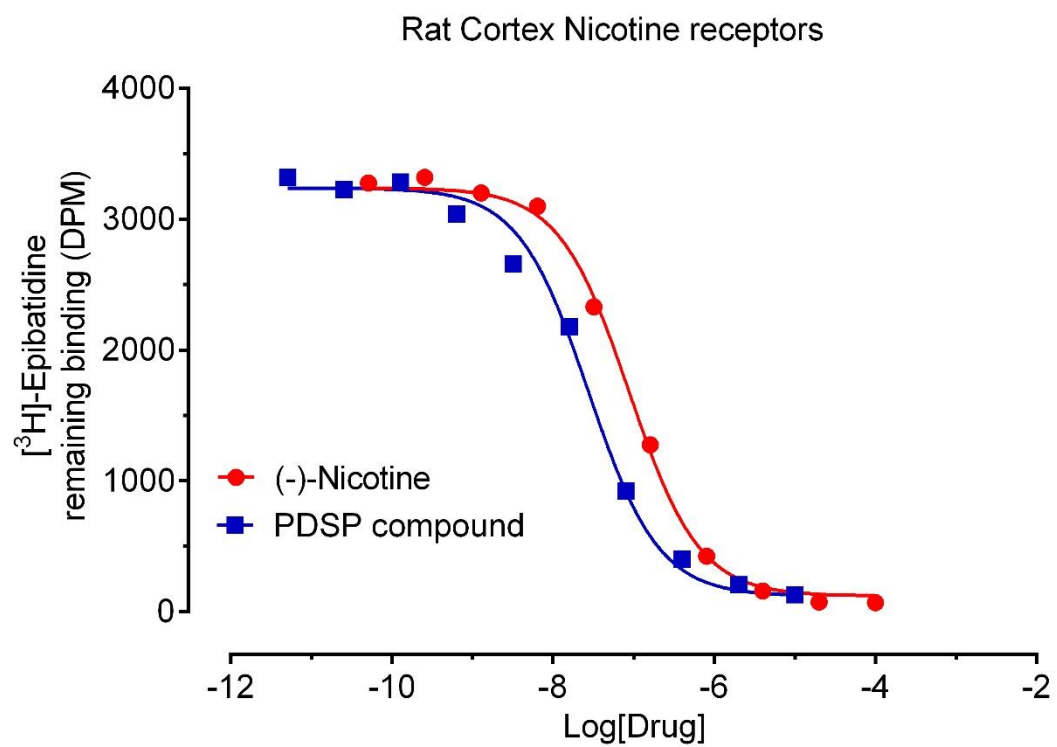
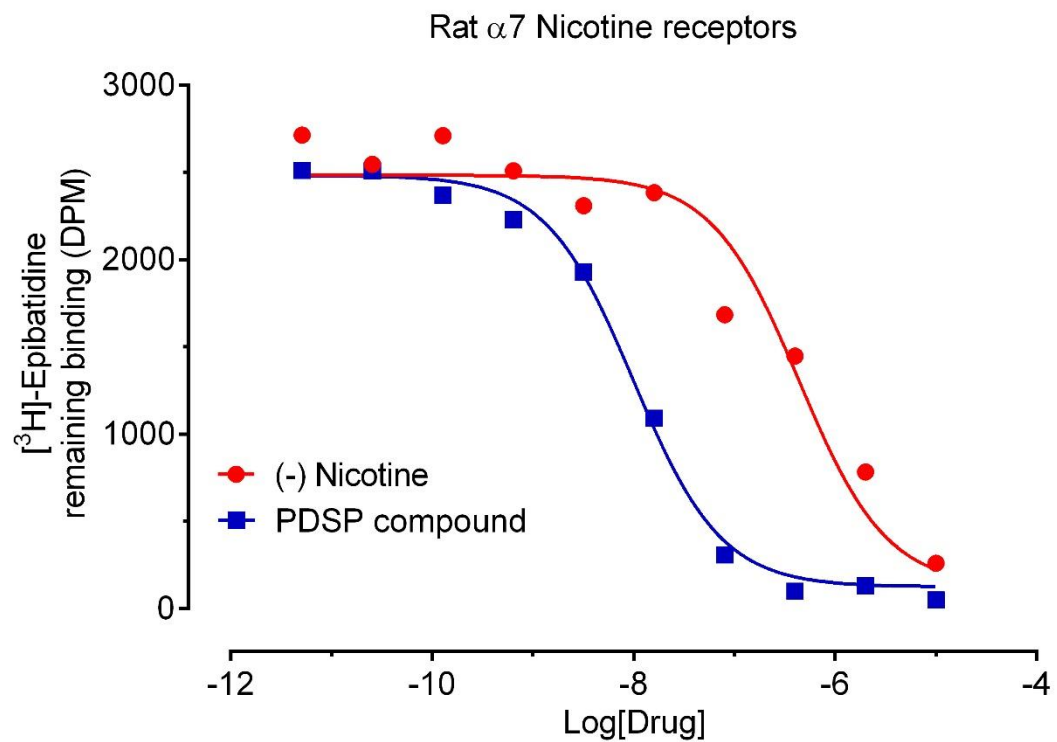


Table 5. Adenosine receptors, radioligand and corresponding concentrations, reference compound, and buffers for primary and secondary radioligand binding assays. Historical reference K_i values from the last > 2 years are also included for quality control.

Adenosine receptors				
Adenosine Binding Buffer: 50 mM Tris HCl, 1U/ml adenosine deaminase, pH 7.4, RT				
Standard Washing Buffer: 50 mM Tris HCl, pH 7.4, cold				
Target	Radioligand pK _d ± SEM (K _d , nM)	Radioligand used (nM)	Reference Ligand pK _d ± SEM (K _d , nM)	Literature
A ₁	[³ H] DPCPX 8.31 ± 0.16 (4.95)	5.0	CGS15943 7.88 ± 0.26 (13.3)	(40, 41)
A _{2A}	[³ H] ZM241385 8.34 ± 0.20 (4.60)	2.0 - 5.0	ZM-241385 8.11 ± 0.19 (7.85)	(42, 43)
			NECA 6.24 ± 0.07 (575)	
A _{2B}	Being developed			
A ₃	Being developed			

Figure 13. Representative competitive binding curves for adenosine receptors

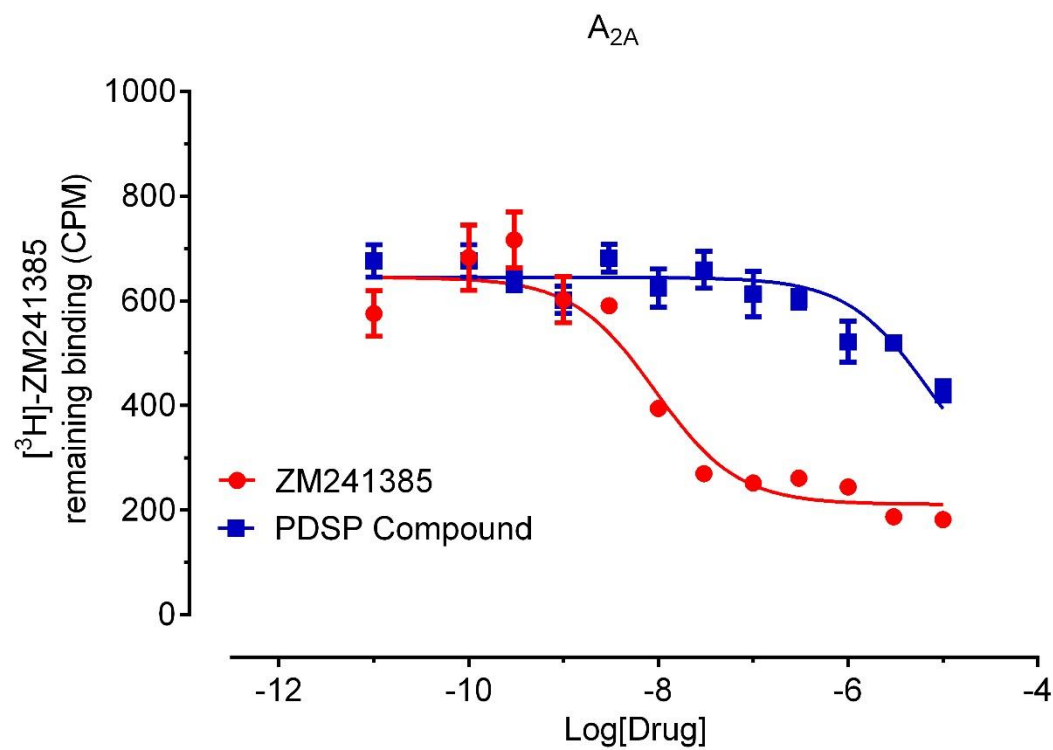
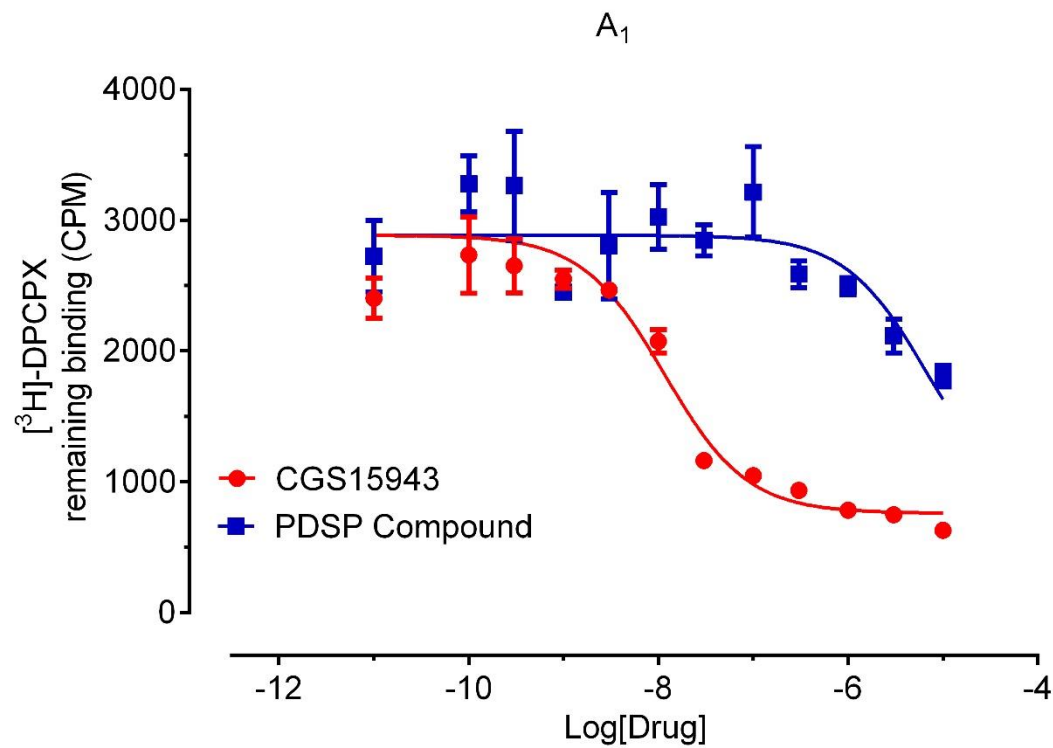
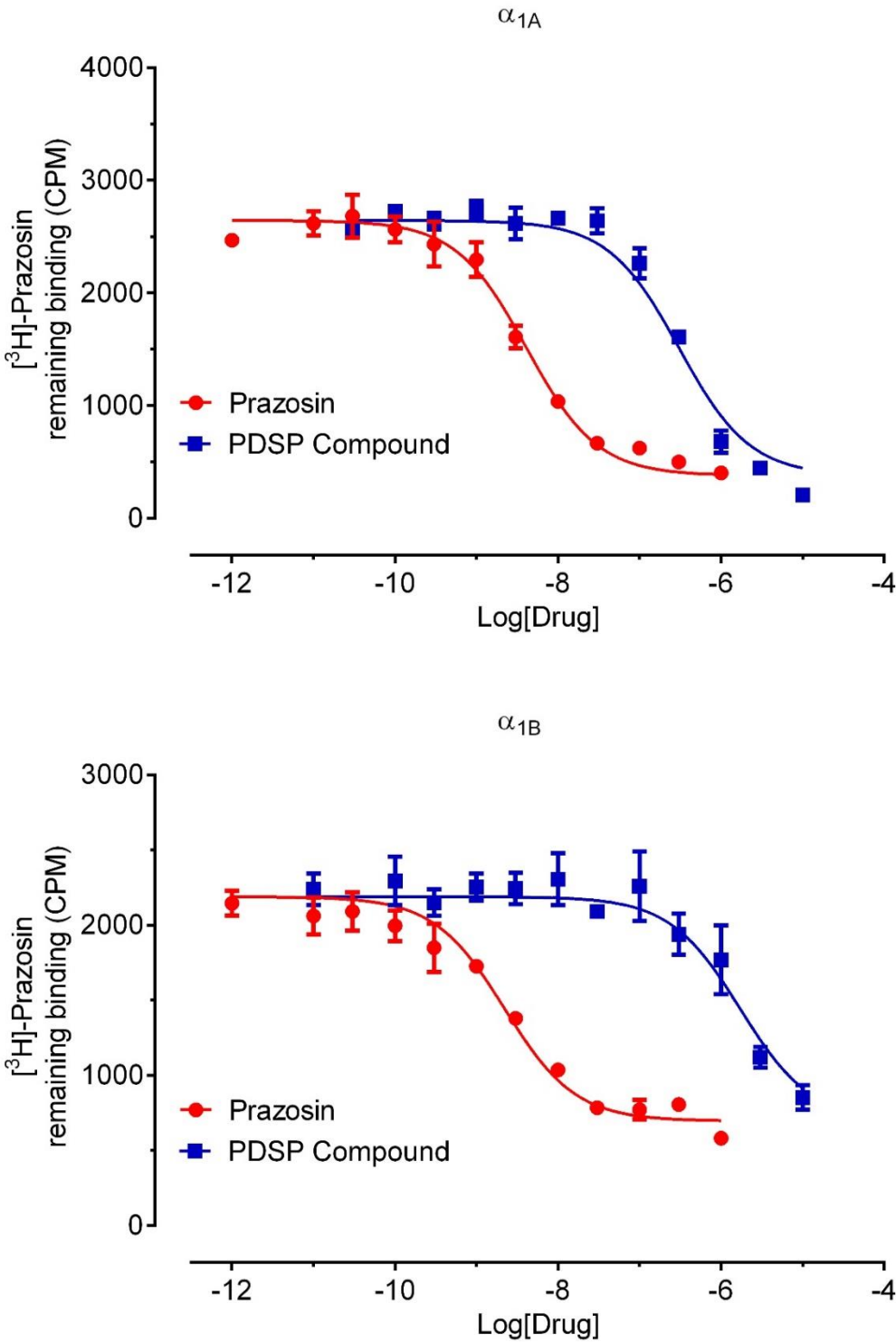
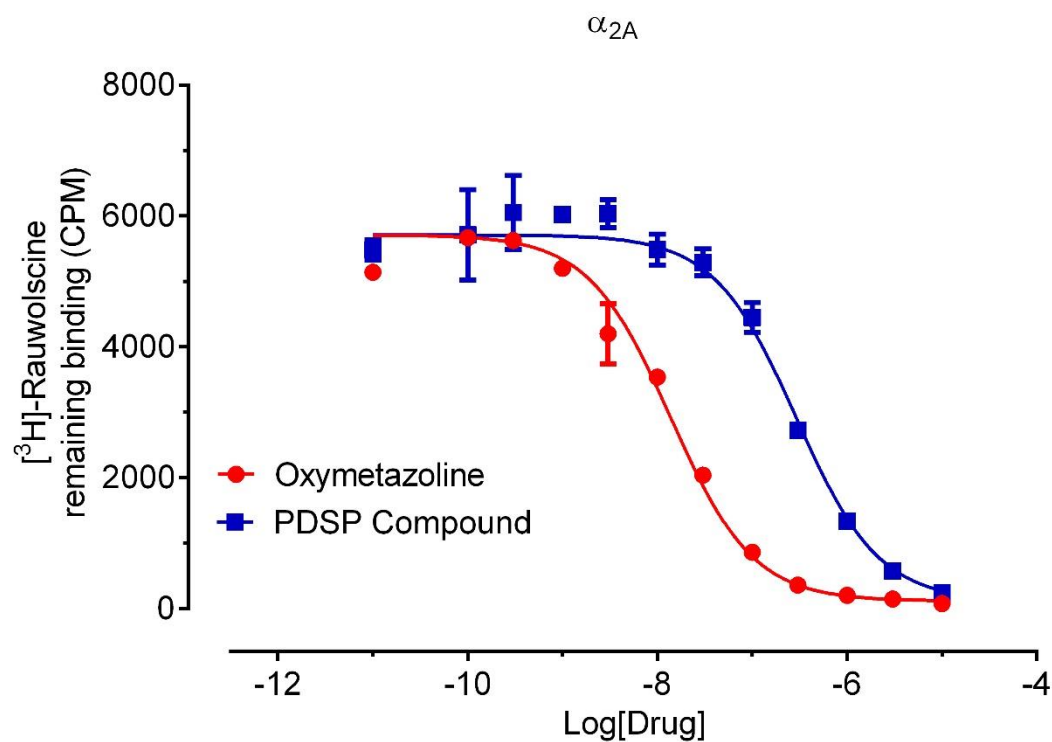
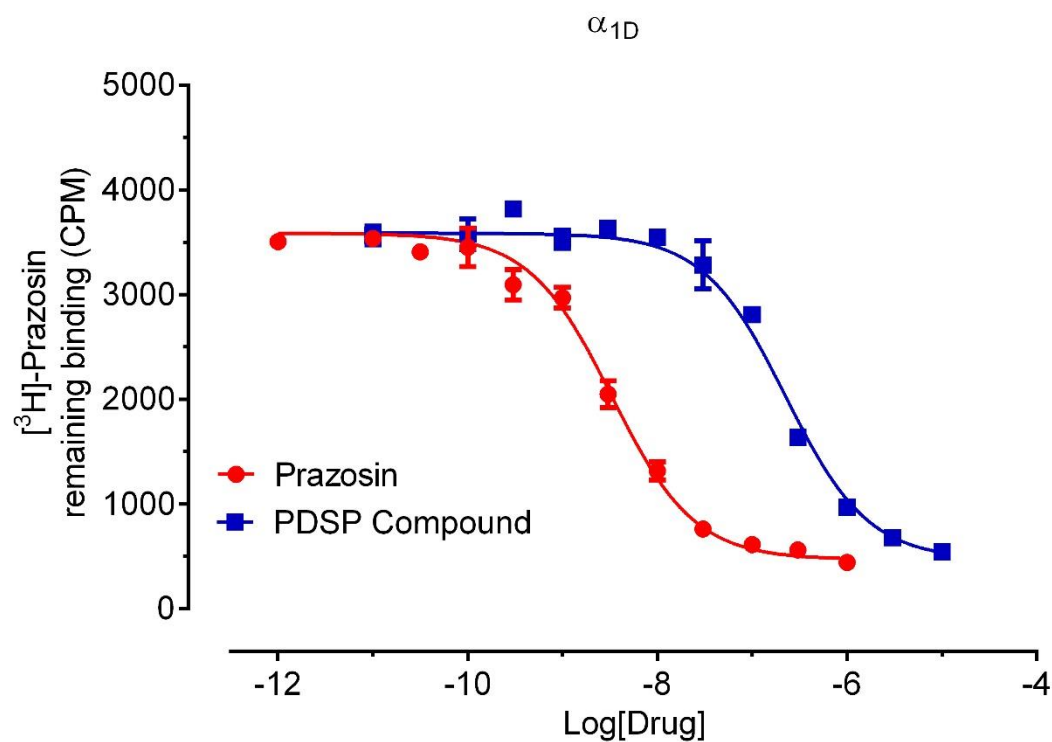


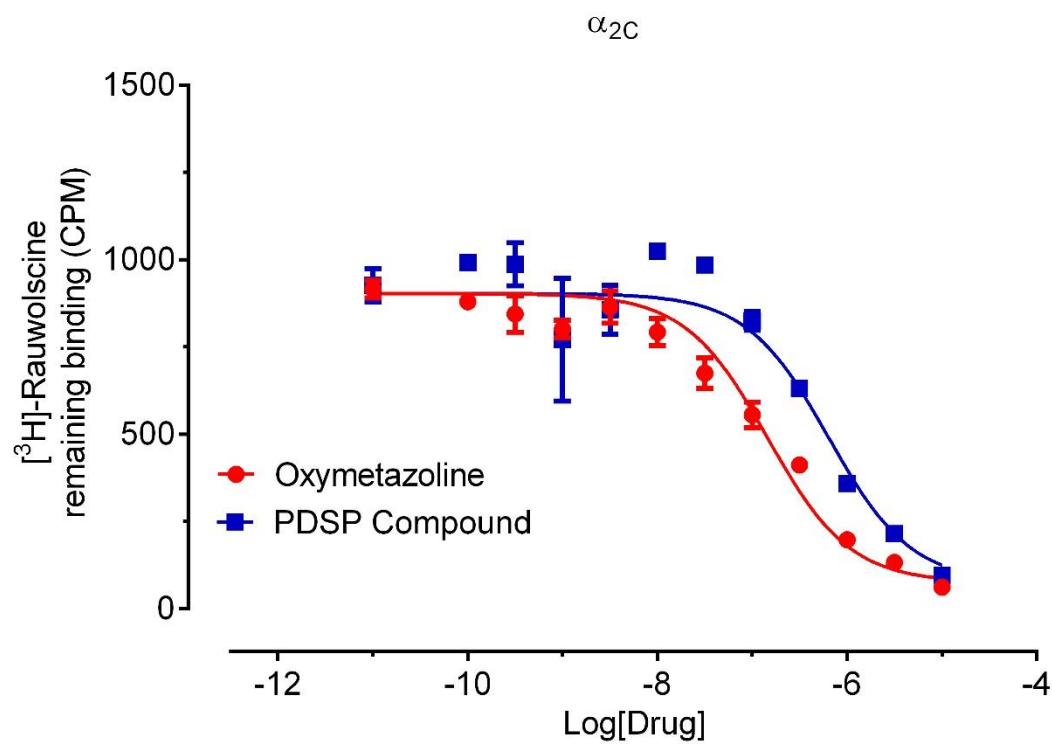
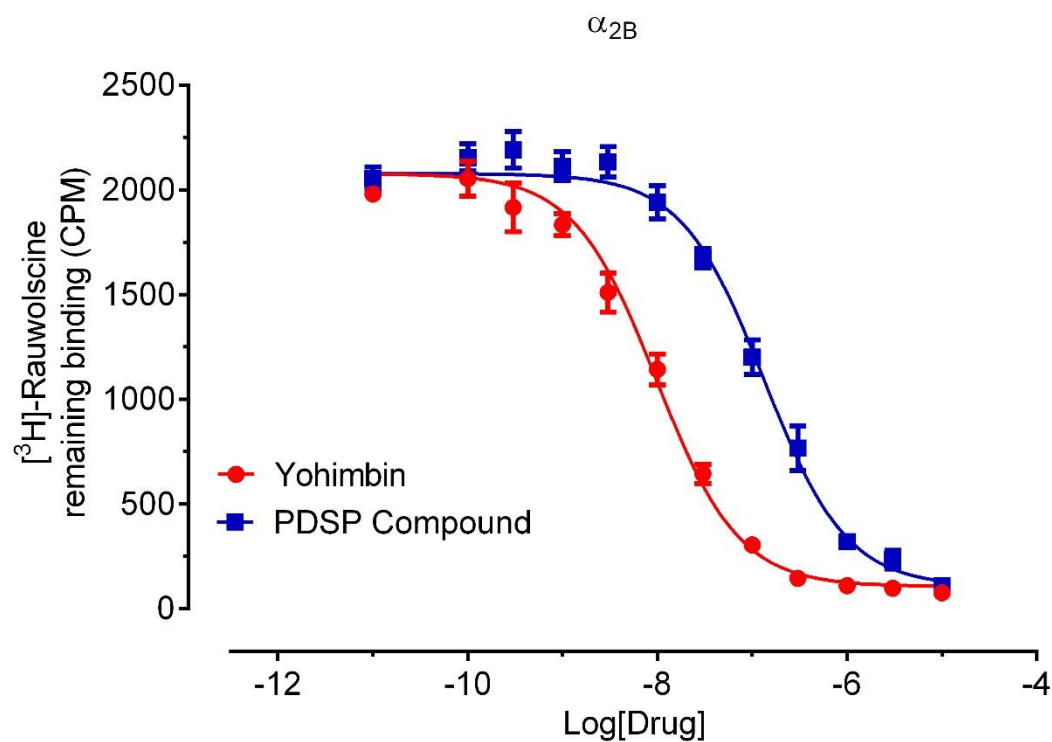
Table 6. Adrenergic receptors, radioligands and corresponding K_d values, reference compounds, and buffers for primary and secondary radioligand binding assays. Historical reference K_i values from the last >2 years are also listed.

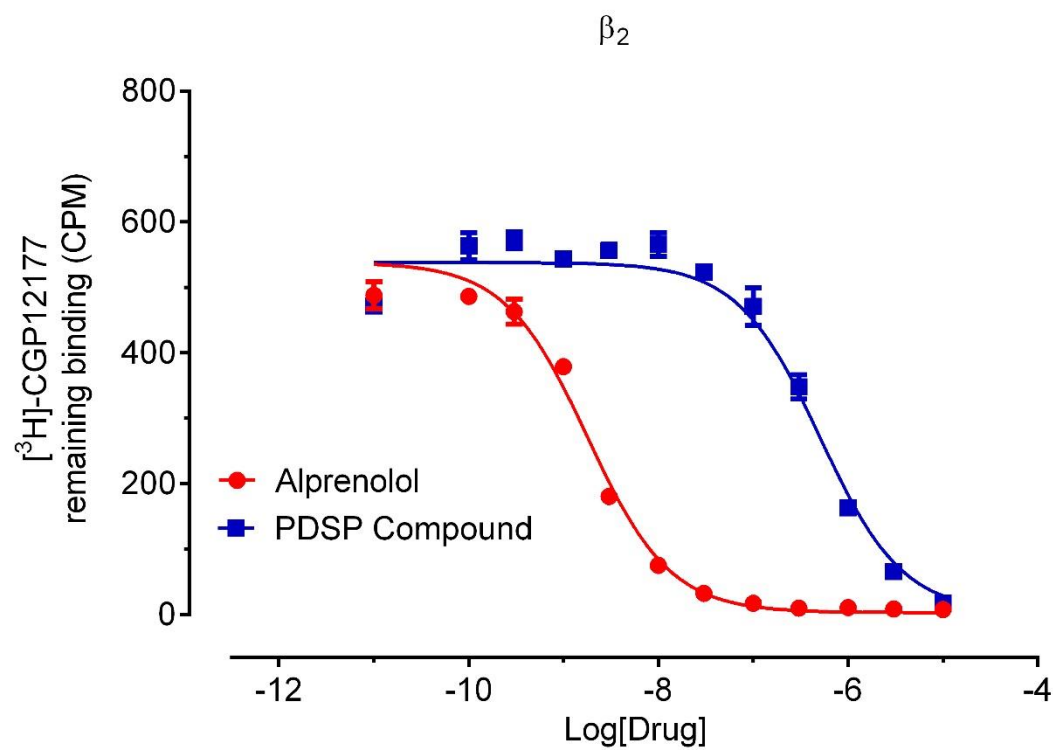
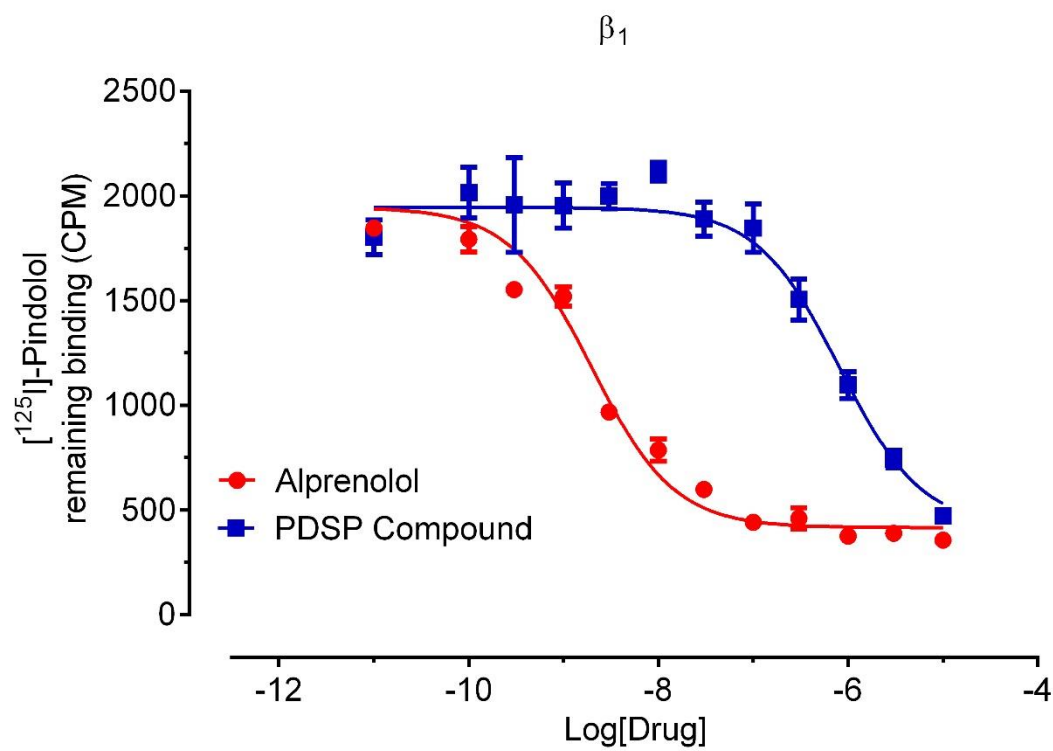
Adrenergic receptors				
α_1 Binding Buffer: 20 mM Tris HCl, 145 mM NaCl, pH 7.4, RT α_2 Binding Buffer: 50 mM Tris HCl, 5 mM $MgCl_2$, pH 7.7, RT β Binding Buffer: 50 mM Tris HCl, 3 mM $MgCl_2$, pH 7.7, RT Standard Wash Buffer: 50 mM Tris HCl, pH 7.4, cold				
Target	Radioligand $pK_d \pm SEM (K_d, nM)$	Radioligand used (nM)	Reference ligand $pK_i \pm SEM (K_i, nM)$	Literature
α_{1A}	[3H]-Prazosin $9.36 \pm 0.07 (0.43)$	0.2 - 1.0	Prazosin $9.16 \pm 0.03 (0.70)$	(44, 45)
α_{1B}	[3H]-Prazosin $9.23 \pm 0.29 (0.58)$	0.3 – 1.0	Prazosin $9.05 \pm 0.03 (0.88)$	
α_{1D}	[3H]-Prazosin $9.21 \pm 0.07 (0.62)$	0.3 – 1.0	Prazosin $9.20 \pm 0.03 (0.63)$	
α_{2A}	[3H]-Rauwolscine $8.46 \pm 0.16 (3.47)$	1.0 – 3.0	Oxymetazoline $8.35 \pm 0.02 (4.51)$	(46–48)
α_{2B}	[3H]-Rauwolscine $8.74 \pm 0.13 (1.81)$	1.5 – 2.0	Yohimbine $8.24 \pm 0.02 (5.81)$	
α_{2C}	[3H]-Rauwolscine $9.02 \pm 0.10 (0.96)$	0.5 – 1.0	Oxymetazoline $7.38 \pm 0.02 (41.6)$	
β_1	[^{125}I]-Pindolol $10.06 \pm 0.09 (0.10)$	0.1 – 0.2	Alprenolol $8.73 \pm 0.03 (1.85)$	(49–52)
β_2	[3H]-CGP12177 $9.15 \pm 0.16 (0.71)$	0.5 - 1.0	Alprenolol $8.79 \pm 0.03 (1.61)$	
β_3	[3H]-CGP12177 $7.50 \pm 0.16 (31.8)$	20		
β_3	[^{125}I]-Pindolol $9.45 \pm 0.15 (0.36)$	0.2 – 0.5	Alprenolol $7.64 \pm 0.03 (23.0)$	

Figure 14. Representative competition binding curves with adrenergic receptors









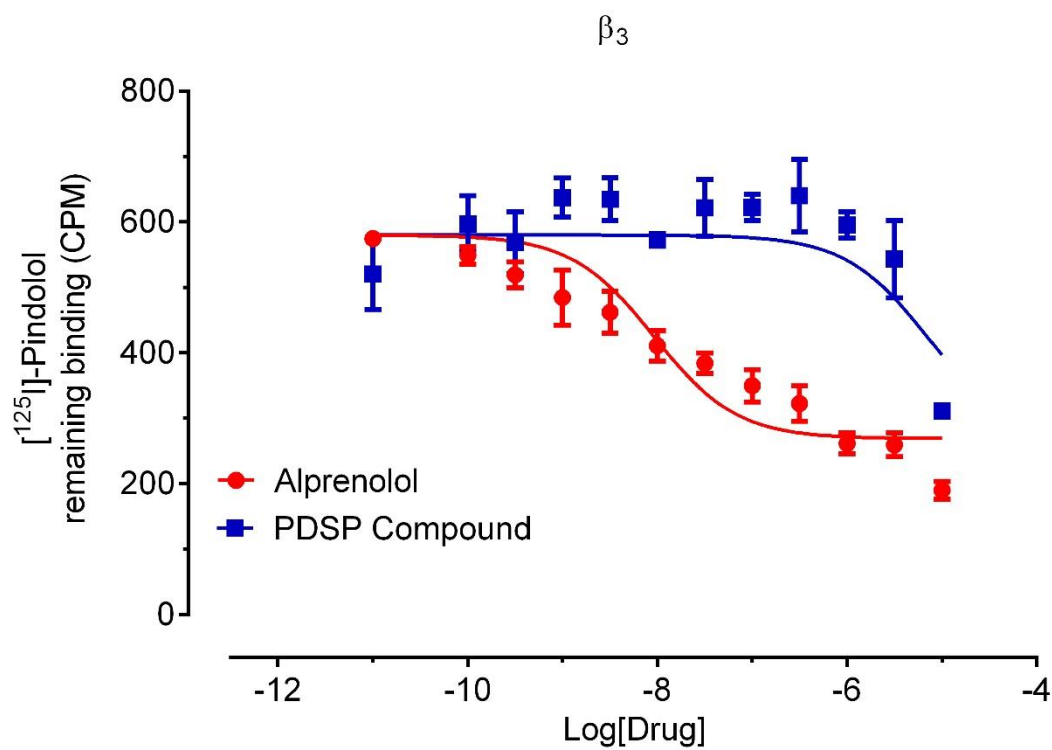
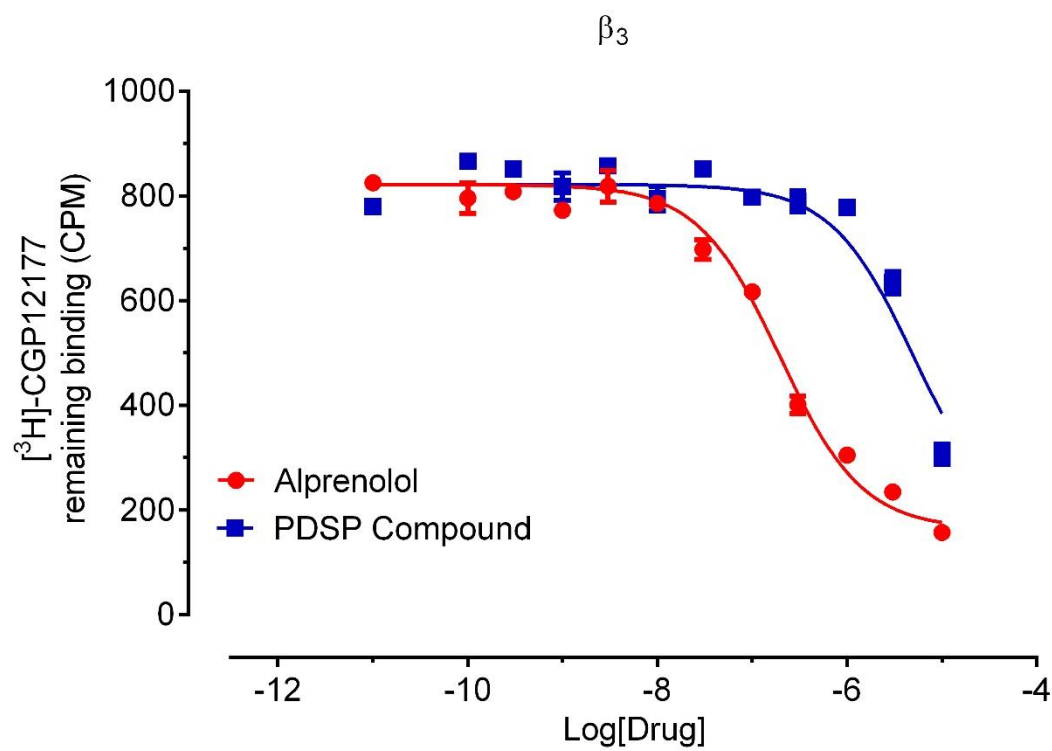


Table 7. Cannabinoid receptors, radioligand and corresponding concentrations, reference compounds, and buffers for primary and secondary radioligand binding assays. Historical reference K_i values from the last >2 years are also included.

Cannabinoid receptors				
Cannabinoid Binding Buffer: 50 mM Tris HCl, 5 mM MgCl ₂ , 1 mM EDTA, 1 mg/ml BSA, pH 7.4, RT Cannabinoid Wash Buffer: cannabinoid binding buffer + 1 mg/ml BSA, pH 7.4, cold				
Target	Radioligand $pK_d \pm SEM (K_d, nM)$	Radioligand used (nM)	Reference Ligand $pK_i \pm SEM (K_i, nM)$	Literature
CB ₁ (rat brain)	[³ H]-CP55940 $8.73 \pm 0.22 (1.85)$	0.5 – 2.0	CP-55940 $8.23 \pm 0.05 (5.87)$	(53–55)
CB ₂	[³ H]-CP55940 $8.47 \pm 0.11 (3.37)$	1.0 – 3.0	CP-55940 $8.06 \pm 0.05 (8.77)$	

Figure 15. Representative competitive binding curves for cannabinoid receptors.

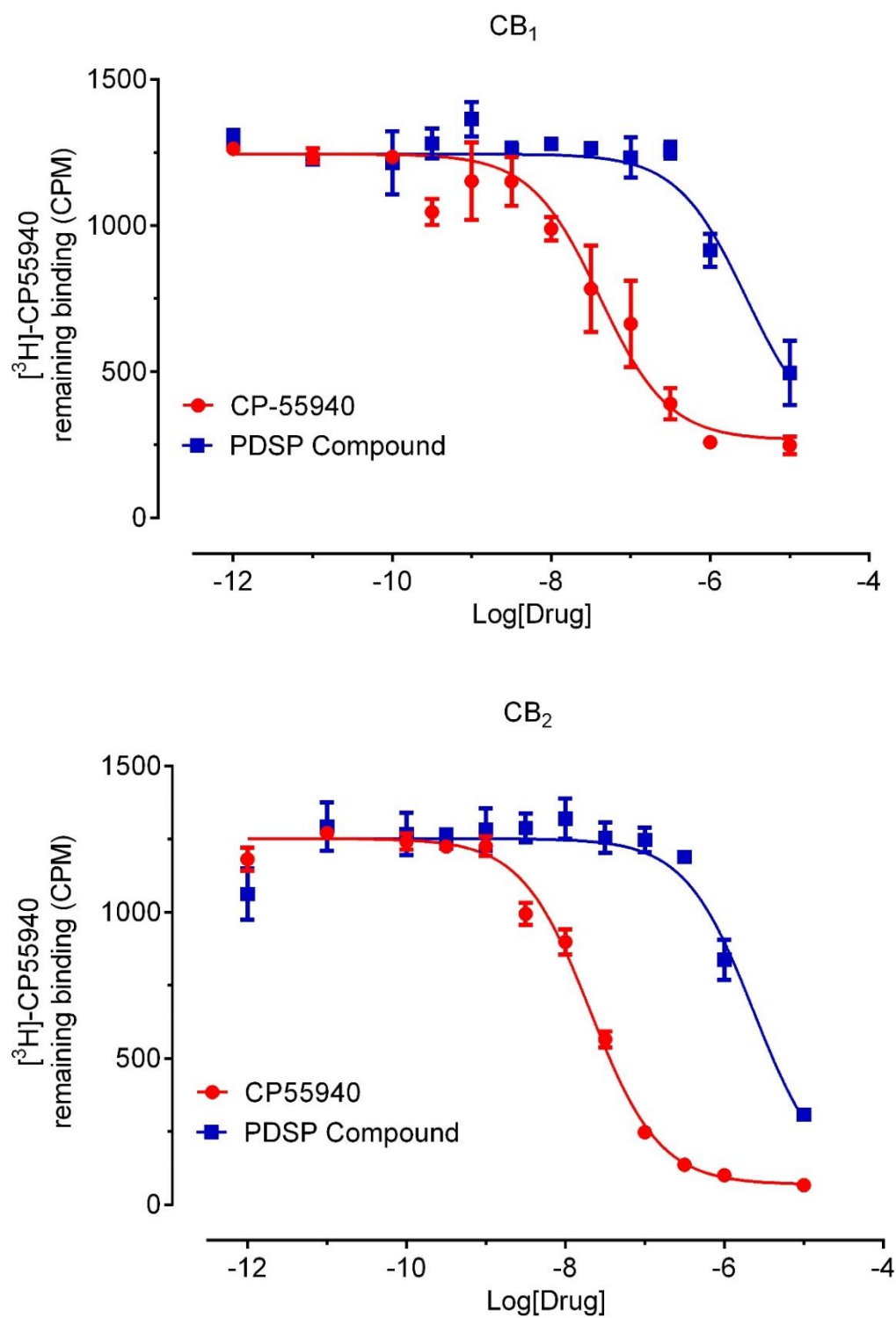
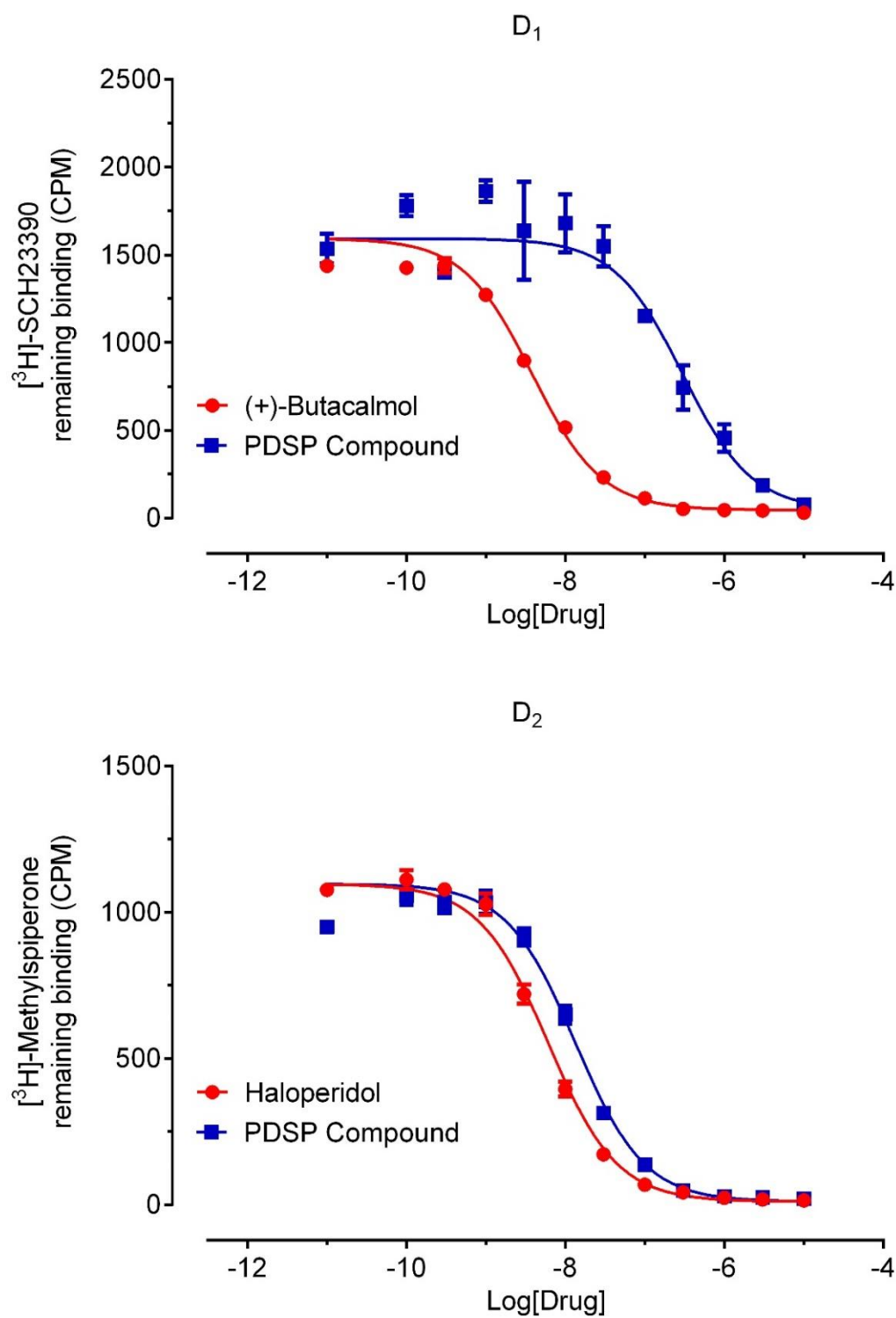
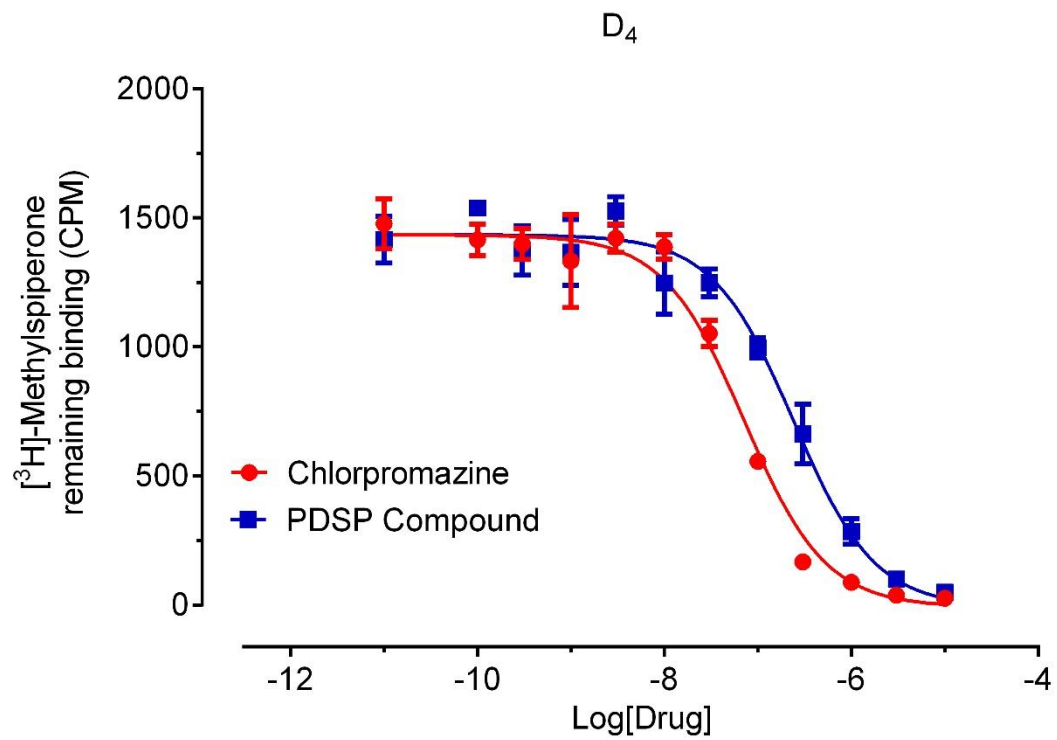
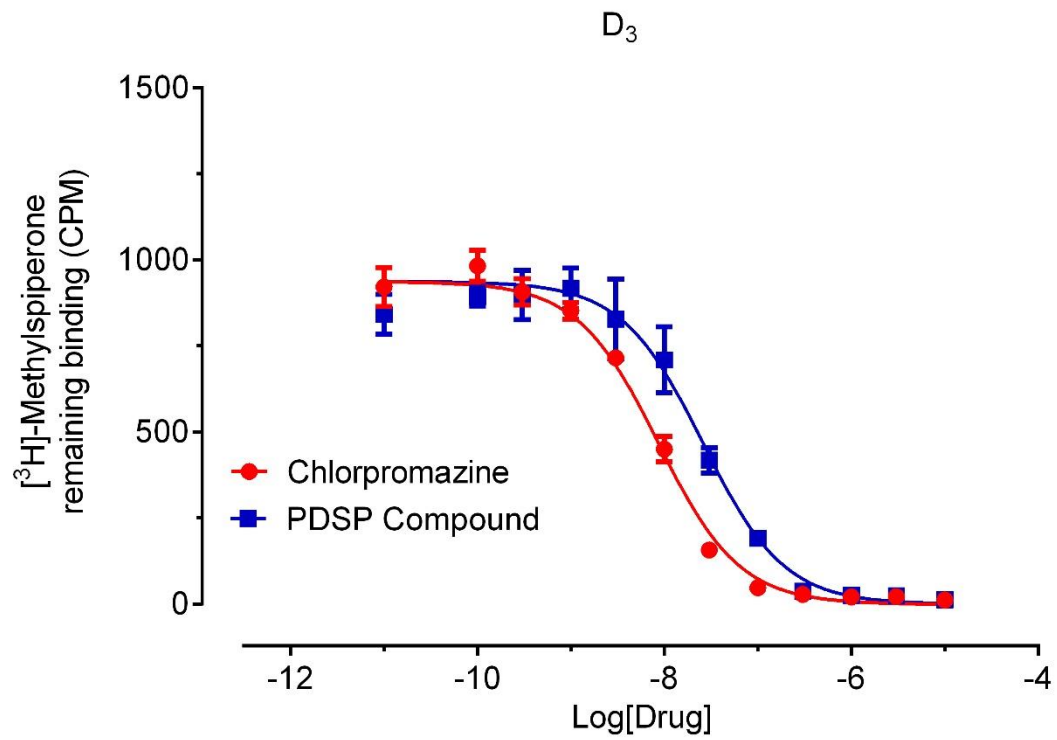


Table 8. Dopamine receptors, radioligands and corresponding K_d values, reference compounds, and buffers for primary and secondary radioligand binding assays. Historical reference K_i values from >2 years are also included.

Dopamine receptors				
Dopamine Binding Buffer: 50 mM HEPES, 50 mM NaCl, 5 mM MgCl ₂ , 0.5 mM EDTA, pH 7.4, RT Standard Wash Buffer: 50 mM Tris HCl, pH 7.4, cold				
Target	Radioligand $pK_d \pm SEM (K_d, nM)$	Radioligand used (nM)	Reference Ligand $pK_i \pm SEM (K_i, nM)$	Literature
D ₁	[³ H]-SCH23390 9.13 \pm 0.05 (0.74)	0.6 – 1.3	(+)-Butaclamol 8.51 \pm 0.02 (3.07)	(56)
D ₂	[³ H]-N-methylspiperone 9.33 \pm 0.06 (0.47)	0.4 – 1.0	Haloperidol 8.15 \pm 0.02 (7.15)	(57, 58)
D ₃	[³ H]-N-methylspiperone 9.44 \pm 0.09 (0.36)	0.5 – 1.8	Chlorpromazine 7.99 \pm 0.02 (10.30)	
D ₄	[³ H]-N-methylspiperone 9.07 \pm 0.06 (0.86)	0.6 – 1.7	Chlorpromazine 7.49 \pm 0.02 (32.62)	
D ₅	[³ H]-SCH23390 8.69 \pm 0.05 (2.03)	2.0 – 3.0	SKF38393 8.59 \pm 0.02 (2.59)	(59)

Figure 16. Representative competitive binding curves with Dopamine receptors.





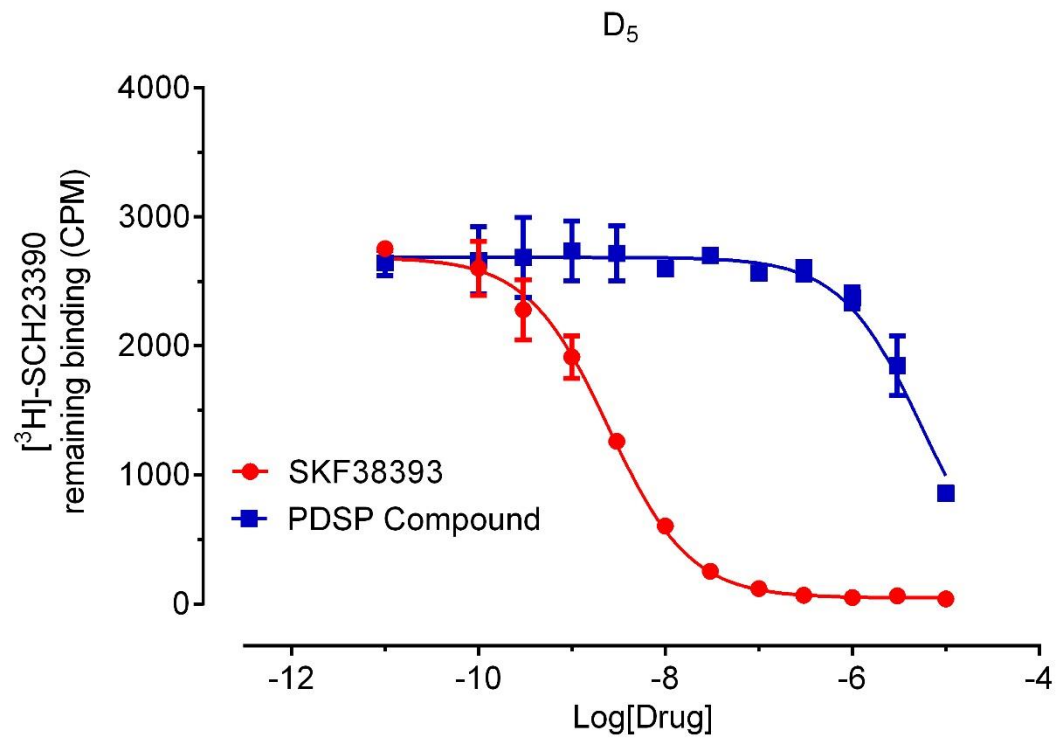
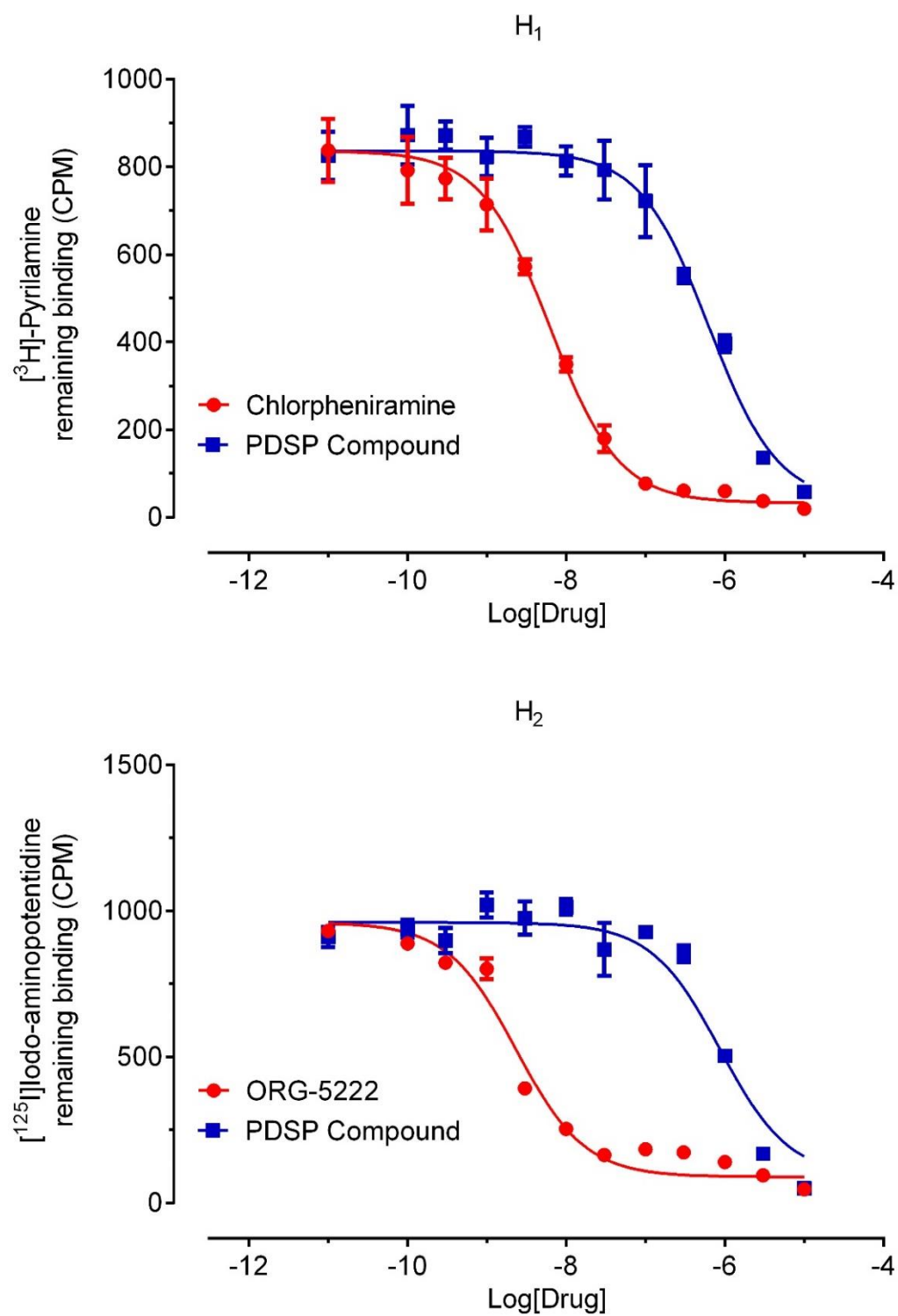


Table 9. Histamine receptors, radioligands and corresponding concentrations, reference compounds, and buffers for primary and secondary radioligand binding assays. Historical reference K_i values from >2 years are also included.

Histamine receptors				
Histamine Binding Buffer: 50 mM Tris HCl, 0.5 mM EDTA, pH 7.4, RT Standard Wash Buffer: 50 mM Tris HCl, pH 7.4, cold Filter: GF/B				
Target	Radioligand $pK_d \pm SEM (K_d, nM)$	Radioligand used (nM)	Reference Ligand $pK_i \pm SEM (K_i, nM)$	Literature
H ₁	[³ H]-Pyrilamine 9.01 ± 0.05 (0.97)	0.6 – 2.0	Chlorpheniramine 8.78 ± 0.02 (1.64)	(60, 61)
H ₂	[¹²⁵ I]-Iodo- aminopotentidine 10.47 ± 0.12 (0.03)	0.02 – 0.05	ORG-5222 9.05 ± 0.04 (0.90)	(62)
H ₃	[³ H]- α -methylhistamine 9.11 ± 0.07 (0.78)	0.5 – 1.0	Histamine 8.30 ± 0.03 (4.99)	(63)
H ₄	[³ H]-Histamine 8.26 ± 0.08 (5.46)	1.0 – 5.0	Clozapine 6.60 ± 0.06 (250)	(64, 65)

Figure 17. Representative competitive binding curves with Histamine receptors.



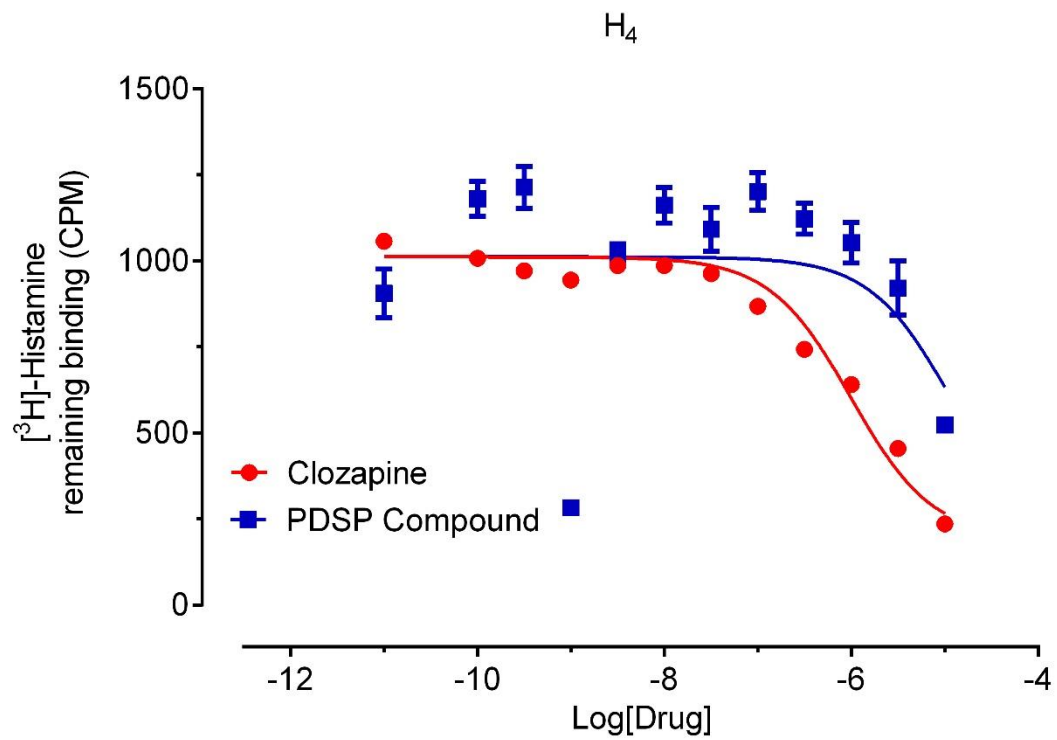
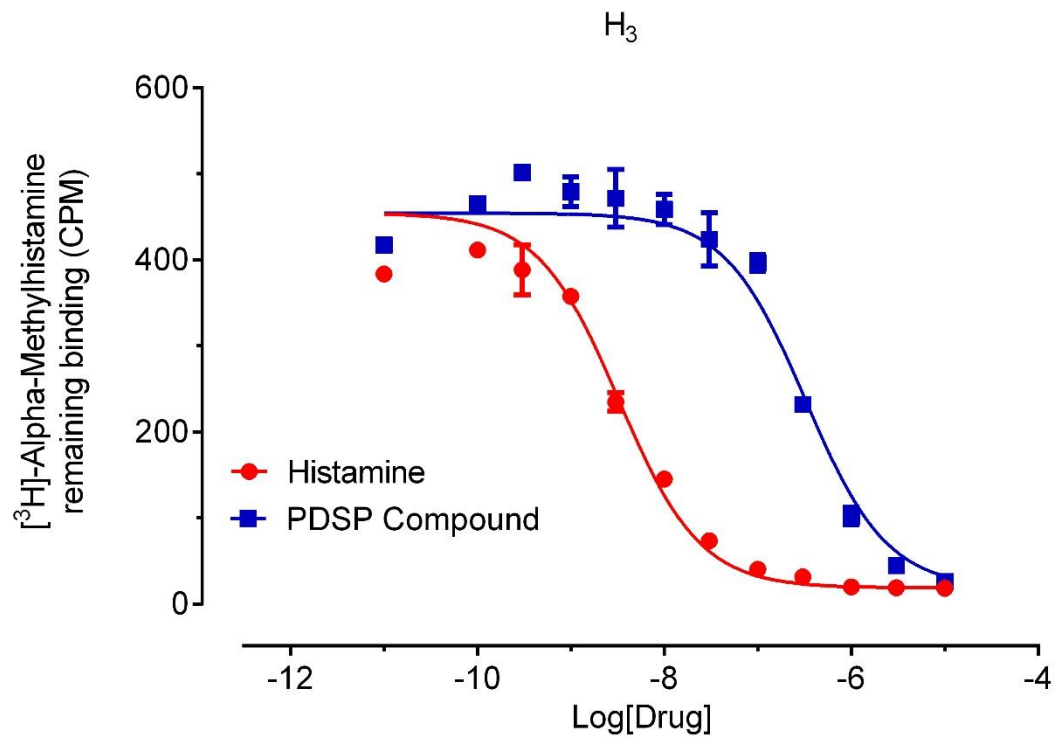
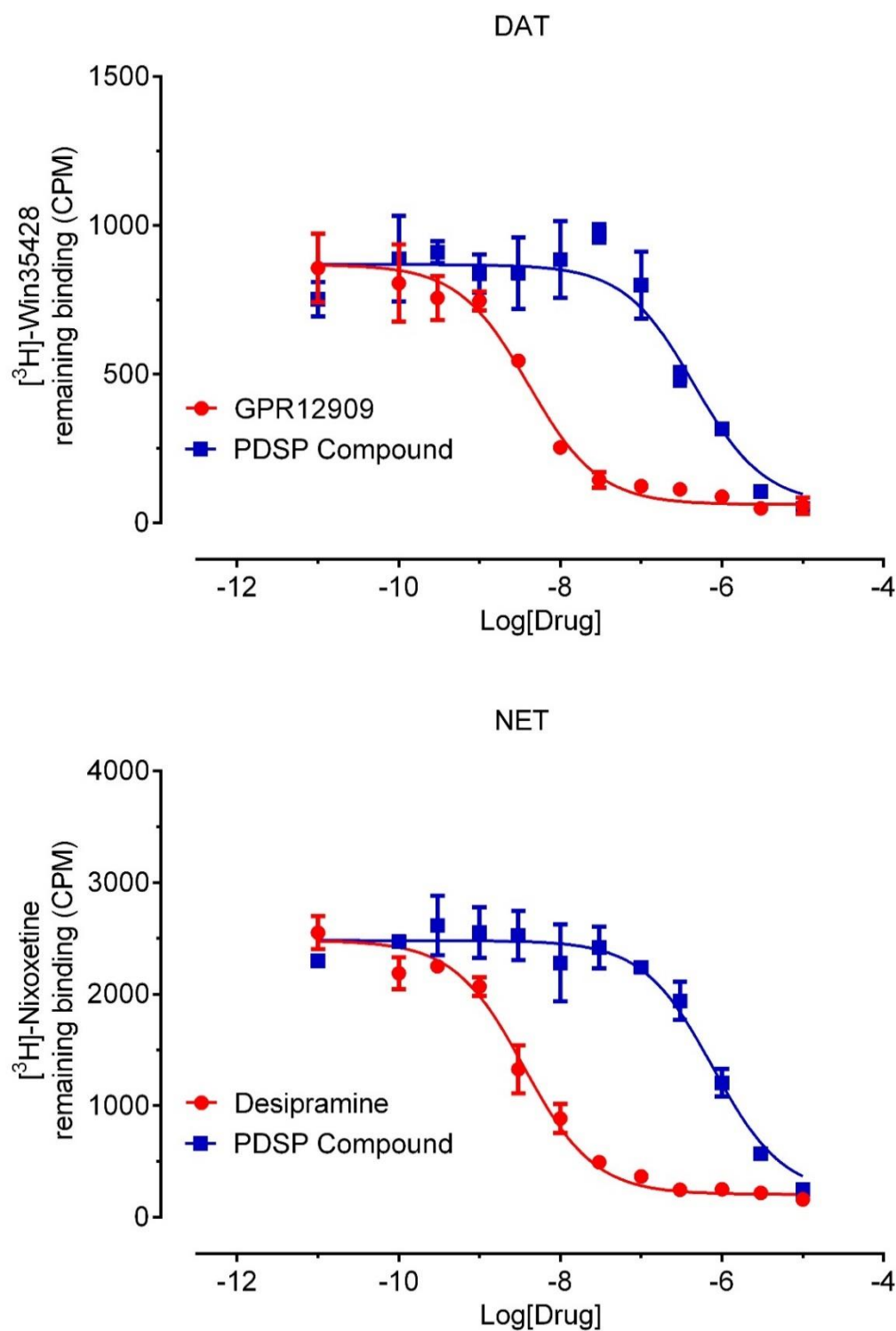


Table 10. Neurotransmitter transporters, radioligands and corresponding concentrations, reference compounds, and buffers for primary and secondary radioligand binding assays. Historical reference K_i values from >2 years are also included.

Neurotransmitter transporters				
Transporter Binding Buffer: 10 mM HEPES, 135 mM NaCl, 5 mM KCl, 0.8 mM MgCl ₂ , 1 mM ETGA, pH 7.4, RT				
Transporter Wash Buffer: Transporter binding buffer, pH 7.4, cold				
Target	Radioligand $pK_d \pm SEM$ (K_d , nM)	Radioligand used (nM)	Reference Ligand $pK_i \pm SEM$ (K_i , nM)	Literature
DAT	[³ H]-Win35428 8.02 ± 0.04 (9.47)	3.6 – 16.0	GBR12909 8.33 ± 0.02 (4.73)	(66, 67)
NET	[³ H]-Nisoxetine 8.42 ± 0.06 (3.83)	1.3 – 5.0	Desipramine 8.65 ± 0.01 (2.24)	(68, 69)
SERT	[³ H]-Citalopram 8.58 ± 0.11 (2.63)	1.5 – 2.0	Amitriptyline 8.26 ± 0.02 (5.53)	(70, 71)

Figure 18. Representative competitive binding curves with neurotransmitter transporters.



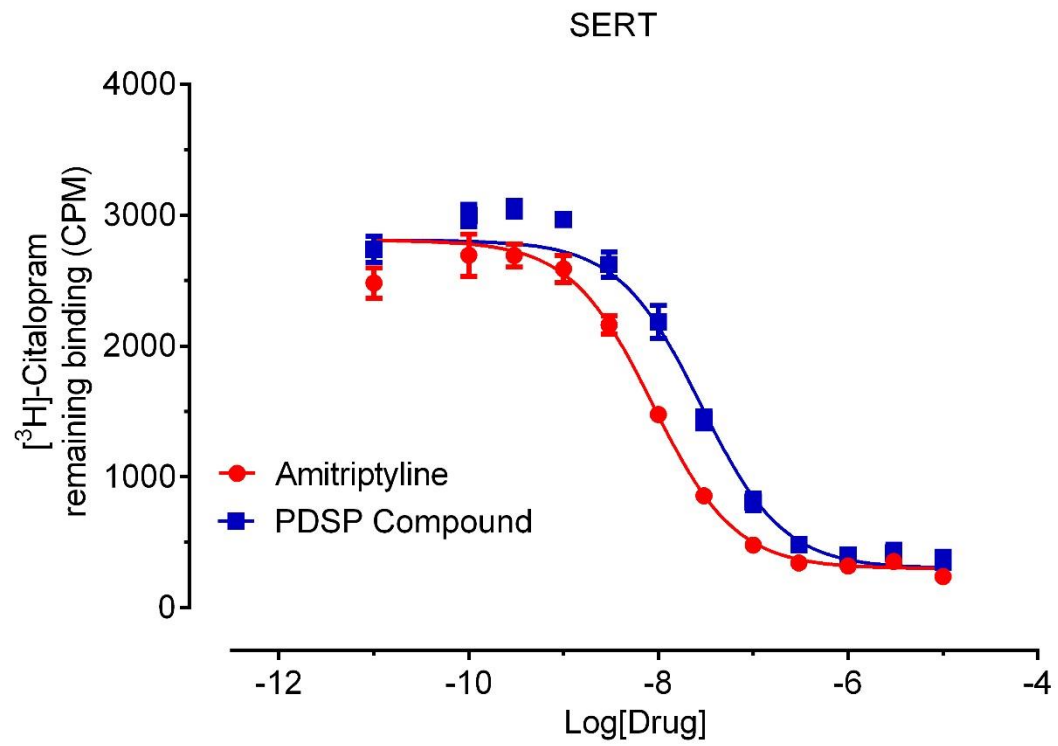
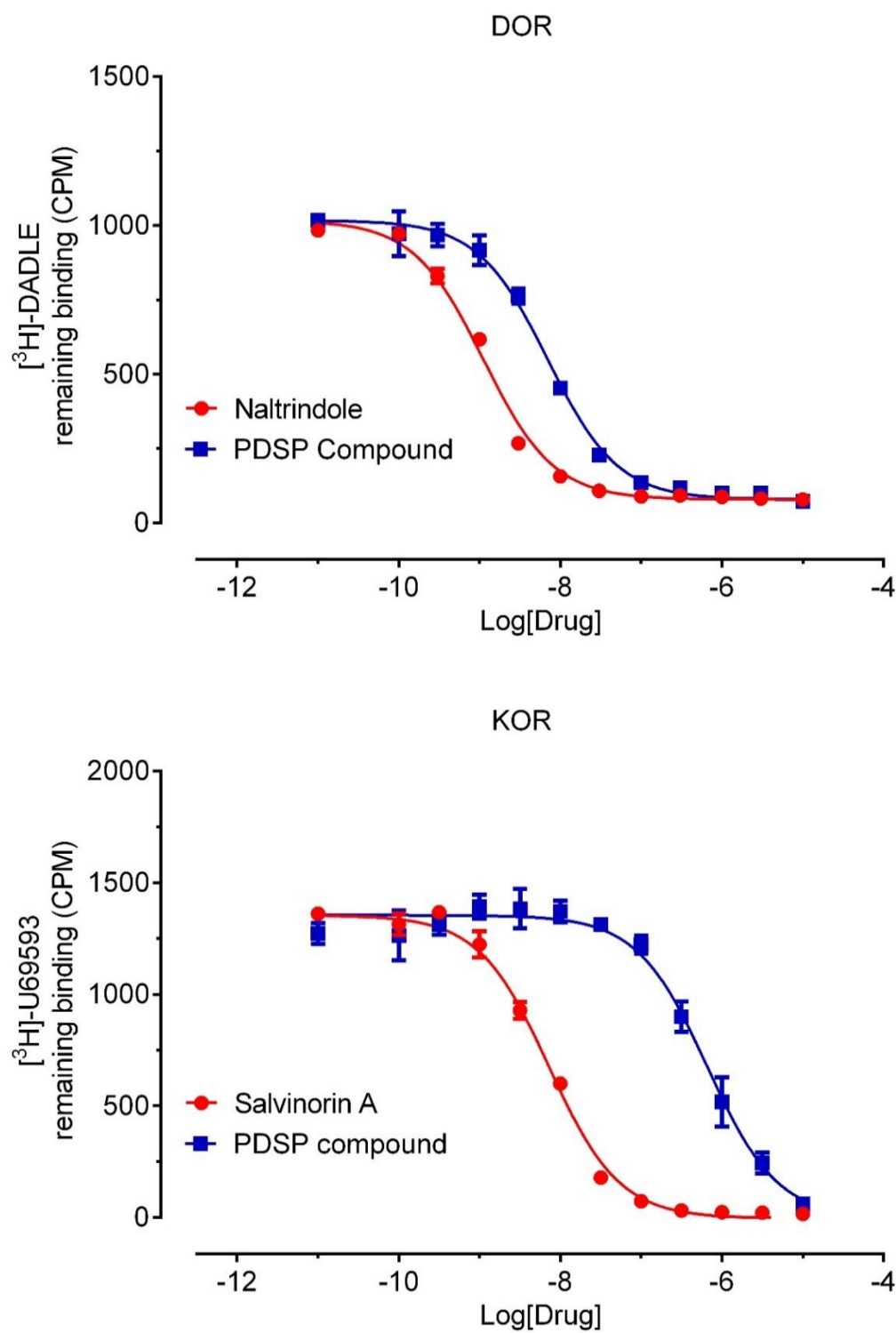


Table 11. Opioid receptors, radioligands and corresponding concentrations, reference compounds, and buffers for primary and secondary radioligand binding assays. Historical reference K_i values from >2 years are also included.

Opioid receptors				
Standard Binding Buffer: 50 mM Tris HCl, 10 mM MgCl ₂ , 0.1 mM EDTA, pH 7.4, RT Standard Wash Buffer: 50 mM Tris HCl, pH. 7.4, 4 °C to 8 °C				
Target	Radioligand $pK_d \pm SEM (K_d, nM)$	Radioligand used (nM)	Reference Ligand $pK_i \pm SEM (K_i, nM)$	Literature
DOR	[³ H]-DADLE 8.57 ± 0.05 (2.69)	1.0 – 2.0	Naltrindole 9.30 ± 0.02 (0.50)	(72, 73)
KOR	[³ H]-U69593 9.08 ± 0.04 (0.83)	0.6 – 1.2	Salvinorin A 8.53 ± 0.02 (2.98)	(74, 75)
MOR	[³ H]-DAMGO 8.92 ± 0.05 (1.20)	1.0 – 2.0	DAMGO 8.75 ± 0.02 (1.76)	(76, 77)
NOP	[³ H]-Nociceptin 9.11 ± 0.12 (0.78)	0.5 – 2.0	JDTiC 7.94 ± 0.06 (11.56) SB612111 8.59 ± 0.10 (2.59)	(78, 79)

Figure 19. Representative competitive binding curves with opioid receptors.



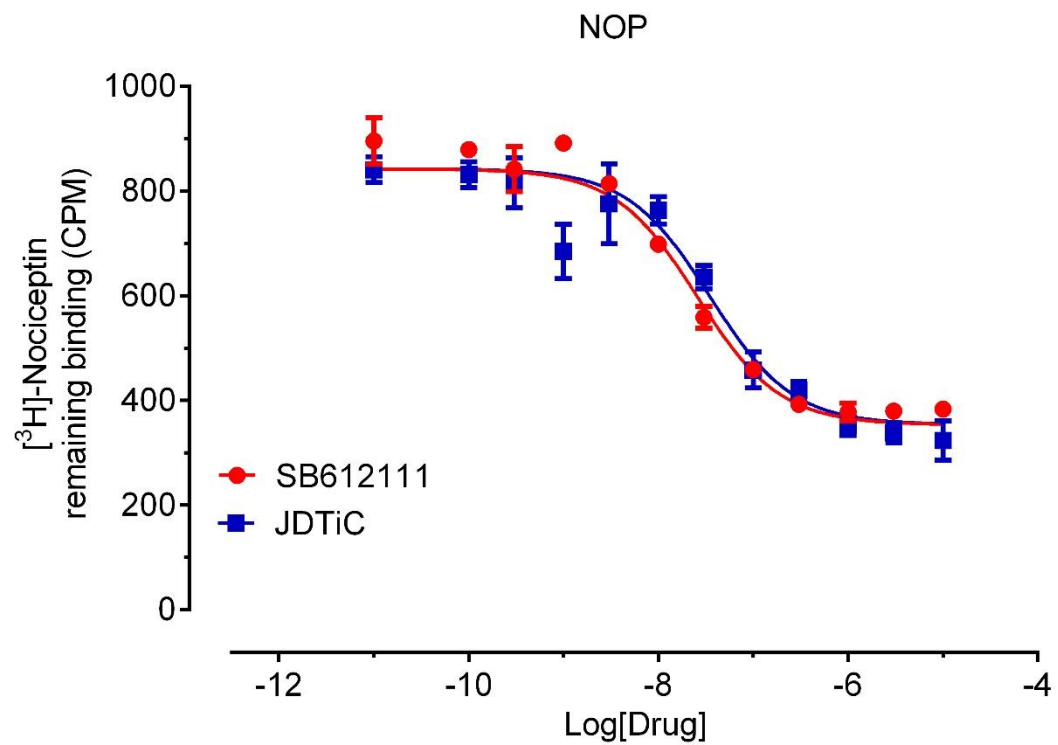
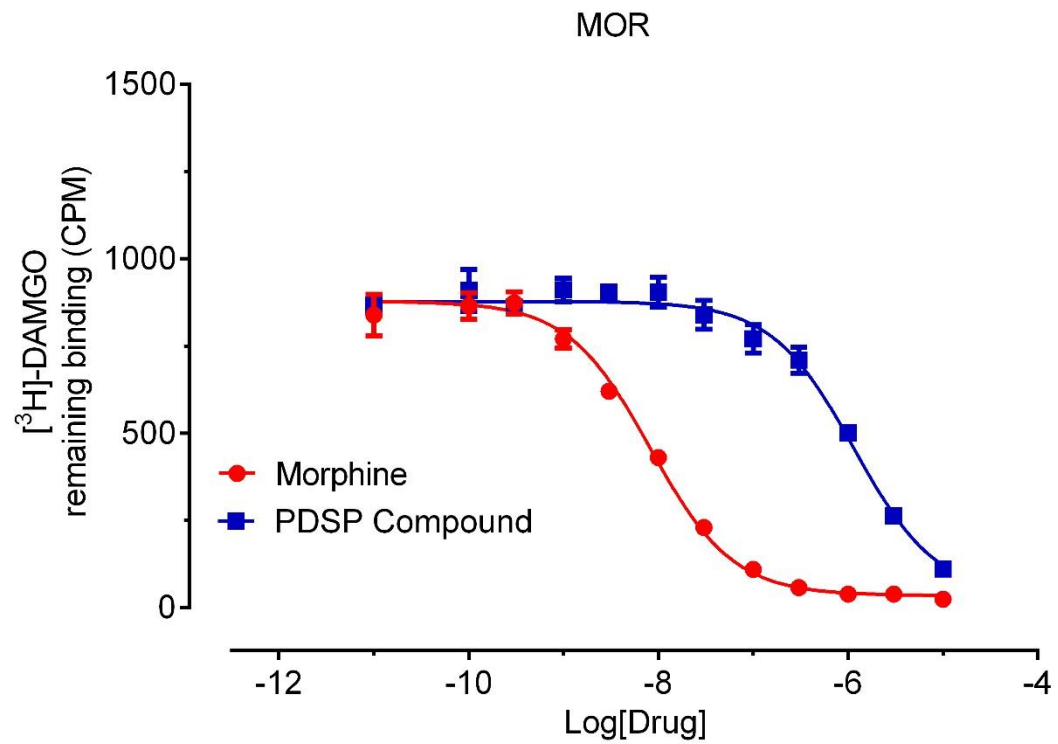


Table 12. HCA₂ receptors, radioligands and corresponding concentrations, reference compounds, and buffers for primary and secondary radioligand binding assays. Historical reference K_i values from > 6 months are also included.

HCA ₂ receptors				
HCA2 Binding Buffer: 50 mM Tris HCl, 1 mM MgCl ₂ , pH 7.4				
Standard Wash Buffer: 50 mM Tris HCl, pH 7.4, cold				
Target	Radioligand pK _d ± SEM (K _d , nM)	Radioligand used (nM)	Reference Ligand pK _i ± SEM (K _i , nM)	Literature
HCA ₂	[³ H]-Niacin 7.90 ± 0.13 (12.47)	4.0 – 20.0	Niacin	(80–82)

Figure 20. Representative competitive binding curves with HCA₂ receptors.

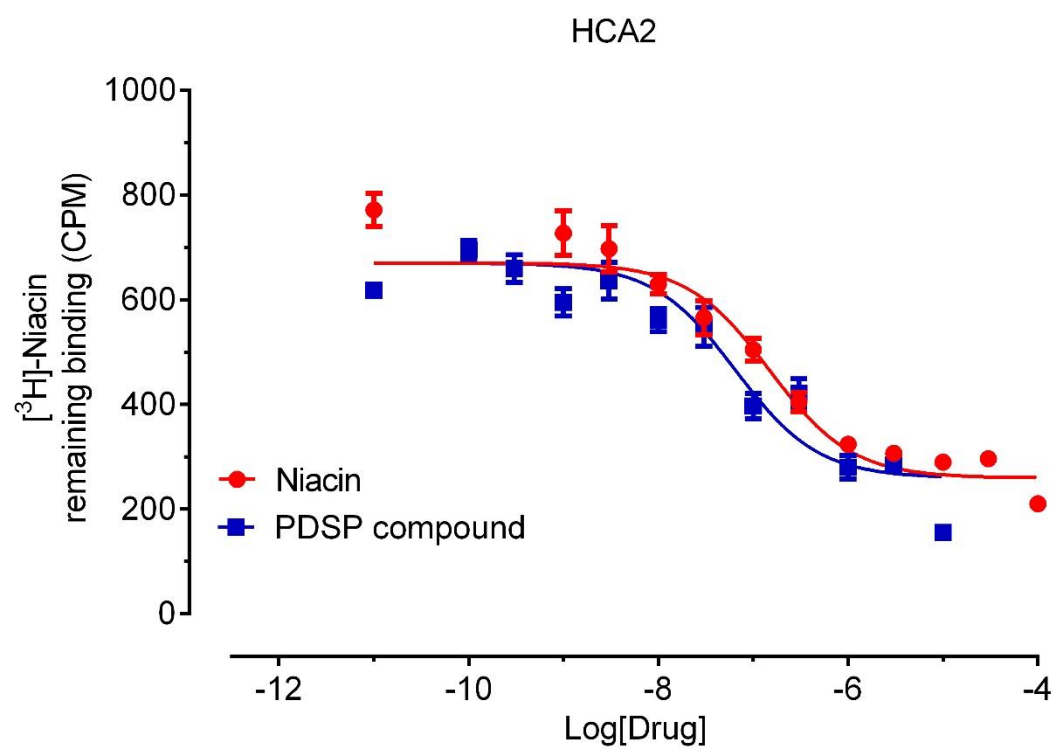
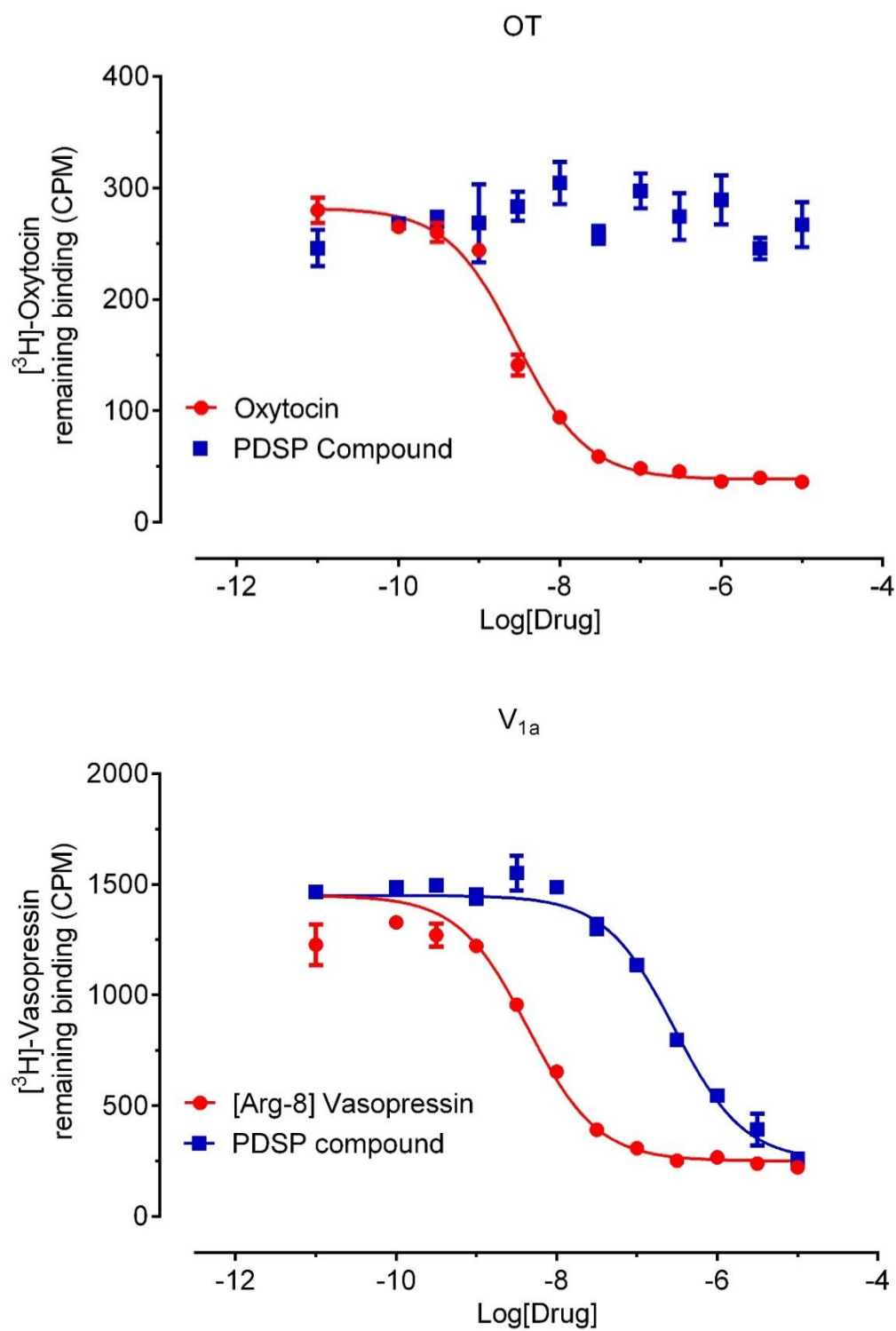


Table 13. Oxytocin and Vasopressin receptors, radioligands and corresponding concentrations, reference compounds, and buffers for primary and secondary radioligand binding assays. Historical reference K_i values from > 2 years are also included.

Oxytocin and Vasopressin receptors				
Oxytocin Binding Buffer: 50 mM HEPES, 10 mM $MgCl_2$, pH 7.4				
Vasopressin Binding Buffer: 20 mM Tris HCl, 100 mM NaCl, 10 mM $MgCl_2$, 0.1 mg/ml bacitracin, 1 mg/ml BSA, pH 7.4, RT				
Standard Wash Buffer: 50 mM Tris HCl, pH 7.4, cold				
Target	Radioligand $pK_d \pm SEM$ (K_d , nM)	Radioligand used (nM)	Reference Ligand $pK_i \pm SEM$ (K_i , nM)	Literature
Oxytocin	$[^3H]$ -Oxytocin 8.89 ± 0.06 (1.28)	1.5 – 2.0	Oxytocin 8.56 ± 0.04 (2.73)	(83–85)
V _{1a}	$[^3H]$ -Vasopressin 9.17 ± 0.06 (0.68)	0.4 – 1.5	Vasopressin 8.76 ± 0.05 (1.73)	(86, 87)
V _{1b}	$[^3H]$ -Vasopressin 9.00 ± 0.05 (0.99)	0.5 – 2.0	Vasopressin 8.88 ± 0.05 (1.32)	
V ₂	$[^3H]$ -Vasopressin 8.54 ± 0.05 (2.91)	0.6 – 1.7	Vasopressin 8.61 ± 0.05 (2.44)	

Figure 21. Representative competitive binding curves with Oxytocin and Vasopressin receptors.



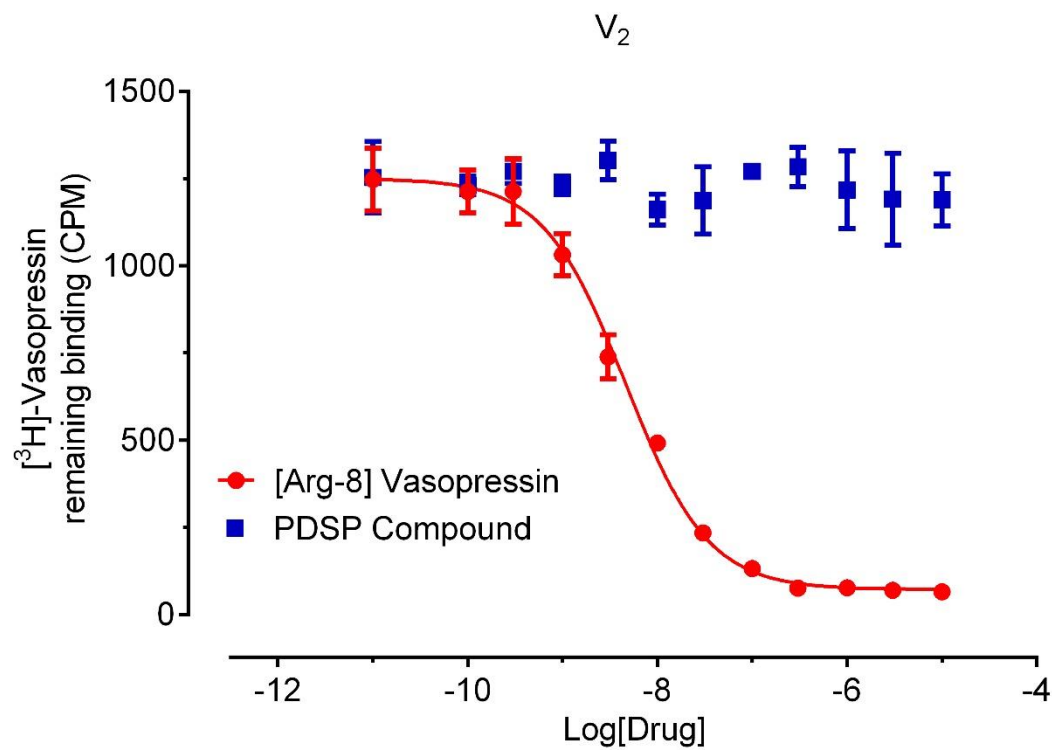
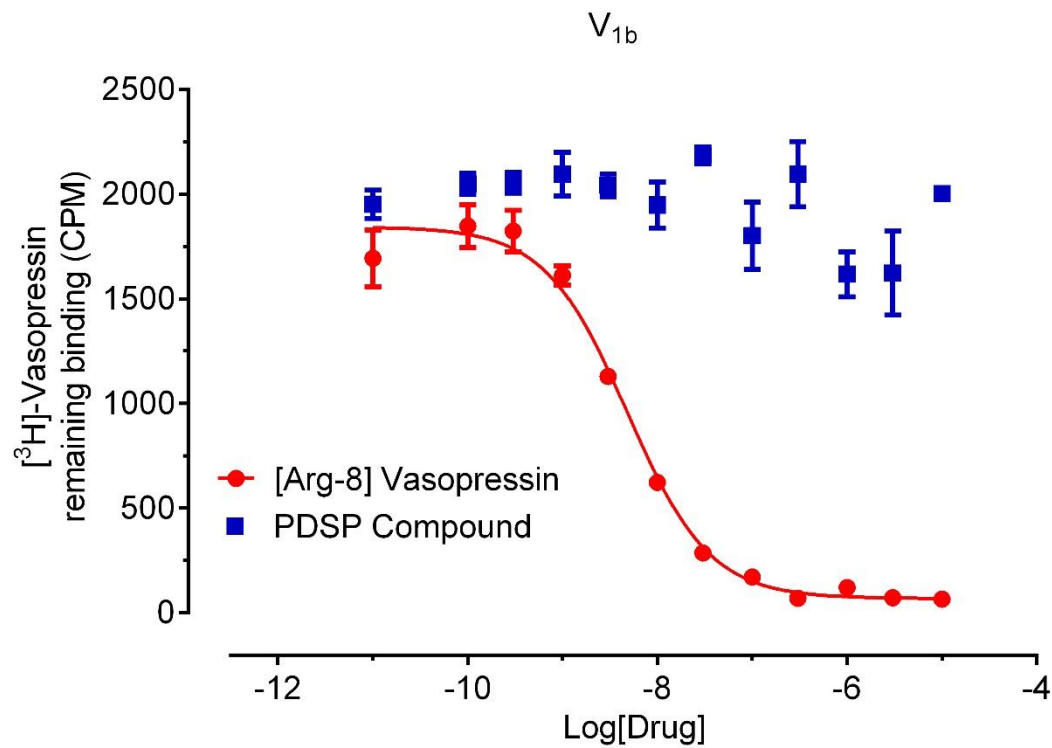


Table 14. Smoothened receptor, radioligands and corresponding concentrations, reference compounds, and buffers for primary and secondary radioligand binding assays. Historical reference K_i values from >2 years are also included.

Smoothened receptor				
SMO Binding Buffer: 50 mM HEPES, 3 mM MgCl ₂ , Protease inhibitors, 0.1mg/ml BSA, pH 7.2, RT SMO Wash Buffer: PBS, pH 7.2, cold				
Target	Radioligand $pK_d \pm SEM (K_d, nM)$	Radioligand used (nM)	Reference Ligand $Pk_i \pm SEM (K_i, nM)$	Literature
SMO	[³ H]-Cyclopamine $8.42 \pm 0.08 (3.81)$	2.6 – 5.0	SAG $8.05 \pm 0.28 (8.93)$ LY2490680 $7.76 \pm 0.07 (17.57)$ Cyclopamine $785 \pm 0.09 (13.98)$	(88, 89)

Figure 22. Representative competitive binding curves with SMO receptors.

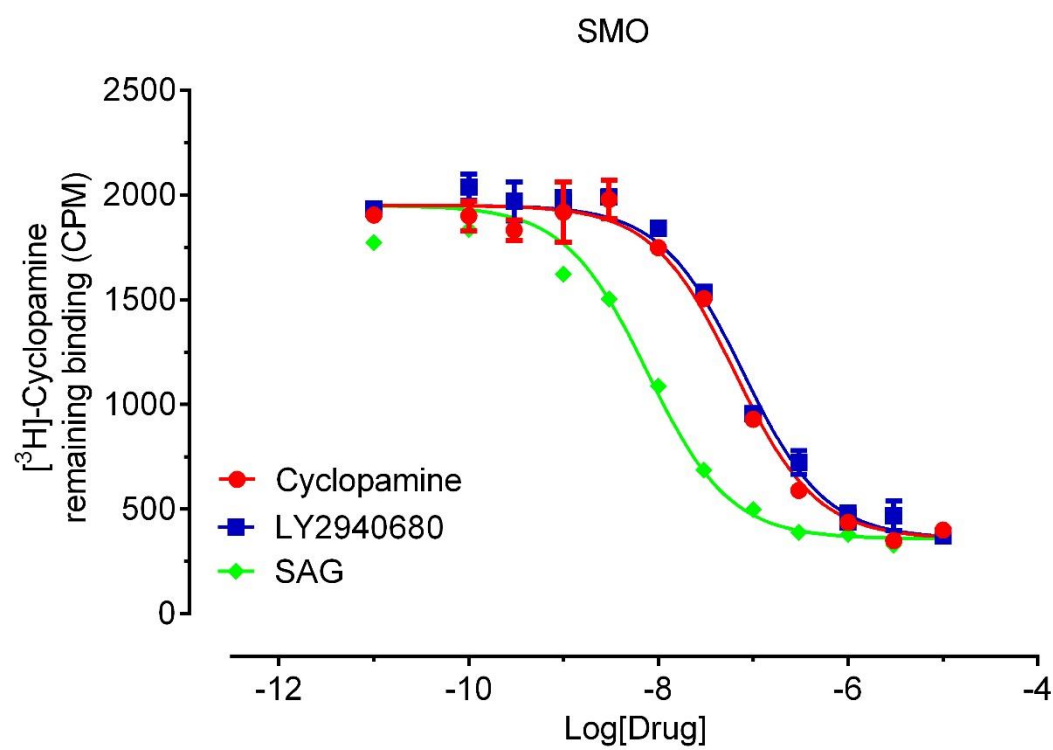


Table 15. Prostanoid receptors, radioligands and corresponding concentrations, reference compounds, and buffers for primary and secondary radioligand binding assays. These assays are seldom requested and were not carried out in the last 5 years.

Prostanoid receptors			
Prostanoid binding buffer: 25 mM Tris HCl, 10 mM MgCl ₂ , 1 mM EDTA, pH 7.4, RT Standard wash buffer: 50 mM Tris HCl, pH 7.4, cold			
Target	Radioligand	[Radioligand] used (nM)	Literature
EP3	[³ H]-PGE2	10	(90, 91)
EP4	[³ H]-PGE2	10	

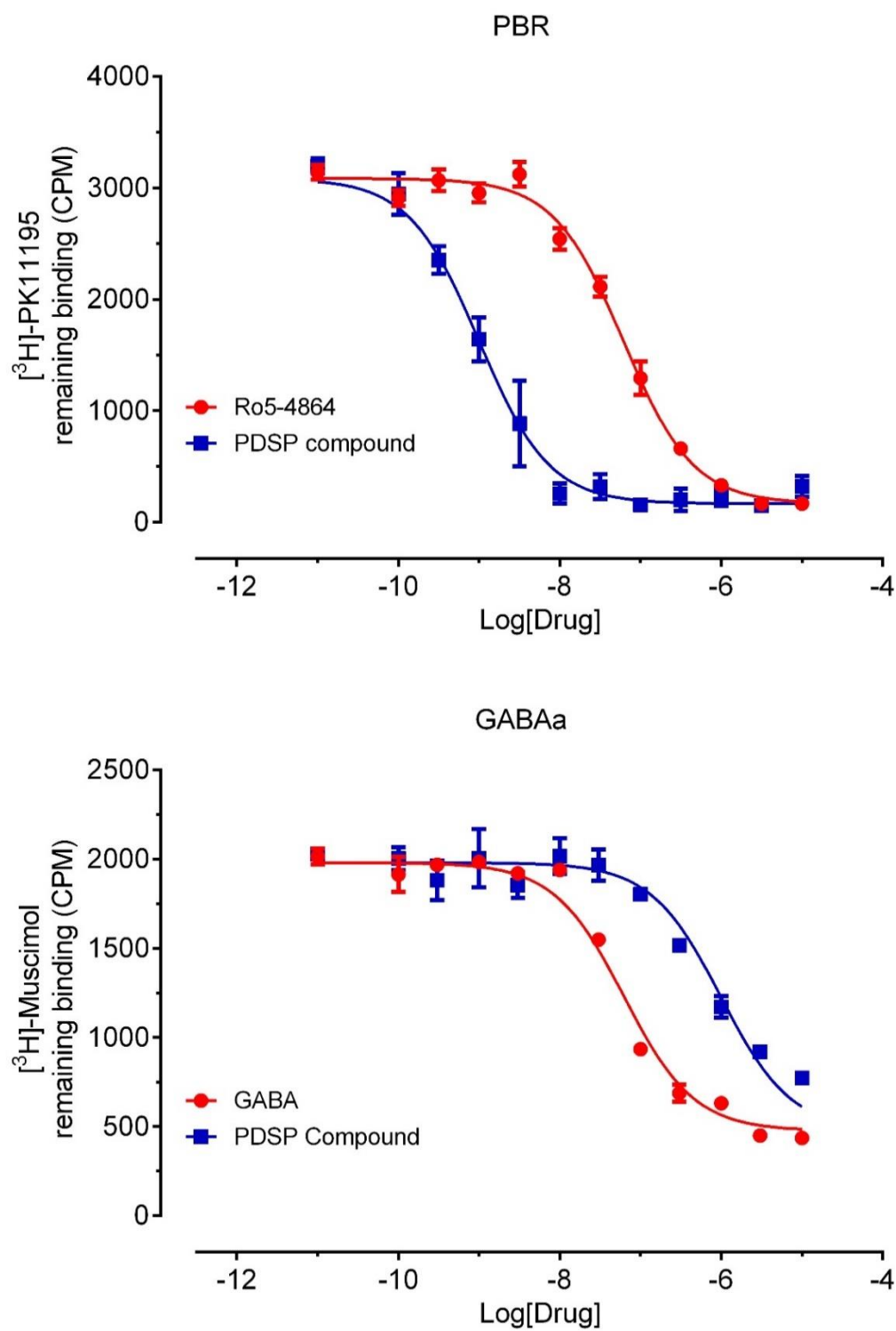
Table 16. PKC subunits, radioligands and corresponding concentrations, reference compounds, and buffers for primary and secondary radioligand binding assays. These assays are seldom requested and were not carried out in the last 5 years.

PKC			
PKC Binding Buffer: 50 mM Tris HCl, 1 mM CaCl ₂ , 4 mg/ml BSA, 100 µg/ml phosphatidylserine, pH 7.4, RT Standard Wash Buffer: 50 mM Tris HCl, pH 7.4, cold			
Target	Radioligand	[³ H] in nM	Literature
PKC α	[³ H]-PDBU	3	(92–94)
PKC β	[³ H]-PDBU	3	
PKC γ	[³ H]-PDBU	3	
PKC δ	[³ H]-PDBU	3	
PKC ϵ	[³ H]-PDBU	3	

Table 17. GABAA receptors, radioligands and corresponding concentrations, reference compounds, and buffers for primary and secondary radioligand binding assays. Historical reference K_i values from >2 years are also included.

GABA receptors				
GABA/PBR Binding Buffer: 50 mM Tris Acetate, pH 7.4, RT				
Benzodiazepin (BZP) Binding Buffer: 50 mM Tris HCl, 2.5 mM CaCl ₂ , pH 7.4, RT				
Standard Wash Buffer: 50 mM Tris HCl, pH 7.4, cold				
Target	Radioligand $pK_d \pm SEM$ (K_d , nM)	Radioligand used (nM)	References	Literature
GABA/PBR (rat brain)	[³ H]-PK11195 9.00 (1.0)	0.3 – 2.0	Ro5-4864 7.82 \pm 0.02 (14.97)	(95, 96)
GABAA (rat brain)	[³ H]-Muscimol 8.11 \pm 0.06 (7.70)	9.50 – 25.0	GABA 6.86 \pm 0.08 (137.5)	(97, 98)
GABAA/BZP (rat brain)	[³ H]-Flunitrazepam 8.79 \pm 0.14 (1.64)	0.6 – 4.0	Clonazepam 8.99 \pm 0.03 (1.03)	(99, 100)

Figure 23. Representative competitive binding curves with GABA receptors.



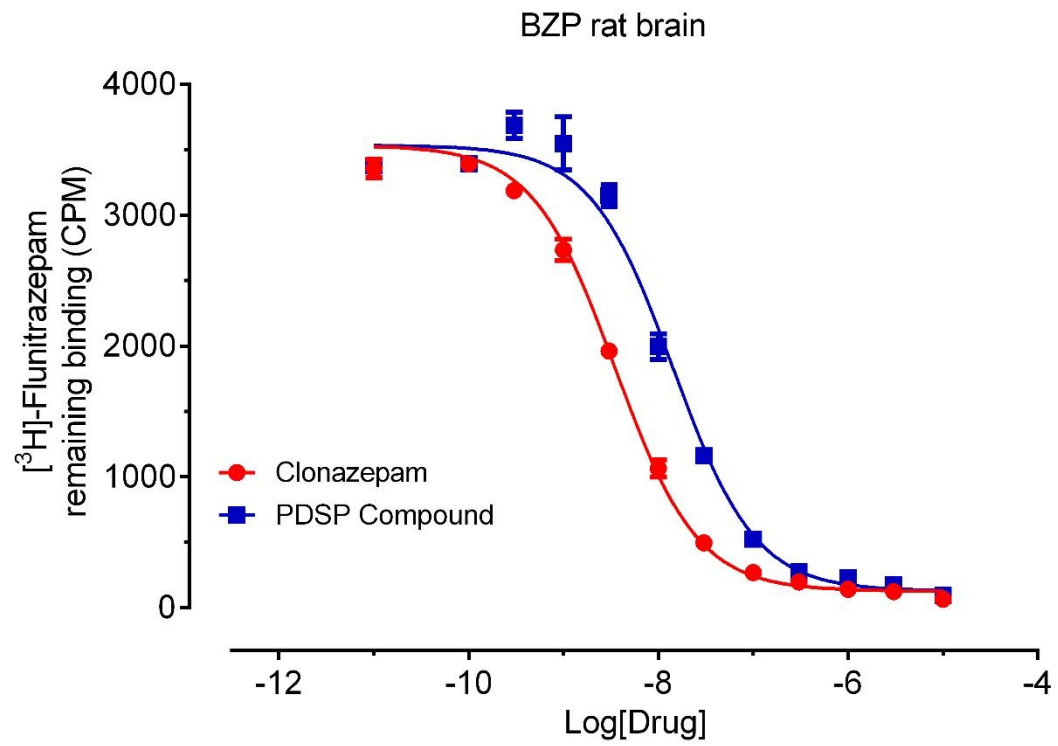
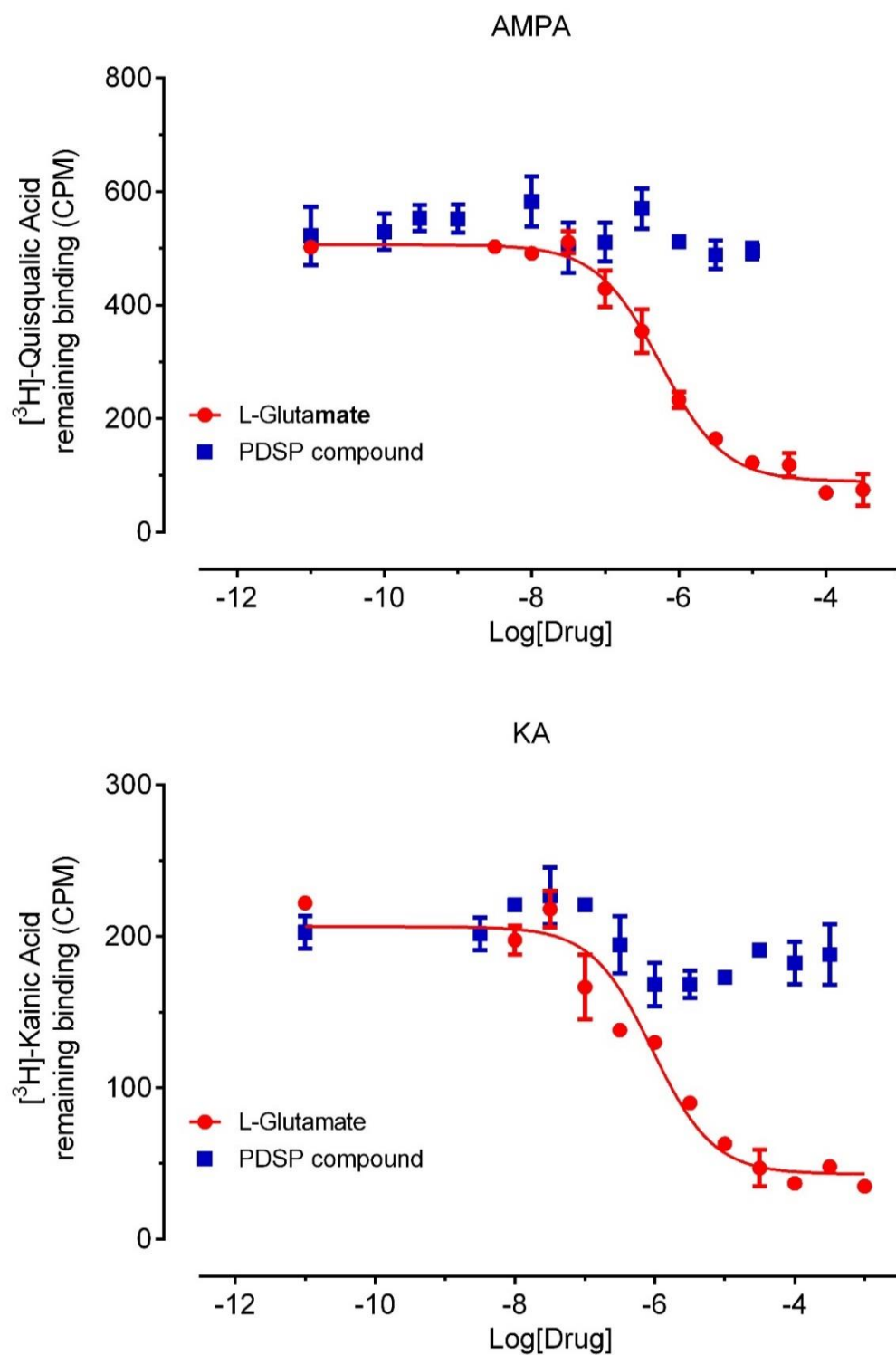
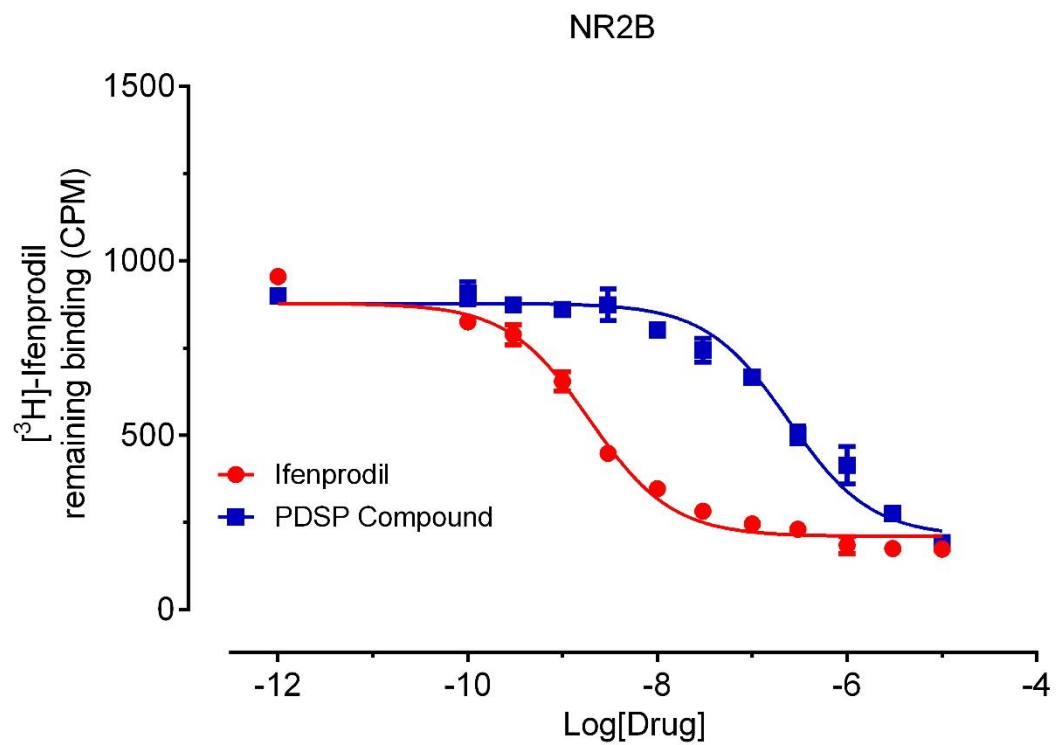
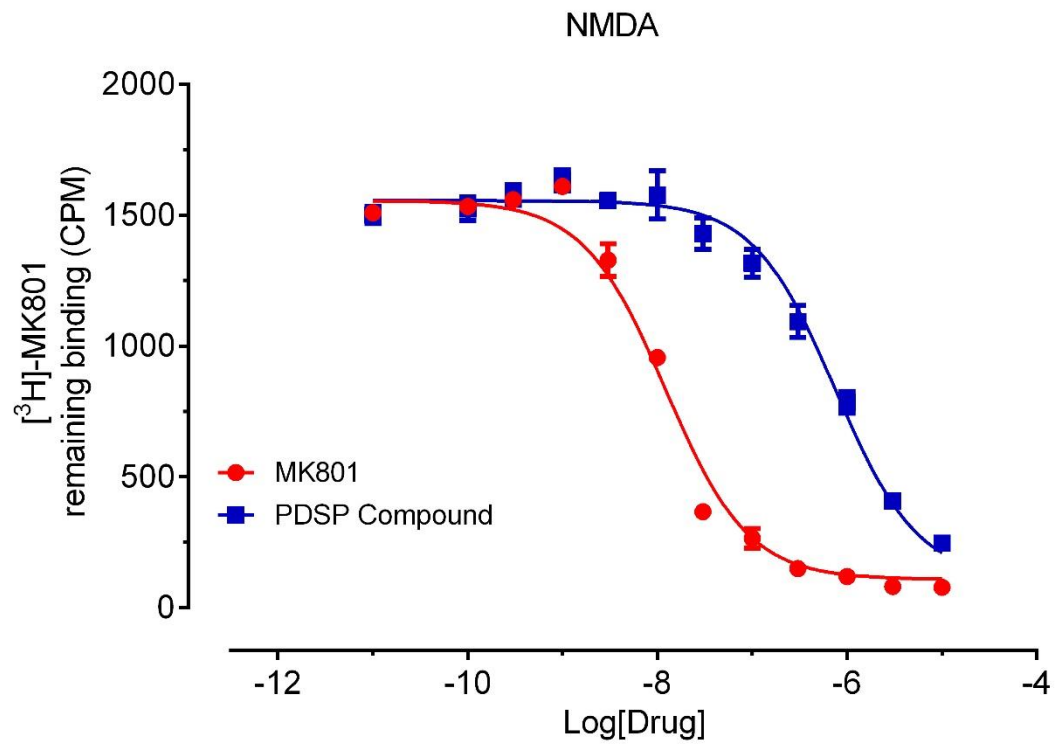


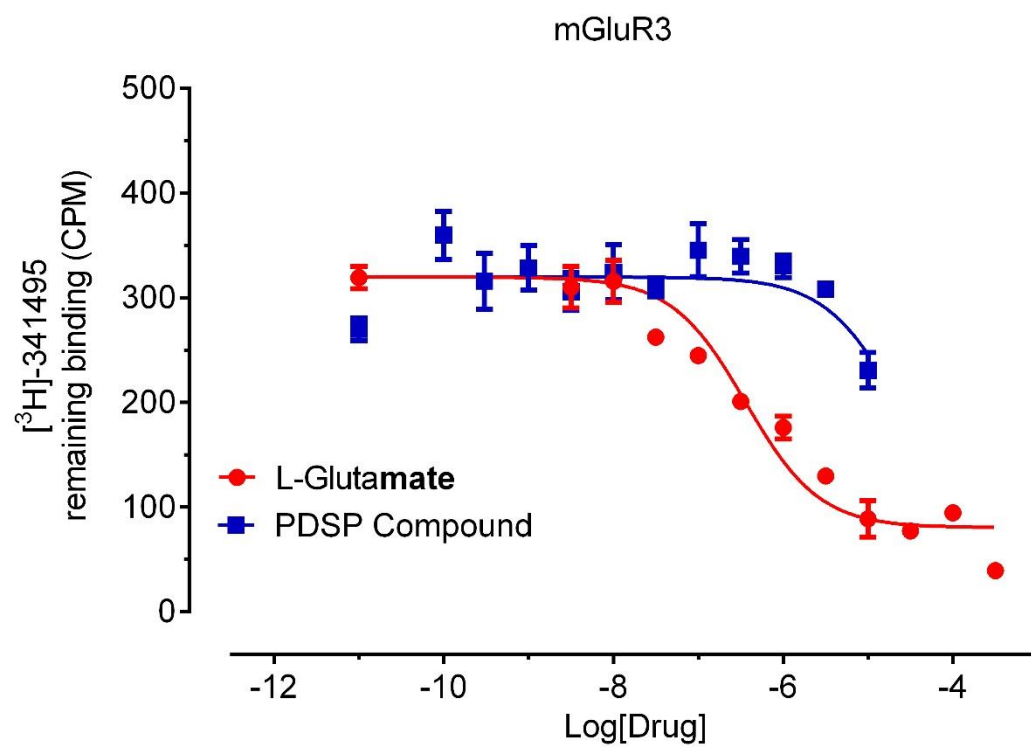
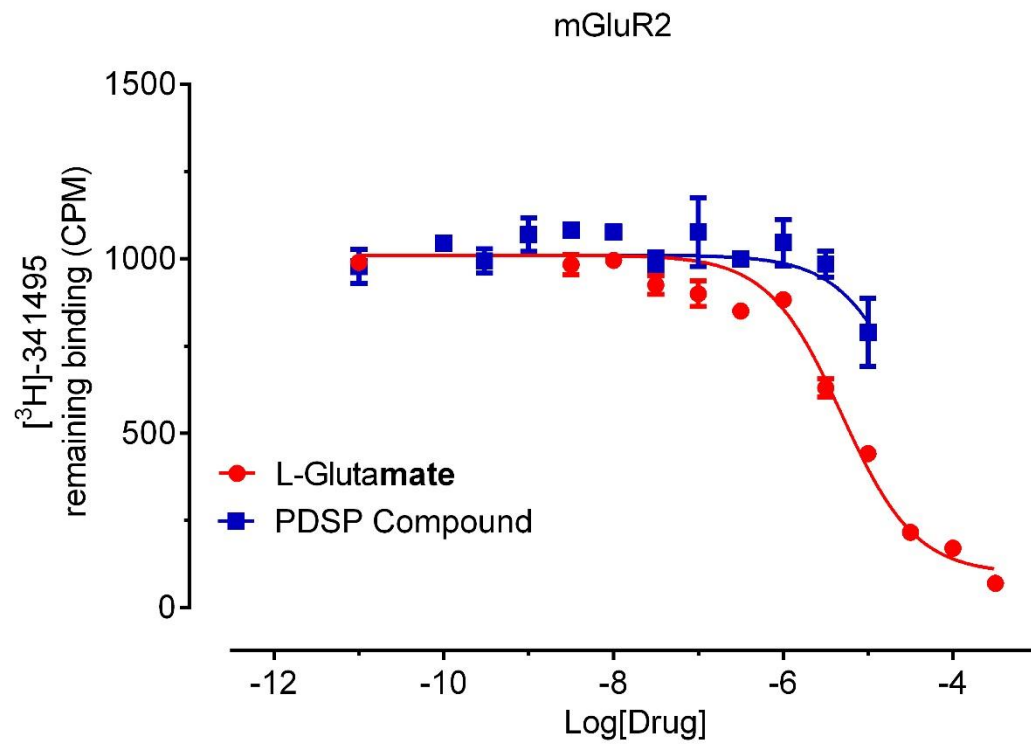
Table 18. Glutamate receptors radioligands, corresponding concentrations, reference compounds, and buffers for primary and secondary radioligand binding assays. Historical affinity results from the last >2 years are listed.

Glutamate receptors				
NMDA Binding Buffer: 20 mM HEPES, 1 mM EDTA, 100 μM L-Glutamate, 100 μM Glycine, pH 7.0, RT mGluR Binding Buffer: 50 mM Tris HCl, 10 mM MgCl2, 0.1 mM EDTA, pH 7.4, RT Standard Wash Buffer: 50 mM Tris HCl, pH 7.4, cold				
Target	Radioligand pK _d ± SEM (K _d , nM)	Radioligand used (nM)	Reference Ligand pK _i ± SEM (K _i , nM)	Literature
NMDA (rat brain)	[³ H]-MK801 8.47 ± 0.07 (3.38)	1.4 – 13.0	MK801 8.41 ± 0.04 (3.88)	(101–103)
NR2B	[³ H]-Ifenprodil (3.27)	3.0 – 5.0	Ifenprodil 8.96 ± 0.03 (1.10)	(104–107)
AMPA	[³ H]-Quisqualic Acid (30)	25.0 – 32.0	L-Glutamate 6.19 ± 0.09 (647)	
KA	[³ H]-Kainic Acid 8.02 ± 0.15 (9.58)	8.0 – 12.0	L-Glutamate 6.22 ± 0.14 (596)	(108, 109)
mGluRs				
mGlu ₁	Being developed			
mGlu ₂	[³ H]-LY341495 8.66 ± 0.07 (2.17)	2.1 – 4.6	L-Glutamate 5.51 ± 0.05 (3090)	(110–112)
mGlu ₃	[³ H]-LY341495 8.43 ± 0.17 (3.71)	1.8 – 2.5	L-Glutamate 6.48 ± 0.10 (3340)	
mGlu ₄	Being developed			
mGlu ₅	[³ H]-MPEP 8.47 ± 0.16 (3.40)	1.0 – 5.0	Fenobam 7.85 ± 0.08 (14.0)	(113)
mGlu ₆	[³ H]-LY341495 8.47 ± 0.16 (3.40)	3.0 – 5.0	L-Glutamate 7.45 ± 0.37 (35.5)	(114)
mGlu ₇	Being developed			
mGlu ₈	Being developed			

Figure 24. Representative competitive binding curves for NMDA and mGluR5 receptors.







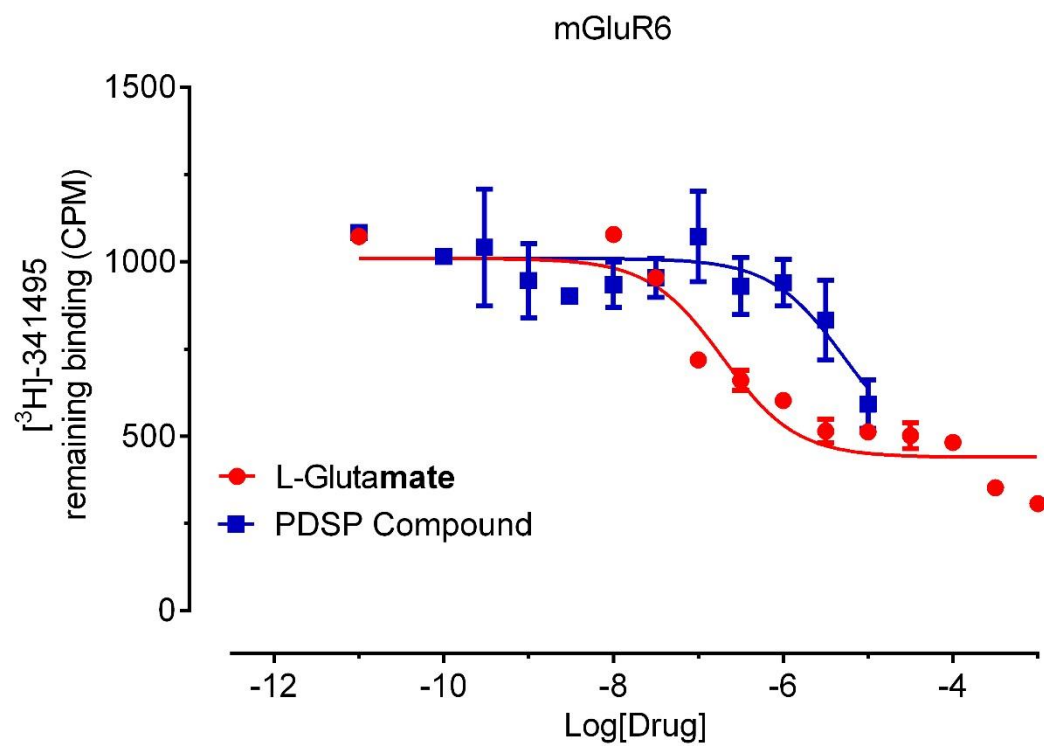
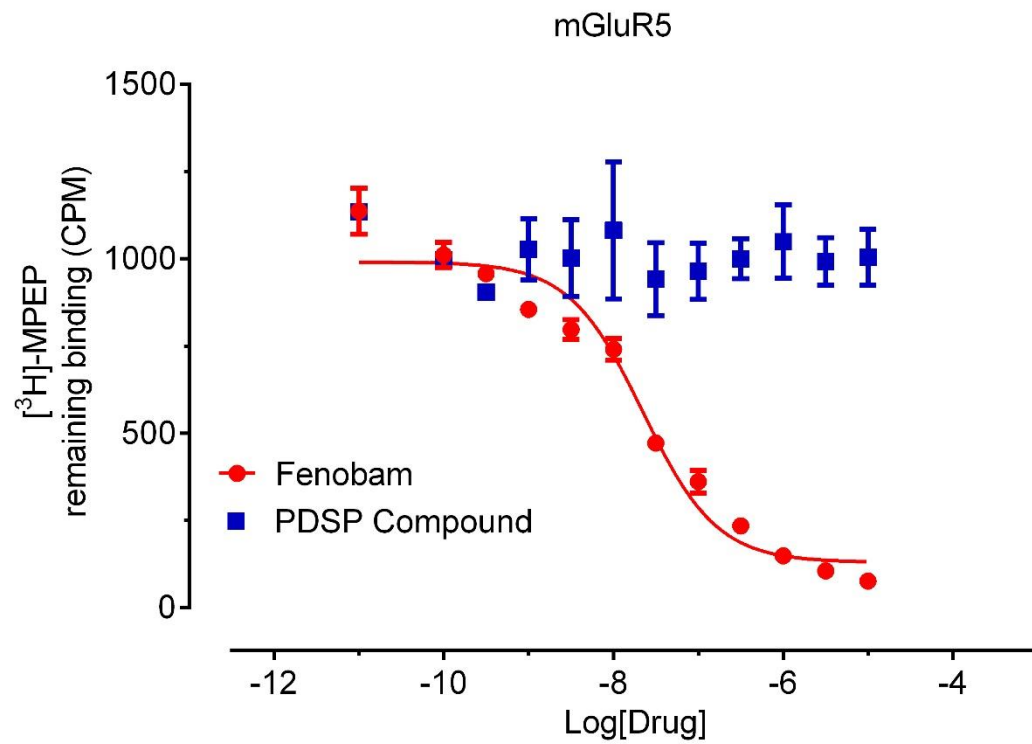
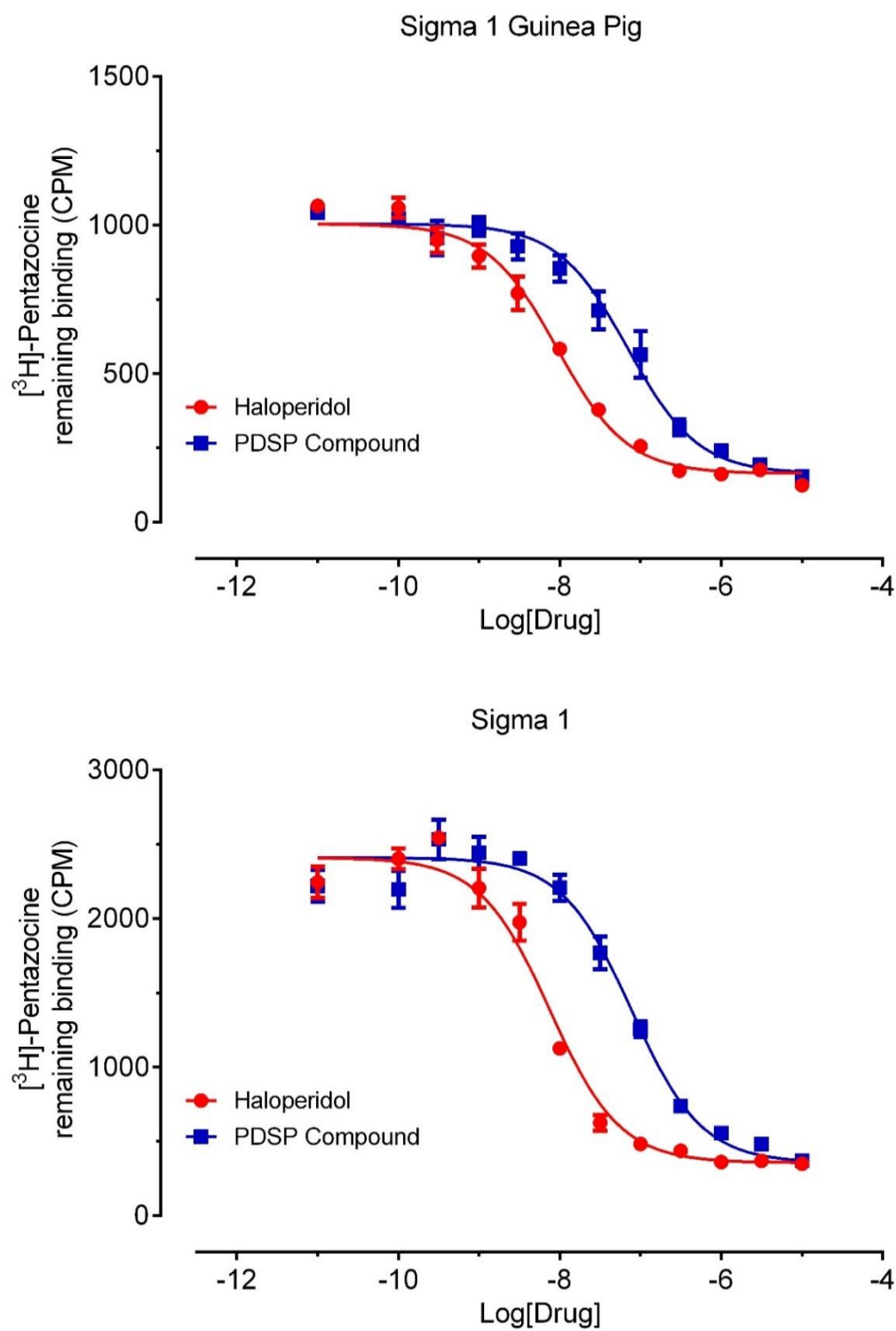


Table 19. Sigma receptors, radioligands and corresponding concentrations, reference compounds, and buffers for primary and secondary radioligand binding assays. Historical reference K_i values from > 6 months are also included.

Sigma receptors				
Sigma Binding Buffer: 50 mM Tris HCl, pH 8.0, RT Standard Wash Buffer: 50 mM Tris HCl, pH 7.4, cold				
Target	Radioligand $pK_d \pm SEM (K_d, nM)$	Radioligand used (nM)	Reference Ligand $pK_i \pm SEM (K_i, nM)$	Literature
Sigma 1 (Guinea pig)	[³ H]-Pentazocine $8.19 \pm 0.18 (6.50)$	2.0 – 10.0	Haloperidol $8.45 \pm 0.01 (3.54)$	(115–117)
Sigma 1 (Human)	[³ H]-Pentazocine $8.08 \pm 0.12 (8.32)$	4.0 – 5.0	Haloperidol $8.14 \pm 0.04 (6.77)$	
Sigma 2 (PC12)	[³ H]-DTG $8.00 \pm 0.03 (9.90)$	5.0 – 7.0	Haloperidol $7.86 \pm 0.01 (13.91)$	
Sigma 2 (Human)	[³ H]-DTG $7.55 \pm 0.18 (27.93)$	5.0	Haloperidol $7.80 \pm 0.04 (15.87)$	

Figure 25. Representative competitive binding curves with Sigma receptors.



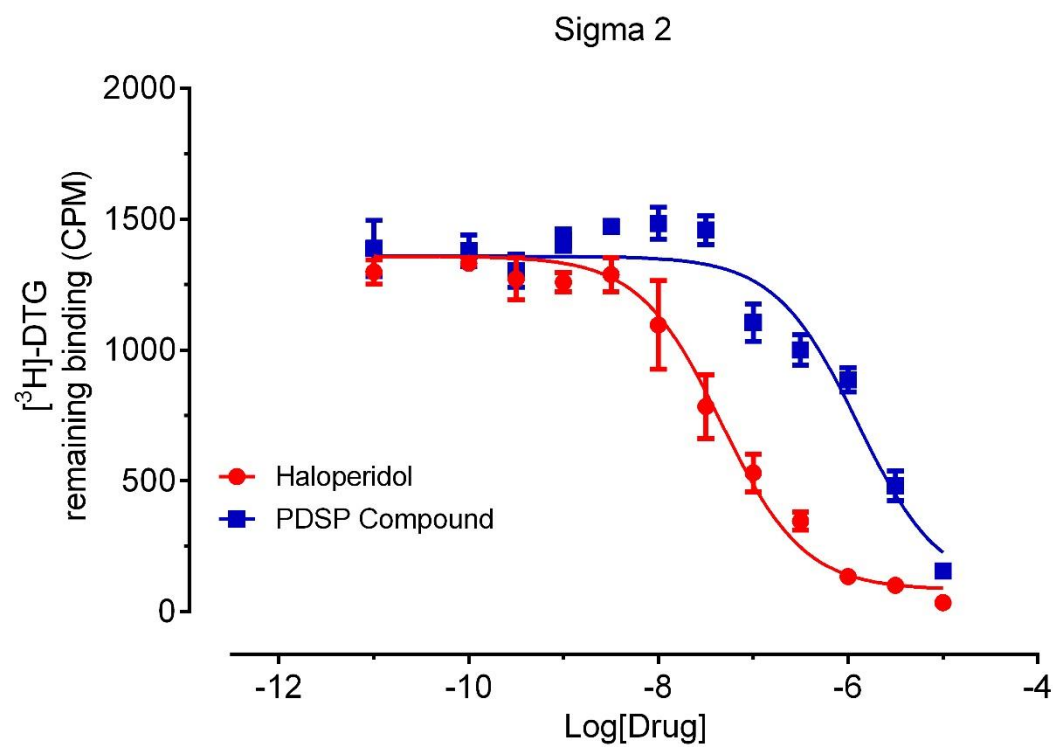
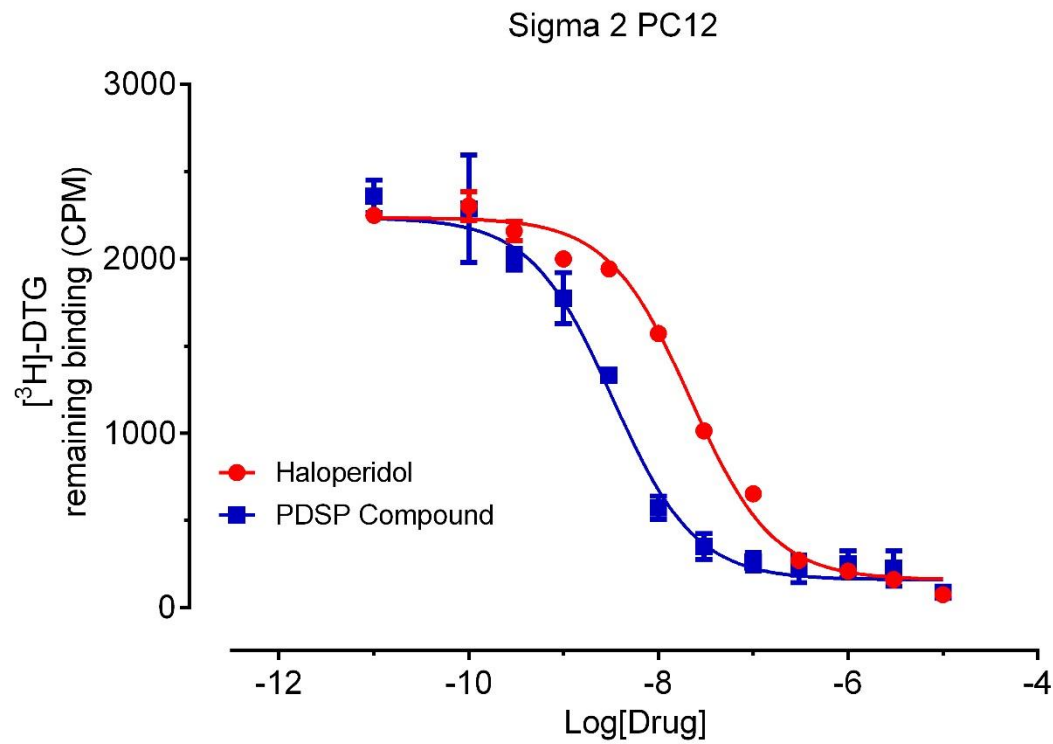


Table 20. Angiotensin II receptors, radioligands and corresponding concentrations, reference compounds, and buffers for primary and secondary radioligand binding assays. Historical reference K_i values (if available) from > 6 months are also included.

Angiotensin receptors				
Angiotensin Binding Buffer: 50 mM Tris HCl, 150 mM NaCl, 5 mM MgCl ₂ , 0.5 mg/ml BSA, 100 mM Bacitracin, pH 7.4, RT				
Standard Wash Buffer: 50 mM Tris HCl, pH 7.4, cold				
Target	Radioligand $pK_d \pm SEM (K_d, nM)$	[³ H] in nM	Reference Ligand $pK_i \pm SEM (K_i, nM)$	Literature
AT ₁	[³ H]-Angiotensin II	0.1	Candesartan	(118, 119)
AT ₂	[³ H]-Angiotensin II 8.19 ± 0.28 (6.52)	3.50	PD123319 7.52 ± 0.06 (30.0)	

Figure 26. Representative binding curve for AT₂ receptors.

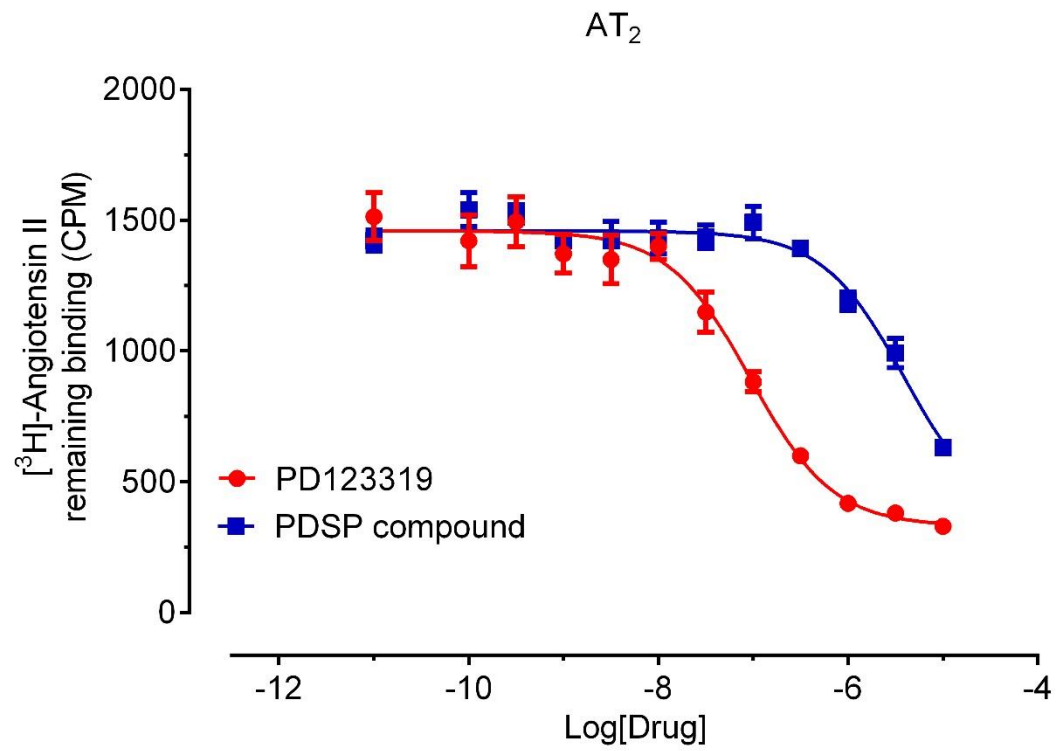


Table 21. Neurotensin receptors, radioligands and corresponding concentrations, reference compounds, and buffers for primary and secondary radioligand binding assays. Historical reference K_i values (if available) from > 6 months are also included.

Neurotensin receptors				
Neurotensin binding buffer: 50 mM Tris HCl, 0.2% BSA				
Standard Wash Buffer: 50 mM Tris HCl, pH 7.4, cold				
Target	Radioligand $pK_d \pm SEM (K_d, nM)$	Radioligand used (nM)	Reference Ligand $pK_i \pm SEM (K_i, nM)$	Literature
NTS ₁	[³ H]-Neurotensin 8.25 ± 0.15 (5.65)	1.0 – 4.0	Neurotensin 8.40 ± 0.07 (3.95)	(120–122)
NTS ₂	[³ H]-Neurotensin	1.2	Neurotensin	

Figure 27. Representative binding curve for Neurotensin receptors.

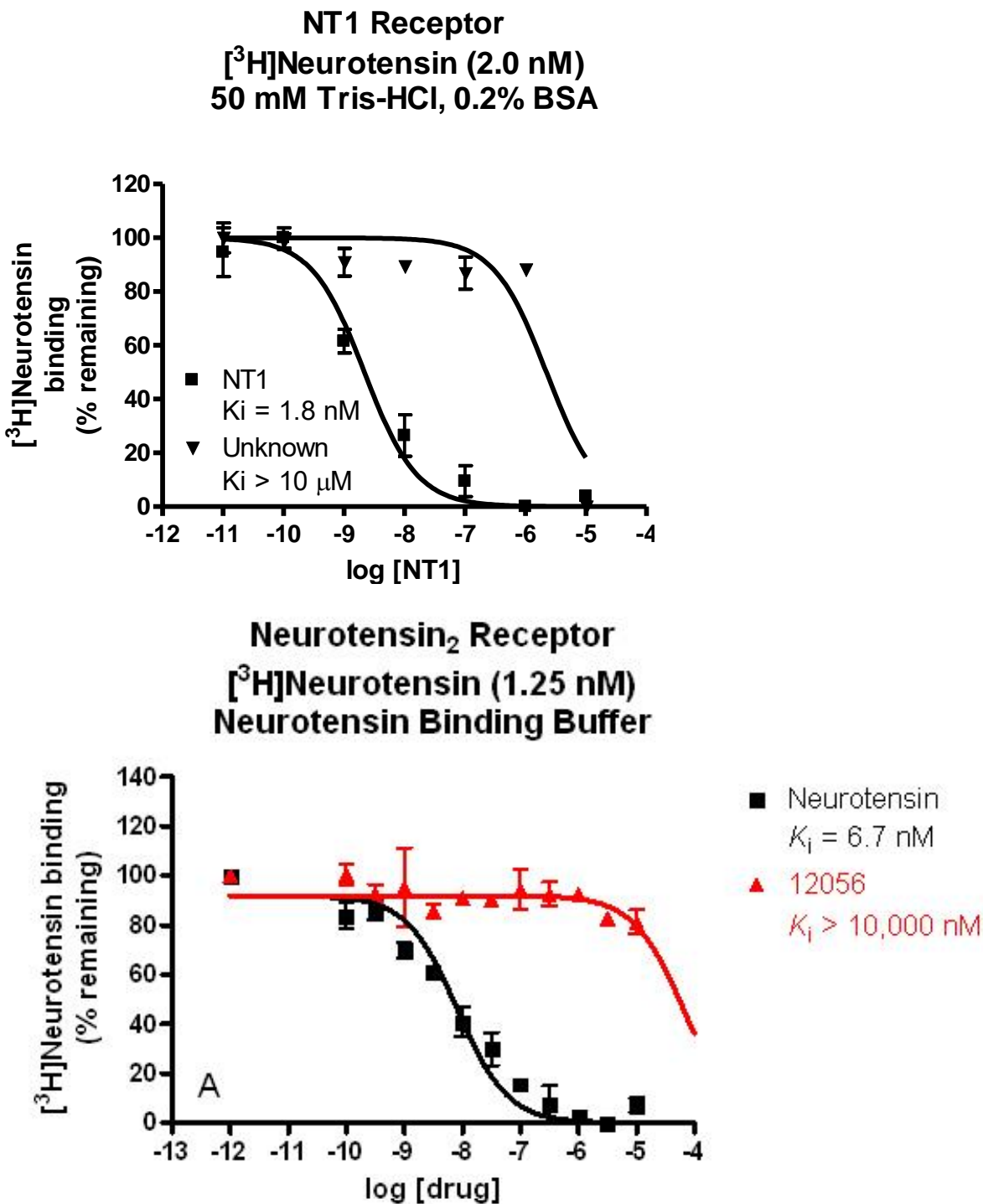


Table 22. VMAT2 transportor, radioligand and corresponding concentration, reference compound, and buffers for primary and secondary radioligand binding assays.

VMAT2 transporter				
VMAT2 binding buffer: 50 mM Tris HCl, 0.2% BSA Standard Wash Buffer: 50 mM Tris HCl, pH 7.4, cold				
Target	Radioligand	Radioligand used (nM)	Reference Ligand	Literature
VMAT2	[³ H]-Tetrabenazine	1.5	Reserpine	(123)

Figure 28. Representative binding curve for VMAT2 transporters.

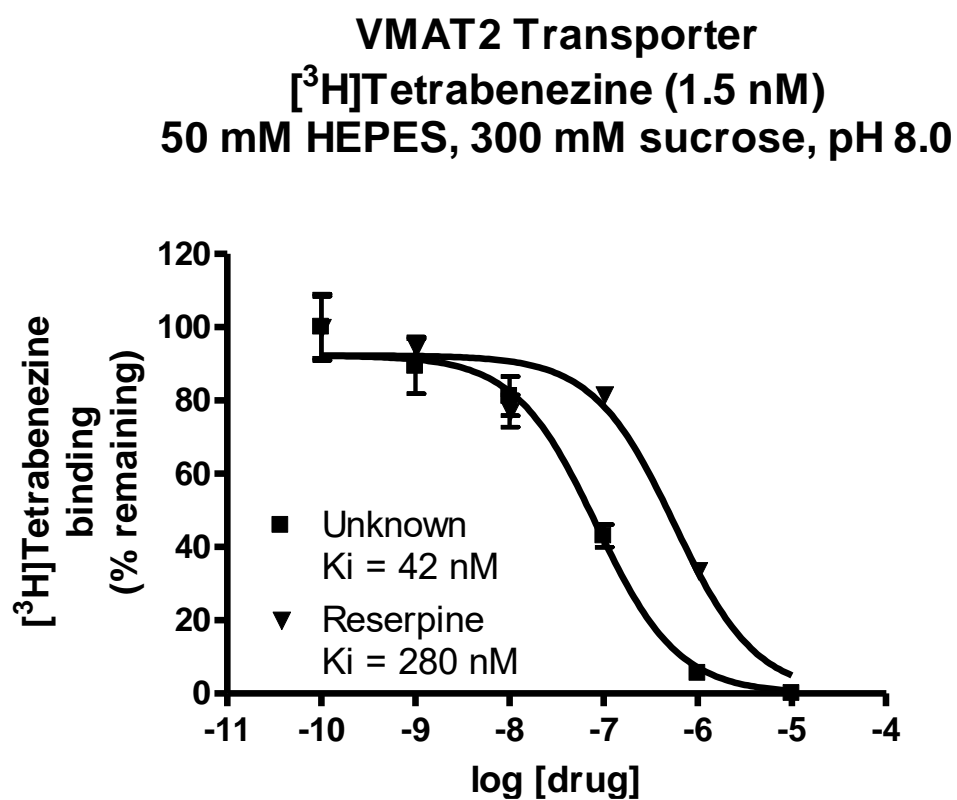


Table 23. Calcium and sodium channels, radioligands and corresponding concentrations, reference compounds, and buffers for primary and secondary radioligand binding assays. Historical reference K_i values (if available) from > 6 months are also included.

Calcium and Sodium channels				
Calcium channel Binding Buffer: 50 mM Tris HCl, 50 mM NaCl, 1 mM CaCl_2 , pH 7.4, RT Sodium channel Binding Buffer: 50 mM HEPES, 130 mM Choline Cl, 5.4 mM KCl, 0.8 mM MgSO_4 , 5.5 mM Glucose, 1 μM tetrodotoxin, 1 mg/ml BSA, 30 μg /well scorpion verom, pH 7.4, 37°C. Standard Wash Buffer: 50 mM Tris HCl, pH 7.4, cold				
Target	Radioligand $\text{pK}_d \pm \text{SEM} (K_d, \text{nM})$	[Radioligand] used (nM)	Reference Ligand $\text{pK}_i \pm \text{SEM} (K_i, \text{nM})$	Literature
Ca^{2+} channel	$[^3\text{H}]\text{-PN200110}$ $8.52 \pm 0.12 (3.04)$	2.0 – 3.0	Nifendipine $8.05 \pm 0.17 (8.85)$	(124, 125)
	$[^3\text{H}]\text{-Nitrendipine}$ $8.21 \pm 0.25 (6.20)$	3.0 – 5.0	Nifendipine	(126, 127)
Na^{+} channel	$[^3\text{H}]\text{-Batrachotoxin}$		Veratridine	(128, 129)

Figure 29. Representative figure for Ca^{2+} channel binding assay.

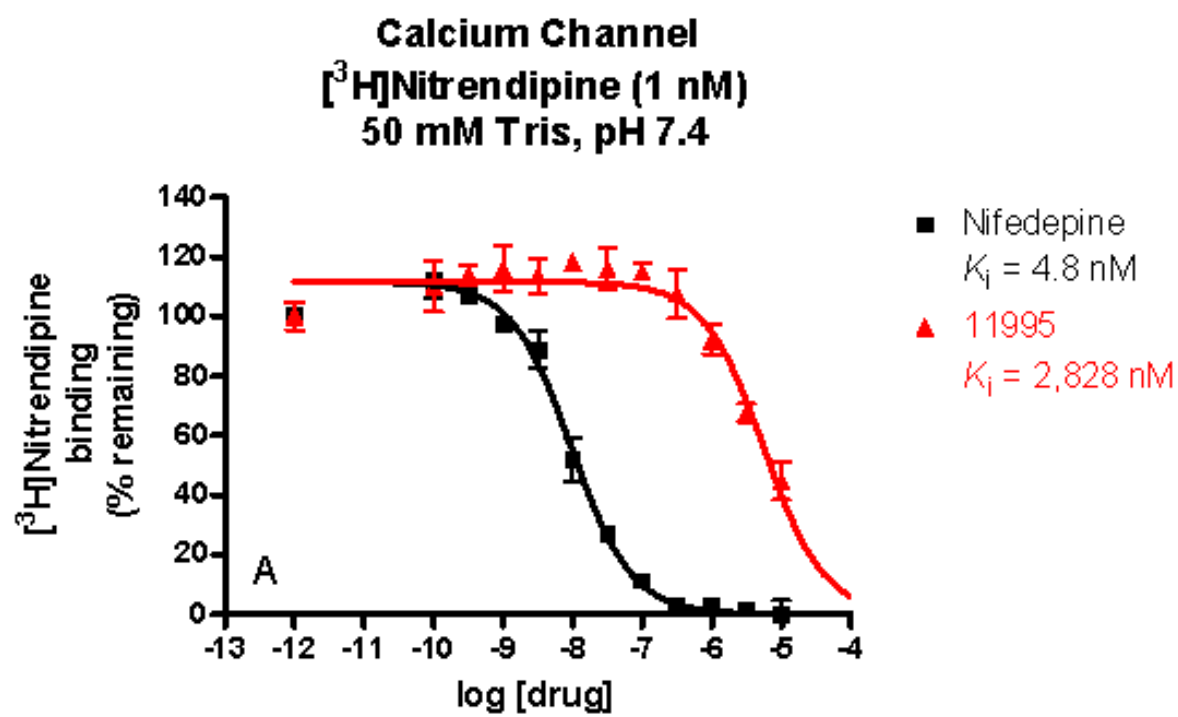


Table 24. HERG potassium channel, radioligand and corresponding concentration, reference compound, and buffers for primary and secondary radioligand binding assays. The concentration of radioligand used for competition binding assay is usually near the K_d value, or as listed. Historical reference K_i values from >2 years are also included.

hERG channel				
hERG binding buffer: 10 mM HEPES, 135 mM NaCl, 5 mM KCl, 0.8 mM MgCl ₂ , 1 mM EGTA, 1 mg/ml BSA, pH 7.4, RT hERG wash buffer: hERG binding buffer, pH 7.4, cold				
Target	Radioligand $pK_d \pm SEM (K_d, nM)$	[Radioligand] used (nM)	Reference Ligand $pK_i \pm SEM (K_i, nM)$	Literature
hERG	[³ H]-Dofetilide 8.39 \pm 0.03 (4.07)	3.0 – 5.0	Dofetilide 8.37 \pm 0.08 (4.29)	(130, 131)

Figure 30. Representative binding curve with hERG potassium channel.

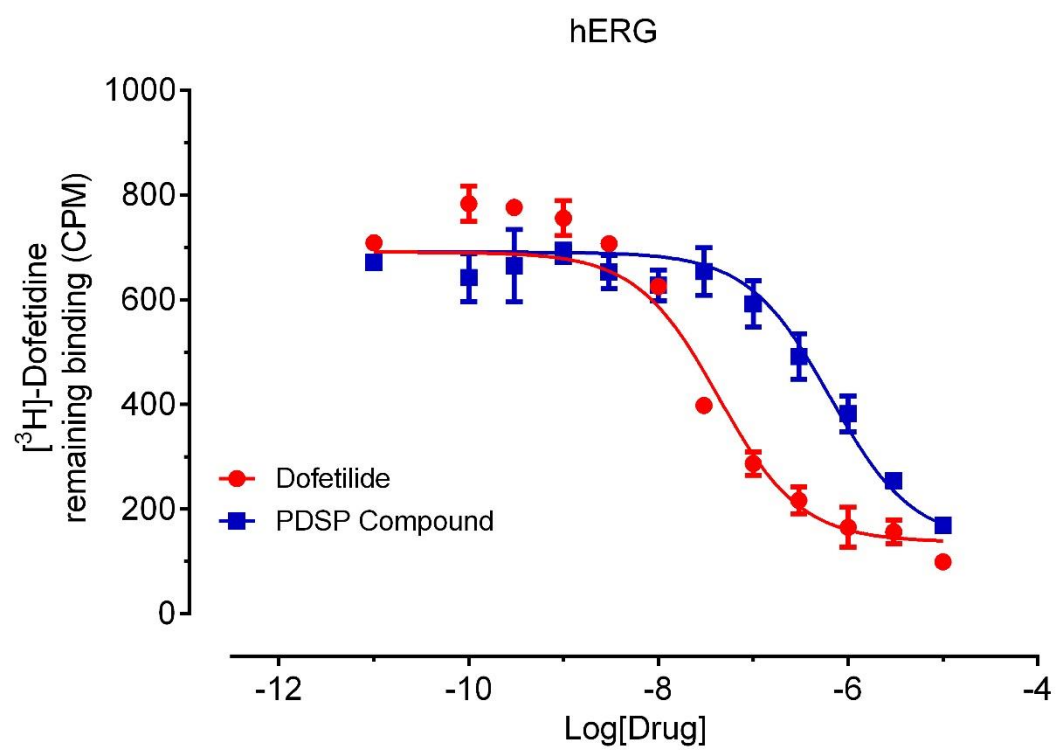


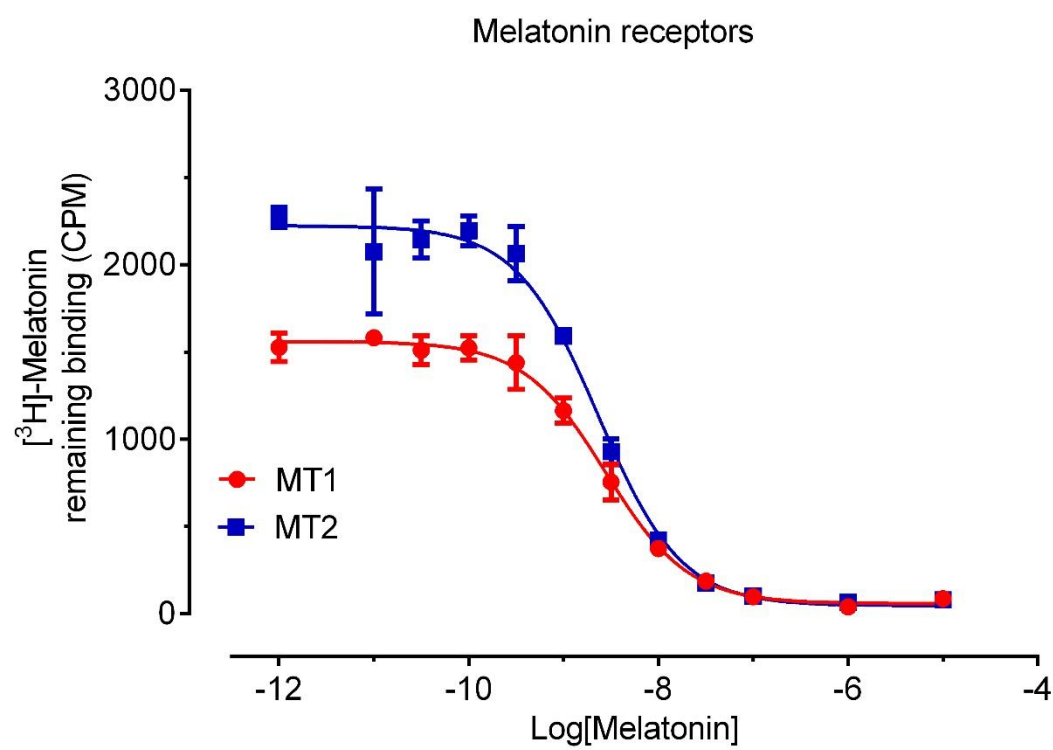
Table 25. Imidazoline receptor, radioligand and corresponding concentration, reference compound, and buffers for primary and secondary radioligand binding assays. The concentration of radioligand used for competition binding assay is usually near the K_d value, or as listed.

Imidazoline				
Imidazoline binding buffer: 5 mM Tris HCl, 5 mM HEPES, 0.5 mM EGTA, 0.5 mM EDTA, 0.5 mM MgCl ₂ , pH 8.0, RT Standard wash buffer: 50 mM Tris HCl, pH 7.4, cold				
Target	Radioligand	Radioligand used (nM)	Reference Ligand	Literature
Imidazoline 1	[³ H]-Clonidine	0.1 nM	Naphazoline	(132, 133)

Table 26. Melatonin receptors, radioligand and corresponding concentration, reference compound, and buffers for primary and secondary radioligand binding assays. These are new binding assays, and thus have no legacy data.

Melatonin receptors (Being developed and optimized)				
Standard binding buffer: 50 mM Tris HCl, 10 mM MgCl ₂ , 0.1 mM EDTA, pH 7.4, RT Standard wash buffer: 50 mM Tris HCl, pH 7.4, cold				
Target	Radioligand pK _d ± SEM (K _d , nM)	[Radioligand] used (nM)	Reference Ligand pK _i ± SEM (K _i , nM)	Literature
MT ₁	[³ H]-Melatonin	0.5 - 1.0	Melatonin	(134–136)
MT ₂	[³ H]-Melatonin	0.5 – 1.0	Melatonin	

Figure 31. Representative binding curves with melatonin receptors.



Section 2: Functional assays

2.1. Drug plate preparations for functional assays: Drug plates for functional assays are either manually prepared or made by STAR robotics. The following drug plate maps are the ones routinely used for functional assays.

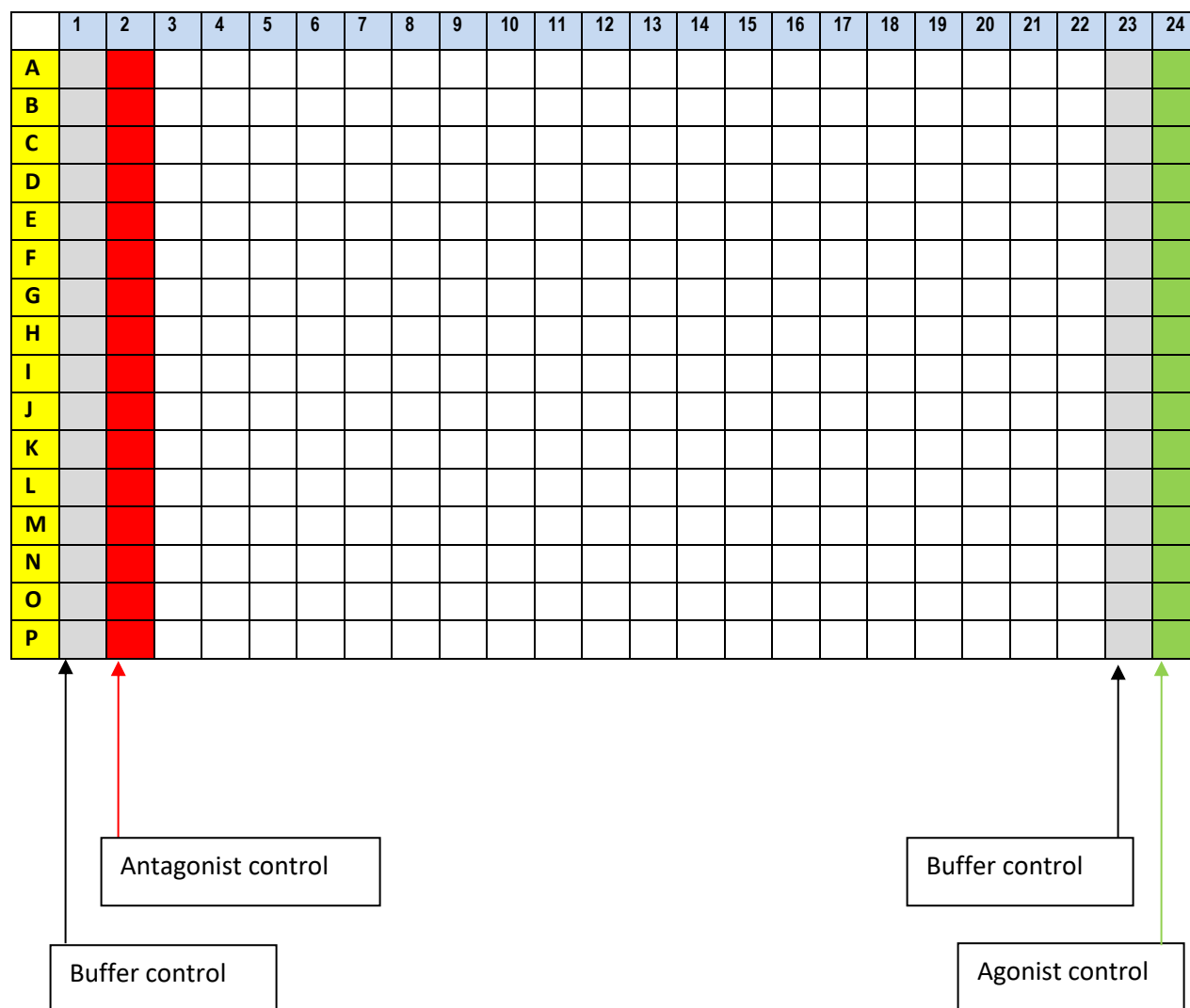


Figure 32. 384-well drug plate map #1 for primary screening: Singlet format (first addition). A total of 320 different compounds can be plated in singlet format in a 384-well drug plate. Columns 1, 2, 23, and 24 are reserved for positive and negative controls.

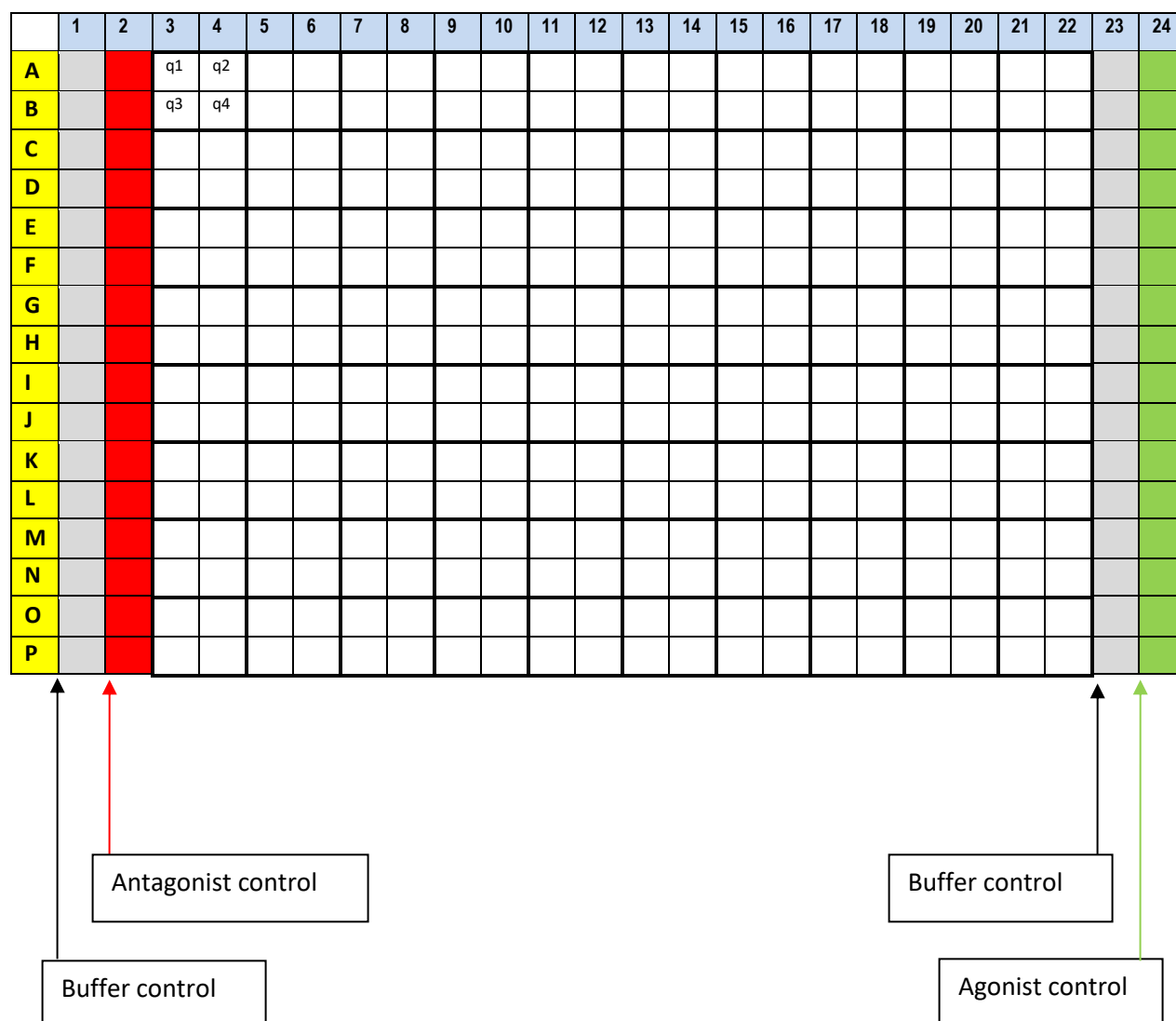


Figure 33. 384-well drug plate map #2 for primary screening: quadrant format (first addition). A total of 80 different compounds can be plated in quadrant format (q1, q2, q3, and q4) in a 384-well drug plate. Columns 1, 2, 23, and 24 are reserved for positive and negative controls.

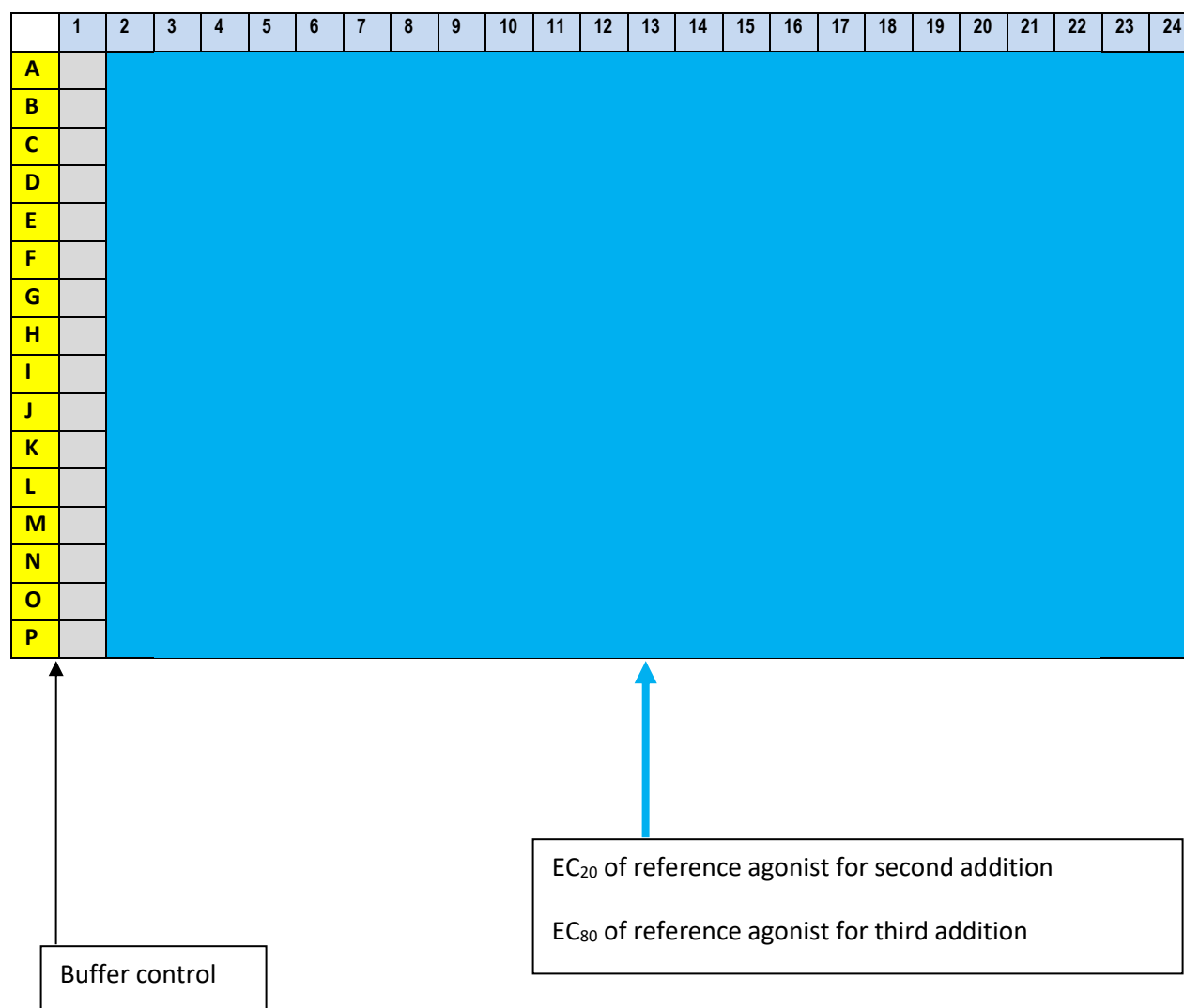


Figure 34. 384-well drug plate map #3: second or third addition in primary screening assays (second addition). Except for Column 1 (which serves as negative control with assay buffer for all additions), all the other wells receive EC₂₀ or EC₈₀ of the reference agonist to determine allosteric potentiator or antagonist activity.

	1	2	3	4	5	6	7	8	9	10	11	12	13	14	15	16	17	18	19	20	21	22	23	24	[X] (M)
A																									0
B																									3E-12
C																									1E-11
D																									3E-11
E																									1E-10
F																									3E-10
G																									1E-09
H																									3E-09
I																									1E-08
J																									3E-08
K																									1E-07
L																									3E-07
M																									1E-06
N																									3E-06
O																									1E-05
P																									3E-05

8	Drug A	Drug B	Drug C	Drug D	Drug E	Drug F	Drug G	Drug H
---	--------	--------	--------	--------	--------	--------	--------	--------

6	Drug A'	Drug B'	Drug C'	Drug D'	Drug E'	Drug F'
---	---------	---------	---------	---------	---------	---------

Figure 35. 384-well drug plate map #4: agonist or antagonist dose-responses for secondary screenings (first addition): Serial dilutions of eight compounds can be made in triplicate (Drug A to H) or six in quadruplicate (Drug A' to F') (indicated below the plate template) from high to low concentrations (final concentrations are indicated to the right of plate template). Either format is used; one of the compounds is a positive control with a known agonist and/or antagonist, such as acetylcholine and/or atropine for muscarinic receptors.

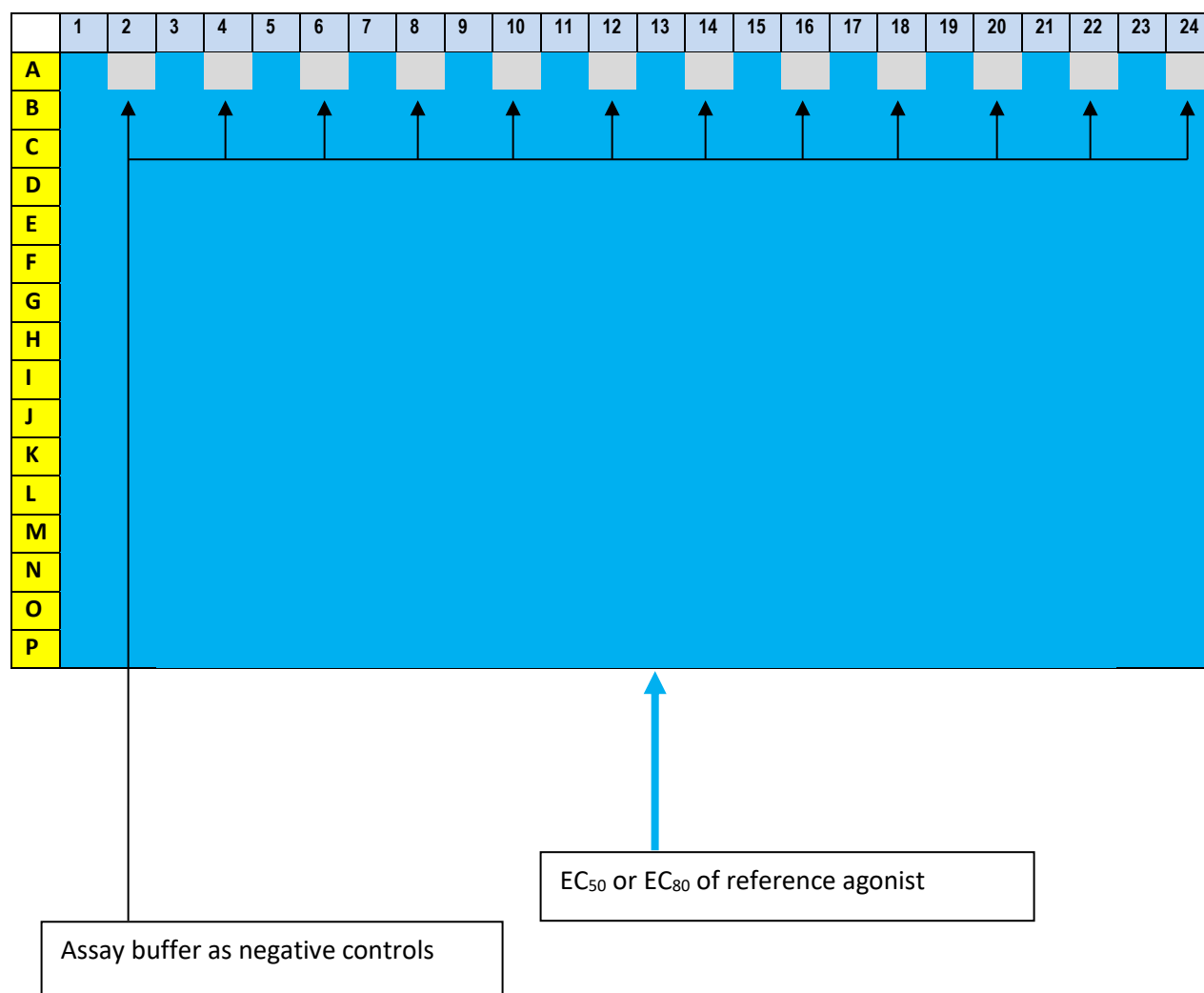


Figure 36. 384-well drug plate map #5: EC₅₀ or EC₈₀ of reference agonist as second addition for antagonist activity (second addition). The even-numbered wells in row A serve as negative controls with assay buffer; while the other wells on the plate contain EC₅₀ or EC₈₀ concentrations of the reference agonist.

	1	2	3	4	5	6	7	8	9	10	11	12	13	14	15	16	17	18	19	20	21	22	23	24
A																								
B																								
C																								
D																								
E																								
F																								
G																								
H																								
I																								
J																								
K																								
L																								
M																								
N																								
O																								
P																								

X	Buffer	30 nM	100 nM	300 nM	1 μ M	3 μ M	10 μ M	30 μ M
---	--------	-------	--------	--------	-----------	-----------	------------	------------

Figure 37. 384-well drug plate map #6 for Schild plot analysis (first addition): Antagonist or allosteric modulator is made in 7 concentrations as indicated below the drug plate template. Each concentration (including the buffer control) has three columns.

	1	2	3	4	5	6	7	8	9	10	11	12	13	14	15	16	17	18	19	20	21	22	23	24	[X] (M)
A																									0
B																									3E-12
C																									1E-11
D																									3E-11
E																									1E-10
F																									3E-10
G																									1E-09
H																									3E-09
I																									1E-08
J																									3E-08
K																									1E-07
L																									3E-07
M																									1E-06
N																									3E-06
O																									1E-05
P																									3E-05

Figure 38. 384-well drug plate map #7 for Schild plot analysis (second addition). Reference agonist is made in the following serial dilutions (as indicated to the right of the drug plate template). Each concentration (including the buffer control) has one complete row.

2.2. General procedures for PDSP functional assays:

In general, PDSP functional assays are carried out in two steps, primary and secondary assays (unless otherwise stated). In primary screening assays, compounds are tested in triplicate or quadruplicate at final concentration of 10 μ M (or 10 μ g/ml for crude extracts) or specific concentrations upon request for agonist and antagonist activities (see 384-well drug plate maps #1, #2, and #3 for detailed setups). Results are normalized and transformed to percentage values. For agonists, the reference agonist activity at 10 μ M is set as 100% and the basal activity with buffer as 0%. **For orphan GPCRs without a known agonist as a reference, activity is expressed as percentage value of basal (with buffer).** For antagonists, the basal activity with buffer is set as 100% inhibition and the activity of an EC₈₀ concentration of the reference agonist as 0% inhibition. For allosteric potentiators, the activity of the EC₂₀ concentration of the reference agonist is set as 0% potentiation. Compounds with a minimum of 30% agonist activity, or 50% antagonist activity, or 30% potentiation above control are flagged for secondary screening (dose-response) assays.

In secondary functional assays, potential agonist hits are tested in full dose-response curves to determine efficacy and potency (see 384-well drug plate map #4). Potential antagonist hits are tested in full dose-response curves to determine IC₅₀ values against EC₅₀ to EC₈₀ concentrations of reference agonist (see 384-well drug plate map #5 for detailed setup). Potential antagonist hits and positive allosteric modulators are further characterized, if necessary, in Schild plot analysis to obtain pK_B values (see 384-well drug plate maps #6 and #7 for detailed setup). Schild plot analysis is designed to obtain full agonist dose-response curves in the absence and presence of increasing concentrations of potential antagonists or allosteric modulators. For those antagonists shifting agonist dose-response curves to the right and also reducing E_{max}, a modified Lew and Angus analysis is applied to obtain pK_B values. For allosteric modulators, secondary dose-response curves are also analyzed using the allosteric operational model to obtain modulation parameters (such as α and β). For studies of ligand functional selectivity and bias among multiple signaling pathways, dose-response results are analyzed using the Black and Leff operational model to quantify bias. Detailed procedures for these secondary assays are given in the following data analysis sections.

Secondary functional assays provide the following parameters for the PDSP database: maximum activation or inhibition after normalization (therefore in percentage values), concentration range used in the assay (lowest and highest concentrations), Hill slope of the dose-response curve, and corresponding potency.

2.3. Data analysis for functional assays

Unless otherwise stated, all functional results are analyzed using GraphPad Prism v5.0 using its built-in functions.

2.3.1: Agonist activity: Functional assay results are plotted against concentrations and analyzed with following 4-parameter built-in agonist dose-response function in GraphPad Prism v5.0.

$$Response = Bottom + \frac{(Top - Bottom)}{1 + 10^{(LogEC_{50} - X)n}}$$

In which, **Top** and **Bottom** are the maximum response (E_{max}) and basal level, respectively; **X** is the agonist concentration and **n** is the Hill slope; **EC₅₀** is the concentration that generated a 50% response.

2.3.2: Antagonist activity: To determine antagonist activity, agonist responses are measured at a fixed EC₈₀ concentration of the reference agonist and in the presence of serial dilutions of the antagonist. Results are fitted with the following inhibitory dose-response function to determine the IC₅₀.

$$Response = Bottom + \frac{(Top - Bottom)}{1 + 10^{(LogIC_{50} - X)n}}$$

The IC₅₀ is then converted to K_i using Cheng-Prusoff equation (7):

$$K_i = \frac{IC_{50}}{1 + \frac{L}{EC_{50}}}$$

in which K_i is the ligand binding affinity determined from antagonist dose-response assay; IC_{50} is the antagonist concentration at which point 50% inhibition is reached; L is the reference agonist concentration used in the assay (usually EC_{50} to EC_{80} concentration of the reference agonist); EC_{50} is the predetermined potency of the reference agonist.

2.3.3. Schild plot analysis: The PDSP has adopted nonlinear regression analysis with the modified Lew and Angus method to estimate antagonist potency pA_2 value. For Schild plot analysis, agonist dose-responses are designed and performed in the absence and presence of 7 concentrations of antagonist in a 384-well plate (see above). Each agonist dose-response is in triplicate. Eight agonist dose-responses share the same X-axis and each set of measured responses is arranged in a Y column titled antagonist concentrations (M). Results are analyzed using the agonist dose-response function as above to determine Bottom and Top values for each dose-response curve. To normalize using Prism's built-in normalization function, the data set is transformed into percentage values with the shared **bottom** as 0% and **Top** of the reference agonist under control conditions as 100%. An equiactive agonist concentration (such as an agonist concentration to generate 20 – 50% response) is selected for all or most curves if possible and corresponding agonist concentrations in the absence and presence of increasing concentrations of antagonist are obtained. Prism 5 has a built-in feature that provides equiactive agonist concentrations if the radio button for “Interpolate unknowns from standard curve” is selected. This feature is at the bottom of the Analyze>Fit tab. The equiactive agonist concentrations are plotted in $-\log$ format (i.e., pEC_{20} or pEC_{50}) against corresponding antagonist (B) concentrations (M). The results are fitted with following equation to obtain $LogK_B$ and n values.

$$Y = -Log(X^n + 10^{LogK_B}) - LogC$$

In which Y is the equiactive agonist concentration in $-\log$ format (such as pEC_{25} or other equally-active agonist concentration values) at corresponding antagonist concentration (X); n is the Schild slope; K_B is the apparent binding affinity of the tested antagonist. The pA_2 value can be calculated from pK_B/n . If $n = 1$ or is not significantly different from 1, $pA_2 = pK_B$, and the tested antagonist is

concluded to be competitive with the agonist; otherwise, antagonist may not be competitive with the agonist.

Representative figures and examples are shown on Pages 169, 170, and 171.

2.3.4. Quantifying bias and functional selectivity analysis (see Pages 171-174). To quantify functional selectivity and bias factors, we analyze functional dose-response results using the Black and Leff operation model as outlined by Kenakin et al., 2012 (137).

$$Response = Basal + \frac{(E_m - Basal)[A]^n \tau^n}{[A]^n \tau^n + ([A] + K_A)^n}$$

Functional dose-response results are analyzed using the above equation in GraphPad Prism V5.0, in which **E_m** is the maximal possible response the system can have, and **basal** is the response in the absence of test drugs (i.e., buffer only). The **E_m** and **Basal** values are usually 100 and 0 if the responses are normalized to percentage of reference activity (100%). **K_A** is the equilibrium dissociation constant of the agonist (**A**), **τ** is the operational agonist efficacy of the agonist (**A**) and is defined as **R_T/K_E** (where **R_T** is the receptor density and **K_E** is the intrinsic efficacy of the agonist (**A**) in a particular signaling pathway, **n** is the transducer slope for the function between agonist occupancy and measured responses. The fitting parameters **E_m** and **n** are cell-specific and should be shared by all agonists that are being tested at the same pathway. **Log(τ/K_A)** is defined as the “transduction coefficient” for a particular agonist at a measured signaling pathway.

To quantify ligand bias (see following equations and steps), drug activity is measured in two or more pathways for a group of ligands (e.g., agonists) to determine corresponding **log(τ/K_A)** values. For each pathway, **Δlog(τ/K_A)** values are calculated by subtracting the reference agonist’s **log(τ/K_A)** (usually the endogenous agonist). The same reference agonist should be used for the different pathways tested. For each agonist, **ΔΔlog(τ/K_A)** values are calculated by subtracting **Δlog(τ/K_A)** for pathway I with the corresponding **Δlog(τ/K_A)** for pathway II. Bias is quantified as **10^{ΔΔlog(τ/K_A)}**. If the value is 1, the agonist has no bias at all; if the value is larger than 1, it is biased towards pathway I; otherwise, it is biased towards pathway II.

Step 1: dose-responses for 2 or more pathways to determine 'transduction coefficient' $\text{Log}(\tau/K_A)$ values for each ligand at each pathway;

Step 2: calculate transduction coefficient difference $\Delta\text{Log}(\tau/K_A)$ between different ligands in the same pathway by subtracting transduction coefficient of the tested sample from that of the reference, usually endogenous, ligand, such as 5-HT for serotonin receptors;

$$\Delta\text{Log}\left(\frac{\tau}{K_A}\right) = \text{Log}\left(\frac{\tau}{K_A}\right) \text{ of sample} - \text{Log}\left(\frac{\tau}{K_A}\right) \text{ of reference}$$

Step 3: calculate transduction coefficient difference $\Delta\Delta\text{Log}(\tau/K_A)$ between the different pathways for the same tested ligand by subtracting the $\Delta\text{Log}(\tau/K_A)$ for one pathway from that of the other pathway;

$$\Delta\Delta\text{Log}\left(\frac{\tau}{K_A}\right) = \Delta\text{Log}\left(\frac{\tau_1}{K_{A1}}\right) - \Delta\text{Log}\left(\frac{\tau_2}{K_{A2}}\right)$$

Step 4: calculate bias factor as below:

$$\text{Bias} = 10^{\Delta\Delta\log\left(\frac{\tau}{K_A}\right)}$$

Step 5: to determine if the calculated bias is statistically significant, a statistical analysis is done with $\Delta\Delta\text{Log}(\tau/K_A)$ values. In addition to the comprehensive methods to estimate SEM values as outlined by Kenakin (137), an alternative (and simpler) method to estimate SEM values is given below, as suggested by Christopoulos et al. (138).

To calculate sem for $\Delta\log(\tau/K_A)$:

$$\text{SEM} = \sqrt{\text{Sample sem}^2 + \text{Reference sem}^2}$$

To calculate sem for $\Delta\Delta\log(\tau/K_A)$:

$$\text{SEM} = \sqrt{\text{pathway I sem}^2 + \text{pathway II sem}^2}$$

2.3.5. Allosteric operational analysis (see Figure 44 on p. 175 for an example). For ligands with allosteric modulator activity, we apply the allosteric operational model to analyze functional results. The functional assay is carried out in the same way as for Schild plot analysis (**Section 2.3.3**), in which the orthosteric agonist dose-response is measured in the absence and presence of increasing concentrations of a potential allosteric modulator. Results are then analyzed with the following equation as described by Leach et al., 2007 (139).

$$Effect = Basal + \frac{(E_{Max} - Basal) (\tau_A[A](K_B + \alpha\beta[B]) + \tau_A[B]K_A)^n}{([A]K_B + K_AK_B + K_A[B] + \alpha[A][B])^n + (\tau_A[A](K_B + \alpha\beta[B]) + \tau_B[B]K_A)^n}$$

In which **Effect** is the measured functional readout in the presence of the orthosteric agonist [**A**] and the allosteric modulator [**B**]; **E_{max}** is the maximal possible system activity; **K_A** and **K_B** are the equilibrium binding affinity for the orthosteric agonist (**A**) and the allosteric modulator (**B**), respectively; **α** and **β** are the allosteric effects on ligand binding (mutual effect between **A** and **B**) and agonist efficacy (with **α** = 1 for neutral cooperativity; **α** >1 for positive cooperativity; **α** <1 for negative cooperativity); **τ_A** and **τ_B** are the capacity of the orthosteric agonist (**A**) and the allosteric ligand (**B**) to exhibit agonism, respectively; **n** is a slope fitting factor.

When doing non-linear least-square regression curve-fitting in Prism v5.0, the **E_{max}** values should be shared for all assays carried out under the same conditions, and should be set to a fixed value which is the maximal system efficacy. **K_A** should be the equilibrium binding affinity and can be estimated by a radioligand binding assay. If the tested allosteric modulator itself has no agonist activity, then **τ_B** = 0. See **Figure 41** on p. 148 for a representative figure.

2.3.6. List of different functional assays PDSP carries out routinely:

- Calcium mobilization assay with FLIPR^{TETRA} for G_q coupled GPCRs.
- Intracellular inositol phosphate accumulation assay.
- Split luciferase-based biosensor cAMP assay for G_i or G_s coupled GPCRs.
- GPCR Tango assay for G-protein independent β -arrestin translocation.
- PRESTO-Tango GPCRome screening
- FluxOR assay for hERG potassium channel function.
- PatchXpress automated patch clamp assay for hERG potassium channels.
- Neurotransmitter transporter assays for DAT, NET, and SERT.
- ⁸⁶Rb⁺ efflux assays for nAChRs
- Multidrug resistance transporter-1 (MDR-1) assay
- Enzyme activity assays
 - HDAC assay
 - MAO A and B assay
 - PKC assay
 - CHK2 assay
- Nicotinic acetylcholine receptors (nAChRs) activity assay (⁸⁶Rb⁺ efflux)

2.4. Functional assays for G_q coupled GPCRs

2.4.1. Calcium mobilization assays (with FLIPR^{TETRA})

Main equipment: FLIPR^{TETRA} from Molecular Devices (Sunnyvale, CA)

Main reagents: Fluo-4 Direct[®] from Invitrogen (Carlsbad, CA)

FLIPR Drug buffer: 20 mM HEPES, 1x HBSS, 2.5 mM Probenecid, pH 7.40, room temperature

2.4.1.1. Cell culture: Cells, either stably expressing target receptors or transiently transfected with target receptor DNA (see below for transfection protocol) are grown overnight, and then plated into Poly-L-Lysine (PLL) coated 384-well black clear bottom cell culture plates with DMEM supplemented with 1% dialyzed FBS (dFBS) and at density of 15 – 20K cells in a volume 40 µl per well. The plates are cultured for a minimum of 6 hours, or overnight, before assays.

2.4.1.2. Calcium Precipitation transfection: The calcium phosphate transfection method (1, 140, 141) is used for most transfections in PDSP assays, mainly with HEK 293T cells. HEK 293T cells are subcultured into either 10-cm dishes (3 million cells per dish) or 15-cm dishes (8 million cells per dish) and incubated overnight. Alternatively, HEK 293T cells are seeded at density of 6 million per 10-cm dish 4 hours prior to transfection. For each 10-cm dish of HEK 293T cells, 10 µg receptor DNA construct in 440 µl distilled water is mixed with 60 µl of 2 M CaCl₂; the DNA/CaCl₂ solution is then added dropwise into 500 µl 2x HBS solution (50 mM HEPES, 280 mM NaCl, 10 mM KCl, 1.5 mM Na₂HPO₄, pH 7.00) while shaking. The mixture is incubated at room temperature for 10 min, then added to cells dropwise, which are then incubated overnight. For transfections in 15-cm dishes, reagents and DNA amounts are increased by 2.5 fold per dish.

2.4.1.3. Calcium mobilization assays with FLIPR^{TETRA}. The protocol for calcium release assays with the FLIPR^{TETRA} is modified from previously published procedures (142, 143). On the day of assay, medium is removed and cells are loaded with 20 µl/well of 1x Fluo-4 Direct Calcium dye (prepared in FLIPR drug buffer). Plates are incubated for 60 min at 37°C, followed by 10 min incubation at room temperature in the dark, and then loaded into the FLIPR. The FLIPR is programmed to take 10

readings (1 read per second) initially as a baseline before addition of 10 μ l of 3x drug solutions. The fluorescence intensity is recorded for 2 minutes after drug addition (first addition, see 384-well drug plate maps #1 and #2 for detailed setup) for agonist activity. To measure antagonist activity, drug stocks are prepared at 4x final concentration, added as above for potential effects on basal levels for 2 minutes first, followed by a 10 min incubation before addition of 10 μ l of 4x of reference agonist at final concentration equal to the EC₈₀ (see 384-well drug plate map #3) to measure remaining agonist activity. To detect positive allosteric modulator activity, the second addition is a 4x concentration of reference agonist at final concentration equal to the EC₂₀ (usually endogenous agonist, see 384-well drug plate map #3) to determine effects on agonist activity. The EC₂₀ or EC₈₀ concentrations are predetermined separately using the same batch of transfected cells. Before the second and/or third additions, FLIPR is programmed to wash tips, first with 10% EtOH, and then with distilled water while recording fluorescence intensity. The incubation time between each addition can be adjusted accordingly to accommodate any preincubation requirements.

2.4.1.4. Schild analysis: To further examine antagonist activity at a particular receptor, we also carry out agonist dose-response studies in the absence and presence of 7 concentrations of selected PDSP compounds. In brief, cell plates are prepared in the same way as for primary or secondary functional assays using PLL-coated 384-well black clear bottom cell culture plates with DMEM + 1% dFBS for a minimum of 6 hours, or overnight. Selected antagonist drug plates are prepared as shown in the above 384-well drug map #6, and are used for the first addition to determine if the testing drug has any effect on basal levels. Reference agonist drug plates are prepared as shown in above 384-well drug map #7, and are used for the second addition to measure effect of antagonist on remaining agonist activity.

2.4.1.5. FLIPR data processing: In calcium mobilization assays with the FLIPR^{TETRA}, every well of the 384-well plate has its own basal activity, defined as the average value of the 10 readings before corresponding drug addition. We take maximal fluorescence intensity readings (RFU, Relative Fluorescence Units) within a minute after drug addition as the agonist activity and these values are exported in the format of “fold of basal” using FLIPR’s ScreenWorks® built-in batch export function. Normalization, when needed, is carried out using Prism’s built-in normalization function, in which

basal is transformed to 0% and the E_{max} of the reference agonist in the same assay plate is transformed to 100%.

2.4.2. Intracellular inositol phosphate accumulation for G_q coupled GPCRs

2.4.2.1. Primary screening assays – Single concentration and data analysis: Each new compound is tested on all receptors at a single concentration (10 μ M) for activity as an agonist or an antagonist. Testing for antagonism is performed in presence of the EC₅₀ concentration of a typical agonist (as described above). Each compound is tested in duplicate in two separate experiments performed on different lots of cells. In addition to the tested compounds, each 96-well plate contains wells for determination of basal activity, maximal agonist stimulation, agonist EC₅₀ concentrations (i.e., concentration-response isotherm), and the IC₅₀ concentration of a known antagonist for purposes of positive control and for activity calculations. The reported results for each compound are calculated for agonists as the % of maximal activity (as obtained with maximal agonist concentrations) and for antagonist as the percent of inhibition of receptor activity (in presence of an EC₅₀ concentration of the agonist). Results are expressed as means \pm SEM from four replicates.

2.4.2.2. Secondary screening assays: Dose-responses and data analysis. Compounds determined to be active as agonists or antagonists may be tested for their potency in concentration-response experiments. Six-point concentration-response curves are done in duplicate twice on two separate lots of cells (sometimes a third curve may be needed if, in the first experiment, the range of concentrations used is outside of the active range). For antagonists, these curves are performed in the presence of the EC₅₀ concentration of the agonist. For each compound, the results from four replicates are averaged, and then either EC₅₀ or IC₅₀ values are calculated by non-linear regression using the 4-parameter logistic equation as indicated in **Section 2.3**. Results are reported as EC₅₀ or IC₅₀ values for each tested compound (and receptor), and also include the EC₅₀ or IC₅₀ values of a known agonist or antagonist for comparison purposes.

2.4.2.3. The following table lists GPCRs for which the PDSP has validated functional assays to measure G_q protein activation via calcium mobilization using FLIPR^{TETRA} or intracellular inositol phosphate accumulation. Representative results are analyzed using Prism v5.0.

Table 27. List of GPCRs for which the PDSP has validated G_q protein mediated calcium mobilization or inositol phosphate (IP) accumulation assays, and their pharmacological parameters. The PDSP will also develop additional calcium mobilization assays for other GPCRs upon request and approval. Assays are carried out according to the above procedures and results are analyzed in Prism. Representative results are from single assays done either in triplicate or quadruplicate.

Receptor	Cell line	Ligands * (references)	E _{max} (fold)	pEC ₅₀ (EC ₅₀ nM) pIC ₅₀ (IC ₅₀ nM)	Hill slope
M ₁	CHO	Acetylcholine	3.4	8.69 (2.1)	1.58
M ₁ D	CHO	CNO (37)	1.5	7.66 (21.8)	0.84
M ₃	CHO	Acetylcholine	2.8	8.91 (1.2)	0.95
M ₃ D	Flp-In CHO	CNO	2.7	7.44 (36.1)	1.01
M ₅	CHO	Acetylcholine	3.4	8.25 (5.6)	1.03
M ₅ D	CHO	CNO	2.1	7.44 (36.5)	0.82
5-HT _{2A}	Flp-In HEK	5-HT	2.4	8.82 (1.5)	1.19
		Ketanserin (antagonist)	2.5	6.80 (159)	-2.92
5-HT _{2B}	Flp-In HEK	5-HT	4.8	8.85 (1.4)	1.25
		Clozapine (antagonist)	2.3	7.43 (37.1)	-1.65
5-HT _{2C} INI	Flp-In HEK	5-HT	3.3	10.11 (0.7)	1.89
		Clozapine (antagonist)	3.3	6.37 (432)	-3.31
5-HT _{2C} VNV	Flp-In HEK	5-HT	2.5	9.26 (0.5)	1.53
5-HT _{2C} VSV	Flp-In HEK	5-HT	5.7	9.08 (0.8)	1.87
α _{1A}	Fibroblast, rat	Norepinephrine	2.3	8.34 (4.5)	1.89
α _{1B}	Fibroblast, rat	Norepinephrine	1.6	8.76 (1.7)	0.86
α _{1D}	Fibroblast, rat	Norepinephrine	4.1	8.61 (2.4)	1.14
AT _{1A}	HEK	Angiotensin II	1.8	9.39 (0.4)	0.72
BB ₁	HEK T	Bombesin	5.6	7.82 (15.3)	1.36
		BIM 187	5.7	7.21 (61.1)	1.73
		Neuromedin B	5.5	8.40 (4.0)	1.40
BB ₂	HEK T	Bombesin	4.4	8.76 (1.7)	0.67
		BIM 187 (144)	4.7	8.49 (3.3)	0.95
		Neuromedin B	4.6	6.58 (262)	1.29
B ₂	HEK T	Bradykinin	1.7	9.57 (0.3)	0.88
CCK ₁	HEK T	Gastrin	4.1	9.83 (0.15)	1.29
CCK ₂	HEK T	Gastrin	4.2	9.84 (0.14)	1.17
Ghrelin	HEK	L-692,585	1.7	9.05 (0.9)	0.80

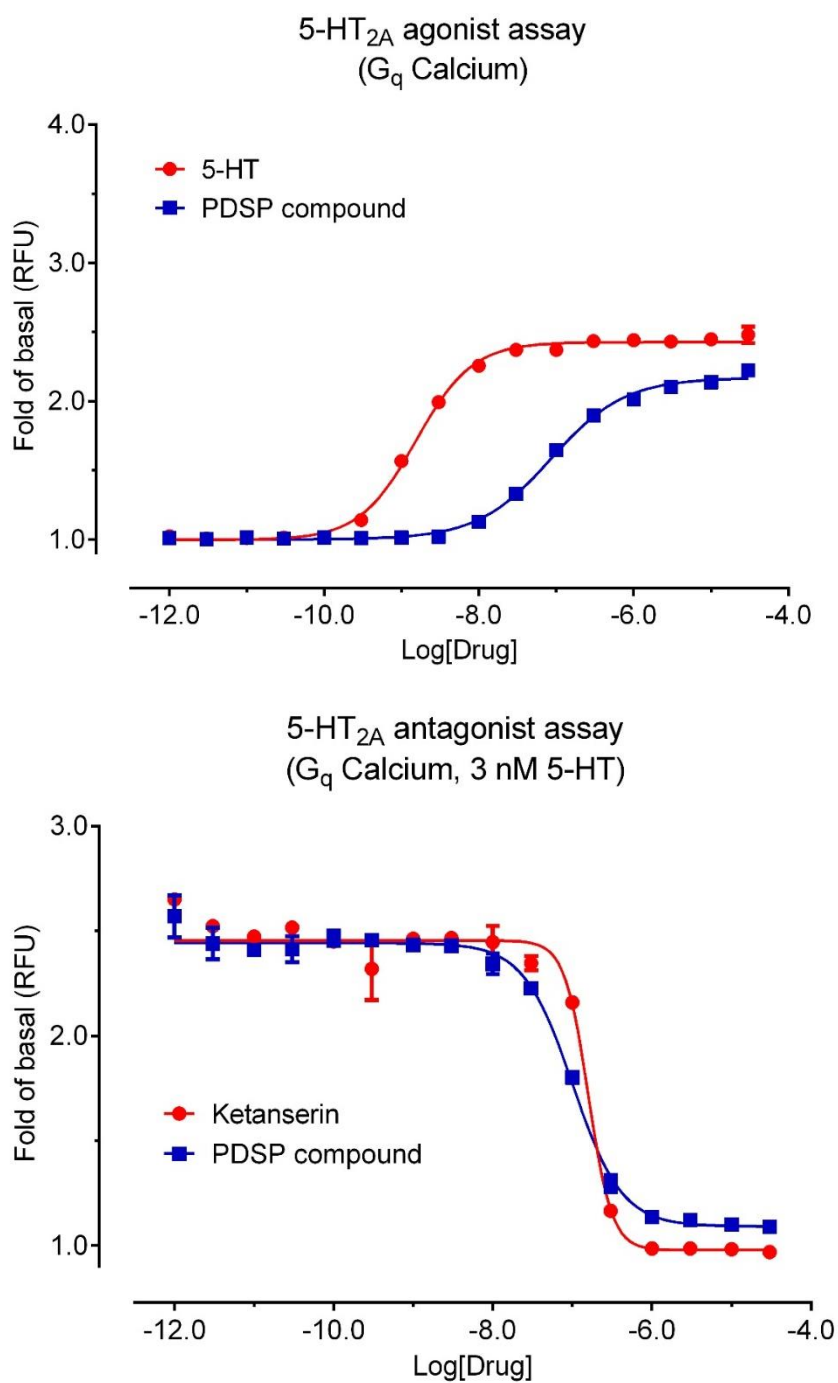
Receptor	Cell line	Ligands * (references)	E _{max} (fold)	pEC ₅₀ (EC ₅₀ nM) pIC ₅₀ (IC ₅₀ nM)	Hill slope
H ₁	HEK	Histamine	2.4	7.77 (16.9)	1.22
H ₂	HEK T	Histamine	1.5	6.24 (577)	1.42
mGlu ₁	HEK	L-Glutamate	3.8	6.02 (964)	2.20
		FTIDC (antagonist)	3.6	7.93 (11.7)	-1.82
mGlu ₅	HEK	L-Glutamate	2.3	5.89 (1397)	2.27
		MTEP (antagonist)	2.3	8.03 (9.4)	-0.63
NK ₁	HEK	Substance P	2.7	7.64 (22.8)	0.79
NK ₂	HEK	Neurokinin A	4.7	7.56 (27.6)	0.66
NK ₂	HEK	Neurokinin B	4.4	6.90 (123)	0.79
NK ₃	HEK	Neurokinin B	4.0	8.41 (3.9)	0.83
NTS ₁	HEK	Neurotensin	3.5	7.99 (10.1)	0.78
		JMV-449 (145)	3.5	8.76 (1.8)	0.93
P2Y ₁	1321N1	ADP	3.1	6.65 (226)	1.31
		UTP	2.0	5.94 (1140)	1.10
P2Y ₂	1321N1	ATP	2.1	6.88 (132)	1.26
		ADP	2.1	5.48 (3306)	1.59
		UTP	1.9	8.03 (9.5)	1.54
		UDP	1.9	5.47 (3400)	1.50
P2Y ₄	1321N1	UTP	2.4	7.65 (22.3)	1.60
		UDP	2.4	5.22 (6088)	1.63
P2Y ₆	1321N1	ATP	1.7	4.59 (25470)	3.17
		ADP	3.5	5.26 (5517)	2.04
		UTP	3.6	7.33 (46.8)	1.22
P2Y ₁₁	1321N1	ATP	3.6	5.70 (2009)	1.78
		UTP	1.9	5.80 (1579)	1.12
PAR1	KOLF, mouse	TRAP	3.9	6.86 (138)	1.17
PAF	HEK	PTAF	1.9	8.06 (87.4)	0.65
V _{1A}	CHO	Vasopressin	3.7	8.09 (8.1)	0.77
		Oxytocin	3.2	5.66 (2193)	1.55
V _{1B}	CHO	Vasopressin	3.3	8.20 (6.3)	0.99
		Oxytocin	3.1	5.42 (3849)	2.03
V ₂	CHO	Vasopressin	2.7	7.42 (38.2)	1.57
OT	CHO	Oxytocin	3.1	7.29 (51.0)	1.21
GPR39	HEK T	GPR39-C3 (146–148)	1.4	6.08 (83.1)	2.72
GPR40	HEK T	GW9508 (149, 150)	1.6	6.53 (294)	0.54
		AS2034178 (151)	1.6	5.85 (1423)	0.72
		AM4668 (152)	1.7	6.93 (118)	0.42
GPR41	HEK T	Propionate	4.1	7.18	
GPR43	HEK T	Propionate		6.43	

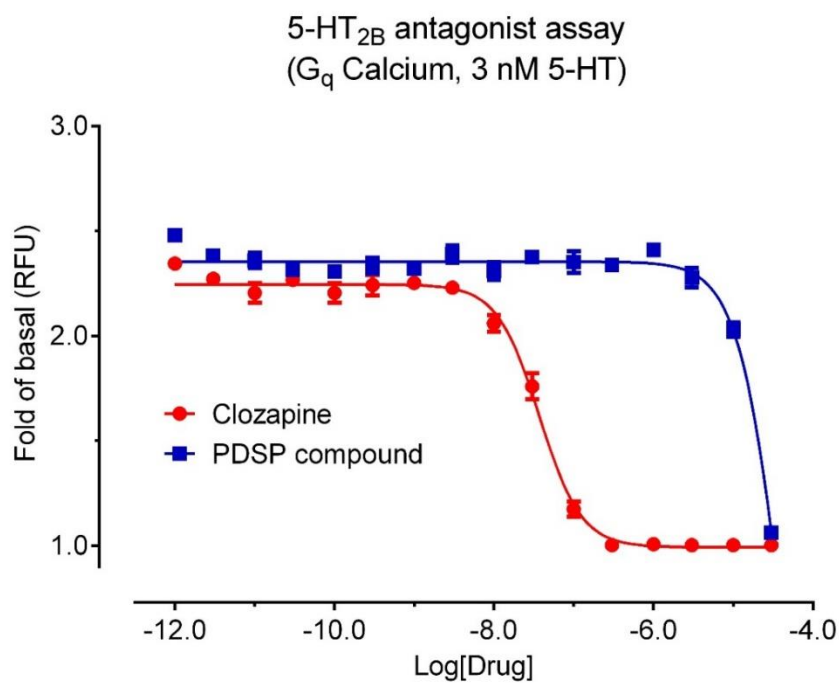
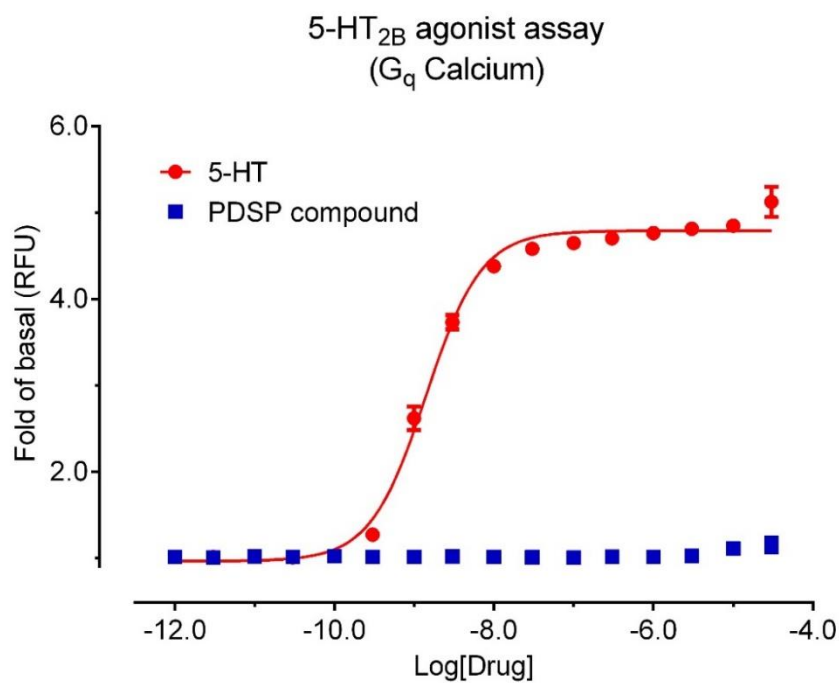
Receptor	Cell line	Ligands * (references)	E _{max} (fold)	pEC ₅₀ (EC ₅₀ nM) pIC ₅₀ (IC ₅₀ nM)	Hill slope
MRGPRX2	Flp-In HEK	TAN-67 (153)	4.5	6.25 (557)	1.02
MRGPRX4	Flp-In HEK	Nateglinide (154)	4.3	5.66 (2208)	3.00

Notes

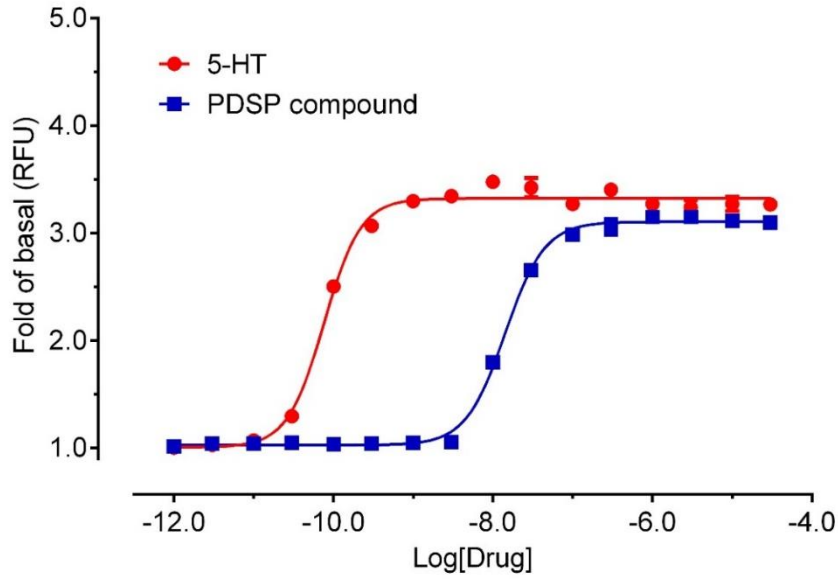
*: Reference antagonist in antagonist assays is indicated individually

Figure 39. Representative dose-response curves of calcium mobilization for G_q -coupled GPCRs, obtained from the FLIPR^{TETRA}. Some curves are presented after normalization with reference agonist activity as 100% and basal as 0%.

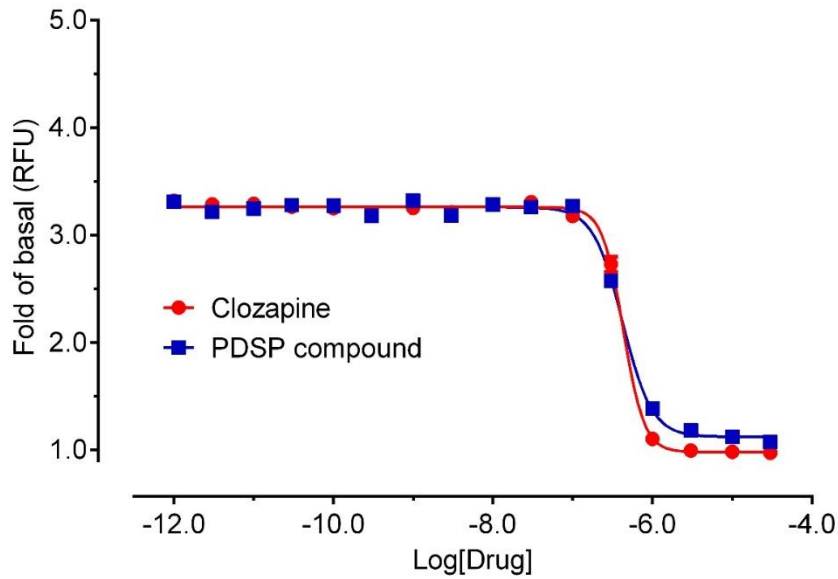




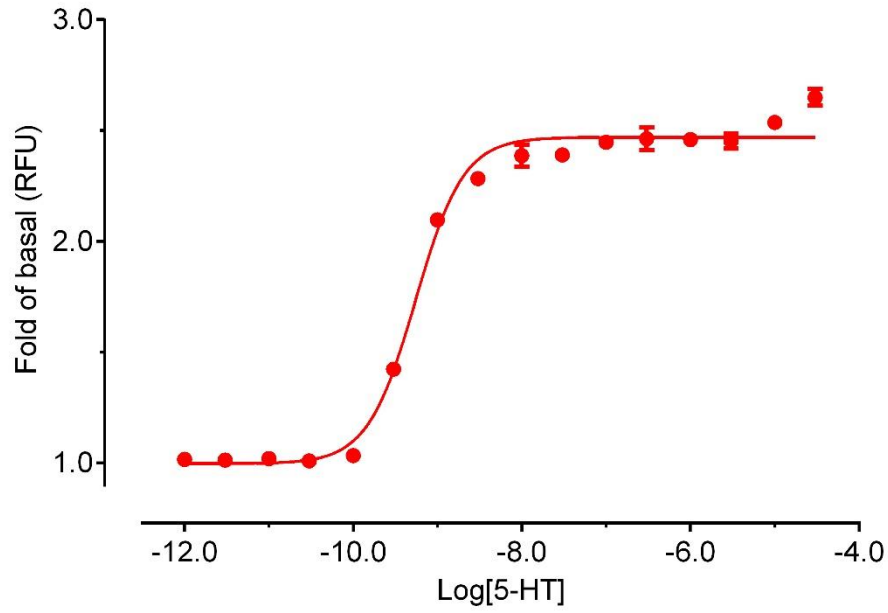
5-HT_{2C} agonist assay
(G_q Calcium)



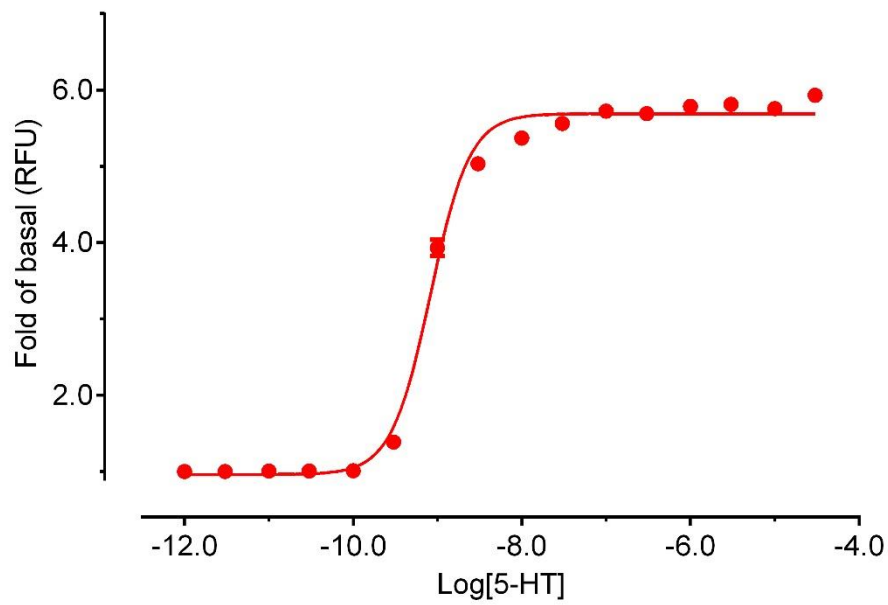
5-HT_{2C} antagonist assay
(G_q Calcium, 3 nM 5-HT)

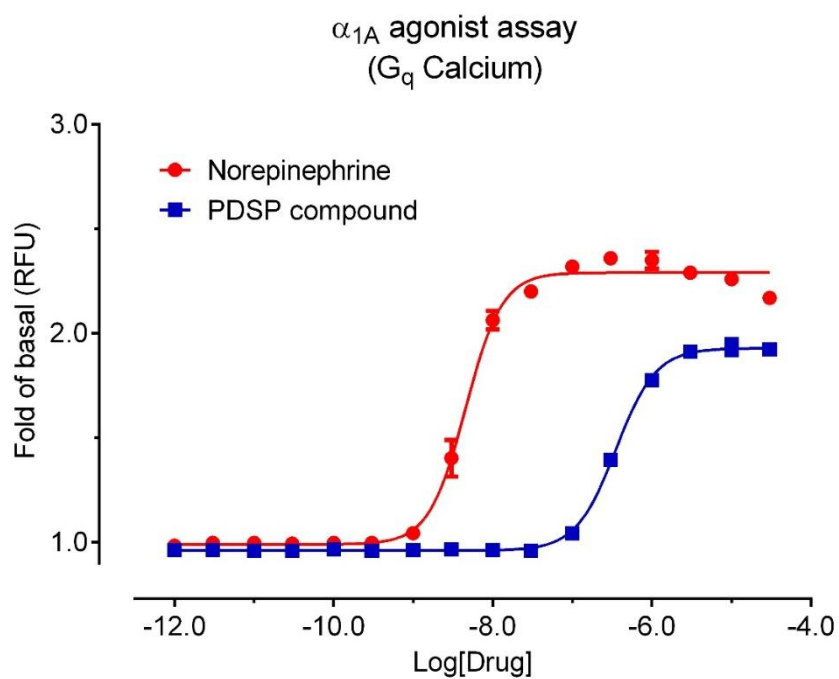
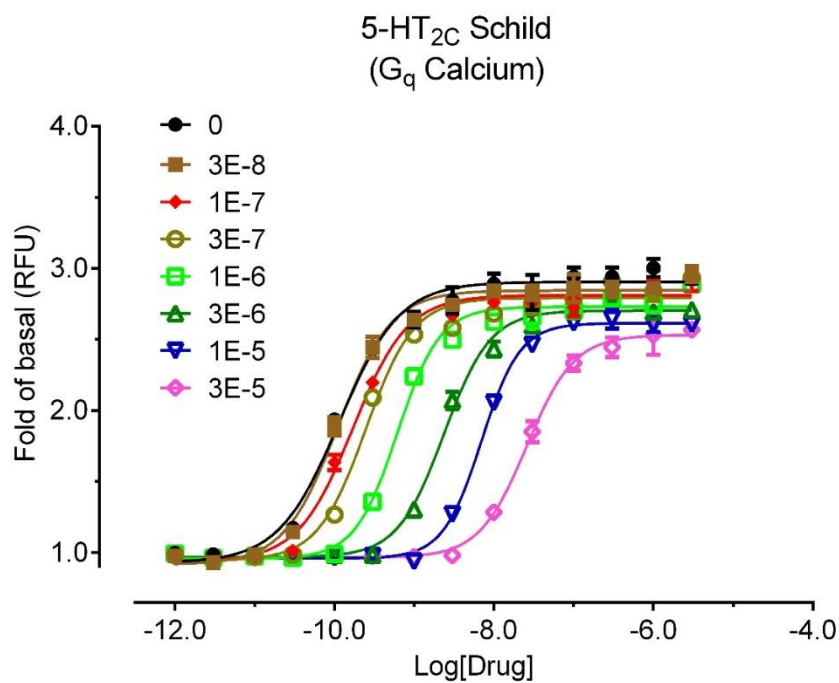


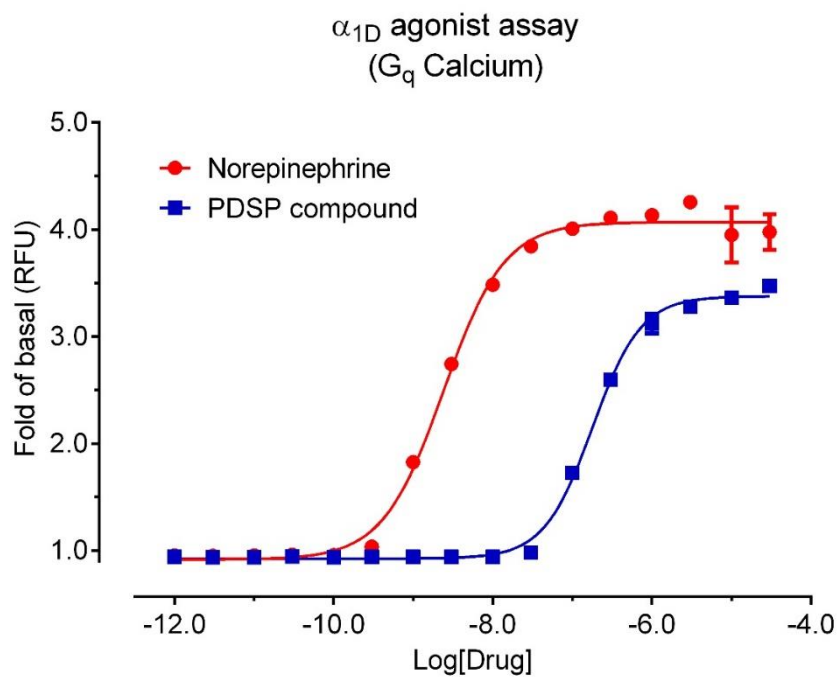
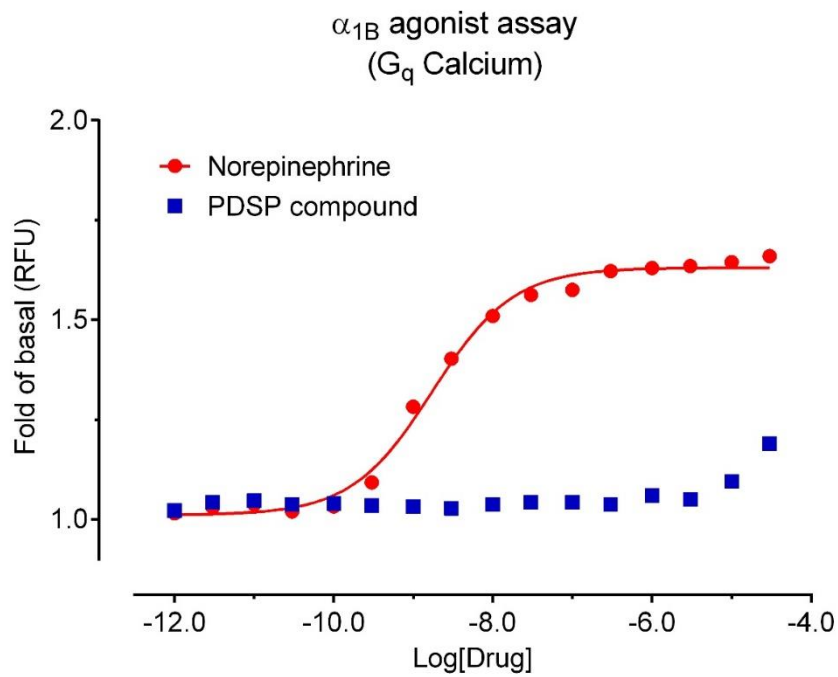
5-HT_{2C} VNV agonist assay
(G_q Calcium)



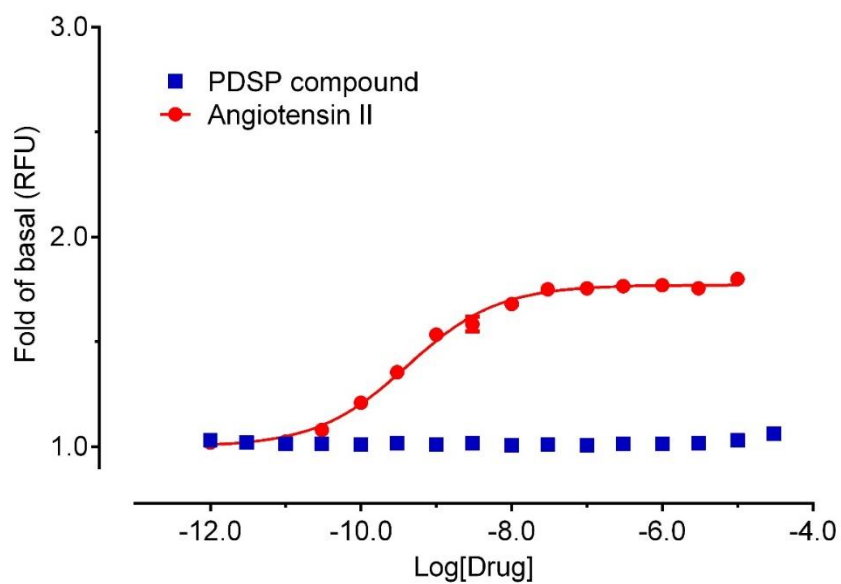
5-HT_{2C} VSV agonist assay
(G_q Calcium)



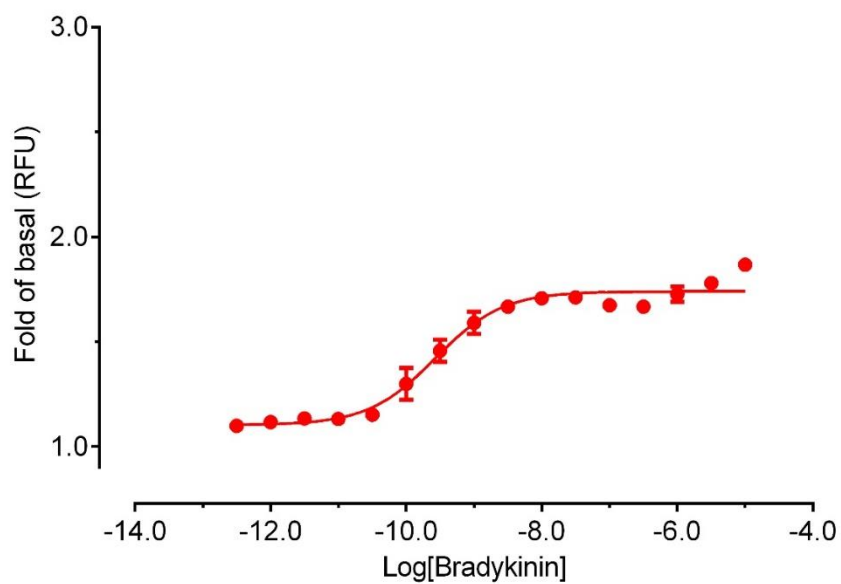


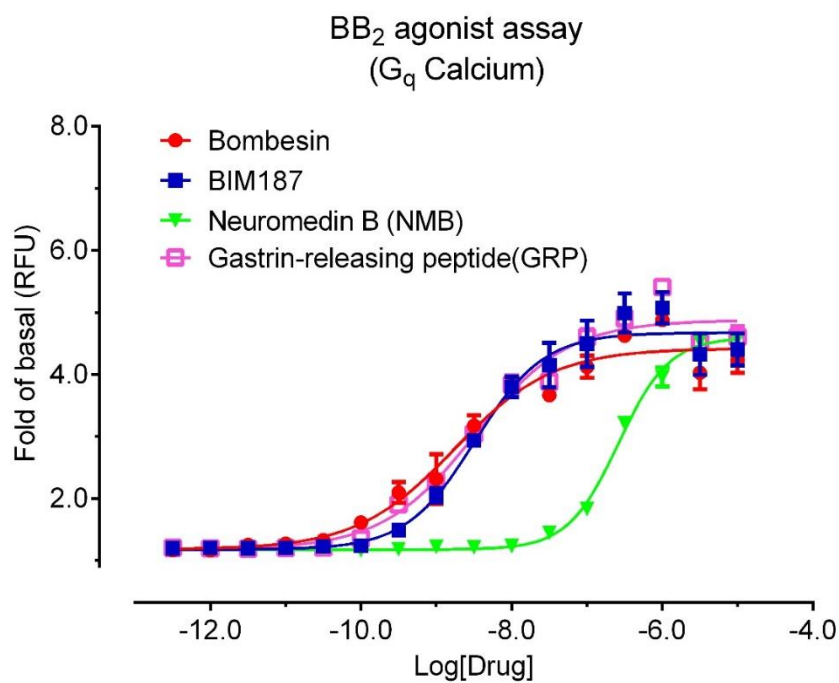
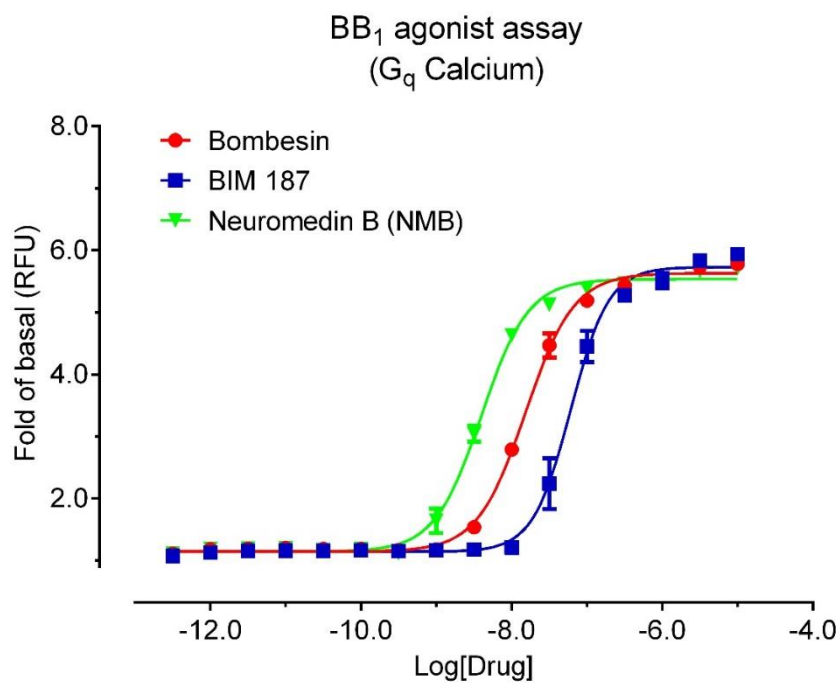


AT₁ agonist assay
(G_q Calcium)

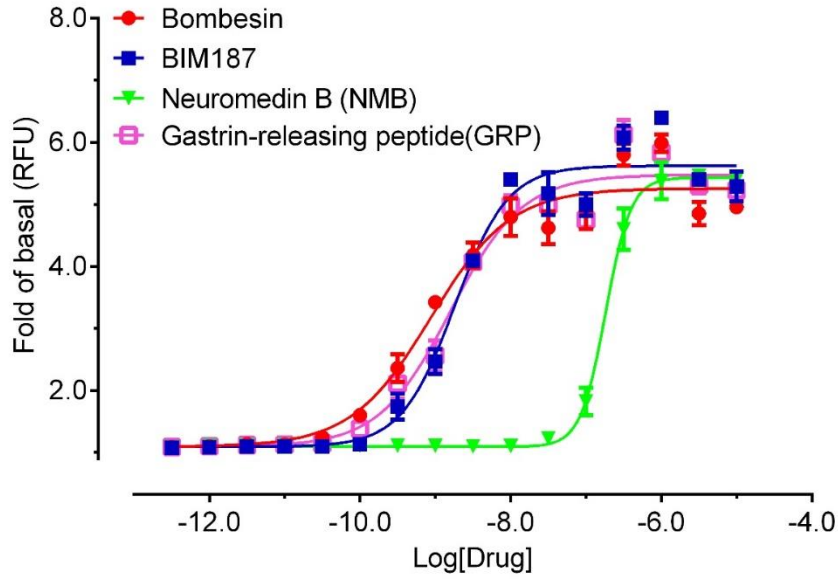


B₂ agonist assay
(G_q Calcium)

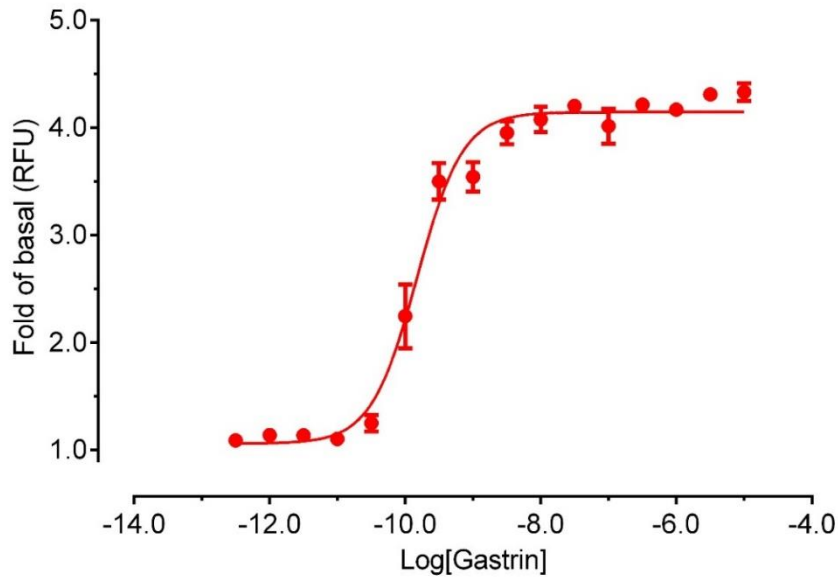


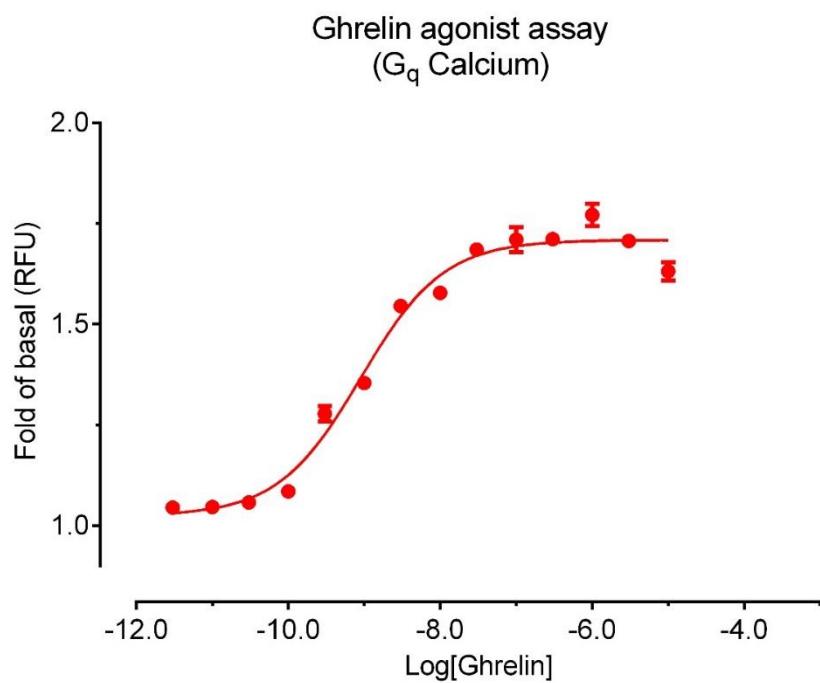
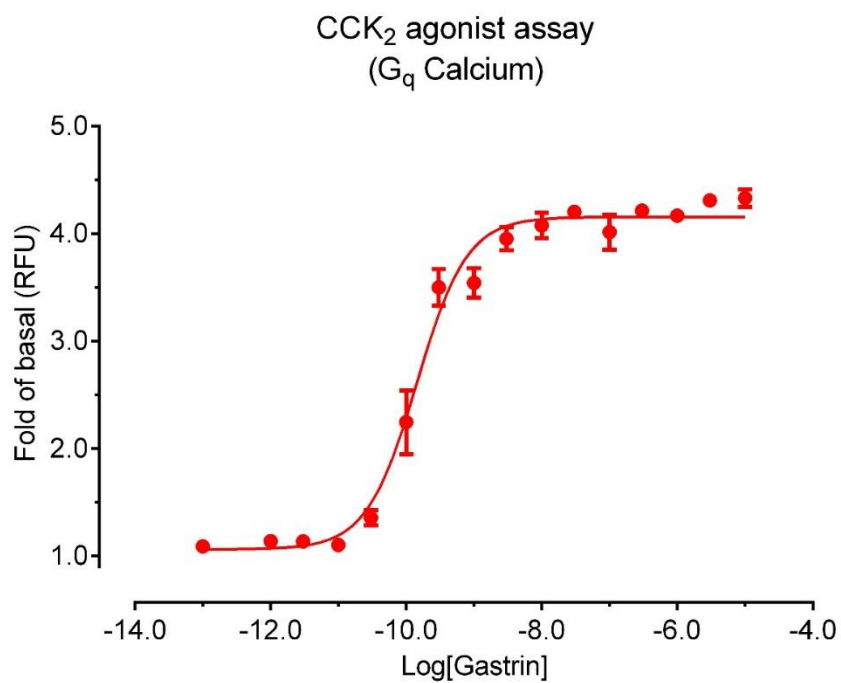


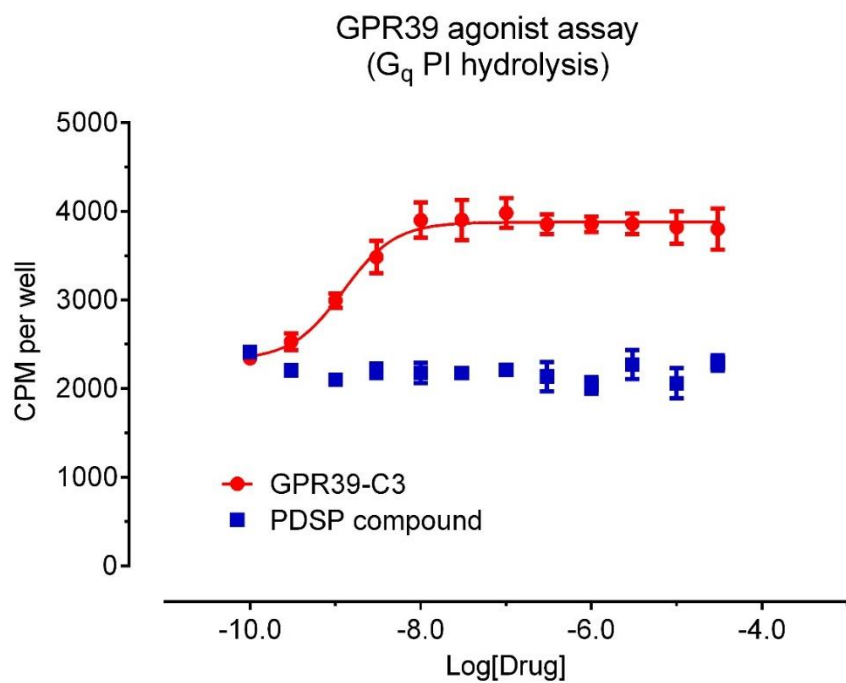
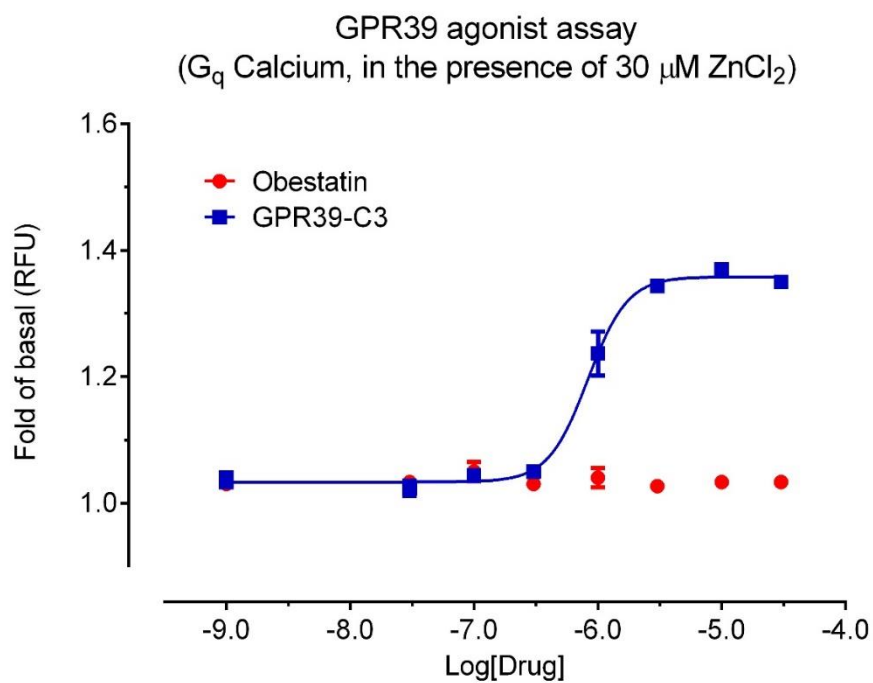
Mouse BB₂ agonist assay
(G_q Calcium)



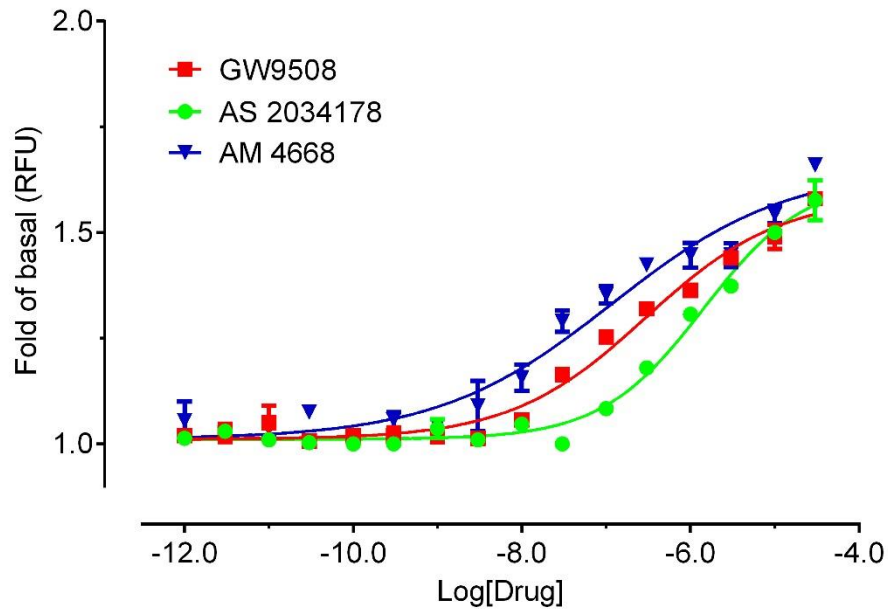
CCK₁ agonist assay
(G_q Calcium)



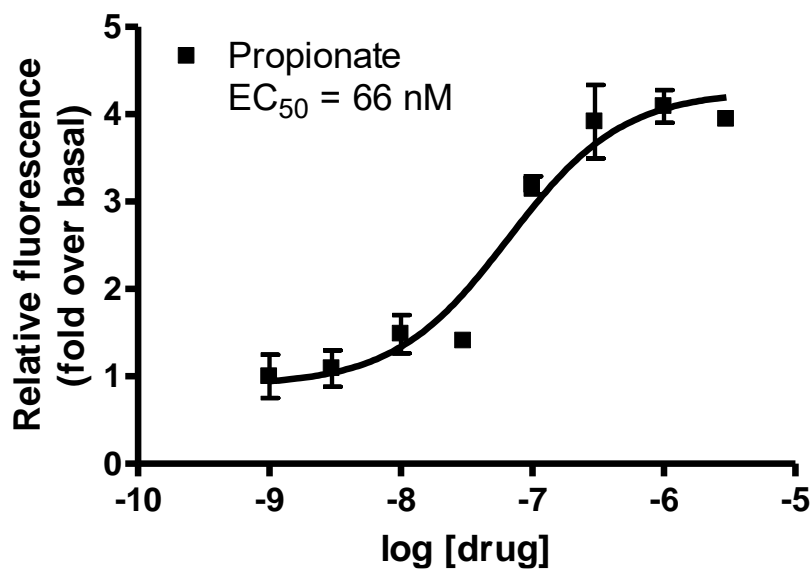




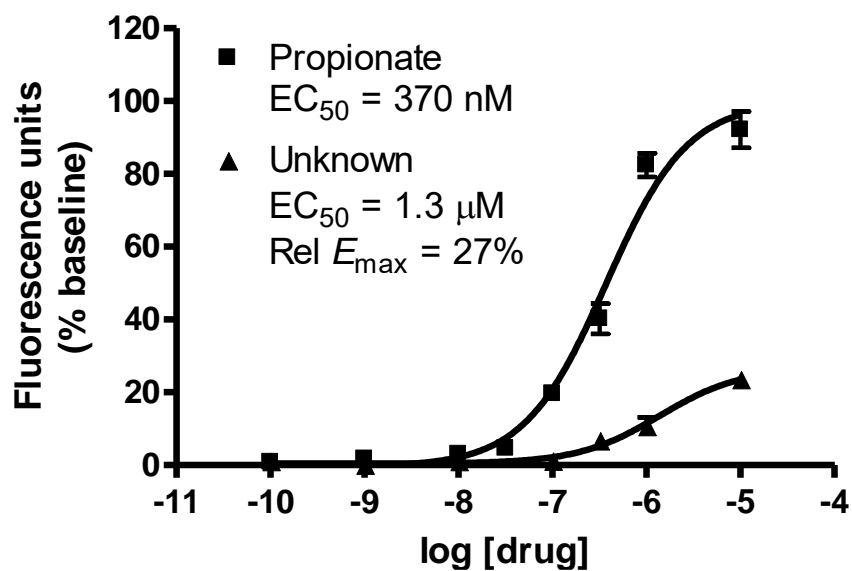
FFA1 agonist assay
(G_q Calcium, GPR40)



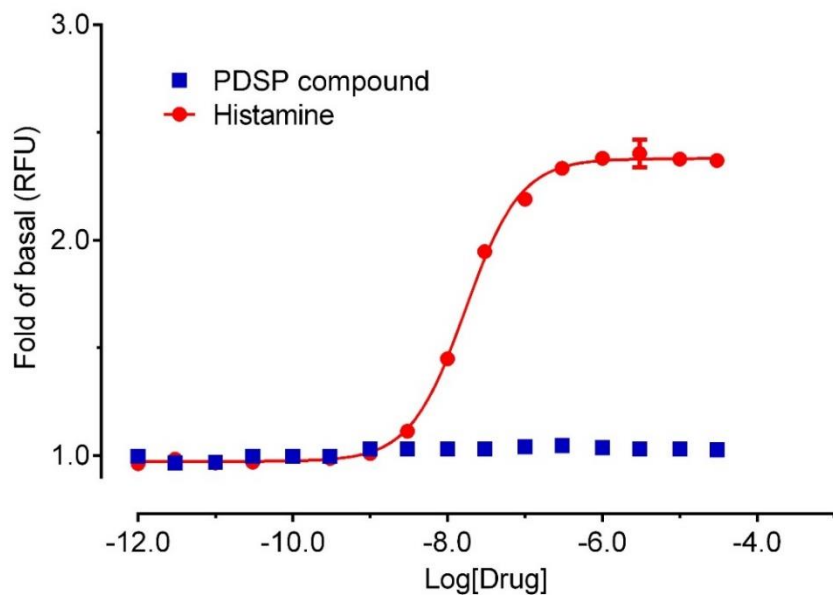
GPR41 Receptor
Hank's Balanced Salt Solution,
20 mM HEPES, 2.5 mM probenecid

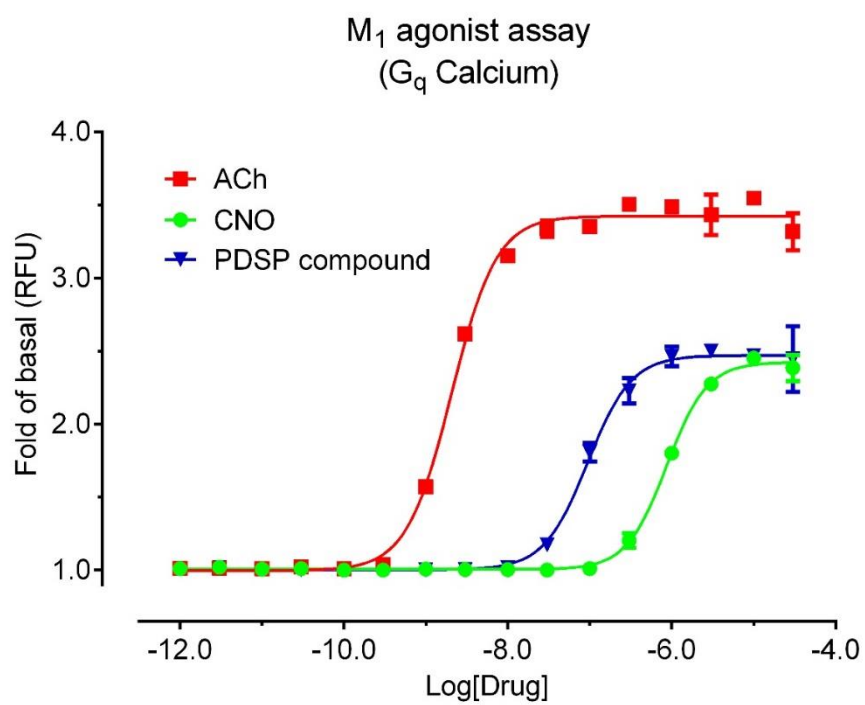
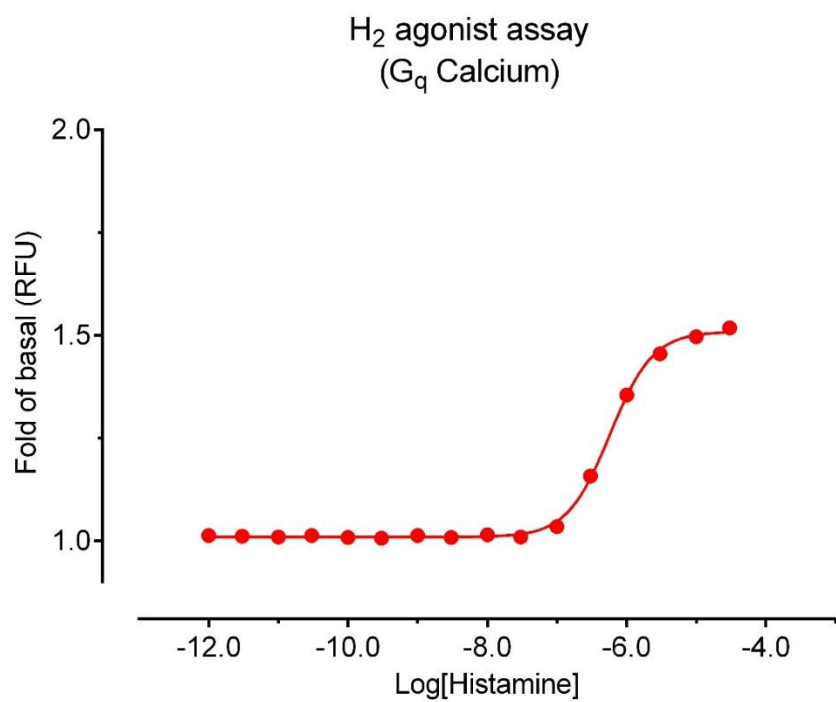


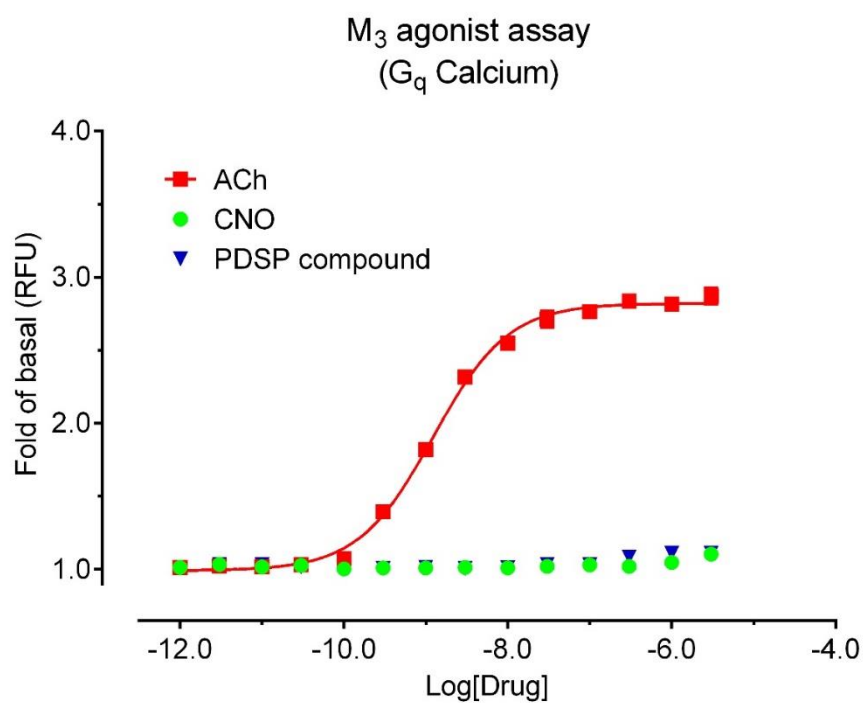
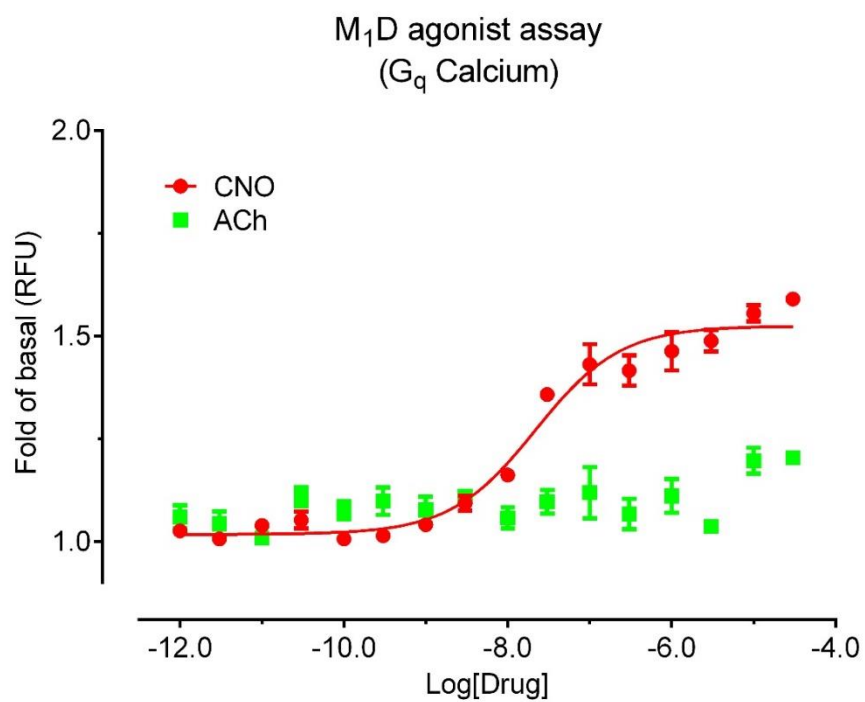
GPR43 Receptor
Hank's Balanced Salt Solution,
20 mM HEPES, 2.5 mM probenecid

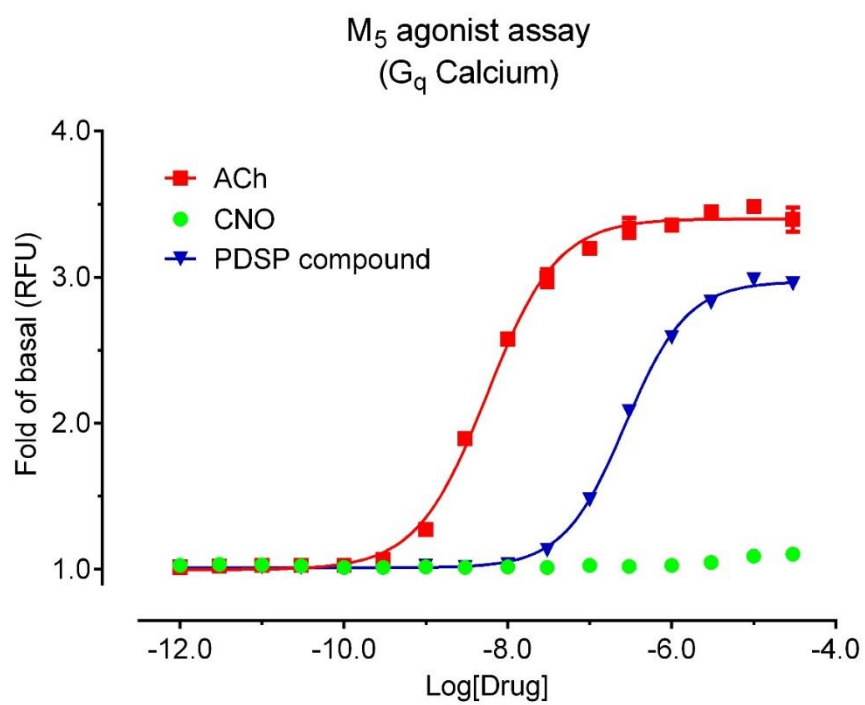
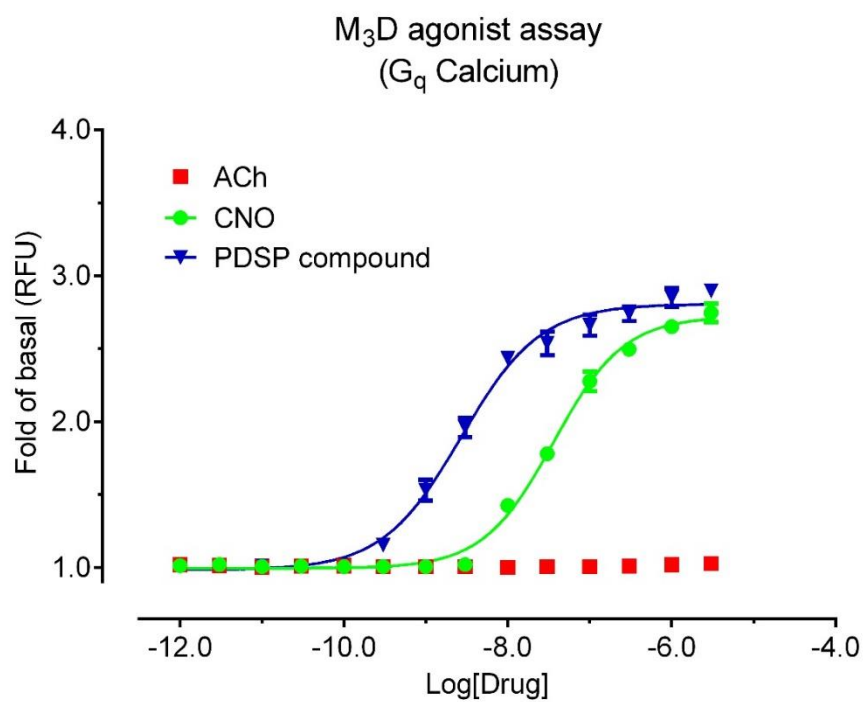


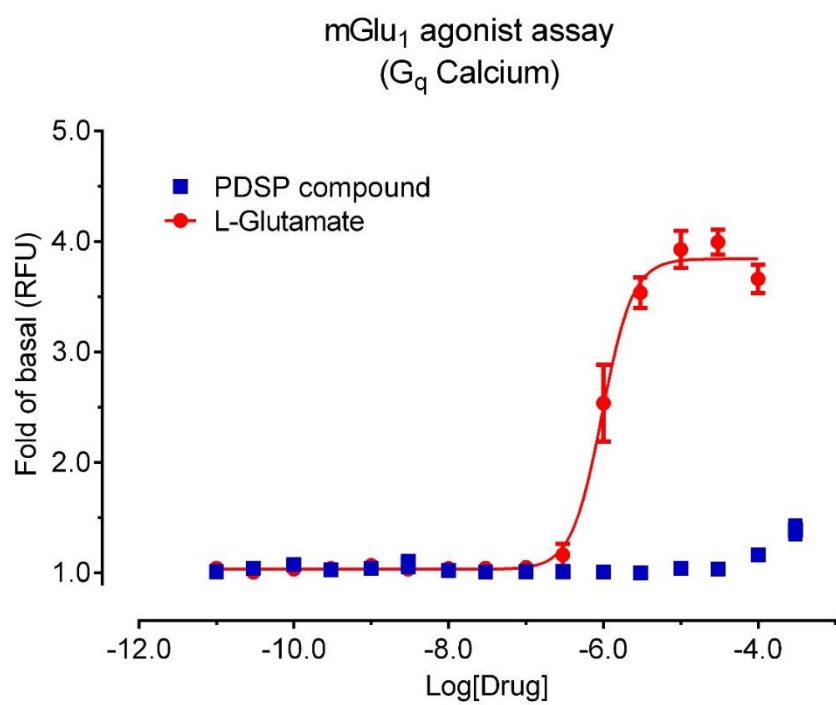
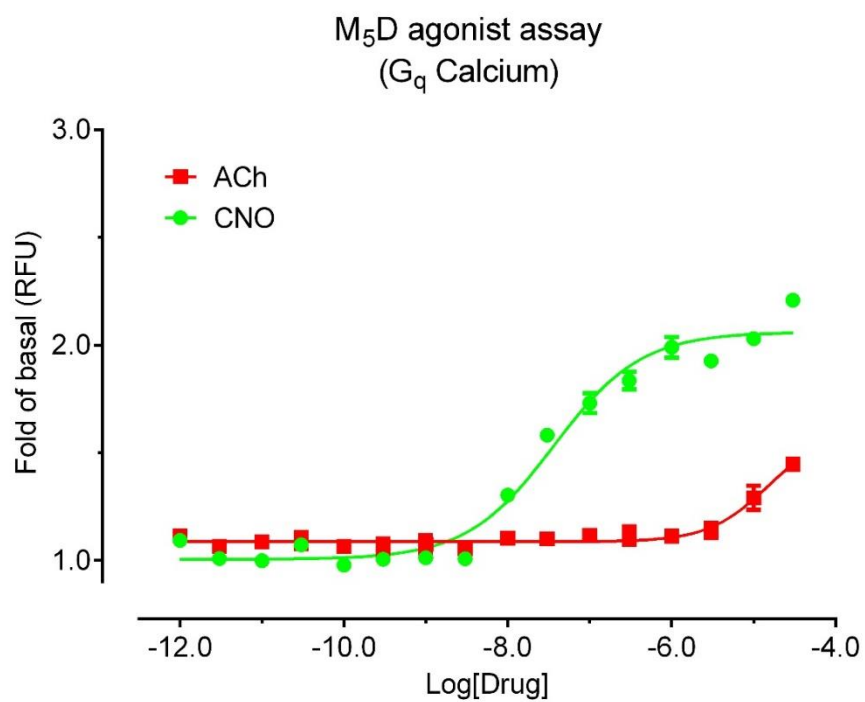
H_1 agonist assay
 (G_q Calcium)

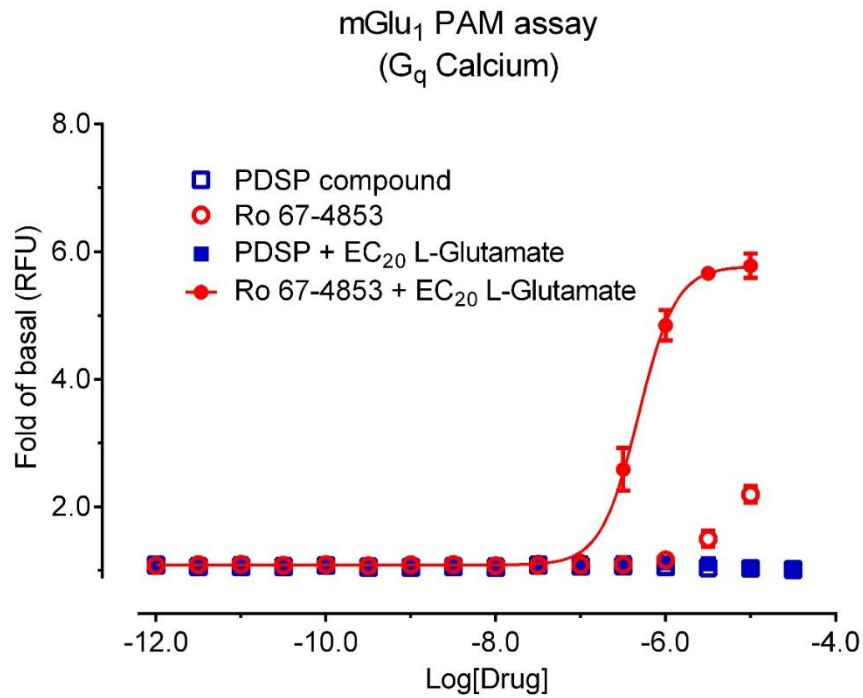
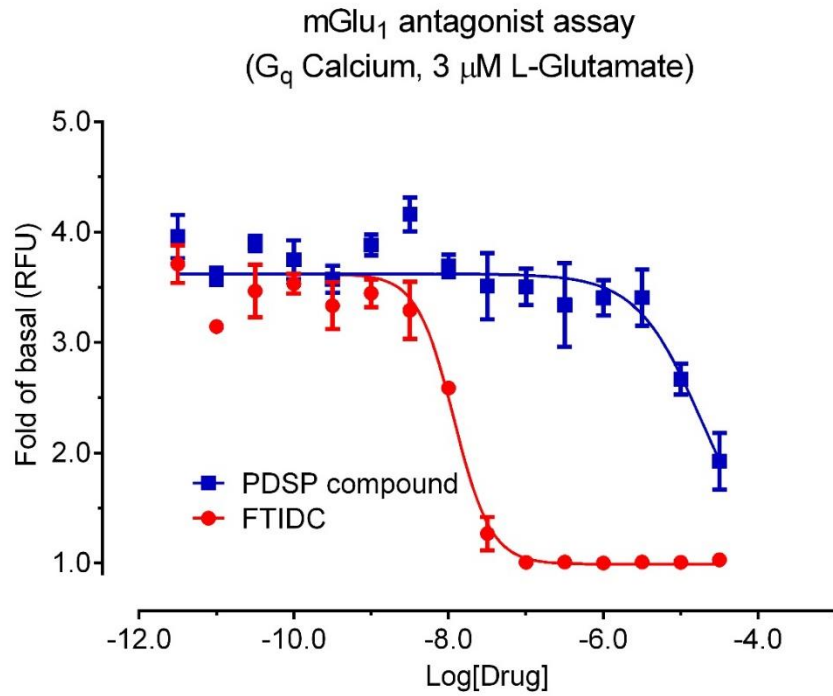


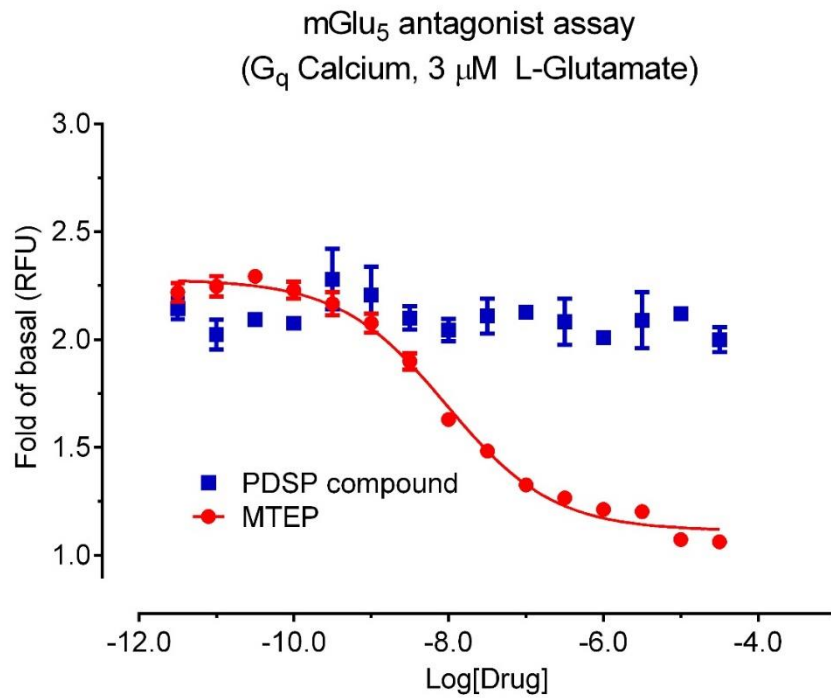
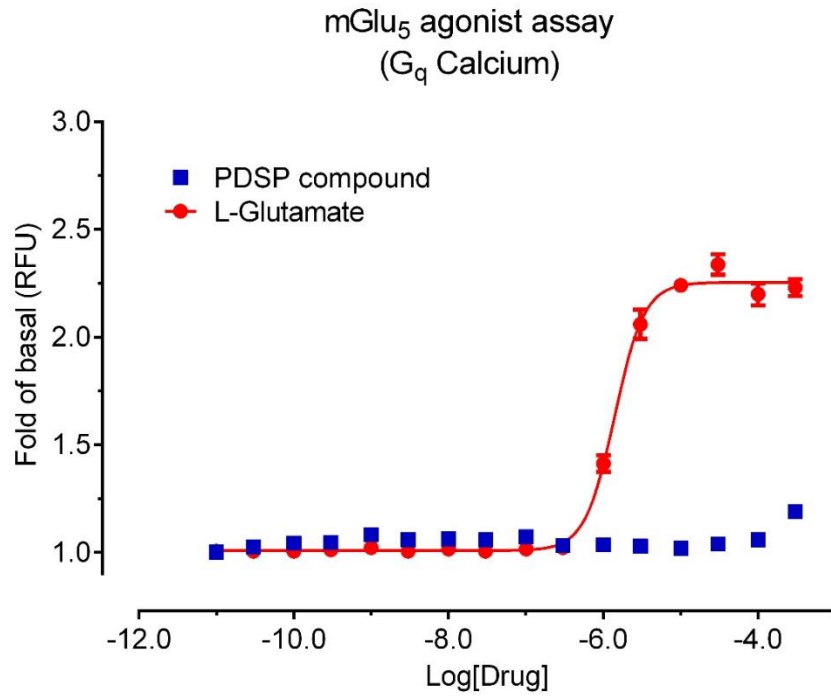


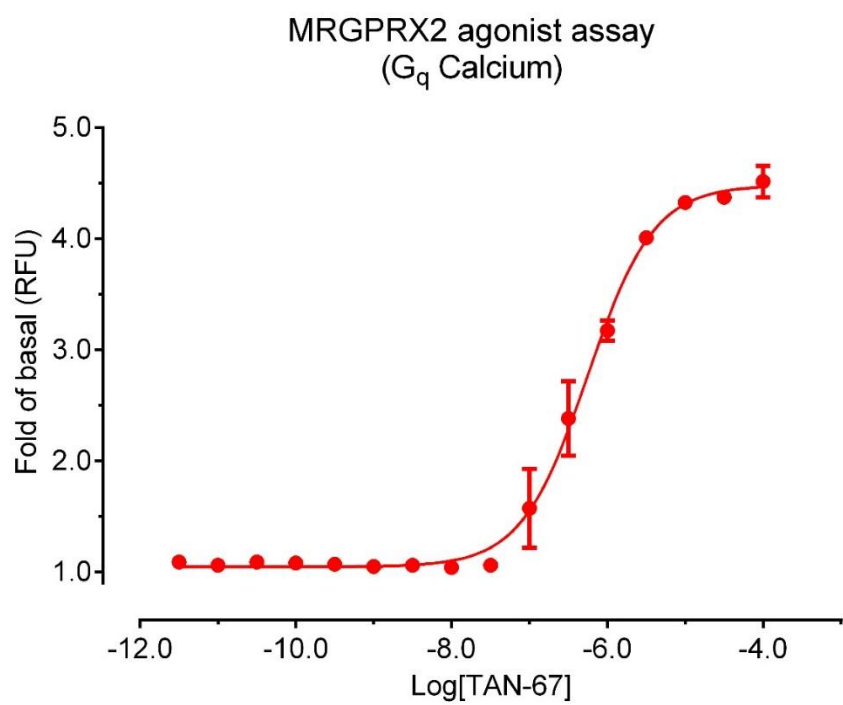
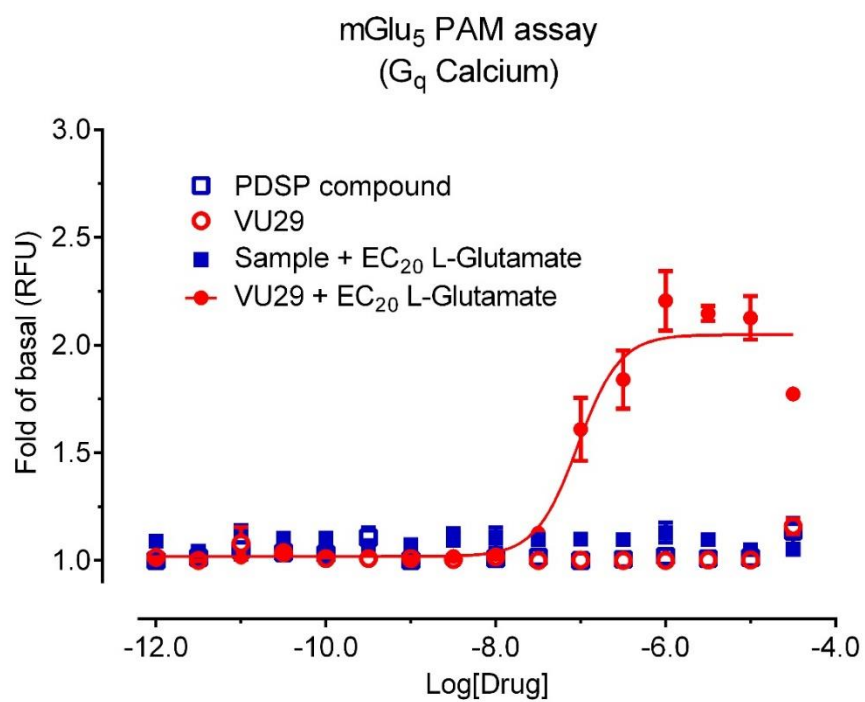




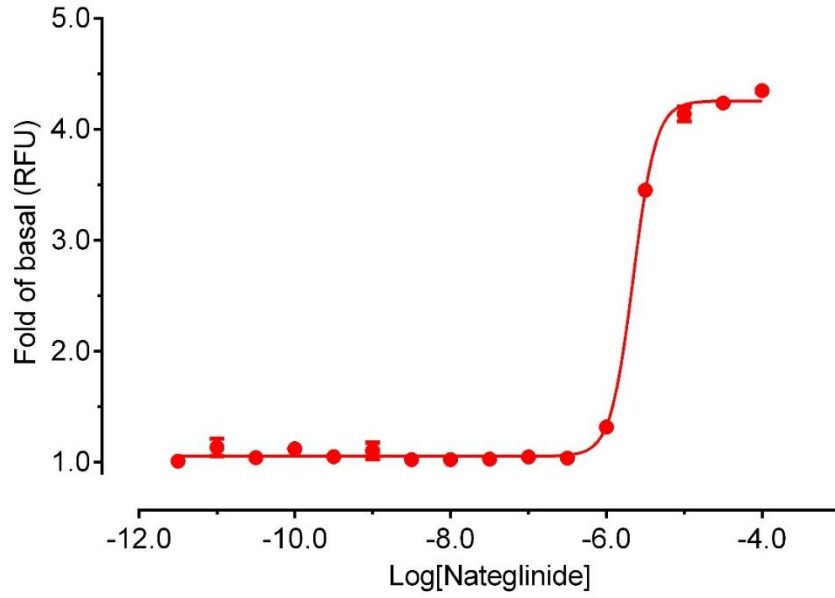




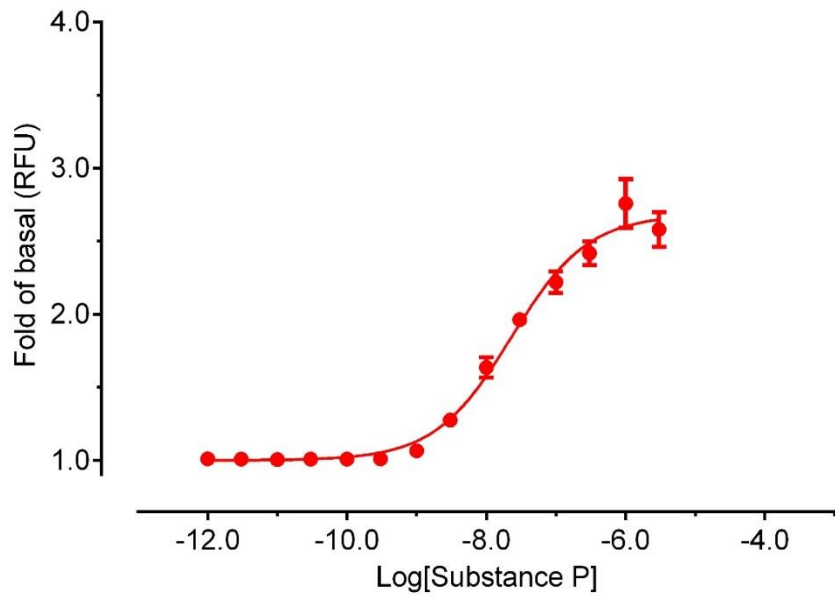


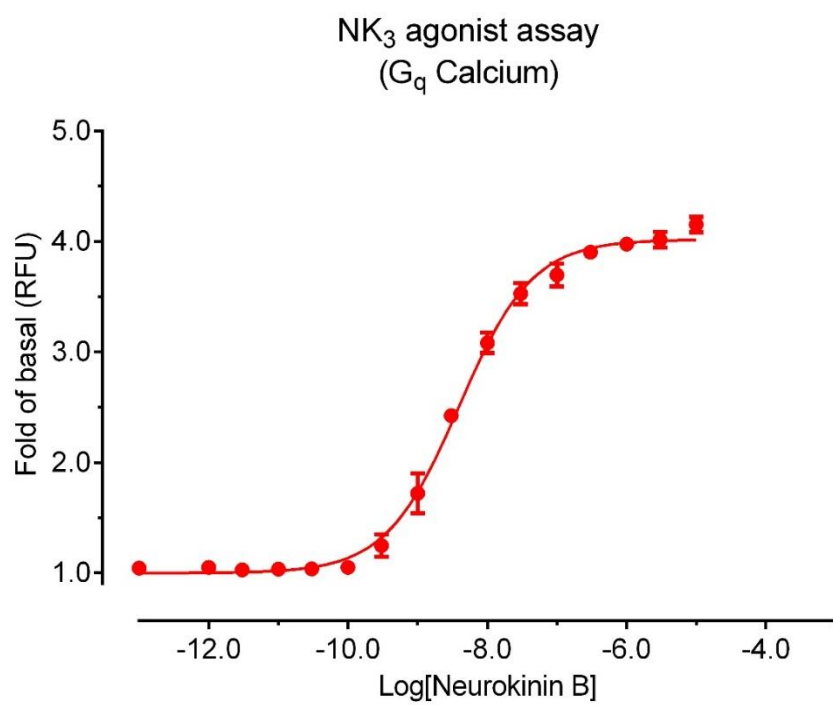
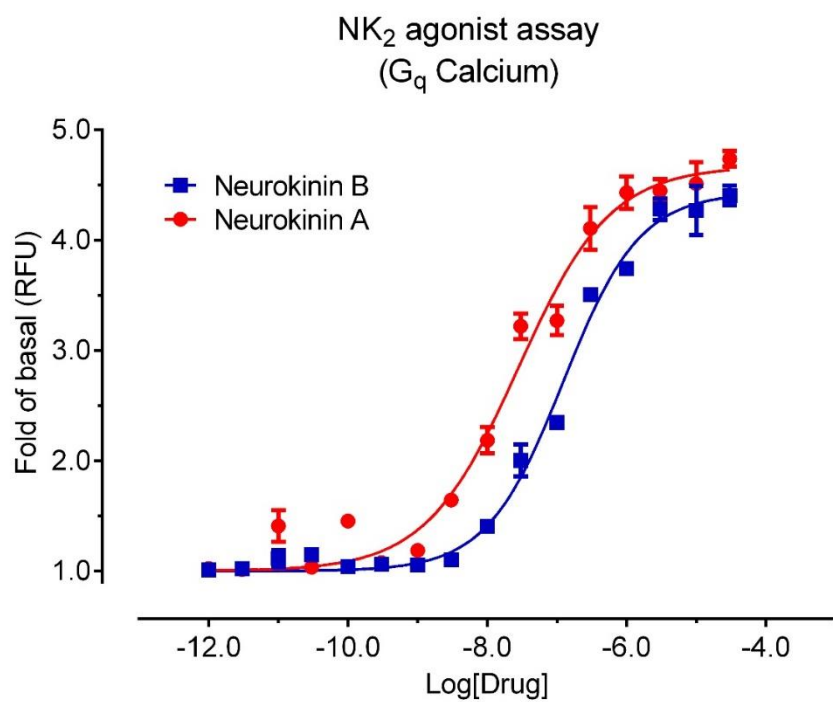


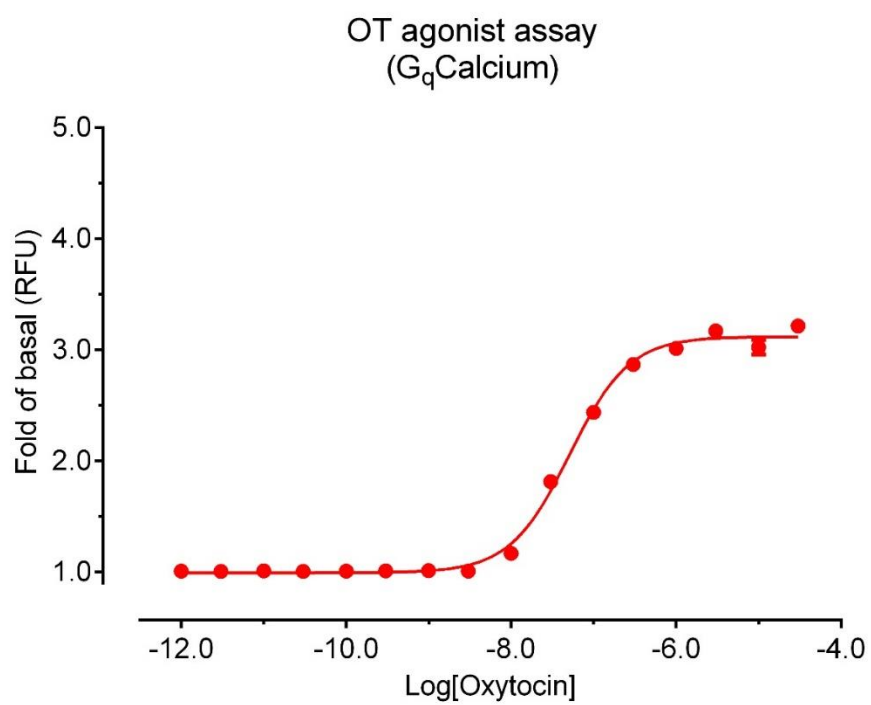
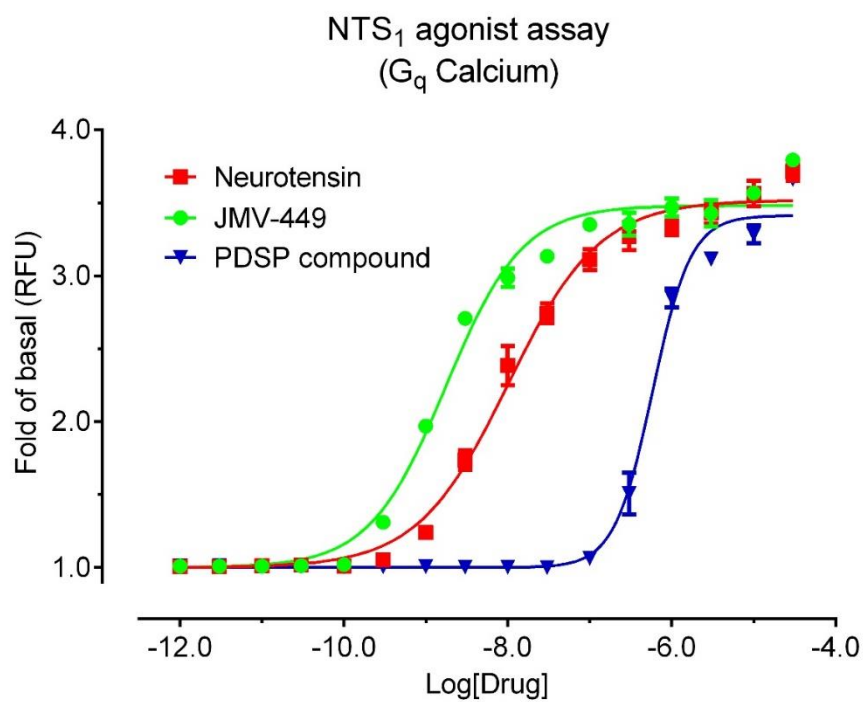
MRGPRX4 agonist assay
(G_q Calcium)

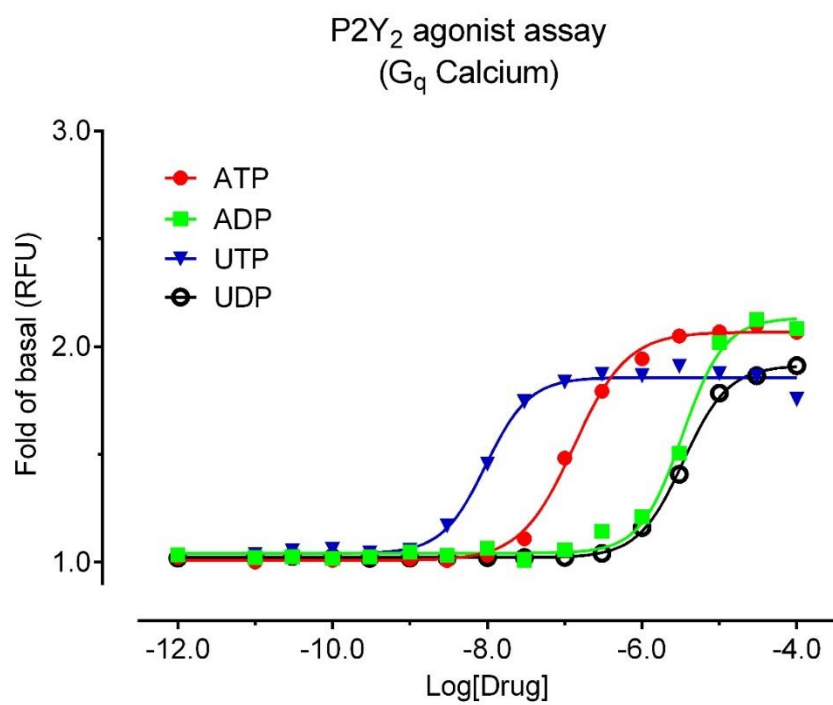
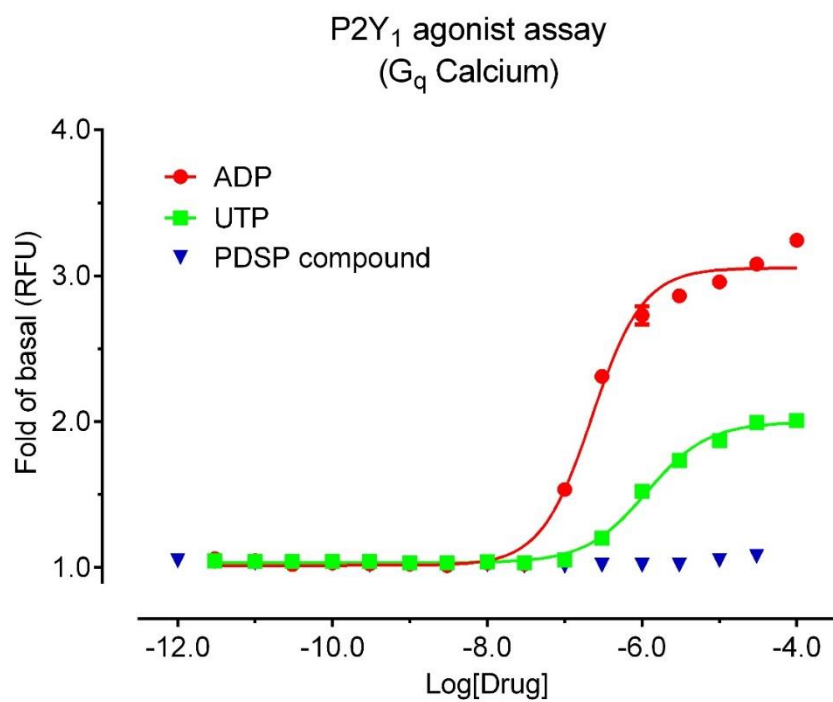


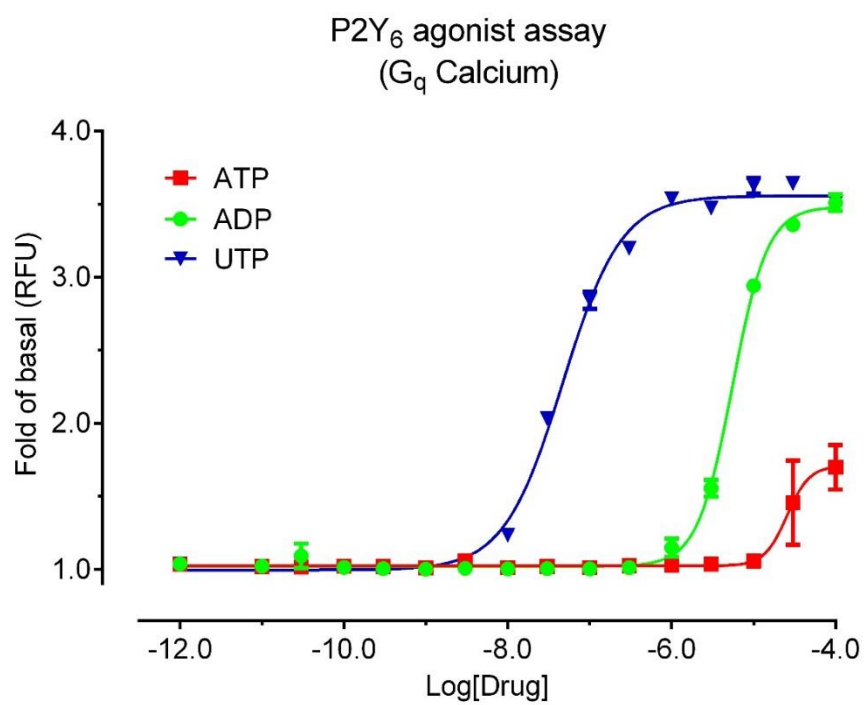
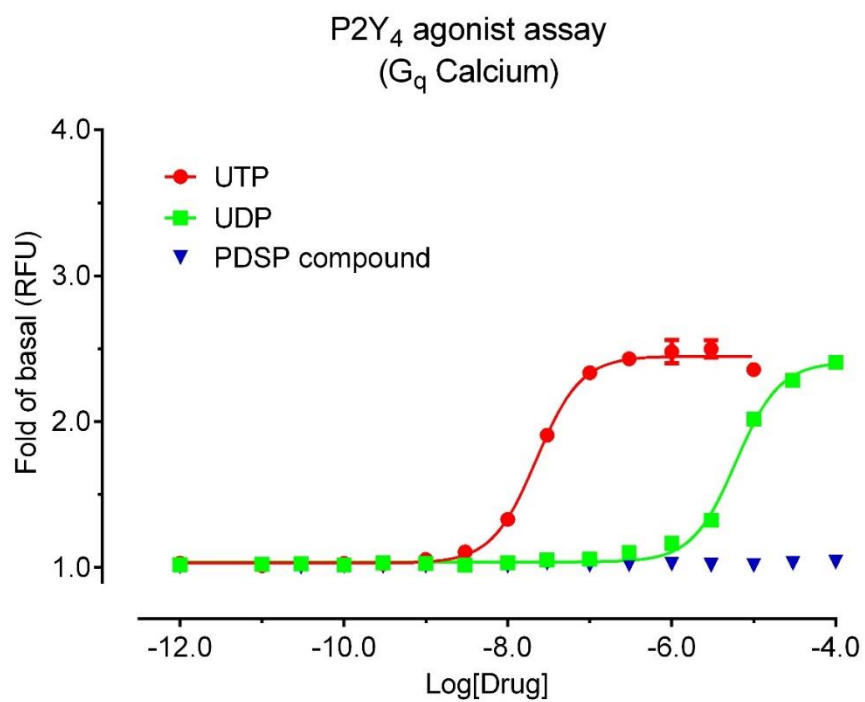
NK₁ agonist assay
(G_q Calcium)

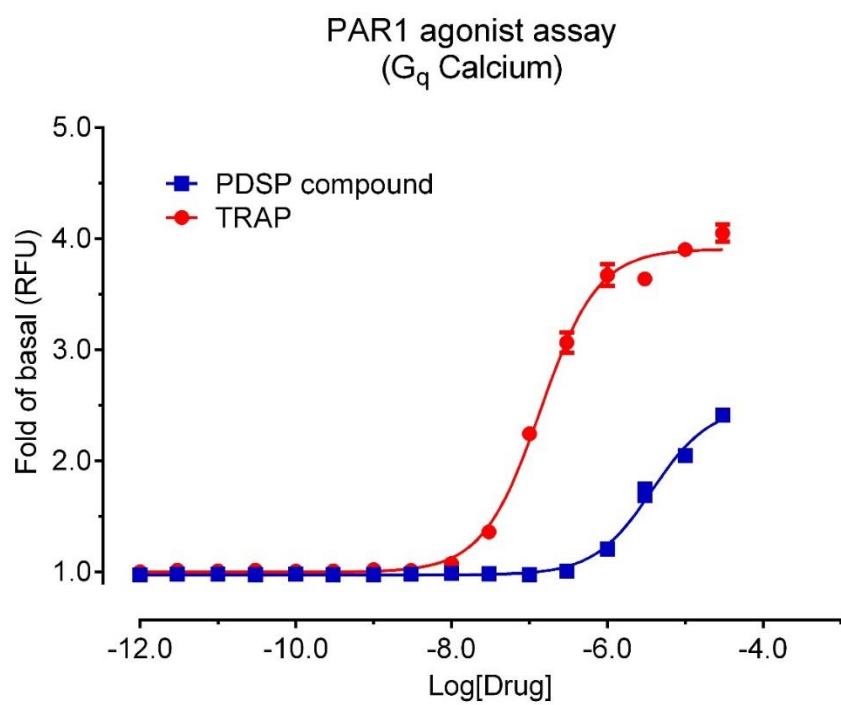
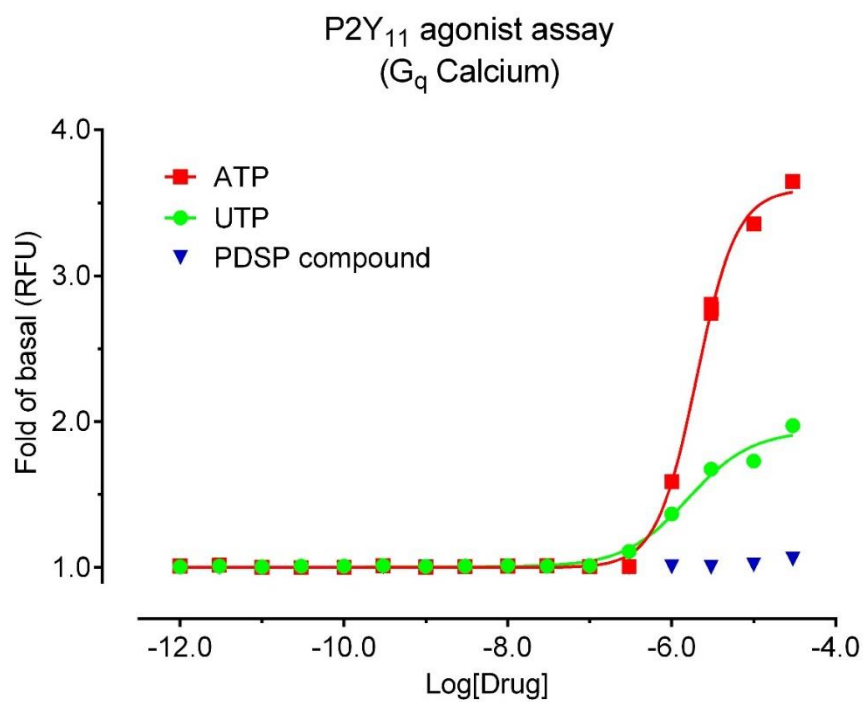


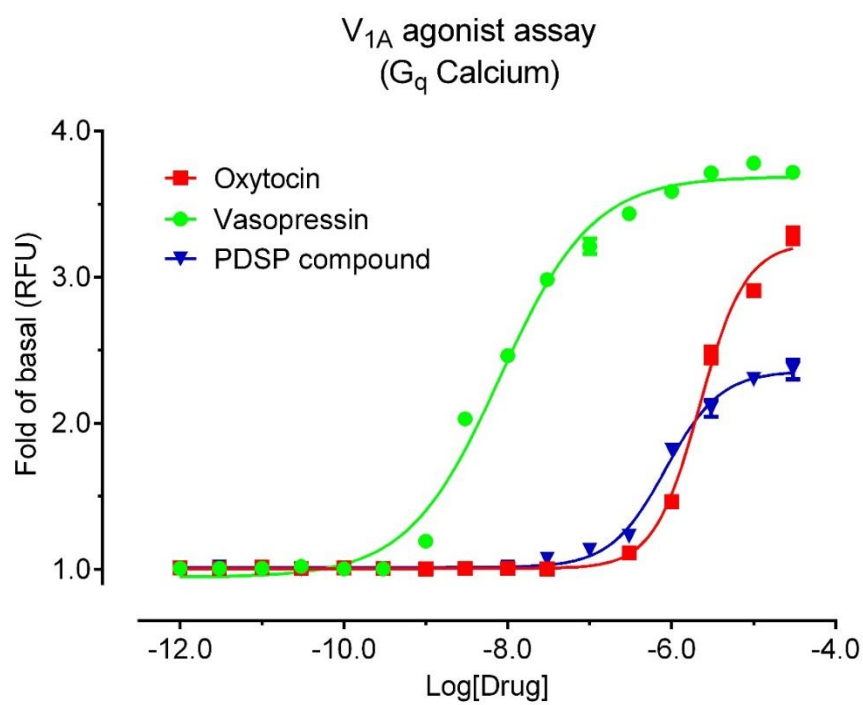
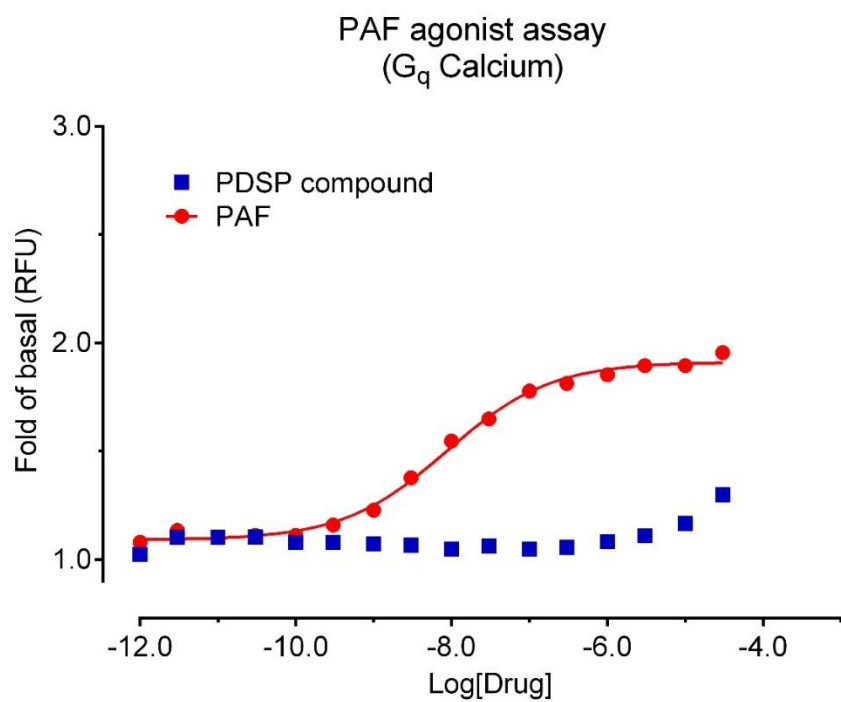












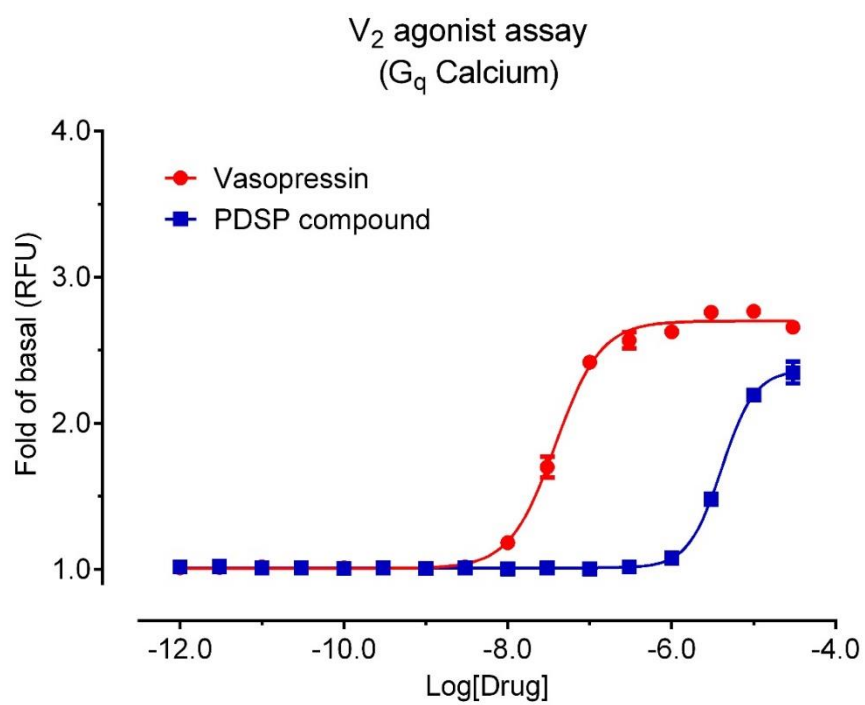
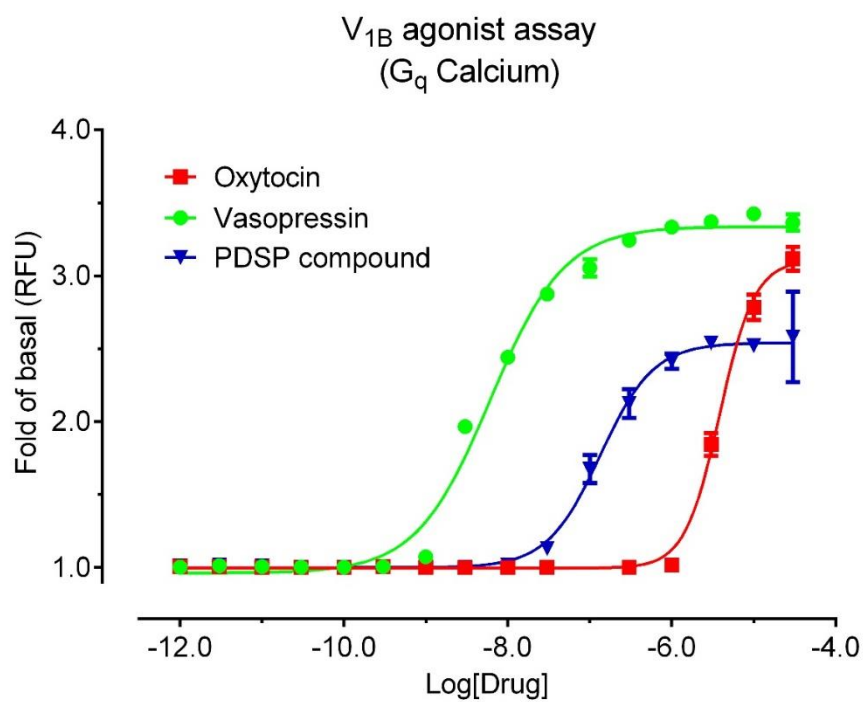


Figure 40. Schild analysis with a PDSP compound at 5-HT_{2A} receptors (G_q Calcium, FLIPR). Results are analyzed according to published procedures (155–157).

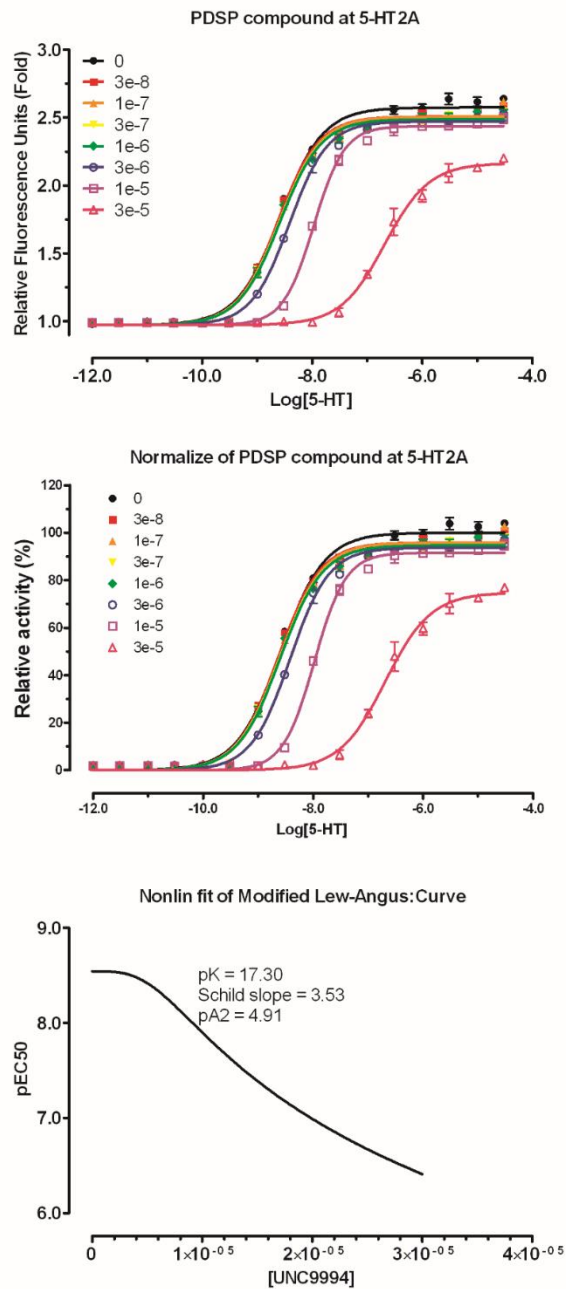
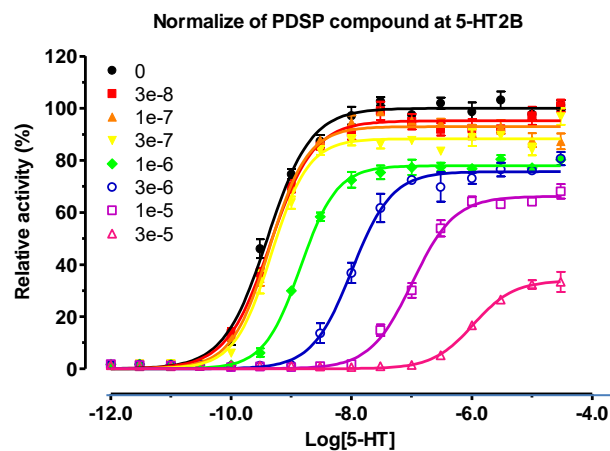
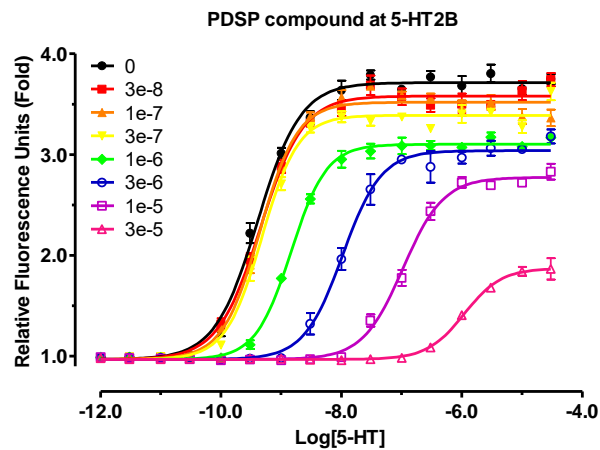
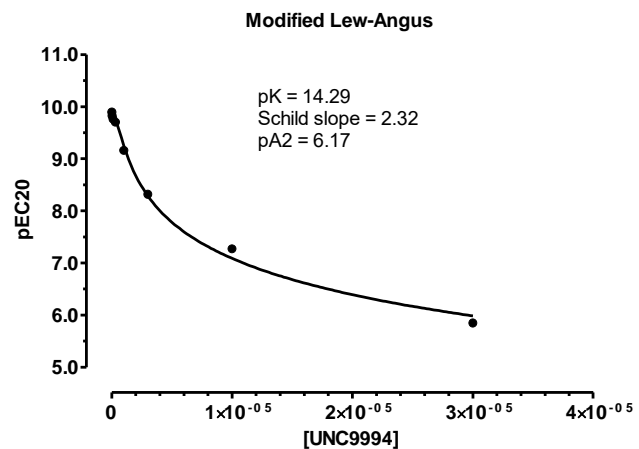


Figure 41. Schild analysis of a PDSP compound at 5-HT_{2B} receptors (G_q Calcium, FLIPR). Results are analyzed according to published procedures (155–157).

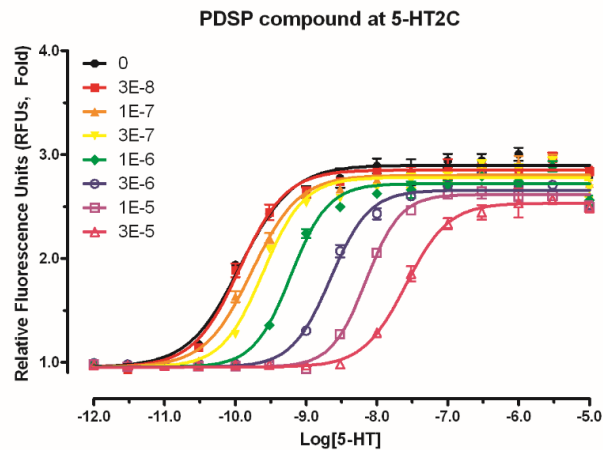


Normalization

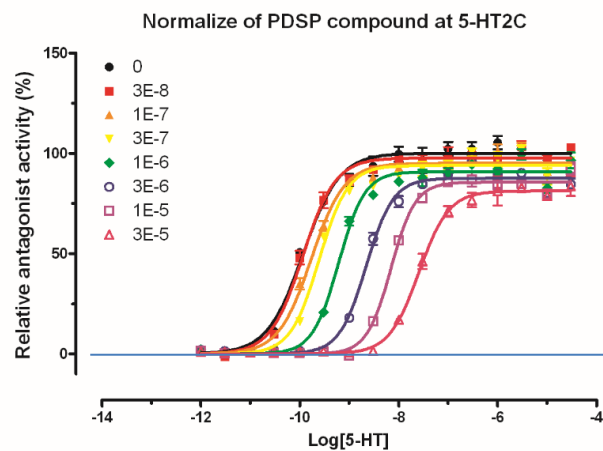


Equiactive agonist
concentration at 20%: pEC₂₀

Figure 42. Schild analysis with a PDSP compound at 5-HT_{2C} receptors (G_q Calcium, FLIPR). Results are analyzed according to published procedures (155–157).



Normalization



Equiactive agonist
concentration at 40%: pEC₄₀

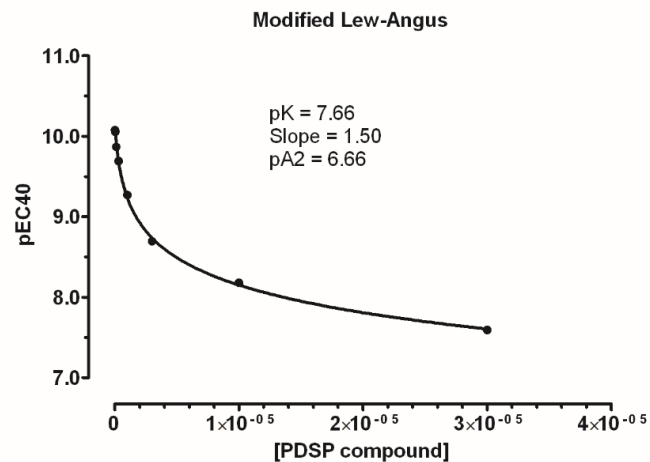


Figure 43. Representative figures for bias analysis. LSD and Ergotamine (ERG) agonist activity in G_i (for 5-HT_{1B}) or G_q (for 5-HT_{2B}) or β -arrestin signaling pathways were determined at 5-HT_{1B} and 5-HT_{2B} receptors as outlined in the functional assay section, and results were normalized to corresponding 5-HT activity and analyzed in Prism using Black and Leff operational model to estimate transduction coefficient, $\text{Log}(\tau/K_A)$, as listed in the Table on the next page. Results are from published papers (142, 158) and modified for presentation here.

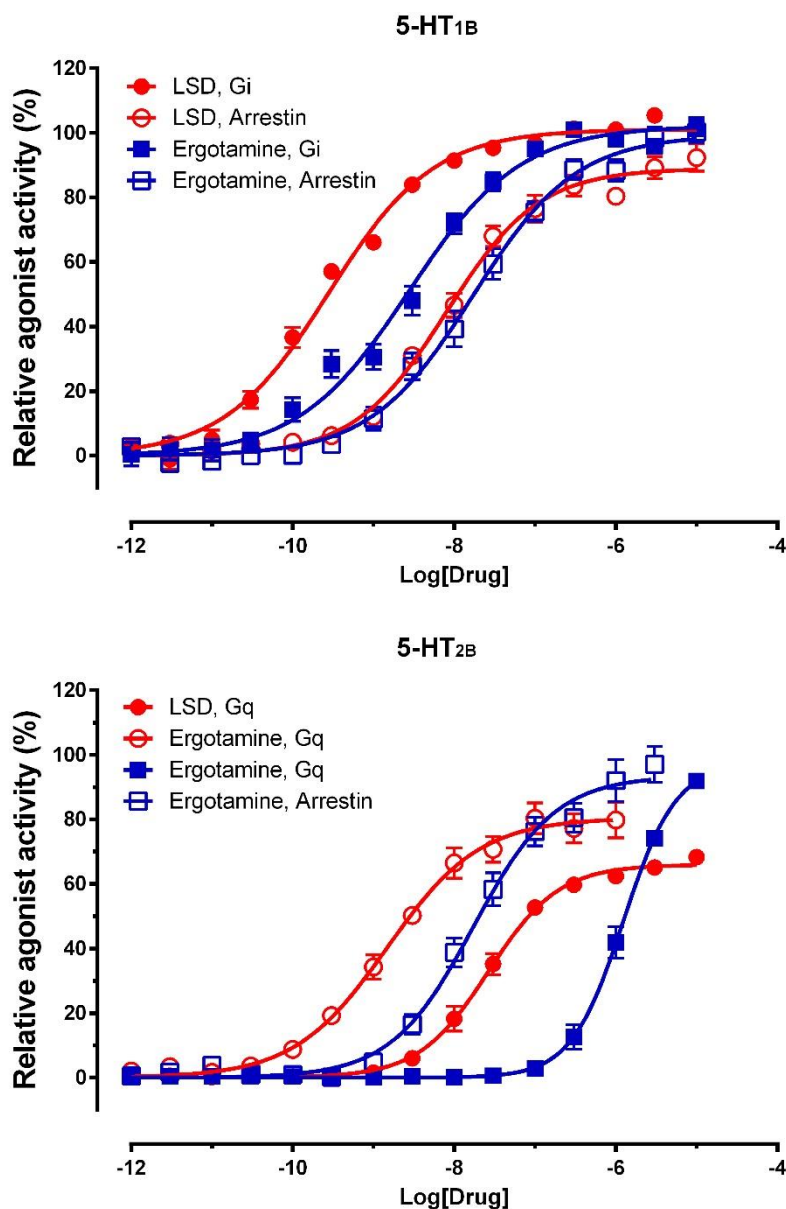


Table 28. Transduction coefficients, $\text{Log}(\tau/K_A)$, and bias factor calculations for indicated pathways of agonists at 5-HT_{1B}. See representative dose-response curves in **Figure 43** on previous page. Bias factor = $10^{\Delta\Delta\text{Log}(\tau/K_A)}$. Results are from published papers (142, 158) and are modified for presentation here.

Ligands	Bias calculation at 5-HT _{1B} receptors					
	G _i pathway	$\Delta\text{Log}(\tau/K_A)$	β -arrestin pathway	$\Delta\text{Log}(\tau/K_A)$	$\Delta\Delta\text{Log}(\tau/K_A)$	Bias Factor
5-HT	9.54 ± 0.08	0	7.47 ± 0.13	0	0	1.0
LSD	9.53 ± 0.09	-0.01	8.08 ± 0.29	0.61	0.62	4.2
Ergotamine	8.53 ± 0.18	-1.01	7.82 ± 0.20	0.35	1.36	22.9
DHE	8.89 ± 0.21	-0.65	7.87 ± 0.19	0.40	1.05	11.2
MTE	9.41 ± 0.12	-0.13	7.72 ± 0.15	0.25	0.38	2.4
Pergolide	7.82 ± 0.25	-1.72	6.41 ± 0.11	-1.06	0.66	4.6
Cabergoline	6.58 ± 0.08	-2.96	6.32 ± 0.14	-1.15	1.81	64.6
Ro 60-0175	6.37 ± 0.35	-3.17	5.32 ± 0.53	-2.15	1.02	10.5
Sumatriptan	8.16 ± 0.19	-1.38	6.94 ± 0.11	-0.53	0.85	7.1
Donitriptan	9.51 ± 0.37	-0.03	8.13 ± 0.18	0.66	0.69	4.9
Eletriptan	8.13 ± 0.29	-1.41	7.07 ± 0.29	-0.40	1.01	10.2
Rizatriptan	7.80 ± 0.43	-1.74	6.63 ± 0.21	-0.84	0.90	7.9

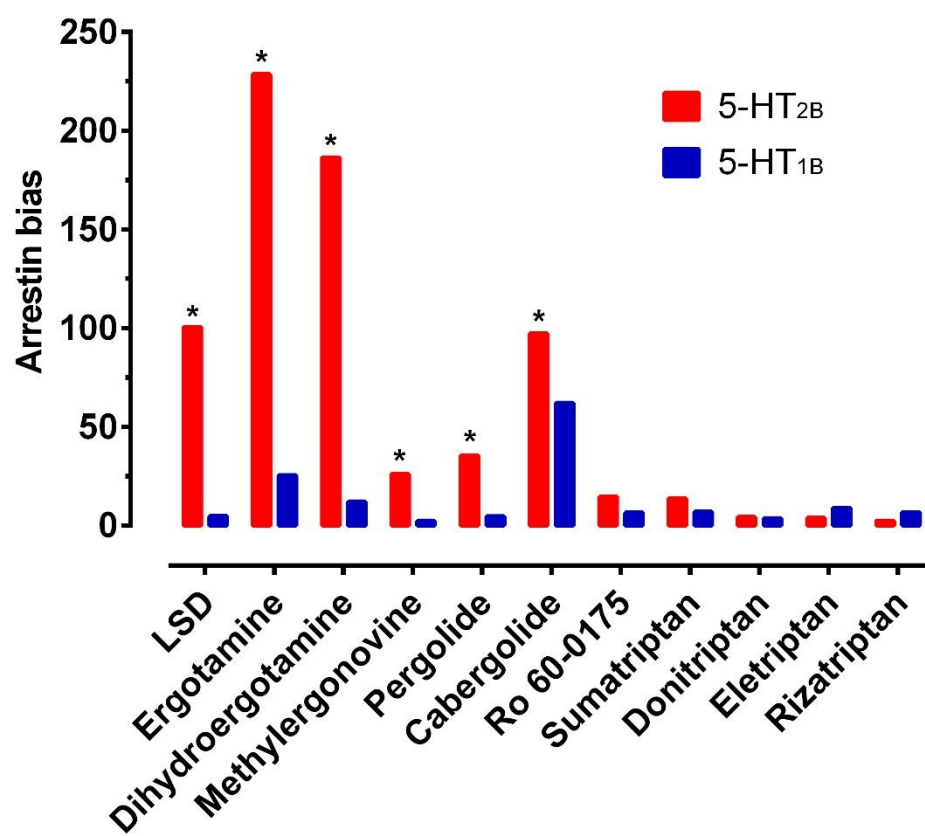
DHE = Dihydroergotamine; MTE = Methylergonovine

Table 29. Transduction coefficients, $\text{Log}(\tau/K_A)$, and bias factor calculation for indicated pathways of agonists at 5-HT_{2B}. See representative dose-response curves in **Figure 43** on previous page. Results are from published papers (142, 158) and are modified for presentation here.

Ligands	Bias calculation at 5-HT _{2B} receptors					
	G _q pathway	$\Delta\text{Log}(\tau/K_A)$	β -arrestin pathway	$\Delta\text{Log}(\tau/K_A)$	$\Delta\Delta\text{Log}(\tau/K_A)$	Bias Factor
5-HT	9.61 ± 0.05	0	8.30 ± 0.09	0	0	1.0
LSD	7.63 ± 0.15	-1.98	8.38 ± 0.09	0.08	2.06	114.8
Ergotamine	5.95 ± 0.10	-3.66	7.05 ± 0.16	-1.25	2.41	257.0
DHE	6.03 ± 0.07	-3.58	7.13 ± 0.33	-1.17	2.41	257.0
MTE	7.93 ± 0.23	-1.68	8.05 ± 0.20	-0.25	1.43	26.9
Pergolide	7.50 ± 0.22	-2.11	7.96 ± 0.08	-0.34	1.77	58.9
Cabergoline	6.92 ± 0.18	-2.69	7.76 ± 0.22	-0.54	2.15	141.3
Ro 60-0175	9.04 ± 0.15	-0.57	9.00 ± 0.10	0.7	1.27	18.6
Sumatriptan	5.24 ± 0.12	-4.37	5.17 ± 0.89	-3.13	1.24	17.4
Donitriptan	6.65 ± 0.12	-2.96	5.92 ± 0.04	-2.38	0.58	3.8
Eletriptan	6.17 ± 0.05	-3.44	5.41 ± 0.20	-2.89	0.55	3.5
Rizatriptan	5.86 ± 0.15	-3.75	5.03 ± 0.03	-3.27	0.48	3.0

DHE = Dihydroergotamine; MTE = Methylergonovine

Figure 44. Comparison of bias factors of various ligands at 5-HT_{1B} and 5-HT_{2B} receptors. Values are taken from **Tables 28 and 29** and **Figure 43**. * indicates significant difference $p < 0.0001$ (two-way ANOVA). Results are from published papers (142, 158) and are modified for presentation here.



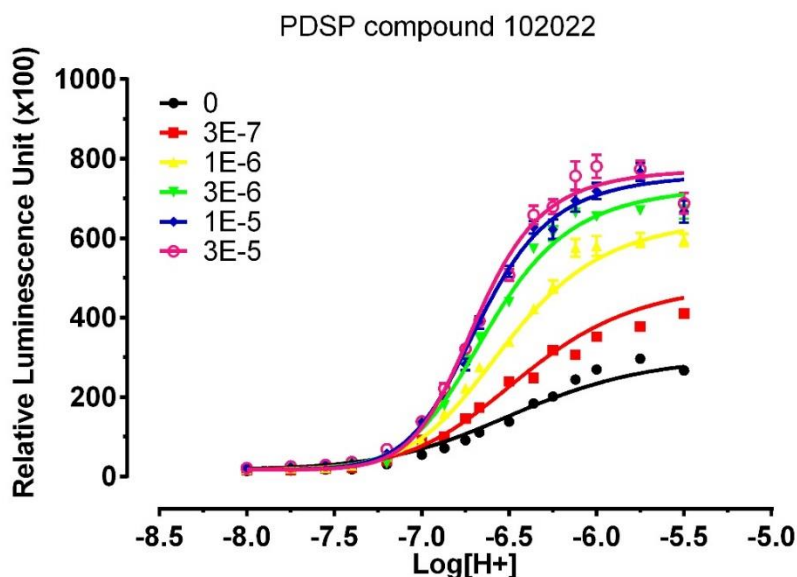


Figure 44. Representative curves for the allosteric operational model. GPR68-mediated cAMP production was determined in the absence and presence of increasing concentration of PDSP compound #102022. Results are analyzed using the allosteric operational model and best-fit values are listed in the following table. In the curve-fitting, $\text{Log}(K_A)$ is set at -6.50 (equivalent to the pEC_{50} value of protons in the absence of #102022), while the E_{max} is constrained to 800 (which is the maximum activity of the system); τ_B is constrained to “0”, since #102022 has no agonist activity by itself.

[102022] M	0	3.00E-7	1.00E-6	3.00E-6	1.00E-5	3.00E-5	Global (shared)
Best-fit values							
$\text{Log}K_A$	(= -6.50)	(= -6.50)	(= -6.50)	(= -6.50)	(= -6.50)	(= -6.50)	
$\text{Log}K_B$	-6.14	-6.14	-6.14	-6.14	-6.14	-6.14	-6.14
Basal	16.32	16.32	16.32	16.32	16.32	16.32	16.32
E_{max}	(=800)	(=800)	(=800)	(=800)	(=800)	(=800)	
τ_A	0.678	0.678	0.678	0.678	0.678	0.678	0.678
α	0.877	0.877	0.877	0.877	0.877	0.877	0.877
β	4.055	4.055	4.055	4.055	4.055	4.055	4.055
B	= 0.0	3.00E-07	1.00E-06	3.00E-06	1.00E-05	3.00E-05	
τ_B	= 0.0	= 0.0	= 0.0	= 0.0	= 0.0	= 0.0	
n	1.443	1.993	2.441	2.799	3.116	3.451	

2.5. Functional assays for G_i or G_s coupled GPCRs - Split luciferase cAMP assay

Main equipment: luminescence counter

Reagents: GloSensor cAMP construct from Promega and Luciferin

Assay buffer: 20 mM HEPES, 1x HBSS, pH 7.40

2.5.1. Cell culture and transfection: To determine G_i or G_s GPCR-mediated cAMP production, the PDSP uses Promega's split luciferase based GloSensor cAMP biosensor technology. With the cells stably expressing target receptors, we transfect with the GloSensor cAMP DNA construct overnight; otherwise, we co-transfect HEK 293T cells with target receptor DNA and GloSensor cAMP DNA construct overnight. For detailed transfection protocol, see above section "Calcium precipitation transfection". To prepare plates for assays, cells are seeded into PLL-coated 384-well white clear bottom cell culture plates in DMEM supplemented with 1% dFBS at a density of 15-20K cells in a volume of 40 µl per well. The plates can be used for assays after 6 hours or overnight.

2.5.2. Split luciferase biosensor cAMP assay – Luciferin first protocol: The GloSensor cAMP assays have been widely used in determining G_i- or G_s-GPCR mediated cAMP production in live cells (142, 147, 158–161). The PDSP uses these assays for cell-based functional assays with G_i- or G_s-coupled GPCRs. On the day of assay, cells are removed from culture medium and loaded with 20 µl of 4 mM luciferin prepared in assay buffer for 60 min at 37°C. All the following steps are carried out at room temperature. To measure agonist activity at G_s-coupled receptors, 10 µl of 3x drug solutions are added and the plate is counted for chemiluminescence after 15 minutes. To measure antagonist activity at G_s-coupled receptors, cells are preincubated with drugs for 15 minutes before addition of an EC₈₀ concentration of a reference agonist, and chemiluminescence is counted after 15 minutes. To measure agonist activity at G_i-coupled receptors, 10 µl 3x drug solutions is added for 15 minutes before addition of 5 µl of isoproterenol at a final concentration of 200 nM, and the plate is counted for chemiluminescence after 15 minutes. An alternative way to directly activate adenylyl cyclases is by the use of 30 µM forskolin(162–164), especially when cells that do not have enough β₂-AR mediated adenylyl cyclase activity (such as CHO cells) are used for GloSensor cAMP assays. To

measure antagonist activity at G_i -coupled receptors, cells are preincubated with drugs for 15 minutes before the addition of an EC_{80} concentration of a reference agonist for another 15 minutes, followed by the addition of 5 μ l isoproterenol at a final concentration of 200 nM and counting after 15 minutes. Isoproterenol is used to activate the endogenous G_s protein through endogenous β_2 adrenergic receptors. Different receptors and different cell lines might need different preincubation times; preliminary assays are done to determine the best count window before large-scale screening assays.

2.5.3. Split luciferase biosensor cAMP assay - Drug first protocol: On the day of assay, cells are removed from culture medium and receive 20 μ l/well assay buffer, followed by addition of 10 μ l of 3x drug solutions for 15 minutes at room temperature. To measure agonist activity for G_s -coupled receptors, 10 μ l of 4 mM luciferin prepared in assay buffer is added, and counting is done after 15 minutes. To measure agonist activity for G_i -coupled receptors, 10 μ l of 4 mM Luciferin supplemented with Isoproterenol at final of 200 nM is added, and counting is done after 15 minutes. To measure antagonist activity at G_i -coupled receptors, cells are preincubated with drugs for 15 minutes before addition of an EC_{80} concentration of a reference agonist for another 15 minutes, followed by addition of 10 μ l of 4 mM luciferin supplemented with isoproterenol at a final concentration of 200 nM and counting after 15 minutes. Different receptors and different cell lines might need different preincubation times; therefore, a preliminary assay are performed to determine the best count window before large-scale screening assays.

2.5.3.1. Primary assays - Single concentration assays. Each new compound is tested on all receptors at a single concentration (10 μ M) for activity as an agonist or an antagonist. Testing for antagonism is performed in presence of the EC_{50} concentration of a typical agonist (as described above). Each compound is tested in duplicate in two separate experiments performed on different lots of cells. In addition to the tested compounds, each 96-well plate contains wells for the determination of basal activity, maximal agonist stimulation, agonist EC_{50} concentrations (i.e., concentration-response isotherm), and the IC_{50} concentration of a known antagonist for purposes of positive control and for activity calculations. The reported results for each compound are calculated for agonists as the % of maximal activity (as obtained with maximal agonist concentrations), and for antagonists as the %

inhibition of receptor activity (in presence of an EC₅₀ concentration of the agonist). Results are expressed as means \pm SEM from four replicates.

2.5.3.2. Secondary assays - Dose-response assays. Compounds determined to be active as agonists or antagonists may be tested for their potency in dose-response experiments. Eight-point dose-response curves are performed in duplicate twice on two separate lots of cells (sometimes a third curve may be needed if in the first experiment the range of concentrations used is outside of the active range). For antagonists, these curves are performed in the presence of the EC₅₀ concentration of the agonist. For each compound, the results from four replicates are averaged and then either EC₅₀ or IC₅₀ values are calculated by non-linear regression using the 4-parameter logistic equation. Results are reported as EC₅₀ or IC₅₀ values for each tested compound (and receptor) and include the EC₅₀ or IC₅₀ values of a known agonist or antagonist for comparison purposes.

2.5.4. Data processing and analysis: The luminescence counter records chemiluminescence in relative luminescence units (RLU) and saves files in 384-well format in Excel sheet for easy processing. Results in RLU are plotted and analyzed in GraphPad Prism v5.0 as outlined in **Section 2.3**.

2.5.5. Table and Figures. List of GPCRs for which the PDSP provides functional assays to determine G_i, G_s, or G_{olf} activity, and their corresponding dose-response curves. PDSP will also provide functional assays for other G_i or G_s coupled GPCRs upon request.

Table 30. List of GPCRs for which the PDSP provides cAMP measurements using GloSensor cAMP technology for G_i or G_s coupled receptors, and representative figures. PDSP will also design and develop functional assays for other G_i- or G_s-coupled GPCRs upon request and approval.

Receptor	G _i or G _s	Cell	Ligands (references)	E _{max} (fold)*	pEC ₅₀ (nM) or pIC ₅₀ (nM)	Hill slope
5-HT _{1A}	G _i	HEK T	5-HT	5.9	8.71 (1.9)	-1.02
5-HT _{1B}	G _i	HEK T	5-HT	5.1	9.71 (0.20)	-0.94
5-HT _{1D}	G _i	HEK T	5-HT	2.0	9.45 (0.36)	-1.77
5-HT _{1E}	G _i	HEK T	5-HT	3.2	9.12 (0.77)	-0.87
5-HT ₄	G _s	HEK T	5-HT	2.3	10.17 (0.07)	0.97
5-HT _{5A}	G _s	CHO	5-HT	Being developed		
5-HT ₆	G _s	HEK T	5-HT	14.6	9.29 (0.5)	0.78
5-HT _{7A}	G _s	HEK T	5-HT	9.1	7.75 (17.6)	0.81
			Clozapine (inverse agonist)	7.9	6.91 (123)	-0.77
M ₂	G _i	HEK T	Acetylcholine	2.1	7.62 (24.1)	-0.74
M _{2D}	G _i	HEK T	CNO	3.4	6.30 (497)	-0.79
M ₄	G _i	HEK T	Acetylcholine	2.7	8.23 (5.8)	-0.94
M _{4D}	G _i	HEK T	CNO	2.6	9.46 (0.35)	-1.25
G _s -DREADD	G _s	HEK T	CNO	13.3	7.89 (12.9)	1.44
			Acetylcholine	8.3	4.60 (25 μM)	1.91
A ₁	G _i	HEK T	NECA	3.6	9.11 (0.78)	-0.99
			DPCPX (antagonist)	11.0	5.18 (6.6 μM)	0.81
A _{2A}	G _s	HEK T	NECA	2.4	9.58 (0.26)	0.74
			CCPA	1.9	7.80 (15.8)	1.42
			CGS21680	2.2	9.67 (0.22)	0.72
			CGS15943 (inverse agonist)	10.4	7.65 (22.5)	-1.27
A _{2B}	G _s	HEK T	NECA	30.4	8.03 (9.4)	1.09
			CGS15943 (antagonist)	24.3	6.44 (366)	-0.74
CRF-1	G _s	HEK T	CRF	95.8	8.55 (2.8)	0.78
CRF-2	G _s	HEK T	CRF	125.0	7.26 (54.7)	0.95
D ₁	G _s	HEK T	Dopamine	153.6	8.18 (6.7)	0.94
D ₂	G _i	HEK T	Dopamine	2.9	8.98 (1.1)	-0.97
D ₃	G _i	HEK T	Dopamine	Being developed		
D ₄	G _i	HEK T	Dopamine	2.0	9.19 (0.6)	-1.67
D ₅	G _s	HEK T	Dopamine	37.6	9.24 (0.6)	0.80
H ₂	G _s	HEK T	Histamine	40.0	8.07 (84.7)	1.08
			Cimetidine (antagonist)	16.6	5.98 (1039)	-1.45
H ₃	G _i	HEK T	Histamine	4.6	8.90 (1.3)	-0.70

Receptor	G _i or G _s	Cell	Ligands (references)	E _{max} (fold)*	pEC ₅₀ (nM) or pIC ₅₀ (nM)	Hill slope
β ₁	G _s	HEK T	Isoproterenol	20.8	11.10 (7.9 pM)	1.32
β ₂	G _s	HEK T	Isoproterenol	54.3	10.71 (19.3 pM)	0.94
			Salmeterol	42.7	9.78 (0.17)	0.86
β ₃	G _s	HEK T	Isoprotenerol	30.5	8.22 (6.0)	0.62
Control HEK T (endogenous β receptors)	G _s	HEK T	Isopreternol	16.3	7.89 (12.9)	1.19
			Norepinephrine	7.8	6.28 (520)	0.89
			Cimaterol	10.7	7.98 (11.8)	0.98
			Dobutamine	7.5	5.51 (3090)	0.98
			Fenoterol	19.5	7.37 (44.0)	0.63
			Metaproterenol	8.0	5.94 (1159)	1.55
			Salbuterol	6.4	6.94 (116)	1.34
			Terbutaline	7.8	6.16 (691)	0.87
HCA ₁	G _i	CHO	Niacin	1.5	4.94 (11.6 μM)	0.43
			Acifran	1.5	4.25 (56.7 μM)	0.55
HCA ₂	G _i	CHO	Acifran	1.5	4.25 (56.7 μM)	0.55
			Acifran	2.8	6.36 (438)	0.69
HCA ₃	G _i	CHO	Niacin	2.0	3.43 (376 μM)	0.56
			Acifran	3.6	4.31 (49.3 μM)	0.67
GLP-1	G _s	HEKT	GLP-1	173.6	7.24 (58.1)	0.81
			Glucagon	175.4	8.19 (6.5)	0.95
DOR	G _i	HEK T	DADLE	2.7	7.36 (43.6)	-0.94
			Naltrindole (antagonist)	1.6	7.73 (18.7)	1.46
KOR	G _i	HEK T	Salvinorin A	2.4	9.43 (0.37)	-1.33
			GNTI (antagonist)	3.2	8.13 (7.4)	1.54
MOR	G _i	HEK T	DAMGO	3.2	8.94 (1.2)	-0.75
			Naltrexone (antagonist)	2.6	7.70 (20.2)	0.67
NOP	G _i	HEK T	Nociceptin	3.6	8.64 (2.3)	-1.06
			SB612111 (antagonist)	1.8	7.66 (22.0)	1.64
Oxoglutarate	G _i	HEK T	α-Ketoglutaric Acid	2.2	3.49 (327 μM)	-1.52
MC ₁	G _s	HEK T	α-MSH	19.1	7.45 (35.5)	1.14
			Melanotan II	21.2	7.89 (13.0)	0.87
MC ₃	G _s	HEK T	α-MSH	91.0	7.06 (87.4)	1.26
			Melanotan II	86.1	7.62 (23.9)	0.93
MC ₄	G _s	HEK T	α-MSH	80.6	9.19 (64.0)	0.98
			Melanotan II	89.1	7.72 (18.9)	0.76
MC ₅	G _s	HEK T	α-MSH	35.9	6.49 (327)	1.65
			Melanotan II	29.8	6.81 (156)	1.54
MT ₁	G _i	HEK T	Melatonin	2.5	10.51 (0.031)	-1.84

Receptor	G _i or G _s	Cell	Ligands (references)	E _{max} (fold)*	pEC ₅₀ (nM) or pIC ₅₀ (nM)	Hill slope
MT ₂	G _i	HEK T	Melatonin	1.9	10.85 (0.014)	-1.18
mGlu ₂	G _i	HEK	L-Glutamate	5.8	5.14 (7287)	-1.13
			LY379268	5.8	8.39 (4.1)	-0.89
			LY341495 (antagonist)	4.1	7.27 (53.5)	1.52
mGlu ₃	G _i	HEK	L-Glutamate	2.3	6.30 (505)	-1.05
			LY341495 (antagonist)	3.2	7.27 (53.2)	2.13
mGlu ₄	G _i	HEK	L-SOP	4.8	5.80 (1590)	-1.02
			LY341495 (antagonist)	2.3	5.27 (5381)	3.38
mGlu ₆	G _i	HEK	L-Glutamate	1.9	4.84 (14.5 μM)	-1.25
			L-SOP	1.9	6.17 (684)	-1.01
			LY341495 (antagonist)	2.8	5.90 (1264)	1.33
mGlu ₇	G _i	Not available yet, in development				
mGlu ₈	G _i	HEK	L-Glutamate	3.6	5.87 (1336)	-0.68
			LY341495 (antagonist)	2.6	6.79 (163)	1.28
NPBW ₁	G _i	HEK T	Neuropeptide W-23 (165)	2.1	8.05 (8.8)	-0.88
NPBW ₂	G _i	HEK T		1.6	9.56 (0.27)	-0.38
RXFP1	G _s	HEK T	Relaxin-2	95.7	9.15 (0.7)	0.92
RXFP2	G _s	HEK T	Relaxin-2	21.1	7.48 (33.4)	0.96
RXFP3	G _i	HEK T	Relaxin-3	2.4	9.85 (0.14)	-1.40
RXFP4	G _i	HEK T	Relaxin-3	2.4	9.19 (0.06)	-0.78
SSTR5	G _i	HEK T	Somastotatin	7.7	8.63 (2.4)	-1.66
TP	G _s	HEK T	U46619(166)	27	5.98 (1055)	0.98
			S18886 (antagonist)(167)	26	8.29 (5.2)	-1.21
GPR88	G _i	HEK T	PDSP reference [#]	6.1	5.99 (1030)	-0.74
GPR4	G _s	HEK T	H ⁺ (161, 168)	5.9	7.99 (10.1)	5.53
GPR65	G _s	HEK T		9.1	7.44 (36.4)	3.56
GPR68	G _s	HEK T		13.6	6.80 (157)	3.36
GPR39	G _s	HEK T	GPR39-C3 (146–148)	16.2	6.28 (527)	1.13

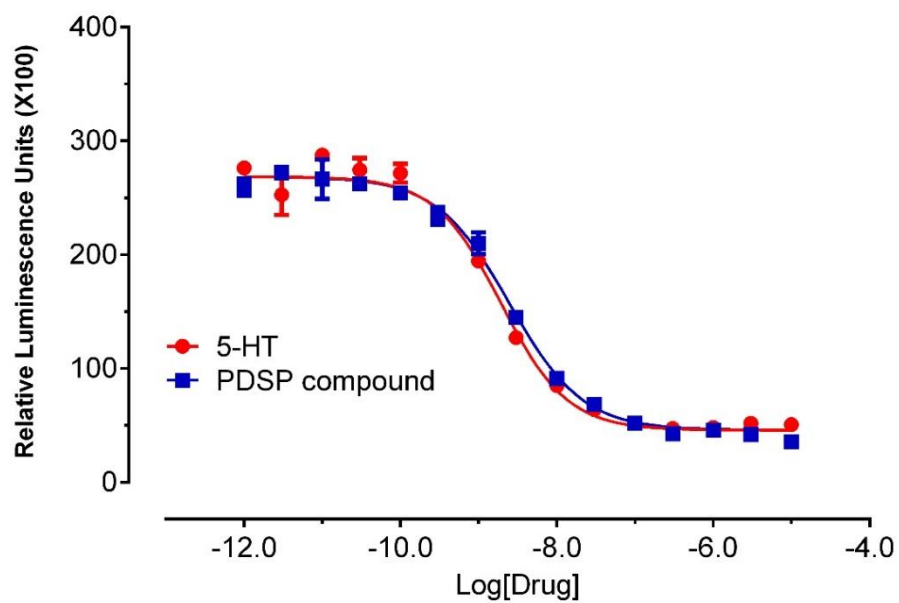
Notes:

#: Roth lab unpublished results

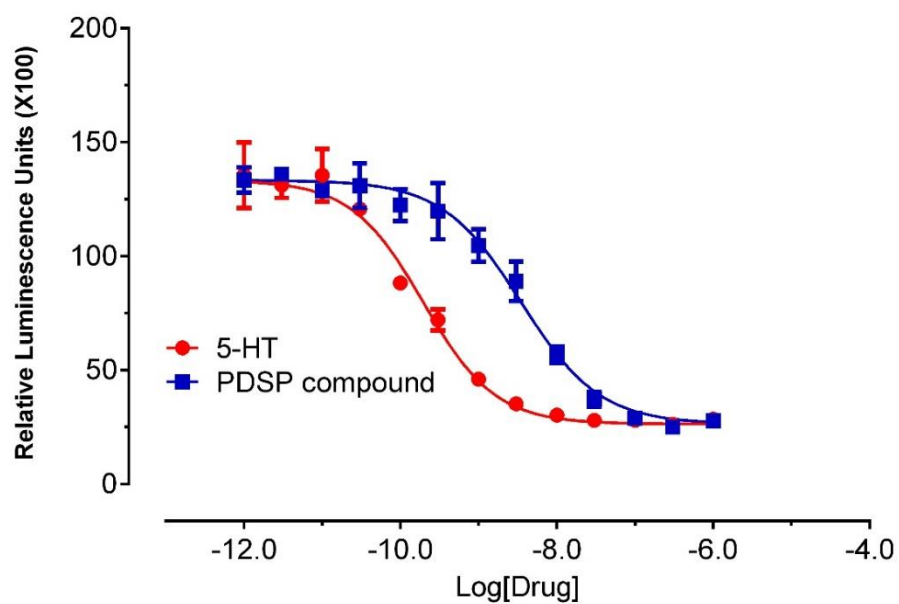
*: E_{max} in fold for G_i pathway represents the ratio of basal vs maximal inhibition; E_{max} in fold for G_s pathway represents the ratio of maximal activation vs basal.

Figure 45. Representative curves for the GloSensor cAMP assay. The assays were conducted according to above procedures and analyzed in GraphPad Prism 6.0.

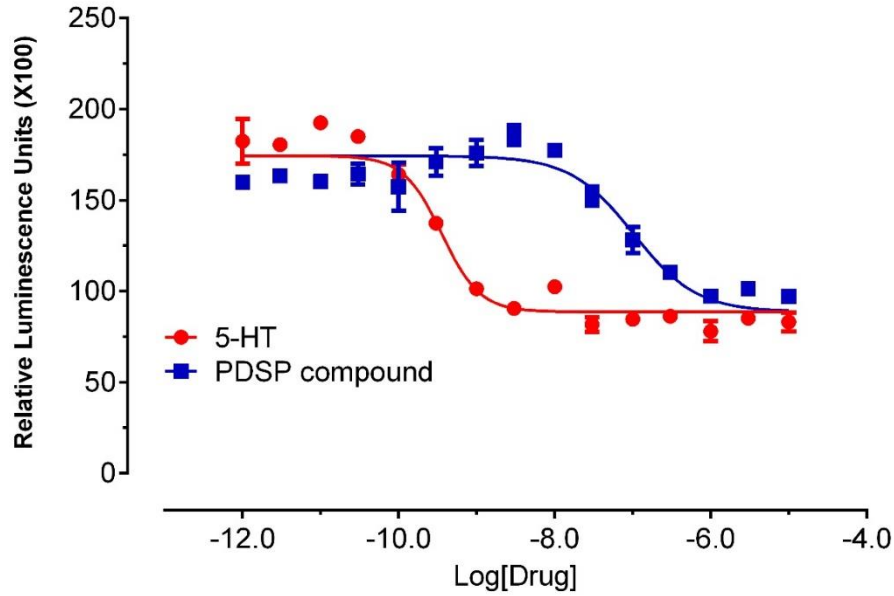
5-HT_{1A} G_i agonist assay
(GloSensor cAMP)



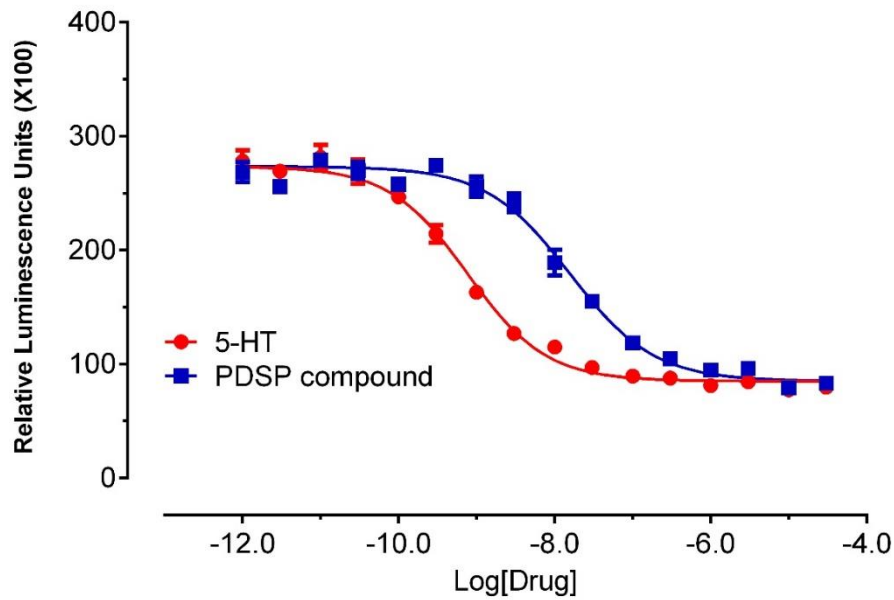
5-HT_{1B} G_i agonist assay
(GloSensor cAMP)

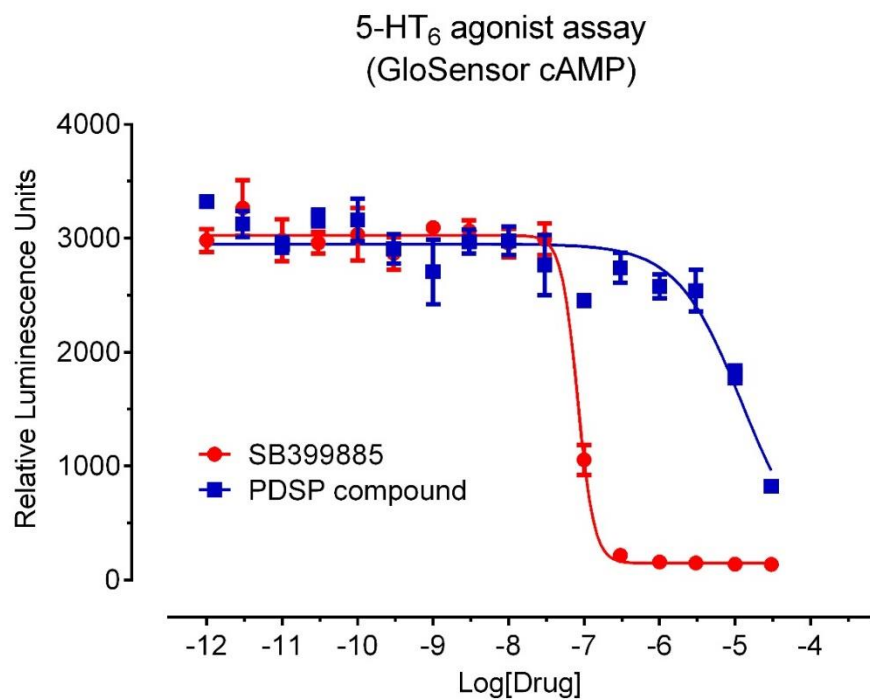
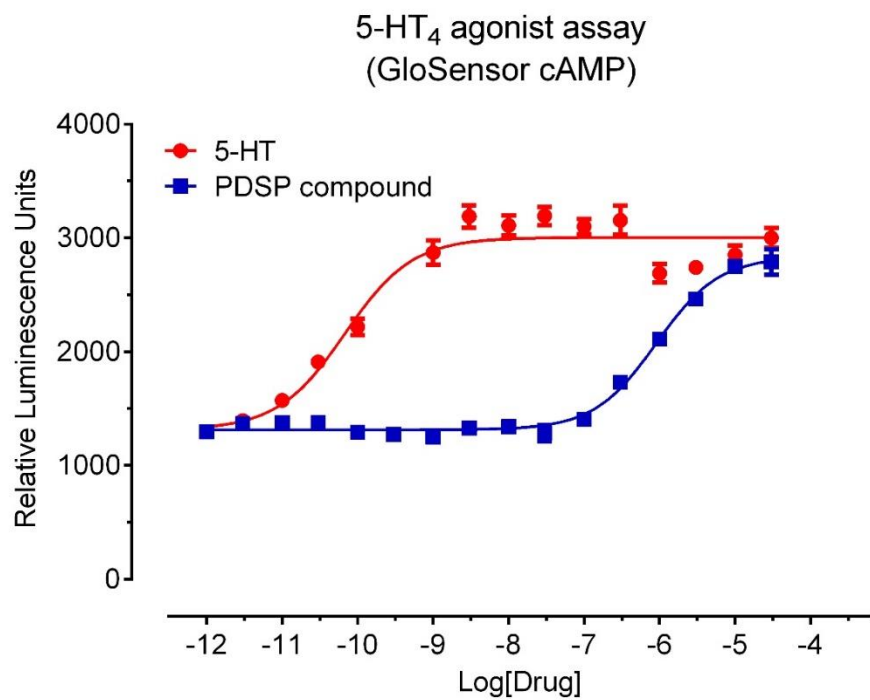


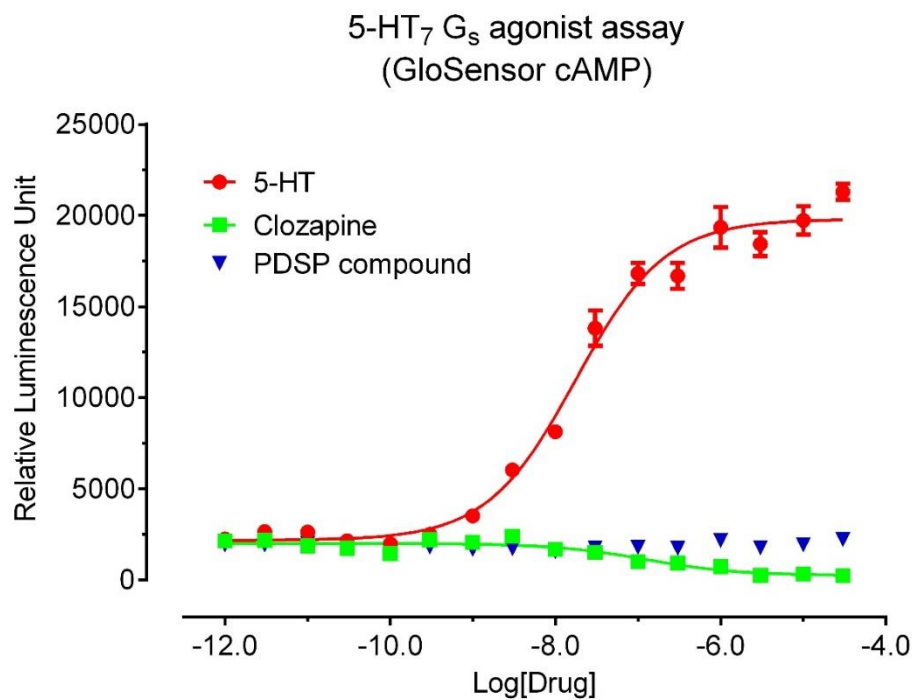
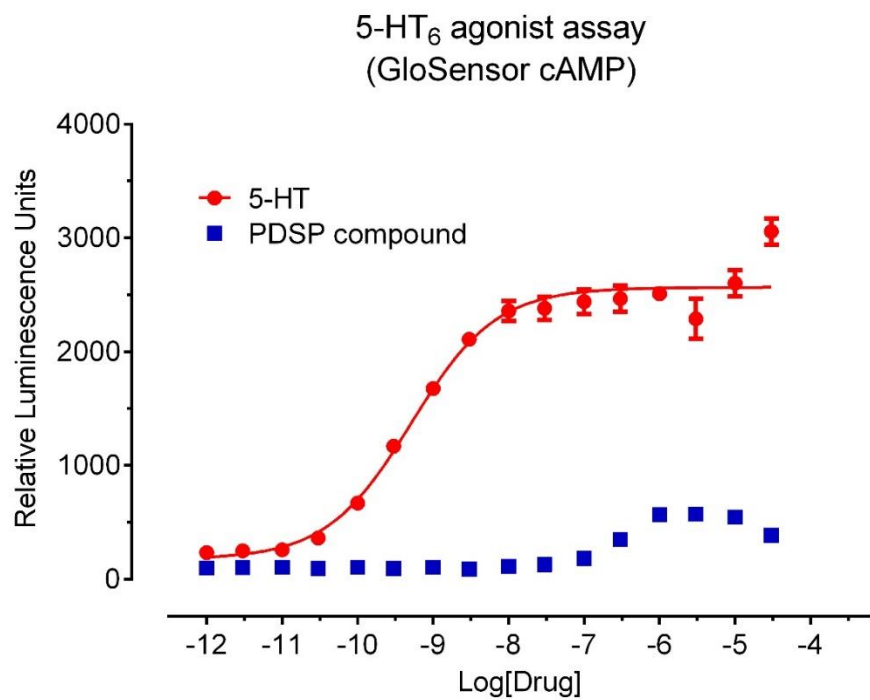
5-HT_{1D} G_i agonist assay
(GloSensor cAMP)



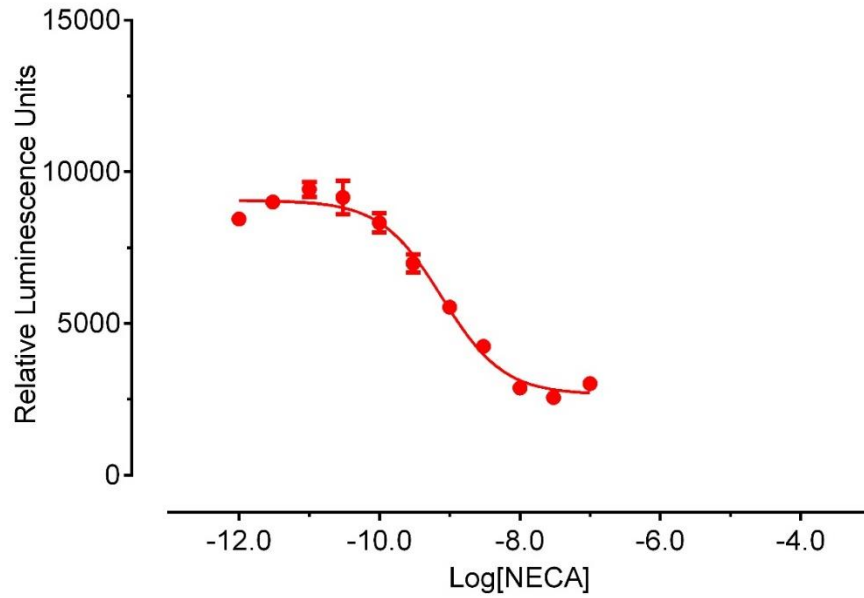
5-HT_{1E} G_i agonist assay
(GloSensor cAMP)



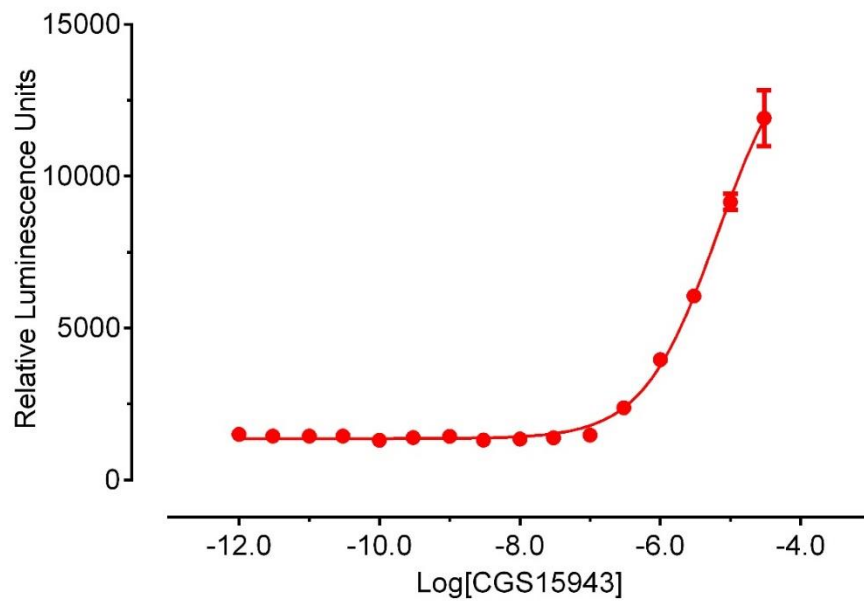


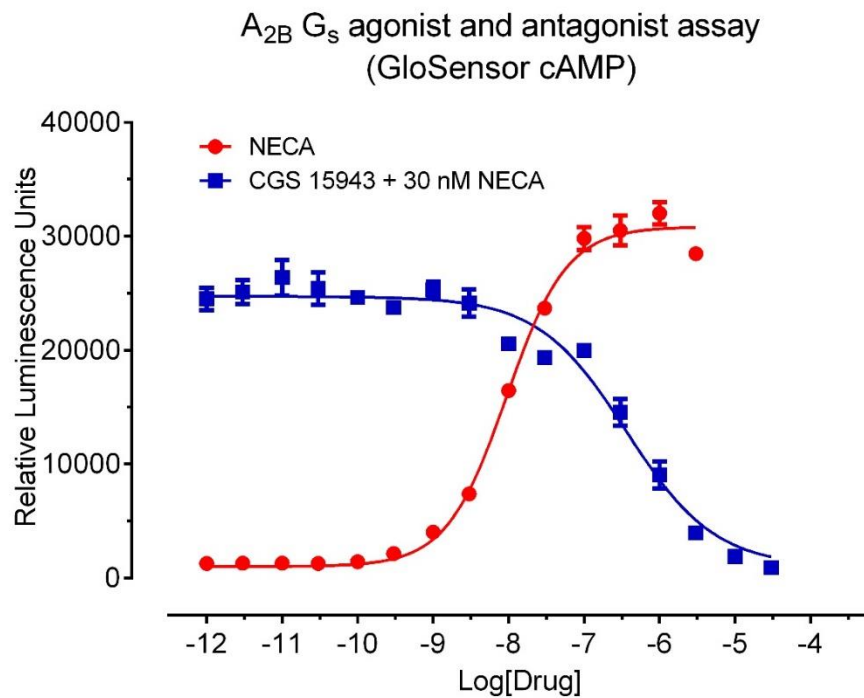
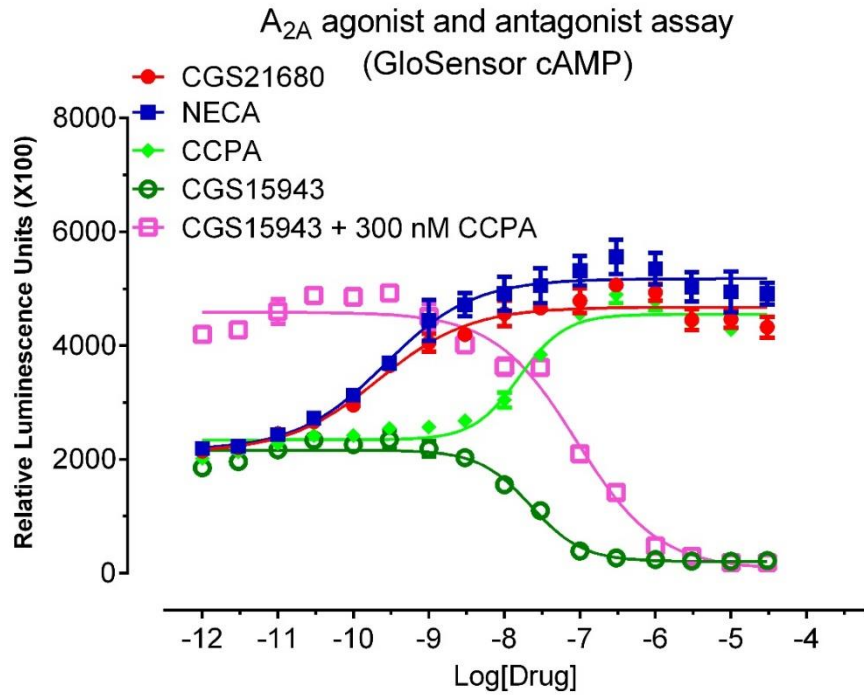


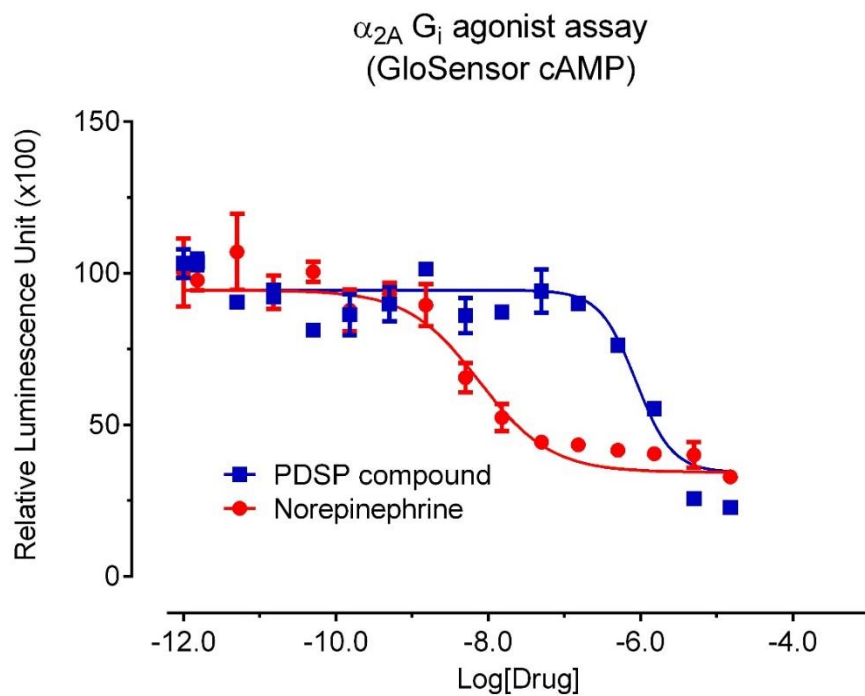
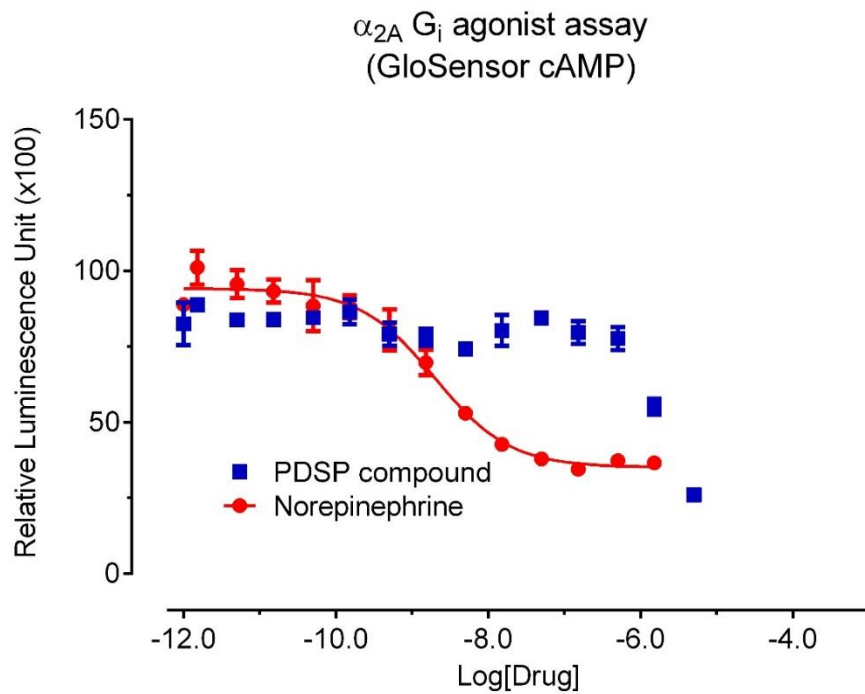
A₁ G_i agonist assay
(GloSensor cAMP)

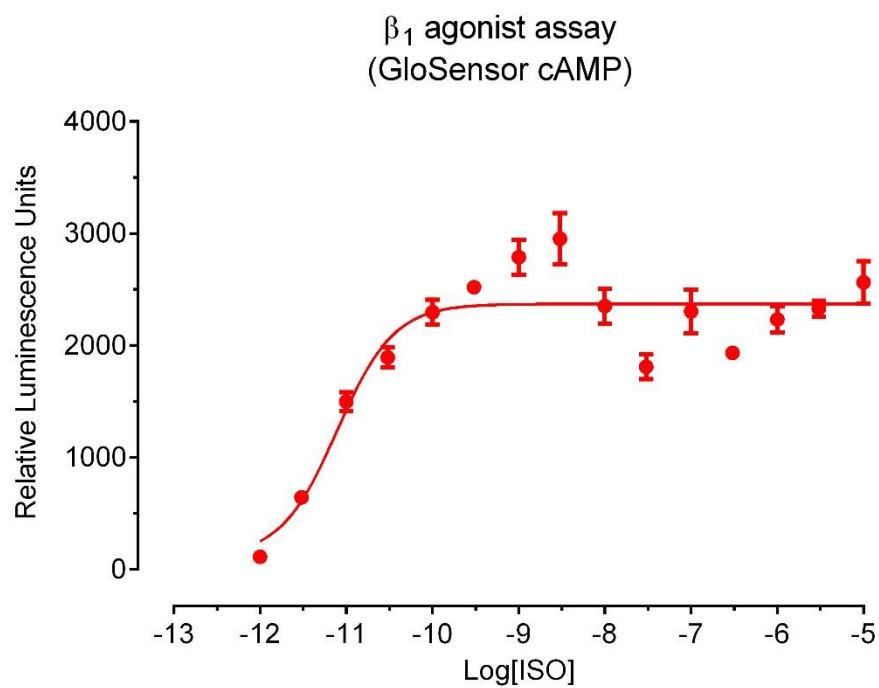
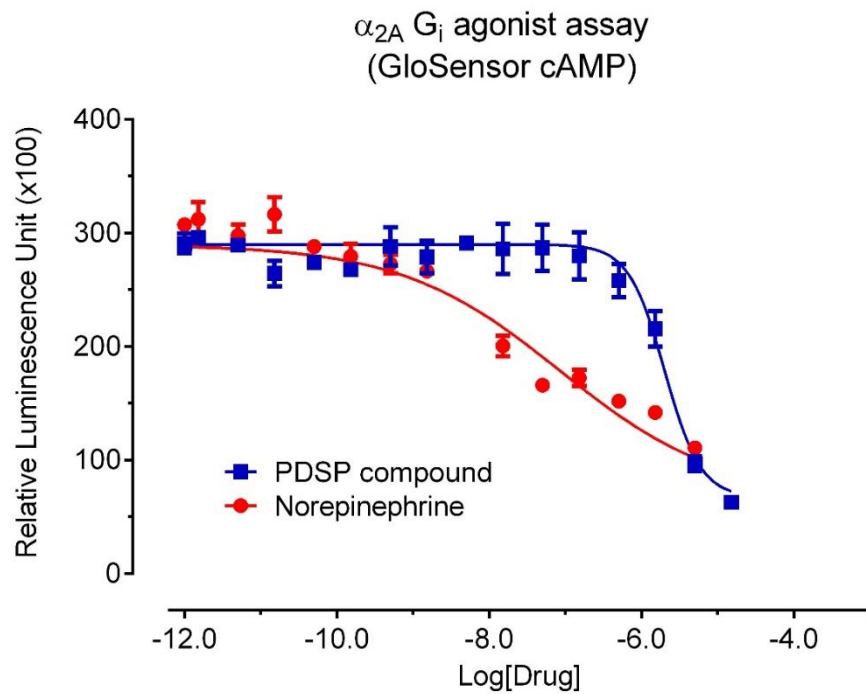


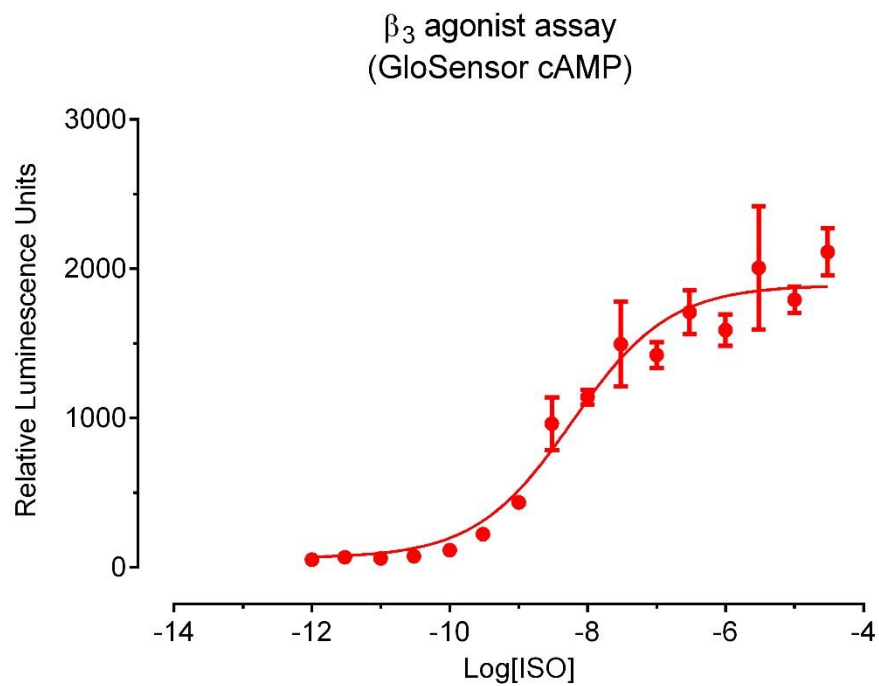
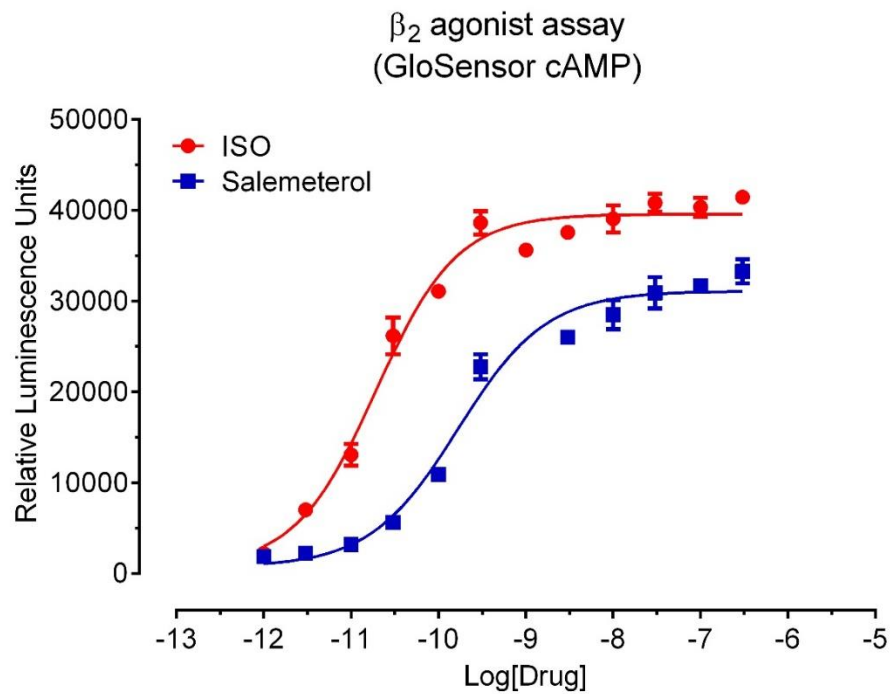
A₁ G_i antagonist assay
(GloSensor cAMP, 10 nM NECA)

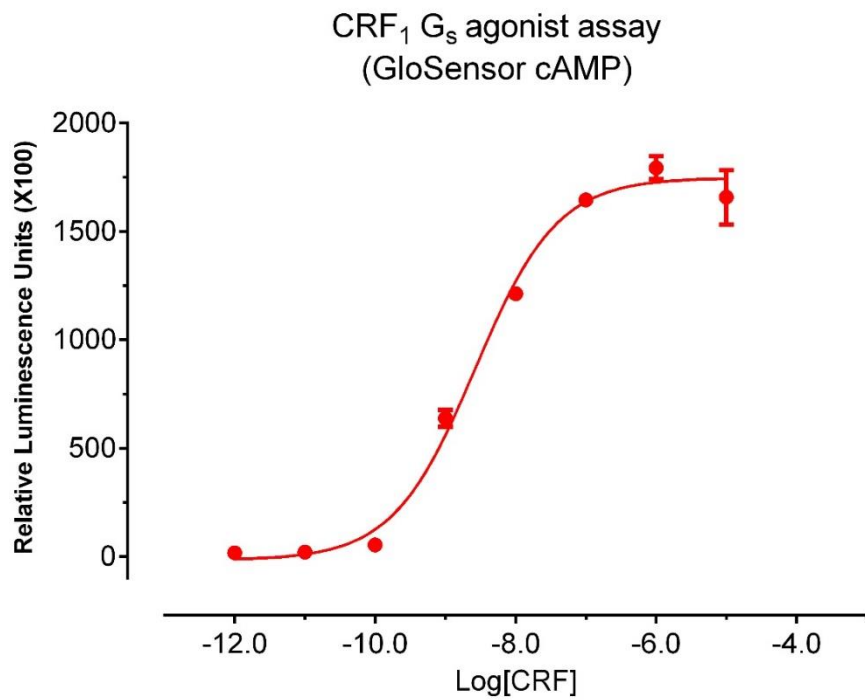
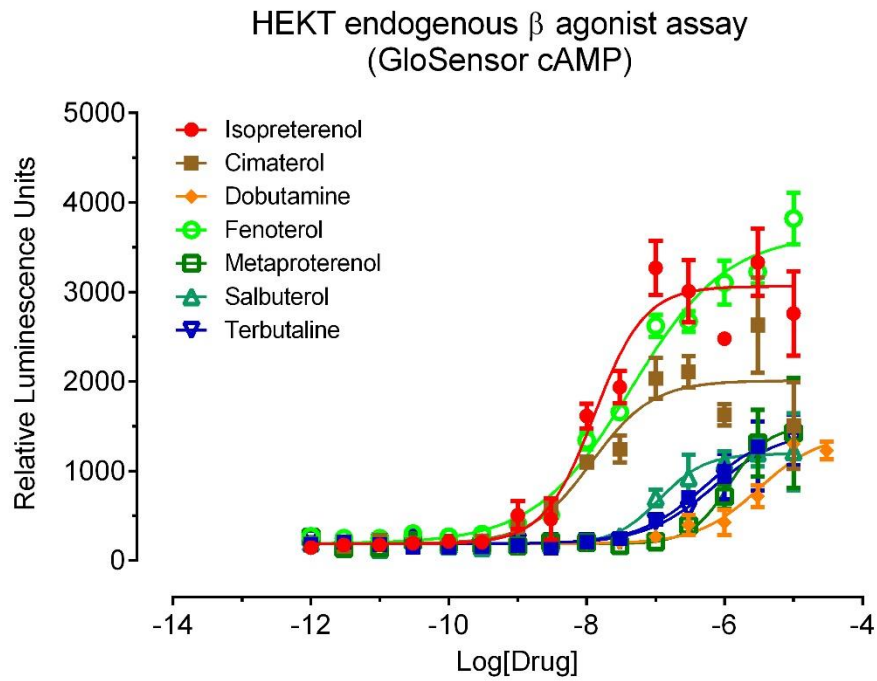


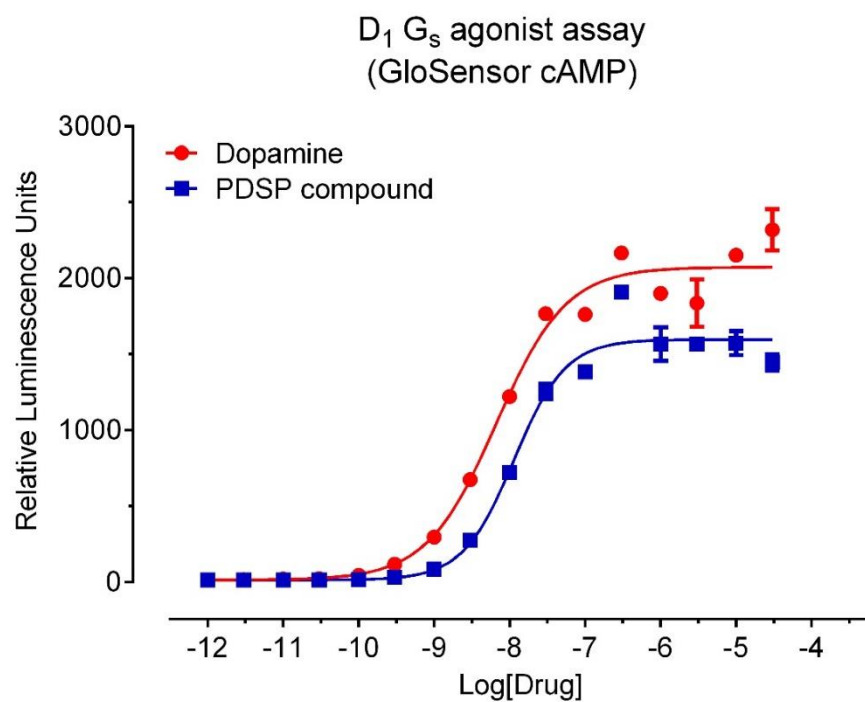
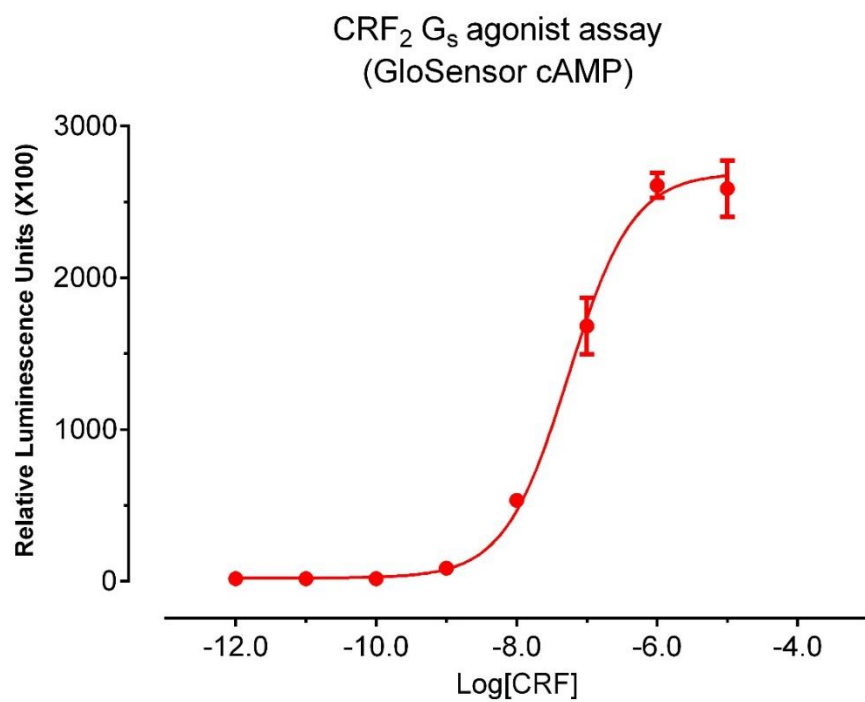


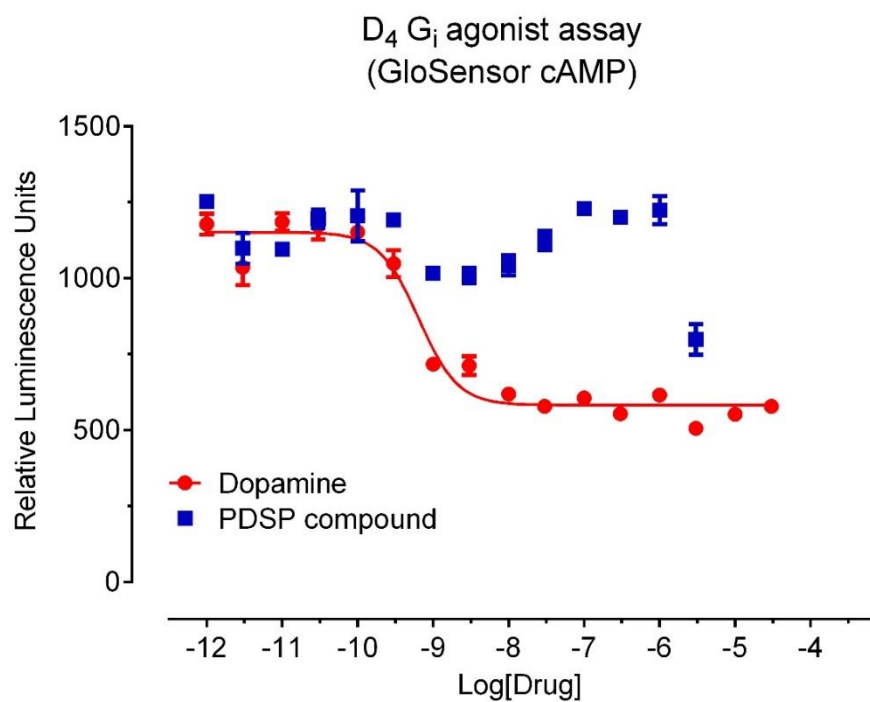
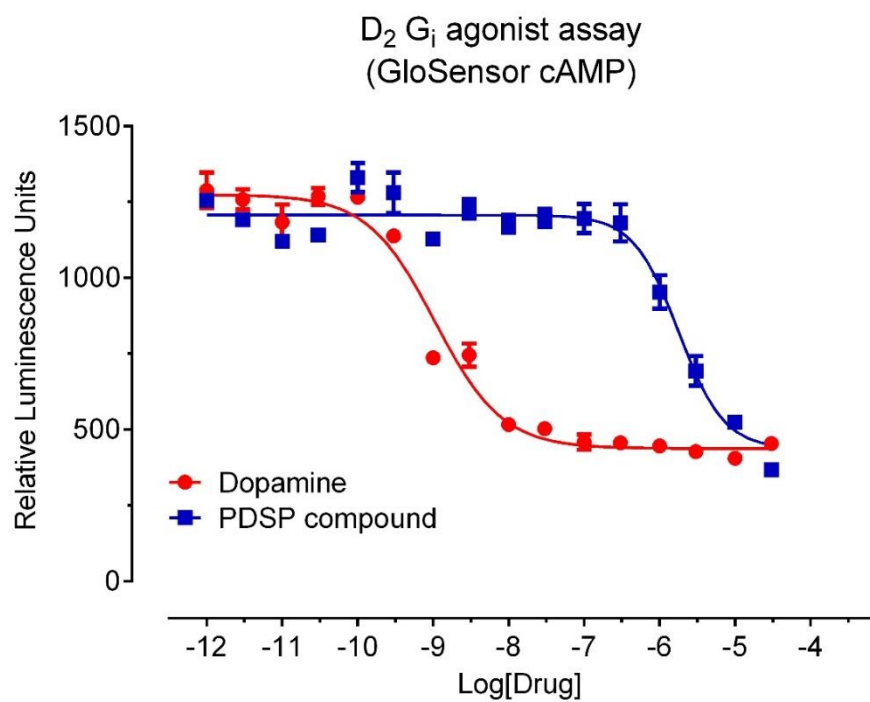


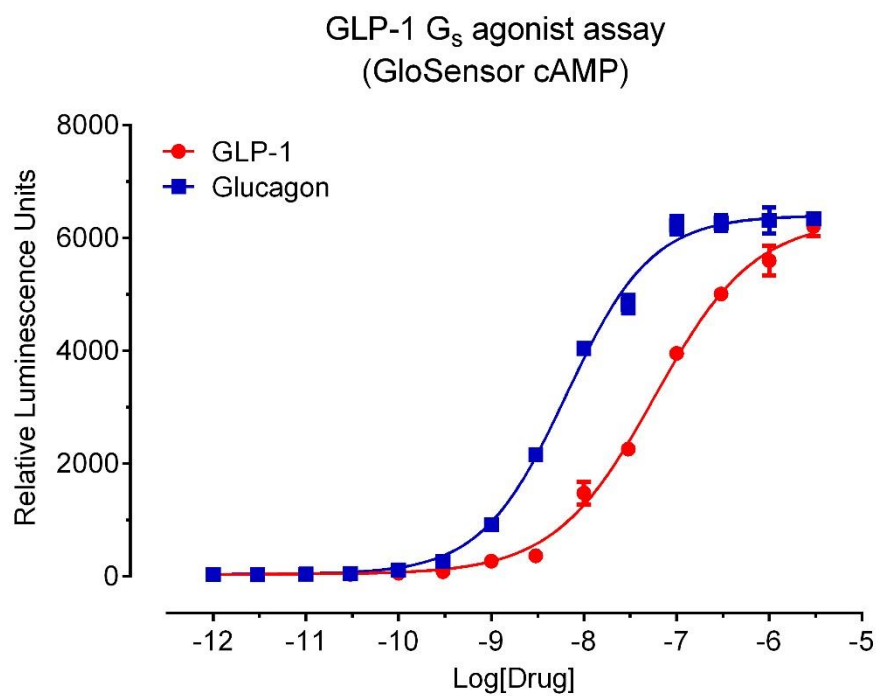
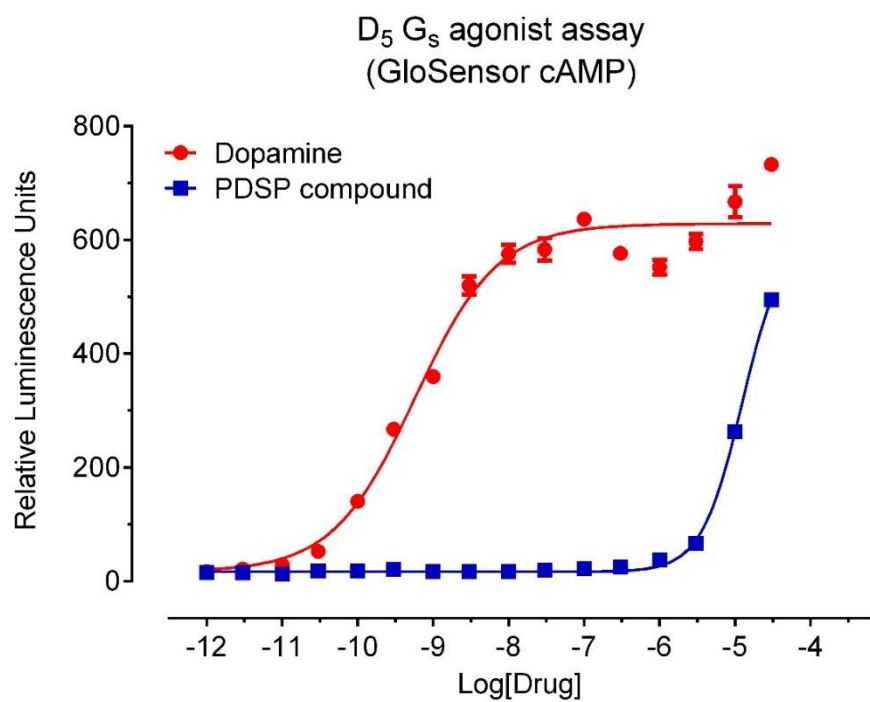




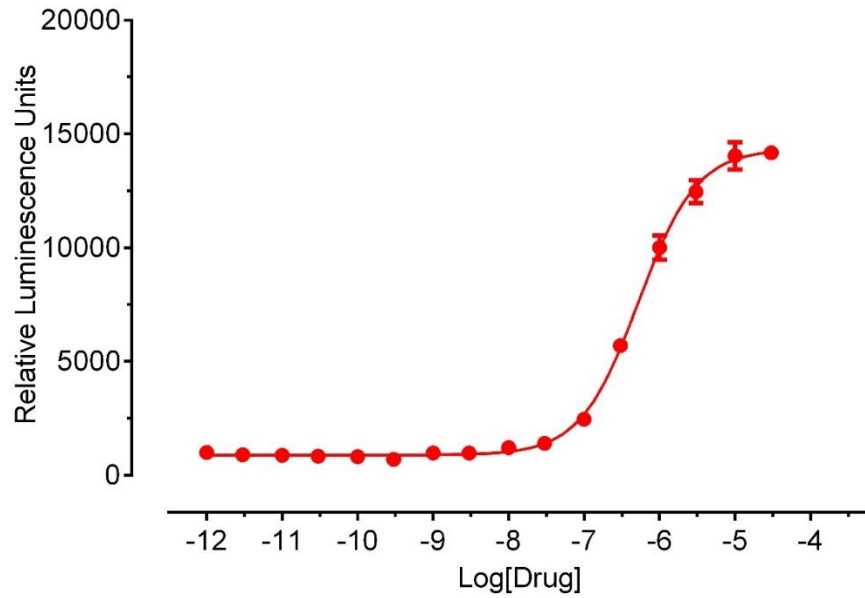




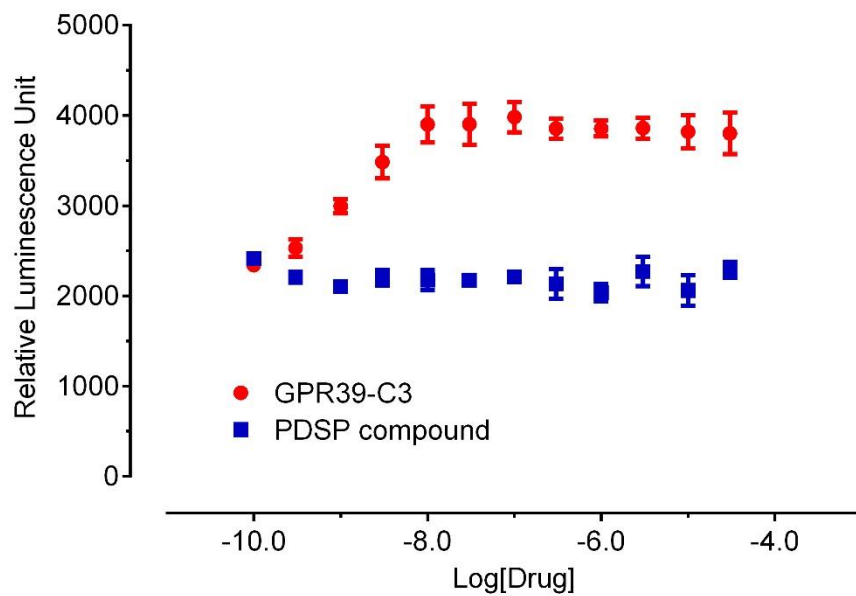




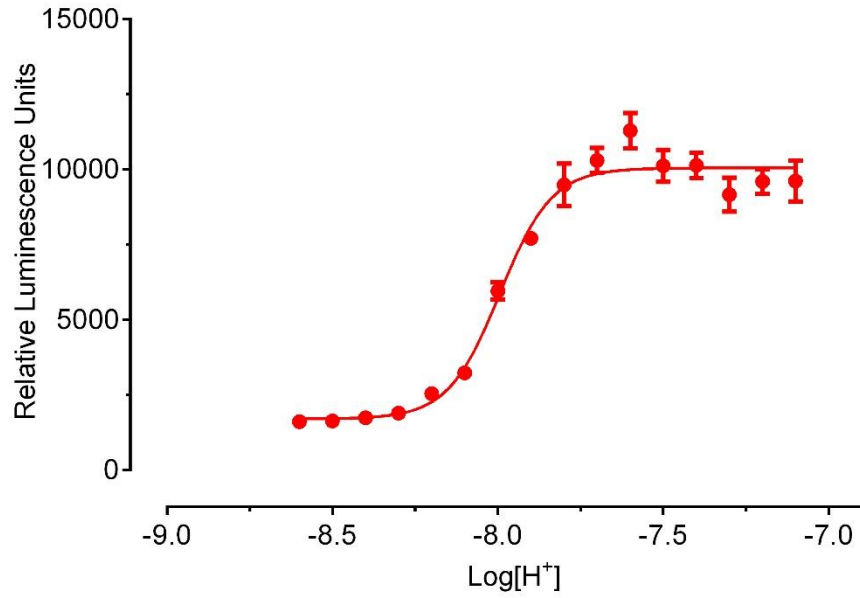
GPR39 G_s agonist assay
(GloSensor cAMP)



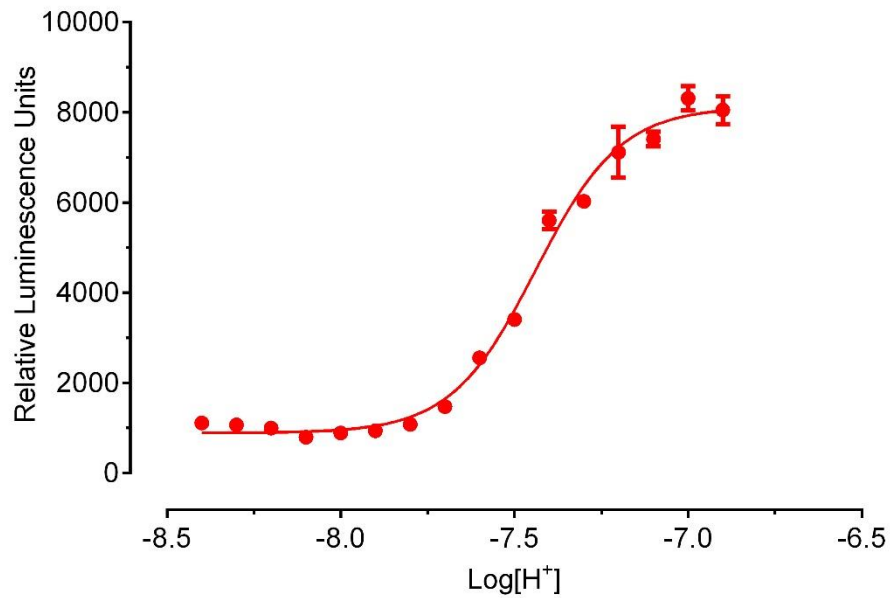
GPR39 agonist assay
(G_q PI hydrolysis)

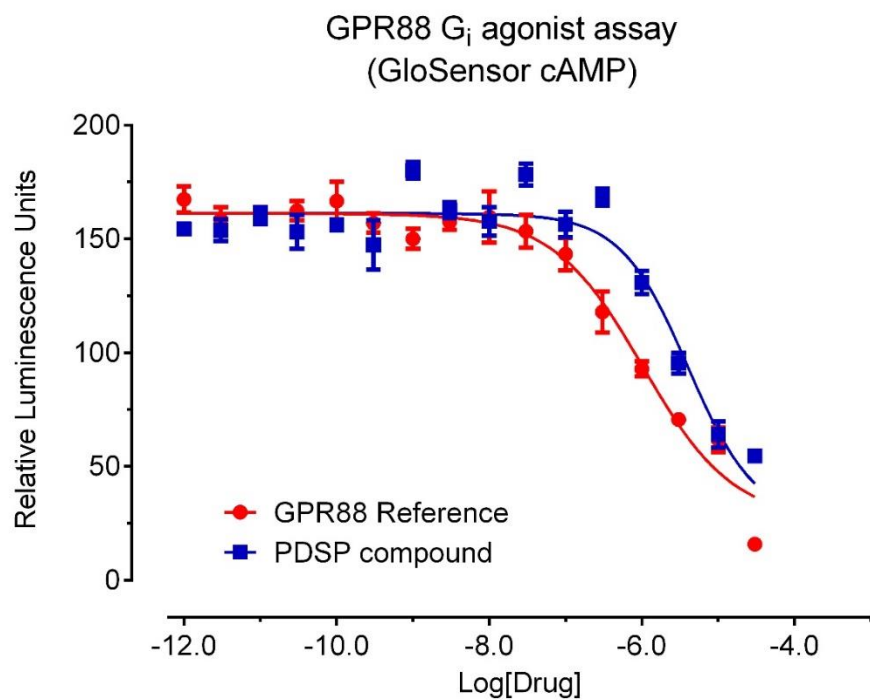
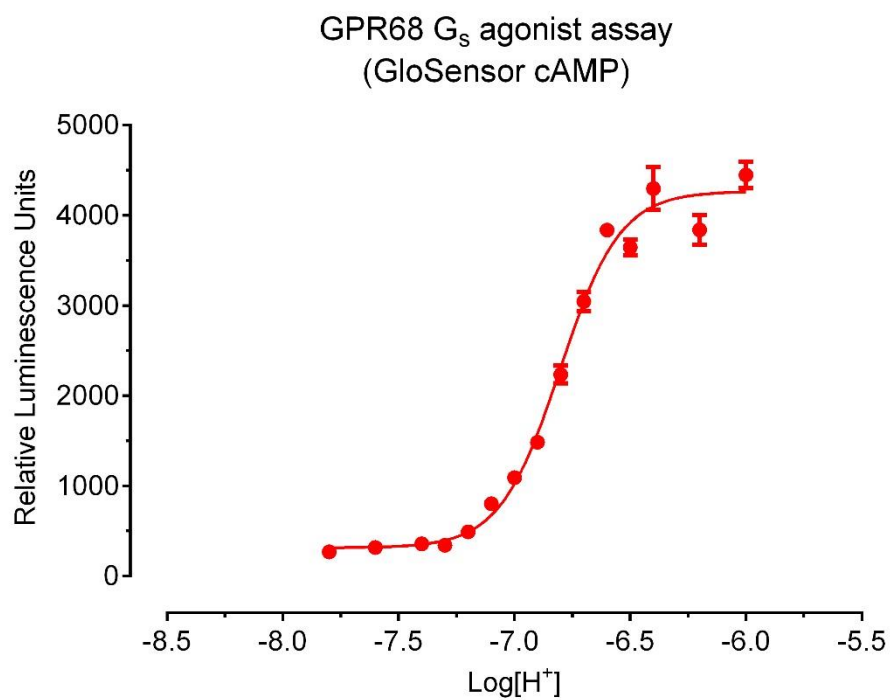


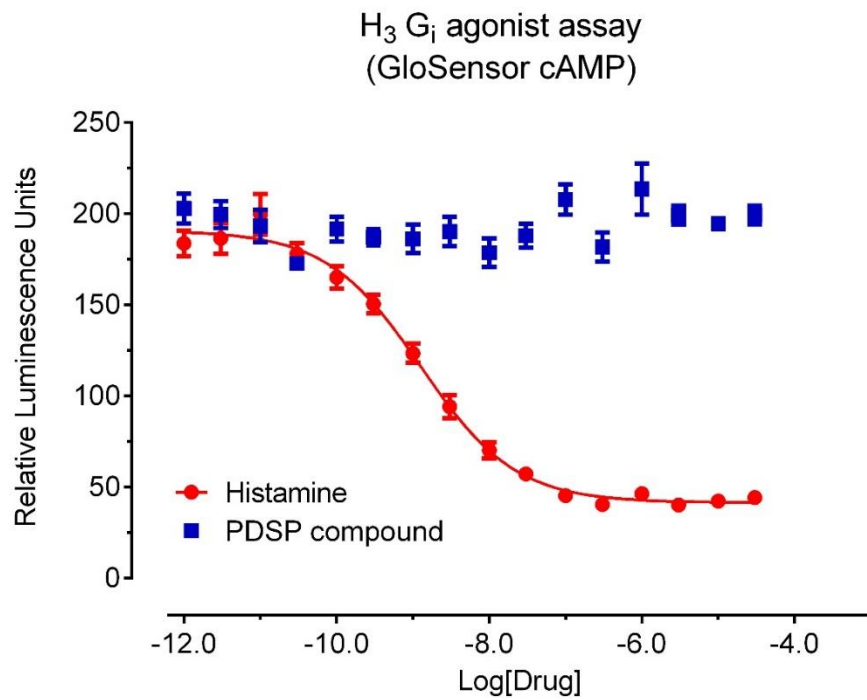
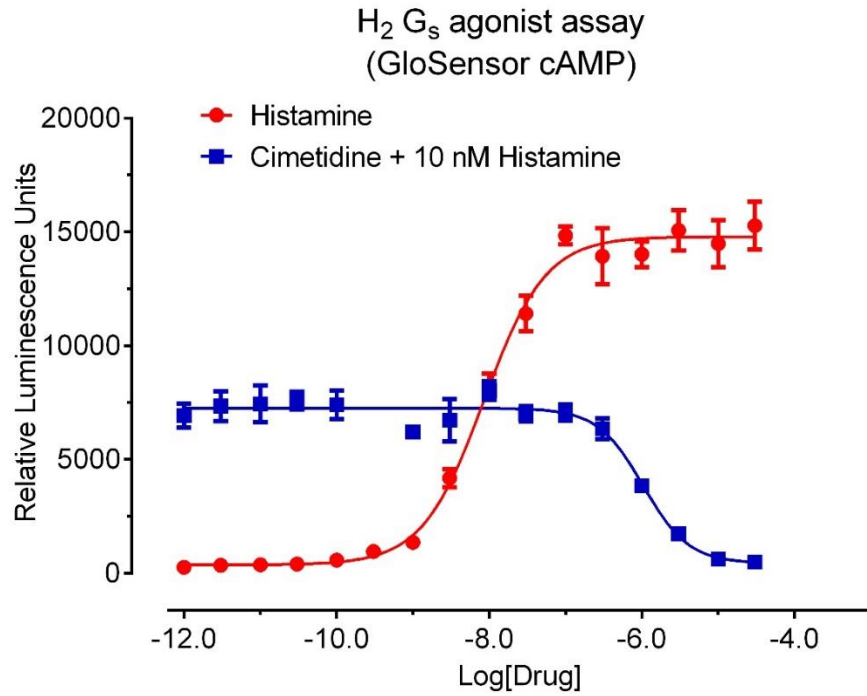
GPR4 G_s agonist assay
(GloSensor cAMP)

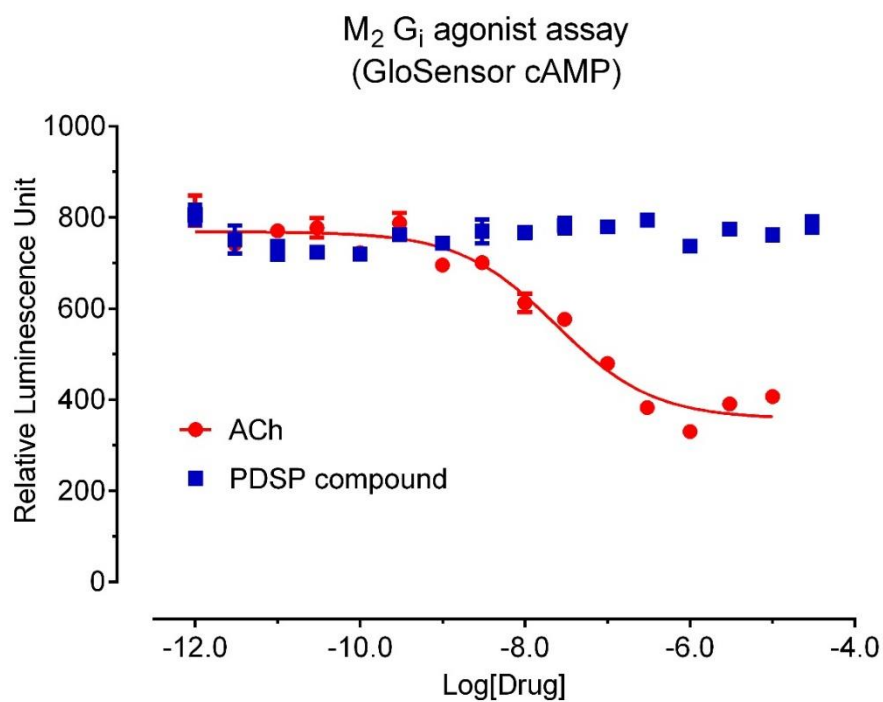
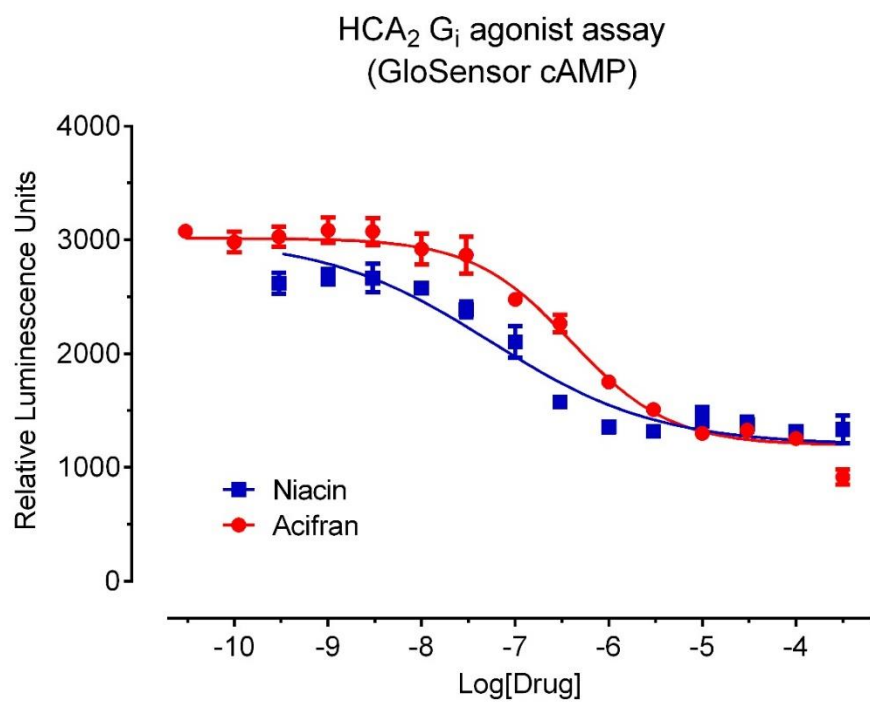


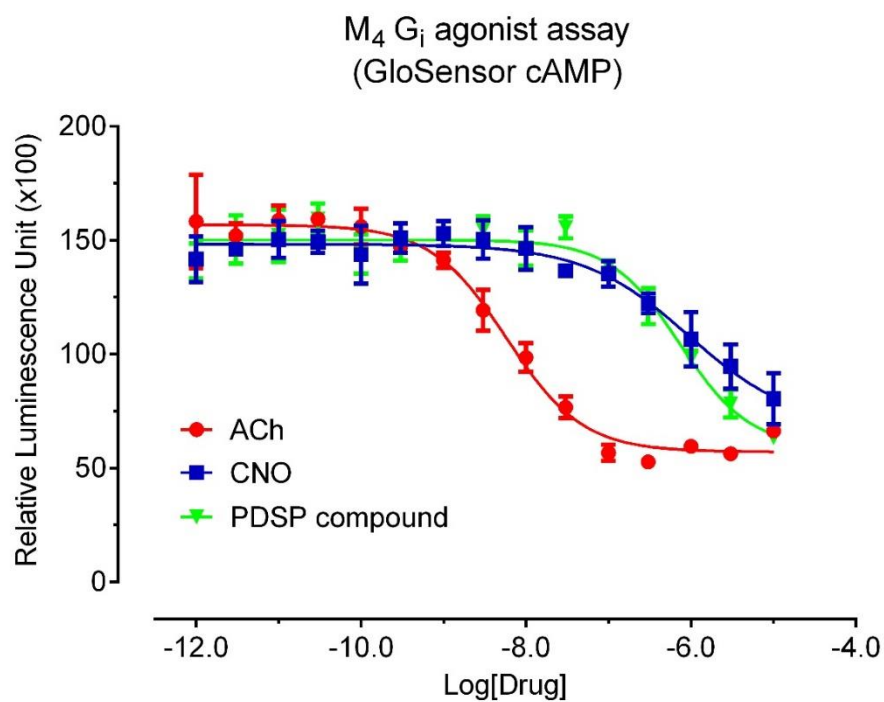
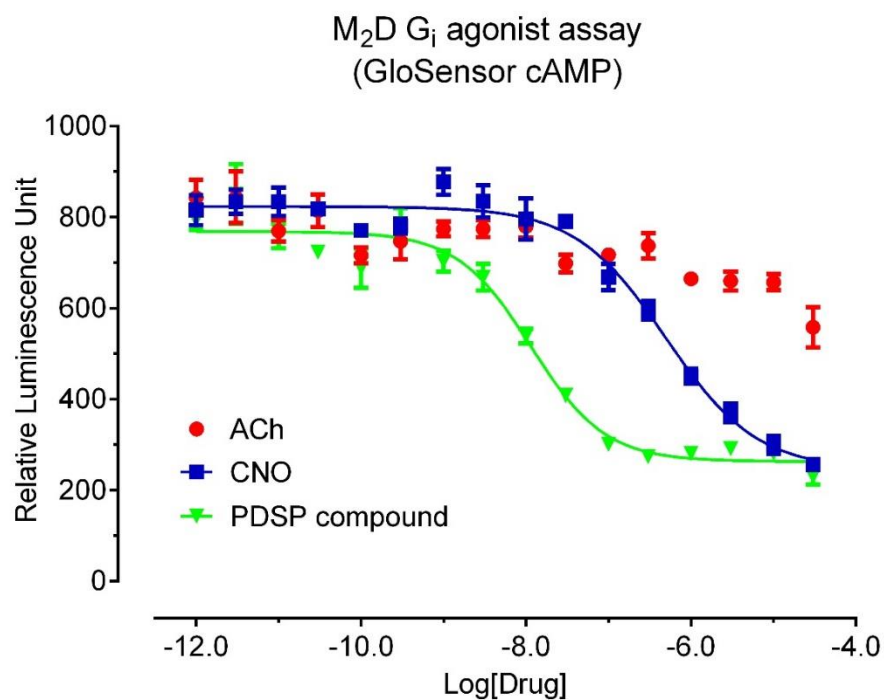
GPR65 G_s agonist assay
(GloSensor cAMP)

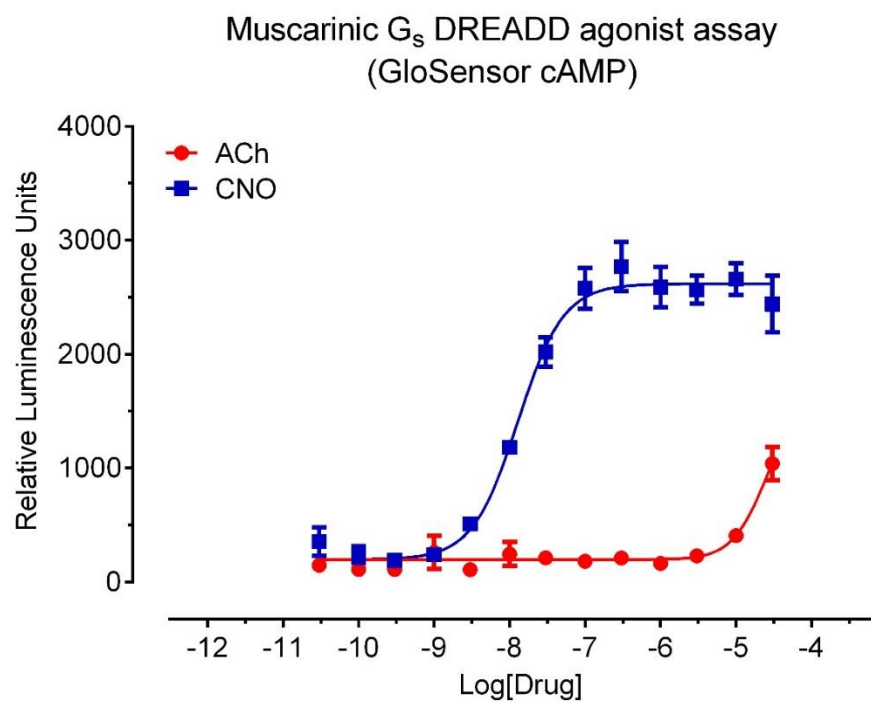
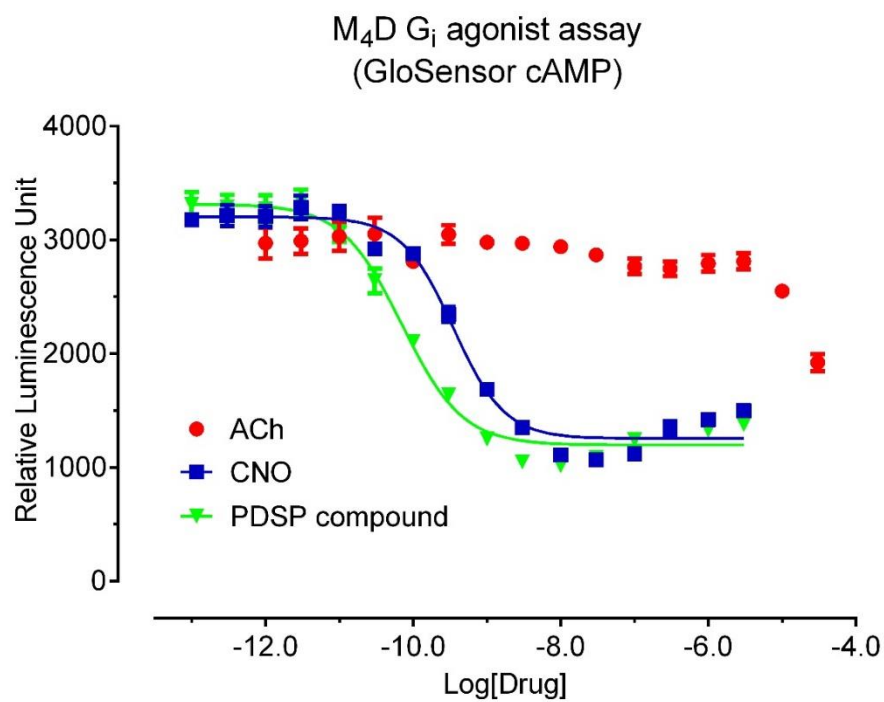




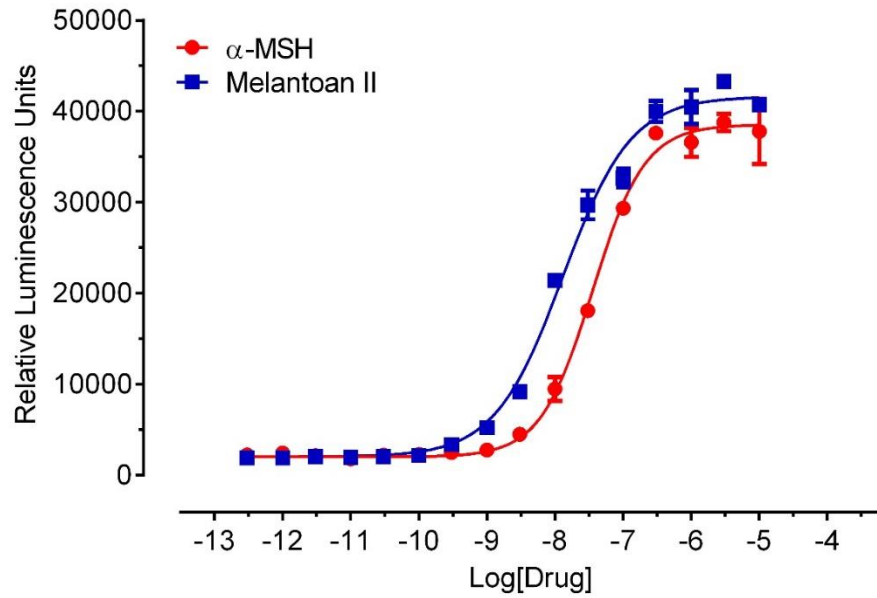




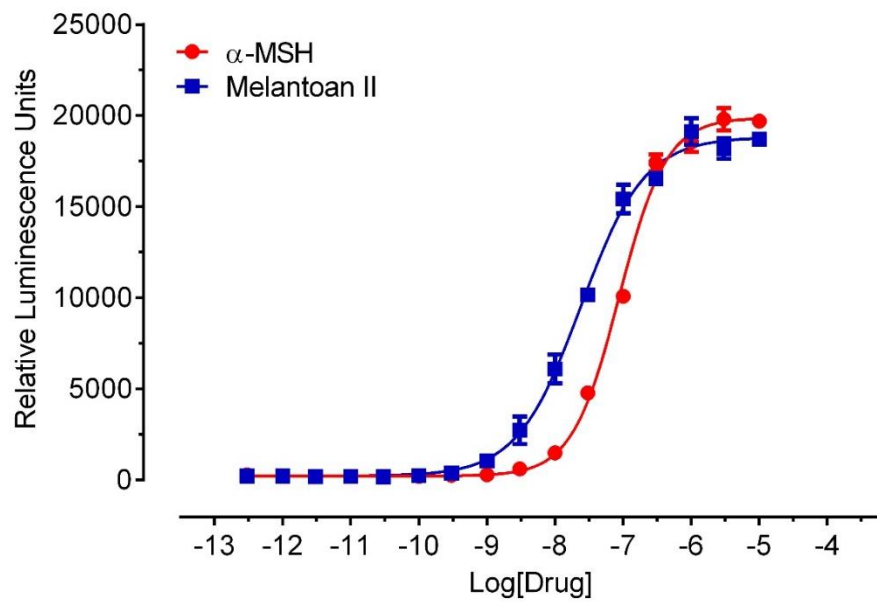


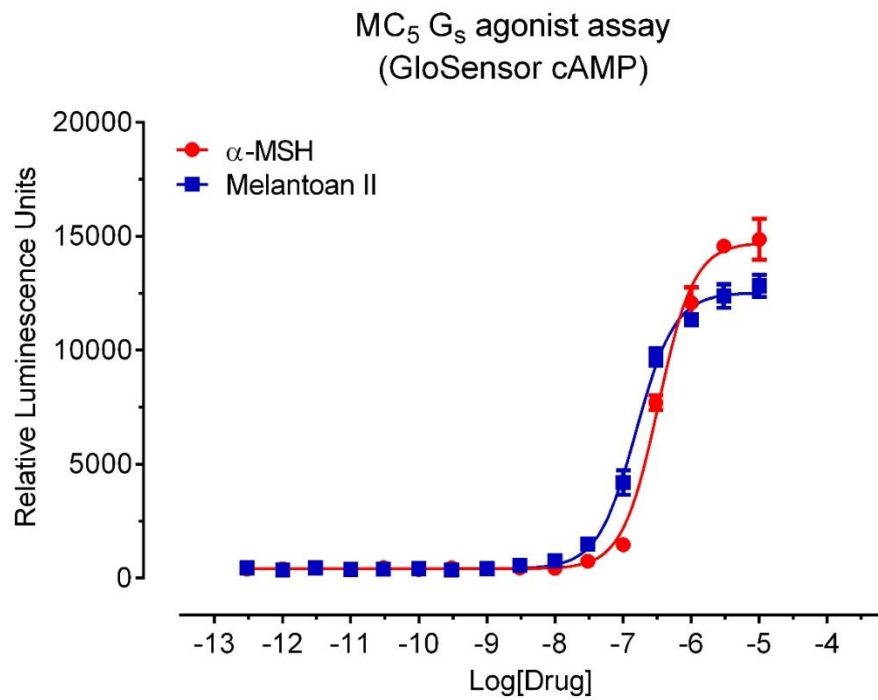
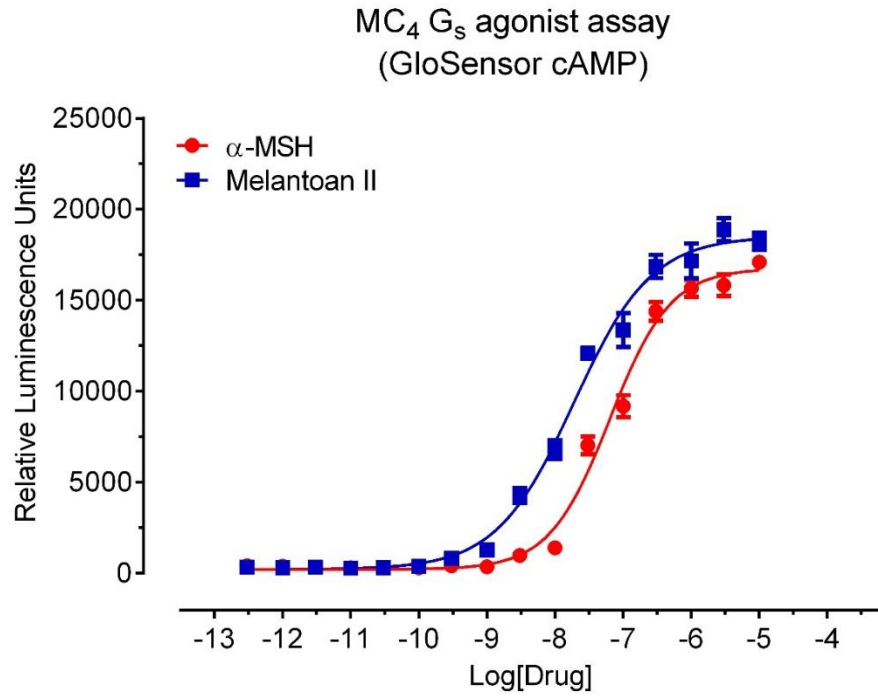


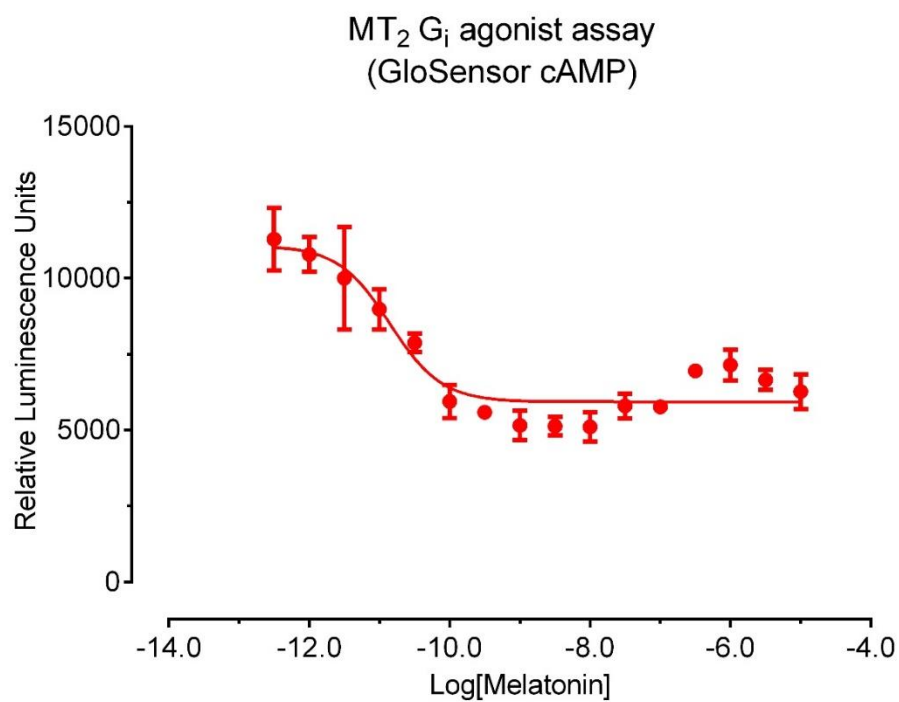
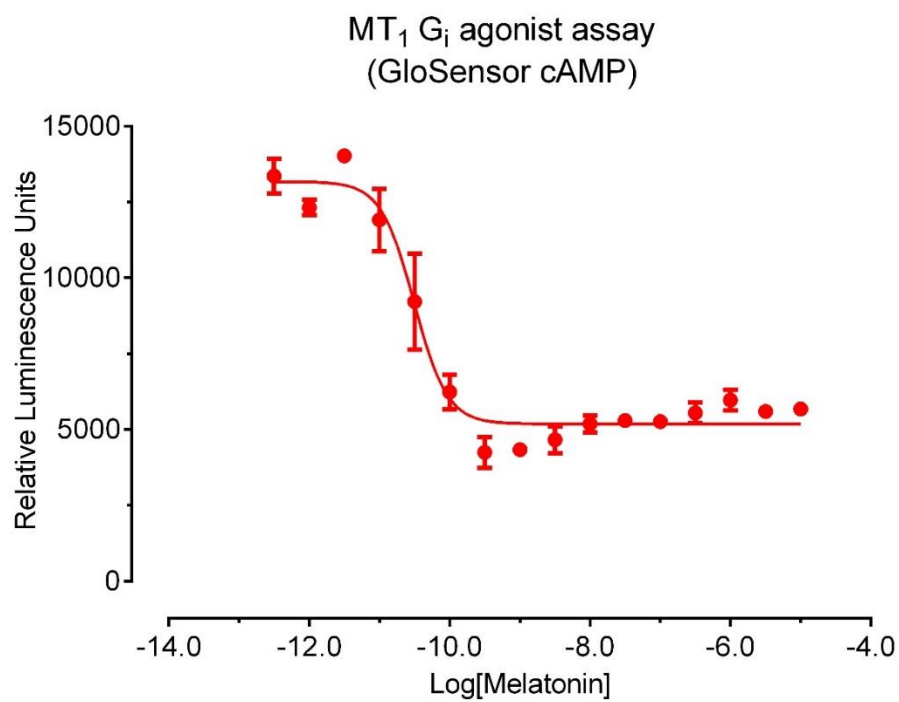
MC₁ G_s agonist assay
(GloSensor cAMP)

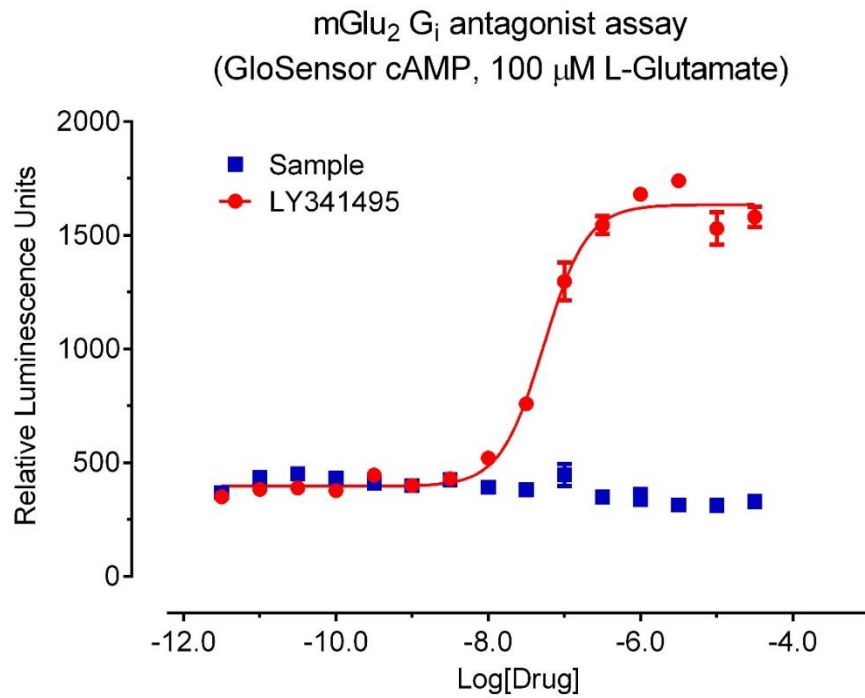
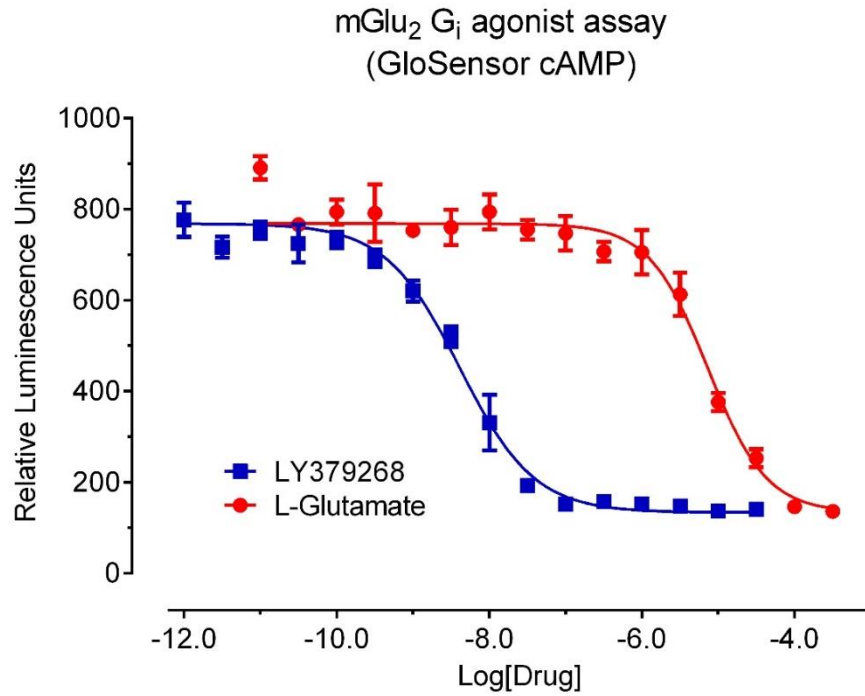


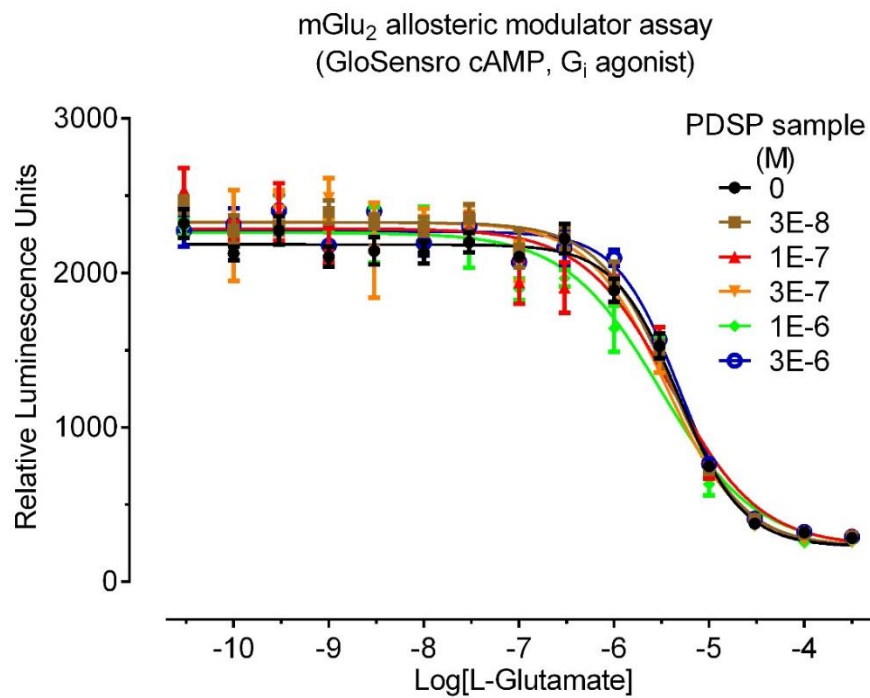
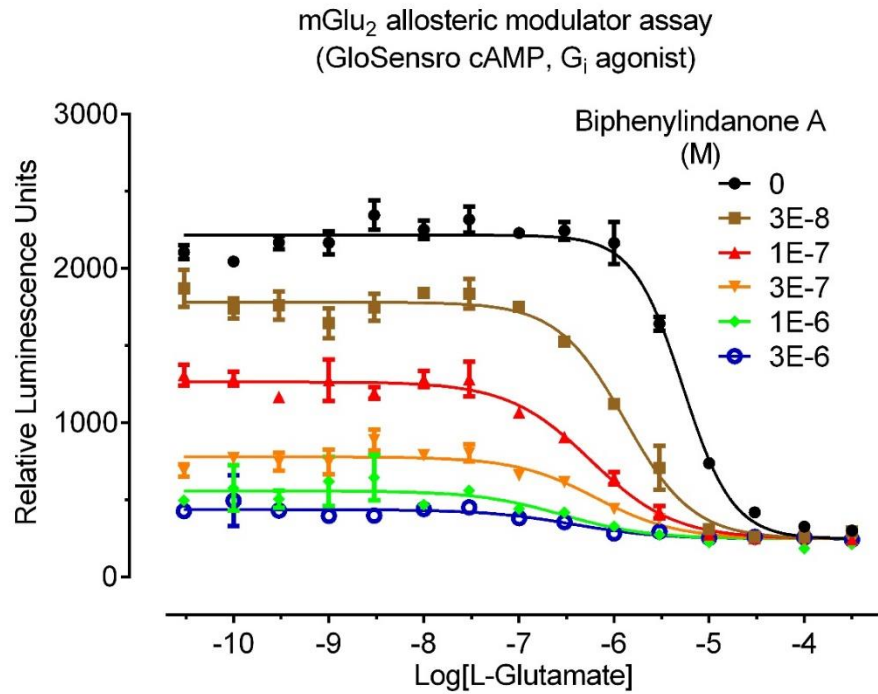
MC₃ G_s agonist assay
(GloSensor cAMP)

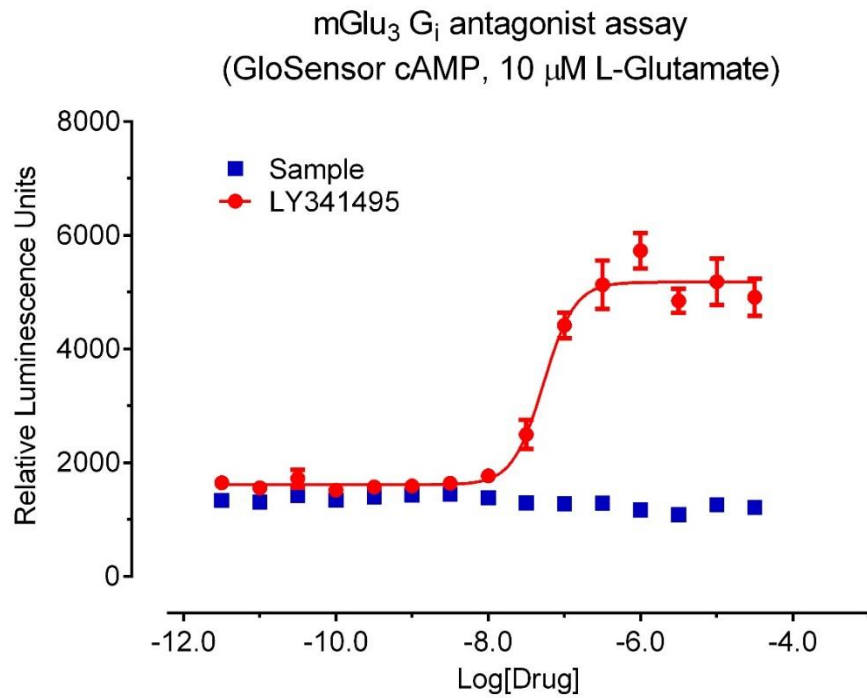
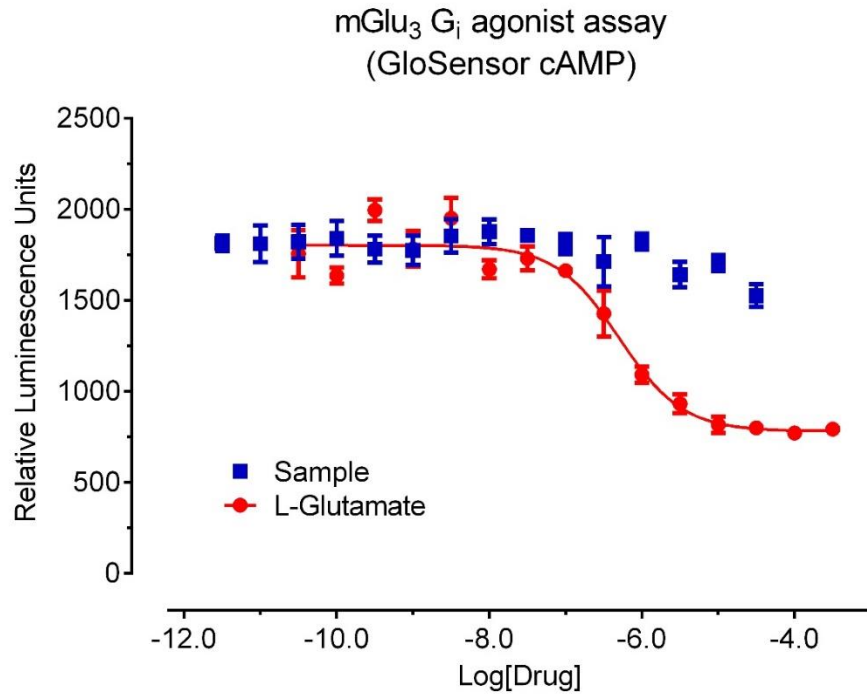


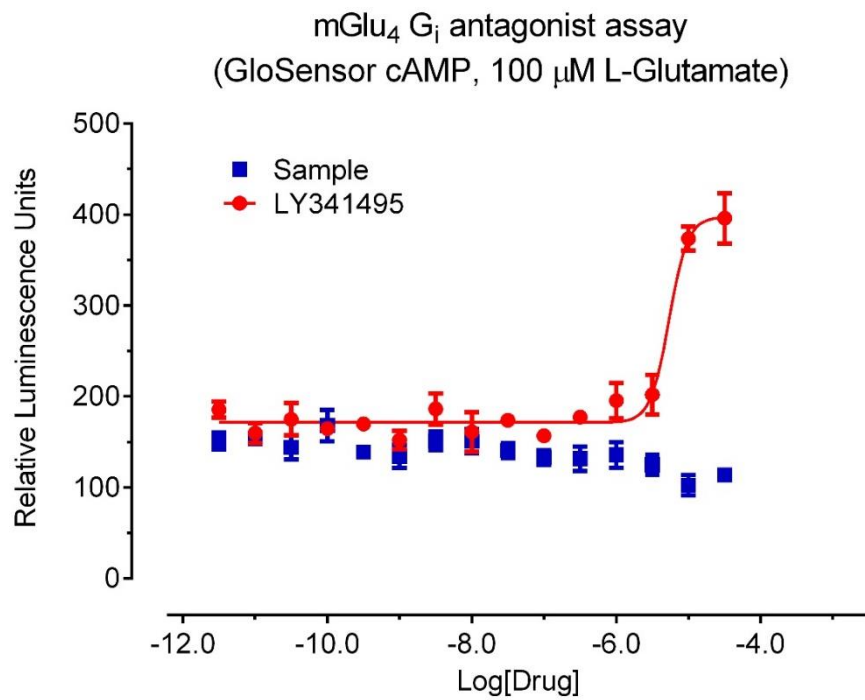
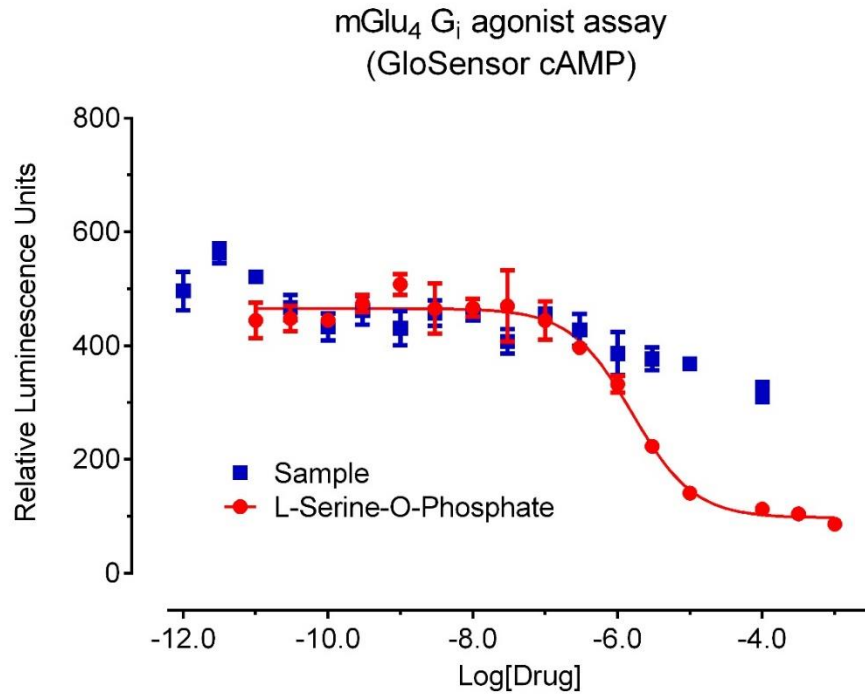


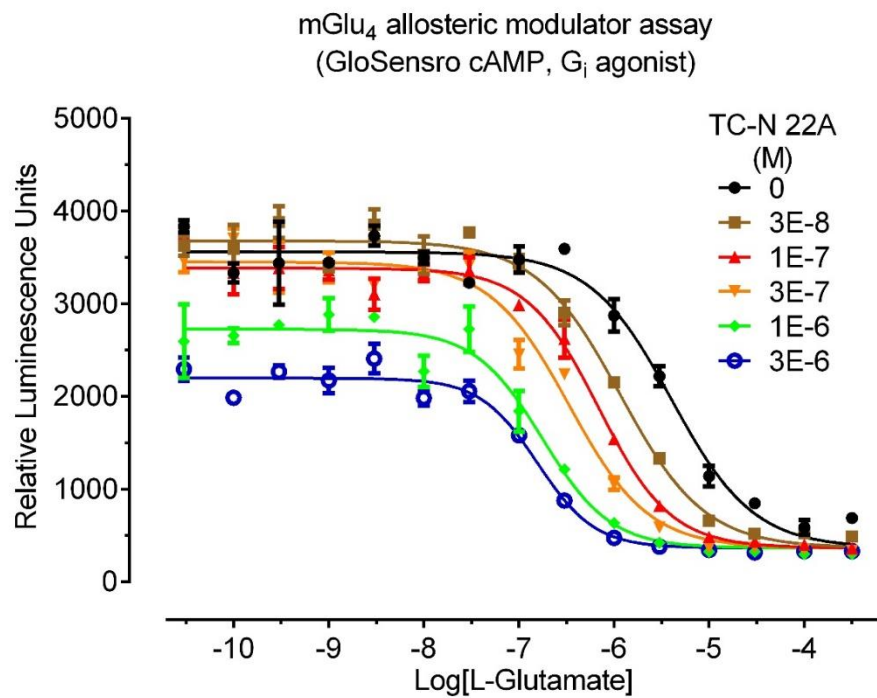
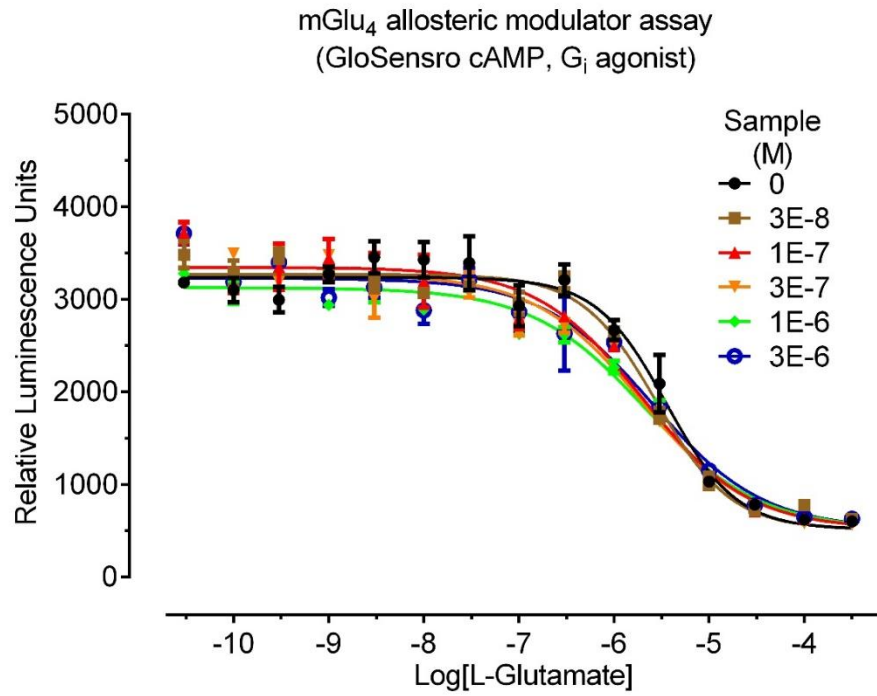


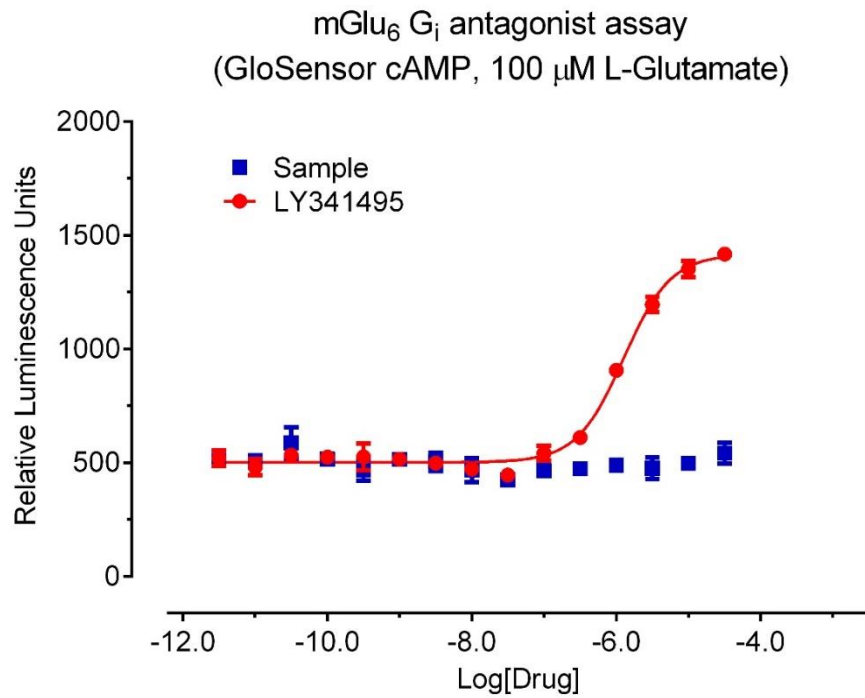
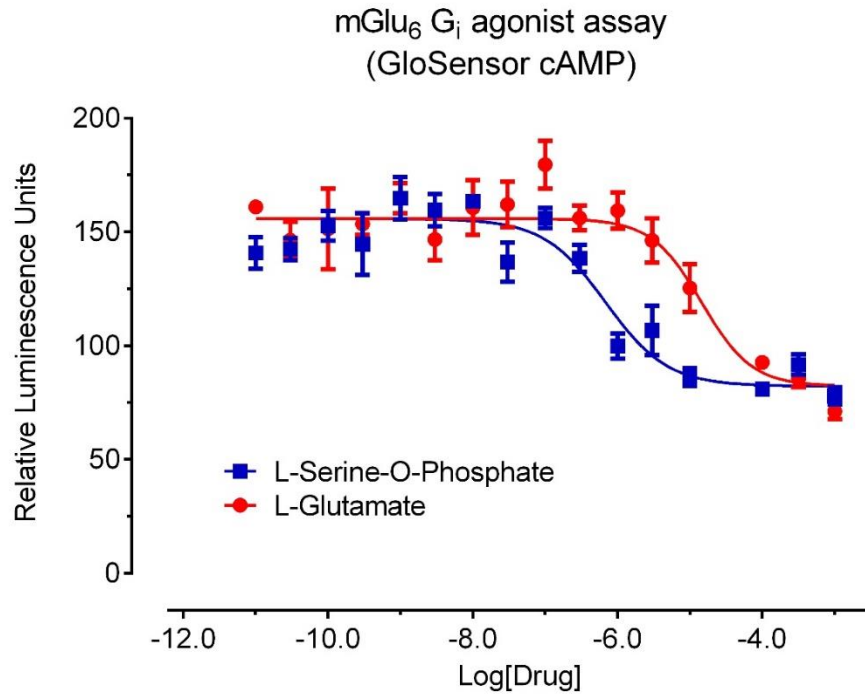


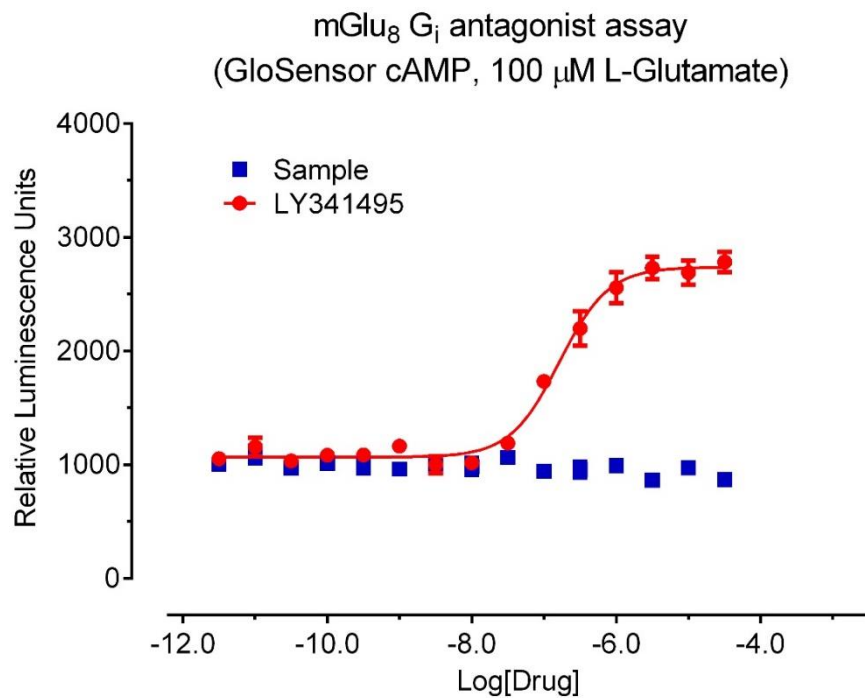
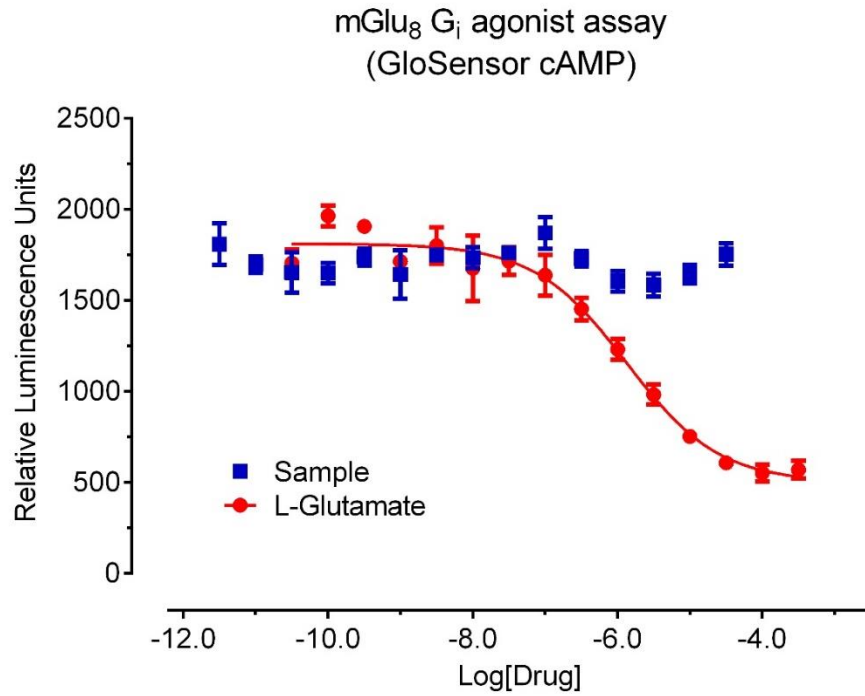


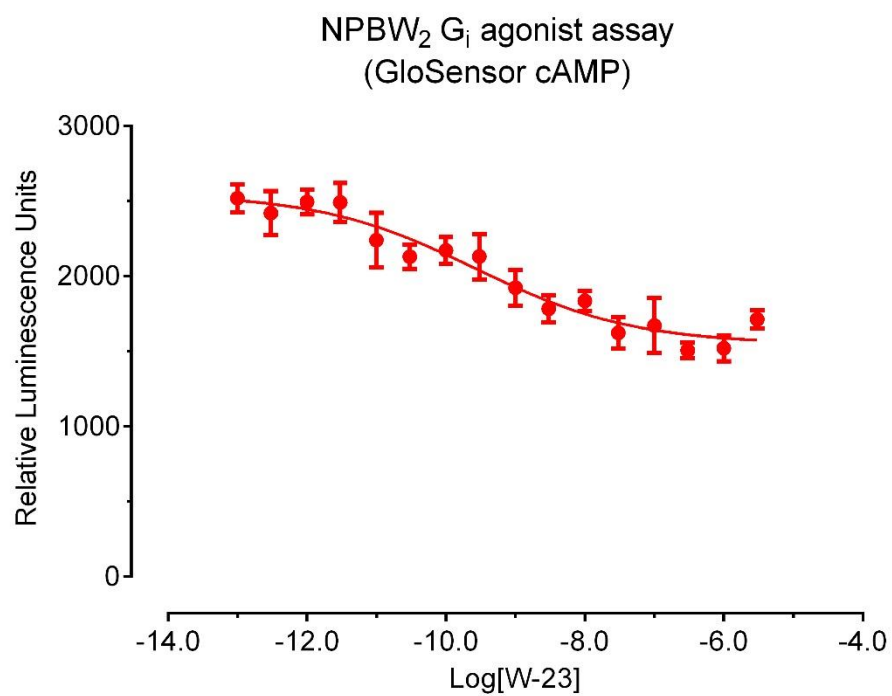
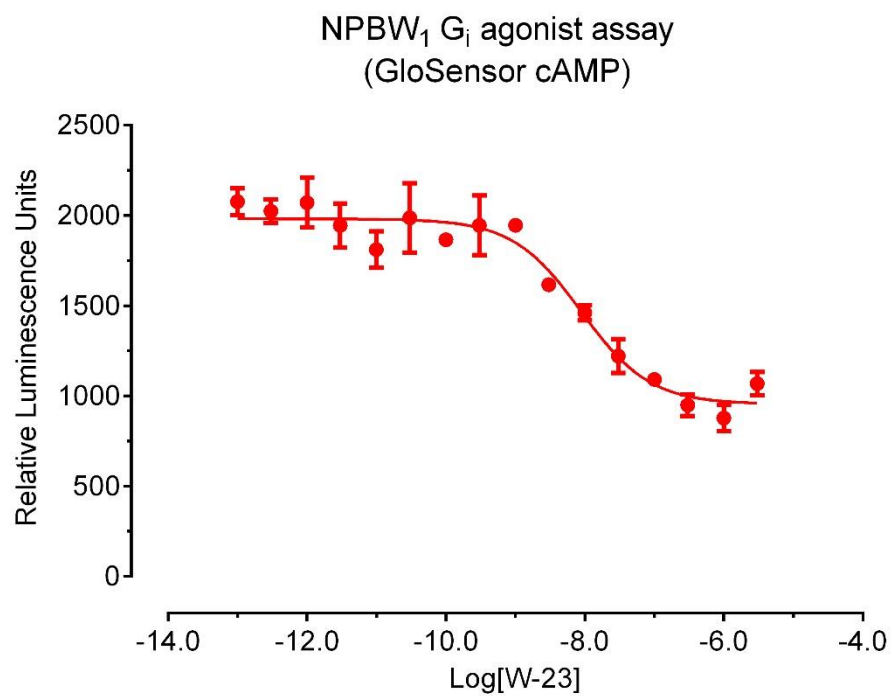


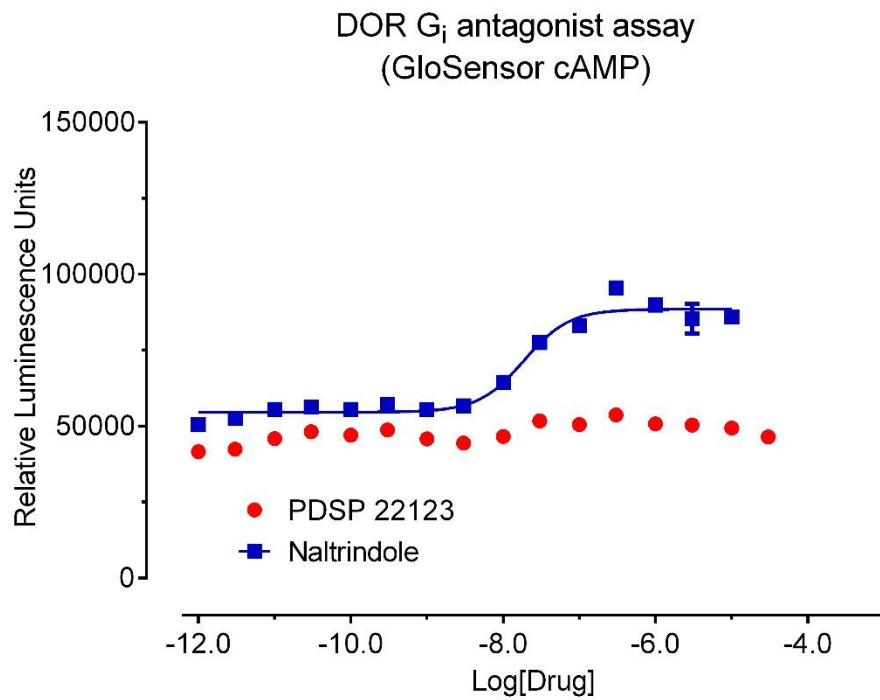
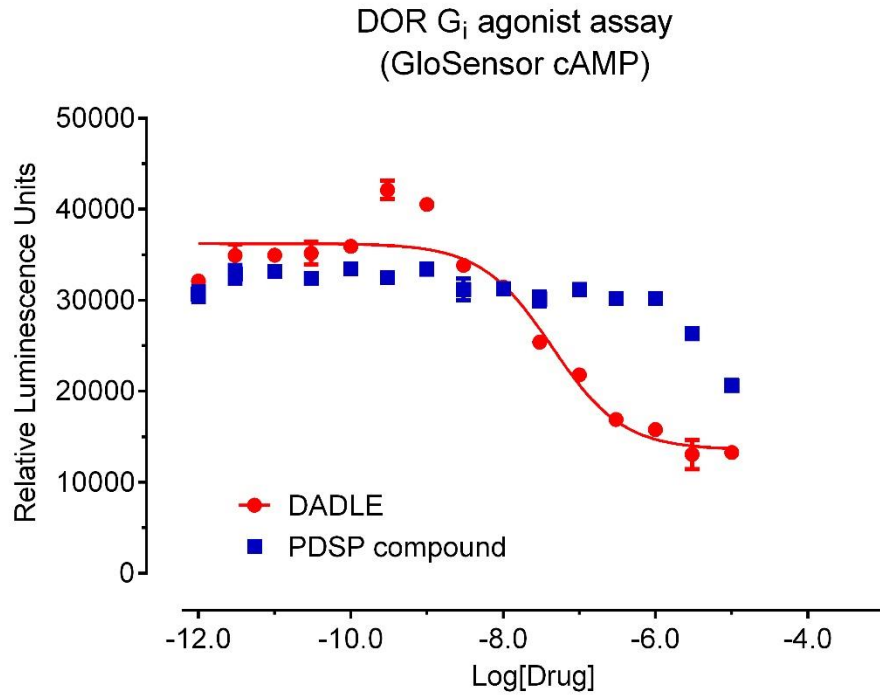


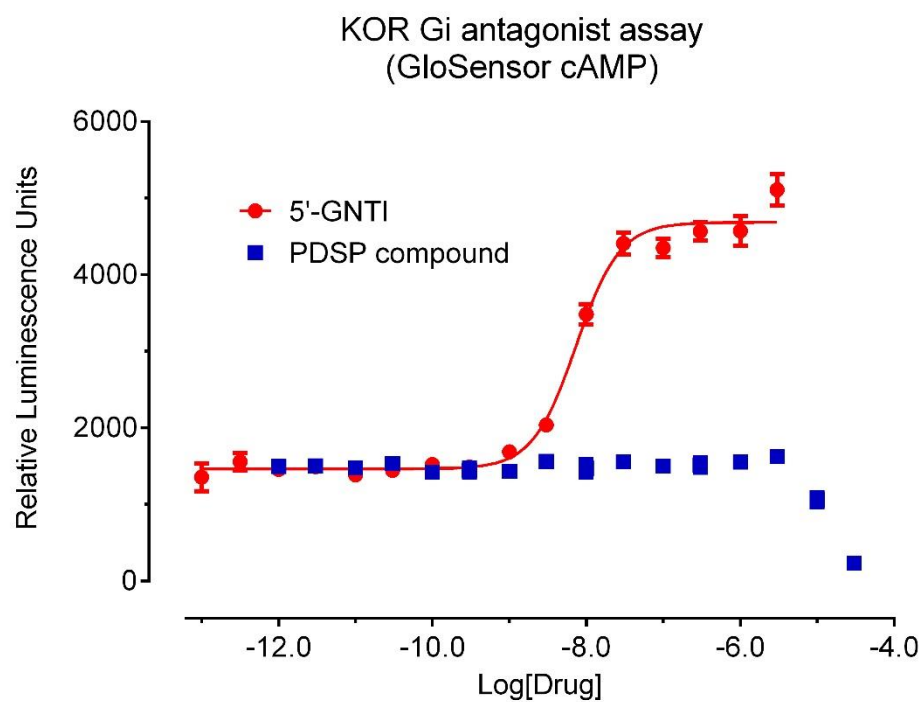
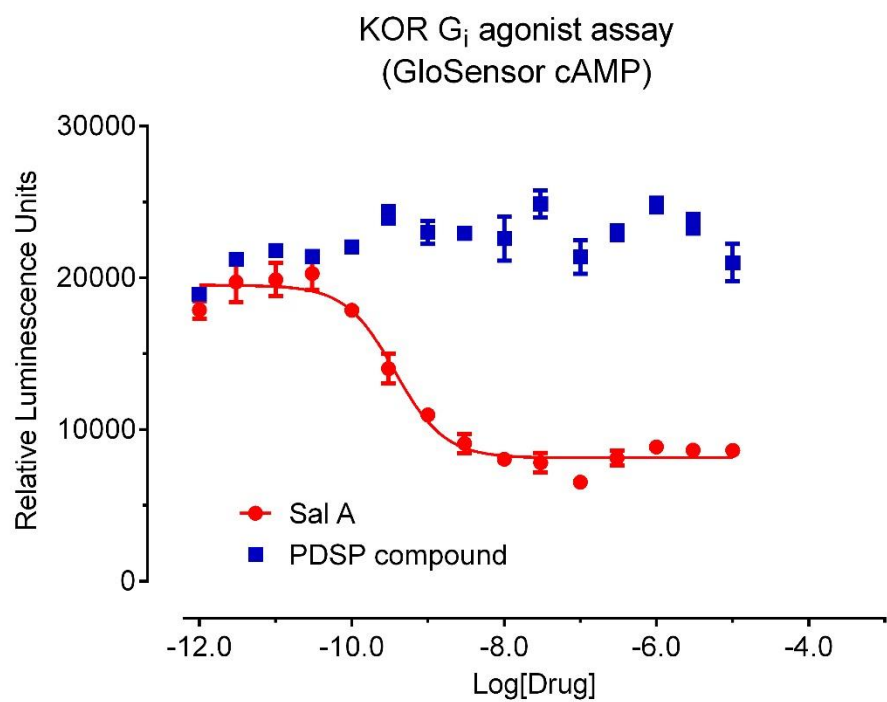


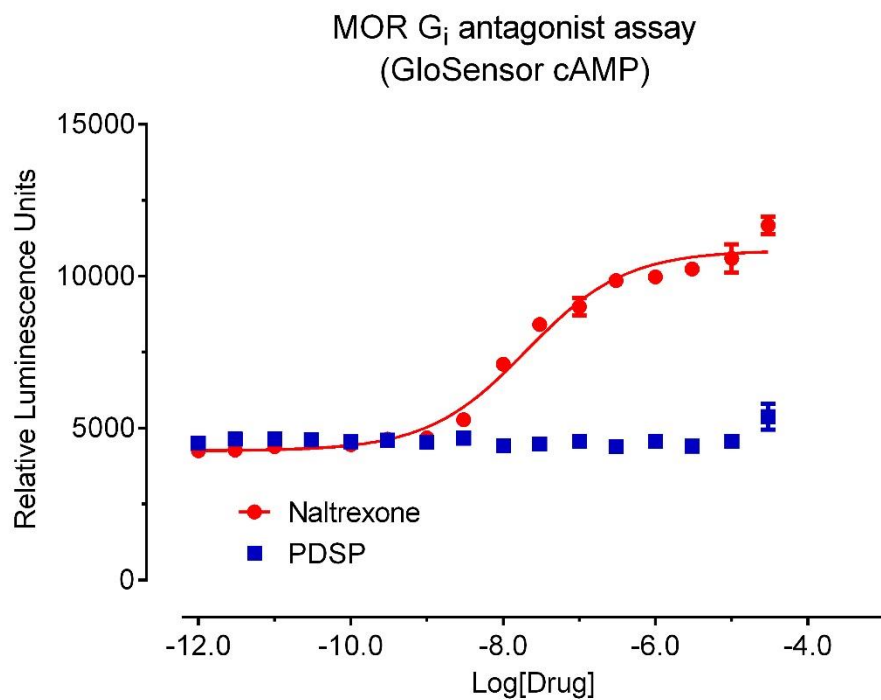
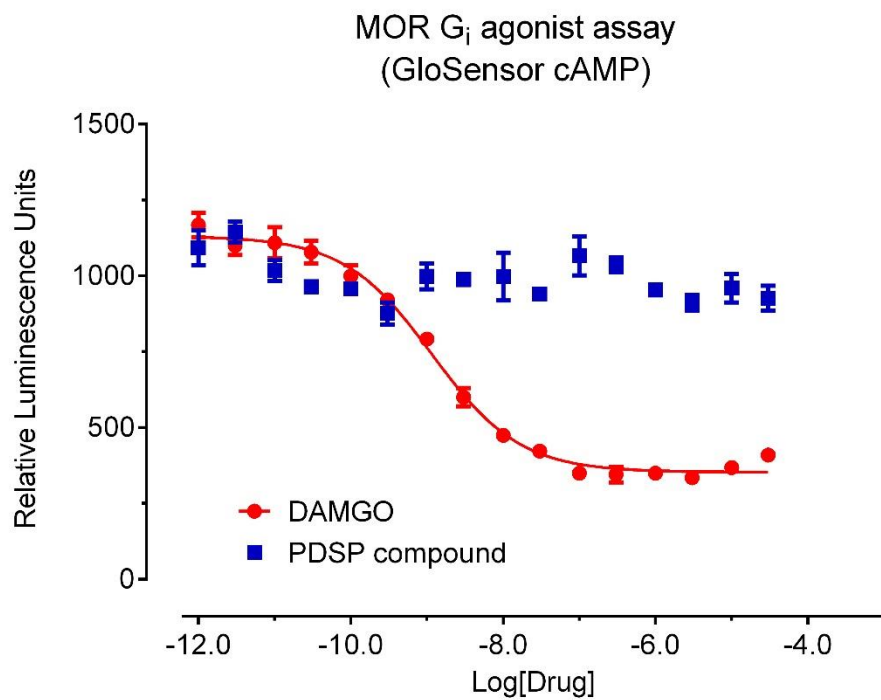


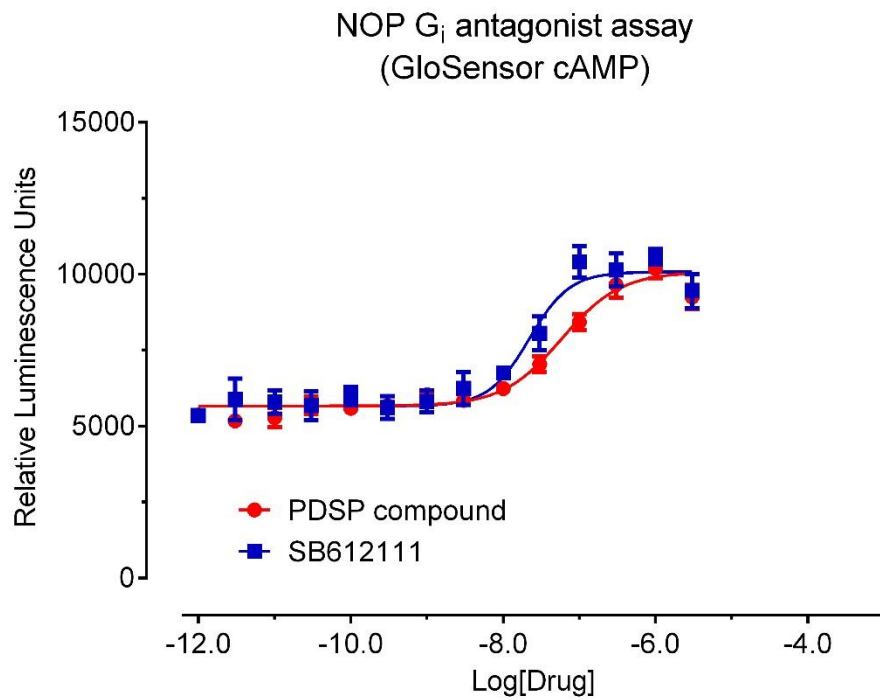
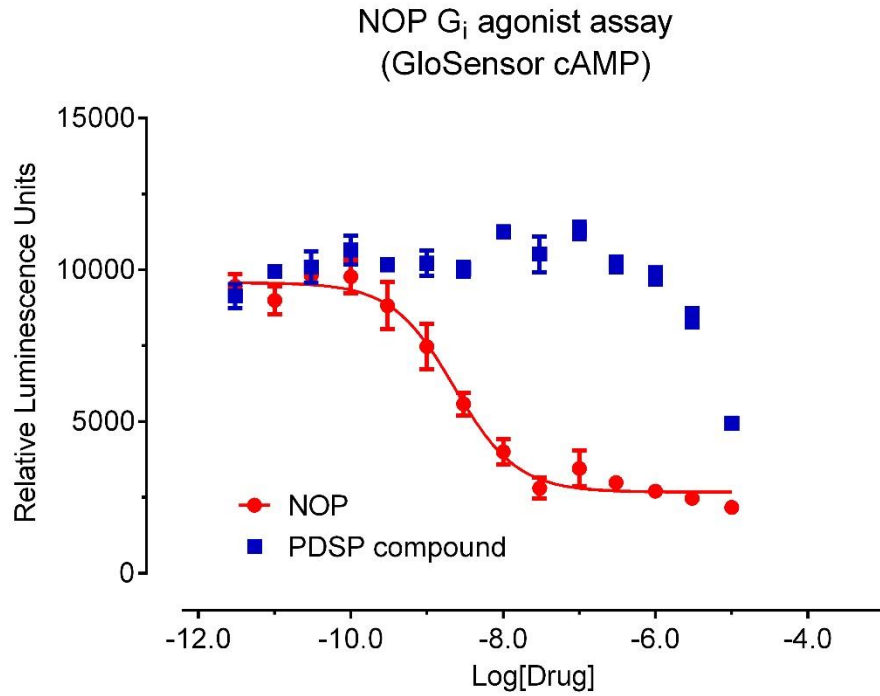


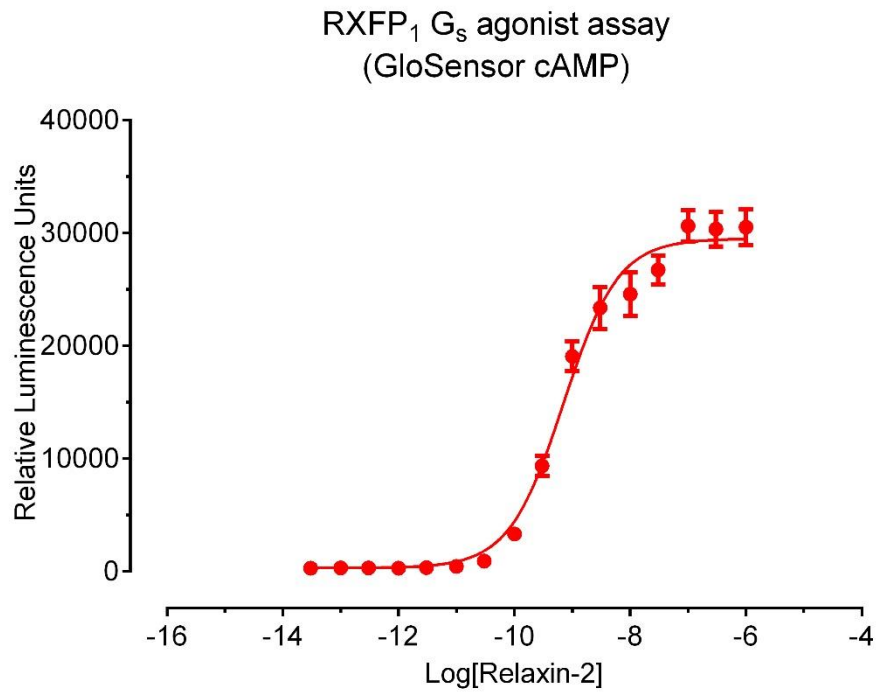
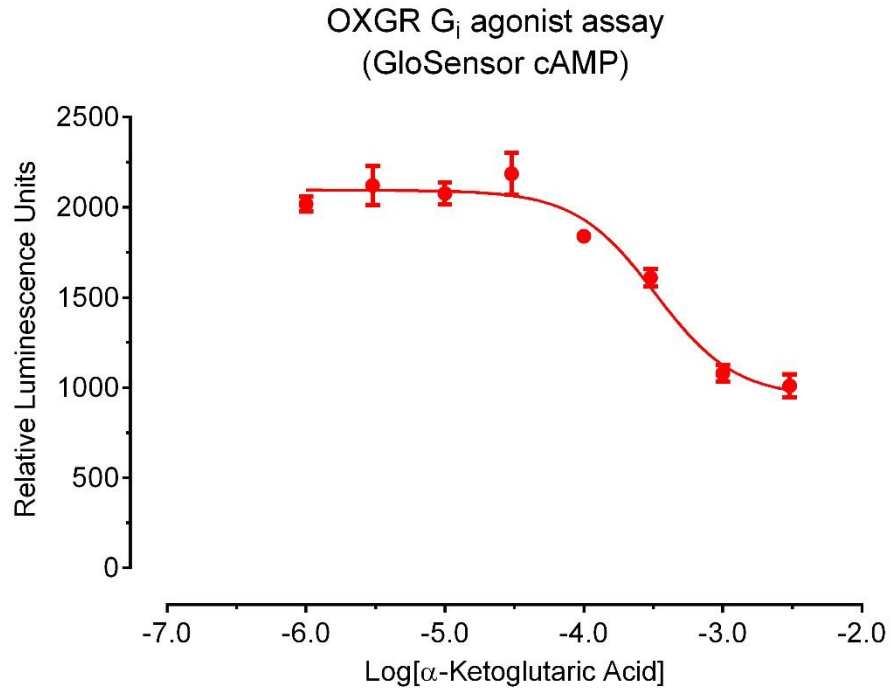


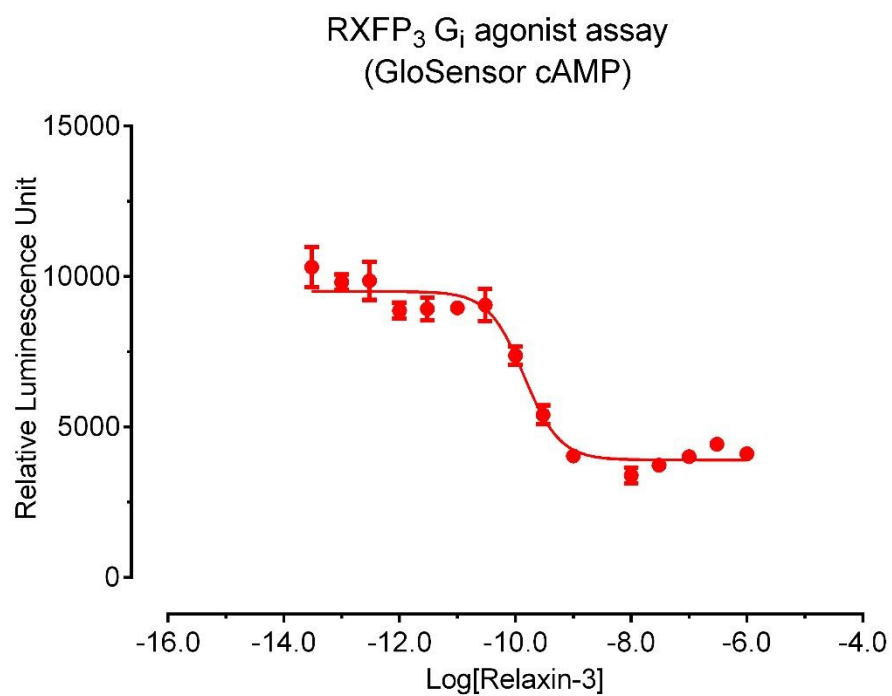
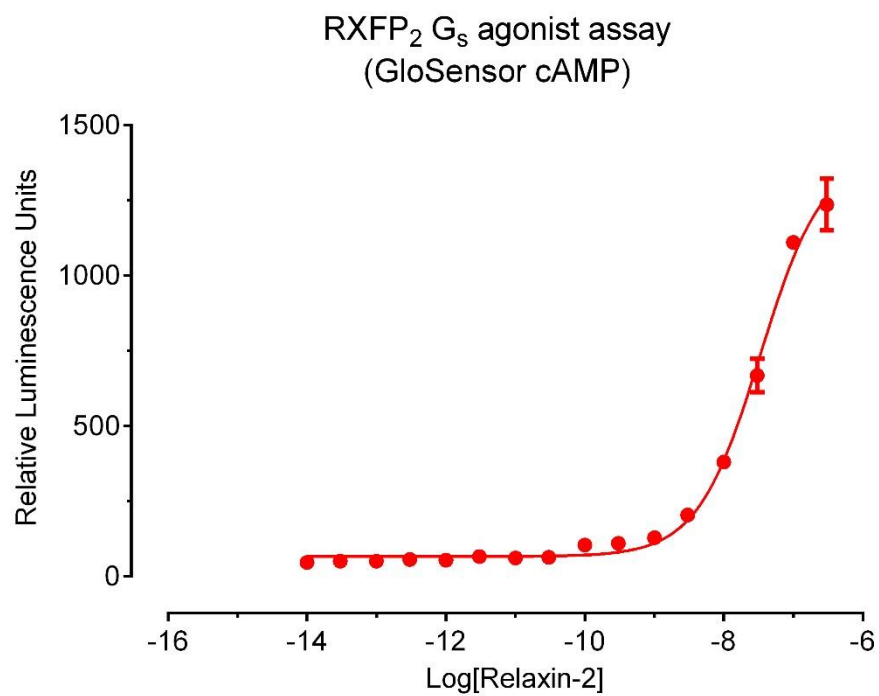


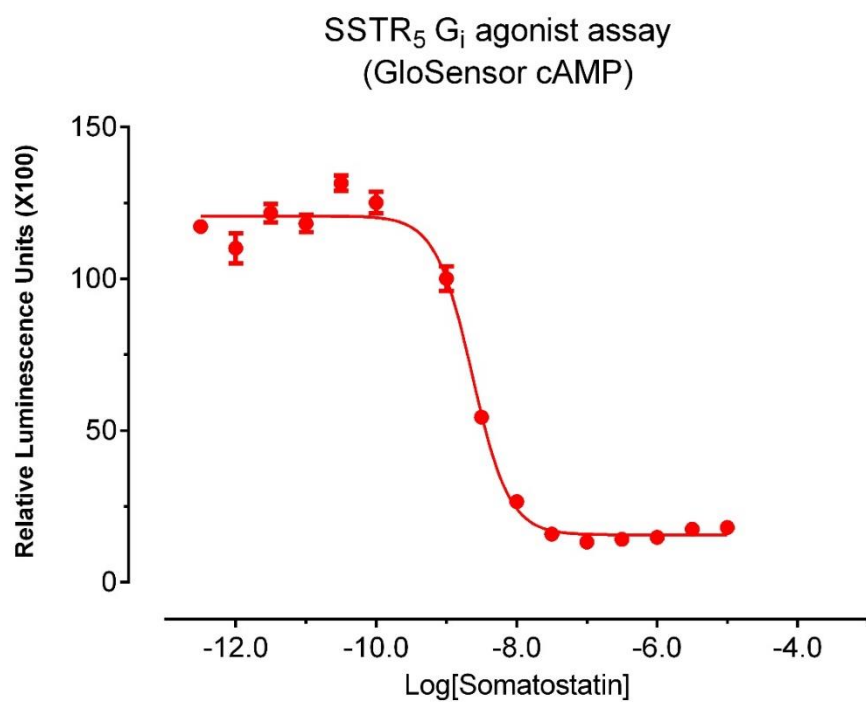
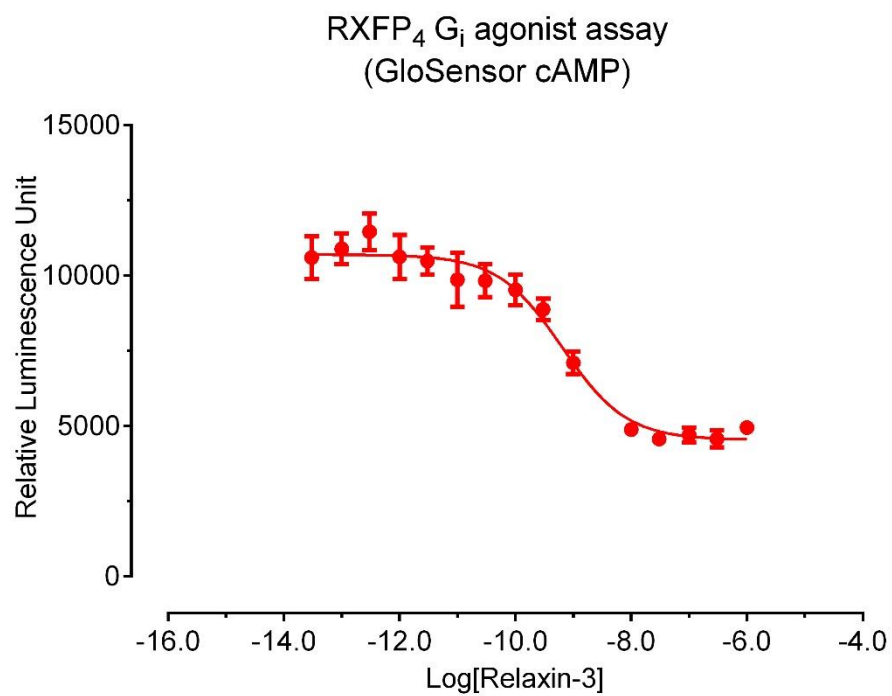


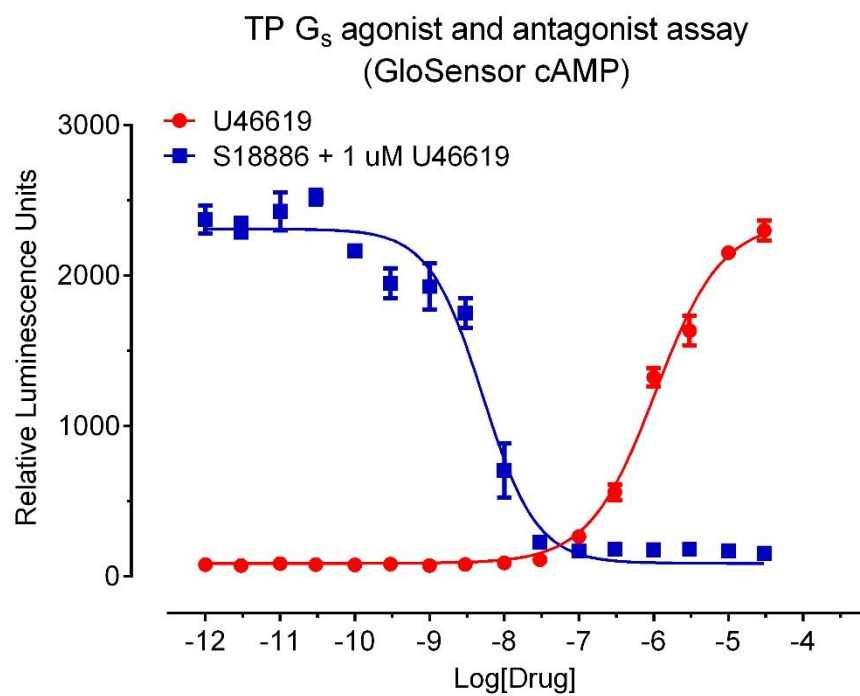












2.6. GPCR Tango assays: G-protein independent β -arrestin recruitment

Main equipment: Luminescence counter

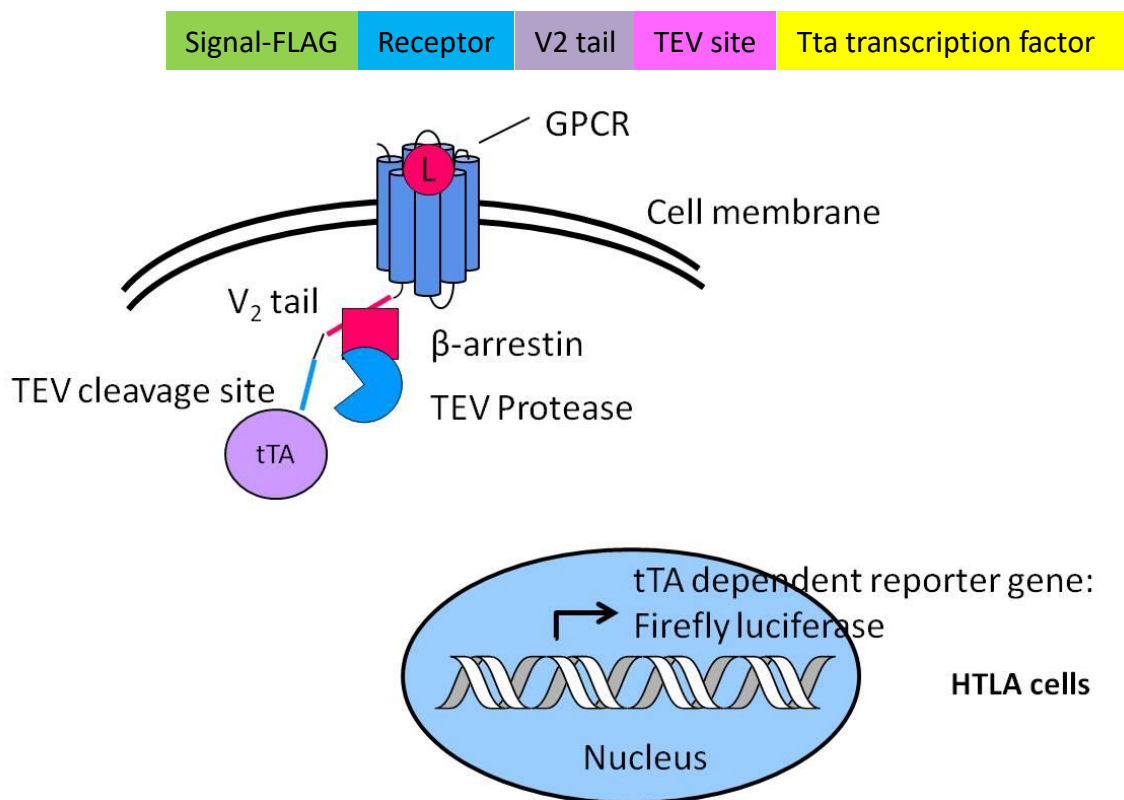
Main reagents: BrightGlo® reagents from Promega

Tango assay buffer: 20 mM HEPES, 1x HBSS, pH 7.40

2.6.1. Tango construct design and cell culture: To measure GPCR mediated β -arrestin translocation activity, we adopted the Tango assay system originally developed by Richard Axel and his colleagues (169). GPCR Tango constructs (**Figure 42**, below) were codon optimized for better expression in mammalian cell lines and total synthesis was by Blue Heron Biotech (Bothell, WA), with independent sequencing confirmation (154). HTLA cells (an HEK293 cell line stably expressing a tTA-dependent luciferase reporter and a β -arrestin2-TEV fusion gene, **Figure 34**, bottom) was gifted from Richard Axel's lab, and are maintained in DMEM supplemented with 10% FBS and 2 μ g/ml Puromycin and 100 μ g/ml Hygromycin. The FLAG tag was designed into the GPCR Tango constructs for confirmation of surface expression (**Figure 43**) and comparison of expression levels.

2.6.2. GPCR Tango assay: HTLA cells are transfected with GPCR tango constructs overnight (see calcium mobilization section for detailed transfection protocol) and are plated in DMEM supplemented with 1% dialyzed FBS in Poly-L-Lys (PLL)-coated 384-well white clear bottom cell culture plates at a density of 15,000 cells in a volume of 40 μ l per well. Cells are incubated for at least 6 hours (or overnight) to allow them to recover before receiving drug stimulation. Drug stimulation solutions are prepared in sterile-filtered Tango assay buffer at 5x concentration and added to cells (10 μ l per well) overnight. To measure antagonist activity, drug solutions are made at 6x of the final concentration and are preincubated with cells for 30 min before addition of 10 μ l of a final EC₈₀ concentration of reference agonist. The EC₈₀ concentration is determined in separate preliminary dose-response assays. On the day of measurement, medium and drug solutions are removed and 20 μ l per well of BrightGlo reagent (diluted 20-fold with Tango assay buffer) are added. Plates are incubated for 20 min at room temperature in the dark before being counted on a luminescence counter.

Figure 46. Tango construct design (**top**) and GPCR tango assay principle (**bottom**). GPCR Tango constructs were designed as indicated (top). Each construct contains these elements in the following order (1) signal/FLAG tag; (2) gene of interest; (3) Vasopressin 2 C-tail; (4) TEV protease site; (5) tTA transcription factor. The GPCR Tango assay is carried out in transiently transfected HEK T cells that are genetically modified to express β -arrestin2 fused with a TEV protease and a Tta mediated luciferase reporter gene. Activation of the transfected GPCR leads to β -arrestin translocation, which guides TEV protease to cleave the Tta transcription factor from the GPCR tail. The free Tta transcription factor then activates the luciferase reporter gene in the nucleus.



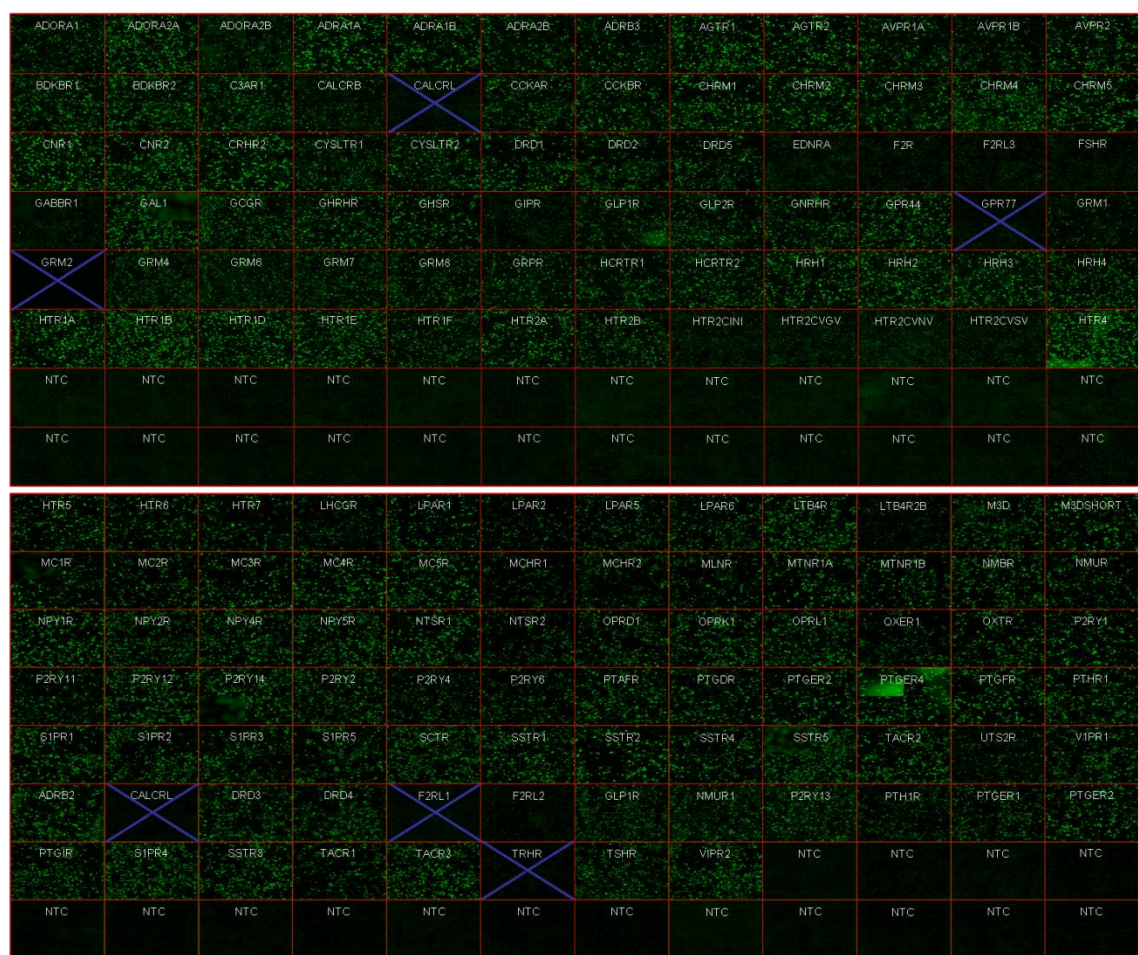


Figure 47. Confirmation of surface expression of FLAG-tagged non-orphan non-olfactory GPCRs used for the β -arrestin recruitment assay. Cells were pre-fixed with paraformaldehyde (PFA) for 30 min, blocked using rabbit anti-FLAG antibody (primary), and incubated for 1h at room temperature and then overnight at 4°C. On day 2, the plate was incubated with Alexa Fluor 594 goat anti-rabbit antibody (secondary) and Hoechst 33342 dye for 1 h. After thorough washing, the plate was post-fixed with PFA and stored at 4°C in the dark. Images were taken using the B-D Pathway High Throughput Bioimager. Blue crosses indicated constructs that were not expressed.

2.6.3. Data processing and analysis: Luminescence counter records chemiluminescence in relative luminescence units (RLU) and saves files in 384-well format in Excel sheet for easy processing.

Results in RLU are plotted against concentrations and analyzed in GraphPad Prism v5.0 as outlined in **Section 2.3**.

Table 31. List of GPCR Tango constructs with representative agonist activity curves. All DNA constructs are human clones, designed according to the original design by Barnea et al., (2008) (169), codon optimized, synthesized by Blue Heron Biotech, and sequence-confirmed (154). Most representative curves were recently published (154) and modified for this protocol book. Some receptors have high variations in E_{\max} for different reference agonists (such as 5-HT vs LSD at 5-HT receptors) because they were not tested from the same batch of transfected cells, and different assays/transfections may have different efficiency. In addition, some constructs were not optimized when the results were obtained, such as the HTR2C constructs – the ones without N-terminal Signal/FLAG peptide work better than the ones with the Signal/FLAG peptide (Roth lab, unpublished results).

Gene Name	IUPHAR Receptor Name	Agonists (references)	E_{\max} (fold of basal)	pEC ₅₀ (EC ₅₀ nM)	Hill slope
HTR1A	5-HT _{1A}	5-HT	15	6.35 (448)	0.67
		LSD	139	7.22 (59.0)	1.16
HTR1B	5-HT _{1B}	5-HT	3.2	7.49 (32.7)	0.66
		LSD	1.6	8.62 (2.4)	0.99
HTR1D	5-HT _{1D}	5-HT	3.4	7.16 (698)	0.70
		LSD	3.4	8.39 (4.0)	0.56
HTR1E	5-HT _{1E}	5-HT	3.6	8.39 (4.0)	0.94
		LSD	1.4	8.61 (2.4)	0.98
HTR1F	5-HT _{1F}	5-HT	77	7.27 (54.2)	0.54
		LSD	13	7.75 (17.9)	0.62
HTR2A	5-HT _{2A}	5-HT	17	6.60 (254)	0.79
		LSD	123	8.97 (1.1)	0.66
HTR2B	5-HT _{2B}	5-HT	2.7	8.65 (2.2)	1.20
		LSD	1.7	8.95 (1.1)	0.39
HTR2C	5-HT _{2C} INI	5-HT	2.0	7.42 (38.4)	0.92
		LSD	4.3	7.09 (81.4)	0.43
	5-HT _{2C} VGV	5-HT		<4.50 (>30 μ M)	0.49
	5-HT _{2C} VNV	5-HT	37	<4.50 (>30 μ M)	0.64
		LSD	1.9	8.30 (5.1)	0.79
	5-HT _{2C} VSV	5-HT		<4.50 (>30 μ M)	0.69
		LSD	1.6	8.89 (1.3)	0.76
	5-HT ₄	5-HT	59	7.59 (25.7)	1.18

Gene Name	IUPHAR Receptor Name	Agonists (references)	E _{max} (fold of basal)	pEC ₅₀ (EC ₅₀ nM)	Hill slope
HTR4	5-HT ₄	LSD	2.0	5.49 (3265)	3.14
HTR5A	5-HT _{5A}	5-HT	11	8.06 (8.7)	0.66
		LSD	16	9.74 (0.18)	0.71
HTR6	5-HT ₆	5-HT	40	6.52 (301)	0.93
		LSD	16.1	8.65 (2.2)	0.76
HTR7A	5-HT _{7A}	5-HT	1.9	7.13 (73.4)	2.23
CHRM1	M ₁	Acetylcholine	2.1	4.58	
		Carbachol	1.6	6.66 (218)	0.74
		Arecoline	3.7	<5	
CHRM2	M ₂	Acetylcholine	8.1	6.41	
		Carbachol	3.8	6.62 (243)	0.96
		Arecoline	23	5.67	
CHRM3	M ₃	Acetylcholine	>10	<5	
		Carbachol	18	5.36 (4388)	0.90
		Arecoline	>10	<5	
	M _{3D}	CNO	27	7.68 (21.1)	1.14
	M _{4D}	CNO	6.1	8.60 (2.5)	1.01
CHRM4	M ₄	Acetylcholine	11.5	5.61	
		Carbachol	35	5.62 (2428)	1.06
		Arecoline	33.8	5.62	
CHRM5	M ₅	Acetylcholine	<2	<5	
		Carbachol	1.6	6.88 (131)	1.36
		Arecoline	8.9	<5	
ADORA1	A ₁	NECA	4.8	7.93 (11.7)	1.10
ADRA1A	α _{1A}	Oxymetazoline	3.6	7.97 (10.6)	0.82
ADRA1B	α _{1B}	Epinephrine	11	6.61 (244)	0.90
ADRA1D	α _{1D}	Norepinephrine	7.6	5.95 (1118)	1.49
ADRA2A	α _{2A}	Clonidine	5.4	8.36 (4.4)	0.99
ADRA2B	α _{2B}	Norepinephrine	8.9	7.20 (63.1)	0.89
ADRA2C	α _{2C}	Clonidine	61	7.20 (63.3)	1.30
ADRB1	β ₁	Epinephrine	22	5.74 (1838)	2.06
ADRB2	β ₂	Epinephrine	17	6.21 (613)	1.70
ADRB3	β ₃	Carvedilol	44	5.53 (2934)	2.51
AGTR1	AT ₁	Angiotensin II	13	7.95 (11.1)	0.57
APLNR	Apelin	Apelin-17	6.5	8.80 (1.6)	0.68
GPBAR1	GPBA	Taurodeoxycholate	>2.3	<5	~0.85
NMBR	BB ₁	Bombesin	4.6	7.06 (86.9)	1.75

Gene Name	IUPHAR Receptor Name	Agonists (references)	E _{max} (fold of basal)	pEC ₅₀ (EC ₅₀ nM)	Hill slope
		Gastrin-releasing peptide (GRP)	4.6	6.98 (105)	2.00
		Neuromedin B	6.0	8.68 (2.1)	0.87
GRPR	BB ₂	Bombesin	6.2	8.50 (3.2)	1.39
		Gastrin-releasing peptide (GRP)	6.1	8.32 (4.8)	1.21
		Neuromedin B	5.3	7.49 (32.6)	1.16
BRS3	BB ₃	Saquinavir (154)	7.5	7.22 (61.0)	0.97
BDKRB1	B ₁	Bradykinin	14	4.60 (25220)	0.53
BDKRB2	B ₂	Bradykinin	6.8	9.00 (1.0)	0.65
CNR1	CB ₁	WIN 55212-2	3.2	6.24 (583)	3.04
		CP55940	19	7.07 (84.5)	1.14
CNR2	CB ₂	CP55940	53	8.30 (5.0)	1.44
CCR6	CCR6	CCL20 (Exodus-1)	2.3	7.84 (14.6)	1.07
CXCR1	CXCR1	IL-8	46	8.44 (3.7)	0.72
		CXCL6	3.5	6.60 (252)	0.99
		CXCL8 (IL-8)	4.1	6.95 (111)	1.05
CXCR2	CXCR2	IL-8	1.9	8.59	1.55
		CXCL6	2.6	6.49 (322)	0.29
		CXCL8 (IL-8)	2.3	6.35 (451)	0.43
CXCR4	CXCR4	CXCL12 (SDF1- α)	2.0	8.65 (2.2)	1.14
CXCR6	CXCR6	CXCL16 (SRPOX)	>10	<5	
ACKR3	ACKR3	CXCL12 (SDF1- α)	49	8.85 (1.4)	1.66
CX3CR1	CX ₃ CR1	CX3CL1	5.8	9.52 (0.3)	2.87
CCKAR	CCK ₁	[Thr28, Nle31]CCK(25-33)	3.4	7.50 (31.4)	1.81
C3AR1	C3a	C3a (70-77)	22	6.24 (582)	2.60
DRD1	D ₁	Cabergoline	17	4.69 (2033)	0.73
DRD2	D ₂	LSD	68	9.29 (0.5)	1.64
DRD3	D ₃	Quinpirole	35	7.33 (46.3)	0.75
DRD4	D ₄	Lisuride	5.5	7.05 (88.5)	0.39
		Quinpirole	7.0	6.61 (243)	0.70
DRD5	D ₅	LSD	28	6.62 (238)	1.39
FPR1	FPR1	fMLP	84	8.61 (2.5)	0.88
FPR2	FPR2/ALX	fMLP	>18	<5	
FPR3	FPR3	fMLP	1.2	6.61 (247)	0.99
GAL1	GAL ₁	Galanin	16	5.71 (1940)	0.70
GAL2	GAL ₂	Galnon	3.6	8.29	
GAL3	GAL ₃	Galanin	3.4	9.92 (1.2)	1.63

Gene Name	IUPHAR Receptor Name	Agonists (references)	E _{max} (fold of basal)	pEC ₅₀ (EC ₅₀ nM)	Hill slope
GHSR	Ghrelin	Ghrelin	1.8	7.10 (8.0)	0.70
GLP-1R	GLP-1	Glucagon	8.8	<5	
SCTR	Secretin	Secretin	5.5	5.39 (4116)	1.10
GNRHR	GnRH	Leuprolide	2.8	8.43 (3.8)	1.96
CYSLTR1	CysLT1	Leukotriene D4	4.0	7.61 (24.8)	1.82
EDNRA	ET _A	Endothelin-1	70	9.21 (0.6)	1.03
HRH1	H ₁	N-Methylhistaprodifen	1.3	7.19 (65.2)	1.37
HRH2	H ₂	Histamine	6.9	5.40 (3982)	2.94
HRH3	H ₃	N-Methylhistamine	21	7.71 (19.6)	0.76
HRH4	H ₄	Histamine	3.2	6.81 (155)	0.94
HCAR2	HCA ₂	Niacin	1.9	5.11 (7729)	0.71
HCRT1R	OX ₁	Orexin-A	86	7.82 (15.3)	1.53
HCRT2R	OX ₂	Orexin-A	60	8.14 (7.2)	1.94
LTB4R	BLT ₁	Leukotriene D4	96	6.71 (196)	0.61
	BLT ₁ *	Leukotriene D4	28	7.55 (28.2)	0.69
LPAR1	LPA ₁	1-oleoyl LPA	6.0	5.36 (4380)	1.35
LPAR2	LPA ₂	1-oleoyl LPA	69	<5	
LPAR5	LPA ₅	1-oleoyl LPA	14	<5	
S1PR1	S1P ₁	Sphingosine-1-phosphate	9.3	5.46 (3435)	0.67
S1PR2	S1P ₂	Sphingosine-1-phosphate	>8	<5	
S1PR3	S1P ₃	Sphingosine-1-phosphate	17	<5	
MCHR1	MCH ₁	[Ala-17]-MCH	6.9	7.67 (21)	1.01
MCHR2	MCH ₂	[Ala-17]-MCH	20	8.39 (4.1)	0.90
MC1R	MC ₁	α-MSH	2.4	7.41 (38.5)	1.64
MC3R	MC ₃	Melanotan II	11	8.15 (7.1)	0.87
MC4R	MC ₄	ACTH	4.6	6.14 (734)	1.15
MC5R	MC ₅	α-MSH	>1.7	<5	
MTNR1A	MT ₁	Melatonin	15	10.81 (0.02)	0.52
MTNR1B	MT ₂	Melatonin	8.1	8.87 (1.3)	0.61
MLNR	Motilin	Motilin	159	8.04 (9.2)	0.97
NMUR1	NMU1	Neuromedin S	34	8.04 (9.1)	1.33
NMUR2	NMU2	Neuromedin S	8.1	7.83 (14.9)	1.05
NPS	NPS	Neuropeptide S	44	6.25 (566)	1.33
NPBWR2	NPBW2	Neuropeptide W-23	35	<5	
NPY1R	Y ₁	Pancreatic polypeptide	3.9	9.27 (0.5)	0.85
NPY2R	Y ₂	Pancreatic polypeptide	23	8.73 (1.9)	0.80
NPY4R	Y ₄	Neuropeptide Y	1.9	7.44 (36.0)	7.05
NTSR2	NTS ₂	SR48692(154)	11	6.23 (589)	1.04

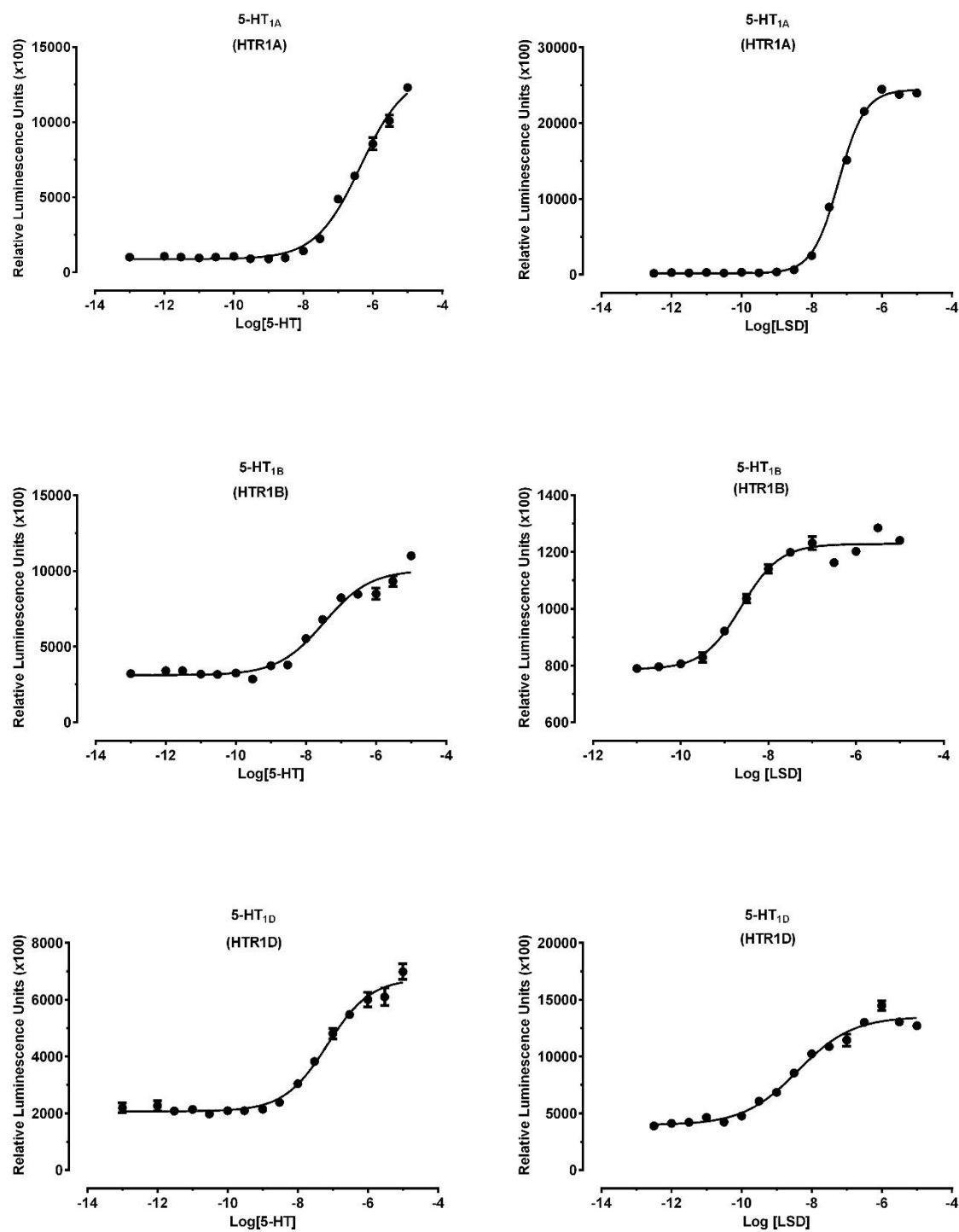
Gene Name	IUPHAR Receptor Name	Agonists (references)	E _{max} (fold of basal)	pEC ₅₀ (EC ₅₀ nM)	Hill slope
OPRD1	δ (DOR)	DADLE	7.8	9.14 (0.7)	0.84
KOR	κ (KOR)	Salvinorin A	9.3	7.49 (32.5)	1.29
OPRM1	μ (MOR)	Morphine	10		
OPRL1	NOP	Orphanin	110	7.92 (12.1)	1.04
P2RY1	P2Y ₁	2-MeS-ADP	46	5.31 (4957)	0.69
P2RY2	P2Y ₂	UTP	44	<5	
P2RY4	P2Y ₄	UTP	5.9	5.13 (735)	1.04
P2RY6	P2Y ₆	UTP	2.5	5.74 (1824)	1.03
P2YR11	P2Y ₁₁	ATP	4.7	<5	
P2RY12	P2Y ₁₂	2-MeS-ADP	46	7.34 (46.1)	0.86
P2RY13	P2Y ₁₃	2-MeS-ADP	2.3	8.20 (6.3)	0.48
P2RY14	P2Y ₁₄	UDP-Glucose	1.6	6.16 (696)	0.65
PTHR1	PTH1	PTH (1-42)	9.0	6.63 (234)	1.05
PTAFR	PAF	PAF (C16)	1.3	9.32 (0.5)	1.18
PTGDR2	DP ₂	Prostaglandin D2	2.8	7.19 (64.9)	1.21
PTGER1	EP ₁	Prostaglandin E2	9.6	7.23 (59.5)	0.73
PTGER2	EP ₂	Prostaglandin E2	49	5.78 (1652)	0.58
PTGER3	EP ₃	Prostaglandin E2	3.7	8.14 (7.3)	0.82
PTGER4	EP ₄	Prostaglandin E2	29	8.92 (1.2)	1.16
PTGFR	FP	Prostaglandin F2α	26	6.98 (104)	0.86
PTGIR	IP	Iloprost	19	<5	
SSTR1	SST ₁	Somatostatin	9.6	5.47 (3372)	0.64
SSTR2	SST ₂	Somatostatin	129	5.59 (2583)	0.89
SSTR3	SST ₃	Somatostatin	124	5.31 (4948)	0.99
SSTR4	SST ₄	Somatostatin	72	5.93 (1175)	0.87
SSTR5	SST ₅	Somatostatin	177	5.86 (1388)	1.09
TACR1	NK ₁	Substance P	3.0	6.74 (180)	2.36
TACR2	NK ₂	Substance P	15	8.72 (1.9)	2.09
TACR3	NK ₃	Substance P	3.0	6.73 (187)	2.28
TA1	TA ₁	β-Phenylethylamine	4.5	3.96 (110 μM)	1.63
UTSR	UT	Urotensin II	8.9	8.72 (1.9)	1.47
AVPR1A	V _{1A}	Vasopressin	145	8.58 (2.6)	0.97
AVPR1B	V _{1B}	Vasopressin	8.9	8.65 (2.2)	0.81
AVPR2	V ₂	Vasopressin	13	8.18 (6.6)	0.72
OXTR	Oxytocin	Oxytocin	35	7.88 (13.2)	0.92
VIPR1	VPAC ₁	Vasoactive Intestinal Peptide (VIP)	2.8	5.00 (10 μM)	2.66

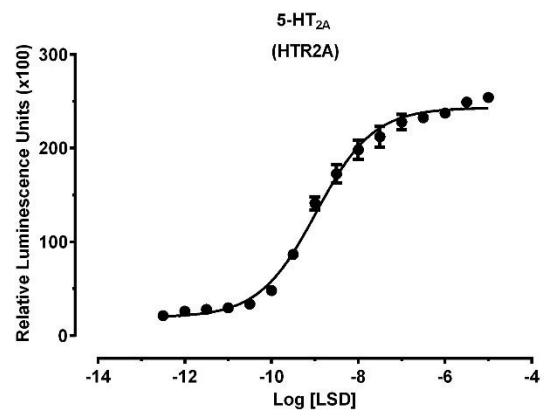
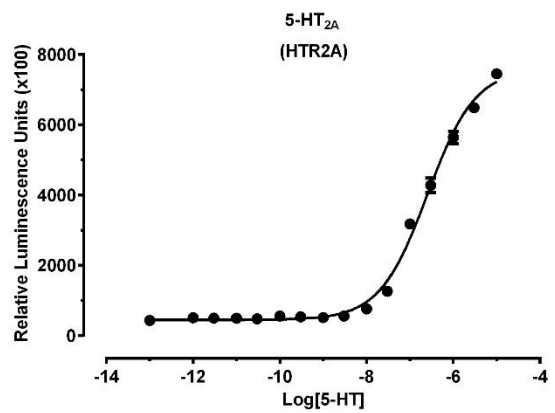
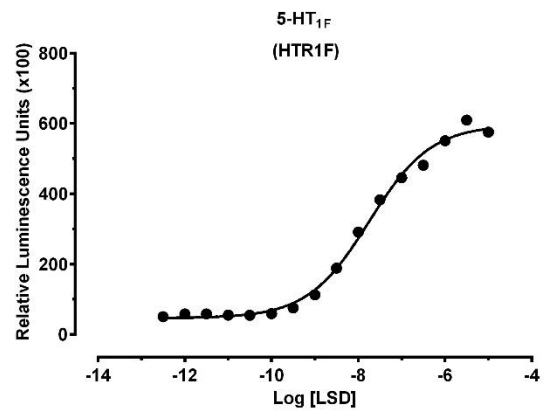
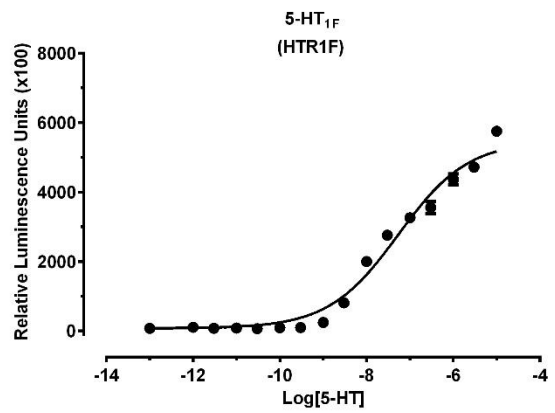
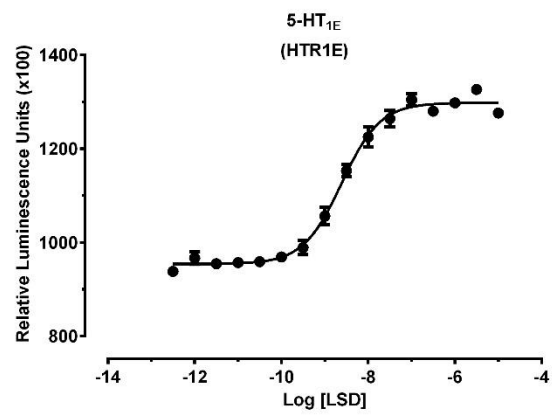
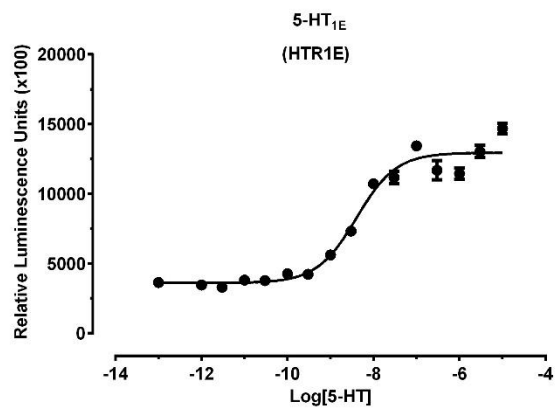
Gene Name	IUPHAR Receptor Name	Agonists (references)	E _{max} (fold of basal)	pEC ₅₀ (EC ₅₀ nM)	Hill slope
VIPR2	VPAC ₂	Vasoactive Intestinal Peptide (VIP)	>5	<5	
GPR35	GPR35	PDSP reference [#]	4.5	7.59 (25.5)	1.05
GPR39	GPR39	GPR39-C3 (146–148)	209	5.98 (1052)	0.57
GPR55	GPR55	Rimonabant (SR141716)	>10	<5	
GPR183	GPR183	7 α ,25-dihydroxy Cholesterol (170, 171)	60	7.32 (48.1)	0.88
MAS1	MAS1	PDSP reference [#]	2.4	5.85 (1425)	1.01
MRGRPX1	MRGPRX1	PDSP reference [#]	1.5	<5	
MRGRPX2	MRGPRX2	TAN-67 (153)	3.1	5.73 (1880)	1.11
MRGRPX4	MRGPRX4	Nateglinide (154)	38	6.37 (423)	1.78

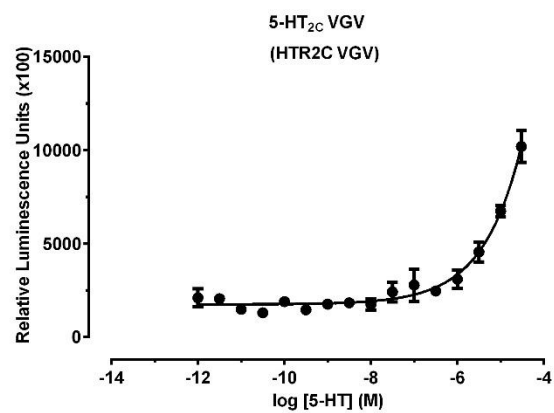
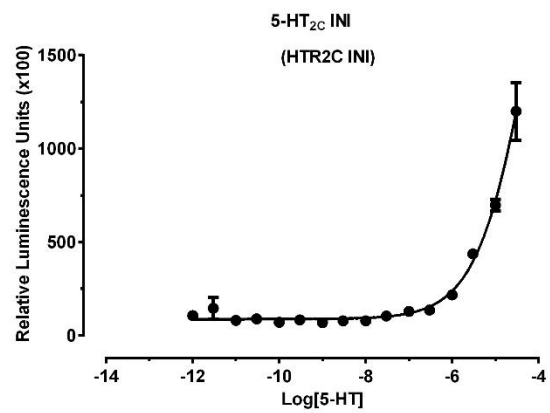
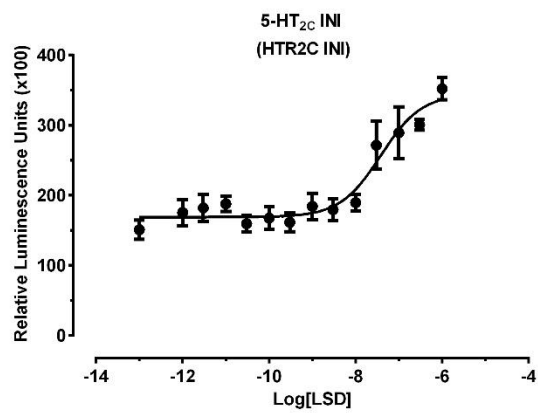
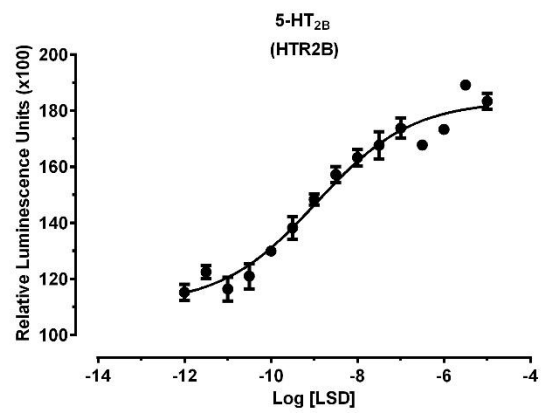
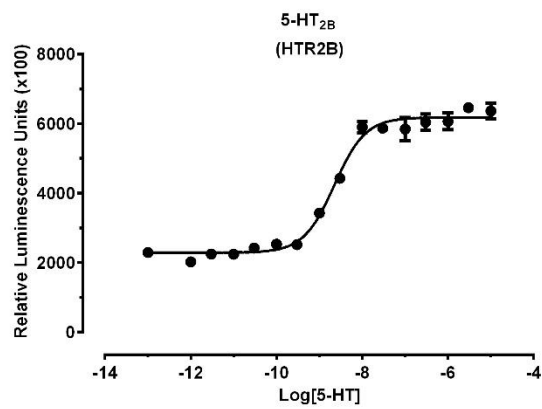
Notes

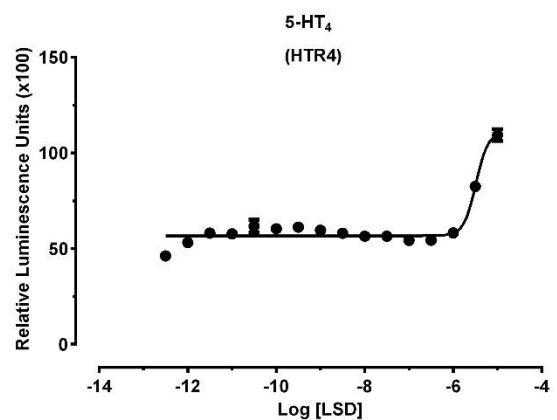
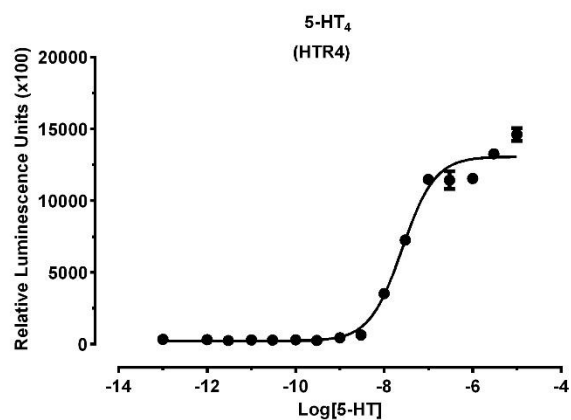
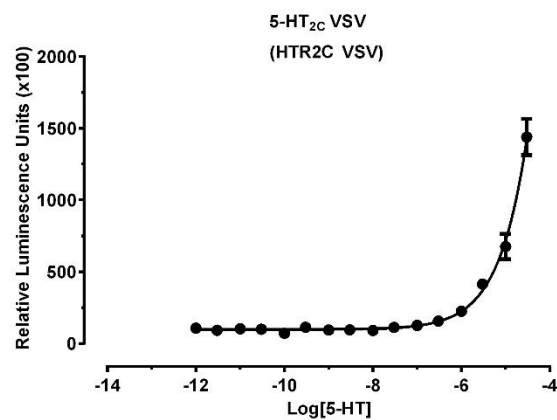
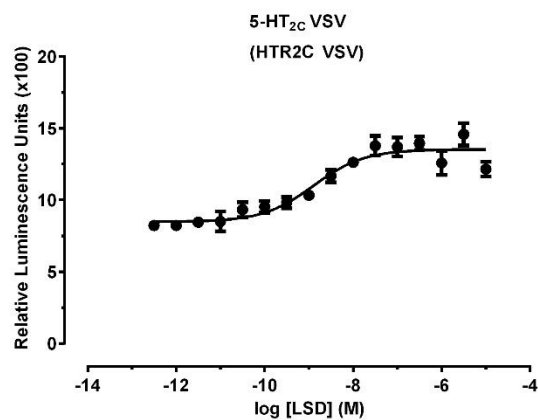
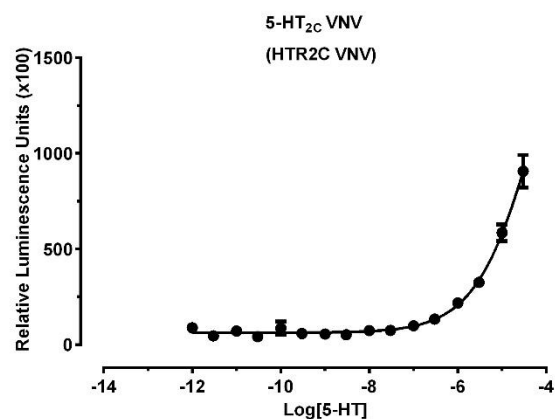
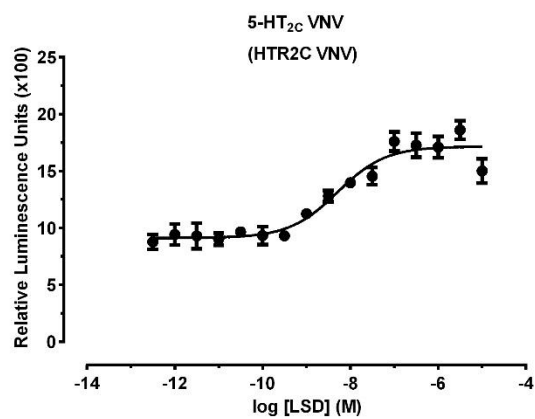
1. * Modified Tango construct without V2 tail
2. # Roth lab unpublished results

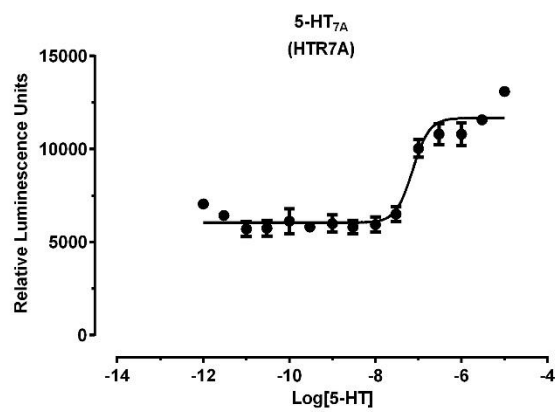
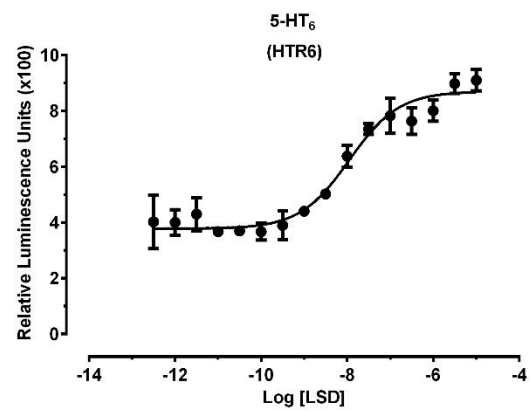
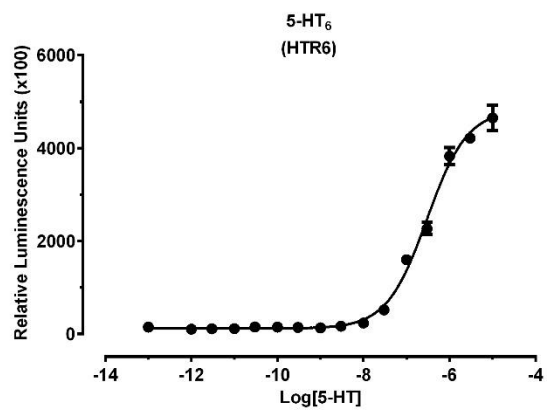
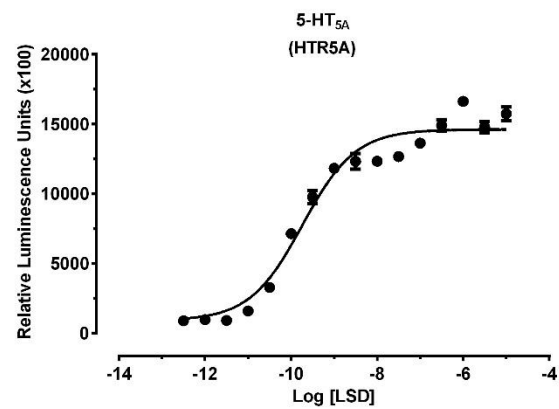
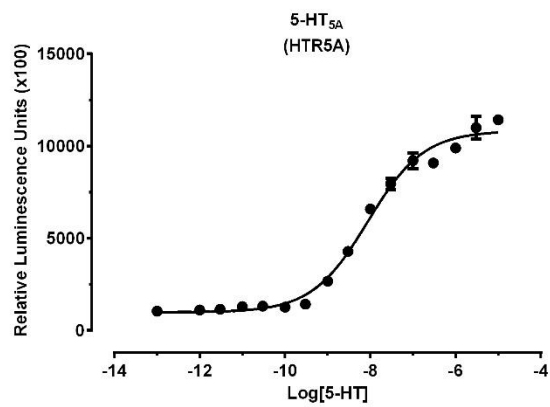
Figure 48. Representative agonist dose-response curves for GPCR mediated β -arrestin translocation.

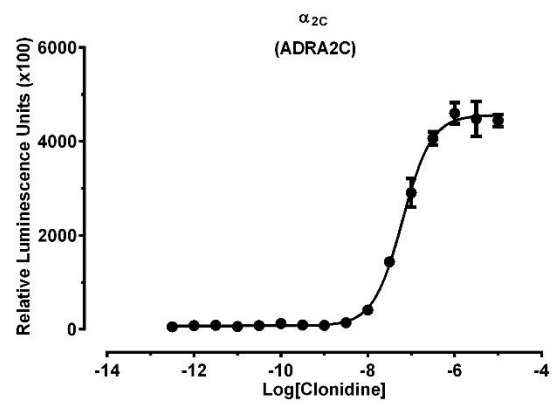
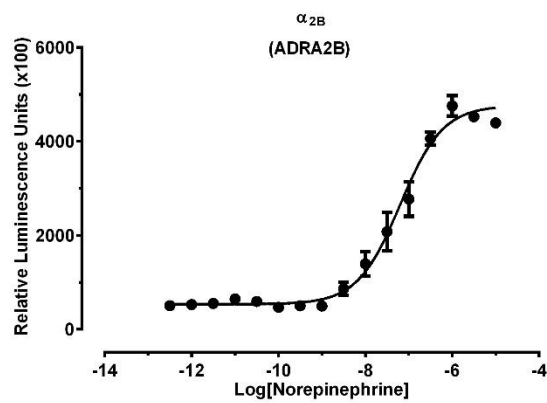
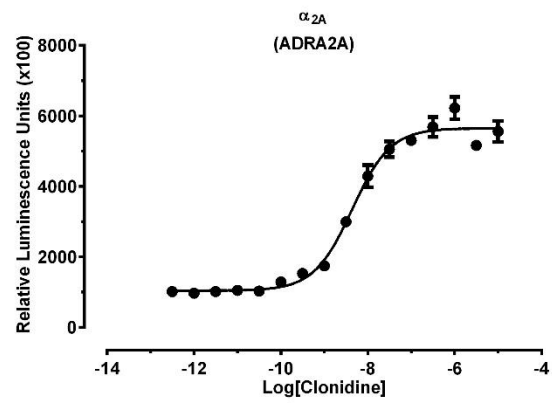
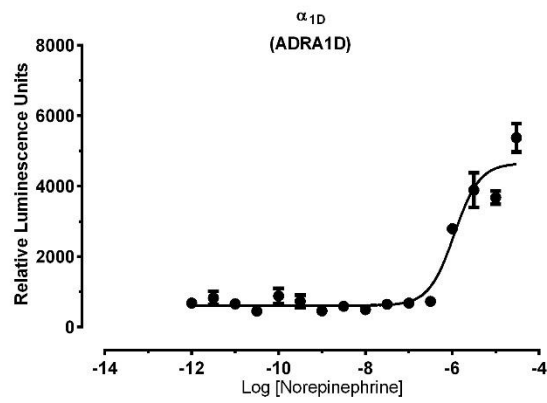
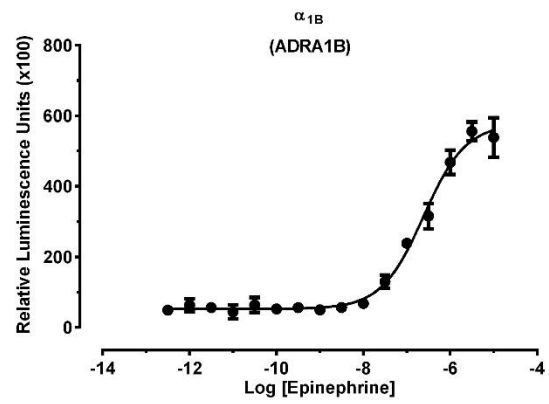
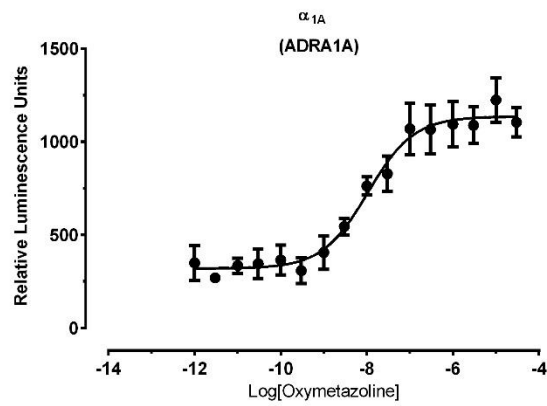


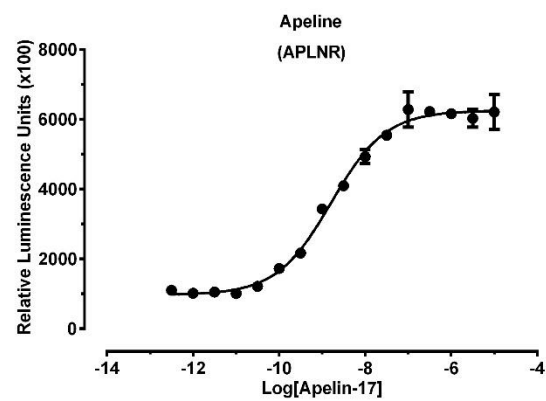
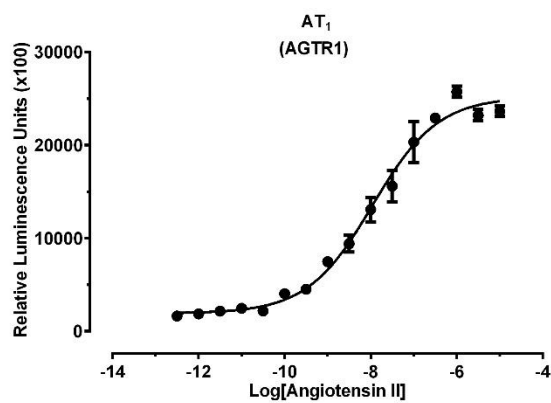
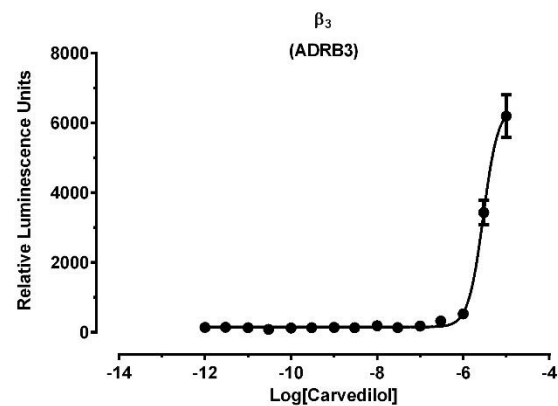
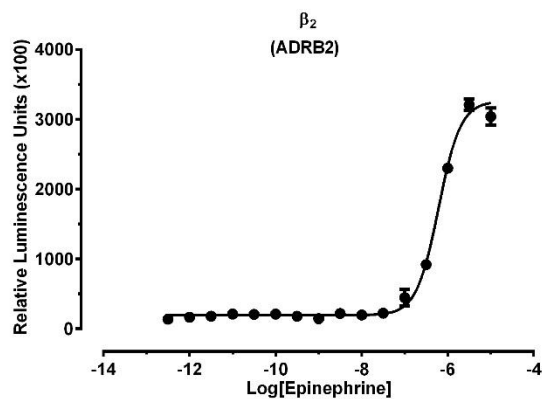
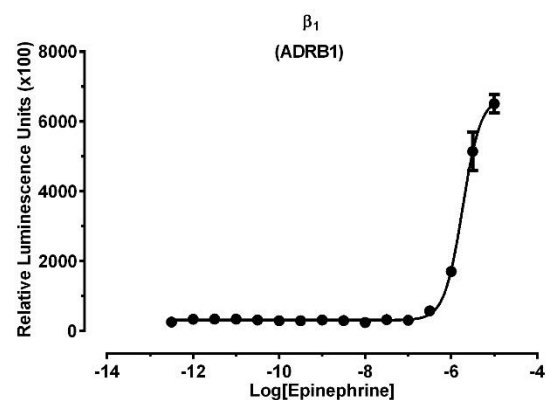
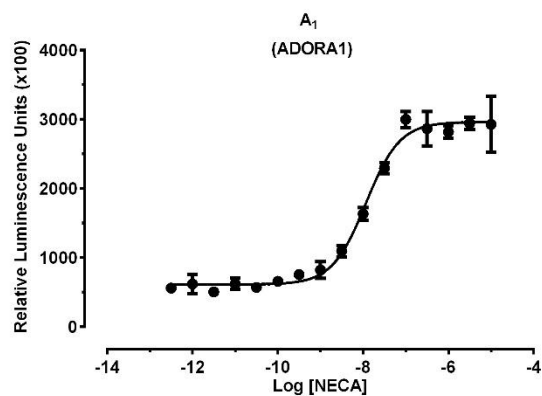


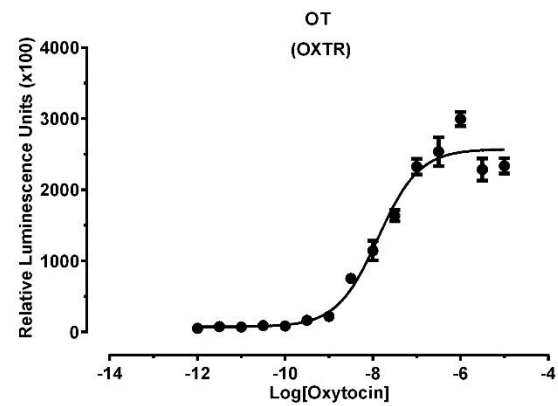
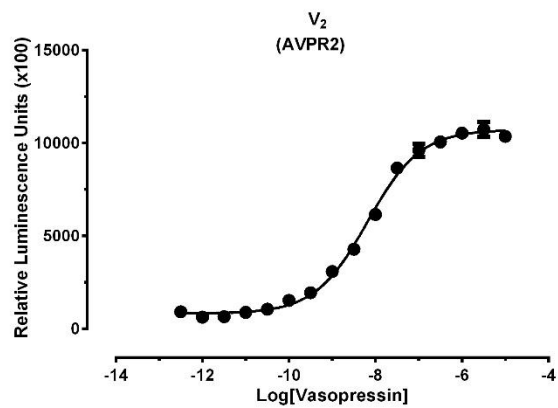
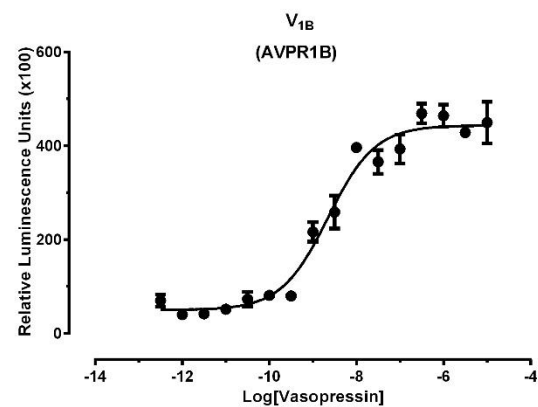
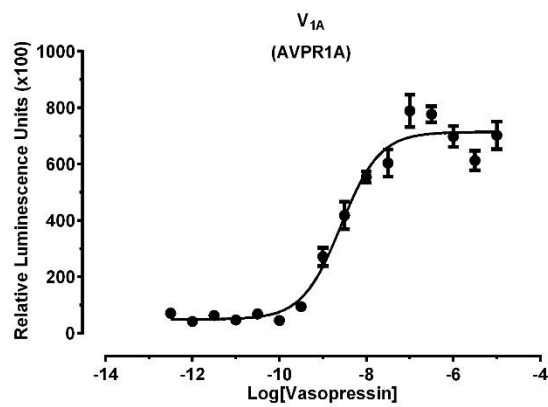


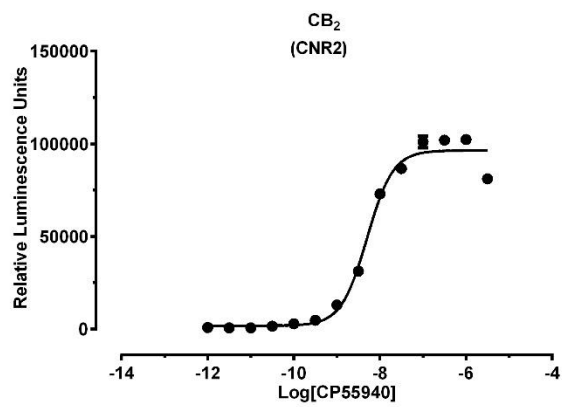
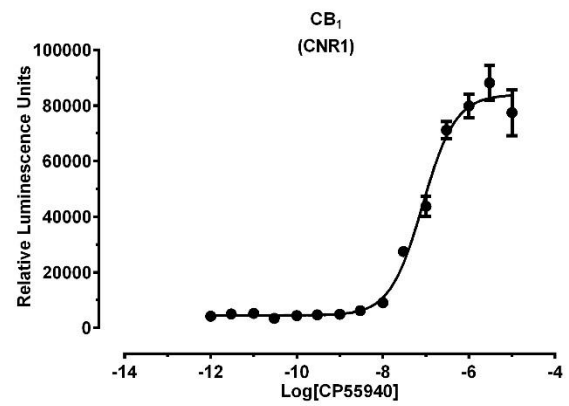
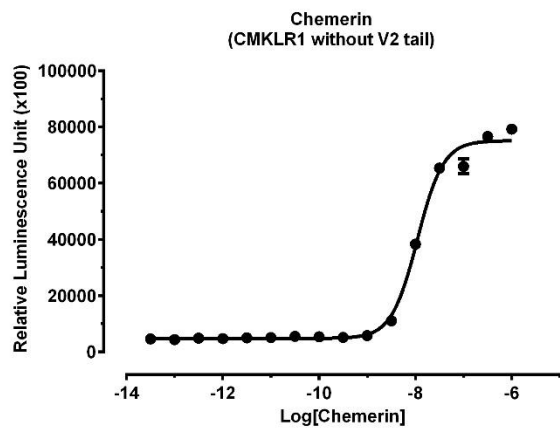
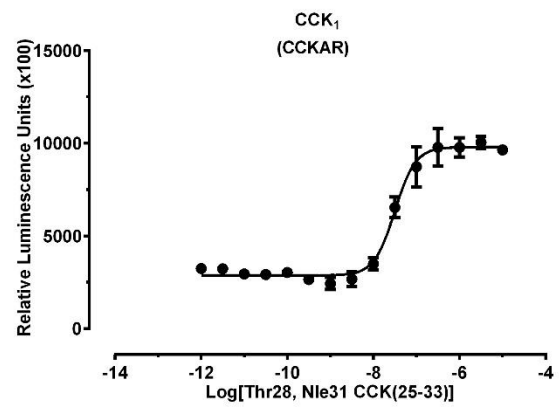
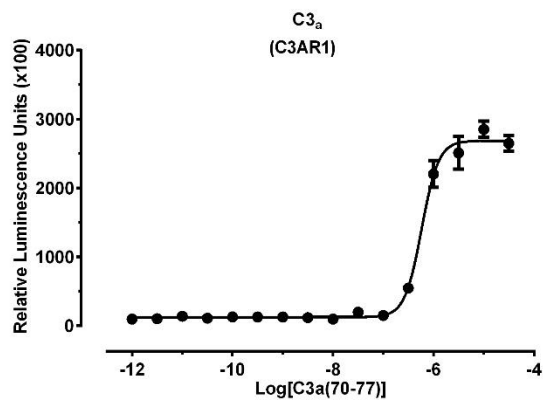


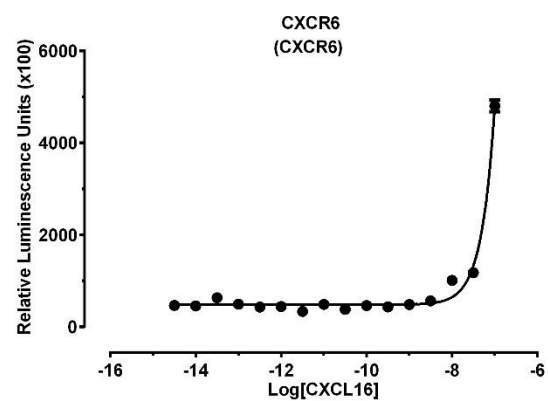
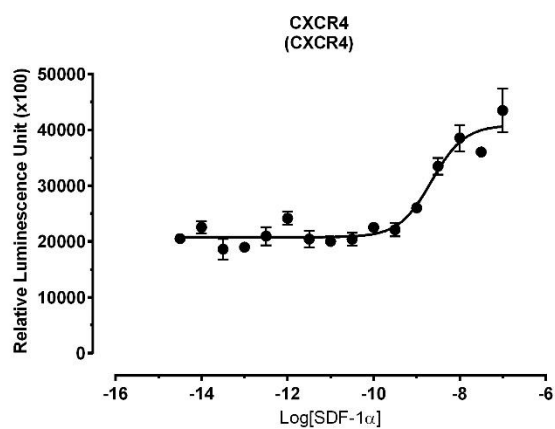
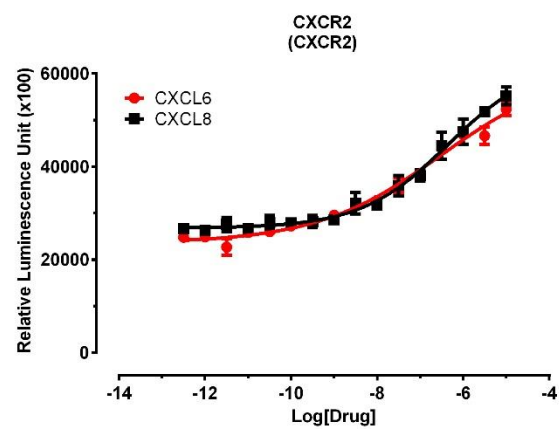
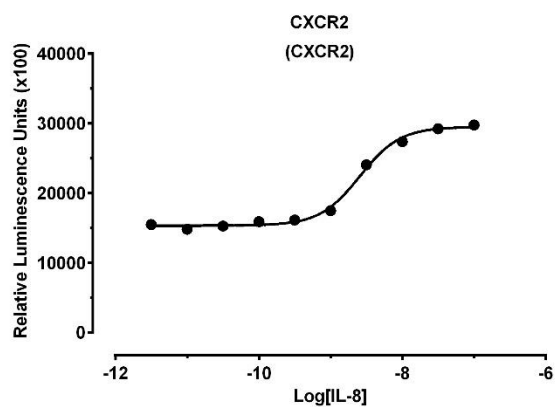
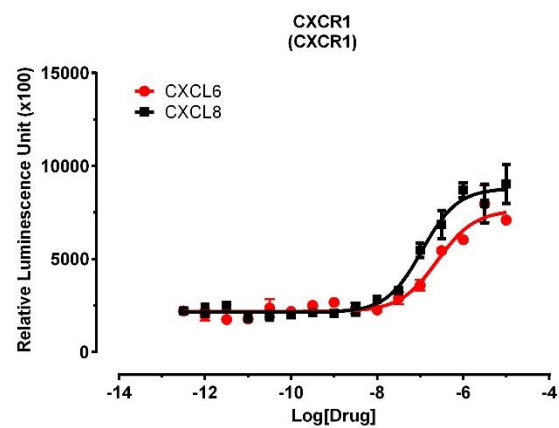
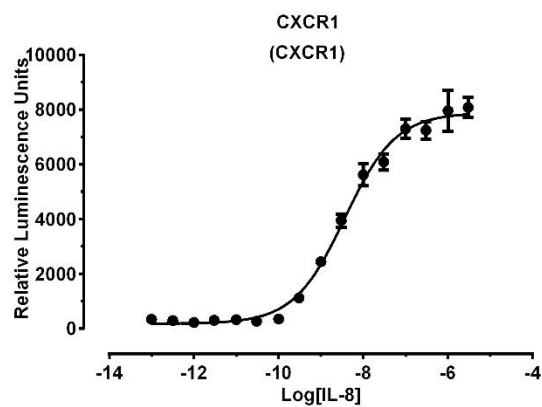


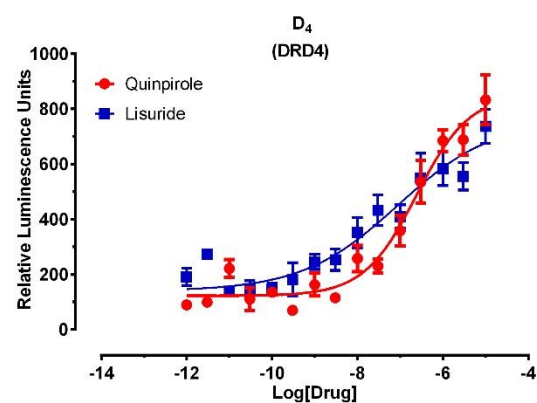
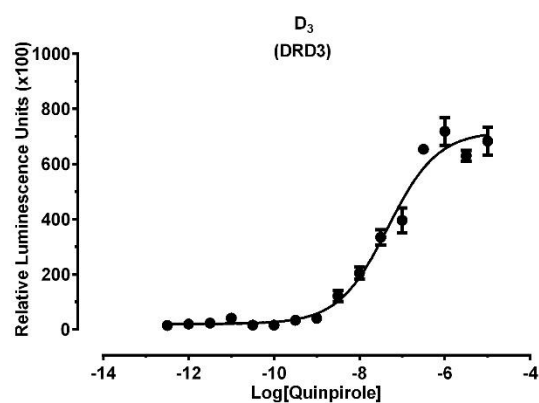
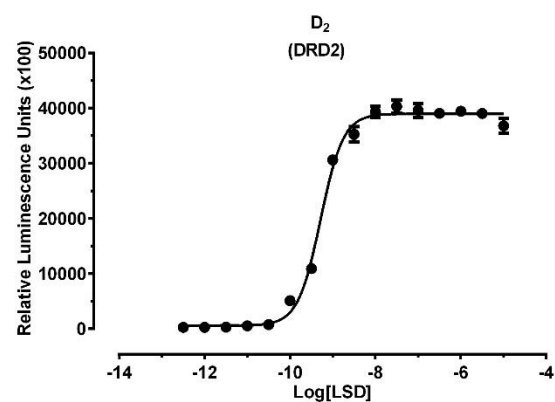
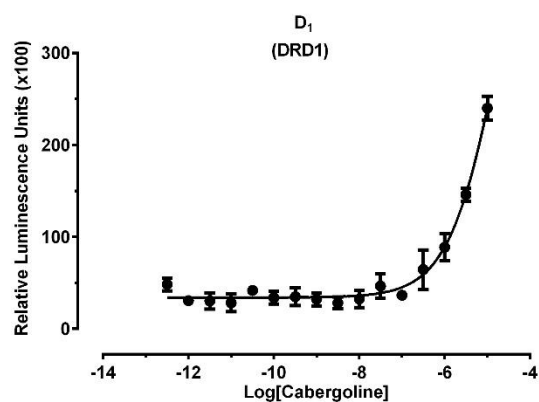
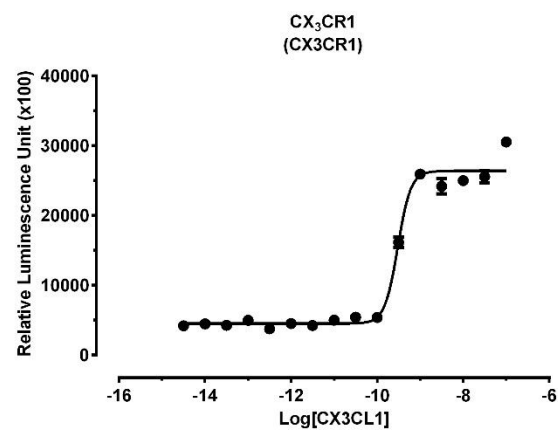
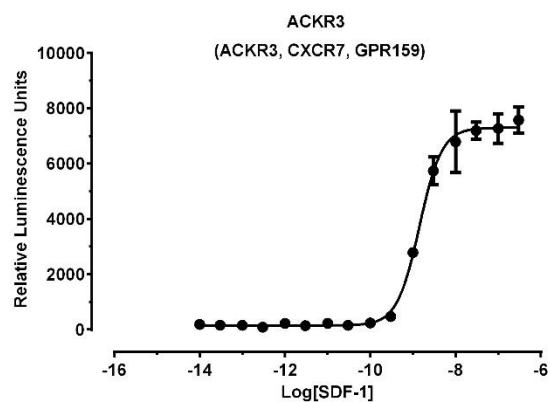


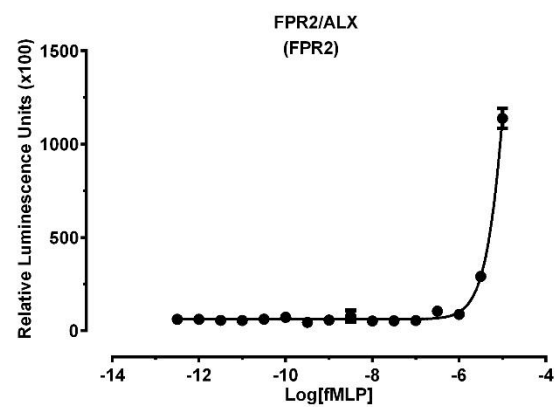
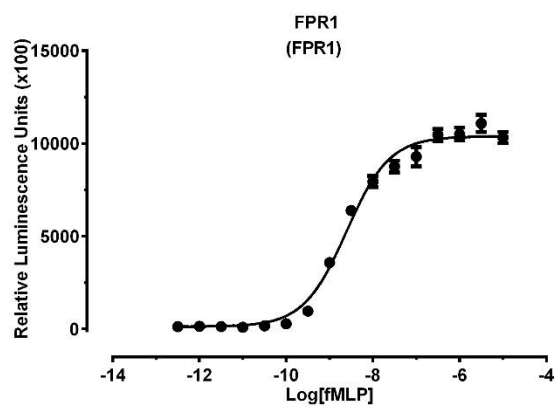
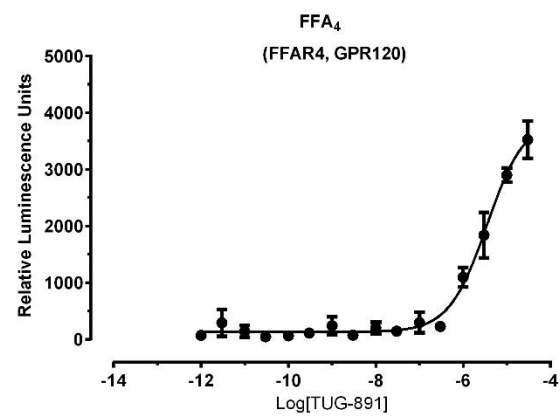
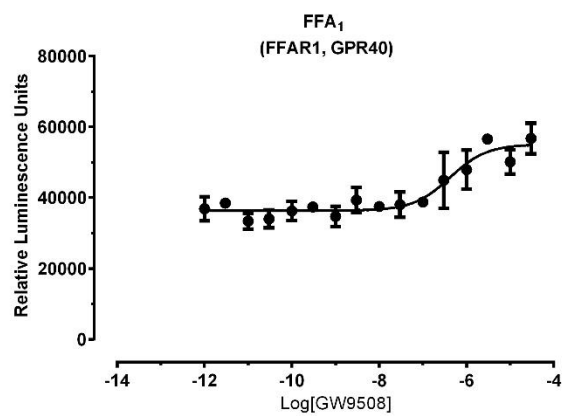
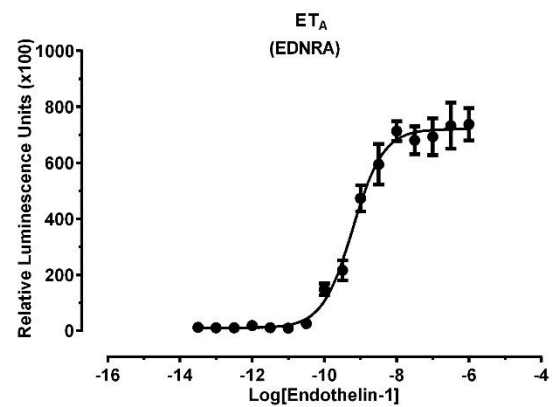
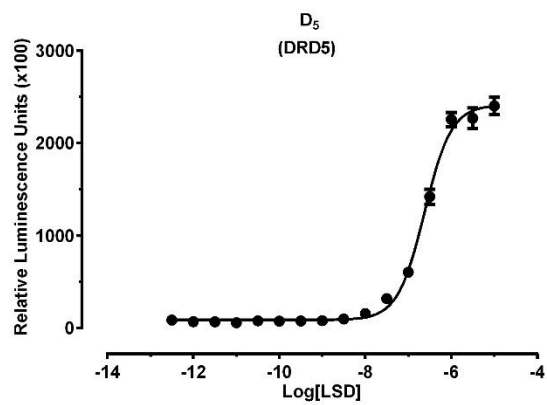


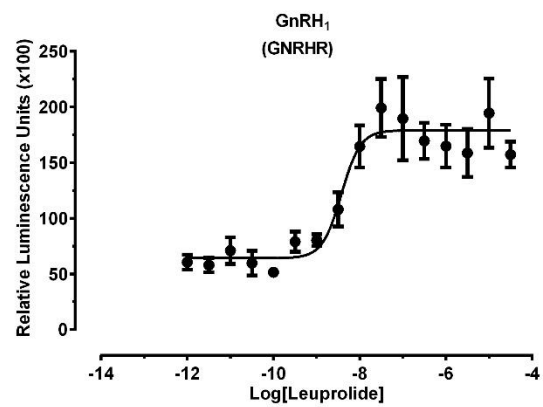
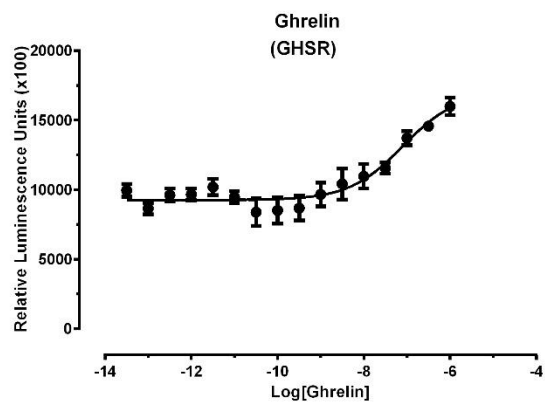
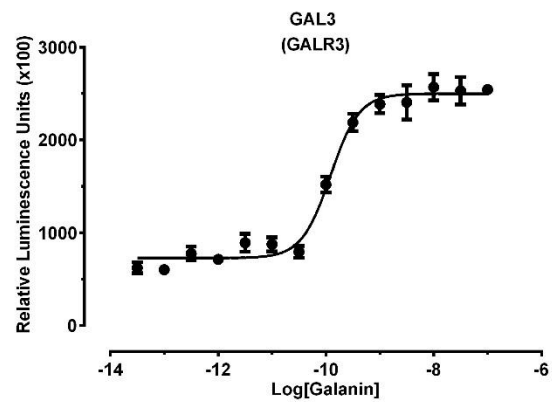
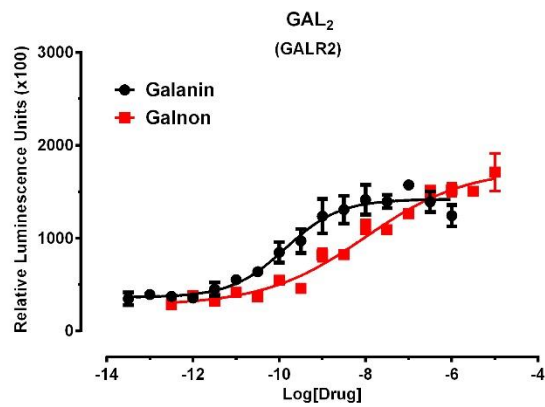
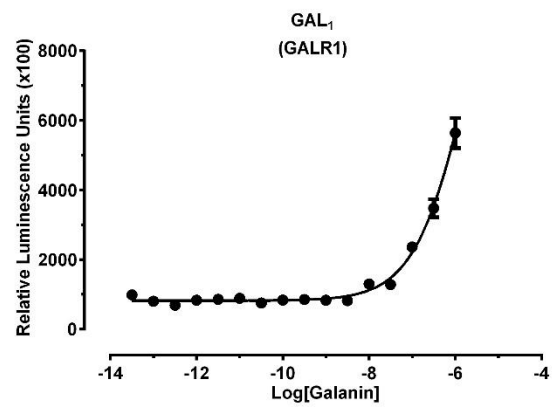
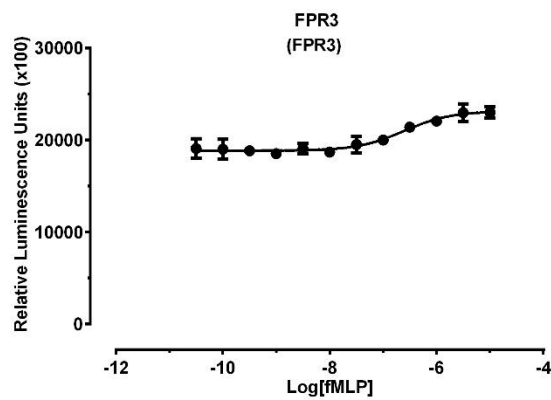


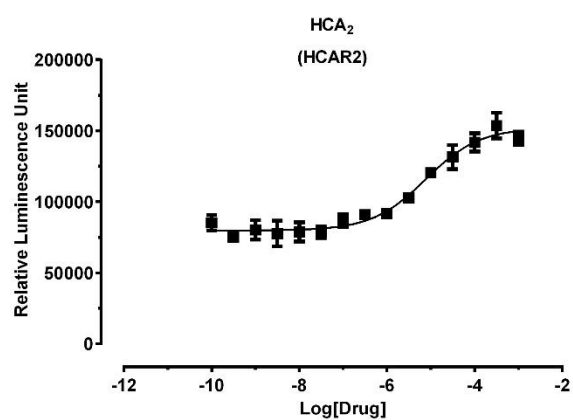
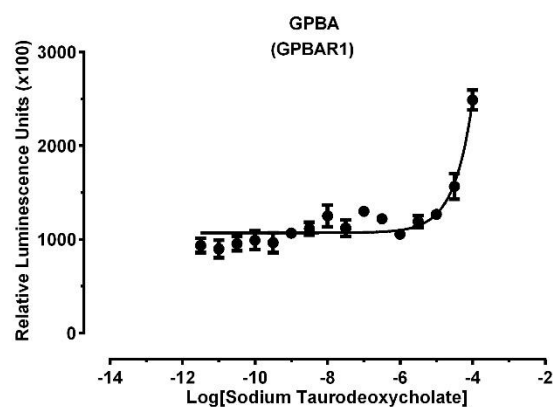
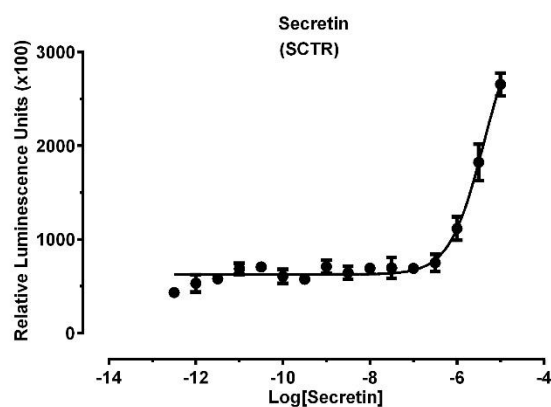
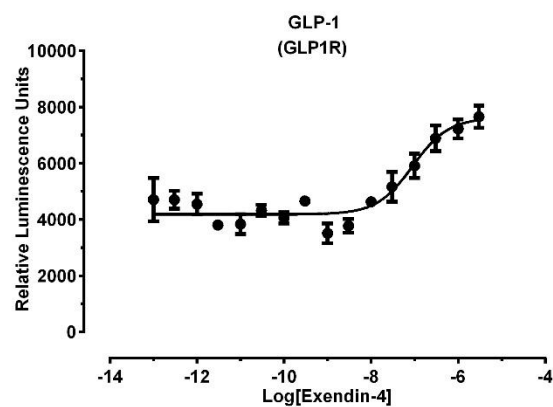
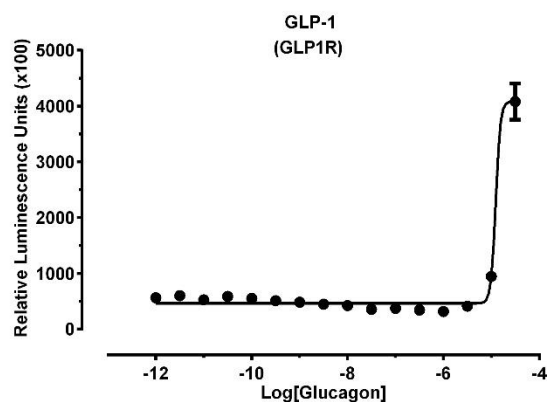


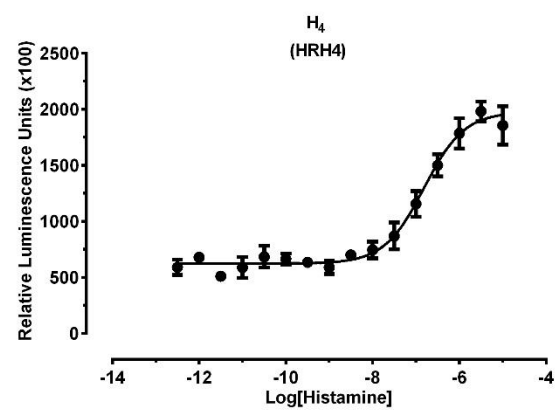
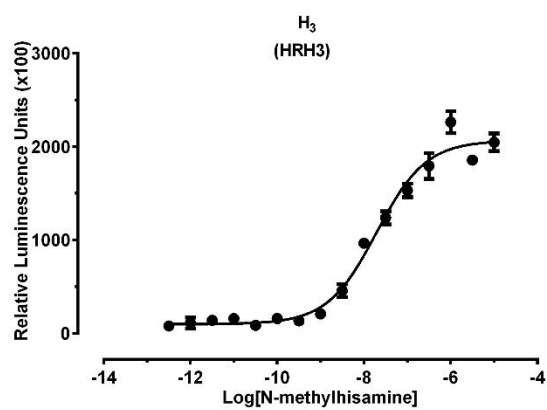
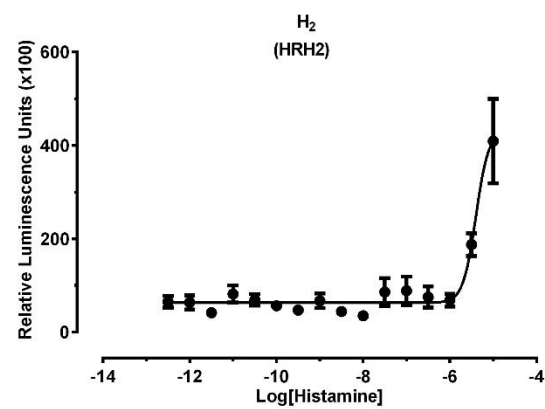
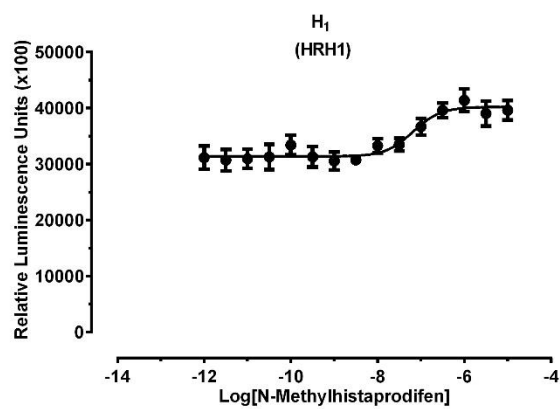
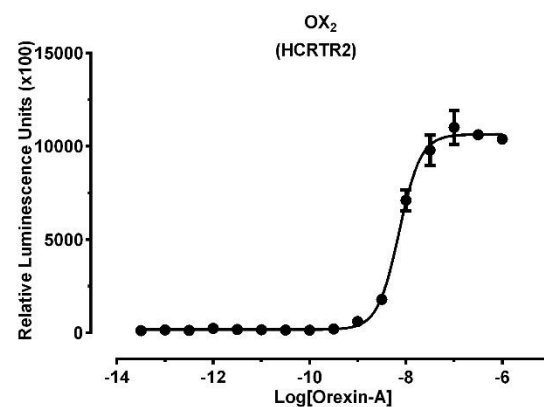
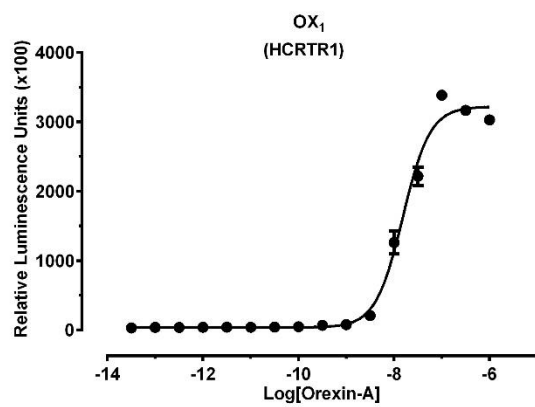


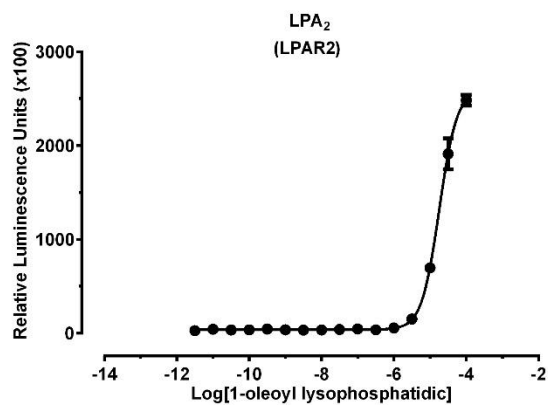
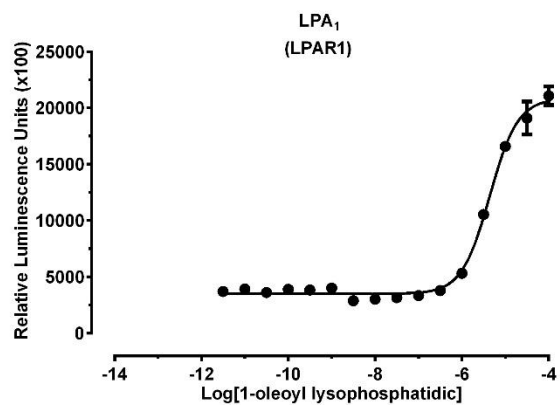
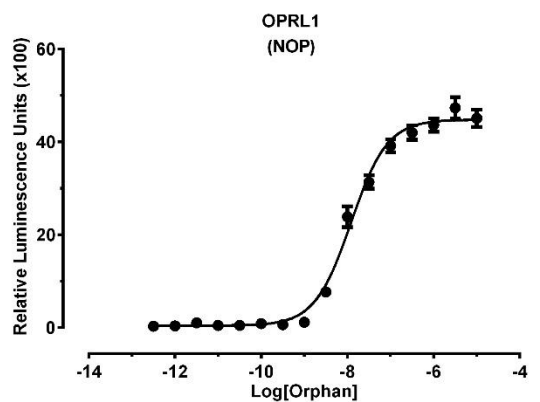
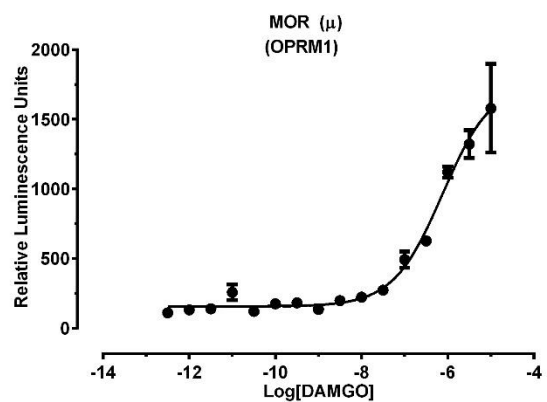
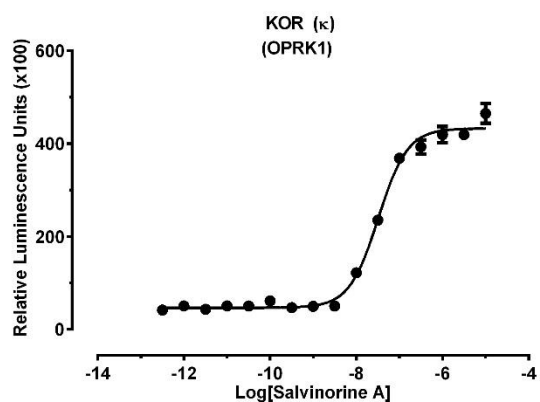
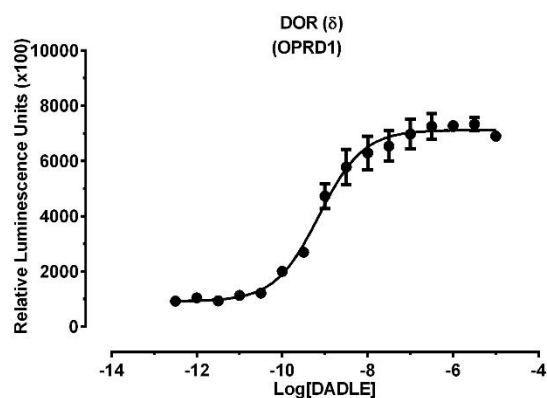


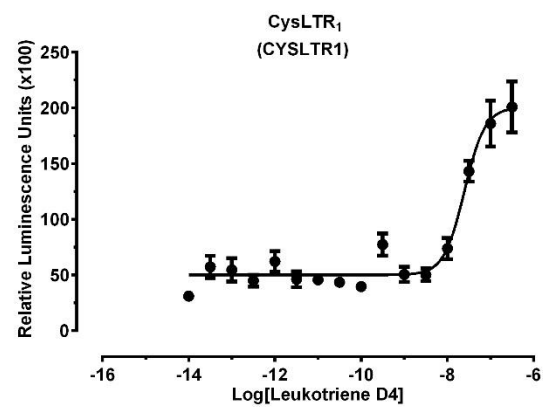
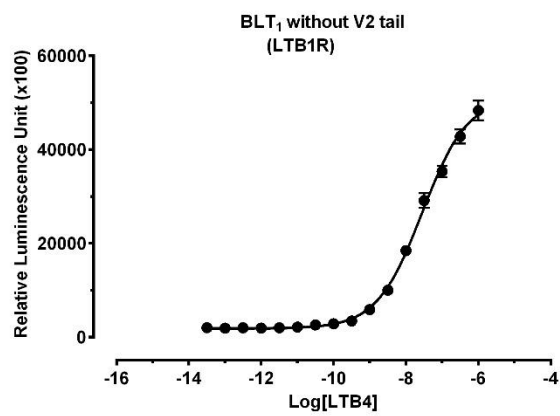
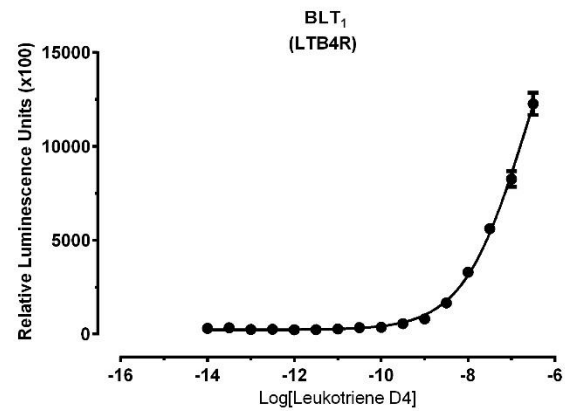
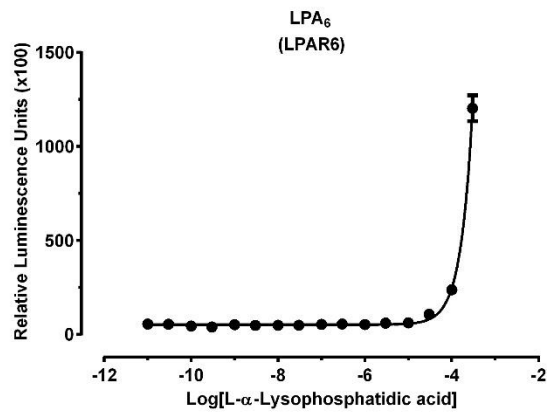
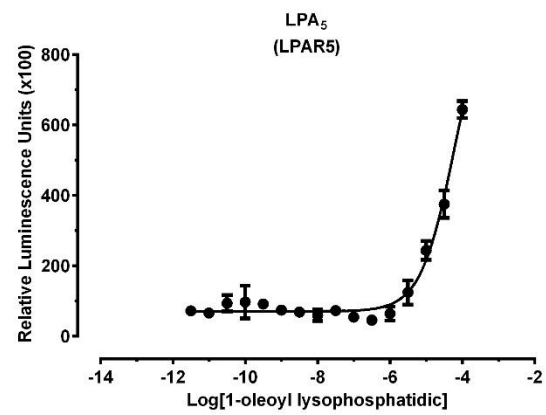
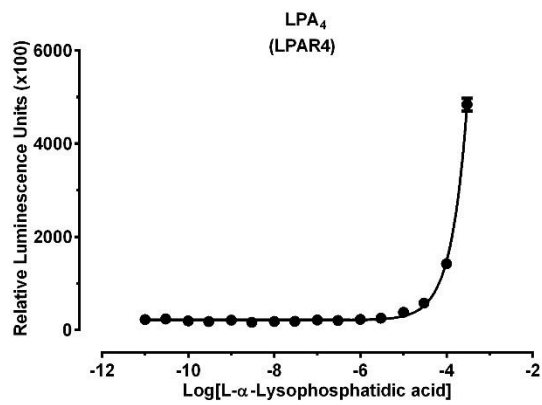


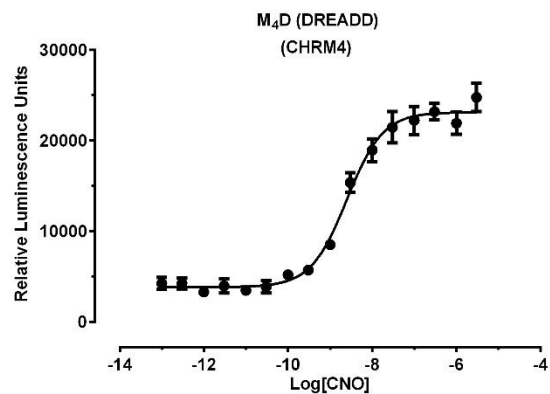
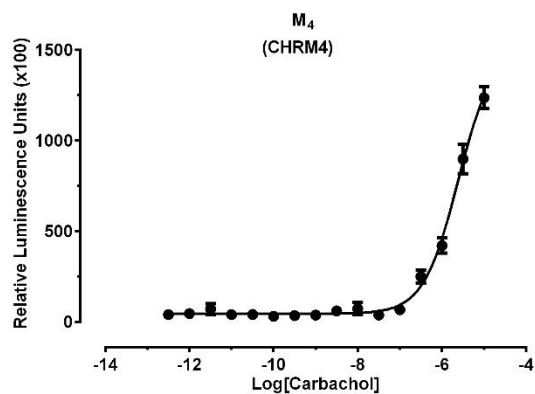
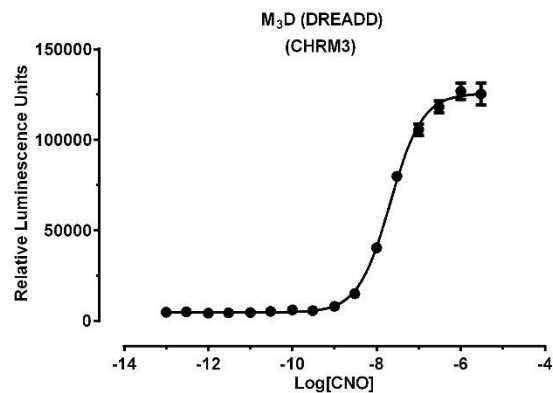
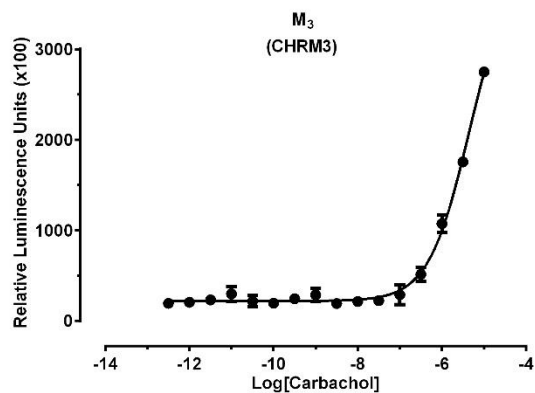
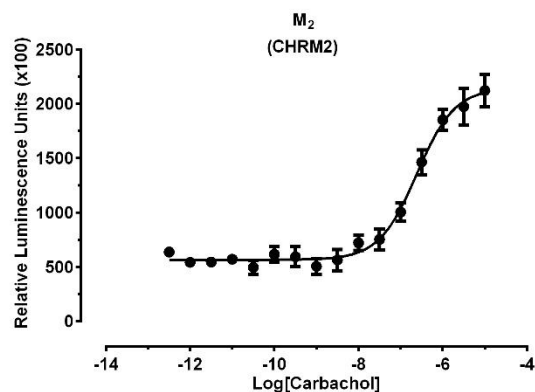
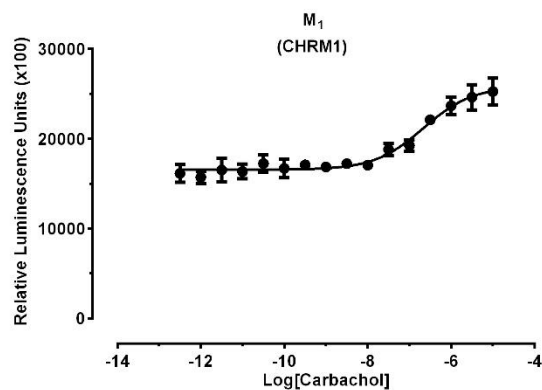


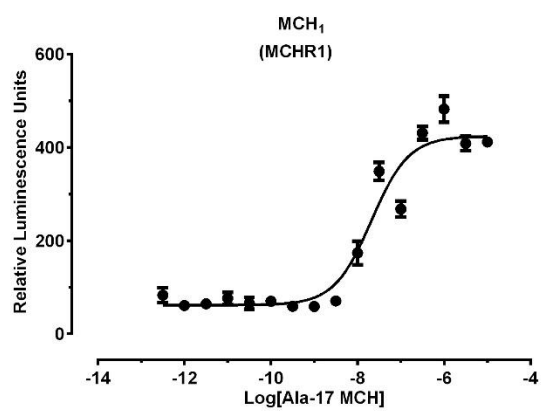
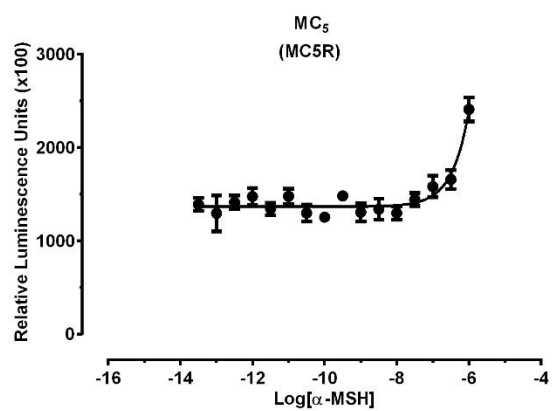
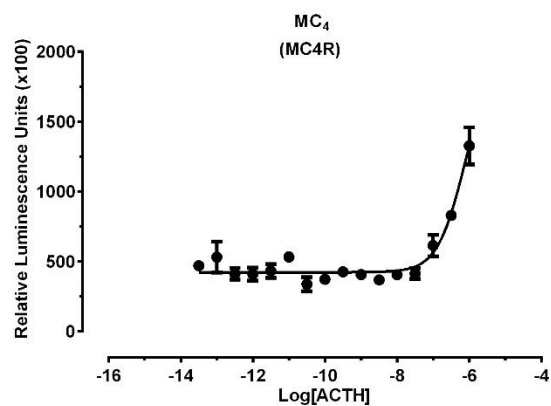
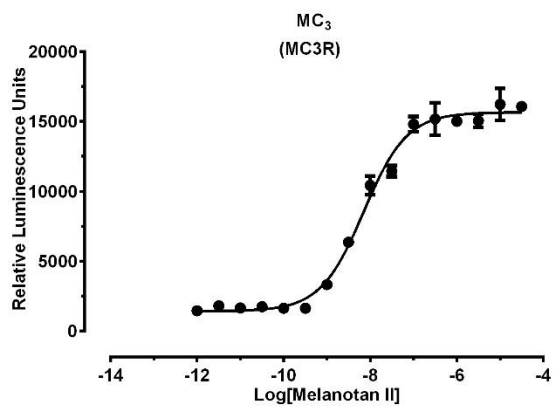
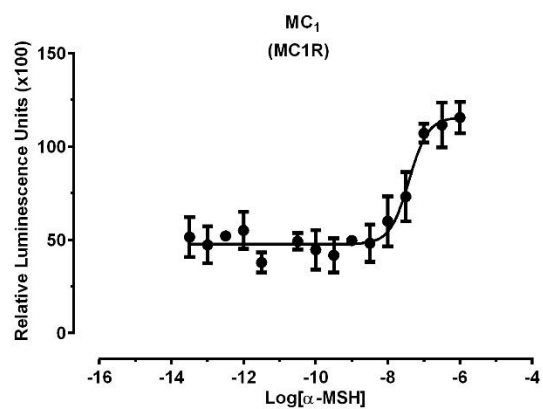
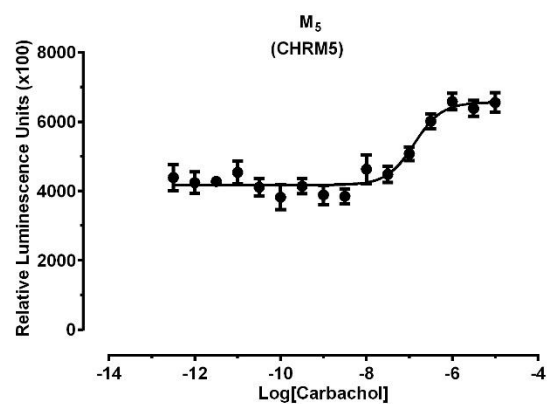


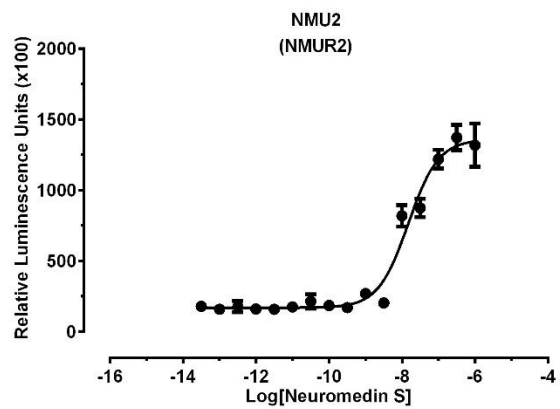
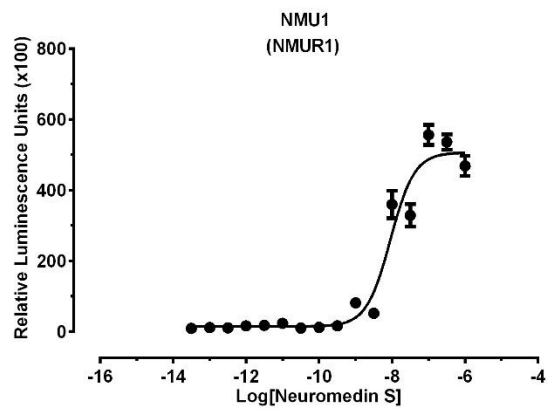
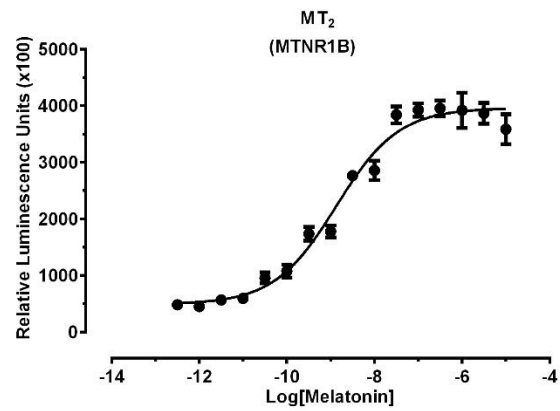
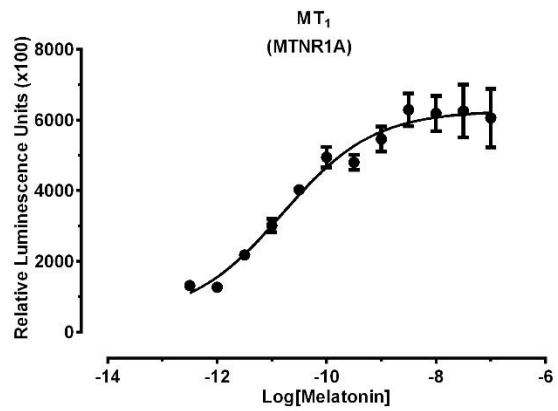
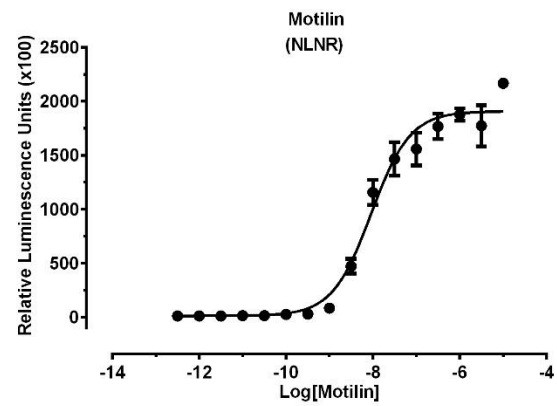
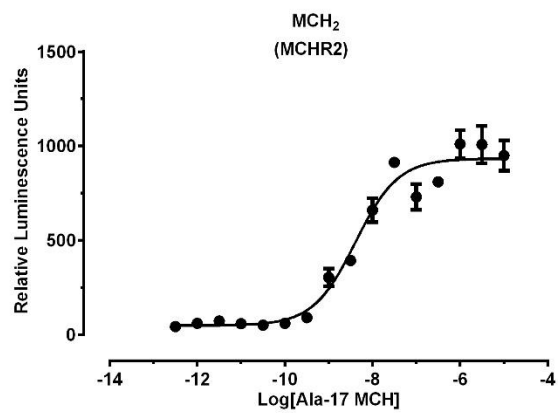


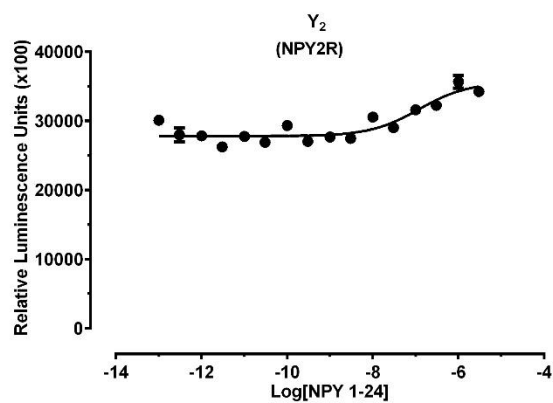
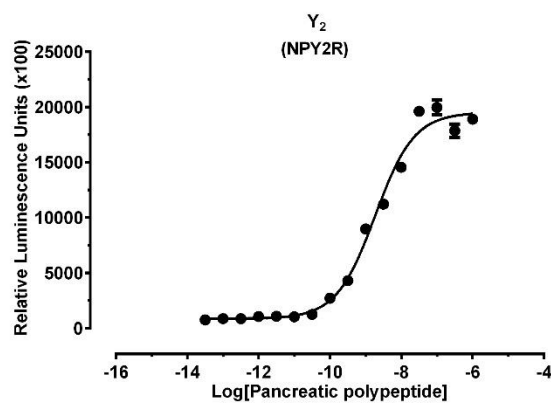
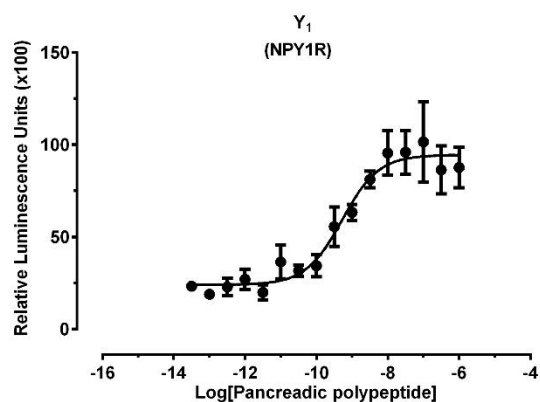
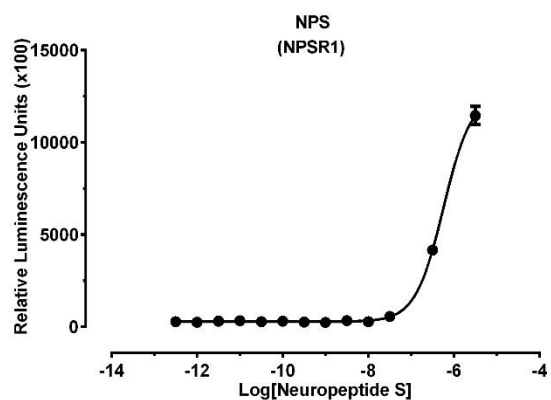
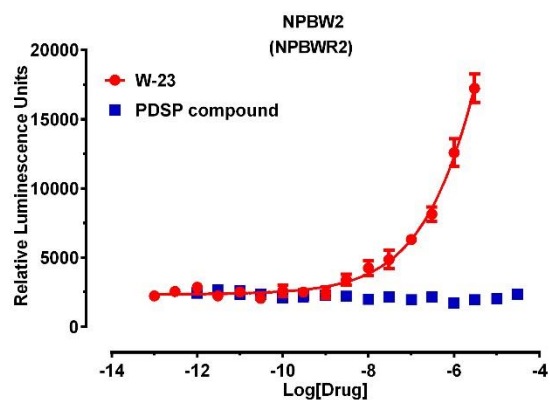
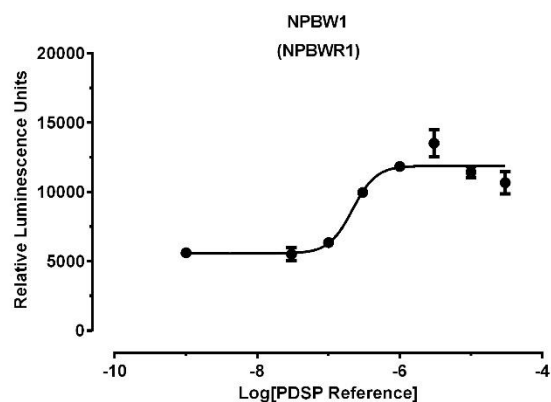


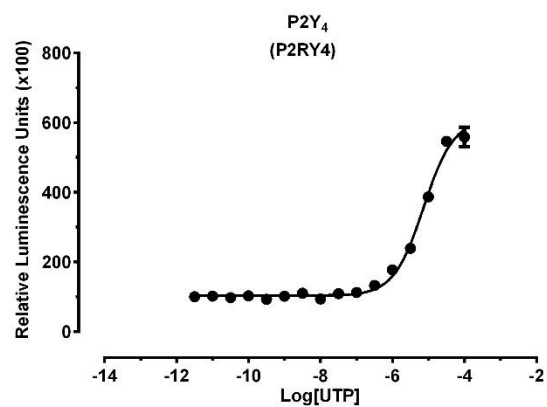
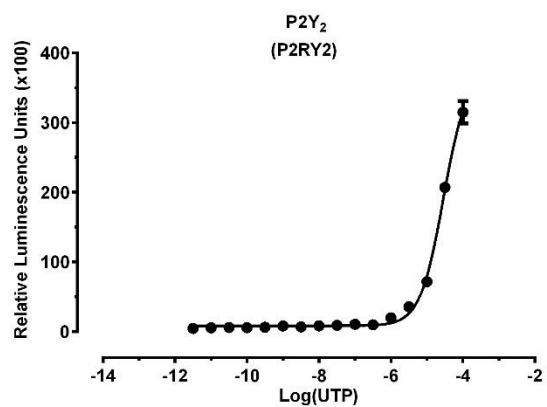
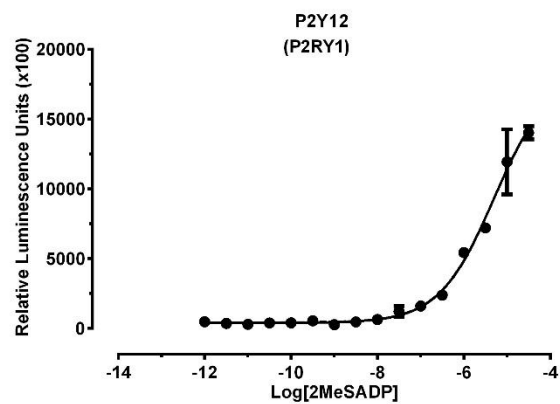
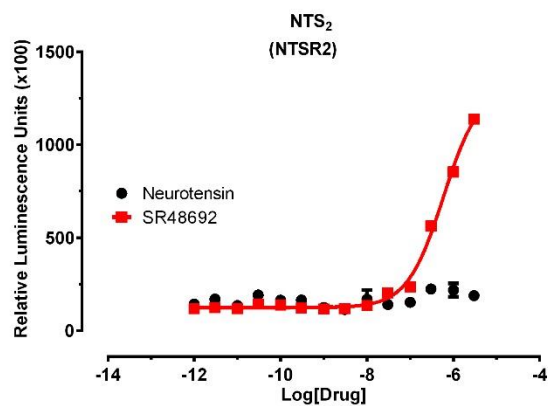
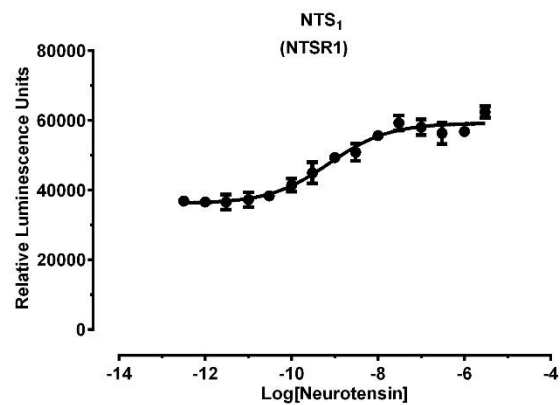
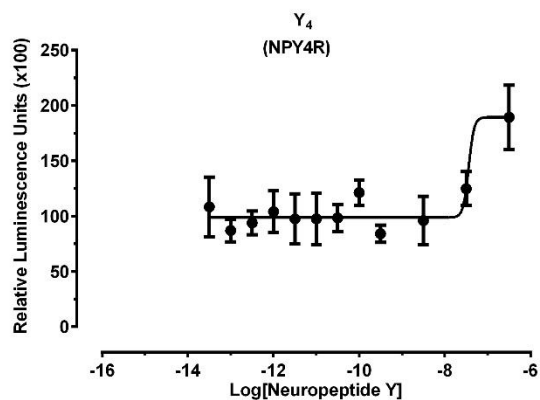


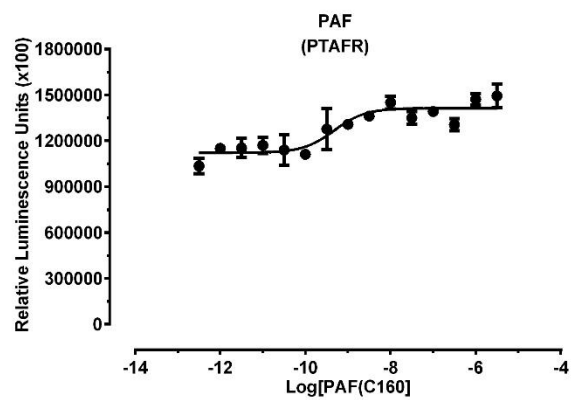
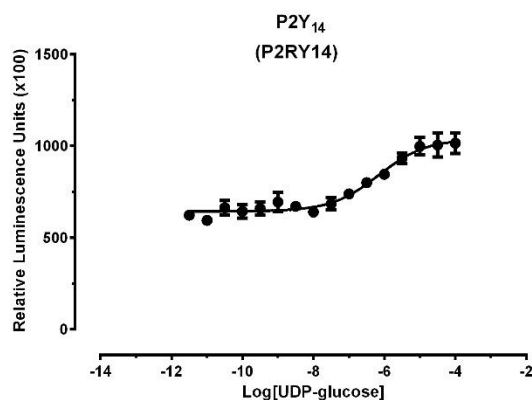
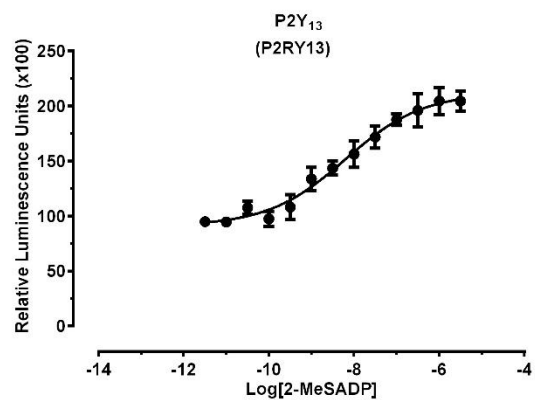
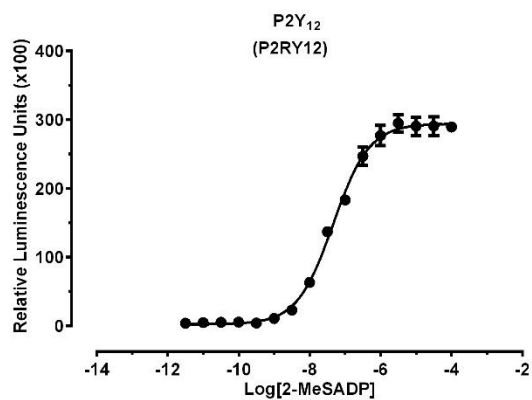
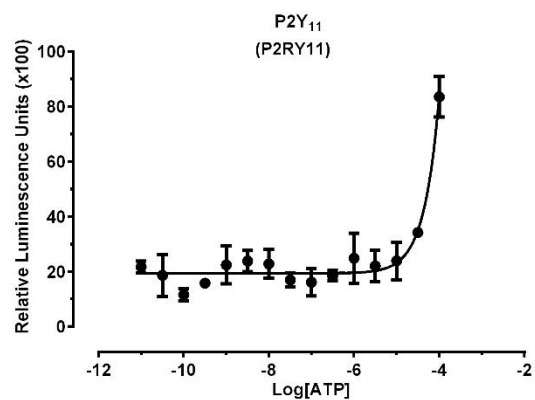
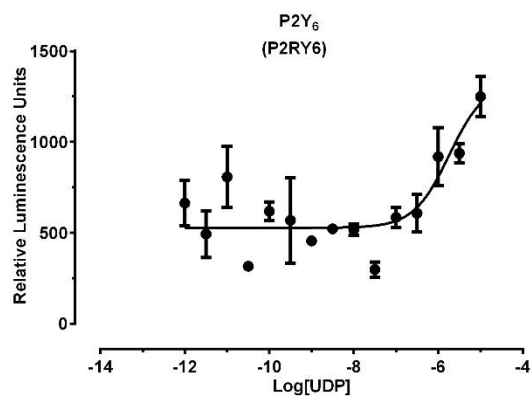


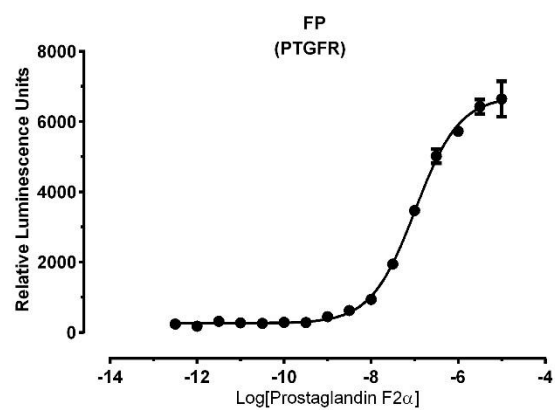
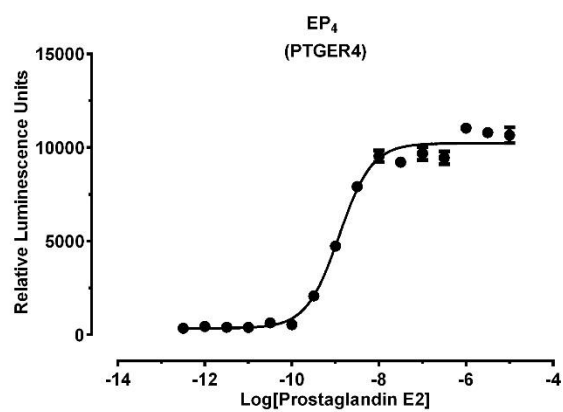
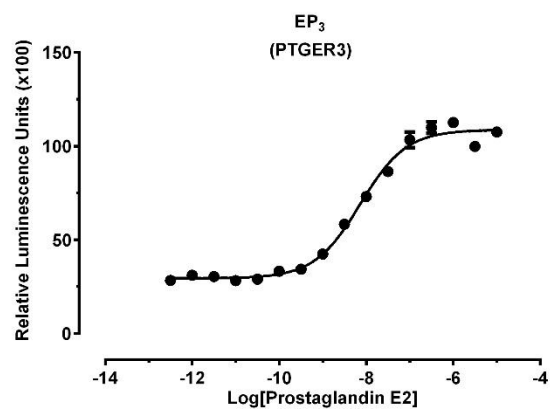
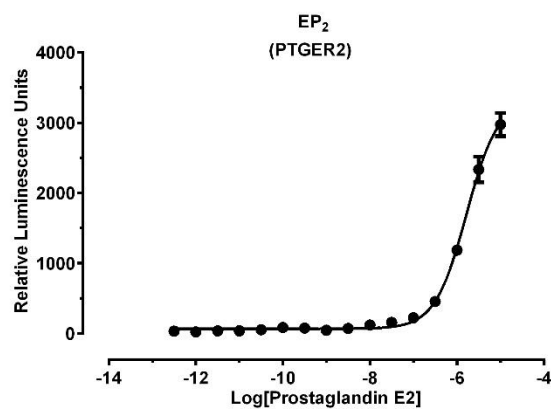
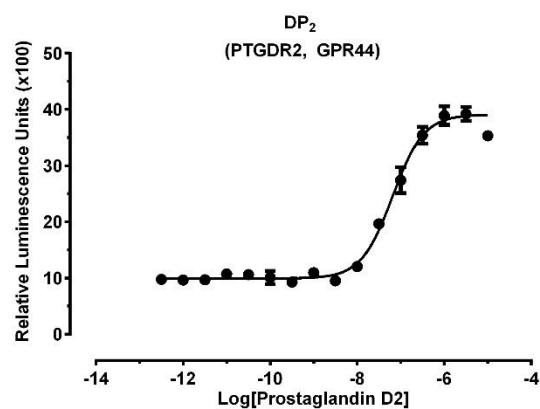
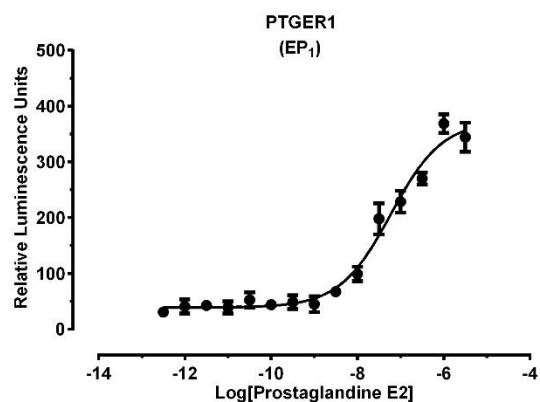


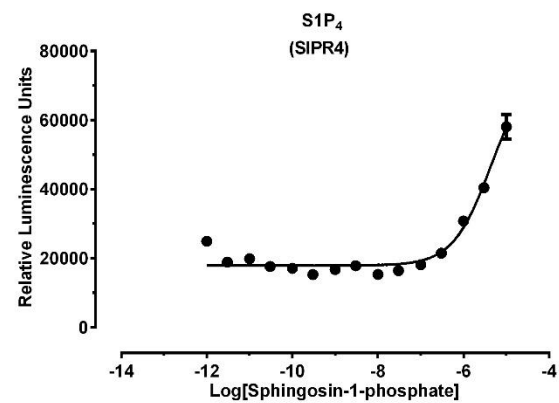
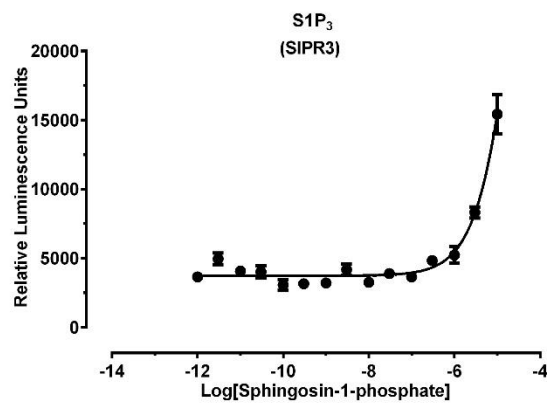
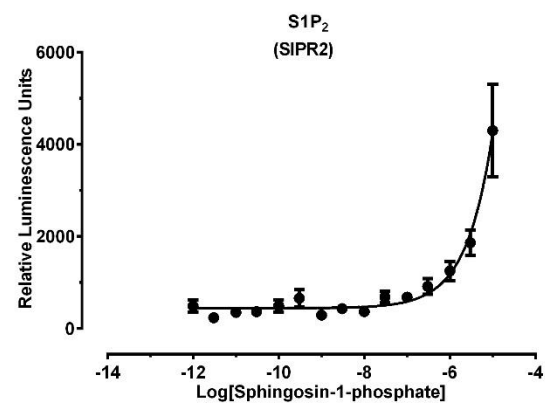
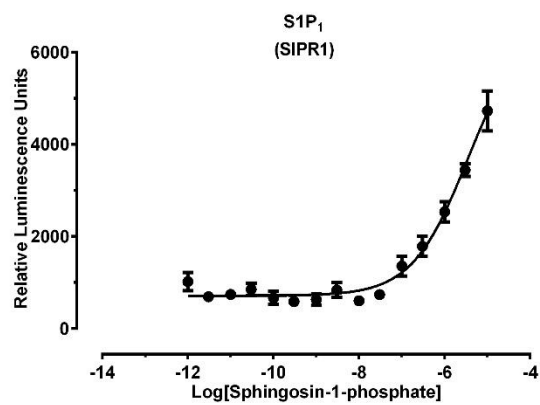
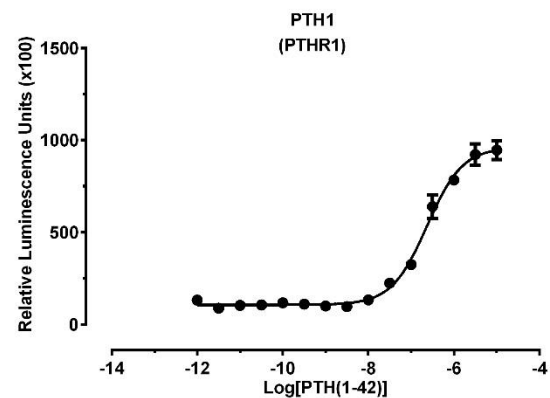
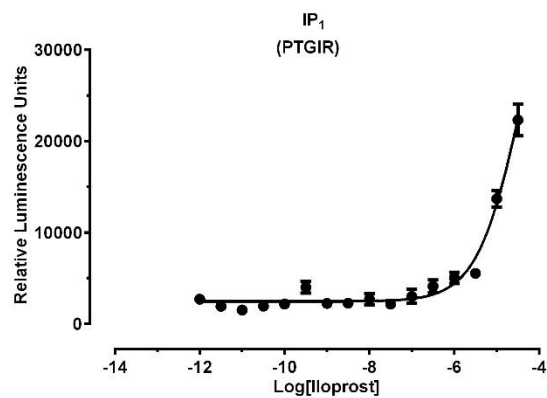


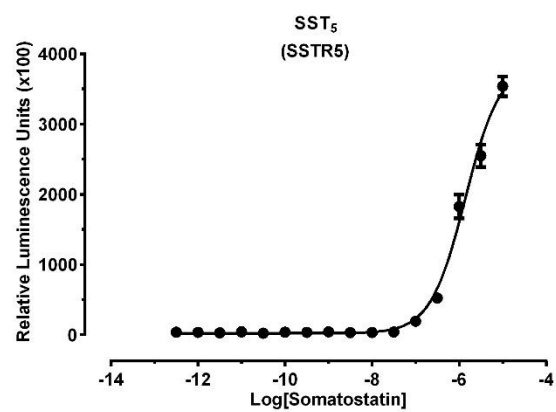
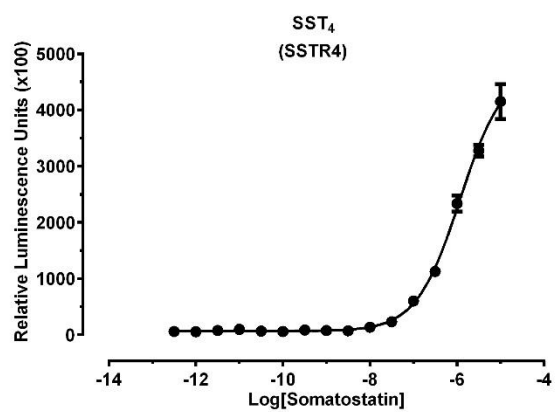
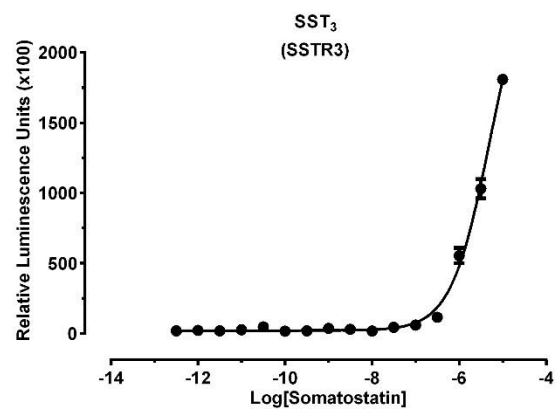
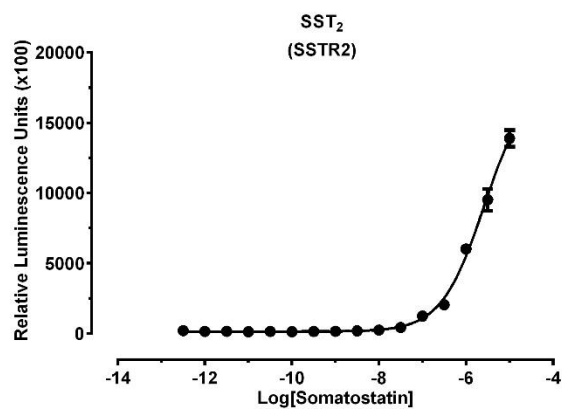
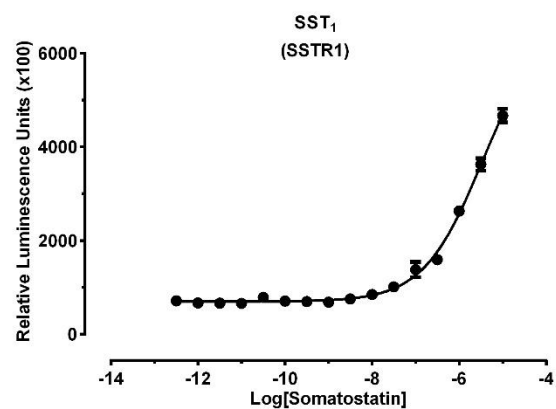
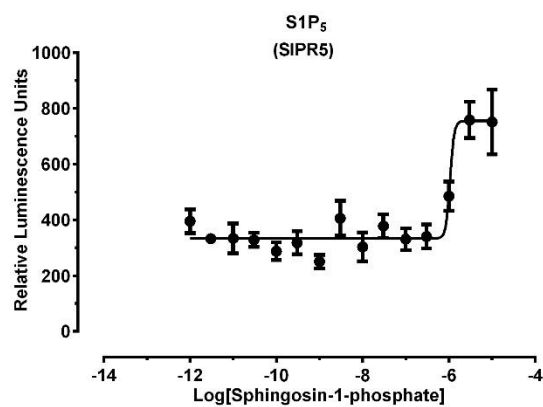


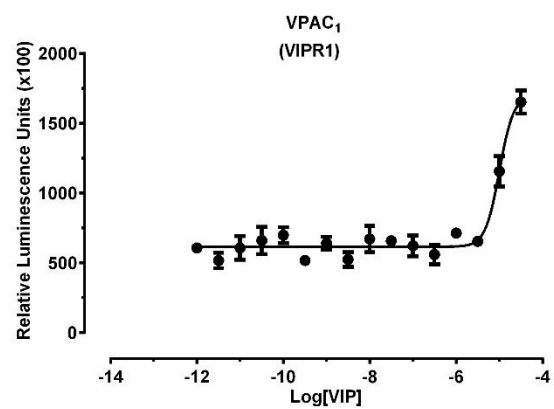
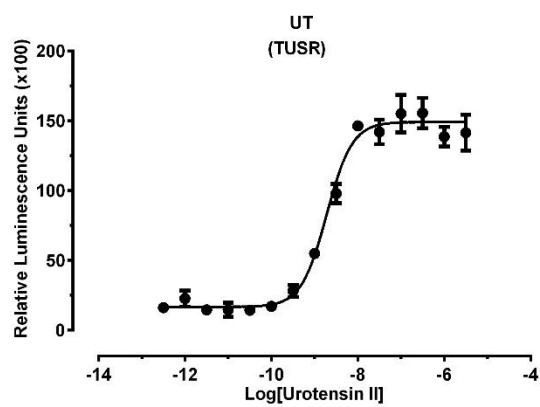
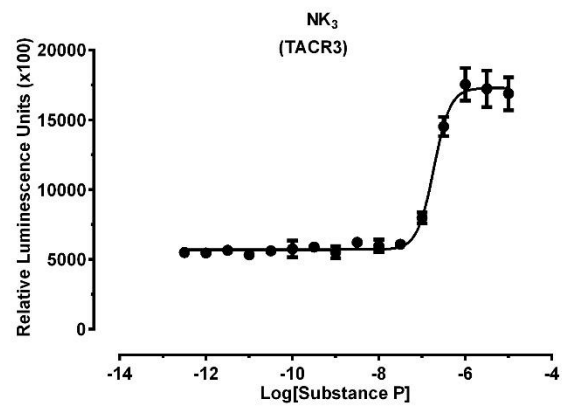
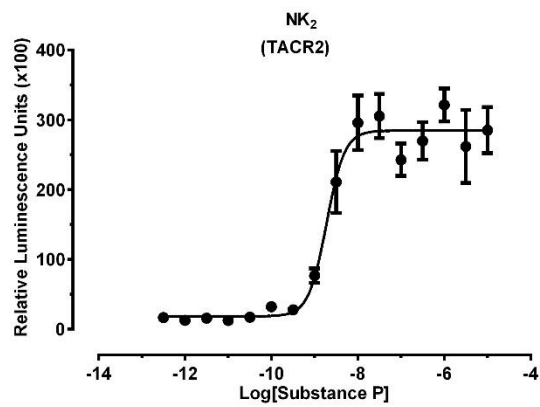
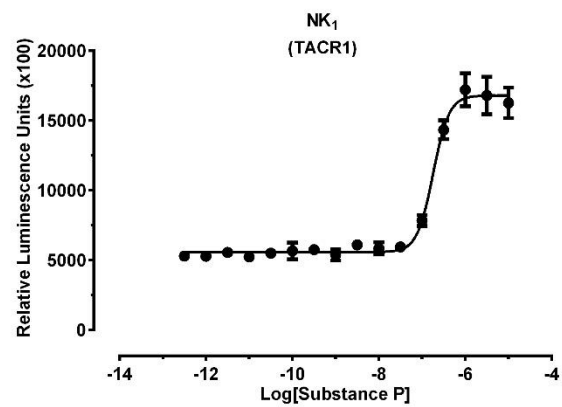
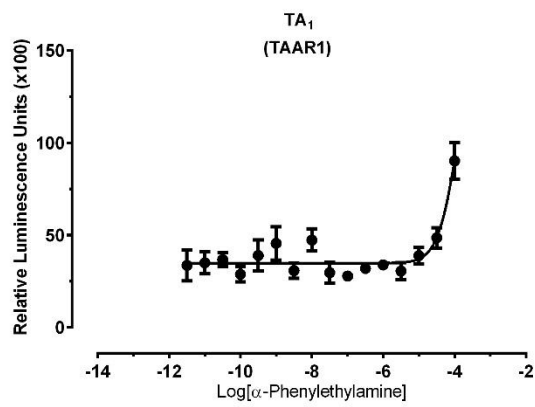


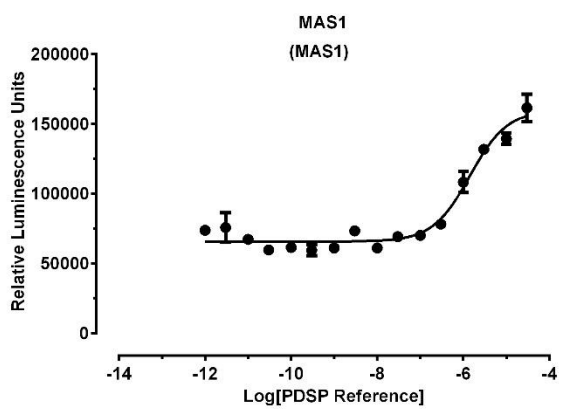
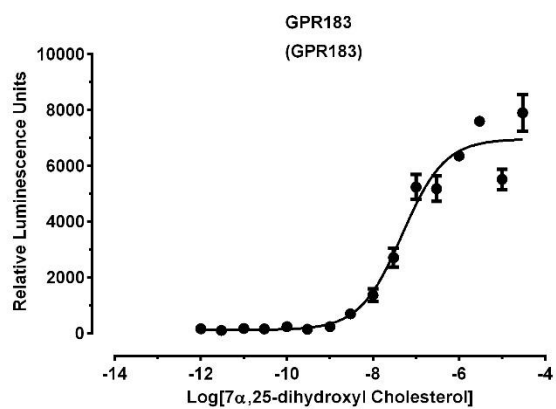
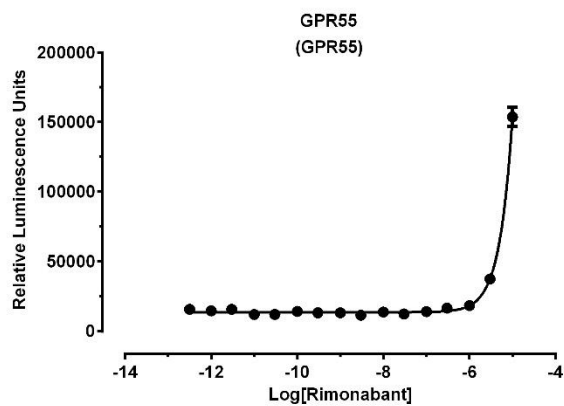
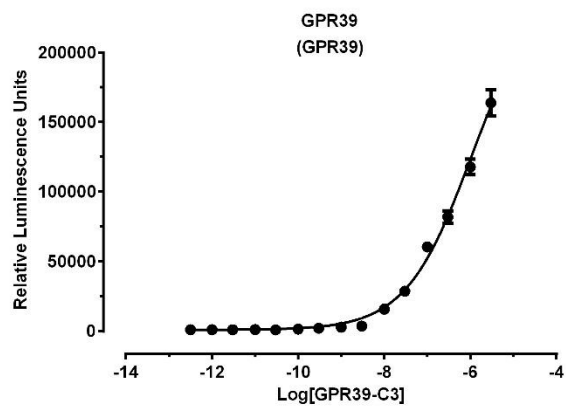
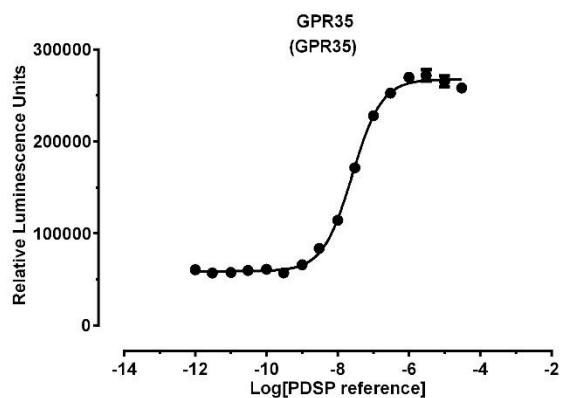
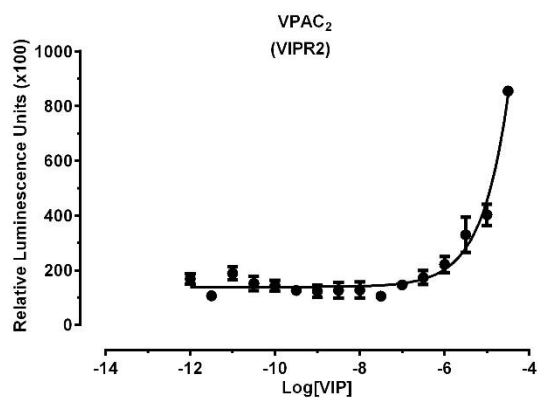












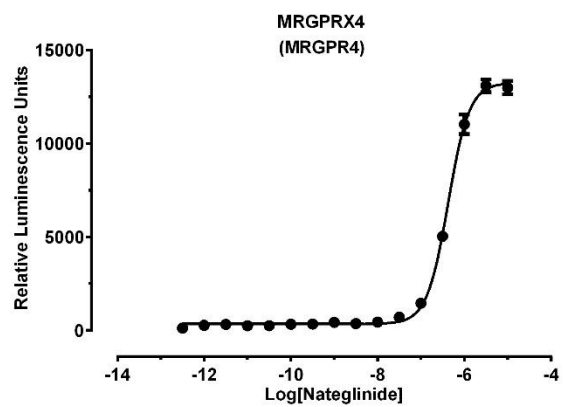
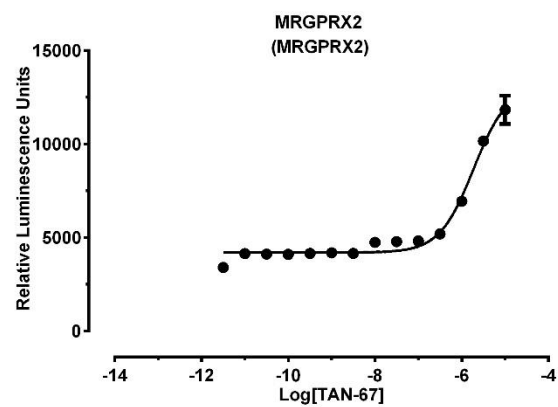
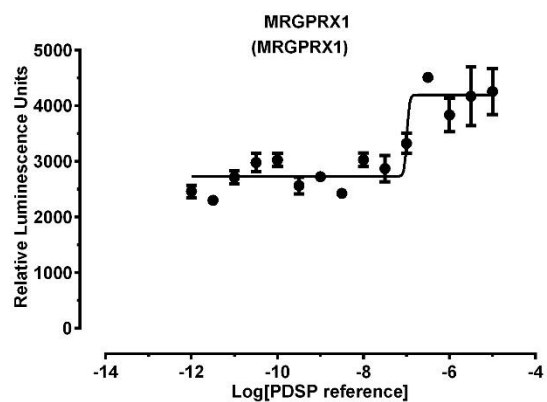


Table 31. List of GPCR Tango constructs with representative antagonist activity assay conditions. Results are analyzed in GraphPad Prism 6.0. Representative curves are attached below in **Figure 49**. PDSP will develop Tango antagonist assays for other GPCRs upon request and approval, as long as reference agonist(s) and antagonist(s) are provided or commercially available. E_{\max} lists the ratio of the top over bottom from the corresponding curves as an indication of signal windows, which is dependent on the concentration of reference agonist for antagonist assay.

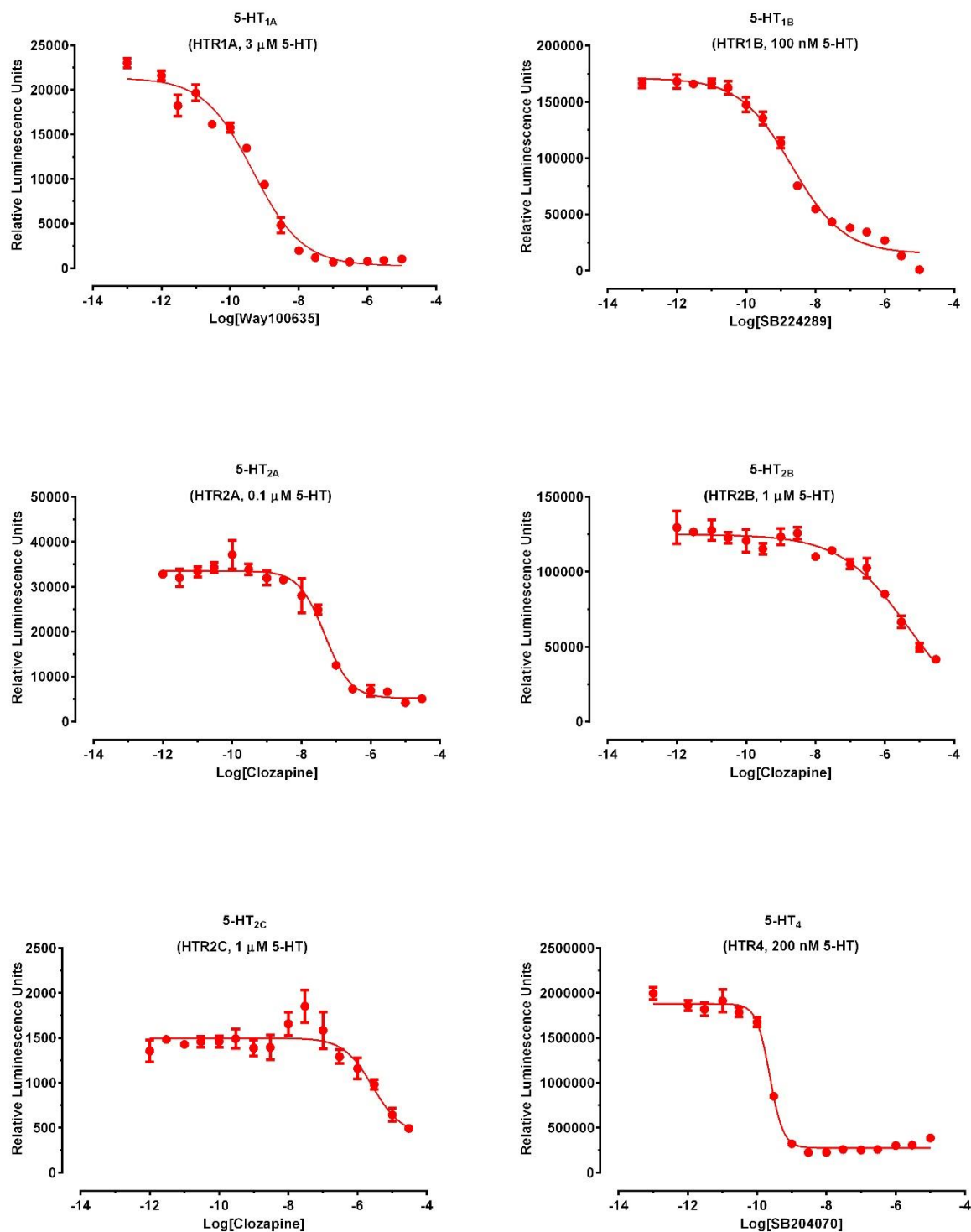
Note: # = Roth lab unpublished results.

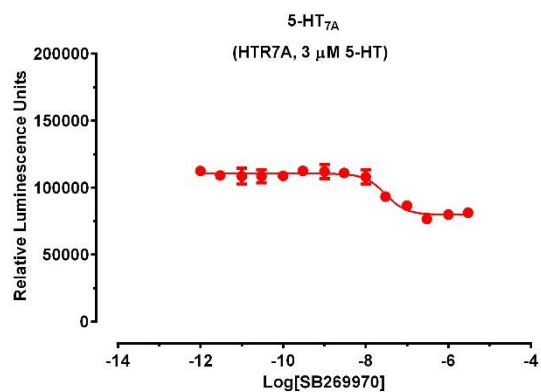
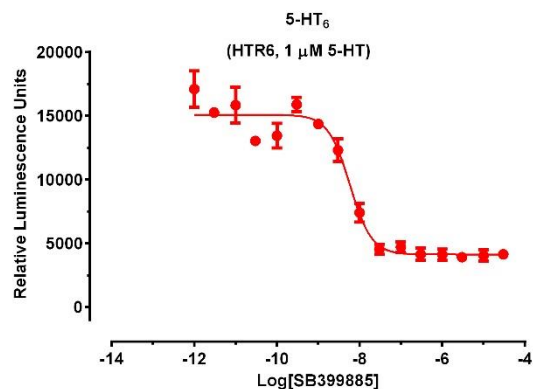
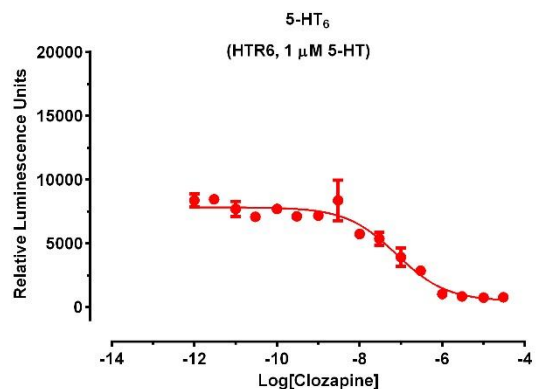
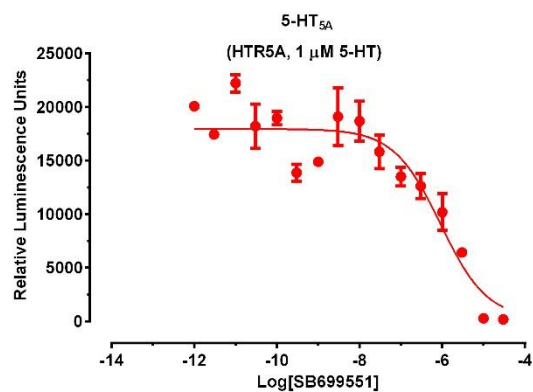
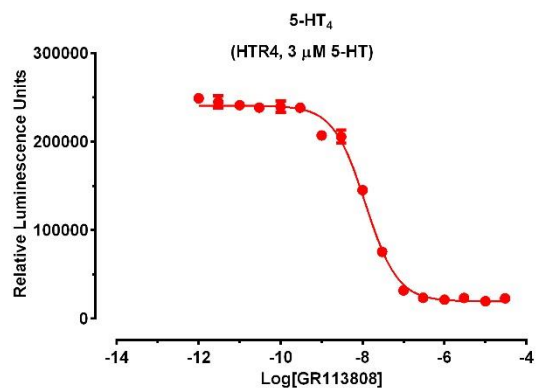
Gene Name	IUPHAR Receptor Name	Reference agonist Reference antagonist	E_{\max} (fold of basal)	pIC ₅₀ (IC ₅₀ nM)	Hill slope
HTR1A	5-HT _{1A}	5-HT (3 μ M) Way100635	83	9.33 (0.47)	-0.60
HTR1B	5-HT _{1B}	5-HT (10 nM) SB224289	114	8.68 (2.1)	-0.58
HTR2A	5-HT _{2A}	5-HT (0.1 μ M) Clozapine	6.5	7.33 (47.0)	-1.16
HTR2B	5-HT _{2B}	5-HT (1 μ M) Clozapine	242	5.31 (4853)	-0.44
HTR2C	5-HT _{2C}	5-HT (1 μ M) Clozapine	3.5	5.57 (2709)	-1.03
HTR4	5-HT ₄	5-HT (200 nM) SB204070	6.8	9.63 (2.3)	-2.24
		5-HT (3 μ M) GR113808	12	7.93 (11.8)	-1.11
HTR5A	5-HT _{5A}	5-HT (1 μ M) SB699551	98	6.04 (91.3)	-0.77
HTR6	5-HT ₆	5-HT (1 μ M) Clozapine	16	7.11 (77.9)	-0.72
		5-HT (1 μ M) SB399885	3.7	8.24 (5.8)	-1.65
HTR7A	5-HT _{7A}	5-HT (1 μ M) SB269970	1.4	7.52 (30.2)	-1.73
CHRM1	M ₁	Carbachol (10 μ M) Atropine	72	7.03 (93.0)	-0.85
CHRM2	M ₂	Carbachol (1 μ M) NMS	11	8.87 (1.3)	-1.13
CHRM3	M ₃	Carbachol (3 μ M) NMS	47	9.58 (0.3)	-0.93
CHRM4	M ₄	Carbachol (1 μ M)	413	10.55 (0.03)	-1.40

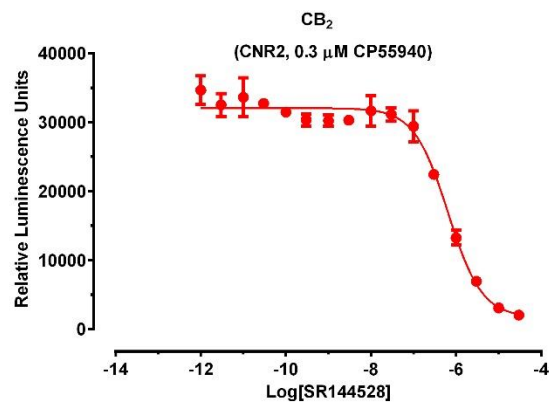
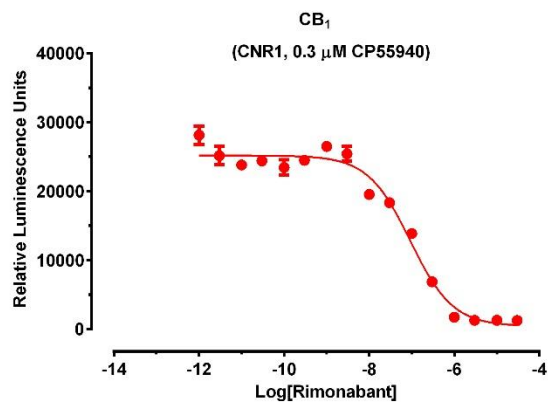
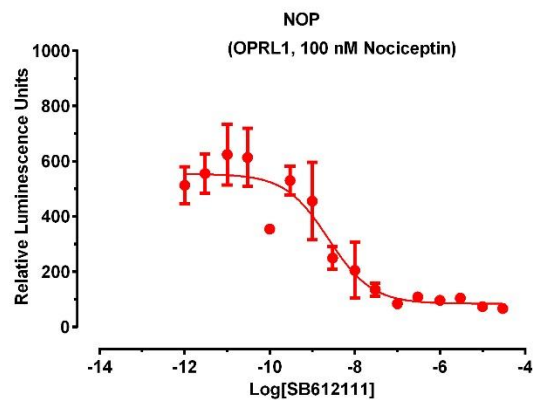
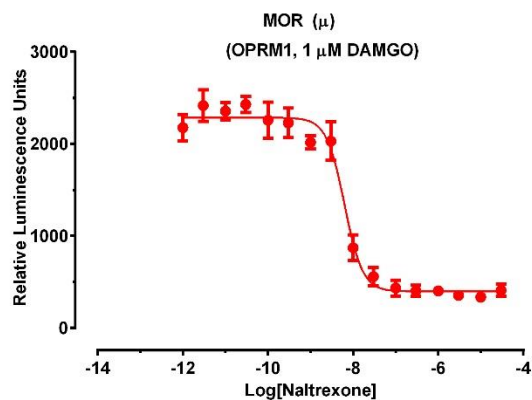
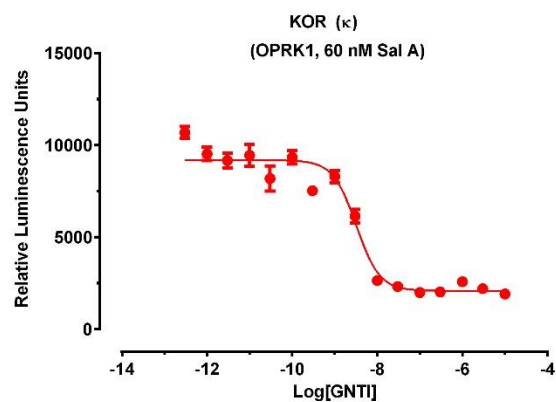
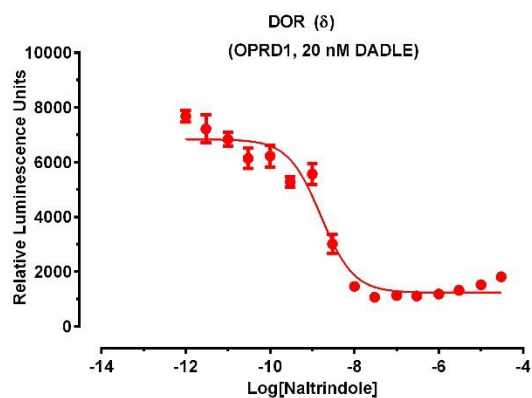
Gene Name	IUPHAR Receptor Name	Reference agonist Reference antagonist	E _{max} (fold of basal)	pIC ₅₀ (IC ₅₀ nM)	Hill slope
		Atropine			
CHRM5	M ₅	Carbachol (10 μM) NMS	2.8	8.97 (1.1)	-0.88
DRD1	D ₁	SKF81297 (3 μM) SCH23390	23	7.28 (52.4)	-1.27
DRD2	D ₂	Quinpirole (10 nM) Haloperidol	24	8.90 (1.3)	-2.31
DRD3	D ₃	Quinpirole (100 nM) Haloperidol	58	7.38 (41.5)	-1.16
DRD4	D ₄	Lisuride (100 nM) Nemonapride	3.6	6.80 (160)	-2.91
DRD5	D ₅	SKF81297 (3 μM) SCH23390	22	6.99 (103)	-1.07
ADRA1A	α _{1A}	Norepinephrine (1 μM) Prazosin	2.0	7.63 (23.3)	-0.88
ADRA1B	α _{1B}	Norepinephrine (1 μM) Prazosin	5.8	8.99 (1.0)	-1.19
ADRA1D	α _{1D}	Norepinephrine (1 μM) Prazosin	5.6	9.60 (0.3)	-1.17
ADRA2A	α _{2A}	Norepinephrine (300 nM) Rauwolscine	10	8.58 (2.6)	-0.97
ADRA2B	α _{2B}	Norepinephrine (300 nM) Rauwolscine	7.3	7.29 (51.9)	-0.94
ADRA2C	α _{2C}	Clonidine (300 nM) Rauwolscine	42	7.94 (11.4)	-1.06
ADRB1	β ₁	Norepinephrine (10 μM) Carvedilol	28	8.56 (2.8)	-1.02
ADRB2	β ₁	Norepinephrine (10 μM) Carvedilol	63	9.15 (0.7)	-0.70
ADORA1	A ₁	NECA (100 nM) CGS15943	44	7.46 (34.6)	-0.88
CNR1	CB ₁	CP55940 (300 nM) Rimonabant	59	7.03 (92.8)	-0.87
CNR2	CB ₂	JWH-018 (300 nM) SR144528	18	6.19 (651)	-1.09
HRH1	H ₁	Histamine (1 μM) Pyrilamine	2.2	6.53 (294)	-0.98
MLNR	Motilin	Motilin (1 μM)	44	8.47 (3.4)	-1.17

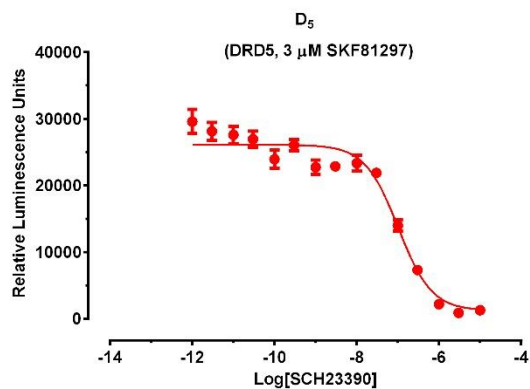
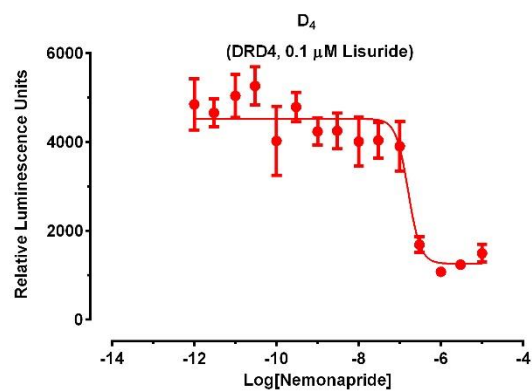
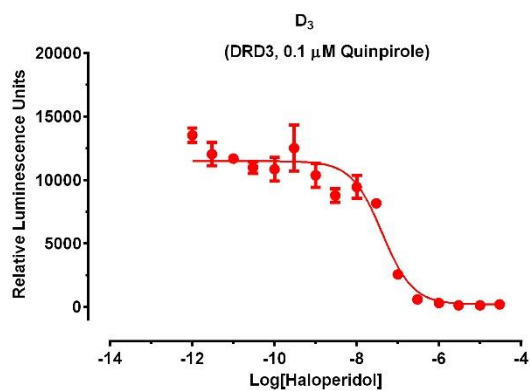
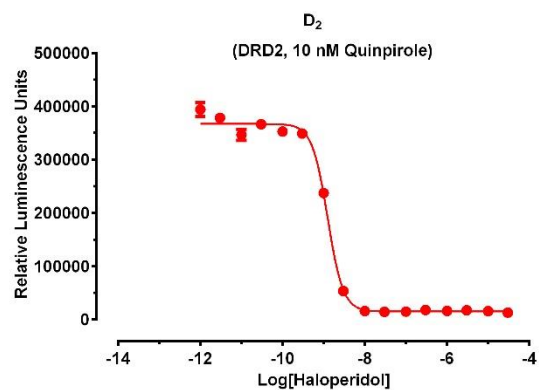
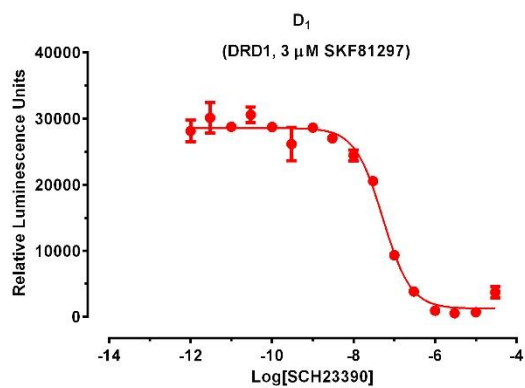
Gene Name	IUPHAR Receptor Name	Reference agonist Reference antagonist	E _{max} (fold of basal)	pIC ₅₀ (IC ₅₀ nM)	Hill slope
		MS 2029			
NMUR2	NMU2	Neuromedin S (1 µM) PDSP reference [#]	2.2	7.23 (59.6)	-0.75
OPRD1	DOR (δ)	DADLE (20 nM) Naltrindole	5.5	8.79 (1.6)	-1.12
OPRK1	KOR (κ)	Salvinorin A (60 nM) GNTI	4.4	8.49 (3.2)	-1.58
OPRM1	MOR (μ)	DAMGO (1 µM) Naltrexone	5.8	8.20 (6.3)	-2.04
OPRL1	NOP	Nociceptin (100 nM) SB612111	6.6	8.62 (2.4)	-0.85
OXTR	OT	Oxytocin (3 µM) PDSP reference [#]	15	5.89 (1299)	-0.92
P2RY1	P2Y ₁	2MeS-ADP (3 µM) MRS 2179	4.6	6.26 (546)	-0.61
P2RY2	P2Y ₂	UTP (10 µM) AR-C 118925XX	4.5	6.39 (408)	-0.82
PTGER4	EP ₄	Prostaglandin E2 (10 nM) L-161982	1.9	7.49 (32.1)	-1.25

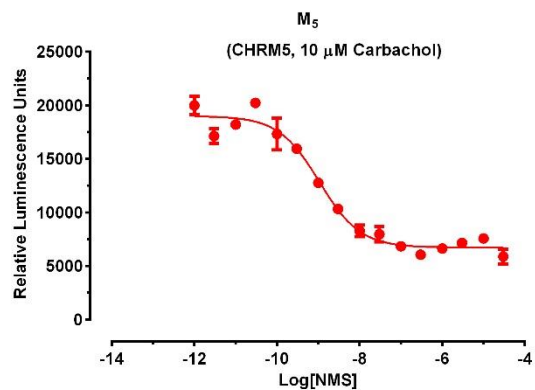
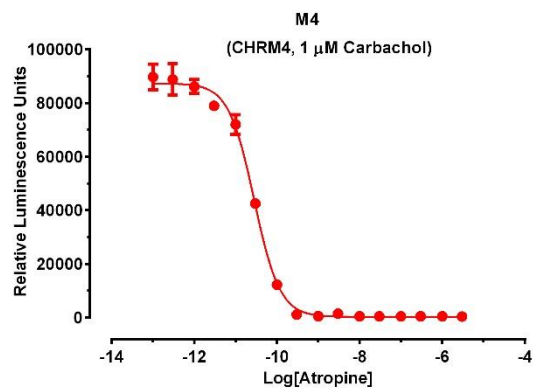
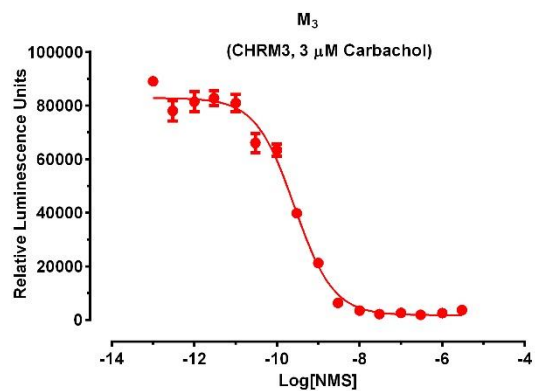
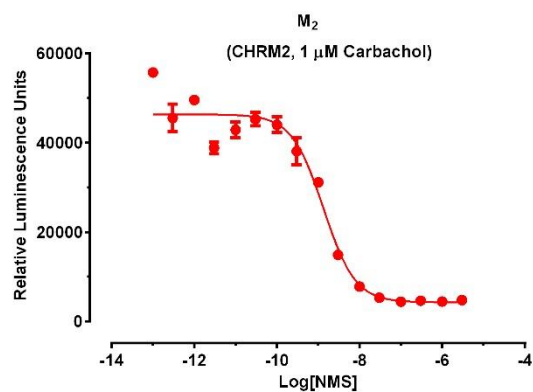
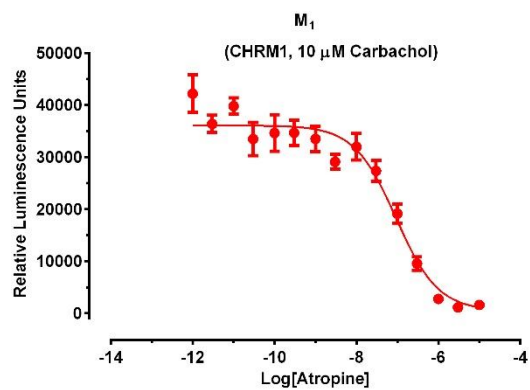
Figure 49. Representative curves for GPCR Tango antagonist assays.

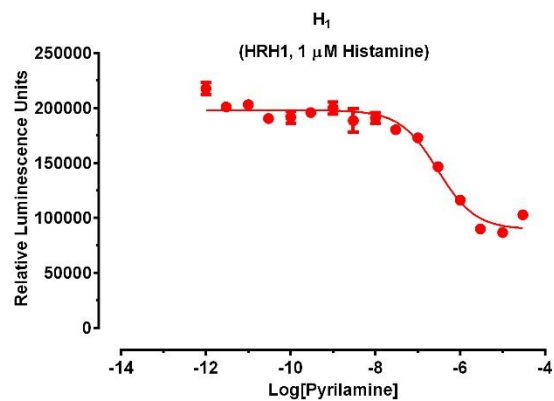
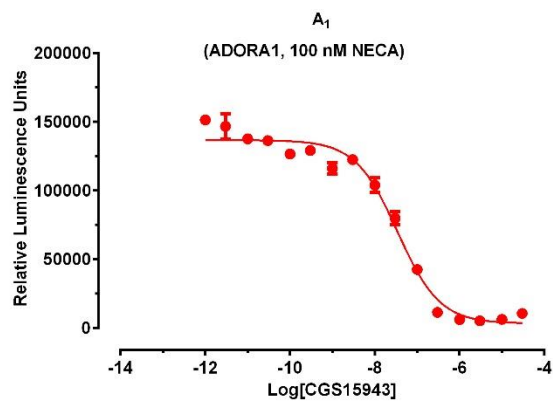
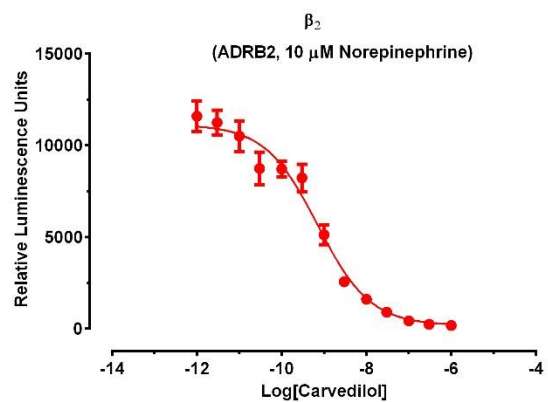
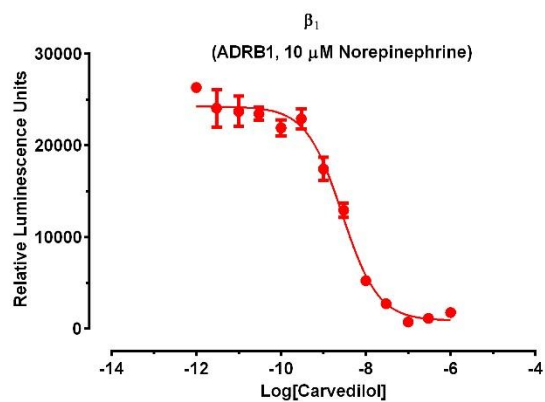
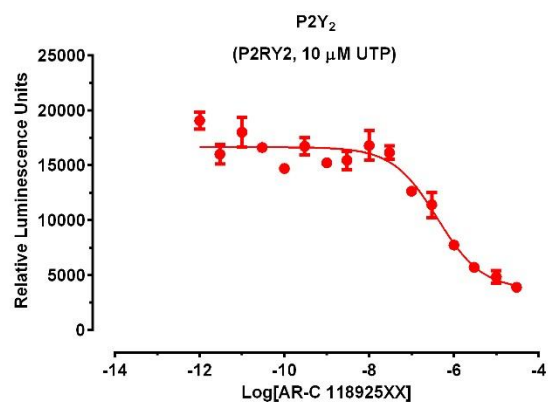
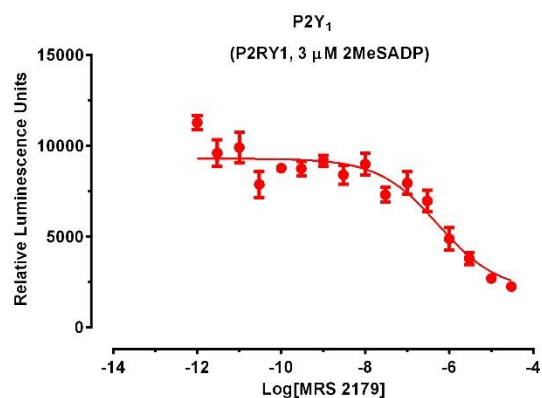


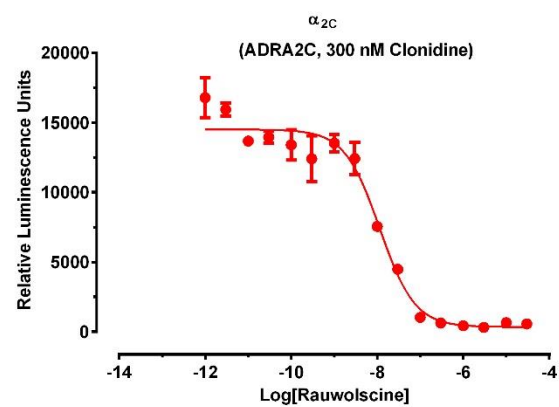
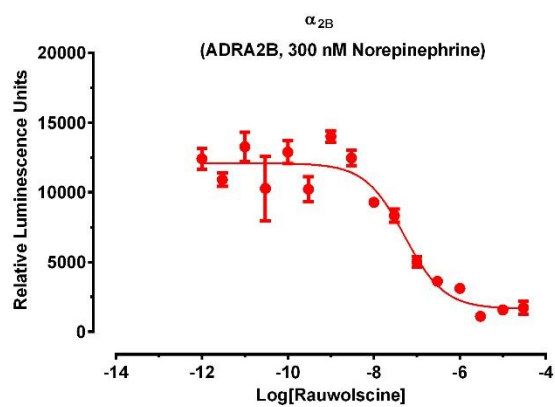
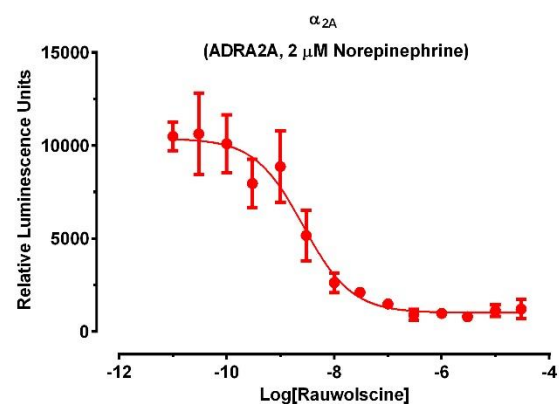
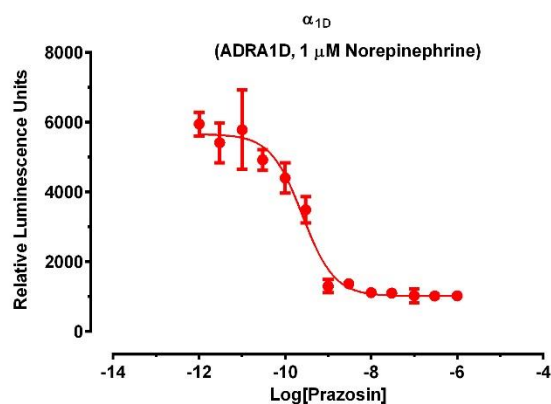
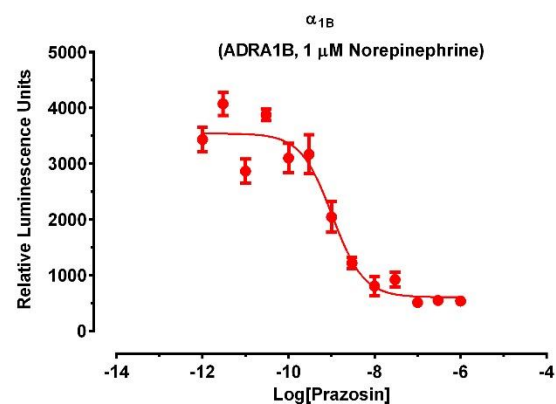
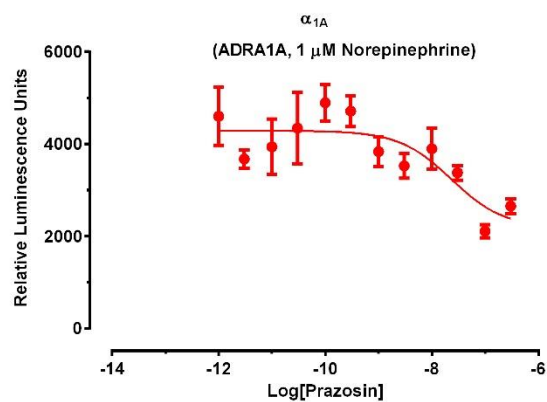


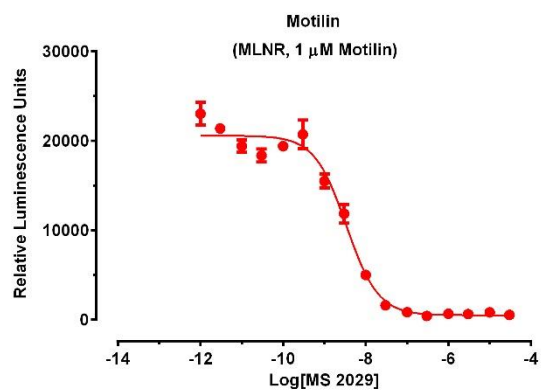
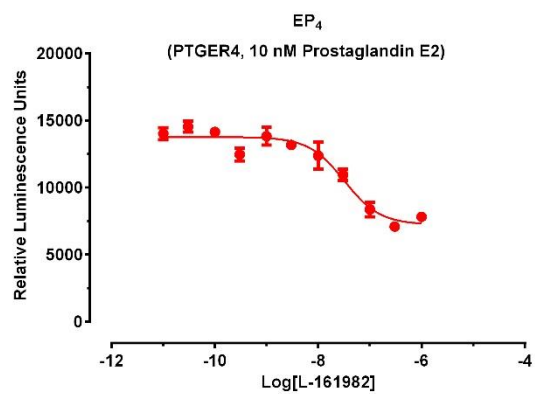
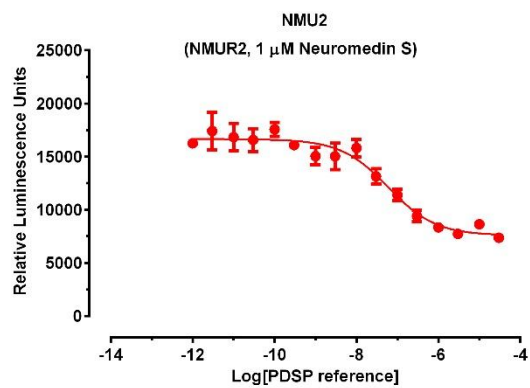












2.7. PRESTO-Tango GPCRome screening

Main equipment: Liquid handling workstation for 96- and 384-well plates, luminescence counter

Main reagent: BrightGlo® from Promega

Assay buffer: 20 mM HEPES, 1x HBSS, pH 7.40

2.7.1. Cell culture. HTLA cells (a gift from Dr. Richard Axel), stably expressing a tTA-dependent luciferase reporter and a β -arrestin2-TEV protease fusion gene, are maintained in DMEM supplemented with 10% FBS, pen-strep, and 2 μ g/ml Puromycin and 100 μ g/ml Hygromycin. To set up the cells for transfection, HTLA cells are plated in DMEM supplemented with 10% dialyzed FBS in Poly-L-Lys (PLL)-coated 384-well white clear bottom cell culture plates at a density of 10,000 cells in a volume of 40 μ l per well and incubated overnight. At least 1hr before transfections (below), we feed the cells with 10 μ l/well DMEM supplemented with 50% FBS, using a Multidrop automated liquid dispenser.

2.7.2. DNA plate. Each single DNA plasmid is plated using the liquid handling workstation in one well of a 96-well plate at 0.5 μ g/well (20 ng per well in 384-well plate and 8 wells per DNA, usually for 10x 384-well plates, see **Fig 50 and 51** for DNA plate designs). Each plate includes 80 receptor DNA samples, assay controls in column 1 with DRD2 and negative controls in column 2 with buffer. DNA plates, if not used immediately, can be dried in a cell culture hood for storage at (-20°C). Immediately before transfection (see below), DNA samples are resuspended in 0.25 M CaCl₂ and manually transferred into 384-well plates with an equal volume of 2x HBS for transfection (see **Figs 50 and 51** for DNA map in 96-and 384-well plates) followed by the next step for transfection (see below).

2.7.3. Transfection using Calcium phosphate precipitation protocol. HTLA cells are set up as indicated above overnight before transfection. The following protocol is designed for transfection on the following scale: one 384-well DNA plate (**Fig 51**) provides DNA for a total of 10 384-well cell plates. Briefly, the plated DNA in a 96-well plate (**Fig 50**) is first resuspended with 0.25 M CaCl₂ to a final volume of 380 μ l/well and manually aliquoted into a 384-well plate (**Figure 51**), 45 μ l/well for a total of 8 wells, to mix with equal volume of 2x HBS (50 mM HEPES, 280 mM NaCl, 10 mM KCl, 1.5 mM Na₂HPO₄, pH 7.00). We then use Hamilton Microlab Star with a 384-well pipette head to transfer

6 μ l/well of DNA/CaCl₂/HBS mixture into each of 10 384-well cell plates. A mixing step (10 μ l x 5-time up and down pipetting) is programmed into the transfection procedure before each transfer. Each 384-well DNA plate is usually used within 20 min after being mixed with 2x HBA solutions. Transfected cells are returned to the incubator for overnight incubation. Under this setting, DNA samples from rows A-D in a 96-well DNA plate are made into a 384-well plate, therefore each 96-DNA plate is sufficient for 2 different 384-well plate layouts. One GPCRome (up to 320 Tango constructs) screening for each compound consists of a total of 8 384-well assay plates, with each receptor being screened in quadruplicate. Thus, a total of eighty 384-well assay plates are needed for a routine screening with 10 PDSP compound samples.

2.7.4. Compound addition and incubation. After overnight transfection and incubation, cells are removed from medium and receive 40 μ l/well fresh DMEM supplemented with 1% dFBS about 2 hrs before compound stimulation. To make drug plates (**Fig 52**), the assay control quinpirole is added into column 1 (where the dopamine DRD2 receptor is expressed), the medium negative control is in columns 2-4 and all the odd numbered columns in a 384-well plate, while test sample is added into all the even numbered columns from 6-24 in the 384-well plate. Compounds and assay control (quinpirole) are made in DMEM with 1% dFBS at 5x working concentration, 105 μ l/well. Drugs are transferred using the Hamilton Microlab Star with a 384-well pipetting head again, 10 μ l/well, one drug plate for eight 384-well cell plates. Assay plates are then incubated overnight at 37°C. The following day, medium and drug solutions are removed and 20 μ l per well of BrightGlo reagent (diluted 20-fold with Tango assay buffer) are added. Plates are incubated for 20 minutes at room temperature in the dark before luminescence is measured.

2.7.5. Data processing and analysis. The luminescence counter records relative luminescence units (RLU) and saves files in 384-well format in Excel sheets for easy processing. The GPCRome screening assay is designed to have 4 replicate wells for samples and 4 replicate wells for basal levels for each construct. In each assay plate, the average background (columns 3-4, usually around 50 RLU) is shared for all constructs in the same plate. Results are expressed in the fold of corresponding average basal, calculated according to the following formula:

$$\textit{Fold of basal} = \frac{(\text{Sample RLU}) - (\text{Avg background RLU})}{(\text{Avg basal RLU}) - (\text{Avg background RLU})}$$

In general, the assay control, DRD2 with 100 nM quinpirole, shows 30x to 100x of basal activity, while the activity seen with most ligand-receptor combinations generally ranges from 0.5x to 2.0x fold of basal. Usually, follow-up studies are not done when the observed activity is less than 3.0x fold of basal. An activity of <0.5x fold of basal, if corresponding basal activity is relatively high, can be a sign of inverse agonist activity, and will be recommended for followup assays. See **Figures 54-55** for representative GPCRome screening results.

	1	2	3	4	5	6	7	8	9	19	11	12
A			1	2	3	4	5	6	7	8	9	10
B			11	12	13	14	15	16	17	18	19	20
C			21	22	23	24	25	26	27	28	29	30
D			31	32	33	34	35	36	37	38	39	40
E			41	42	43	44	45	46	47	48	49	50
F			51	52	53	54	55	56	57	58	59	60
G			61	62	63	64	65	66	67	68	69	70
H			71	72	73	74	75	76	77	78	79	80
	DRD2	Buffer	Tango constructs (#1 - #80)									

Figure 50. 96-well DNA map. **Green** wells (Column 1) have DRD2 plasmid as assay control. **White** wells (Column 2) have no DNA as negative controls. **Grey** wells (Columns 3 – 12) have DNA plasmids (DNA sample #1 to #80). A total of 4 96-well plates would be needed for a complete GPCRome Tango experiment.

	1	2	3	4	5	6	7	8	9	10	11	12	13	14	15	16	17	18	19	20	21	22	23	24
A					1	1	2	2	3	3	4	4	5	5	6	6	7	7	8	8	9	9	10	10
B					1	1	2	2	3	3	4	4	5	5	6	6	7	7	8	8	9	9	10	10
C					1	1	2	2	3	3	4	4	5	5	6	6	7	7	8	8	9	9	10	10
D					1	1	2	2	3	3	4	4	5	5	6	6	7	7	8	8	9	9	10	10
E					11	11	12	12	13	13	14	14	15	15	16	16	17	17	18	18	19	19	20	20
F					11	11	12	12	13	13	14	14	15	15	16	16	17	17	18	18	19	19	20	20
G					11	11	12	12	13	13	14	14	15	15	16	16	17	17	18	18	19	19	20	20
H					11	11	12	12	13	13	14	14	15	15	16	16	17	17	18	18	19	19	20	20
I					21	21	22	22	23	23	24	24	25	25	26	26	27	27	28	28	29	29	30	30
J					21	21	22	22	23	23	24	24	25	25	26	26	27	27	28	28	29	29	30	30
K					21	21	22	22	23	23	24	24	25	25	26	26	27	27	28	28	29	29	30	30
L					21	21	22	22	23	23	24	24	25	25	26	26	27	27	28	28	29	29	30	30
M					31	31	32	32	33	33	34	34	35	35	36	36	37	37	38	38	39	39	40	40
N					31	31	32	32	33	33	34	34	35	35	36	36	37	37	38	38	39	39	40	40
O					31	31	32	32	33	33	34	34	35	35	36	36	37	37	38	38	39	39	40	40
P					31	31	32	32	33	33	34	34	35	35	36	36	37	37	38	38	39	39	40	40
	DRD2		Negative		Tango constructs																			

Figure 51. 384-well DNA plate for calcium precipitation transfection. Tango constructs are transferred from 96-well plates into 384-well plates in the above layout. **Green wells** (Columns 1-2) are DRD2-transfected wells as assay control. **White wells** (Columns 3-4) have no DNA as negative controls (background). **Grey wells** (Columns 5-24) are for Tango constructs, each construct is transfected in 8 wells as highlighted in a block. In this setting, one 96-well DNA plate will need two 384-well plates, therefore, the entire GPCRome experiment requires a total of eight 384-well plates.

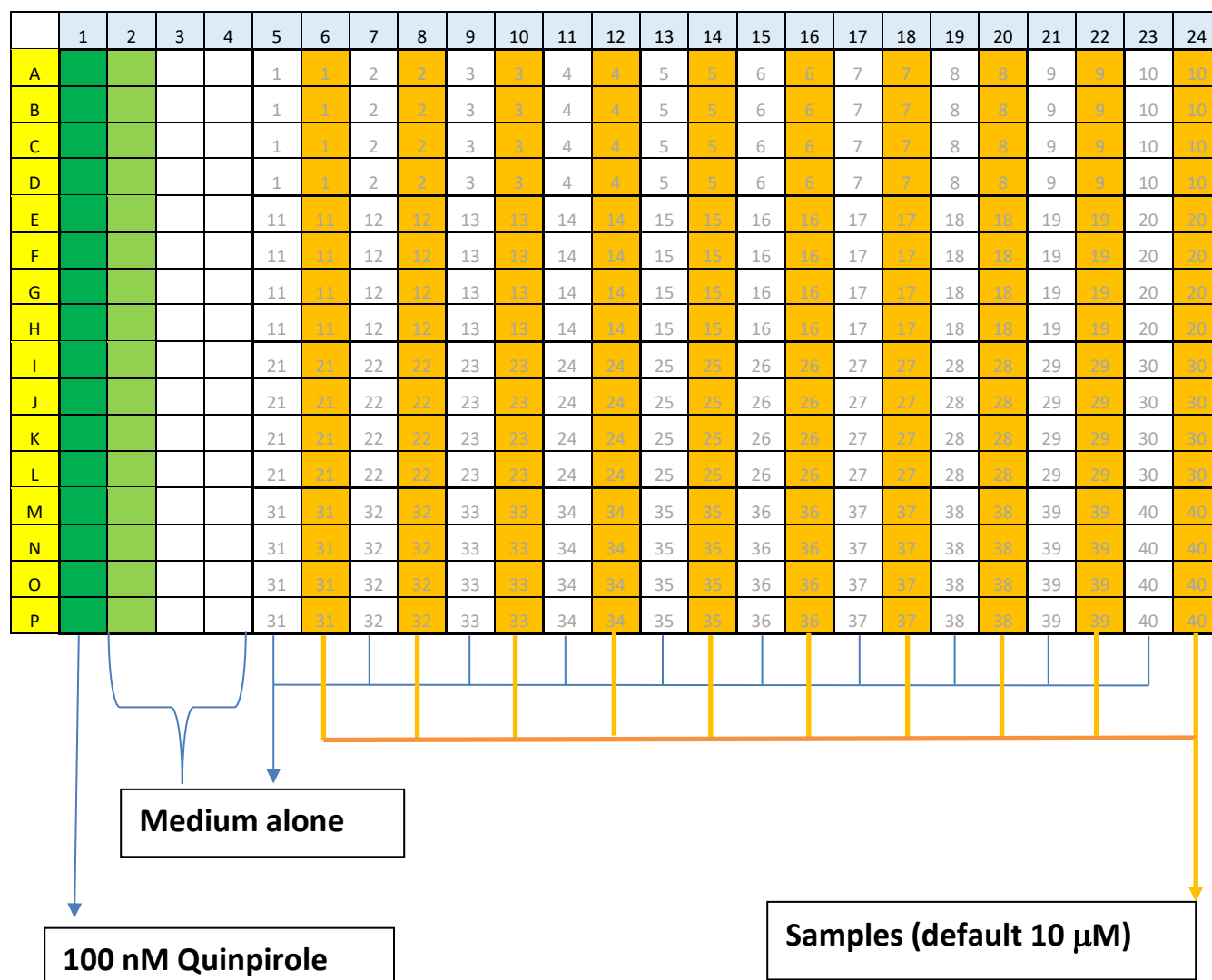


Figure 52. 384-well drug plate layout for stimulation. Column 1 receives 100 nM quinpirole, while Column 2 receives medium only (DMEM + 1% dFBS) to serve as “DRD2 basal”. Columns 3 and 4 receive medium only to serve as background activity. For the rest of the plate, odd numbered columns receive medium (DMEM + 1% dFBS) and even numbered columns receive test sample (prepared in DMEM + 1% dFBS). Therefore, each Tango constructs has 4 sample wells and 4 basal wells. Results are expressed as fold of average basal for each construct.

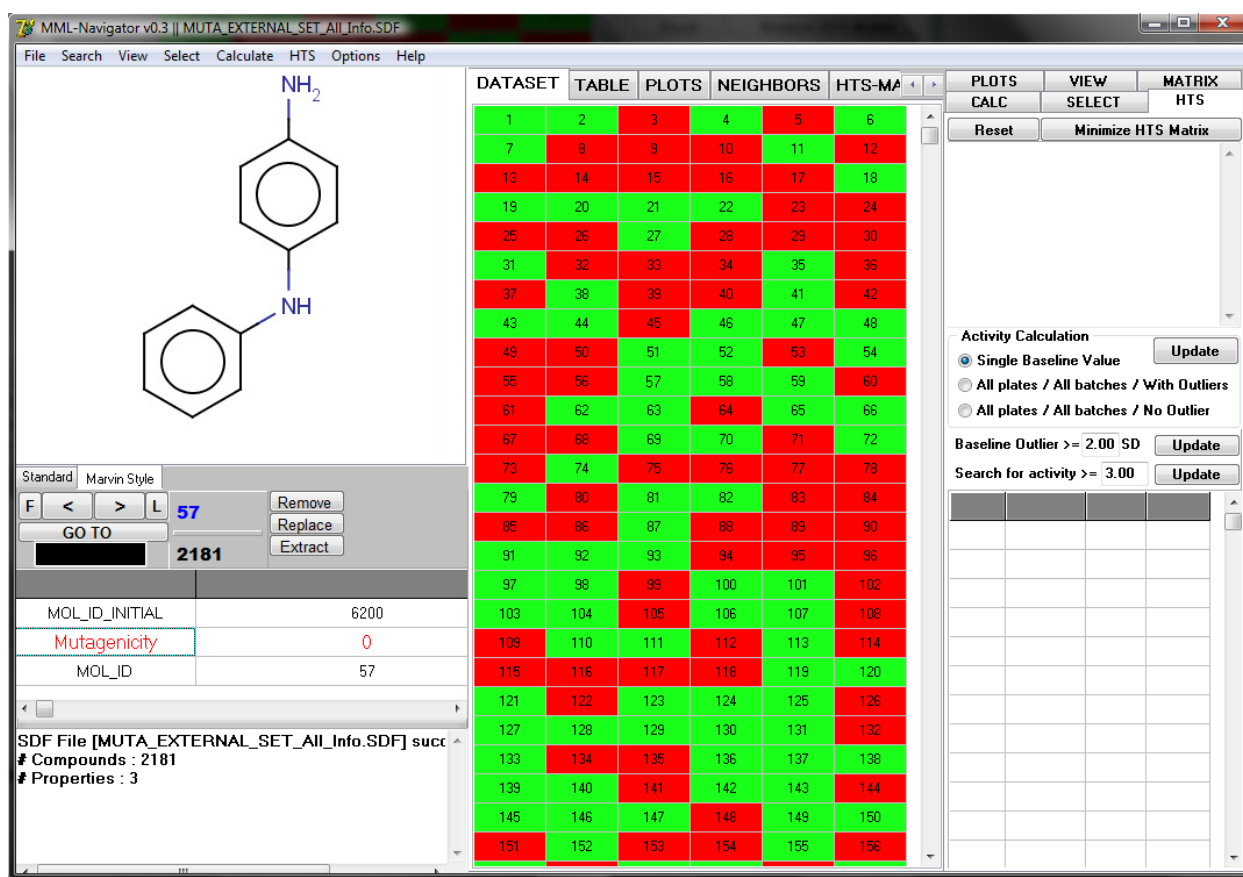


Figure 53. Navigator interface. This software readily calculates activation (%) relative to positive control as well as relative to baseline. Compound structures, number of plates and compounds tested per assay, and calculated values for every receptor/compound pair can be viewed on the main screen.

Alternatively, to calculate and report these values, we also use the Navigator software (custom made and developed in-house by the Molecular Modeling Laboratory, College of Pharmacy, UNC at Chapel Hill). The Navigator takes raw output files in Excel sheets and calculates relative activation as indicated above. A screen shot of the Navigator interface is shown in **Figure 53**.

2.7.6. Representative figures. As a proof of concept, we screened three compounds (LSD, Rimonabant, and Fluoxetine) against 143 GPCRs (non-orphan, non-olfactory GPCRs) at final concentration of 1 μ M. Results (fold of baseline) are reported below in **Figure 54**. Representative GPCRome screening with ergotamine is shown in **Figure 55**.

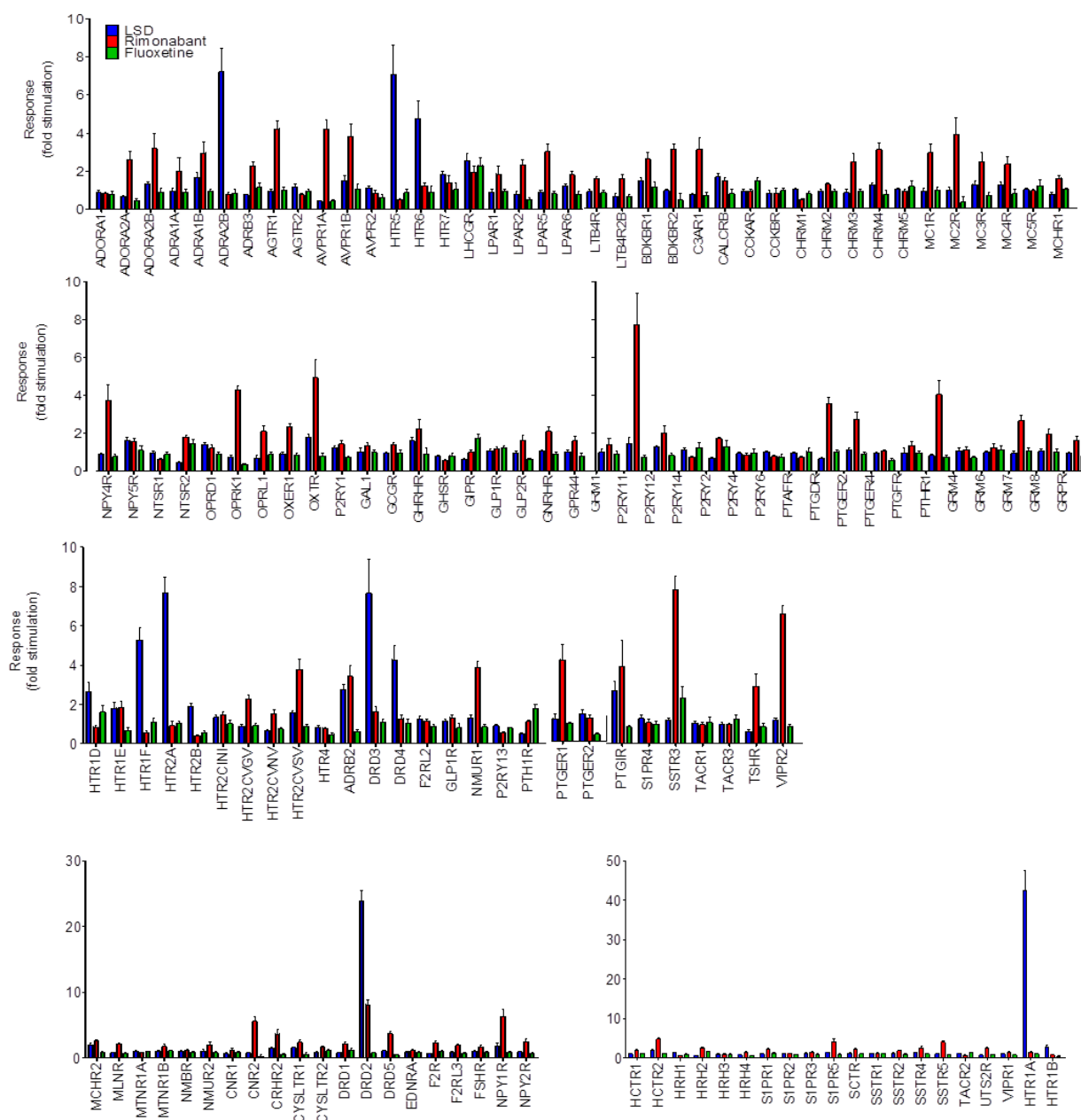


Figure 54. Sample parallel primary screening for 143 non-orphan non-olfactory GPCRs using β -arrestin recruitment assay (Tango). Activity is reported as Response (fold stimulation over baseline) for LSD (blue), rimonabant (red), and fluoxetine (green).

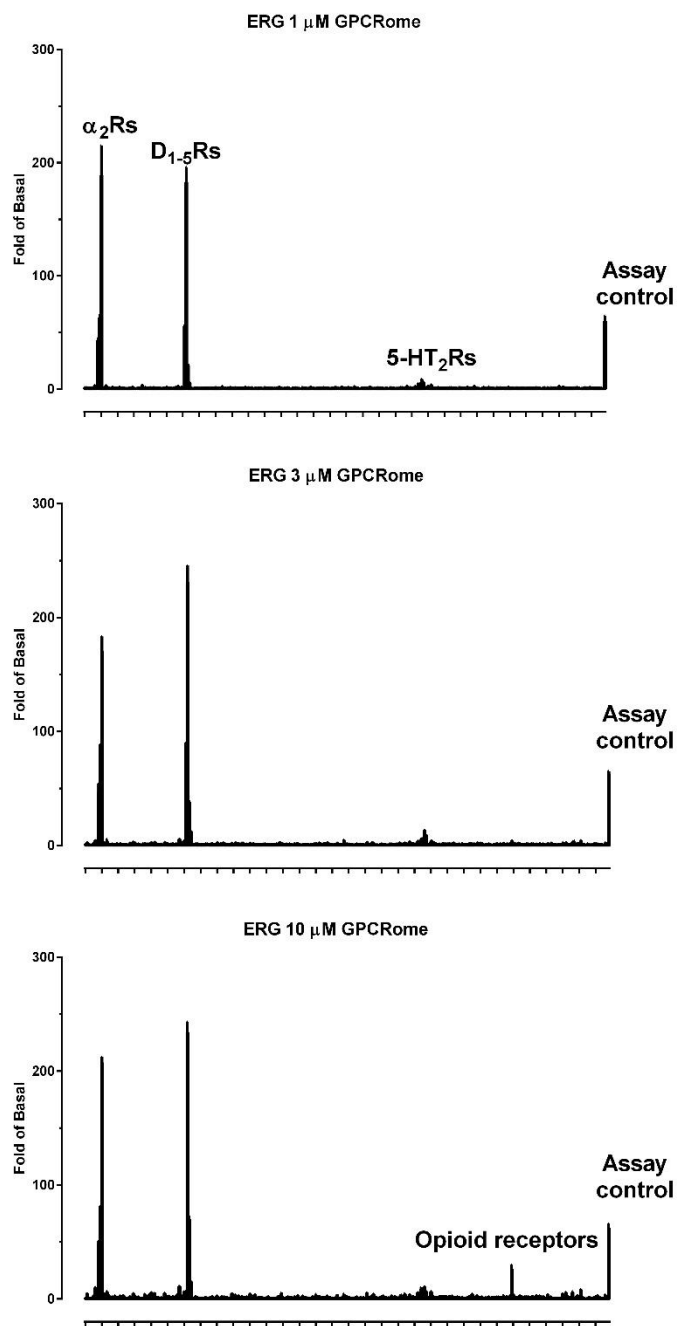


Fig 55. GPCRome screening with ergotamine (ERG) at 1, 3, and 10 μ M. The assay control is 100 nM quinpirole at DRD2. Results were reformatted from a recent paper (172).

2.8. BRET-based transducerome assays

2.8.1. Introduction: G Protein Coupled Receptors (GPCRs) are membrane proteins that transduce extracellular signals to the intracellular environment through the activation of a heterotrimeric complex consisting of an α -subunit (G_α) and a dimerized pair of β and γ subunits ($G_{\beta\gamma}$). Upon receptor activation by an agonist, the receptor mediates an exchange of Guanosine Diphosphate (GDP) for a Guanosine Triphosphate (GTP) in the G_α subunit, leading to dissociation from the receptor/ G_α / $G_{\beta\gamma}$ complex and subsequent activation of downstream effectors by these G proteins. Traditionally, GPCRs have been classified partially by the set of G_α proteins activated by the receptors. These are grouped into families based on the similarity of their downstream effector pairings (**Table 32**). The degree to which one receptor may activate one or multiple species of G proteins is of considerable physiological importance, as different cellular contexts, containing different G protein complements, may produce markedly different responses following the activation of the same receptor. Because of the similarity of signaling pathways within G protein families, the ability to differentiate relative specific efficacies has been fraught with complications. Moreover, the different cell types used in functional assays can produce different responses, depending on whether the full complement of the effector pathway is intact. For example, the Adenosine 2_A receptor (A_{2A}) can couple effectively to G_{olf} , but measuring its stimulation of cAMP production depends on the presence of adenylyl cyclase V (173), which is not present in all cell types (e.g. HEK293, **Fig 56**). Reconstitution of this complete effector pathway allows for a functional G_{olf} readout, but requires *a priori* knowledge of these relevant details.

Table 32. G-protein alpha subunits and their primary effectors

G-protein α subunits	Primary effector pathways
G _q , G ₁₁ , G ₁₄ , G ₁₅	Activation of PLC/Trio/P63RhoGEF
G _{i1} , G _{i2} , G _{i3} , G _z	Inhibition of Adenylyl Cyclases
G _s long, G _s short, G _{olf}	Activation of Adenylyl Cyclases
G ₁₂ , G ₁₃	Activation of Rho/Rac GTPases

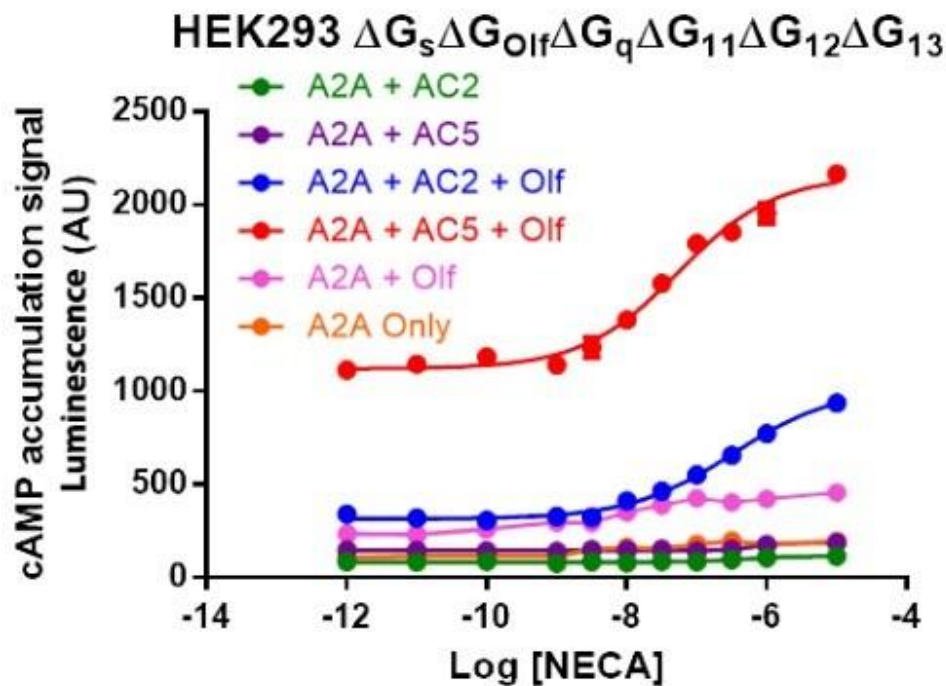


Figure 56. Adenosine 2A (A_{2A}) mediated G_s-cAMP production signaling in HEK293 cells lacking G_s, G_q, G₁₂ family G-proteins (174) requires Adenylyl Cyclase 5 (AC5). G_s-cAMP production was measured using GloSensor cAMP method.

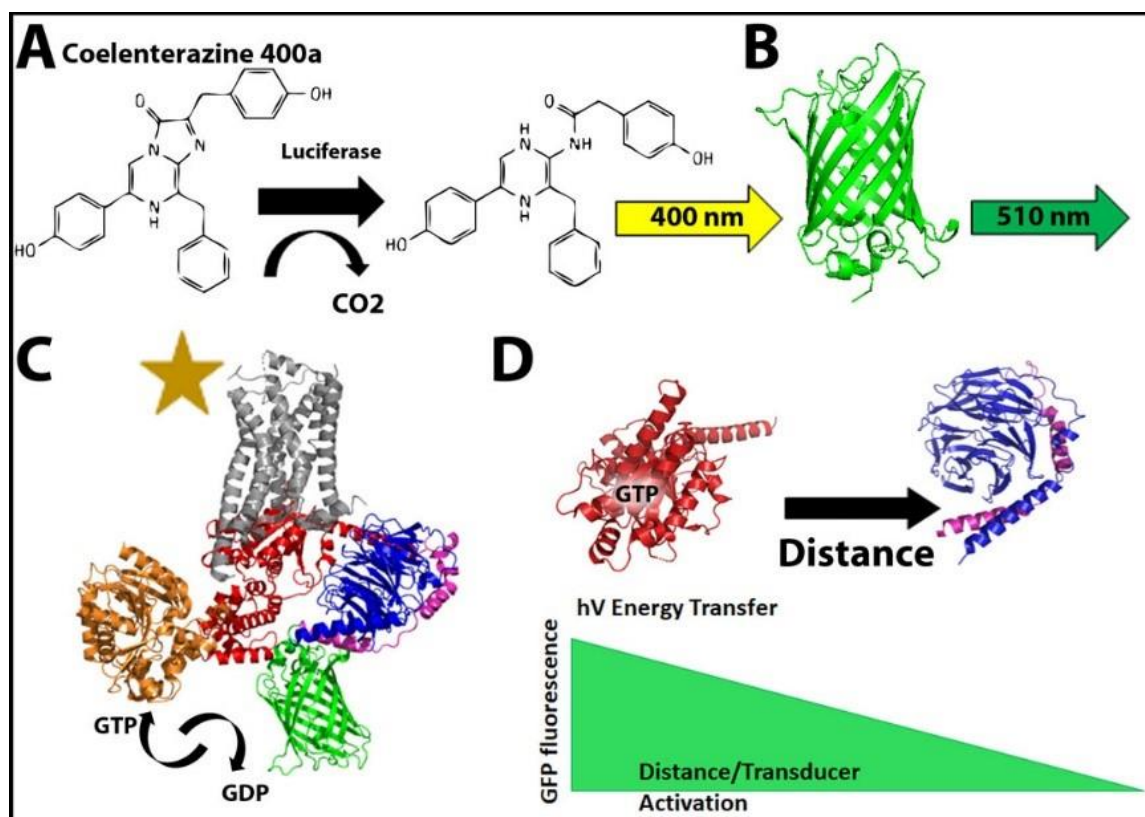


Fig 57. (A) Coelenterazine 400a is oxidized to produce luminescence at 400 nm. (B) This wavelength excites the fluorophore GFP² which emits a fluorescent signal at 510 nm. (C) An active GPCR facilitates the exchange of GDP for GTP in its G_α subunit, leading to the dissociation of the G_{αβγ} and the subsequent activation of their effectors. (D) Labeling the heterotrimeric subunits with the luciferase and GFP² allows measuring the association of the inactive trimer, and the dissociation as a proxy for GPCR-mediated activation.

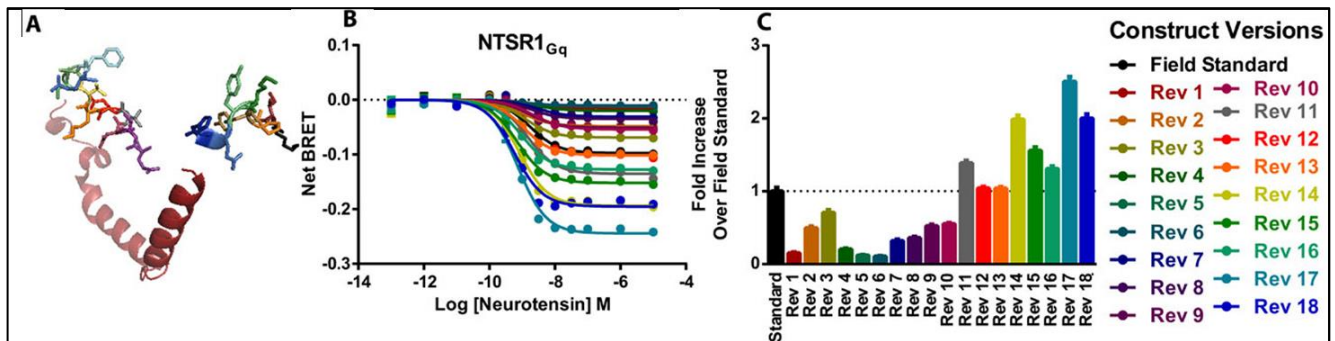


Fig 58. (A) rLuc was inserted at positions in the G α subunit (green) most proximal to the c-terminus of the G γ subunit (burgundy), which is fused to GFP². (B) Function and dynamic range of the BRET pairs were assayed using the human Neurotensin 1 receptor (NTSR1). (C) Dynamic range measured as the change in BRET following receptor activation was used to assess the optimal construct (greatest improvement over the current published standard).

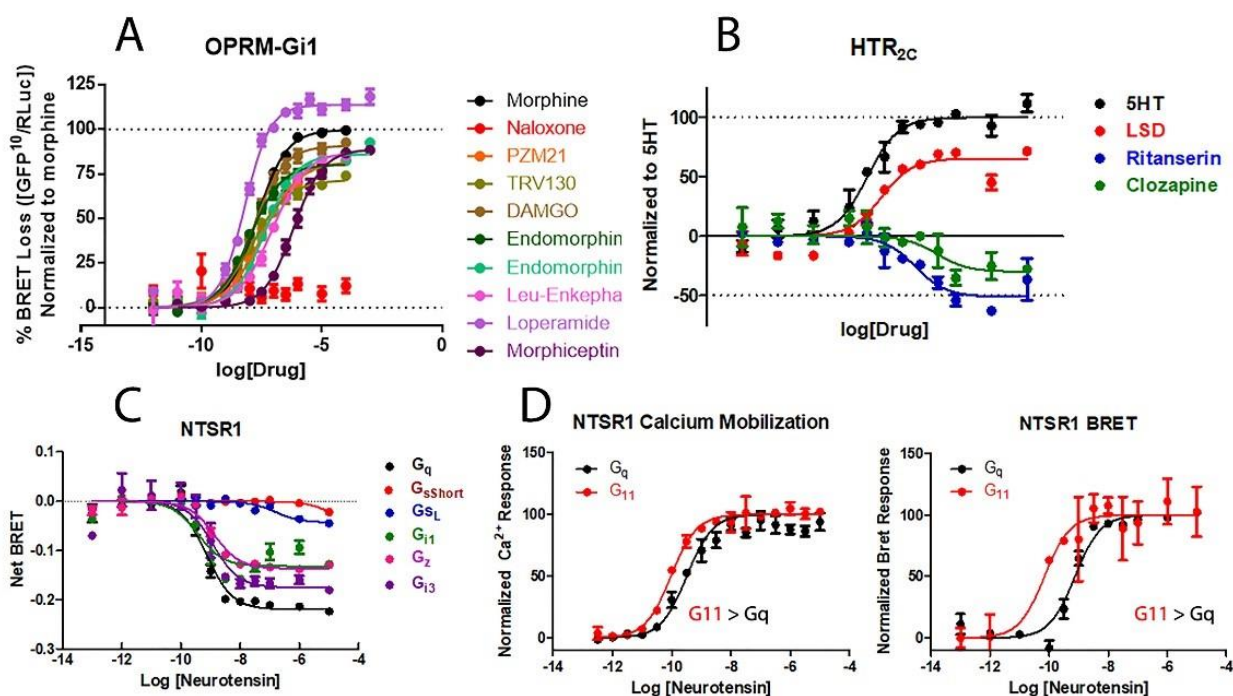


Fig 59. (A) Relative potencies and efficacies for μ opioid (MOR, OPRM1) receptor agonists through the G_{i1} pathway. (B) Full, partial, and inverse agonism at the HTR_{2C} (5-HT_{2C}) receptor. (C) Relative potencies through multiple G protein families at the neurotensin 1 receptor (NTS₁). (D) Using G protein-deficient CRISP HEK293 cells, increased potency at the G_{i1} pathway relative to its familial G_q counterpart can be confirmed.

Bioluminescence Resonance Energy Transfer (BRET) (175, 176) is an experimental tool used to study the association of two or more proteins. Briefly, an enzyme (Renilla luciferase) catalyzes a reaction with a chemical substrate (**Fig 57A**) to produce luminescence, which excites a proximal fluorophore when the emission/excitation of the substrate/ fluorophore are resonant (**Fig 57B**). Thus, the ratio of the fluorescent signal to the (constant) luminescent output can be used as a proxy for the degree of association between the two proteins. In the case of GPCR signaling, this can be used to study the association of the G_α and $G_{\beta\gamma}$ subunits, which make up the primary signaling complex downstream of receptor activation. An agonist-bound GPCR facilitates the exchange of Guanosine Diphosphate (GDP) for a Guanosine Triphosphate (GTP) in the G_α subunit (**Fig 57C**), which stabilizes its active state and subsequent dissociation from the $G_{\beta\gamma}$ subunit. The G_α is then free to activate its downstream effectors. By labeling the G_α and the $G_{\beta\gamma}$ with the luciferase and its cognate fluorophore (GFP²), the change in their resonance can be assessed as a measure of primary signal transduction of the GPCR (**Fig 57D**). We have developed a full panel of G_α -luciferase fusion proteins and a cognate panel of GFP²-labeled and unlabeled G_β and G_γ subunits. Although some versions of these constructs have been explored (177) in the literature, many of those exhibited relatively restricted dynamic ranges and thus, questionable utility. Recently, some groups have been attempting to rationally design similar biosensors, but no full panel of academic open-source freely available $G_\alpha/G_{\beta\gamma}$ tools exist yet.

2.8.2. Assay design and optimization. We utilized published crystal structures and modeling approaches to improve and optimize existing luciferase-tagged $G_\alpha/G_{\beta\gamma}$ probes, and expanded the available library to the entire $G_\alpha/G_{\beta\gamma}$ family. Throughout this process, we have generated and tested >400 unique constructs, selecting those showing the greatest dynamic range. These new biosensors exhibit between a 2 and 10-fold increase in dynamic range over the currently published probes, thus greatly enhancing the utility of this platform.

The optimized BRET probes can assay relative efficacies and potencies within transducer/receptor pairs (**Fig 58A**). Additionally, because the system is at equilibrium and is not subject to amplification, basal

activity and inverse agonism can also be measured (**Fig 58B**). Relative potencies among transducers can be assayed (**Fig 58C**), and can be confirmed using orthologous assays (**Fig 58D**).

2.8.3. Assay procedure

Day 1: HEK293T cells are plated at ~60% confluency in DMEM containing 10% dialyzed FBS (dFBS).

Day 2: Receptor + G_{α} -RLuc + G_{β} + G_{γ} -GFP² plasmids are co-transfected at a ratio of 1:1:1:1.

Day 3: Cells are removed from the plate using versene (0.5 mM EDTA in PBS pH 7.4) and plated at a density of 25 to 50K cells/well in poly-lysine-coated 96-well plates in DMEM containing 1% dFBS.

Day 4: DMEM is aspirated or shaken out of the wells, followed by a wash in assay buffer (1x HBSS + 20 mM HEPES pH 7.4). Subsequently, 60 μ l of assay buffer is added to the wells. 10 μ L of 50 μ M Coelenterazine 400a (Nanolight technology, Cat#340) is added to each well and incubated for 5 minutes while protected from light. 30 μ L of drug dilutions (done in assay buffer + 0.3 mg/ml ascorbic acid and 0.3% BSA) are added to the wells and incubated for an additional 5 minutes. At this point, the plate is read using a LB940 Mithras multimode microplate reader (Berthold Scientific) at 1 s per read, using 400 and 510 nm emission filters. BRET is computed as the ratio of GFP² fluorescence (GFP) to coelenterazine signal (rLuc). Signal is calculated as the net decrease in BRET following agonist addition (net BRET, **Fig 59C**) and can be normalized to a reference ligand (**Fig 59A, B, D**).

2.8.4. Additional resources available: In addition to the G_{α} -rLuc probes, we have identified optimal $\beta\gamma$ GFP-tagged acceptors. Throughout the process we have accumulated a complete set of tagged and untagged G_{γ} and G_{β} proteins that can be used to customize assays as requested (**Table 33**).

We plan to expand and validate this approach further, including GPCRs coupled to all four major G_{α} protein families. Once validation is complete, we will make all relevant constructs available for non-commercial use through **AddGene**.

Table 33. Complete list of tagged and untagged donor and acceptor constructs.

Donor	Optimal Acceptor
G_{i1}	γ_2 -GFP
G_{i2}	γ_2 -GFP
G_{i3}	γ_2 -GFP
G_z	γ_2 -GFP
G_{11}	γ_{12} -GFP
G_{12} (optimization in progress)	γ_2 -GFP
G_{13}	γ_2 -GFP
G_{14}	β_4 -GFP
$G_{15/16}$ (optimization in progress)	β_4 -GFP
G_q	γ_1 -GFP
G_s Short	γ_1 -GFP
G_s Long	γ_1 -GFP
G_{olf}	γ_3 -GFP, γ_8 -GFP, or β_4 -GFP

2.9. FluxOR assays for hERG activity

Main equipment: FLIPR^{TETRA} from Molecular Devices (Sunnyvale, CA)

Main reagents: FluxOR kit from Invitrogen (Carlsbad, CA)

FluxOR assay buffer: 20 mM HEPES, 1x HEBSS, 2.5 mM Probenecid, pH 7.40

The following protocol was adapted from a previously published paper(131).

2.9.1. Cell culture: HEK293 cells stably expressing hERG channels were purchased from ChanTest (Cleveland, OH) and maintained accordingly in DMEM supplemented with 10% FBS and 500 µg/ml G418. The hERG HEK293 cells are subcultured when they reach 80-90% confluency.

2.9.2. FluxOR assays for hERG inhibitors: Thallium (Tl⁺) Flux assays are carried out using the FluxOR Potassium Ion Channel Assay kit from Invitrogen according to the manufacturer's instructions with a few modifications. In detail, hERG HEK293 cells are plated into PLL-coated 384-well black clear bottom cell culture plates in DMEM supplemented with 1% dialyzed FBS at a density of 15,000 cells in a final volume of 40 µl per well. The plated cells are incubated overnight before being used for assay. On the day of the assay, FluxOR dye reagents are reconstituted by mixing Component A (1/1000 dilution) and PowerLoad (1/100 dilution) using FluxOR assay buffer and loaded into cells with 20 µl/well of FluxOR reagent for 90 min in the dark. During incubation, drug solutions and stimulation solution are prepared. Stimulation solution is as follows: 2.5ml deionized water, 1ml FluxOR chloride-free buffer (Component E), 1 ml K₂SO₄ (125 mM, Component F), and 0.5 ml Tl₂SO₄ (50 mM, Component G). At the end of the dye loading period, dye is removed, and the FLIPR^{TETRA} is programmed to transfer drugs from drug plates into cell plates (25 µl per well). The cells are incubated with the drugs for 15 min at room temperature in the dark. Stimulation solution (6.3 µl per well) is added with the FLIPR^{TETRA}. The fluorescence intensity (excitation at 490 nm and emission at 525 nm) in each well is measured every second for 10 seconds before addition of stimulation solution (as baseline), and for 90 seconds thereafter by the FLIPR^{TETRA} using ScreenWorks 2.0 software. Alternatively, the FluxOR assays can be performed with cryopreserved hERG HEK293 cells. In brief, frozen cells are washed with growth media once to remove DMSO in the freezing media, and then

plated at 20,000 cells per well as above and assayed 5 hours later. Results using cryopreserved cells are not different from those obtained using fresh cells.

2.9.3. Assay procedure for hERG trafficking modulators: The above protocol was designed to measure the acute effect of drugs on hERG channel activity (such as hERG channel inhibitors or activators). For those drugs without acute inhibitory effect in the TI^+ flux assays, we modified the standard protocol to conduct a longer chronic study to identify compounds that might be acting through indirect mechanisms (e.g., hERG trafficking inhibition, hERG internalization, and $\text{Na}^+\text{-K}^+$ ATPase inhibition). Briefly, cells are first treated with drugs for the desired time period (up to 16 hours) and are washed once with assay buffer before dye loading. The dye solution is then replaced with assay buffer and the fluorescence intensity is measured upon addition of stimulation solution per the standard protocol.

2.9.4. Data processing and analysis: The fluorescence intensity time course of each well in the 384-well assay plate is processed using ScreenWorks 2.0 software to export the slope of curve for the first 15 seconds after addition of the stimulation buffer. The initial slopes are then plotted against drug concentrations and analyzed in Prism 5.0 as outlined in **Section 2.3**.

Figure 60. Raw fluorescence signal traces recorded on FLIPR with HEK293 cells stably expressing hERG channels. Recording started 10 seconds before addition of stimulation solution and continued for another 90 seconds. Cisapride was shown to reduce signals in a dose-dependent manner (error bars not shown for clarity).

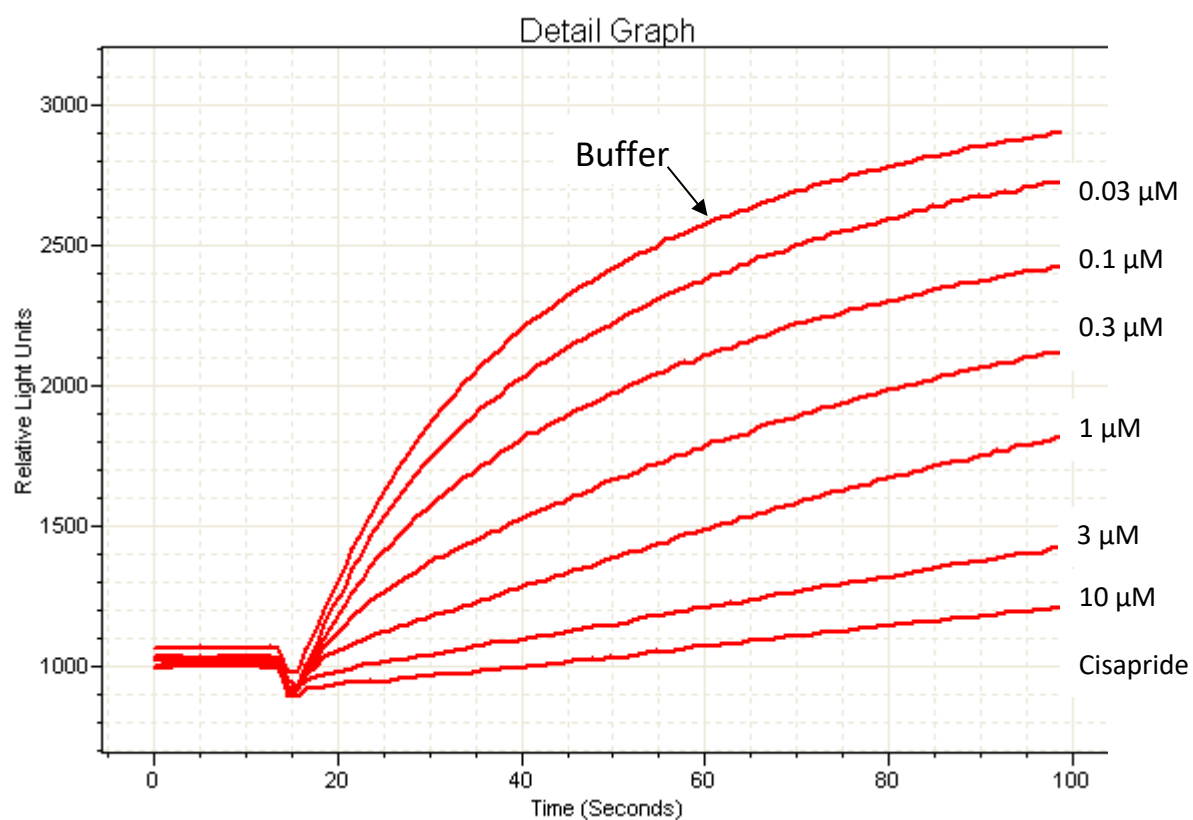


Figure 61. Initial slope of curves from above Figure 30 was exported from FLIPR ScreenWorks, plotted against corresponding concentrations of cisapride, and fitted to a four-parameter logistic function using GraphPad Prism 5.0.

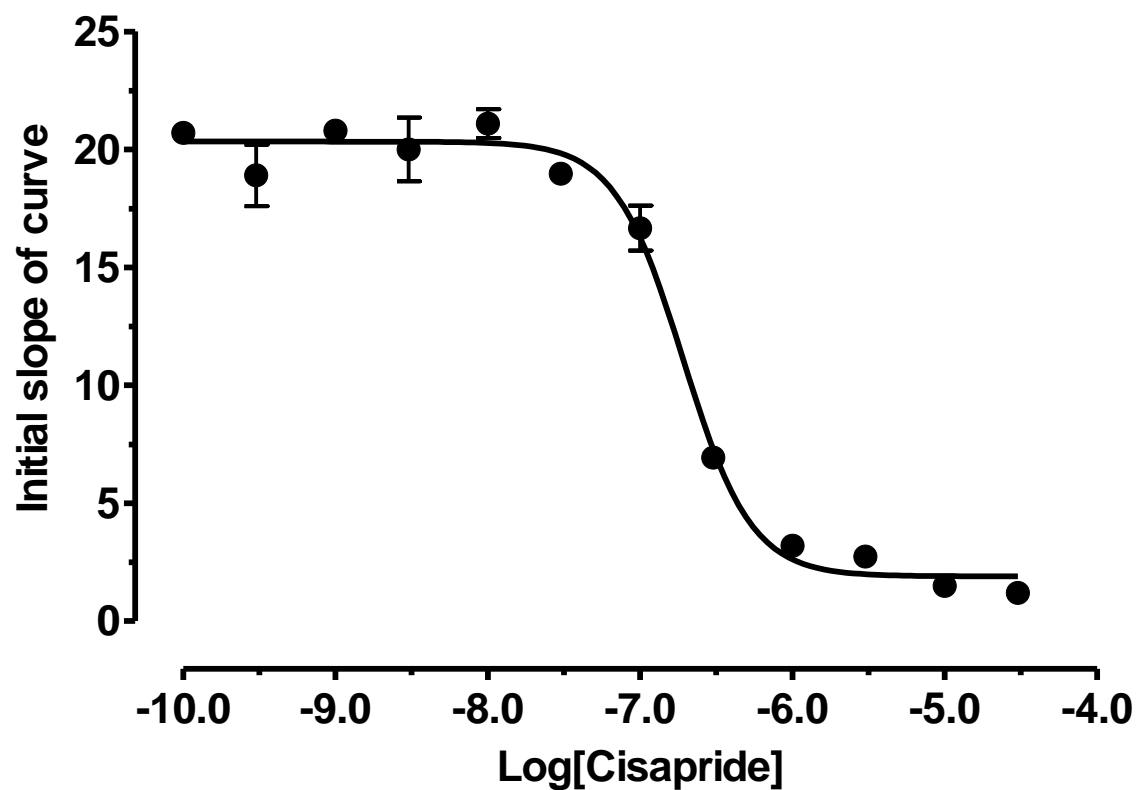


Figure 62. Acute and chronic effect of the hERG trafficking inhibitor ouabain on hERG channel activity. Activity of ouabain was determined with acute TI^+ flux assay (upper) and chronic TI^+ assay (lower). HEK293 cells stably expressing hERG channels were first incubated with ouabain for desired time at 37°C in the incubator; the remaining hERG activity was determined.

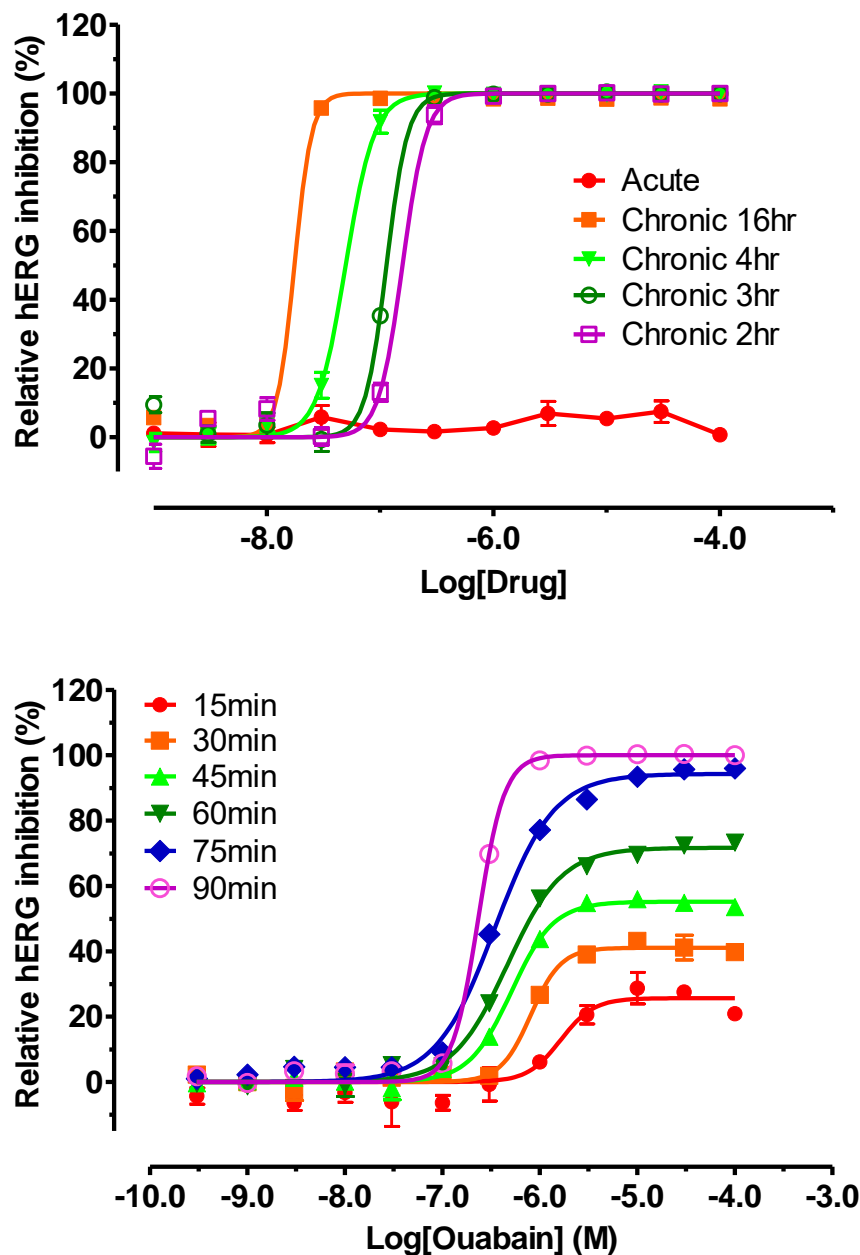
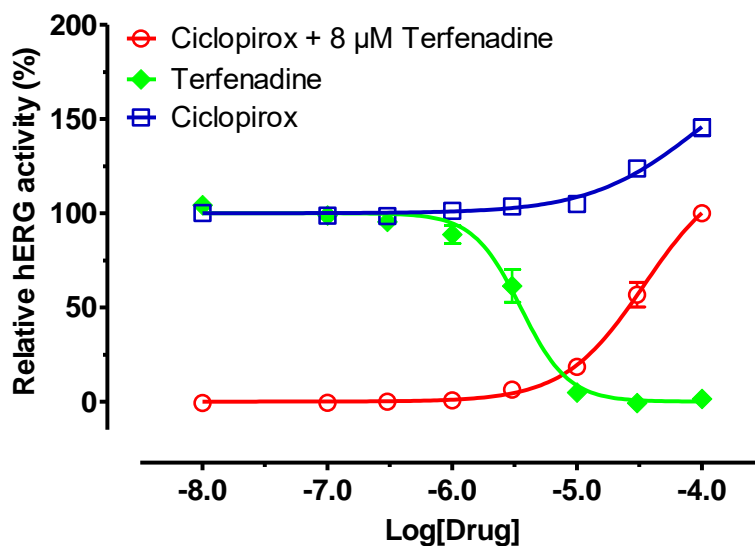
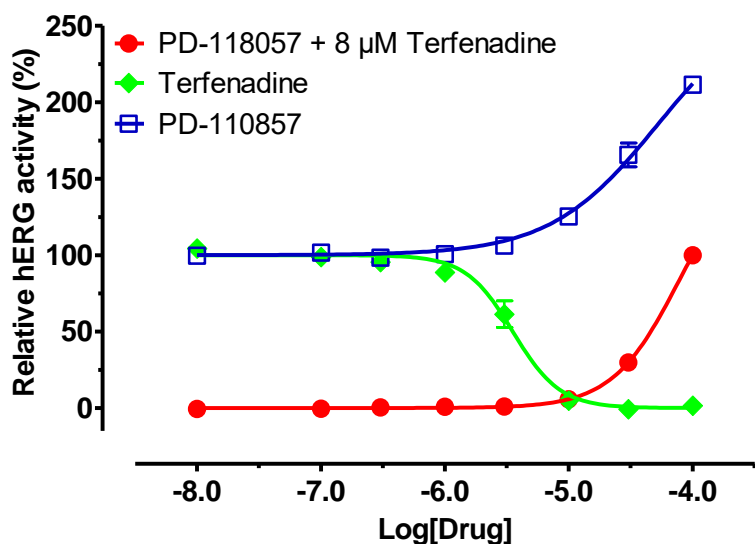


Figure 63. Activation of hERG channels in TI^+ flux assays. Terfenadine completely inhibited hERG channel activity, whereas PD-118057 (upper panel) and ciclopirox (lower panel) were able to activate the hERG channel. For assays done in the presence of terfenadine, terfenadine was added 5 min before PD-118057 or ciclopirox. For hERG activator activity, values were normalized to their corresponding basal activities in percentage: basal activity as 100% in the absence of terfenadine and basal activity as 0% in the presence of terfenadine.



2.10. PatchXpress assays for hERG activity

Main equipment: PatchXpress 7000A (MDS Analytical Technologies, Sunnyvale, CA)

PatchXpress external solution: 137mM NaCl, 4mM KCl, 1.8mM CaCl₂, 1mM MgCl₂, 10mM HEPES, 10mM Glucose, pH7.4 (adjusted with NaOH).

PatchXpress internal buffer: 15mM NaCl, 70mM KF, 60mM KCl, 1mM MgCl₂, 5mM HEPES, 5mM EGTA, 4mM ATP, and 0.4mM GTP, pH 7.2 (adjusted with KOH).

Automated planar patch clamp (APPC): PatchXpress electrophysiology

2.10.1. External and Internal solutions: The PatchXpress assay procedure is adopted from Huang et al., (2010) (131). Fresh external and internal solutions are prepared at room temperature on the day of the assay. The KF-based internal buffer was adopted from a report by Zeng et al., (2009) (178), in which they reported a greater success rate with a KF-based internal buffer than with a traditional KCl-internal solution. We add ATP, GTP, and Mg²⁺ to the KF-based internal solution to prevent potential current run-down. Osmolarity of the buffers is determined with a VAPRO 5520 Vapor Pressure Osmometer (Wescor, INC, Logan UT). The osmolarity is usually at 285 ± 10 mmol/Kg for the external buffer and 295 ± 10 mmol/Kg for the internal buffer. The buffers are vacuum-filtered to remove any air bubbles or small particles.

2.10.2. Cell preparation: For patch clamp assays, hERG HEK 293 cells are maintained as described above and subcultured into 10-cm dishes two days before scheduled assays at 1 – 2 million cells per dish in growth media without G418. Cells are not used if they reach more than 90% confluency. To prepare the cells for patch clamping, we followed ChanTest's recommendations with minor modifications. The goal is to prepare a clean, fresh cell suspension immediately before loading cells onto the PatchXpress. Cells are briefly washed with PBS, treated with Accutase (Sigma, 2.5ml per 10-cm dish) for 4 min at room temperature to detach them, gently transferred and suspended in 20 ml growth media without G418 in a 50-ml centrifuge tube, and allowed to recover from detachment for 30 min at 37°C in an incubator. At the end of the incubation period, 1 million cells are transferred into another 50ml centrifuge tube and pelleted by centrifugation at 250 x g for 2.5 min at room

temperature. The cell pellet is then gently re-suspended into 170 μ l of the external buffer, transferred into a 1.5ml microcentrifuge tube, and loaded into the PatchXpress 7000A (MDS Analytical Technologies, Sunnyvale, CA) in 'waiting mode' for cells. To minimize delay and cell clumping, the APPC system is started well in advance of use and primed with fresh external and internal solutions before preparing cells. The patch clamping procedure is started with a new SealChip right at the end of the 30-min incubation and recovery period. By the time the cell suspension is ready to load into the APPC system, the system has reached the 'waiting mode' for receiving the cells.

2.10.3. Drug plate preparation: While cells are in the incubation and recovery period, drug solutions are prepared in 0.5ml polypropylene round-bottom 96-well drug plate (Fisher Scientific). Drugs in 10 mM DMSO stocks were diluted in the external buffer at a final volume of 360 μ l per well, more than enough for the drug to be tested in two cells (triple addition at each of 50 μ l for one cell at each concentration). The final concentration of DMSO is 0.3% (v/v) for all dilutions (except for several drugs that required 3% DMSO as indicated in Results). For initial assays, 8-point (ranging from 30 nM to 30 μ M with 0.3% DMSO in external buffer as a negative control) concentration-response curves are generated. For subsequent assays, the concentration range can be adjusted as necessary to give full concentration-response curves (0 to 100% inhibition). The drug plate setup information is manually entered into the APPC system before starting the procedure. The assay is started within 15 minutes, and the highest drug concentration is tested within 90 minutes. A new drug plate is prepared for each new SealChip.

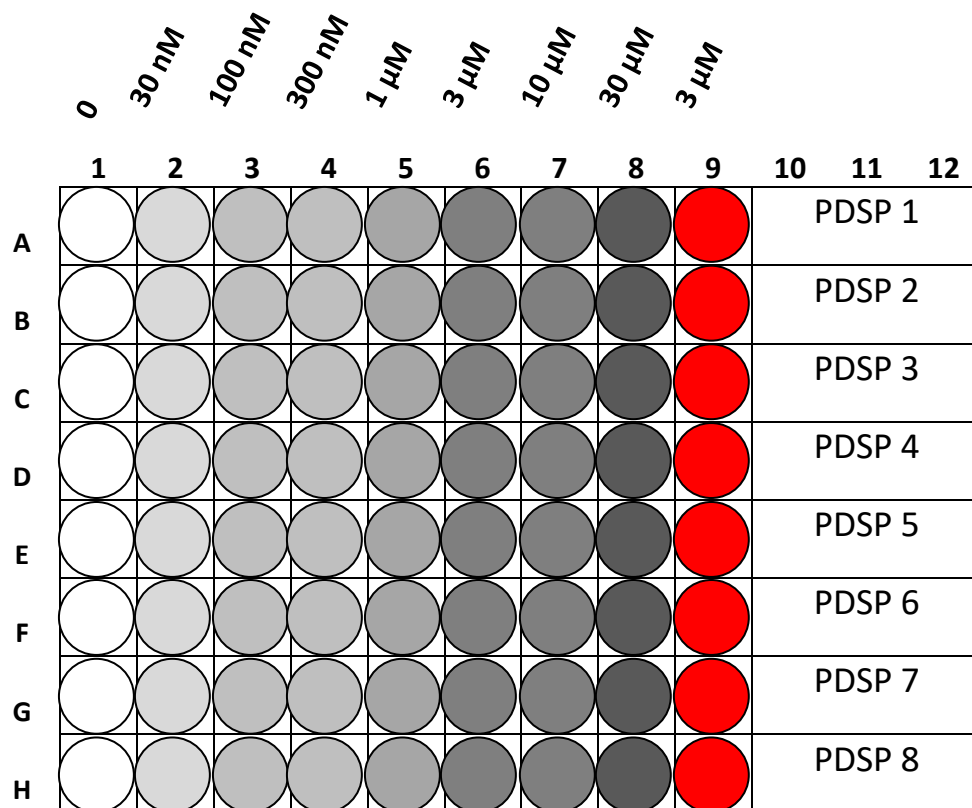


Figure 64. A typical APPC drug plate map (minimum of 360 μ l per well). Each drug has eight serial dilutions 0.5 log unit apart as indicated in the plate map, starting with a buffer control on the left and ending at 30 μ M, followed by a positive control (red) on the right, usually cisapride at 3 μ M.

2.10.4. APPC procedures: The APPC procedure starts with the manual loading of a SealChip₁₆[™] (AVIVA Biosciences, San Diego, CA) and is executed automatically at room temperature. The system requires approximately 7 min to (1) dry and load the SealChip onto the recording station; (2) external and internal solutions are then added; (3) the quality of each of the 16 chambers is confirmed; (4) the machine enters waiting mode and prompts for cell loading, at which point the cell suspension prepared above is immediately loaded. After loading, the single cell suspension is triturated briefly and aliquoted (35 μ l, ~ 20,000 cells) by the on-board robotic Cavo pipette to each chamber on the SealChip. First, positive pressure (6 mmHg) then brief suction with negative pressure (-45 mmHg) are

applied to help the cells descend quickly, and a single cell is drawn onto the top of the electrode hole of each chamber. A negative pressure ramp to 75mmHg (at 5mmHg per second) is then applied repeatedly until the seal resistance reaches 1G Ω (Gigaohm) or greater for Giga-seals and over 300 M Ω (Megaohm) for 2nd seals. After obtaining a seal, another negative pressure ramp from -40mmHg to -250mmHg is applied repeatedly to rupture the patched membrane and achieve the whole cell configuration. Chambers with low seal resistances (i.e. no cell detection) are terminated within 90 seconds; chambers that cannot form seals within 5 minutes are terminated by either a built-in script or user intervention. After achieving whole cell configuration, the voltage protocol is activated, beginning with a 2-minute wash-out and a 5-minute stabilization period. After stabilization, cells with less than 0.2 nA tail current amplitude are terminated. The voltage protocol consists of the following steps: (1) depolarization from holding potential of -80mV to -50mV for 50 milliseconds to measure leak current without activation of the hERG channel; (2) further depolarization to +20mV for 5 seconds to activate the hERG channel (hERG channels are activated and quickly inactivated); (3) repolarization to -50mV for 1.7 seconds to remove inactivation and elicit outward hERG tail current; (4) repolarization to holding potential at -80mV to keep hERG channels closed. This pulse pattern is applied repeatedly every 10 seconds (0.1 Hz). The instantaneous current at -50mV before stepping to +20mV is designated as leak current and is subtracted from corresponding peak tail current for data processing. Each concentration-response study starts with a buffer control to determine the maximal hERG tail current (0% inhibition) in the absence of drugs. Each dose is applied three times (50 μ l each at 25 μ l per second) with 11 seconds between additions, and each addition is preceded by aspiration of buffer or previous drug solution from the chamber down to a 5 μ l dead volume. This triple addition and aspiration protocol fully exchanges the solution in the chamber with negligible dilution within one minute. The built-in DataStable script is activated between each dose. When either drug effect reaches steady state (less than 0.1% difference from last measurement), or after a maximum of 5 minutes, the next dose is queued for delivery. Right after each concentration-response trial, a 5-minute wash-out is applied to monitor recovery of the hERG channels from inhibition. At the end of wash-out, a positive control (usually cisapride at 3 μ M) is applied to inhibit any recovered hERG channel activity or remaining hERG channel activity.

2.10.5. Data processing and analysis: APPC data are collected and automatically deposited into the database program DataXpress V2.0 (MDS Analytic Technologies, Sunnyvale, CA). If a cell has a leak current higher than 1/3 of the total tail current, the data for that cell is excluded. If a cell shows current run-down of more than 25% of the initial total tail current at the first (lowest) drug concentration, the data for that cell is excluded. The drug concentration range is usually adjusted after an initial assay so that, in subsequent assays, the lowest drug concentration inhibits hERG by less than 10%. The hERG tail currents are transformed and normalized to percent inhibition with a built-in script in the DataXpress program (total initial tail current = 0% inhibition, no current = 100% inhibition). Normalized results from multiple assays are pooled and analyzed with Prism's built-in four-parameter logistic functions as outlined in **Section 2.3**. A built-in statistical comparison function in Prism is then used to determine if a model with a variable Hill slope fit the data better than a model with a standard Hill slope (slope of 1); a p value less than 0.05 is considered significant. Finally, the potency value and corresponding Hill slope value from the best-fit model are reported.

Figure 65. Voltage protocol (upper) and corresponding hERG tail current recording (lower) for the automated planar patch clamp assays.

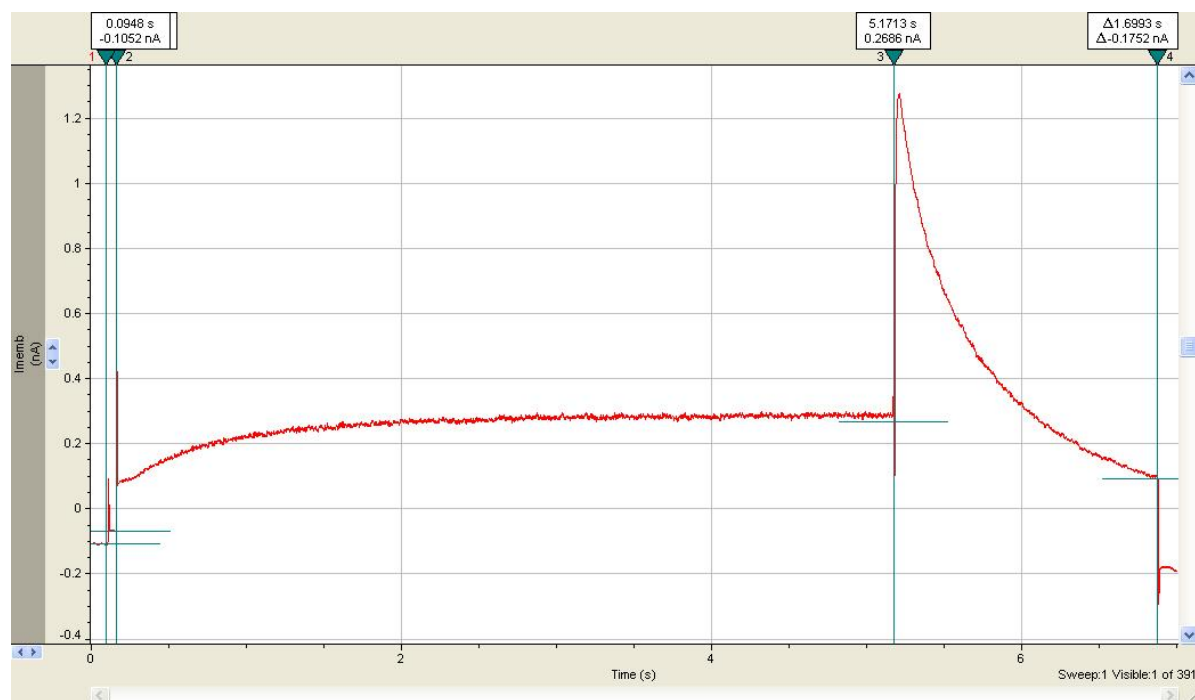
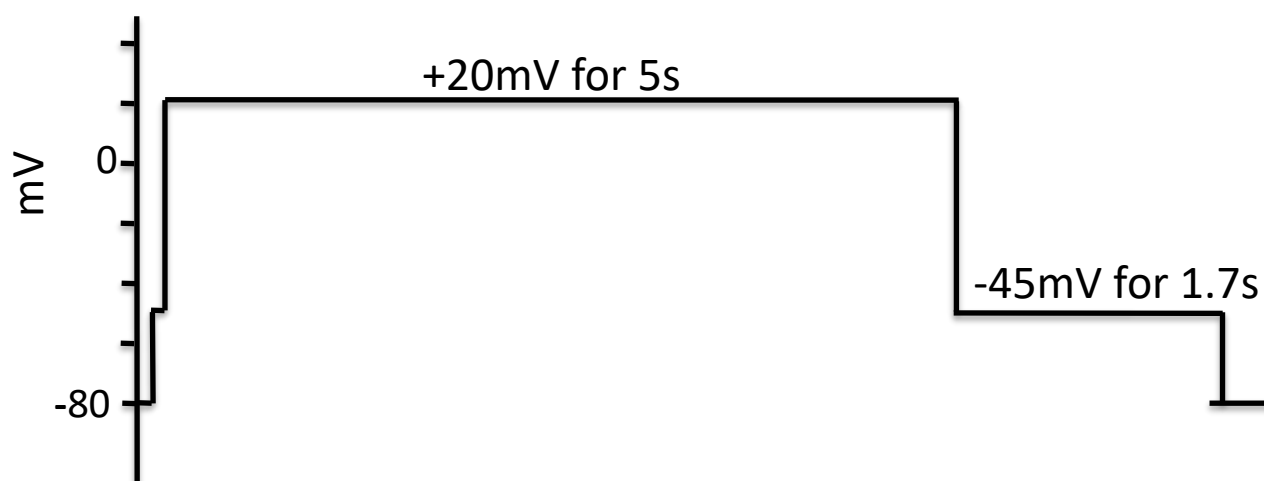


Figure 66. A representative whole-cell patch clamp recording showing inhibition of hERG channel current (nA) by a PDSP compound in a dose-dependent manner, which was partially recovered during a wash-out cycle, and then completely inhibited again by a positive control (3 μ M cisapride). The figure is a captured screen in the DataXpress program showing hERG tail currents in the absence and presence of a PDSP compound. The red vertical line (left) indicates addition of buffer control, green vertical lines indicate triple additions of drugs with concentrations (μ M) above the green lines, the dark blue vertical lines indicated wash-out with buffer, and the pink vertical lines indicate the positive control cisapride. Red crosses indicate the times when the hERG tail current was measured by the system.

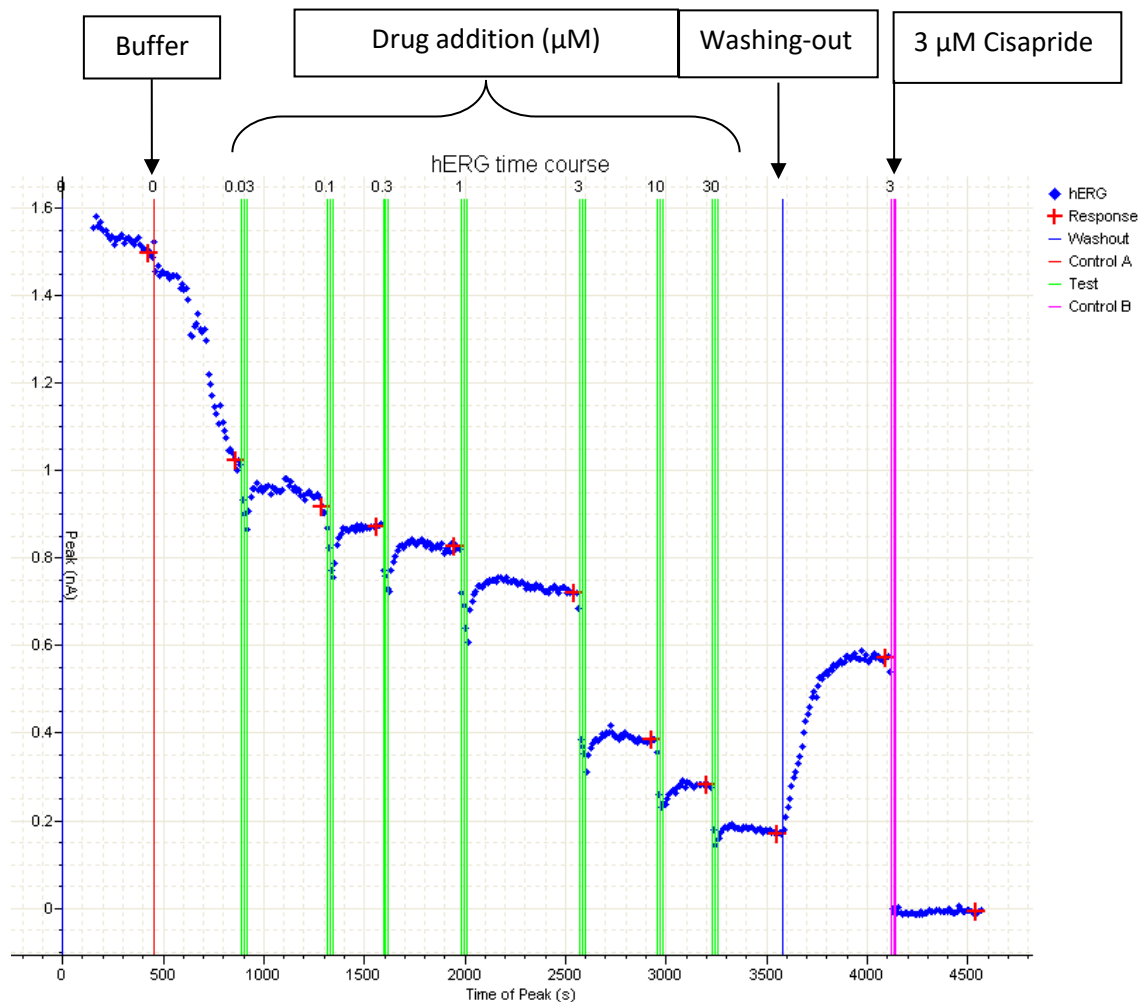


Figure 67. The captured screen in the DataXpress program shows a representative whole-cell patch clamp recording of hERG tail currents in the absence and presence of cisapride. The red vertical line indicates addition of buffer control and the green vertical triple lines indicate triple additions of cisapride with concentrations (μM) listed above the green lines. Red crosses indicate the times when hERG tail current was measured by the system.

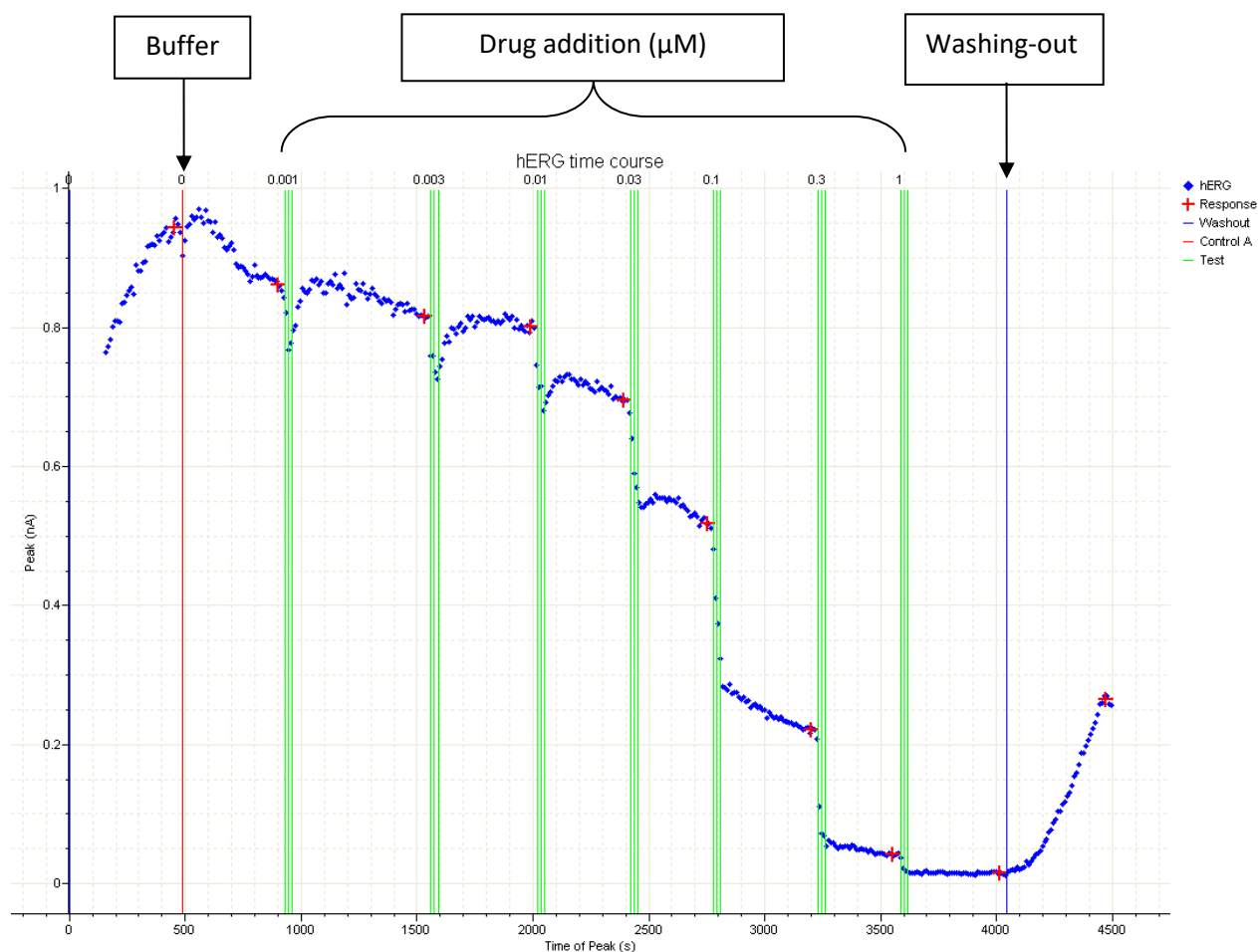


Figure 68. The hERG tail currents in Figure 67 were extracted from the program DataXpress, plotted against cisapride concentrations, and fitted to a four-parameter logistic function using GraphPad Prism 5.0 (131).

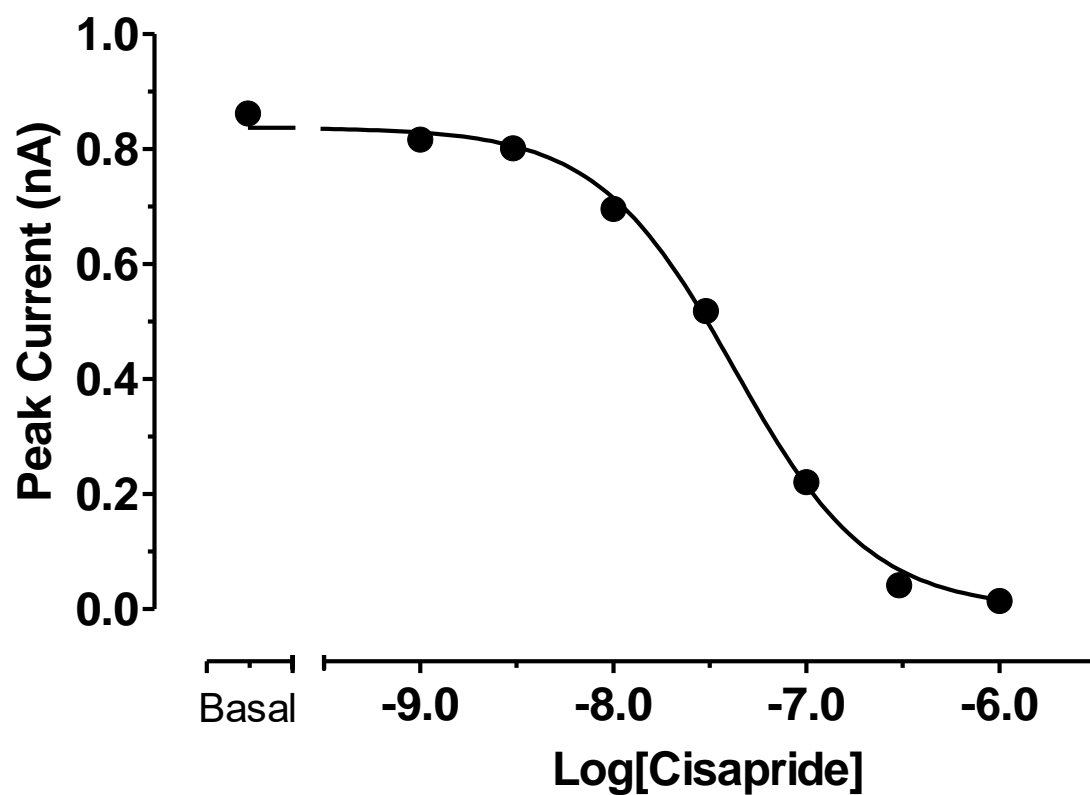
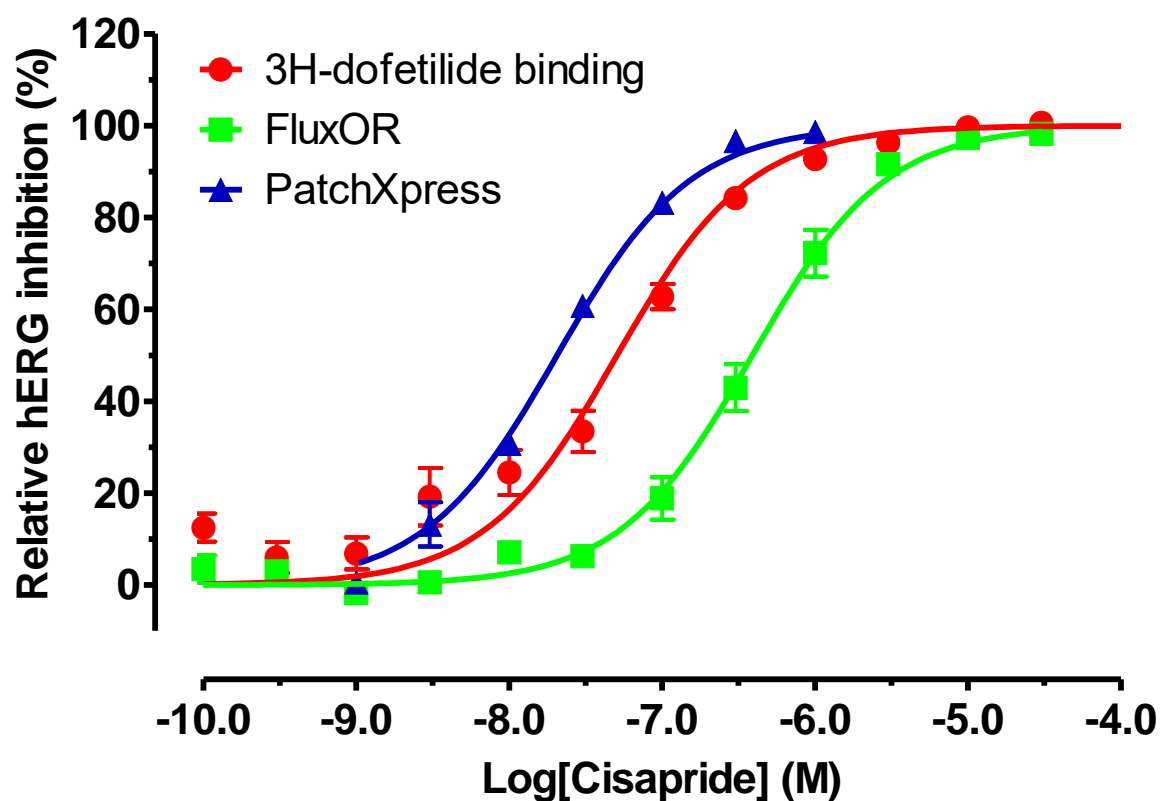


Figure 69. Side-by-side comparison of dose-dependent relations of cisapride in 3H-dofetilide competition binding assay; Ti^+ flux assay, and APPC assay. Results from multiple assays ($n \geq 2$) were normalized to percentage inhibition and pooled for curve-fitting in GraphPad Prism 5.0. Results indicated that the PatchXpress assay was the most sensitive, and the Ti^+ flux assay was the least sensitive (131).



2.11. Neurotransmitter transporter assays for DAT (Dopamine transporter), NET (norepinephrine transporter), and SERT (Serotonin transporter).

Main equipment: FlexStation II (Molecular Devices, Sunnyvale, CA)

Main reagent: Neurotransmitter transporter uptake assay kit (R8174) from Molecular Devices

Assay buffer: 20 mM HEPES, 1x HBSS, pH 7.40, RT

2.11.1. Background and principle: The assay system is designed to use the same fluorophore to measure norepinephrine (NET), dopamine (DAT), and serotonin (SERT) transporter activity (179–184). The proprietary fluorophore mimics biogenic neurotransmitters and is actively transported into the cell through the NET, DAT, or SERT. After incubation with test compounds, the dye solution is added to cells and the fluorescent dye is transported into the cell. External fluorescence is quenched with a masking dye, which cannot enter cells. Therefore, fluorophore fluoresces when it enters the cell and the fluorescence intensity is proportional to the transporter activity. The assay can be performed without a wash step and the fluorescence intensity can be monitored in kinetic mode or end-point modes.

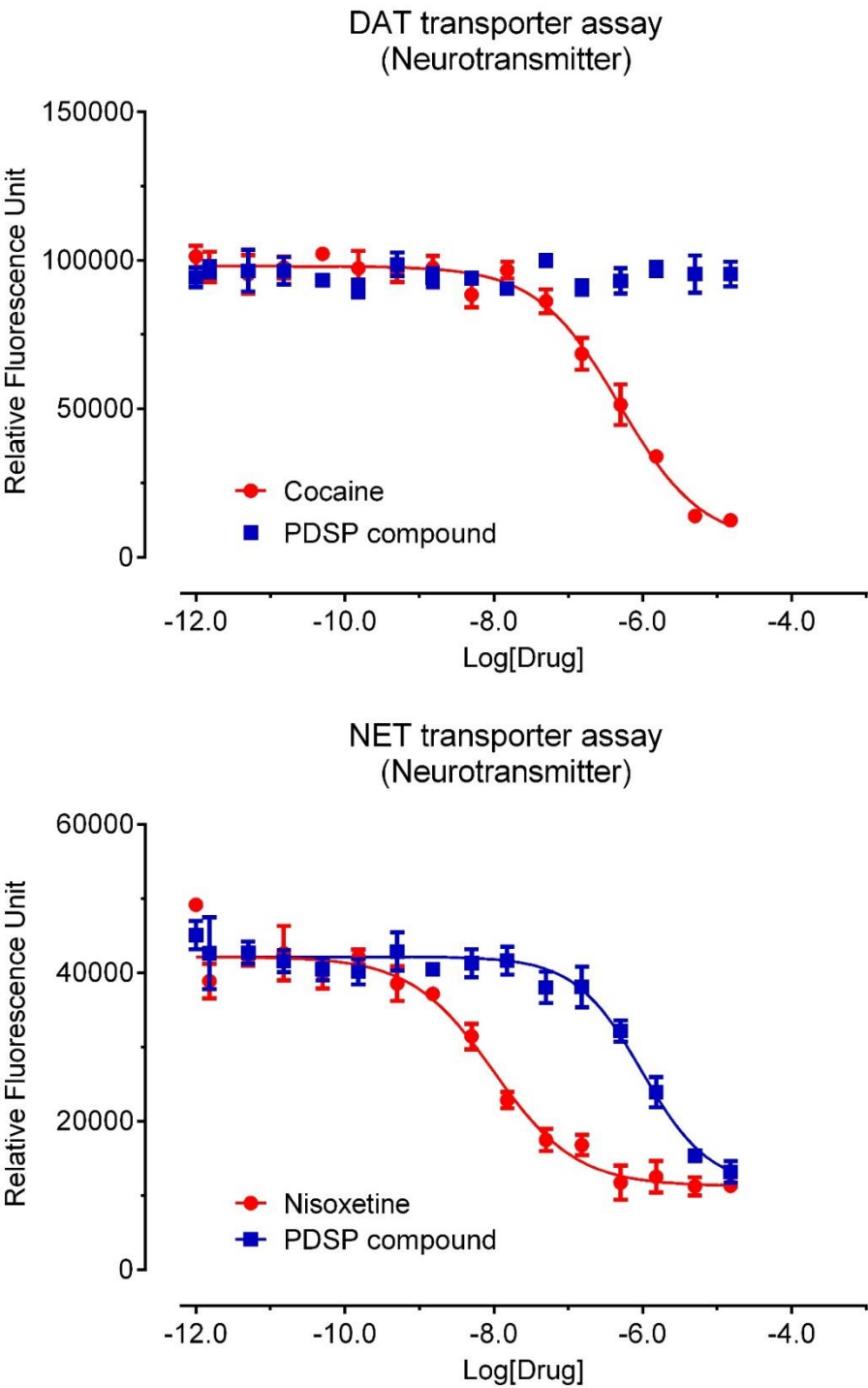
2.11.2. Assay procedure: The neurotransmitter transporter assays are conducted using Molecular Devices' Neurotransmitter Transporter Uptake Assay Kit (R8174) with HEK293 cells stably expressing human DAT, NET, or SERT. In brief, cells are plated in Poly-L-Lys (PLL)-coated 384-well black clear bottom cell culture plates in DMEM + 1% dialyzed FBS, at a density of 15,000 cells per well in a total volume of 40 μ l. The cells are incubated for a minimum of 6 hours before use in assays. First, medium is removed, 20 μ l of assay buffer (20 mM HEPES, 1x HBSS, pH 7.40) is added, followed by 5 μ l of 5x drug solutions (384-well drug plate map #1 or #2, Figure 22, for primary assays and see 384-well drug map #4, Figure 25, in Section 2.1). Plates are incubated at 37°C for 30 min. After incubation, 25 μ l of dye solution is added and fluorescence intensity is measured after 30 min at 37°C, using the FlexStation II (bottom read mode, Excitation at 440 nm, Emission at 520 nm with 510 nm cut-off). Results (Relative Fluorescence Units, RLU) are exported and plotted against drug concentrations in

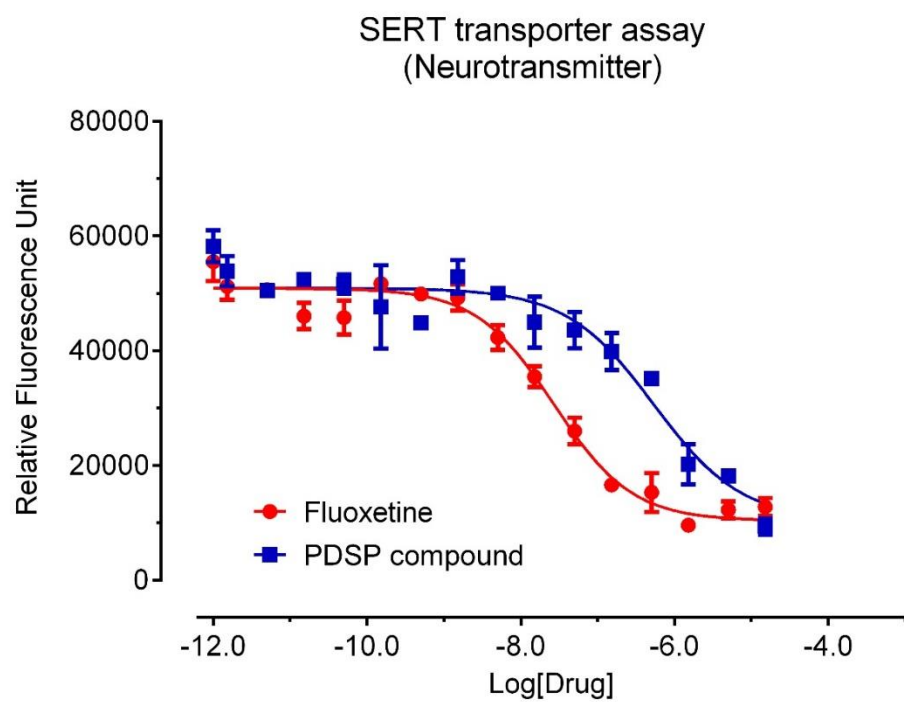
Prism 5.0 for nonlinear regression to obtain inhibitory potency. Cocaine, nisoxetine, and fluoxetine serve as positive controls for DAT, NET, and SERT, respectively.

2.11.2. Data processing and analysis. Fluorescence intensity is exported and analyzed in Prism 5.0 to obtain IC₅₀ values using non-linear least-squares curve fitting.

2.11.3. Representative figures

Figure 70. Representative curves of neurotransmitter reuptake inhibition at DAT, NET, and SERT.





2.12. Multidrug Resistance Transporter (MDR-1) assay.

Main equipment: FlexStation II (Molecular Devices, Sunnyvale, CA)

Assay buffer: Dulbecco's PBS, 10 mM Glucose

Protocol: The MDR assay protocol is adapted from PubChem BioAssay ID 377

(<http://pubchem.ncbi.nlm.nih.gov/assay/assay.cgi?aid=377>)

2.12.1. MDR assay Background: Assays for modulation of MDR activity are performed using Caco-2 cells, a cultured line derived from human colonic epithelium. The assay relies on the fluorescent dye calcein as an indicator. Lipophilic pro-dye calcein acetoxymethyl ester (Calcein-AM) is not fluorescent, and easily gets across the plasma membrane, entering cells by passive diffusion. Calcein-AM is then converted by cellular esterases into highly fluorescent calcein, which is negatively charged and stays inside the cell. MDR can actively transport calcein-AM, but not fluorescent calcein, out of the cells; therefore intracellular fluorescent calcein would be low. Higher MDR activity leads to lower fluorescence. Compounds that compete with calcein-AM for MDR will prevent the removal of calcein-AM from cells, leading to increased fluorescence. Therefore, fluorescence intensity can be used to estimate interaction between compounds and MDR (185–189).

2.12.2. MDR assay procedure: The assay monitors the time-dependent increase in calcein fluorescence in live cells in 96 well plates. This is carried out using a FlexStation II fluorimeter (Molecular Devices). Cells are seeded into glass-bottom 96-well plates one day before assay (80,000 cells per well). On the day of the assay, the medium is removed and replaced with 50 μ l of D-PBS, 10 mM glucose containing no additional compound (negative control), test compound (25 μ M), or reference compound (cyclosporin A) (25 μ M). The cells are incubated for 30 min at 37°C, and then the instrument adds calcein-AM to the cells (500 nM final concentration). The instrument monitors fluorescence over a 4-min period and calculates the slope of the fluorescence increase. All compounds are assayed in quadruplicate and each assay contains wells with no test compound (negative control) and wells with 25 μ M cyclosporin A, an efficient MDR inhibitor as a positive control. Results for test compounds are calculated from the slope of the fluorescence increase and are normalized so the value from untreated cells is 0% and the value for cyclosporin A is 100%.

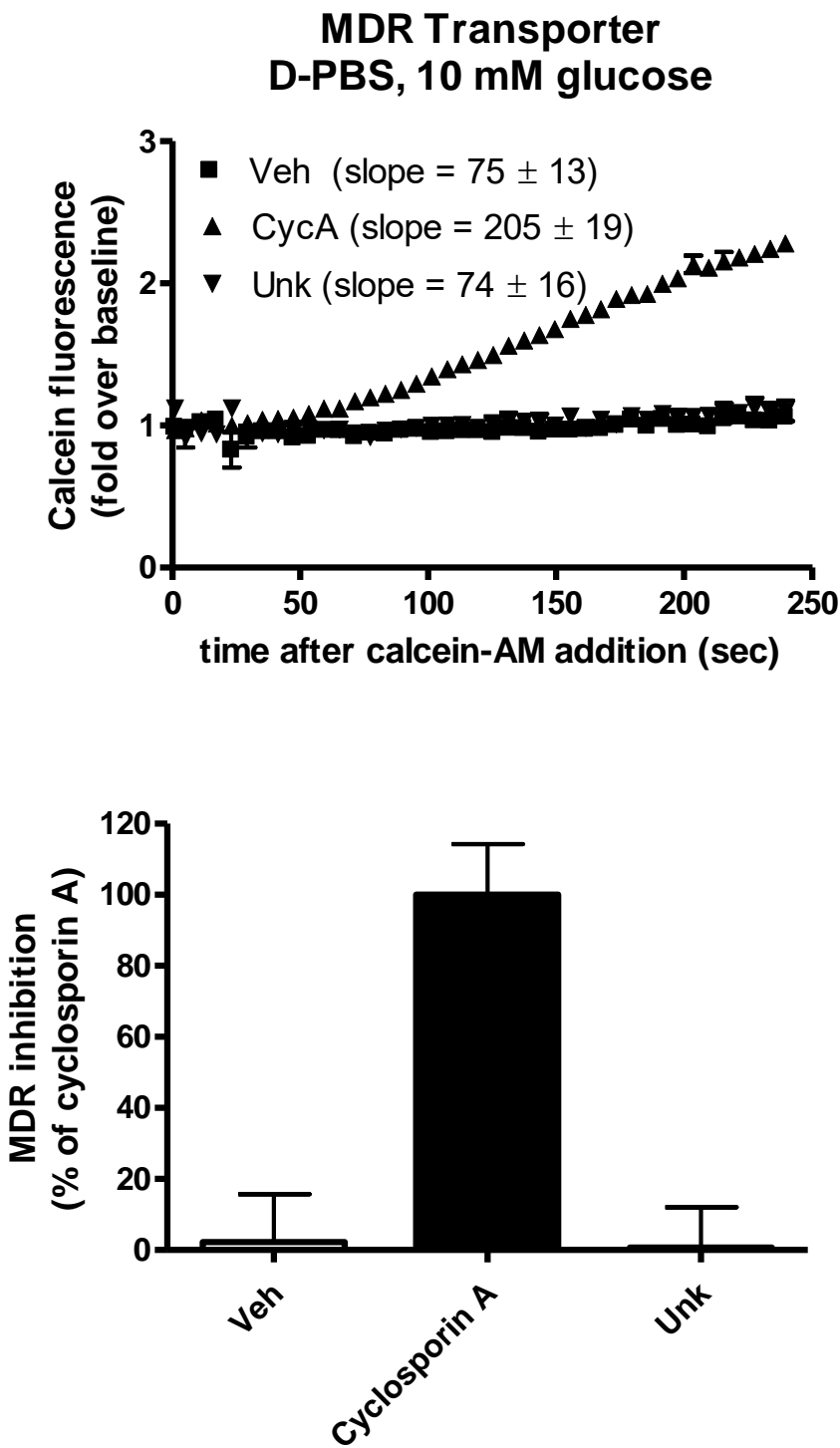
This assay has several features that make it ideal for initial screening of compounds for interaction with MDR. Because the assay is carried out in live cells, compounds must diffuse across lipid bilayers to interact with MDR sites on the cytoplasmic face of the protein. This is similar to the situation in vivo, where compounds must diffuse into the cytoplasm where they interact with MDR. Similarly, the assay provides a means for assessing not only interactions with MDR but also partitioning across cell membranes and thus hydrophobicity.

Although this assay is excellent for initial screening, users should be aware that the assay has several drawbacks. i) The assay does not distinguish between MDR substrates and inhibitors. Both will give similar signals in the assay because they prevent the transport of calcein-AM. ii) Some compounds may give spurious results by inhibiting the esterases that convert calcein-AM to calcein. Finally, (iii) activity depends on the cytoplasmic concentration of the compounds. For a compound that is an MDR substrate, this concentration depends on the rate of diffusion across the plasma membrane and the rate at which MDR pumps the compound out of the cells. At steady state, the cytoplasmic concentration will be lower than the extracellular concentration, but it cannot be measured easily. Consequently, this assay is not the best choice for determining half-maximal concentrations for interacting compounds.

2.12.3. Data process. Fluorescence intensity is exported and analyzed in Prism 5.0 using non-linear least-squares curve fitting.

2.12.4. Representative figures

Figure 71. Representative data from an MDR inhibition assay.



2.13. Histone Deacetylase (HDAC) inhibition assay.

Main equipment: FlexStation II (Fluorescence plate reader) (Molecular Devices, CA)

Assay buffer: 50 mM Tris HCl, 137 mM NaCl; 2.7 mM KCl, 1 mM MgCl₂, pH 8.0

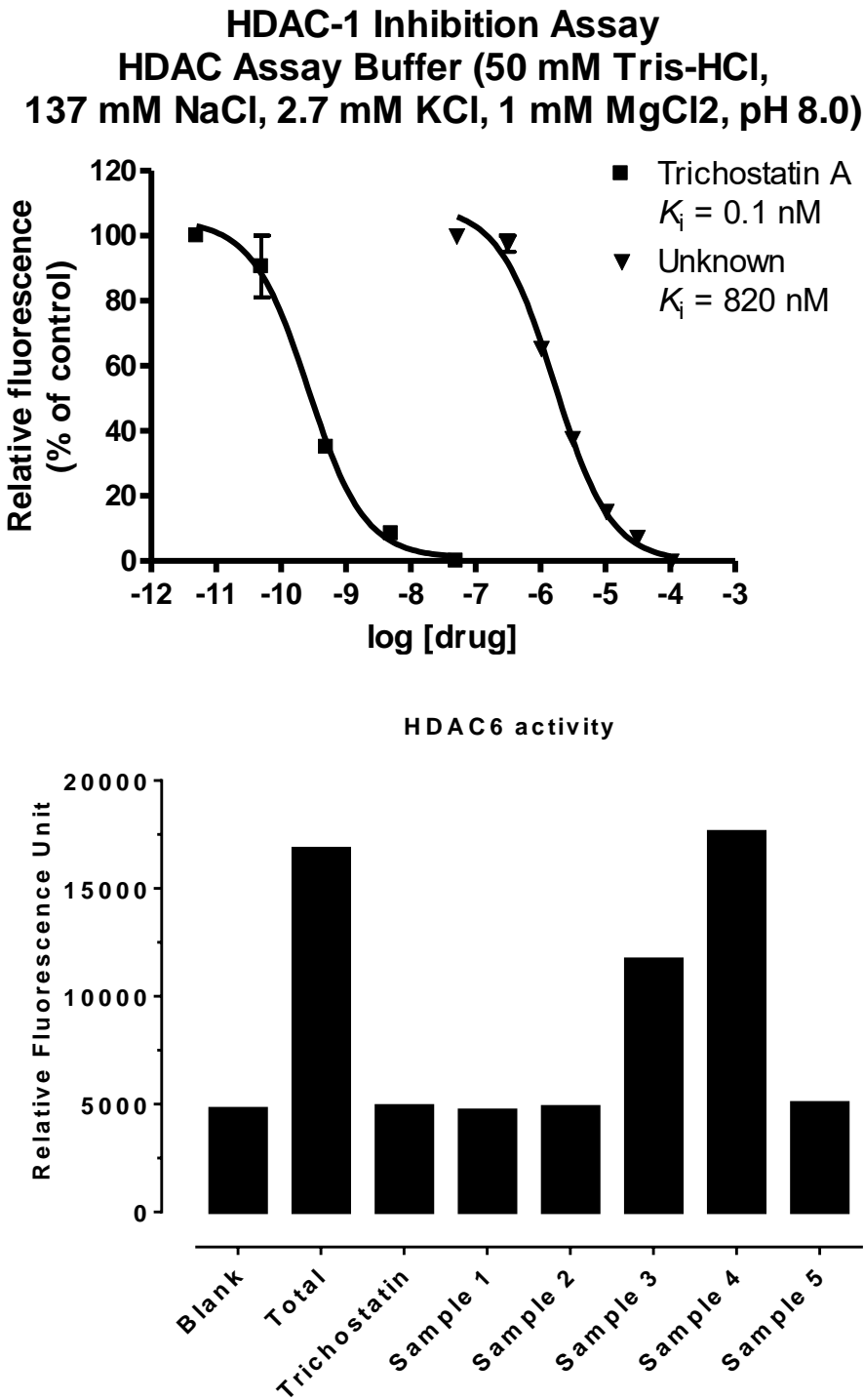
Main reagent: The HDAC assay protocol was adapted from BioMol Fluor de Lys assay system (Plymouth Meeting, PA)

2.13.1. General Assay Procedure. To identify potential inhibitors of HDAC, we utilize the fluorimetric Fluor de Lys HDAC Assay Kit from Biomol as instructed by the manufacturer. Similar procedures have been modified for high throughput screening assays (190–193). Briefly, 4X dilutions of test compound or reference compound (trichostatin A) are prepared (final assay concentrations span from 0.1 nM to 10 μ M) in Assay Buffer, and 12.5 μ l are added to the wells of a 96-well plate (particular to this assay; Biomol). Nuclear extracts containing HDAC activity (procured from Biomol) are diluted to 4X and 12.5 μ l are added to the wells containing test or reference compound (each concentration assayed in triplicate). The samples are incubated at room temperature for 10 min to equilibrate the temperature. Then, 25 μ l of 2X Fluor de Lys HDAC substrate (final HDAC substrate concentration is typically a value between one half its apparent K_M and the apparent K_M ; for HDAC1 a concentration of 50 μ M is used, for HDAC6 a concentration between 10 and 30 μ M is used) are added to each well. Deacetylation of the substrate, which generates a product that can be made fluorescent, is allowed to proceed for 30 min. Next, the reactions are stopped and the fluorescence of the deacetylated product is developed by adding 50 μ l of 2X Assay Developer and incubating at room temperature for 15 min. Finally, fluorescence is read on a FLEXStation II plate reader (Molecular Devices) (excitation 350-380 nm, emission 440-460 nm).

2.13.2. Data processing. Raw data (RFUs) representing deacetylated substrate fluorescence is plotted as a function of the logarithm of the molar concentration of the test or reference compound. Non-linear regression of the normalized (to the fluorescence measured in the absence of HDAC inhibitor and test compound) raw data is performed in Prism 5.0 using the built-in three parameter logistic model describing competitive inhibition (one-site):

2.13.3. Representative figures.

Figure 72. Representative HDAC 1 inhibition curves (upper) and HDAC 6 inhibition in the absence and presence of 10 μ M compounds (bar graph, lower)



2.14. Monoamine Oxidase (MAO) A and B assays.

Main equipment: FlexStation II (Fluorescence plate reader) (Molecular Devices, CA)

Main reagent: Monoamine A and B Detection Kit from Cell Technology (Mountain View, CA)

2.14.1. Background. Monoamine oxidase (MAO) is a flavin-containing enzyme that catalyses the oxidation of amine-containing neurotransmitters such as serotonin, norepinephrine, epinephrine, and dopamine to yield the corresponding aldehydes. MAO has two isoforms, MAO A and MAO B. They exhibit different specificities to substrates and inhibitor selectivities. MAO A acts preferentially on serotonin and norepinephrine and is inhibited by clorgyline. MAO B acts preferentially on 2-phenylethylamine and benzylamine and is inhibited by deprenyl and pargyline. Several fluorescence-based screening assays have been developed over the years (194–198) to screen for inhibitors or to measure MAO activities.

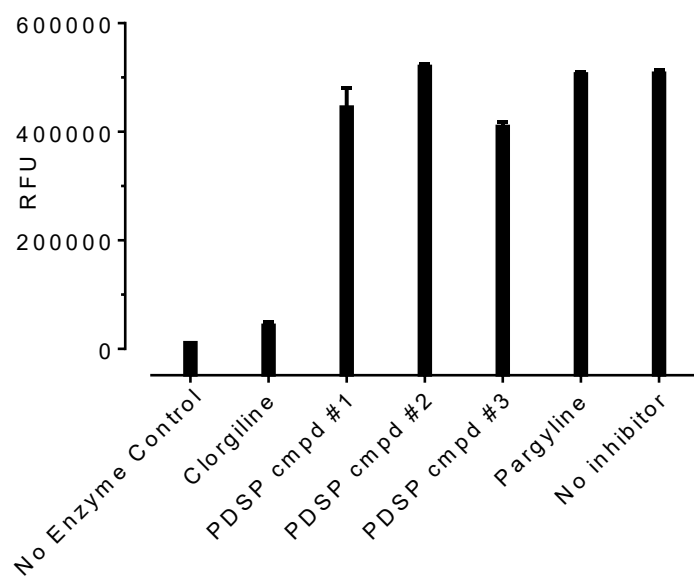
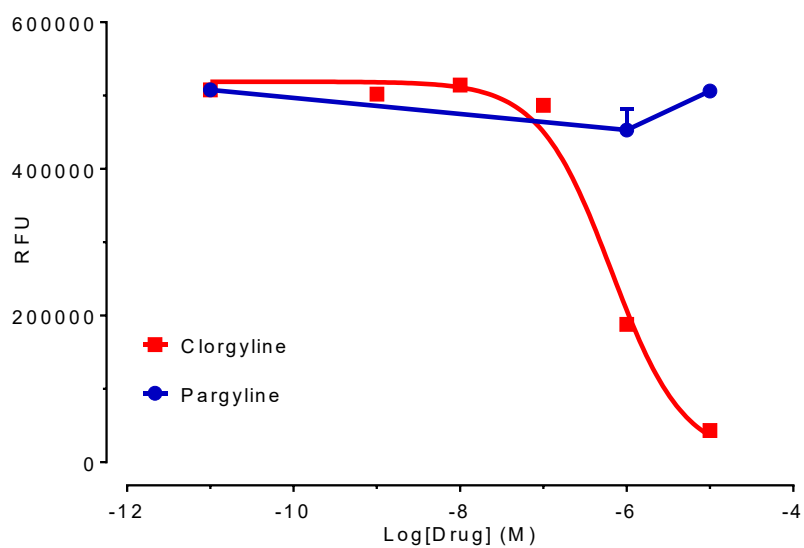
We use the MAO A and B Detection Kit from Cell Technology for Monoamine A and B enzyme assays. The assay system utilizes a non-fluorescent proprietary substrate to detect H_2O_2 released from the conversion of the MAO substrate (Benzylamine for MAO A and Tyramine for MAO B) to its aldehyde. The reaction of H_2O_2 with the non-fluorescent substrate is catalyzed by peroxidase in 1:1 stoichiometry to produce a fluorescent product with emission at 590 – 600 nm and excitation at 530 – 571 nm.

2.14.2. Assay procedure. The MAO A and B assays were performed in 96-well plates according to manufacturer's instructions. In brief, samples (test drugs and controls) are added to designated wells, followed by reaction cocktail containing reaction buffer, non-fluorescent substrate for H_2O_2 , HRP, and substrate for MAO A or B. The reactions are allowed to proceed for 30 minutes at room temperature in the dark. At the end of the 30-minute incubation period, plates are read in the FlexStation II (Molecular Devices, CA) using excitation 570 nm and emission at 590 nm.

2.14.3. Data processing. Fluorescence intensity is exported and analyzed in Prism v 5.0 using non-linear least-squares curve fitting.

2.14.4. Representative figures

Figure 73. Representative curves for MAO A activity in the presence of clorgyline and pargyline (upper) and bar graph showing MAO A activity in the presence of 10 μ M different test compounds (lower).



2.15. PKC activity assay

Main equipment: FlexStation II (Fluorescence plate reader) (Molecular Devices, CA)

Main reagent: Omnia Ser/Thr Recombinant Kit 8 (#KNZ2081) from Invitrogen (Carlsbad, CA)

PKC isoforms: purchased from Invitrogen or Sigma (St. Louis, MO)

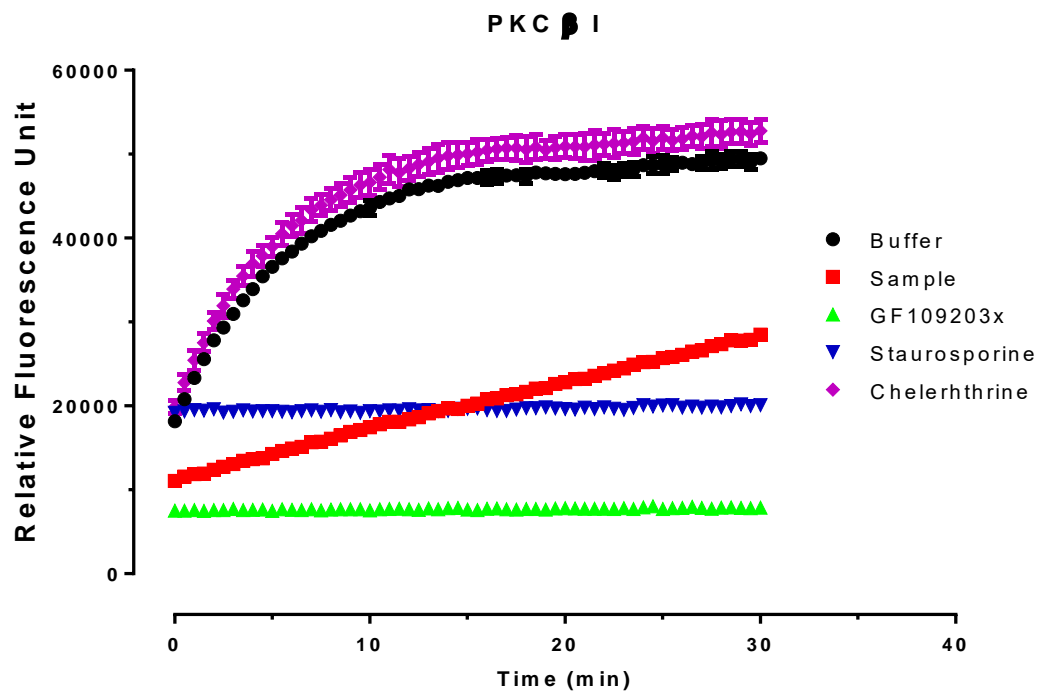
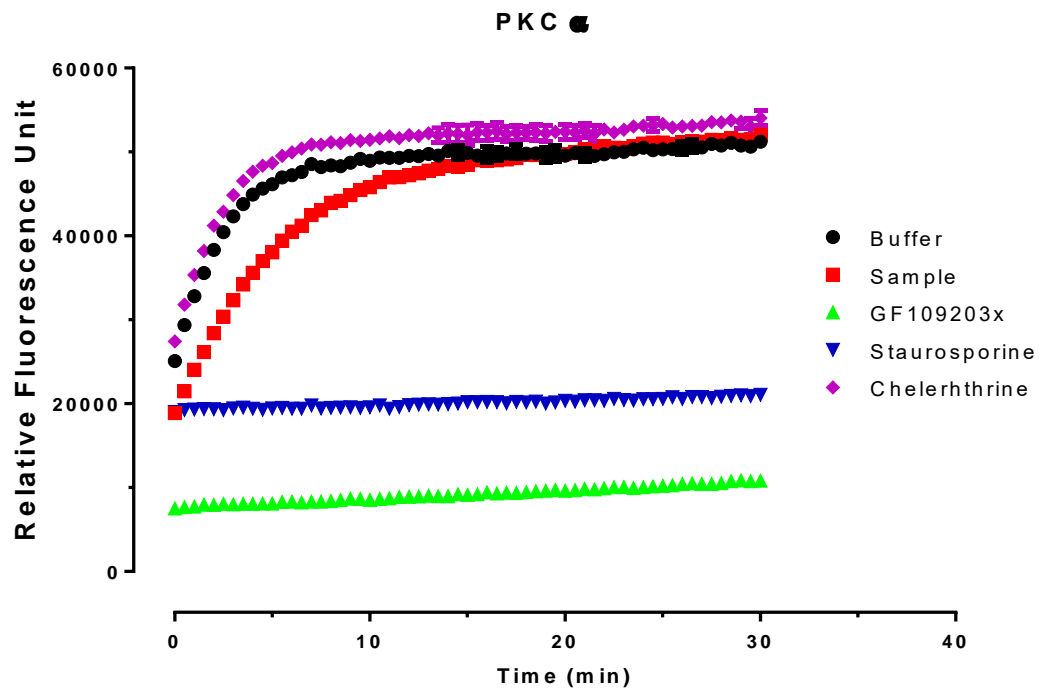
2.15.1. Background. Protein Kinase C (PKC) has 12 isoforms and is classed into three groups (conventional PKCs, Novel PKCs, and Atypical PKCs) based on their requirement of activators (Calcium ion lipids). Conventional PKC isoforms (α , β I, β II, and γ) require calcium, DAG, and phospholipid as activators; novel PKC isoforms (δ , ϵ , η , θ , and μ) require DAG but not calcium; atypical PKC isoforms (ζ and ι) require neither DAG nor calcium. We use Invitrogen's PKC assay kit (Kinase Activity Assay Kit, KNZ2081, aka The Omnia(R) Ser/Thr Recombinant Kit 8) for PKC inhibitor screening assays. The assay uses a Ser/Thr containing peptide substrate conjugated with the chelation-enhanced fluorophore (CHEF) 8-hydro-5-(N,N-dimethylsulfonamido)-2-methylquinoline (Sox). Phosphorylation of the peptide substrate results in Mg^{2+} chelation and formation of an ion-ion interaction bridge between the Sox moiety and phosphate group, leading to an increase in fluorescence at 485 nm when being excited at 360 nm.

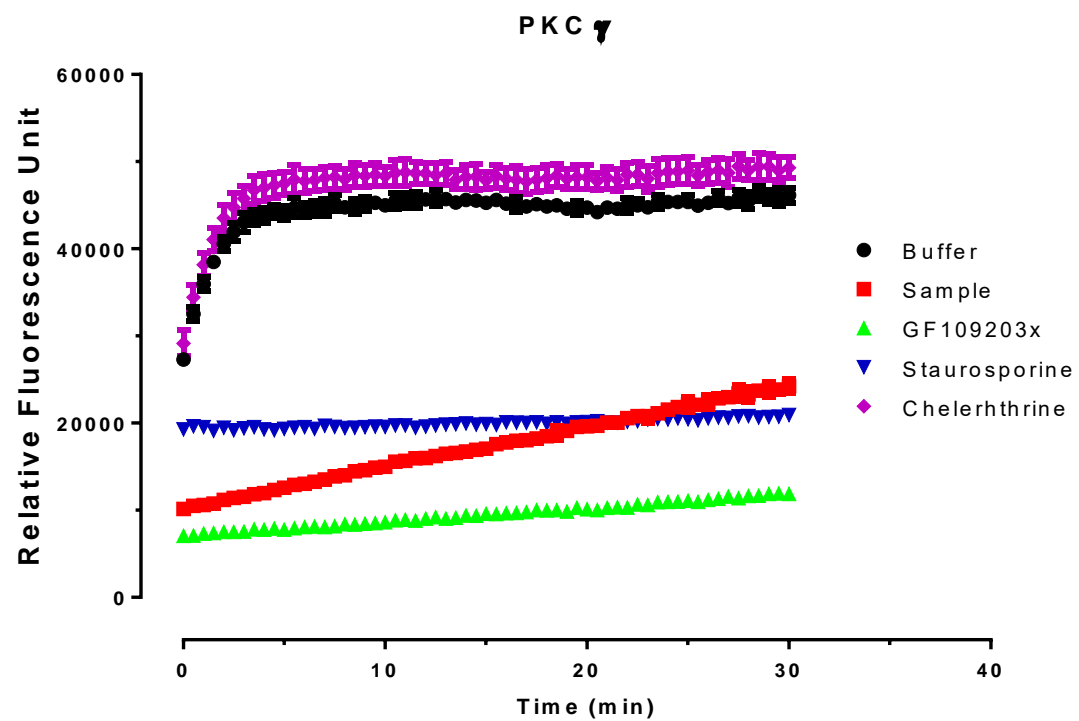
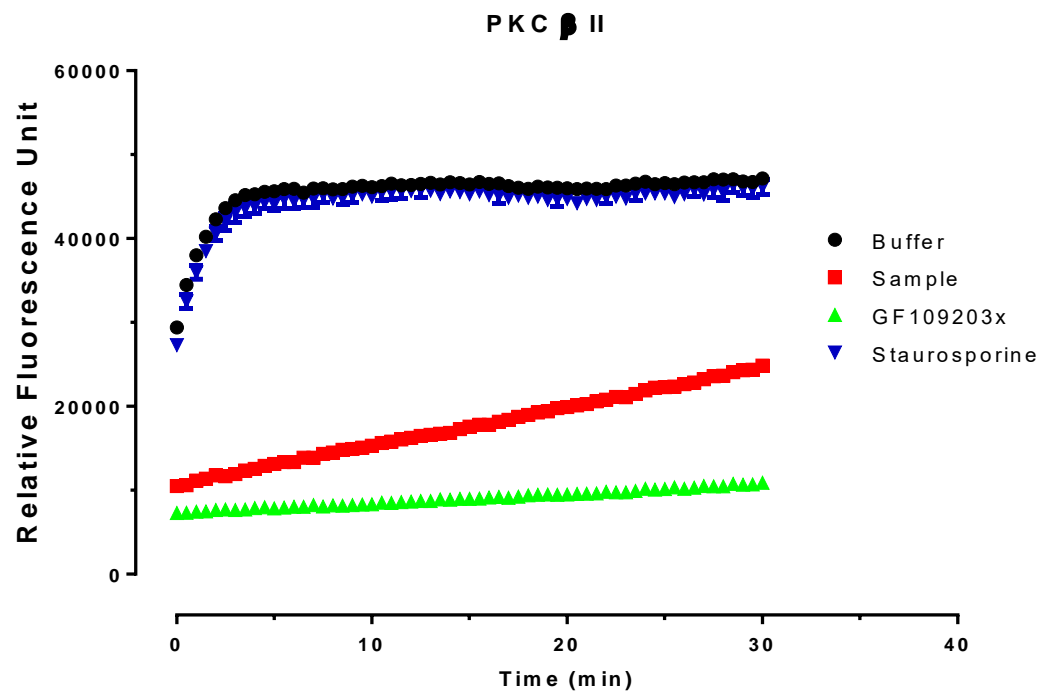
2.15.2. Assay procedure. PKC kinase activity assays are performed in 96-well plates (1/2 area and low protein binding surface) according to the manufacturer's suggested procedure. In brief, a master reaction mix is made with the following components: assay buffer, peptide substrate, ATP, DTT, calcium and/or lipid activator (use buffer for atypical PKC isoforms), and aliquotted to corresponding wells; this is followed by addition of drug working solutions (samples) or buffer (as negative control) or known inhibitors (as positive control). The mixture is warmed up in the FlexStation to 30°C for about 10 min. The reaction starts when PKC isoform is added, and plates are read every minute for 60 min, with excitation at 360 nm and emission at 485 nm.

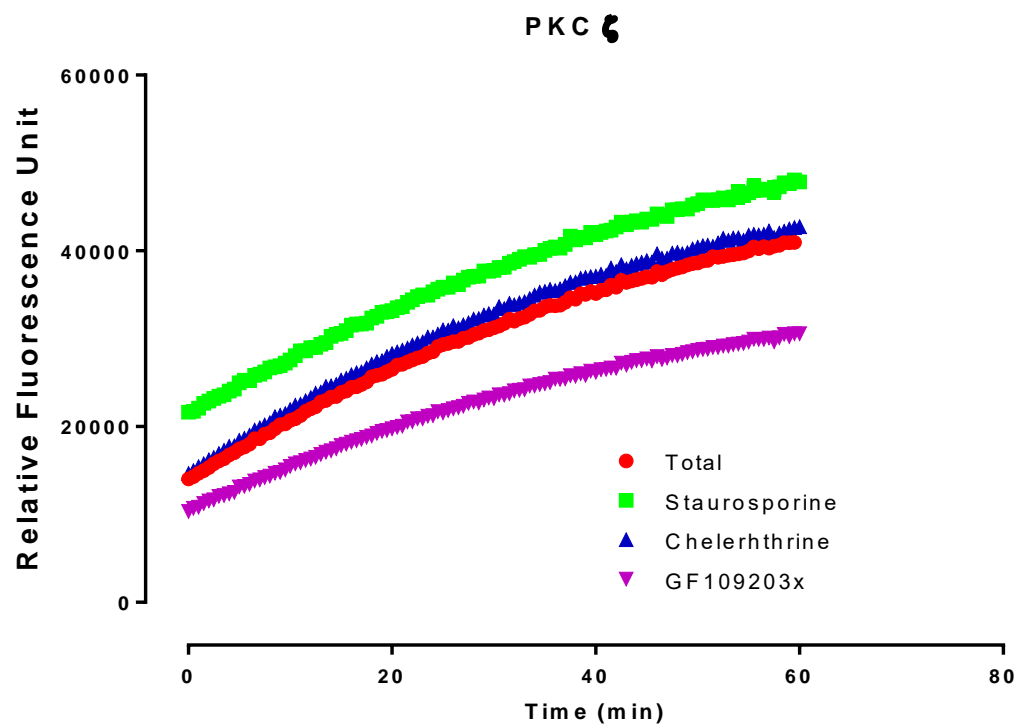
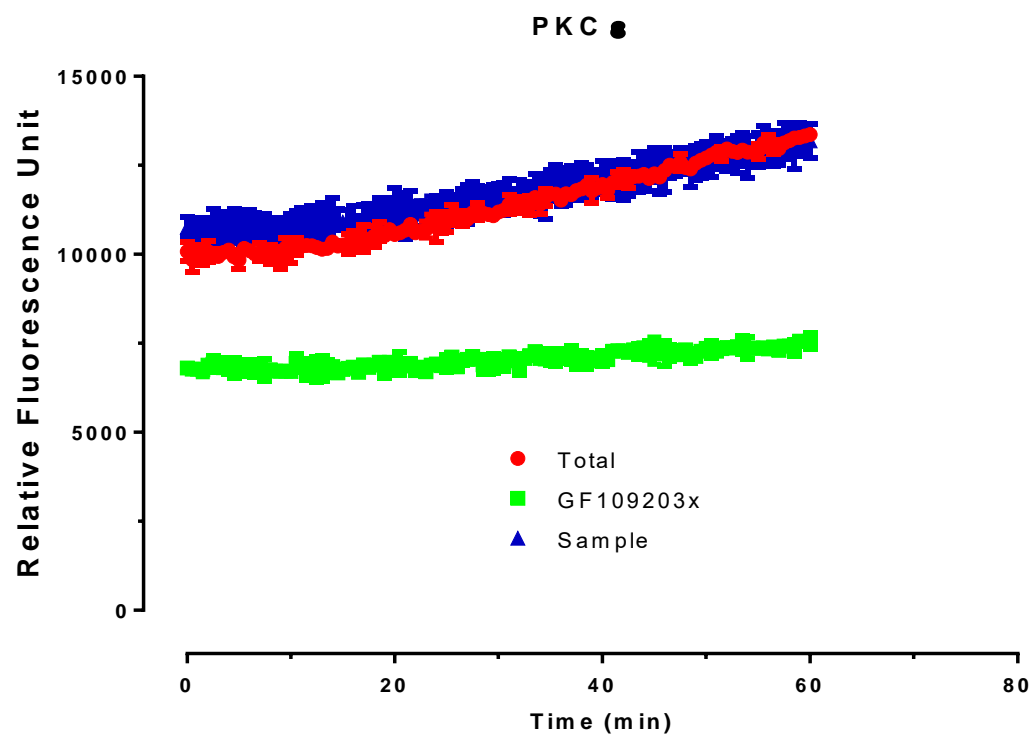
2.15.3. Data analysis. Fluorescence intensity increases over time. Intensity values are exported when the total activity reaches a plateau (or at the 30 min point) and analyzed in Prism v 5.0 using non-linear least-squares curve fitting.

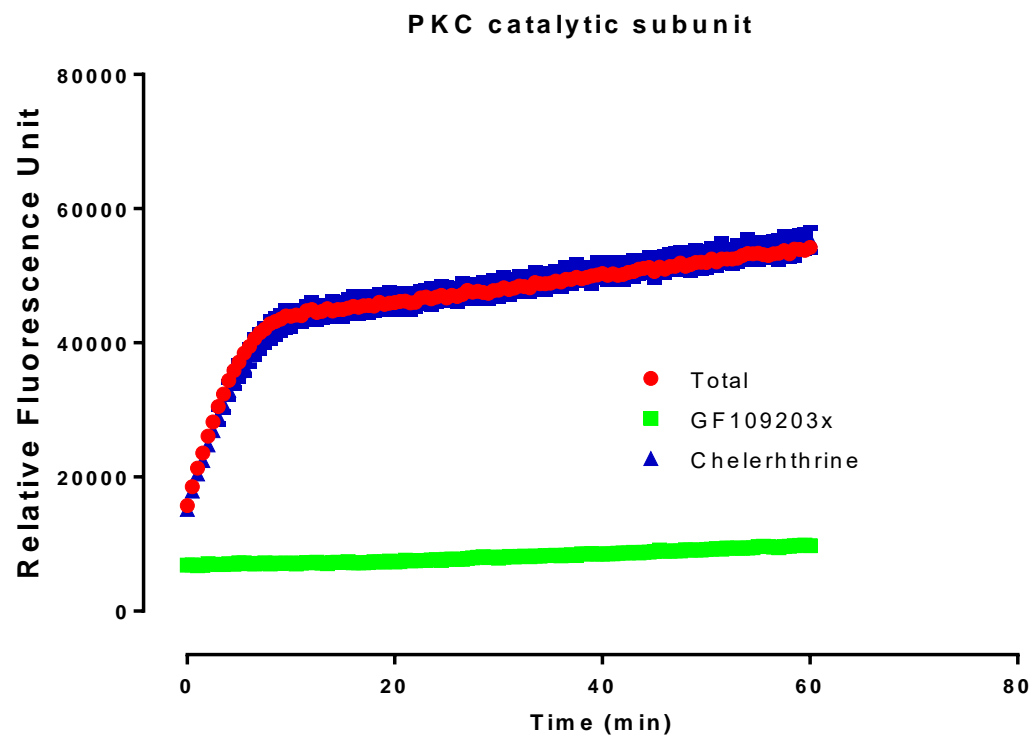
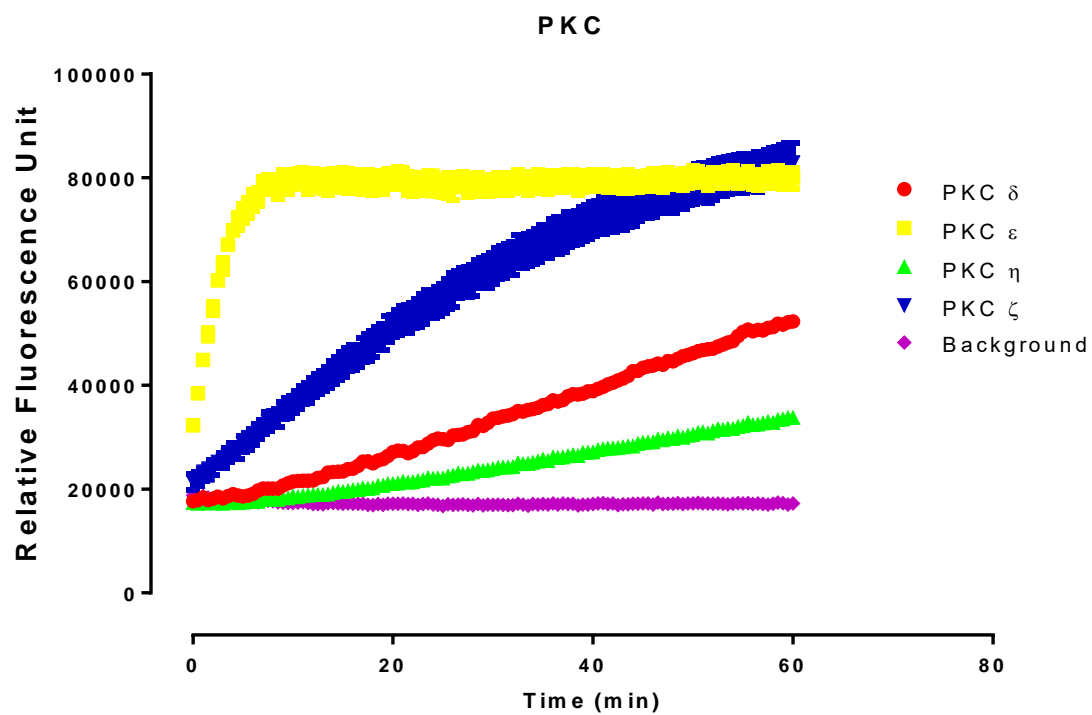
2.15.4. Representative figures.

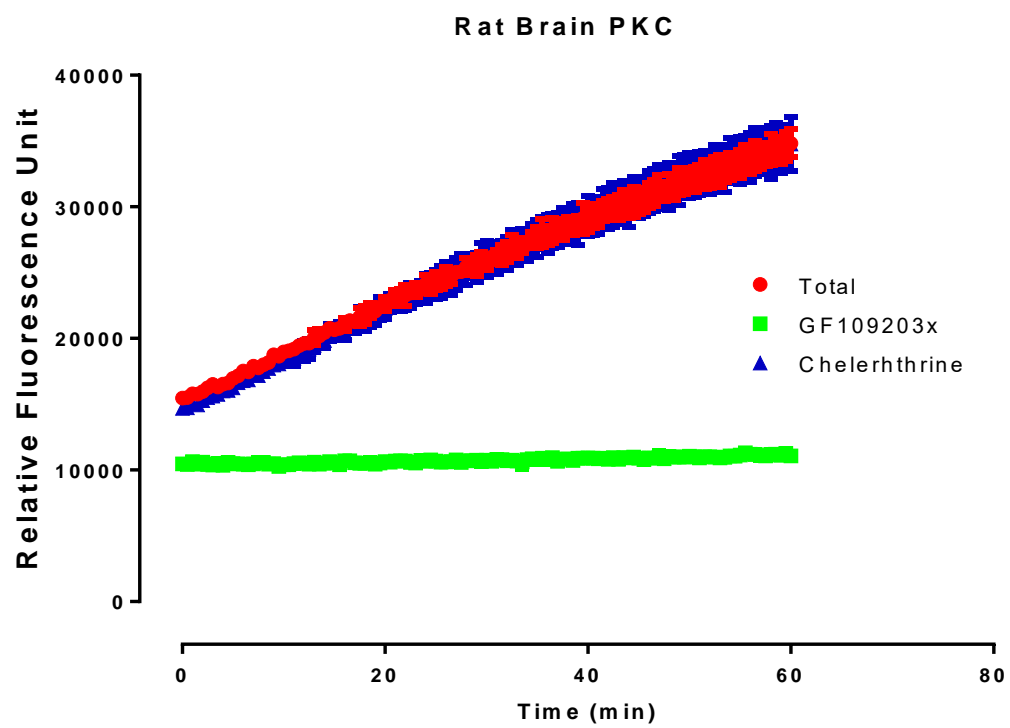
Figure 74. Time course of PKC activity in the absence and presence compounds (10 μ M).











2.16. Checkpoint Kinase 2 (CHK2) assay

Main equipment: FlexStation II (Fluorescence plate reader) (Molecular Devices, Sunnyvale, CA)

Main reagent: Omnia Ser/Thr Recombinant Kit 3 (#KNZ1031) from Invitrogen (Carlsbad, CA)

CHK2 enzyme (#PV3367) was purchased from Invitrogen.

2.16.1. Background. CHK2 is one of the Ser/Thr kinases phosphorylated and activated by upstream signaling apparatus (ATM and ATR) in response to DNA damage. Along with CHK1, CHK2 plays a critical role in determining cellular responses to DNA damage. Inhibitors for kinases like CHK2 could represent novel anticancer therapies.

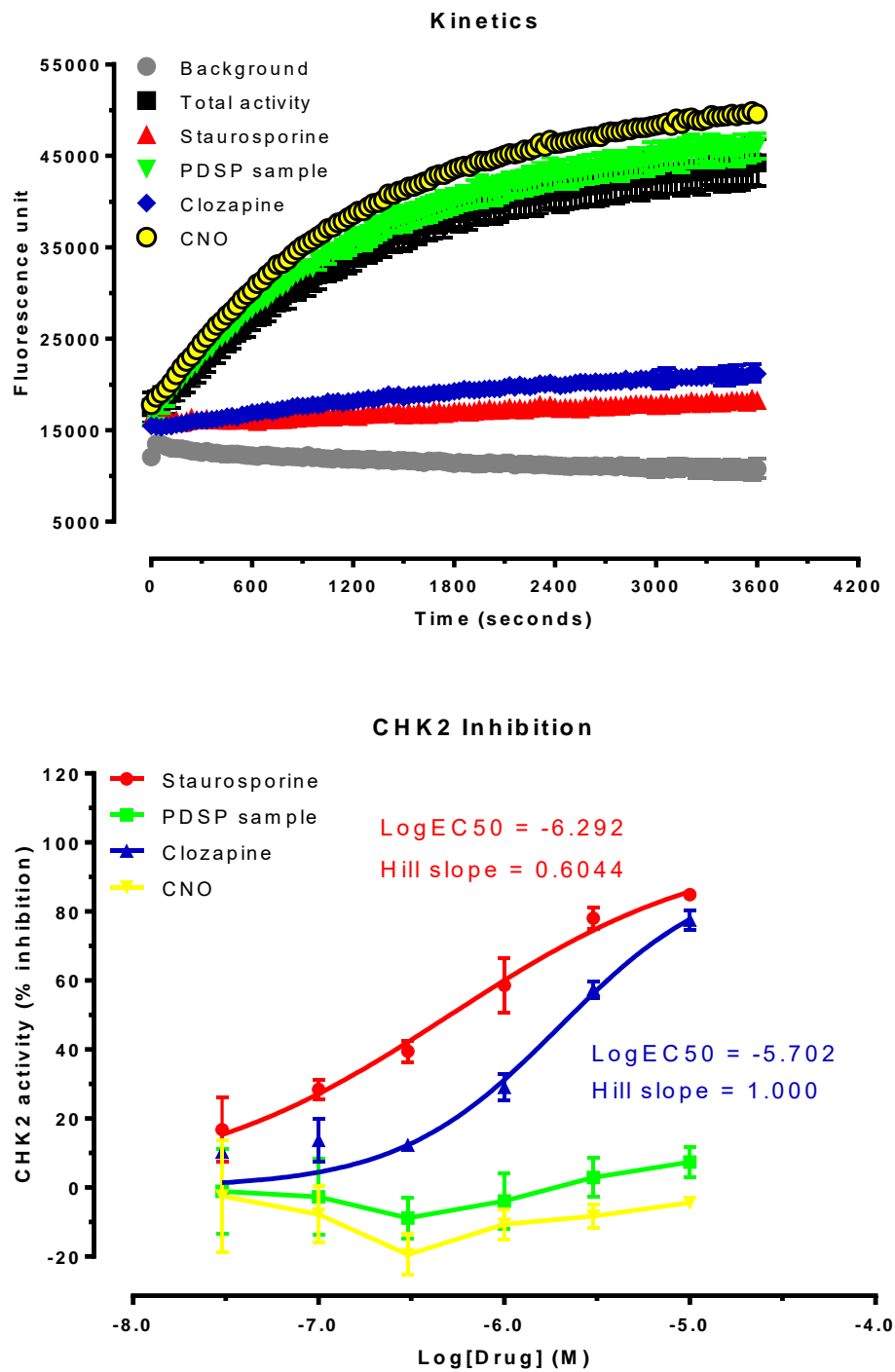
We use Invitrogen's Kinase Activity Assay Kit (#KNZ1031, Omnia Ser/Thr Recombinant Kit 3) to measure CHK2 activity (199–201). The Omnia® Kinase assay uses a Ser/Thr-containing peptide substrate conjugated with the chelation-enhanced fluorophore (CHEF) 8-hydro-5-(N,N-dimethylsulfonamido)-2-methylquinoline (Sox). Phosphorylation of the peptide substrate results in Mg^{2+} chelation and formation of an ion-ion interaction between the Sox moiety and phosphate group, leading to an increase in fluorescence at 485 nm when being excited at 360 nm.

2.16.2. Assay procedure. The PKC kinase activity assays are performed in 96-well plates (1/2 area and low protein binding surface) according to the manufacturer's suggested procedure. In brief, a master reaction mix is made with the following components: assay buffer, peptide substrate, ATP, DTT, calcium and/or lipid activator (use buffer for atypical PKC isoforms), and aliquotted to corresponding wells; drug working solutions (test samples) or buffer (as negative control) or known inhibitors (as positive control) are added, and the mixture is warmed up in the FlexStation to 30°C for about 10 min. The reaction starts when the PKC isoform is added, and plates are read every minute up to 60 min, with excitation of 360 nm and emission of 485 nm.

2.16.3. Data analysis. Fluorescence intensity increases over time. Intensity values are exported when the total activity reaches a plateau (or at the 30 min point) and analyzed in Prism v 5.0 using non-linear least-squares curve fitting.

2.16.4. Representative figures

Figure 75. Representative figures for CHK2 kinase activity kinetics (upper) and percentage inhibition (lower).



2.17. Functional assays with human $\alpha 3\beta 4$ and $\alpha 4\beta 2$ nAChRs – $^{86}\text{Rb}^+$ efflux assay

2.17.1. Background. Nicotinic acetylcholine receptors (nAChRs) are ligand-gated ion channels, different from G protein-coupled muscarinic acetylcholine receptors (mAChRs). Each nAChR contains five subunits symmetrically forming a pore; each subunit has four transmembrane domains with both intracellular N- and C-terminus.

2.17.2. Assay procedure. Agonist and antagonist activities of PDSP compounds on nAChRs are assessed by measuring $^{86}\text{Rb}^+$ efflux in HEK293 cells stably expressing nAChRs as described previously (5, 6). In brief, aliquots of cells in the selection growth medium are plated into Poly-D-Lysine coated 24-well plates. The plated cells are grown at 37°C for 18 to 24 h to reach 70-95% confluence. The cells are then incubated in growth medium (0.5 ml/well) containing $^{86}\text{RbCl}$ (2 $\mu\text{Ci/ml}$) for 4 h at 37°C. This loading mixture is then aspirated, and the cells are washed four times with HEPES buffer (15 mM HEPES, 140 mM NaCl, 2 mM KCl, 1 mM MgSO_4 , 1.8 mM CaCl_2 , 11 mM Glucose, pH 7.4; 1 ml/well). One ml of buffer, with or without agonists, is then added to each well. After incubation for 2 min, the assay buffer is collected and the amount of $^{86}\text{Rb}^+$ in the buffer is determined. Cells are lysed by adding 1 ml of 100 mM NaOH to each well, and the lysate is then collected for determination of the amount of $^{86}\text{Rb}^+$ in the cells at the end of the efflux assay. Radioactivity of assay samples and lysates is measured by liquid scintillation counting. The total amount of $^{86}\text{Rb}^+$ loaded (cpm) is calculated as the sum of the assay sample and the lysate of each well. The amount of $^{86}\text{Rb}^+$ efflux is expressed as a percentage of $^{86}\text{Rb}^+$ loaded. Stimulated $^{86}\text{Rb}^+$ efflux is defined as the difference between efflux in presence of nicotinic agonists and basal efflux measured in the absence of agonists.

2.17.2.1. Primary functional assay. The primary functional assay is carried out with $^{86}\text{Rb}^+$ efflux experiments. For assessing agonist activity, 4 concentrations of a test PDSP compound, 0.1, 1, 10 and 100 μM , are applied. Agonist activity is scaled as % of the stimulation by 100 μM nicotine. If a PDSP test compound shows a concentration-dependent activation, or shows 25% stimulation at any concentration, it is progressed to the secondary functional assay for agonist activity. For assessing antagonist activity, 4 concentrations of a test PDSP compound, 0.1, 1, 10 and 100 μM , are applied in the presence of 100 μM nicotine. Antagonist activity is scaled as % inhibition of the $^{86}\text{Rb}^+$ efflux

stimulated by 100 μ M nicotine. If a PDSP test compound shows a concentration-dependent inhibition, and shows more than 50% of inhibition at 100 μ M, it is progressed to the secondary functional assay for antagonist activity. All efflux assays are performed in quadruplicate. Nicotine is included in assays to define 100% agonist activity as well as to serve as a control.

2.17.2.2. Secondary functional assay. The secondary functional assay is carried out with $^{86}\text{Rb}^+$ efflux experiments. For assessing agonist activity, 8 concentrations of a test PDSP compound are applied. Agonist activity is scaled as % of stimulation by 100 μ M nicotine. For assessing antagonist activity, 8 concentrations of a test PDSP compound are applied in the presence of 100 μ M nicotine. Antagonist activity is scaled as % inhibition of the $^{86}\text{Rb}^+$ efflux stimulated by 100 μ M nicotine. All efflux assays are performed in quadruplicate. Nicotine is included in assays to define 100% agonist activity as well as to serve as a control.

2.17.3. Data analysis. Radioactivity (cpm/well) is exported and analyzed in Prism 5.0 by nonlinear least-squares regression to estimate EC_{50} or IC_{50} values.

2.17.4. Representative figures

Figure 76. Representative figures of agonist activity at nAChRs

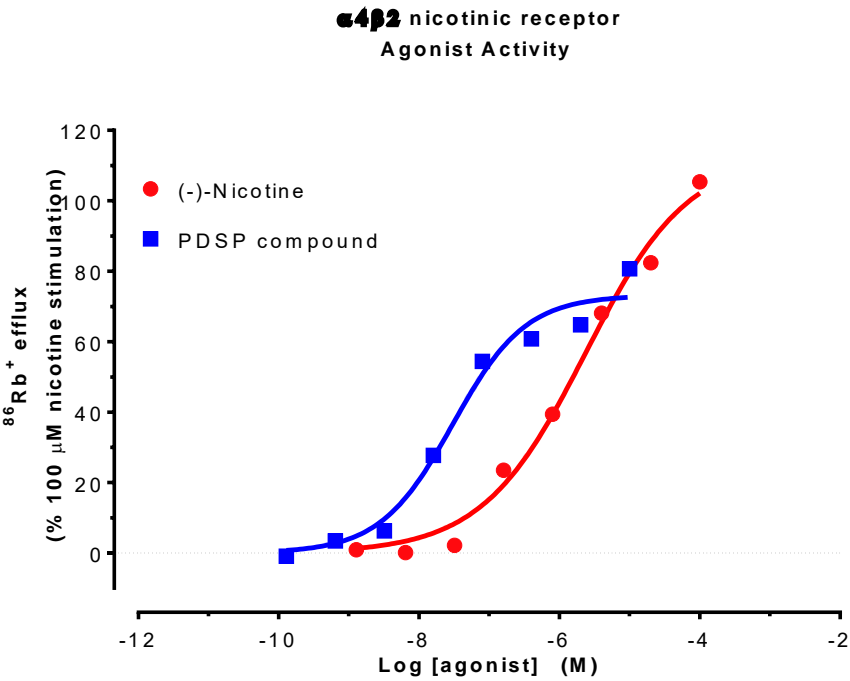
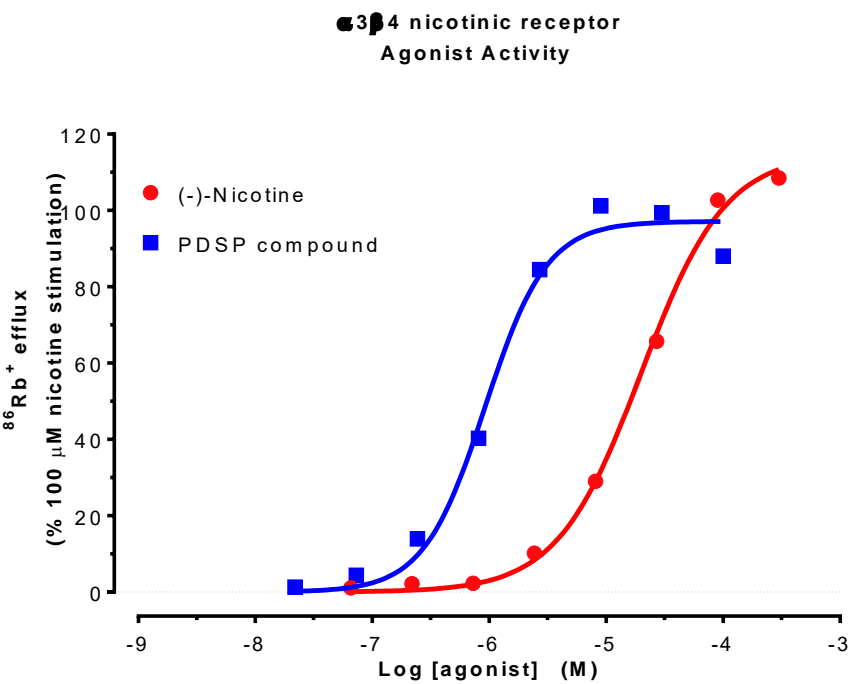


Figure 67. Representative figures of antagonist activity at nAChRs.

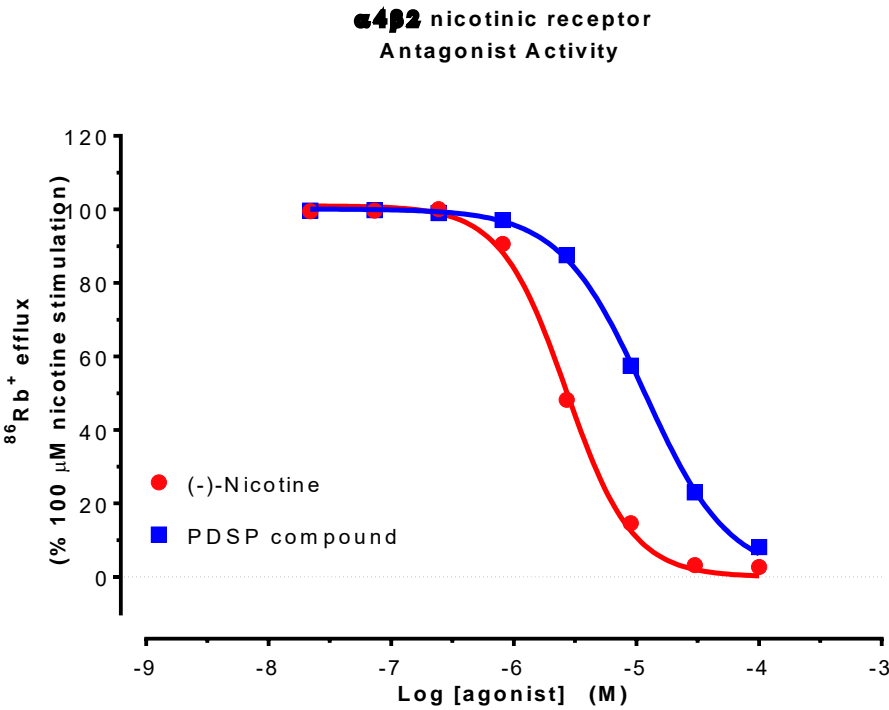
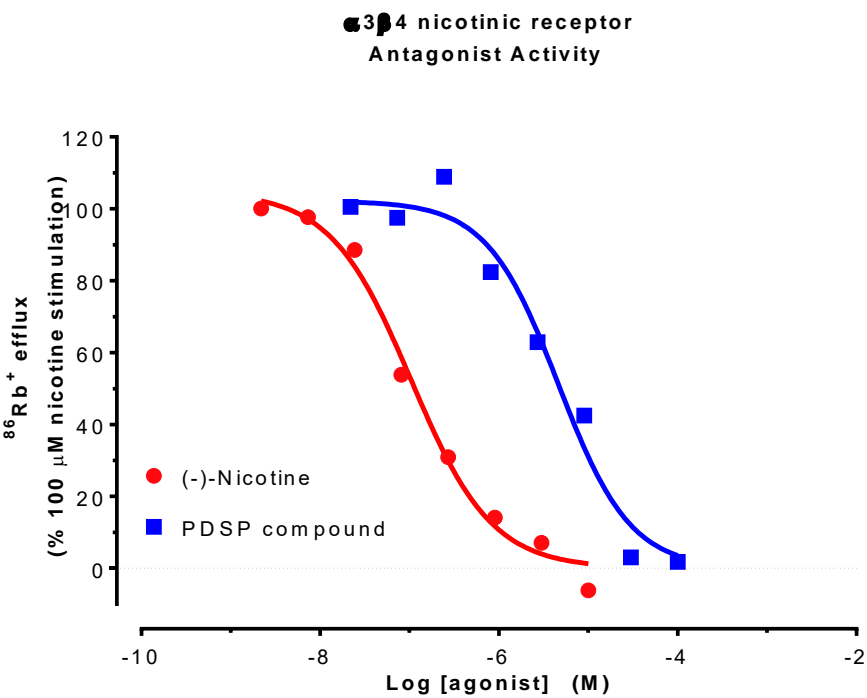


Table 34. Complete list of targets and corresponding available functional and radioligand binding assays at PDSP. ^3H or ^{125}I is for available radioligand binding assays. A checkmark (✓) indicates that the functional assay is available: G_q = Calcium mobilization or Inositol phosphate accumulation assay; G_i or G_s = split luciferase cAMP biosensor assay; β -arrestin = GPCR mediated arrestin translocation assay; “Other Assay” indicates target-specific assays as detailed in the main text as indicated in the specific section; “TBO” indicates assays under development or verification or optimization. Many assays can be developed upon request. BRET assays are being developed and will be made available for the PDSP when they are fully optimized.

*DREADD = Designer Receptors Exclusively Activated by Designer Drugs.

Target (Receptor name)	Available assays at PDSP (new system)					Note
	Binding	G_q	G_i or G_s	β -arrestin	BRET	
5-HT receptors						
5-HT _{1A}	3H		✓	✓		
5-HT _{1B}	3H		✓	✓		
5-HT _{1D}	3H		✓	✓		
5-HT _{1E}	3H		✓	✓		
5-HT _{1F}			✓	✓		
5-HT _{2A}	3H	✓		✓		
5-HT _{2B}	3H	✓		✓		
5-HT _{2C} (INI)	3H	✓		✓		
5-HT _{2C} (VGI)	3H	✓		✓		
5-HT _{2C} (VGV)	3H	✓		✓		
5-HT _{2C} (VNV)	3H	✓		✓		
5-HT _{2C} (VSV)	3H	✓		✓		
5-HT ₃	3H					
5-HT ₄	3H		✓	✓		
5-HT _{5A}	3H		✓	✓		
5-HT ₆	3H		✓	✓		
5-HT _{7A}	3H		✓	✓		
5-HT _{7B}						
5-HT _{7D}						
Acetylcholine (Muscarinic) receptors						
M ₁	3H	✓		✓		
M ₂	3H		✓	✓		
M ₃	3H	✓		✓		
M ₄	3H		✓	✓		

Target (Receptor name)	Available assays at PDSP (new system)					Note
	Binding	G _q	G _i or G _s	β-arrestin	BRET	
M ₅	3H	√		√		
Acetylcholine (Muscarinic) DREADDs						
M ₁ DREADD*	3H	√				DREADD
M ₂ DREADD	3H		√			DREADD
M ₃ DREADD	3H	√		√		DREADD
M ₄ DREADD	3H		√	√		DREADD
M ₅ DREADD	3H	√				DREADD
G _s DREADD	3H	√	√			DREADD
Adhesion class GPCRs						
ADGRA1						GPR123
ADGRA2						GPR124
ADGRA3						GPR125
ADGRB1						BAI1
ADGRB2						BAI2
ADGRB3						BAI3
CELSR1						ADGRC1
CELSR2						ADGRC2
CELSR3						ADGRC3
ADGRD1						GPR133
ADGRD2						GPR144
ADGRE1						EMR1
ADGRE2						EMR2
ADGRE3						EMR3
ADGRE4P						EMR4, GPR127
ADGRE5						CD97
ADGRF1						GPR110
ADGRF2						GPR111
ADGRF3						GPR113
ADGRF4						GPR115
ADGRF5						GPR116
ADGRG1						GPR56
ADGRG2						GPR64
ADGRG3						GPR97
ADGRG4						GPR112
ADGRG5						GPR114
ADGRG6						GPR126
ADGRG7						GPR128
ADGRL1						LPHN1
ADGRL2						LPHN2
ADGRL3						LPHN3
ADGRL4						ELTD1
ADGRV1						GPR98
Adrenergic receptors						

Target (Receptor name)	Available assays at PDSP (new system)					Note
	Binding	G _q	G _i or G _s	β-arrestin	BRET	
α _{1A}	3H	√		√		
α _{1B}	3H	√		√		
α _{1D}	3H	√		√		
α _{2A}	3H		√	√		
α _{2B}	3H		√	√		
α _{2C}	3H		√	√		
β ₁	125I		√	√		
β ₂	3H		√	√		
β ₃	125I		√	√		
Adenosine receptors						
A ₁	3H		√	√		
A _{2A}	3H		√	TBO		
Mouse A _{2A}	3H		√			
A _{2B}	3H		√	TBO		
A ₃	3H			TBO		
Angiotensin II receptors						
AT ₁	3H	√		√		
AT ₂	3H			TBO		
Apelin receptor						
Apelin				√		
Bile Acid receptors						
GPBA				√		
Bombesin receptors						
BB ₁		√		√		
BB ₂		√		√		
BB ₂ , mouse		√				
BB ₃		√		√		
Bradykinin receptors						
B ₁				√		
B ₂		√		√		
Calcitonin receptors						
CT				TBO		Calcitonin receptor
CT-like				TBO		CT-like receptor
Calcium sensing receptors						
CaS				√		
GPRC6				TBO		
Cannabinoid receptors						
CB ₁ (rat brain)	3H					
CB ₁	3H		√	√		
CB ₂	3H		√	√		
GPR18				TBO		Orphan
GPR55				√		Orphan

Target (Receptor name)	Available assays at PDSP (new system)					Note
	Binding	G _q	G _i or G _s	β-arrestin	BRET	
GPR119				TBO		Orphan
Chemokine receptors						
CCR1				TBO		
CCR2				TBO		
CCR3				TBO		
CCR4				√		
CCR5				TBO		
CCR6				√		
CCR7				TBO		
CCR8				TBO		
CCR9				TBO		
CCR10				TBO		
CXCR1				√		
CXCR2				√		
CXCR3				TBO		
CXCR4				√		
CXCR5				TBO		
CXCR6				√		
ACKR3				√		CXCR7, CMKOR1, GPR159
CX ₃ CR1				√		
XCR1						
CCRL1						
CCRL2						
Cholecystokinin receptors						
CCK1		√		√		
CCK2		√		TBO		
Complement peptide receptors						
C3a				√		
C5a1				TBO		
C5a2				TBO		
Corticotropin-releasing factor receptors						
CRF ₁	3H		√	TBO		CRHR1
CRF ₂	3H		√	TBO		CRHR2
Dopamine receptors						
D ₁	3H		√	√		
D ₂	3H		√	√		
D ₃	3H		TBO	√		
D ₄	3H		√	√		
D ₅	3H		√	√		
Endothelin receptors						
ET _A				√		

Target (Receptor name)	Available assays at PDSP (new system)					Note
	Binding	G _q	G _i or G _s	β-arrestin	BRET	
ET _B				TBO		
Estrogen receptor						
GPER				TBO		
Formylpeptide receptors						
FPR1				√		
FPR2/ALX				√		
FPR3				√		
Free fatty acid receptors						
FFA1		√		√		
FFA2				TBO		
FFA3				TBO		
FFA4				√		GPR120
GPR42				TBO		Orphan
Frizzled receptors						
FZD1						
FZD2						
FZD3						
FZD4						
FZD5						
FZD6						
FZD7						
FZD8						
FZD9						
FZD10						
SMO	3H					
GABAB receptors						
GABAB1						
GABAB2						
Galanin receptors						
GAL ₁				√		
GAL ₂				√		
GAL ₃				√		
Ghrelin receptor						
Ghrelin	3H	√		√		
Glucagon receptors						
GHRH				√		
GIP						
GLP-1			√	√		
GLP-2				TBO		
Glucagon				TBO		
Secretin				√		
Glycoprotein receptors						

Target (Receptor name)	Available assays at PDSP (new system)					Note
	Binding	G _q	G _i or G _s	β-arrestin	BRET	
FSH				TBO		
LH				TBO		
TSH				TBO		
Gonadotrophin-releasing hormone receptors						
GnRH ₁				√		
GnRH ₂				TBO		
Histamine receptors						
H ₁	3H	√		√		
H ₂	3H, 125I	√	√	√		
H ₃	3H		√	√		
H ₄	3H			√		
Hydroxycarboxylic acid receptors						
HCA ₁				TBO		GPR81
HCA ₂	3H		√	√		GPR109A
HCA ₃				TBO		GPR109B
Kisspeptin receptor						
Kisspeptin				TBO		
Leukotriene receptors						
BLT ₁				√		
BLT ₂				TBO		
CysLT ₁				√		
CysLT ₂				TBO		
OXE				TBO		
FRP2/ALX				√		
Lysophospholide (LAP) receptors						
LPA ₁				√		
LPA ₂				√		
LPA ₃				TBO		
LPA ₄				TBO		
LPA ₅				√		
LPA ₆				TBO		
Lysophospholipid (S1P) receptors						
S1P ₁				√		
S1P ₂				√		
S1P ₃				√		
S1P ₄				TBO		
S1P ₅				TBO		
Melanin-concentrating hormone receptors						
MCH ₁				√		
MCH ₂				√		
Melanocortin receptors						
MC ₁		√	√	√		
MC ₂				TBO		

Target (Receptor name)	Available assays at PDSP (new system)					Note
	Binding	G _q	G _i or G _s	β-arrestin	BRET	
MC ₃		√	√	TBO		
MC ₄			√	√		
MC ₅			√	√		
Melatonin receptors						
MT ₁			√	√		
MT ₂			√	√		
Metabotropic Glutamate receptors						
mGlu ₁	3H TBO	√		TBO		
mGlu ₂	3H		√	TBO		
mGlu ₃	3H		√	TBO		
mGlu ₄	3H TBO		√	TBO		
mGlu ₅	3H	√		TBO		
mGlu ₅ (rat brain)	3H		√			
mGlu ₆	3H		√	TBO		
mGlu ₇	3H TBO			TBO		
mGlu ₈	3H TBO		√	TBO		
Motilin receptor						
Motilin				√		
Neuromedin U receptors						
NMU1				√		
NMU2				√		
Neuropeptide FF receptors						
NPFF1				TBO		
NPFF2				TBO		
Neuropeptide S receptor						
NPS				√		
Neuropeptide W/Neuropeptide B receptor						
NPBW ₁			√	√		
NPBW ₂			√	√		
Neuropeptide Y receptors						
Y ₁				√		
Y ₂				√		
Y ₄				√		
Y ₅				TBO		
Y ₆				TBO		
Neurotensin receptors						
NTS1	3H	√		√		
NTS2	3H			√		
Opioid receptors						
δ (DOR)	3H		√	√		

Target (Receptor name)	Available assays at PDSP (new system)					Note
	Binding	G _q	G _i or G _s	β-arrestin	BRET	
κ (KOR)	3H		√	√		
μ (MOR)	3H		√	√		
NOP	3H		√	√		
MRGPRX1				√		Orphan
MRGPRX2		√		√		Orphan
MRGPRX3				TBO		Orphan
MRGPRX4		√		√		Orphan
Orexin receptors						
OX ₁				√		
OX ₂				√		
Oxoglutarate						
Oxoglutarate			√	TBO		
P2Y receptors						
P2Y ₁		√		√		
P2Y ₂		√		√		
P2Y ₄		√		√		
P2Y ₆		√		√		
P2Y ₈				TBO		Orphan
P2Y ₁₀				TBO		Orphan
P2Y ₁₁		√		√		
P2Y ₁₂				√		
P2Y ₁₃				√		
P2Y ₁₄				√		
Parathyroid hormone receptors						
PTH1				√		
PTH2				TBO		
QRFP receptor						
QRFP				√		GPR103
Platelet-activating factor receptor						
PAF	3H	√		√		
Prokineticin receptors						
PKR ₁				TBO		PROKR1 (GPR73a)
PKR ₂				TBO		PROKR2 (GPR73b)
Prolactin-releasing peptide receptor						
PrRP				TBO		GPR10
Prostanoid receptors						
DP ₁				TBO		PTGDR
DP ₂				√		PTGDR2
EP ₁	3H			√		PTGER1
EP ₂	3H			√		PTGER2
EP ₃	3H			√		PTGER3
EP ₄	3H			√		PTGER4

Target (Receptor name)	Available assays at PDSP (new system)					Note
	Binding	G _q	G _i or G _s	β-arrestin	BRET	
FP				√		PTGFR
IP1				√		PTGIR
TP			√	TBO		TBXA2R
Protease-activated receptors						
PAR ₁		√		TBO		
PAR ₂				TBO		
PAR ₃				TBO		
PAR ₄				TBO		
Relaxin family peptide receptors						
RXFP ₁			√	TBO		
RXFP ₂			√	TBO		
RXFP ₃			√	TBO		
RXFP ₄			√	TBO		
Somatostatin receptors						
SST ₁				√		
SST ₂				√		
SST ₃				√		
SST ₄				√		
SST ₅			√	√		
Succinate receptor						
Succinate				TBO		GPR91
Tachykinin receptors (Neurokinin receptors)						
NK ₁		√		√		
NK ₂		√		√		
NK ₃		√		√		
Thyrotropin-releasing hormone receptors						
TRH ₁				TBO		
TRH ₂				TBO		
Trace amine receptor						
TA ₁				√		
Urotensin receptor						
UT				√		
Vasopressin and Oxytocin receptors						
V _{1A}	3H	√		√		
V _{1B}	3H	√		√		
V ₂	3H	√		√		
OT	3H	√		√		
VIP and PACAP receptors						
PAC ₁				TBO		ADCYAP1R1
VPAC ₁				√		PVR2
VPAC ₂				√		VIPR1
Class A orphan GPCRs						
CMKLR1				√		

Target (Receptor name)	Available assays at PDSP (new system)					Note
	Binding	G _q	G _i or G _s	β-arrestin	BRET	
GPR1				TBO		
GPR3				TBO		
GPR4			√	TBO		
Mouse GPR4			TBO			
GPR6				TBO		
GPR12				TBO		
GPR15				TBO		
GPR17				TBO		
GPR18				TBO		
GPR19				TBO		
GPR20				TBO		
GPR21				TBO		
GPR22				TBO		
GPR25				TBO		
GPR26				TBO		
GPR27				TBO		
GPR31				TBO		
GPR32				TBO		
GPR33				TBO		
GPR34				TBO		
GPR35				√		
GPR37				TBO		
GPR37L1				TBO		
GPR39				√		
GPR42						FFAR1L
GPR45				TBO		
GPR50				TBO		
GPR52				TBO		
GPR55				√		
GPR61				TBO		
GPR62				TBO		
GPR63				TBO		
GPR65			√	TBO		
Mouse GPR65			TBO			
GPR68		√	√	TBO		
Mouse GPR68			TBO			
GPR75				TBO		
GPR78				TBO		
GPR79						
GPR82				TBO		
GPR83				TBO		
GPR84				TBO		
GPR85				TBO		

Target (Receptor name)	Available assays at PDSP (new system)					Note
	Binding	G _q	G _i or G _s	β-arrestin	BRET	
GPR87				TBO		
GPR88			√	TBO		
GPR101				TBO		
GPR119				TBO		
GPR132				TBO		
GPR135				TBO		
GPR139				TBO		
GPR141				TBO		
GPR142				TBO		
GPR146				TBO		
GPR148				TBO		
GPR149				TBO		
GPR150				TBO		
GPR151				TBO		
GPR152				TBO		
GPR153				TBO		
GPR156				TBO		
GPR157				TBO		
GPR158				TBO		
GPR160				TBO		
GPR161				TBO		
GPR162				TBO		
GPR171				TBO		
GPR173				TBO		
GPR174				TBO		
GPR176				TBO		
GPR182				TBO		
GPR183				TBO		EBI2
LGR4						GPR48
LGR5						GPR49
LGR6						
MAS1				√		
MAS1L				TBO		
MRGPRD				TBO		
MRGPRE				TBO		
MRGPRF				TBO		
MRGPRG				TBO		
MRGPRX1				√		
MRGPRX2		√		√		
MRGPRX3				TBO		
MRGPRX4		√		√		
P2RY8				TBO		
P2RY10				TBO		

Target (Receptor name)	Available assays at PDSP (new system)					Note
	Binding	G _q	G _i or G _s	β-arrestin	BRET	
TAAR2				TBO		GPR58
TAAR3						GPR57
TAAR4P						
TAAR5				TBO		
TAAR6				TBO		
TAAR8				TBO		GPR102
TAAR9				TBO		
Class B orphan GPCRs						
GPR56				TBO		
GPR64				TBO		
GPR97				TBO		
GPR110				TBO		
GPR113				TBO		
GPR114				TBO		
GPR115				TBO		
GPR116				TBO		
GPR123				TBO		
GPR124				TBO		
GPR125				TBO		
GPR126				TBO		
GPR128				TBO		
GPR133				TBO		
GPR144				TBO		
GPR157				TBO		
Class C orphan GPCRs						
GPR156				TBO		
GPR158				TBO		
GPRC5A				TBO		
GPRC5B				TBO		
GPRC5C				TBO		
GPRC5D				TBO		
GPRC6A				TBO		
Opsin receptors						
OPN1LW						
OPN1MW						
OPN1SW						
Rhodopsin						
OPN3				TBO		
OPN4						
OPN5				TBO		GPR136
Other 7TM receptors						

Target (Receptor name)	Available assays at PDSP (new system)					Note
	Binding	G _q	G _i or G _s	β-arrestin	BRET	
GPR107						
GPR137						
OR51E1						GPR136/GPR164
TPRA1						GPR175
GPR143				TBO		
GPR157						

Table 34. PDSP targets other than 7-TMs.

Other targets	Binding	Functional assays	Note
nAChRs			
$\alpha 2\beta 2$	3H	($^{86}\text{Rb}^+$ efflux assay)	Section 2.17 Assays conducted at PDSP subcontractor Georgetown Univ.
$\alpha 2\beta 4$	3H		
$\alpha 3\beta 2$	3H		
$\alpha 3\beta 4$	3H	($^{86}\text{Rb}^+$ efflux assay)	
$\alpha 4\beta 2$	3H	($^{86}\text{Rb}^+$ efflux assay)	
$\alpha 4\beta 4$	3H		
$\alpha 4\beta 2$ (Rat Brain)	3H		
$\alpha 2\beta 2$	3H		
$\alpha 7$	3H		
Imidazoline receptors			
I1 (rat brain)	3H		
I2 (rat brain)	3H		
GABA channels			
GABAA $\alpha 1$	3H, BZP		
GABAA $\alpha 2$	3H, BZP		
GABAA $\alpha 3$	3H, BZP		
GABAA $\alpha 5$	3H, BZP		
GABAA $\alpha 6$	3H, BZP		
GABAA (rat brain)	3H, BZP		
GABAB (rat brain)	3H		
Ion channels			
hERG K+	3H	Tl ⁺ Flux and PatchXpress	Section 2.9 Section 2.10
Ca ²⁺ (rat brain)	3H		
Cav1.2, human	3H		
Na ⁺ site II	3H		
Transporters			
DAT	3H	Neurotransmitter Transporter assay	Section 2.11
NET	3H		
SAT	3H		
VMAT1			
VMAT2	3H		
Sigma receptors			
Sigma 1 (Guinea Pig)	3H		
Sigma 1, human	3H		
Sigma 2 (PC12)	3H		
Sigma 2, human	3H		
Glutamate channels			

Other targets	Binding	Functional assays	Note
NMDA (rat brain)	3H		
AMPA (rat brain)	3H		
PCP (rat brain)	3H		
Kainate (rat brain)	3H		
NR1 (rat brain)	3H		
NR2B (rat brain)	3H		
Other targets			
MDR1		(Caco-2)	
PKC α	3H	Fluorimetric, Omnia Ser/Thr Recombinant assay kits from Invitrogen	Section 2.15
PKC β I	3H		
PKC β II	3H		
PKC γ	3H		
PKC δ	3H		
PKC ϵ	3H		
PKC η			
PKC ζ			
PKC τ			
CHK2		Fluorimetric, Omnia Ser/Thr Recombinant assay kits from Invitrogen	
PBR (rat brain)	3H		
HDAC		Fluorimetric, BioMol Fluor de Lys assay	Section 2.13
MAO A		Fluorimetric, MAO detection kit	Section 2.14
MAO B		Fluorimetric, MAO detection kit	

Bibliography

1. Jordan M, Schallhorn A, Wurm FM (1996) Transfecting mammalian cells: optimization of critical parameters affecting calcium-phosphate precipitate formation. *Nucleic Acids Res* 24(4):596–601.
2. Subedi GP, Johnson RW, Moniz HA, Moremen KW, Barb A (2015) High Yield Expression of Recombinant Human Proteins with the Transient Transfection of HEK293 Cells in Suspension. *J Vis Exp* (106):e53568.
3. Cervera L, et al. (2015) Selection and optimization of transfection enhancer additives for increased virus-like particle production in HEK293 suspension cell cultures. *Appl Microbiol Biotechnol* 99(23):9935–9949.
4. Chiu J, et al. (1999) Chronic ethanol exposure alters MK-801 binding sites in the cerebral cortex of the near-term fetal guinea pig. *Alcohol* 17(3):215–221.
5. Xiao Y, et al. (1998) Rat alpha3/beta4 subtype of neuronal nicotinic acetylcholine receptor stably expressed in a transfected cell line: pharmacology of ligand binding and function. *Mol Pharmacol* 54(2):322–333.
6. Xiao Y, et al. (2006) Sazetidine-A, a novel ligand that desensitizes alpha4beta2 nicotinic acetylcholine receptors without activating them. *Mol Pharmacol* 70(4):1454–1460.
7. Cheng Y, Prusoff WH (1973) Relationship between the inhibition constant (K₁) and the concentration of inhibitor which causes 50 per cent inhibition (I₅₀) of an enzymatic reaction. *Biochem Pharmacol* 22(23):3099–3108.
8. Khawaja X, Ennis C, Minchin MC (1997) Pharmacological characterization of recombinant human 5-hydroxytryptamine_{1A} receptors using a novel antagonist radioligand, [³H]WAY-100635. *Life Sci* 60(9):653–665.
9. Satała G, Duszyńska B, Lenda T, Nowak G, Bojarski AJ (2017) Allosteric Inhibition of Serotonin 5-HT₇ Receptors by Zinc Ions. *Mol Neurobiol*.
10. Andressen KW, et al. (2017) Related GPCRs couple differently to G_s: preassociation between G protein and 5-HT₇ serotonin receptor reveals movement of G_{as} upon receptor activation. *FASEB J*.
11. Middlemiss DN, Fozard JR (1983) 8-Hydroxy-2-(di-n-propylamino)-tetralin discriminates between subtypes of the 5-HT₁ recognition site. *Eur J Pharmacol* 90(1):151–153.
12. Middlemiss DN (1984) Stereoselective blockade at [³H]5-HT binding sites and at the 5-HT autoreceptor by propranolol. *Eur J Pharmacol* 101(3-4):289–293.
13. Piñeyro G, Castanon N, Hen R, Blier P (1995) Regulation of [³H]5-HT release in raphe, frontal cortex and hippocampus of 5-HT_{1B} knock-out mice. *Neuroreport* 7(1):353–359.

14. Hoyer D, Engel G, Kalkman HO (1985) Molecular pharmacology of 5-HT₁ and 5-HT₂ recognition sites in rat and pig brain membranes: radioligand binding studies with [³H]5-HT, [³H]8-OH-DPAT, (-)[¹²⁵I]iodocyanopindolol, [³H]mesulergine and [³H]ketanserin. *Eur J Pharmacol* 118(1-2):13–23.
15. Schiller L, Donix M, Jähkel M, Oehler J (2006) Serotonin 1A and 2A receptor densities, neurochemical and behavioural characteristics in two closely related mice strains after long-term isolation. *Prog Neuropsychopharmacol Biol Psychiatry* 30(3):492–503.
16. Ueki T, et al. (2015) Yokukansan, a traditional Japanese medicine, decreases head-twitch behaviors and serotonin 2A receptors in the prefrontal cortex of isolation-stressed mice. *J Ethnopharmacol* 166:23–30.
17. Rashid M, et al. (2003) Identification of the binding sites and selectivity of sarpogrelate, a novel 5-HT₂ antagonist, to human 5-HT_{2A}, 5-HT_{2B} and 5-HT_{2C} receptor subtypes by molecular modeling. *Life Sci* 73(2):193–207.
18. Stain-Malmgren R, Kjellman BF, Aberg-Wistedt A (1998) Platelet serotonergic functions and light therapy in seasonal affective disorder. *Psychiatry Res* 78(3):163–172.
19. Riccioni T, et al. (2011) ST1936 stimulates cAMP, Ca²⁺, ERK1/2 and Fyn kinase through a full activation of cloned human 5-HT₆ receptors. *Eur J Pharmacol* 661(1-3):8–14.
20. Fitzgerald LW, et al. (1999) High-affinity agonist binding correlates with efficacy (intrinsic activity) at the human serotonin 5-HT_{2A} and 5-HT_{2C} receptors: evidence favoring the ternary complex and two-state models of agonist action. *J Neurochem* 72(5):2127–2134.
21. Van Wijngaarden I, Tulp MT, Soudijn W (1990) The concept of selectivity in 5-HT receptor research. *Eur J Pharmacol* 188(6):301–312.
22. Wong EH, Bonhaus DW, Wu I, Stefanich E, Eglen RM (1993) Labelling of 5-hydroxytryptamine₃ receptors with a novel 5-HT₃ receptor ligand, [³H]RS-42358-197. *J Neurochem* 60(3):921–930.
23. Van den Wyngaert I, et al. (1997) Cloning and expression of a human serotonin 5-HT₄ receptor cDNA. *J Neurochem* 69(5):1810–1819.
24. Mialet J, et al. (2000) Exploration of the ligand binding site of the human 5-HT₄ receptor by site-directed mutagenesis and molecular modeling. *Br J Pharmacol* 130(3):527–538.
25. Bender E, et al. (2000) Structure of the human serotonin 5-HT₄ receptor gene and cloning of a novel 5-HT₄ splice variant. *J Neurochem* 74(2):478–489.
26. Dalwadi DA, et al. (2016) Molecular mechanisms of serotonergic action of the HIV-1 antiretroviral efavirenz. *Pharmacol Res* 110:10–24.

27. Bach T, et al. (2001) 5HT₄(a) and 5-HT₄(b) receptors have nearly identical pharmacology and are both expressed in human atrium and ventricle. *Naunyn Schmiedebergs Arch Pharmacol* 363(2):146–160.
28. Grailhe R, Grabtree GW, Hen R (2001) Human 5-HT(5) receptors: the 5-HT(5A) receptor is functional but the 5-HT(5B) receptor was lost during mammalian evolution. *Eur J Pharmacol* 418(3):157–167.
29. Matthes H, et al. (1993) Mouse 5-hydroxytryptamine_{5A} and 5-hydroxytryptamine_{5B} receptors define a new family of serotonin receptors: cloning, functional expression, and chromosomal localization. *Mol Pharmacol* 43(3):313–319.
30. Boess FG, Monsma FJ, Meyer V, Zwingelstein C, Sleight AJ (1997) Interaction of tryptamine and ergoline compounds with threonine 196 in the ligand binding site of the 5-hydroxytryptamine₆ receptor. *Mol Pharmacol* 52(3):515–523.
31. Stam NJ, et al. (1997) Human serotonin 5-HT₇ receptor: cloning and pharmacological characterisation of two receptor variants. *FEBS Lett* 413(3):489–494.
32. Peralta EG, et al. (1987) Distinct primary structures, ligand-binding properties and tissue-specific expression of four human muscarinic acetylcholine receptors. *EMBO J* 6(13):3923–3929.
33. Christopoulos A, Wilson K (2001) Interaction of anandamide with the M₁ and M₄ muscarinic acetylcholine receptors. *Brain Res* 915(1):70–78.
34. Cembala TM, Sherwin JD, Tidmarsh MD, Appadu BL, Lambert DG (1998) Interaction of neuromuscular blocking drugs with recombinant human m₁-m₅ muscarinic receptors expressed in Chinese hamster ovary cells. *Br J Pharmacol* 125(5):1088–1094.
35. Christopoulos A, Pierce TL, Sorman JL, El-Fakahany EE (1998) On the unique binding and activating properties of xanomeline at the M₁ muscarinic acetylcholine receptor. *Mol Pharmacol* 53(6):1120–1130.
36. Chen X, et al. (2015) The first structure-activity relationship studies for designer receptors exclusively activated by designer drugs. *ACS Chem Neurosci* 6(3):476–484.
37. Armbruster BN, Li X, Pausch MH, Herlitze S, Roth BL (2007) Evolving the lock to fit the key to create a family of G protein-coupled receptors potently activated by an inert ligand. *Proc Natl Acad Sci USA* 104(12):5163–5168.
38. Nawaratne V, et al. (2008) New insights into the function of M₄ muscarinic acetylcholine receptors gained using a novel allosteric modulator and a DREADD (designer receptor exclusively activated by a designer drug). *Mol Pharmacol* 74(4):1119–1131.
39. Wang SZ, el-Fakahany EE (1993) Application of transfected cell lines in studies of functional receptor subtype selectivity of muscarinic agonists. *J Pharmacol Exp Ther* 266(1):237–243.

40. Dalpiaz A, Townsend-Nicholson A, Beukers MW, Schofield PR, IJzerman AP (1998) Thermodynamics of full agonist, partial agonist, and antagonist binding to wild-type and mutant adenosine A1 receptors. *Biochem Pharmacol* 56(11):1437–1445.
41. Townsend-Nicholson A, Schofield PR (1994) A threonine residue in the seventh transmembrane domain of the human A1 adenosine receptor mediates specific agonist binding. *J Biol Chem* 269(4):2373–2376.
42. Gao ZG, Jiang Q, Jacobson KA, IJzerman AP (2000) Site-directed mutagenesis studies of human A(2A) adenosine receptors: involvement of glu(13) and his(278) in ligand binding and sodium modulation. *Biochem Pharmacol* 60(5):661–668.
43. Alexander SP, Millns PJ (2001) [(3)H]ZM241385--an antagonist radioligand for adenosine A(2A) receptors in rat brain. *Eur J Pharmacol* 411(3):205–210.
44. Noguchi H, Muraoka R, Kigoshi S, Muramatsu I (1995) Pharmacological characterization of alpha 1-adrenoceptor subtypes in rat heart: a binding study. *Br J Pharmacol* 114(5):1026–1030.
45. Oshita M, Kigoshi S, Muramatsu I (1991) Three distinct binding sites for [3H]-prazosin in the rat cerebral cortex. *Br J Pharmacol* 104(4):961–965.
46. Chiesa IJ, Castillo LF, Lüthy IA (2008) Contribution of alpha2-adrenoceptors to the mitogenic effect of catecholestrogen in human breast cancer MCF-7 cells. *J Steroid Biochem Mol Biol* 110(1-2):170–175.
47. Nakagawa T, et al. (2012) Yokukansan inhibits morphine tolerance and physical dependence in mice: the role of α_2 A-adrenoceptor. *Neuroscience* 227:336–349.
48. Perry BD, U'Prichard DC (1981) [3H]rauwolscine (alpha-yohimbine): a specific antagonist radioligand for brain alpha 2-adrenergic receptors. *Eur J Pharmacol* 76(4):461–464.
49. Casale TB, Hart JE (1987) (-)[125I]pindolol binding to human peripheral lung beta-receptors. *Biochem Pharmacol* 36(15):2557–2564.
50. Koike K, Takayanagi I (1997) Characteristics of [3H]CGP12177 binding sites at beta 2- and beta 3-adrenoceptors in the guinea pig taenia caecum. *Gen Pharmacol* 28(1):73–76.
51. Joseph SS, Lynham JA, Colledge WH, Kaumann AJ (2004) Binding of (-)-[3H]-CGP12177 at two sites in recombinant human beta 1-adrenoceptors and interaction with beta-blockers. *Naunyn Schmiedebergs Arch Pharmacol* 369(5):525–532.
52. Tsuchihashi H, Yokoyama H, Nagatomo T (1989) Binding characteristics of 3H-CGP12177 to beta-adrenoceptors in rat myocardial membranes. *Jpn J Pharmacol* 49(1):11–19.
53. Showalter VM, Compton DR, Martin BR, Abood ME (1996) Evaluation of binding in a transfected cell line expressing a peripheral cannabinoid receptor (CB2): identification of cannabinoid receptor subtype selective ligands. *J Pharmacol Exp Ther* 278(3):989–999.

54. Ross RA, et al. (1999) Agonist-inverse agonist characterization at CB1 and CB2 cannabinoid receptors of L759633, L759656, and AM630. *Br J Pharmacol* 126(3):665–672.
55. Ross RA, et al. (1998) Comparison of cannabinoid binding sites in guinea-pig forebrain and small intestine. *Br J Pharmacol* 125(6):1345–1351.
56. Zhou QY, et al. (1990) Cloning and expression of human and rat D1 dopamine receptors. *Nature* 347(6288):76–80.
57. Hall H, Wedel I, Halldin C, Kopp J, Farde L (1990) Comparison of the in vitro receptor binding properties of N-[3H]methylspiperone and [3H]raclopride to rat and human brain membranes. *J Neurochem* 55(6):2048–2057.
58. Schmiege N, et al. (2016) Dysbindin-1 modifies signaling and cellular localization of recombinant, human D₃ and D₂ receptors. *J Neurochem* 136(5):1037–1051.
59. Ricci A, Amenta F (1994) Dopamine D5 receptors in human peripheral blood lymphocytes: a radioligand binding study. *J Neuroimmunol* 53(1):1–7.
60. De Backer MD, Loonen I, Verhasselt P, Neefs JM, Luyten WH (1998) Structure of the human histamine H1 receptor gene. *Biochem J* 335 (Pt 3):663–670.
61. Moguilevsky N, et al. (1994) Stable expression of human H1-histamine-receptor cDNA in Chinese hamster ovary cells. Pharmacological characterisation of the protein, tissue distribution of messenger RNA and chromosomal localisation of the gene. *Eur J Biochem* 224(2):489–495.
62. Kühn B, Schmid A, Harteneck C, Gudermann T, Schultz G (1996) G proteins of the Gq family couple the H2 histamine receptor to phospholipase C. *Mol Endocrinol* 10(12):1697–1707.
63. Chen J, Liu C, Lovenberg TW (2003) Molecular and pharmacological characterization of the mouse histamine H3 receptor. *Eur J Pharmacol* 467(1-3):57–65.
64. Gbahou F, et al. (2006) Compared pharmacology of human histamine H3 and H4 receptors: structure-activity relationships of histamine derivatives. *Br J Pharmacol* 147(7):744–754.
65. Liu C, Wilson SJ, Kuei C, Lovenberg TW (2001) Comparison of human, mouse, rat, and guinea pig histamine H4 receptors reveals substantial pharmacological species variation. *J Pharmacol Exp Ther* 299(1):121–130.
66. Hong WC, Amara SG (2010) Membrane cholesterol modulates the outward facing conformation of the dopamine transporter and alters cocaine binding. *J Biol Chem* 285(42):32616–32626.
67. Soucy JP, Mrini A, Lafaille F, Doucet G, Descarries L (1997) Comparative evaluation of [3H]WIN 35428 and [3H]GBR 12935 as markers of dopamine innervation density in brain. *Synapse* 25(2):163–175.

68. Tejani-Butt SM, Brunswick DJ, Frazer A (1990) [3H]nisoxetine: a new radioligand for norepinephrine uptake sites in brain. *Eur J Pharmacol* 191(2):239–243.
69. Wersinger C, Jeannotte A, Sidhu A (2006) Attenuation of the norepinephrine transporter activity and trafficking via interactions with alpha-synuclein. *Eur J Neurosci* 24(11):3141–3152.
70. D’Amato RJ, Largent BL, Snowman AM, Snyder SH (1987) Selective labeling of serotonin uptake sites in rat brain by [3H]citalopram contrasted to labeling of multiple sites by [3H]imipramine. *J Pharmacol Exp Ther* 242(1):364–371.
71. Tsuruda PR, et al. (2010) Influence of ligand binding kinetics on functional inhibition of human recombinant serotonin and norepinephrine transporters. *J Pharmacol Toxicol Methods* 61(2):192–204.
72. Barrett RW, Vaught JL (1983) Evaluation of the interactions of mu and delta selective ligands with [3H]D-Ala2-D-Leu5-enkephalin binding to mouse brain membranes. *Life Sci* 33(24):2439–2448.
73. Akiyama K, Gee KW, Mosberg HI, Hruby VJ, Yamamura HI (1985) Characterization of [3H][2-D-penicillamine, 5-D-penicillamine]-enkephalin binding to delta opiate receptors in the rat brain and neuroblastoma--glioma hybrid cell line (NG 108-15). *Proc Natl Acad Sci USA* 82(8):2543–2547.
74. Meng F, et al. (1993) Cloning and pharmacological characterization of a rat kappa opioid receptor. *Proc Natl Acad Sci USA* 90(21):9954–9958.
75. Lahti RA, Mickelson MM, McCall JM, Von Voigtlander PF (1985) [3H]U-69593 a highly selective ligand for the opioid kappa receptor. *Eur J Pharmacol* 109(2):281–284.
76. Page KJ, et al. (2000) Effects of systemic 3-nitropropionic acid-induced lesions of the dorsal striatum on cannabinoid and mu-opioid receptor binding in the basal ganglia. *Exp Brain Res* 130(2):142–150.
77. Raynor K, et al. (1994) Pharmacological characterization of the cloned kappa-, delta-, and mu-opioid receptors. *Mol Pharmacol* 45(2):330–334.
78. Mollereau C, Moisand C, Butour JL, Parmentier M, Meunier JC (1996) Replacement of Gln280 by His in TM6 of the human ORL1 receptor increases affinity but reduces intrinsic activity of opioids. *FEBS Lett* 395(1):17–21.
79. Dooley CT, et al. (1997) Binding and in vitro activities of peptides with high affinity for the nociceptin/orphanin FQ receptor, ORL1. *J Pharmacol Exp Ther* 283(2):735–741.
80. Wise A, et al. (2003) Molecular identification of high and low affinity receptors for nicotinic acid. *J Biol Chem* 278(11):9869–9874.
81. Soga T, et al. (2003) Molecular identification of nicotinic acid receptor. *Biochem Biophys Res Commun* 303(1):364–369.

82. Tunaru S, et al. (2003) PUMA-G and HM74 are receptors for nicotinic acid and mediate its anti-lipolytic effect. *Nat Med* 9(3):352–355.
83. Jasper JR, Harrell CM, O'Brien JA, Pettibone DJ (1995) Characterization of the human oxytocin receptor stably expressed in 293 human embryonic kidney cells. *Life Sci* 57(24):2253–2261.
84. Kimura T, et al. (1994) Molecular characterization of a cloned human oxytocin receptor. *Eur J Endocrinol* 131(4):385–390.
85. Fuchs AR, Fuchs F, Husslein P, Soloff MS, Fernström MJ (1982) Oxytocin receptors and human parturition: a dual role for oxytocin in the initiation of labor. *Science* (80-) 215(4538):1396–1398.
86. Chini B, et al. (1995) Tyr115 is the key residue for determining agonist selectivity in the V1a vasopressin receptor. *EMBO J* 14(10):2176–2182.
87. Tahara A, et al. (1998) Pharmacological characterization of the human vasopressin receptor subtypes stably expressed in Chinese hamster ovary cells. *Br J Pharmacol* 125(7):1463–1470.
88. Wang C, et al. (2013) Structure of the human smoothened receptor bound to an antitumour agent. *Nature* 497(7449):338–343.
89. Wang C, et al. (2014) Structural basis for Smoothened receptor modulation and chemoresistance to anticancer drugs. *Nat Commun* 5:4355.
90. Wilson RJ, et al. (2006) GW627368X ((N-{2-[4-(4,9-diethoxy-1-oxo-1,3-dihydro-2H-benzo[f]isoindol-2-yl)phenyl]acetyl} benzene sulphonamide): a novel, potent and selective prostanoid EP4 receptor antagonist. *Br J Pharmacol* 148(3):326–339.
91. Abramovitz M, et al. (2000) The utilization of recombinant prostanoid receptors to determine the affinities and selectivities of prostaglandins and related analogs. *Biochim Biophys Acta* 1483(2):285–293.
92. Lewin NE, Blumberg PM (2003) [3H]Phorbol 12,13-dibutyrate binding assay for protein kinase C and related proteins. *Methods Mol Biol* 233:129–156.
93. Johnson MS, Simpson J, Mitchell R (1996) Effect of phorbol 12, 13-dibutyrate on ligand binding, enzyme activity and translocation of protein kinase C isoforms in the alpha T3-1 gonadotrope-derived cell line. *Mol Cell Biochem* 165(1):65–75.
94. Parent A, Dea D, Quirion R, Poirier J (1993) [3H]phorbol ester binding sites and neuronal plasticity in the hippocampus following entorhinal cortex lesions. *Brain Res* 607(1-2):23–32.
95. Papadopoulos V, Guarneri P, Kreuger KE, Guidotti A, Costa E (1992) Pregnenolone biosynthesis in C6-2B glioma cell mitochondria: regulation by a mitochondrial diazepam binding inhibitor receptor. *Proc Natl Acad Sci USA* 89(11):5113–5117.

96. Benavides J, et al. (1984) Characterization of peripheral type benzodiazepine binding sites in human and rat platelets by using [3H]PK 11195. Studies in hypertensive patients. *Biochem Pharmacol* 33(15):2467–2472.
97. Agey MW, Dunn SM (1989) Kinetics of [3H]muscimol binding to the GABAA receptor in bovine brain membranes. *Biochemistry* 28(10):4200–4208.
98. Nadler LS, Raetzman LT, Dunkle KL, Mueller N, Siegel RE (1996) GABAA receptor subunit expression and assembly in cultured rat cerebellar granule neurons. *Brain Res Dev Brain Res* 97(2):216–225.
99. Chang RS, Snyder SH (1978) Benzodiazepine receptors: labeling in intact animals with [3H] flunitrazepam. *Eur J Pharmacol* 48(2):213–218.
100. Sieghart W, Mayer A, Drexler G (1983) Properties of [3H]flunitrazepam binding to different benzodiazepine binding proteins. *Eur J Pharmacol* 88(4):291–299.
101. Reynolds IJ, Miller RJ (1988) [3H]MK801 binding to the NMDA receptor/ionophore complex is regulated by divalent cations: evidence for multiple regulatory sites. *Eur J Pharmacol* 151(1):103–112.
102. Reynolds IJ, Miller RJ (1988) [3H]MK801 binding to the N-methyl-D-aspartate receptor reveals drug interactions with the zinc and magnesium binding sites. *J Pharmacol Exp Ther* 247(3):1025–1031.
103. Reynolds IJ (2001) [3H](+)-MK801 radioligand binding assay at the N-methyl-D-aspartate receptor. *Curr Protoc Pharmacol* Chapter 1:Unit 1.20.
104. Basham ME, Sohrabji F, Singh TD, Nordeen EJ, Nordeen KW (1999) Developmental regulation of NMDA receptor 2B subunit mRNA and ifenprodil binding in the zebra finch anterior forebrain. *J Neurobiol* 39(2):155–167.
105. Höfner G, Wanner KT (2000) [3H]ifenprodil binding to NMDA receptors in porcine hippocampal brain membranes. *Eur J Pharmacol* 394(2-3):211–219.
106. Hashimoto K, London ED (1993) Further characterization of [3H]ifenprodil binding to sigma receptors in rat brain. *Eur J Pharmacol* 236(1):159–163.
107. Kawakami Z, et al. (2009) Neuroprotective effects of yokukansan, a traditional Japanese medicine, on glutamate-mediated excitotoxicity in cultured cells. *Neuroscience* 159(4):1397–1407.
108. Miralles A, Olmos G (1989) [3H]kainic acid binding sites in chick cerebellar membranes. *Comparative Biochemistry and Physiology Part C: Comparative Pharmacology* 93(2):321–325.
109. Crawford N, Lang TK, Kerr DS, de Vries DJ (1999) High-affinity [3H] kainic acid binding to brain membranes: a re-evaluation of ligand potency and selectivity. *J Pharmacol Toxicol Methods* 42(3):121–125.

110. Ornstein PL, et al. (1998) [3H]LY341495, a highly potent, selective and novel radioligand for labeling Group II metabotropic glutamate receptors. *Bioorg Med Chem Lett* 8(14):1919–1922.
111. Wright RA, Arnold MB, Wheeler WJ, Ornstein PL, Schoepp DD (2001) [3H]LY341495 binding to group II metabotropic glutamate receptors in rat brain. *J Pharmacol Exp Ther* 298(2):453–460.
112. Monn JA, et al. (2007) Synthesis and metabotropic glutamate receptor activity of S-oxidized variants of (-)-4-amino-2-thiabicyclo-[3.1.0]hexane-4,6-dicarboxylate: identification of potent, selective, and orally bioavailable agonists for mGlu2/3 receptors. *J Med Chem* 50(2):233–240.
113. Malherbe P, et al. (2003) Mutational analysis and molecular modeling of the binding pocket of the metabotropic glutamate 5 receptor negative modulator 2-methyl-6-(phenylethynyl)-pyridine. *Mol Pharmacol* 64(4):823–832.
114. Wright RA, Arnold MB, Wheeler WJ, Ornstein PL, Schoepp DD (2000) Binding of [3H](2S,1'S,2'S)-2-(9-xanthylmethyl)-2-(2'-carboxycyclopropyl) glycine ([3H]LY341495) to cell membranes expressing recombinant human group III metabotropic glutamate receptor subtypes. *Naunyn Schmiedebergs Arch Pharmacol* 362(6):546–554.
115. Sguazzini E, Schmidt HR, Iyer KA, Kruse AC, Dukat M (2017) Reevaluation of fenpropimorph as a σ receptor ligand: Structure-affinity relationship studies at human σ 1 receptors. *Bioorg Med Chem Lett* 27(13):2912–2919.
116. Alon A, et al. (2017) Identification of the gene that codes for the σ 2 receptor. *Proc Natl Acad Sci USA* 114(27):7160–7165.
117. Schmidt HR, et al. (2016) Crystal structure of the human σ 1 receptor. *Nature* 532(7600):527–530.
118. Pelet C, Mironneau C, Rakotoarisoa L, Neuilly G (1995) Angiotensin II receptor subtypes and contractile responses in portal vein smooth muscle. *Eur J Pharmacol* 279(1):15–24.
119. Widdowson PS, Renouard A, Vilaine JP (1993) Binding of [3H]angiotensin II and [3H]DuP 753 (Losartan) to rat liver homogenates reveals multiple sites. Relationship to AT1a- and AT1b-type angiotensin receptors and novel nonangiotensin binding sites. *Peptides* 14(4):829–837.
120. Lahti RA, Cochrane EV, Roberts RC, Conley RR, Tamminga CA (1998) [3H]Neurotensin receptor densities in human postmortem brain tissue obtained from normal and schizophrenic persons. An autoradiographic study. *J Neural Transm* 105(4-5):507–516.
121. Schotte A, Leysen JE, Laduron PM (1986) Evidence for a displaceable non-specific [3H]neurotensin binding site in rat brain. *Naunyn Schmiedebergs Arch Pharmacol* 333(4):400–405.
122. Kanba KS, Kanba S, Okazaki H, Richelson E (1986) Binding of [3H]neurotensin in human brain: properties and distribution. *J Neurochem* 46(3):946–952.

123. Zucker M, Weizman A, Rehavi M (2001) Characterization of high-affinity [3H]TBZOH binding to the human platelet vesicular monoamine transporter. *Life Sci* 69(19):2311–2317.
124. Rampe D, Kim HS, Lacerda AE, Birnbaumer L, Brown AM (1990) [3H]PN200-110 binding in a fibroblast cell line transformed with the alpha 1 subunit of the skeletal muscle L-type Ca²⁺ channel. *Biochem Biophys Res Commun* 169(3):825–831.
125. Striessnig J, Murphy BJ, Catterall WA (1991) Dihydropyridine receptor of L-type Ca²⁺ channels: identification of binding domains for [3H](+)-PN200-110 and [3H]azidopine within the alpha 1 subunit. *Proc Natl Acad Sci USA* 88(23):10769–10773.
126. Ehlert FJ, Roeske WR, Itoga E, Yamamura HI (1982) The binding of [3H]nitrendipine to receptors for calcium channel antagonists in the heart, cerebral cortex, and ileum of rats. *Life Sci* 30(25):2191–2202.
127. Gould RJ, Murphy KM, Snyder SH (1982) [3H]nitrendipine-labeled calcium channels discriminate inorganic calcium agonists and antagonists. *Proc Natl Acad Sci USA* 79(11):3656–3660.
128. Friesse J, Gleitz J (1998) Kavain, dihydrokavain, and dihydromethysticin non-competitively inhibit the specific binding of [3H]-batrachotoxinin-A 20-alpha-benzoate to receptor site 2 of voltage-gated Na⁺ channels. *Planta Med* 64(5):458–459.
129. Gusovsky F, et al. (1990) Voltage-dependent sodium channels in synaptoneurosome: studies with 22Na⁺ influx and [3H]saxitoxin and [3H]batrachotoxinin-A 20-alpha-benzoate binding. Effects of proparacaine isothiocyanate. *Brain Res* 518(1-2):101–106.
130. Finlayson K, Turnbull L, January CT, Sharkey J, Kelly JS (2001) [3H]dofetilide binding to HERG transfected membranes: a potential high throughput preclinical screen. *Eur J Pharmacol* 430(1):147–148.
131. Huang X-P, Mangano T, Hufeisen S, Setola V, Roth BL (2010) Identification of human Ether-à-go-go related gene modulators by three screening platforms in an academic drug-discovery setting. *Assay Drug Dev Technol* 8(6):727–742.
132. Bricca G, et al. (1994) Human brain imidazoline receptors: further characterization with [3H]clonidine. *Eur J Pharmacol* 266(1):25–33.
133. Molderings GJ, Moura D, Fink K, Bönisch H, Göthert M (1993) Binding of [3H]clonidine to I1-imidazoline sites in bovine adrenal medullary membranes. *Naunyn Schmiedeberg's Arch Pharmacol* 348(1):70–76.
134. Cahill GM, Besharse JC (1989) Retinal melatonin is metabolized within the eye of xenopus laevis. *Proc Natl Acad Sci USA* 86(3):1098–1102.
135. Benítez-King G, Huerto-Delgadillo L, Antón-Tay F (1993) Binding of 3H-melatonin to calmodulin. *Life Sci* 53(3):201–207.

136. Legros C, et al. (2014) Melatonin MT₁ and MT₂ receptors display different molecular pharmacologies only in the G-protein coupled state. *Br J Pharmacol* 171(1):186–201.
137. Kenakin T, Watson C, Muniz-Medina V, Christopoulos A, Novick S (2012) A simple method for quantifying functional selectivity and agonist bias. *ACS Chem Neurosci* 3(3):193–203.
138. Gregory KJ, Sexton PM, Tobin AB, Christopoulos A (2012) Stimulus bias provides evidence for conformational constraints in the structure of a G protein-coupled receptor. *J Biol Chem* 287(44):37066–37077.
139. Leach K, Sexton PM, Christopoulos A (2007) Allosteric GPCR modulators: taking advantage of permissive receptor pharmacology. *Trends Pharmacol Sci* 28(8):382–389.
140. Kingston RE, Chen CA, Rose JK (2003) Calcium phosphate transfection. *Curr Protoc Mol Biol* Chapter 9:Unit 9.1.
141. Calcium phosphate-mediated transfection of eukaryotic cells (2005) *Nat Methods* 2(4):319–320.
142. Wacker D, et al. (2013) Structural features for functional selectivity at serotonin receptors. *Science* (80-) 340(6132):615–619.
143. Huang X-P, et al. (2009) Parallel functional activity profiling reveals valvulopathogens are potent 5-hydroxytryptamine(2B) receptor agonists: implications for drug safety assessment. *Mol Pharmacol* 76(4):710–722.
144. Laferrère B, et al. (1992) Effects of bombesin, of a new bombesin agonist (BIM187) and a new antagonist (BIM189) on food intake in rats, in relation to cholecystokinin. *Eur J Pharmacol* 215(1):23–28.
145. Lugin D, et al. (1991) Reduced peptide bond pseudopeptide analogues of neurotensin: binding and biological activities, and in vitro metabolic stability. *Eur J Pharmacol* 205(2):191–198.
146. Peukert S, et al. (2014) Discovery of 2-Pyridylpyrimidines as the First Orally Bioavailable GPR39 Agonists. *ACS Med Chem Lett* 5(10):1114–1118.
147. Sato S, Huang X-P, Kroeze WK, Roth BL (2016) Discovery and characterization of novel GPR39 agonists allosterically modulated by zinc. *Mol Pharmacol* 90(6):726–737.
148. Bassilana F, et al. (2014) Target identification for a Hedgehog pathway inhibitor reveals the receptor GPR39. *Nat Chem Biol* 10(5):343–349.
149. Briscoe CP, et al. (2006) Pharmacological regulation of insulin secretion in MIN6 cells through the fatty acid receptor GPR40: identification of agonist and antagonist small molecules. *Br J Pharmacol* 148(5):619–628.

150. Nakamoto K, Aizawa F, Nishinaka T, Tokuyama S (2015) Regulation of prohormone convertase 2 protein expression via GPR40/FFA1 in the hypothalamus. *Eur J Pharmacol* 762:459–463.
151. Tanaka H, et al. (2013) Chronic treatment with novel GPR40 agonists improve whole-body glucose metabolism based on the glucose-dependent insulin secretion. *J Pharmacol Exp Ther* 346(3):443–452.
152. Liu JJ, et al. (2014) Optimization of GPR40 agonists for type 2 diabetes. *ACS Med Chem Lett* 5(5):517–521.
153. Lansu K, et al. (2017) In silico design of novel probes for the atypical opioid receptor MRGPRX2. *Nat Chem Biol* 13(5):529–536.
154. Kroeze WK, et al. (2015) PRESTO-Tango as an open-source resource for interrogation of the druggable human GPCRome. *Nat Struct Mol Biol* 22(5):362–369.
155. Lew MJ, Angus JA (1995) Analysis of competitive agonist-antagonist interactions by nonlinear regression. *Trends Pharmacol Sci* 16(10):328–337.
156. Lew MJ, Angus JA (1997) An improved method for analysis of competitive agonist/antagonist interactions by non-linear regression. *Ann N Y Acad Sci* 812:179–181.
157. Christopoulos A, Parsons AM, Lew MJ, El-Fakahany EE (1999) The assessment of antagonist potency under conditions of transient response kinetics. *Eur J Pharmacol* 382(3):217–227.
158. Wang C, et al. (2013) Structural basis for molecular recognition at serotonin receptors. *Science* (80-) 340(6132):610–614.
159. Wu H, et al. (2012) Structure of the human κ -opioid receptor in complex with JDTic. *Nature* 485(7398):327–332.
160. Fenalti G, et al. (2014) Molecular control of δ -opioid receptor signalling. *Nature* 506(7487):191–196.
161. Huang X-P, et al. (2015) Allosteric ligands for the pharmacologically dark receptors GPR68 and GPR65. *Nature* 527(7579):477–483.
162. Insel PA, Ostrom RS (2003) Forskolin as a tool for examining adenylyl cyclase expression, regulation, and G protein signaling. *Cell Mol Neurobiol* 23(3):305–314.
163. Seamon KB, Daly JW (1981) Forskolin: a unique diterpene activator of cyclic AMP-generating systems. *J Cyclic Nucleotide Res* 7(4):201–224.
164. Iyengar R (1993) Molecular and functional diversity of mammalian Gs-stimulated adenylyl cyclases. *FASEB J* 7(9):768–775.
165. Shimomura Y, et al. (2002) Identification of neuropeptide W as the endogenous ligand for orphan G-protein-coupled receptors GPR7 and GPR8. *J Biol Chem* 277(39):35826–35832.

166. Coleman RA, Humphrey PP, Kennedy I, Levy GP, Lumley P (1981) Comparison of the actions of U-46619, a prostaglandin H₂-analogue, with those of prostaglandin H₂ and thromboxane A₂ on some isolated smooth muscle preparations. *Br J Pharmacol* 73(3):773–778.
167. Cimetière B, et al. (1998) Synthesis and biological evaluation of new tetrahydronaphthalene derivatives as thromboxane receptor antagonists. *Bioorg Med Chem Lett* 8(11):1375–1380.
168. Ludwig M-G, et al. (2003) Proton-sensing G-protein-coupled receptors. *Nature* 425(6953):93–98.
169. Barnea G, et al. (2008) The genetic design of signaling cascades to record receptor activation. *Proc Natl Acad Sci USA* 105(1):64–69.
170. Liu C, et al. (2011) Oxysterols direct B-cell migration through EBI2. *Nature* 475(7357):519–523.
171. Hannedouche S, et al. (2011) Oxysterols direct immune cell migration via EBI2. *Nature* 475(7357):524–527.
172. Peng Y, et al. (2018) 5-HT_{2C} Receptor Structures Reveal the Structural Basis of GPCR Polypharmacology. *Cell* 172(4):719–730.e14.
173. Xie K, et al. (2015) Stable G protein-effector complexes in striatal neurons: mechanism of assembly and role in neurotransmitter signaling. *Elife* 4.
174. Grundmann M, et al. (2018) Lack of beta-arrestin signaling in the absence of active G proteins. *Nat Commun* 9(1):341.
175. Hamdan FF, Percherancier Y, Breton B, Bouvier M (2006) Monitoring protein-protein interactions in living cells by bioluminescence resonance energy transfer (BRET). *Curr Protoc Neurosci* Chapter 5:Unit 5.23.
176. Hamdan FF, Audet M, Garneau P, Pelletier J, Bouvier M (2005) High-throughput screening of G protein-coupled receptor antagonists using a bioluminescence resonance energy transfer 1-based beta-arrestin2 recruitment assay. *J Biomol Screen* 10(5):463–475.
177. Saulière A, et al. (2012) Deciphering biased-agonism complexity reveals a new active AT₁ receptor entity. *Nat Chem Biol* 8(7):622–630.
178. Zeng H, et al. (2008) Improved throughput of PatchXpress hERG assay using intracellular potassium fluoride. *Assay Drug Dev Technol* 6(2):235–241.
179. Schwartz JW, Blakely RD, DeFelice LJ (2003) Binding and transport in norepinephrine transporters. Real-time, spatially resolved analysis in single cells using a fluorescent substrate. *J Biol Chem* 278(11):9768–9777.
180. Chen N-H, Reith MEA, Quick MW (2004) Synaptic uptake and beyond: the sodium- and chloride-dependent neurotransmitter transporter family SLC6. *Pflugers Arch* 447(5):519–531.

181. Galli A, DeFelice LJ, Duke BJ, Moore KR, Blakely RD (1995) Sodium-dependent norepinephrine-induced currents in norepinephrine-transporter-transfected HEK-293 cells blocked by cocaine and antidepressants. *J Exp Biol* 198(Pt 10):2197–2212.
182. Pacholczyk T, Blakely RD, Amara SG (1991) Expression cloning of a cocaine- and antidepressant-sensitive human noradrenaline transporter. *Nature* 350(6316):350–354.
183. Blakely RD, DeFelice LJ, Galli A (2005) Biogenic amine neurotransmitter transporters: just when you thought you knew them. *Physiology (Bethesda)* 20:225–231.
184. Bolden-Watson C, Richelson E (1993) Blockade by newly-developed antidepressants of biogenic amine uptake into rat brain synaptosomes. *Life Sci* 52(12):1023–1029.
185. Tiberghien F, Loo F (1996) Ranking of P-glycoprotein substrates and inhibitors by a calcein-AM fluorometry screening assay. *Anticancer Drugs* 7(5):568–578.
186. Wigler PW (1999) PSC833, cyclosporin A, and dextrigulidipine effects on cellular calcein retention and inhibition of the multidrug resistance pump in human leukemic lymphoblasts. *Biochem Biophys Res Commun* 257(2):410–413.
187. Essodaigui M, Broxterman HJ, Garnier-Suillerot A (1998) Kinetic analysis of calcein and calcein-acetoxymethylester efflux mediated by the multidrug resistance protein and P-glycoprotein. *Biochemistry* 37(8):2243–2250.
188. Eneroth A, et al. (2001) Evaluation of a vincristine resistant Caco-2 cell line for use in a calcein AM extrusion screening assay for P-glycoprotein interaction. *Eur J Pharm Sci* 12(3):205–214.
189. Sevin E, et al. (2013) Accelerated Caco-2 cell permeability model for drug discovery. *J Pharmacol Toxicol Methods* 68(3):334–339.
190. Krasteva S, Heiss E, Krenn L (2011) Optimization and application of a fluorimetric assay for the identification of histone deacetylase inhibitors from plant origin. *Pharm Biol* 49(6):658–668.
191. Howitz KT (2015) Screening and profiling assays for HDACs and sirtuins. *Drug Discov Today Technol* 18:38–48.
192. Yeung F, et al. (2004) Modulation of NF-kappaB-dependent transcription and cell survival by the SIRT1 deacetylase. *EMBO J* 23(12):2369–2380.
193. Howitz KT, et al. (2003) Small molecule activators of sirtuins extend *Saccharomyces cerevisiae* lifespan. *Nature* 425(6954):191–196.
194. Peng L, Zhang G, Zhang D, Wang Y, Zhu D (2010) A direct continuous fluorometric turn-on assay for monoamine oxidase B and its inhibitor-screening based on the abnormal fluorescent behavior of silole. *Analyst* 135(7):1779–1784.

195. Zhou M, Panchuk-Voloshina N (1997) A one-step fluorometric method for the continuous measurement of monoamine oxidase activity. *Anal Biochem* 253(2):169–174.
196. Zhou JJ, Zhong B, Silverman RB (1996) Direct continuous fluorometric assay for monoamine oxidase B. *Anal Biochem* 234(1):9–12.
197. Matsumoto T, et al. (1985) A sensitive fluorometric assay for serum monoamine oxidase with kynuramine as substrate. *Clin Biochem* 18(2):126–129.
198. Suzuki O, Noguchi E, Yagi K (1976) A simple fluorometric assay for type B monoamine oxidase activity in rat tissues. *J Biochem* 79(6):1297–1299.
199. Shults MD, Janes KA, Lauffenburger DA, Imperiali B (2005) A multiplexed homogeneous fluorescence-based assay for protein kinase activity in cell lysates. *Nat Methods* 2(4):277–283.
200. Shults MD, et al. (2007) A multiplexed protein kinase assay. *Chembiochem* 8(8):933–942.
201. Shults MD, Imperiali B (2003) Versatile fluorescence probes of protein kinase activity. *J Am Chem Soc* 125(47):14248–14249.